SJL

British Journal of Pharmacology

May 1992

Volume 106 Number 1 pages 1–226

Br. J. Pharmacol. (1992), **106**, 3–8 © Macmillan Press Ltd, 1992

Morphine 6-glucuronide: a metabolite of morphine with greater emetic potency than morphine in the ferret

P.I. Thompson, *S. Bingham, [1]*P.L.R. Andrews, N. Patel, S.P. Joel & M.L. Slevin

Department of Medical Oncology, St Bartholomew's and Homerton Hospitals, London and *Department of Physiology, St Georges Hospital Medical School, London

1 The emetic potencies of morphine and its metabolite morphine 6-glucuronide have been determined in the ferret by constructing dose-response curves for mean total retches and vomits for subcutaneous doses of 0.05 mg kg^{-1} to 5 mg kg^{-1}. Morphine 6-glucuronide induced retching and vomiting at lower doses than morphine and at a maximal dose induced more retching and vomiting than morphine.

2 The emesis induced by both morphine and morphine 6-glucuronide was abolished by the pre-administration of naloxone (0.5 mg kg^{-1} s.c.).

3 The 5-HT$_3$ receptor antagonists granisetron and ondansetron (1 mg kg^{-1}, s.c.) failed to abolish or reduce emesis induced by either compound.

4 At a high-dose (5 mg kg^{-1}), morphine but not morphine 6-glucuronide failed to induce emesis and abolished the emesis induced by the cytotoxic drug, cyclophosphamide (200 mg kg^{-1}, i.p.).

5 Preliminary pharmacokinetic studies of intravenous and subcutaneous morphine and morphine 6-glucuronide revealed that morphine 6-glucuronide accounts for less than 1% of the metabolic product of morphine in the ferret. Peak plasma levels of the two compounds after their subcutaneous administration were obtained within 10 min. The metabolic profile of morphine was not dose-dependent. There was no relationship between plasma level and emetic response for either compound.

Keywords: Emesis; ferret; morphine metabolism; morphine pharmacokinetics; morphine 6-glucuronide pharmacokinetics

Introduction

In 1969 Yoshimura *et al.* demonstrated that in addition to morphine 3-glucuronide (M3G), morphine was metabolized to morphine 6-glucuronide (M6G) in the rabbit. Subsequently M6G was identified in man (Oguri *et al.*, 1970). These investigators were the first to synthesize M6G and administer the compound to mice (Kamata *et al.*, 1969; Shimomura *et al.*, 1971). They found that M6G in contrast to M3G possessed potent antinociceptive activity. In comparison with morphine, M6G appeared to have 4 times the analgesic potency when given systemically and 45 times the potency when given directly into the cerebral ventricles. This has since been confirmed by other workers in rats (Pasternak *et al.*, 1987; Abbott & Palmour, 1988). The LD_{50} of M6G, however, was 86% that of morphine, not 25% as would be expected if the antinociceptive potency directly correlated with toxicity.

The analgesic activity of M6G has now been demonstrated in man with 14 of 16 patients with cancer pain, given 1 mg 70 kg^{-1} to 4 mg 70 kg^{-1} by intravenous injection, experiencing significant pain relief (Osborne *et al.*, 1989). In that phase I study, no patients experienced nausea, dysphoric symptoms or clinically significant cardiorespiratory side effects. In view of the higher LD_{50} of M6G in mice (when corrected for antinociceptive potency) and the lack of toxicity seen in the phase I study, M6G may have an improved therapeutic/toxic ratio in man compared to morphine. The most troublesome side effects of morphine administration in man are nausea and vomiting, constipation, drowsiness and respiratory depression (Comroe & Dripps, 1948; Miller, 1980; Ventafridda, 1984).

The aim of the present study was to assess and quantify the comparative emetic effects of a range of doses of morphine and M6G in the ferret which is considered a good model of emesis in man for cytotoxic drugs (Florczyk *et al.*, 1981). The ability of the opioid receptor antagonist, naloxone, to block emesis was investigated as was the effect of the 5-HT$_3$ receptor antagonists granisetron (BRL 43694) and ondansetron (GR 38032F). Both these compounds have proved to have potent anti-emetic effects against cytotoxic- and radiation-induced vomiting in the ferret (Stables *et al.*, 1987; Bermudez *et al.*, 1988).

Methods

Conscious animals

Forty three fed ferrets weighing between 420 g and 1580 g (mean 850 g) were given morphine or M6G subcutaneously in the shoulder and observed for a minimum of 1 h. The dose-range administered was 0.01 mg kg^{-1} to 5 mg kg^{-1} for M6G and 0.05 mg kg^{-1} to 5 mg kg^{-1} for morphine, the lowest dose for each compound being the highest dose at which none of 5 animals showed an emetic response. Five animals were tested at each dose up to one dose level above the dose achieving a 100% emetic response, and 4 animals at higher dose levels. The ED_{100} is defined as the minimum dose producing an emetic response in all animals tested. The doses used were: 0.01, 0.02, 0.05, 0.1, 0.2, 0.5, 1.0, 2.0 and 5.0 mg kg^{-1}. There was at least one week between the use of any one animal in testing to avoid the development of tolerance.

Pharmacology of the emetic response The reversibility of the emetic response with the opioid receptor antagonist naloxone was investigated. Naloxone (0.5 mg kg^{-1}) was administered by intraperitoneal injection to 6 ferrets. Immediately following this 3 animals were given 0.2 mg kg^{-1} morphine (the ED_{100} dose) by subcutaneous injection and 3 animals 0.05 mg kg^{-1} M6G (the ED_{100} dose). They were then observed for at

[1] Author for correspondence.

least 2 h to ensure the latency to emesis was not just prolonged.

The effectiveness of the 5-HT_3 receptor antagonists, granisetron and ondansetron, was also investigated: 6 animals received granisetron (1 mg kg^{-1}) by subcutaneous injection 30 min before receiving 0.2 mg kg^{-1} morphine subcutaneously and 5 animals received the same dose of granisetron before M6G (0.05 mg kg^{-1} s.c.). Six animals were also given ondansetron (1 mg kg^{-1}) before receiving morphine as above. All animals were observed for 1 h.

Anti-emetic effects of a high-dose of morphine In the cat Costello & Borison (1977) have previously noted an anti-emetic effect of high doses of morphine. This was further studied in the ferret with the cytotoxic agent cyclophosphamide used as the emetic stimulus. Cyclophosphamide was given at a dose of 200 mg kg^{-1} by intraperitoneal injection to 4 animals immediately following a subcutaneous injection of 5 mg kg^{-1} of morphine. This dose of cyclophosphamide has previously been shown to cause emesis in all animals tested with a latency of less than 20 min (Hawthorn *et al.*, 1988).

Analysis and statistics The number and timing of retches and vomits was recorded as well as general behaviour. Dose-response curves were established for each compound for mean number of retches and vomits occurring over 1 h, mean latency of responders, mean duration of response and percentage of animals having an emetic response. The mean duration of response was defined as the mean time from the first to last retch or vomit. Results are expressed as mean (± s.e.mean). The differences at each dose between morphine and M6G for these parameters were compared by the Mann Whitney U test.

Anaesthetized animals

Pharmacokinetics and metabolism The emetic potency of M6G revealed in this study was unexpected. The pharmacokinetics and metabolism of intravenous and subcutaneous morphine and M6G in the ferret was therefore assessed in a preliminary study to determine the differences in metabolism compared to man, and to determine if there was any correlation between plasma levels and emesis. In view of the difficulty in obtaining multiple arterial blood samples in the conscious ferret, anaesthetized animals were used for this pilot pharmacokinetic study. This also enabled the collection of intermittent bile and urine samples. After an overnight fast, 8 ferrets were anaesthetized with urethane (1.5 g kg^{-1}, 50% w/v in 154 mM NaCl) by intraperitoneal injection. The trachea, the external jugular vein and the carotid artery were located and cannulated following a midline incision into the neck. Morphine and morphine-6-glucuronide were administered either subcutaneously into the shoulder or intravenously. Each of the 8 ferrets used in this pilot study received a different drug and drug dose given by either method of administration (see results for details).

The time points at which blood was taken were: 2, 3, 5, 7.5, 10, 15, 30, 60 and 120 min. A final blood sample was taken immediately before the animals were killed at the conclusion of the experiment. At each time point a volume of 0.5 ml blood was taken from the carotid artery cannula to clear the line and put aside for re-injection via the jugular cannula. A further volume of 0.75 to 1 ml blood was then taken for analysis. The blood was immediately separated and the plasma frozen at − 40°C until assay. Blood removed was replaced by an equal volume of 10% dextran administered via the external jugular line. The first replacement was given after the 15 min sample and was equivalent to the total volume removed up to that time. Subsequent replacements were given after the removal of each blood sample.

The plasma concentrations of morphine, M3G and M6G after morphine administration and of morphine-6-glucuronide after morphine-6-glucuronide were examined. The assay method involves a modification (Joel *et al.*, 1988) of the high performance liquid chromatography assay first described by Svensson *et al.* (1982). This assay simultaneously detects morphine and M6G by electrochemical detection and M3G by fluorescence detection. The lower limit of sensitivity for morphine and morphine 6-glucuronide is 2 nmol l^{-1} and for morphine 3-glucuronide is 20 nmol l^{-1}.

Pharmacokinetic calculations Pharmacokinetic profiles for each animal were established by use of the dedicated drug pharmacokinetic computer programme 'STRIPE'. This programme derives the best experimental fit to the log concentration versus time curve using least squares regression analysis.

The elimination half-life ($t_{\frac{1}{2}}$) was calculated from the formula:

$$t_{\frac{1}{2}} = \frac{0.693}{k}$$

where k is the slope of the exponential following the initial distribution phase. The elimination data confomed to a two compartment model. The area under the concentration-time curve from zero to infinity (AUC[0−∞]) was calculated by using the trapezoidal rule from T0 to Tn (where T0 = time of drug administration and Tn = time of the last plasma sample) and adding this to the area from Tn to T∞ calculated by dividing the concentration at Tn (Cn) by the elimination rate constant:

$$AUC[0-\infty] = AUC(0\text{-}Tn) + \frac{Cn}{k}$$

Drugs

Drugs used were cyclophosphamide (Farmatalia Carlo Urba Ltd, UK), granisetron (kindly donated by Smith-Kline Beecham Pharmaceuticals Ltd), morphine 6-glucuronide (Salford Ultrafine Chemicals Ltd, Manchester, UK), morphine sulphate (Evans Medical Ltd, UK), naloxone hydrochloride (Dupont (UK) Pharmacuticals Ltd) and ondansetron (kindly donated by Glaxo, UK). All drugs were either diluted or dissolved in 154 mM NaCl and injected intravenously or subcutaneously in a volume of 0.5 ml kg^{-1}.

Results

Emetic effects of morphine and morphine 6-glucuronide

Table 1 shows the incidence of retches or vomits which occurred at each dose of morphine and M6G. From these data, doses were chosen which elicited an emetic response in all animals tested in that group (ED_{100}). These were 0.2 mg kg^{-1} for morphine and 0.05 mg kg^{-1} for M6G and were used for the subsequent pharmacology studies.

The dose-response curves for mean number of retches and

Table 1 Incidence of retching and vomiting by dose (animals responded/animals tested) of morphine or morphine-6-glucuronide (M6G) given subcutaneously

	Retches		*Vomits*	
	Morphine	*M6G*	*Morphine*	*M6G*
Dose (mg kg^{-1})				
0.01	—	0/5	—	0/5
0.02	—	2/5	—	2/5
0.05	0/5	8/8	0/5	4/8
0.10	2/5	5/5	2/5	5/5
0.20	8/8	4/4	4/8	4/4
0.50	5/5	4/4	4/5	4/4
1.00	2/4	4/4	1/5	3/4
2.00	3/4	4/4	1/4	3/4
5.00	0/4	3/4	0/4	2/4

vomits for both morphine and M6G are shown in Figure 1a and b respectively. At all doses tested M6G evoked more retching and vomiting than morphine. The dose at which an emetic response was first evoked (retching or vomiting) was 0.02 mg kg^{-1} for M6G and 0.1 mg kg^{-1} for morphine. The maximal emetic response for both drugs (greatest number of retches and vomits) was produced by a dose of 0.5 mg kg^{-1}. At this dose the mean latencies to retch following morphine and M6G were 7.5 and 1.5 min respectively ($P < 0.05$). The dose-response curves for both drugs were bell-shaped although the emetic response occurred over a wider dose-range following M6G. At the highest dose of 5 mg kg^{-1}, no animals had an emetic response to morphine whereas 3 out of 4 animals receiving M6G still demonstrated an emetic response. Only one of the four animals receiving morphine 5 mg kg^{-1} alone was noticeably sedated. The dose-response curves for retching and vomiting (Figure 1a and b) show a decreasing magnitude of response with doses of M6G above 0.5 mg kg^{-1}. This, coupled with the decrease in the percentage of animals responding at these dose levels, suggests that higher doses of M6G may have resulted in a reduction of effect similar to that observed with morphine. However, sedation became particularly noticeable at 5 mg kg^{-1} and higher doses were therefore not administered.

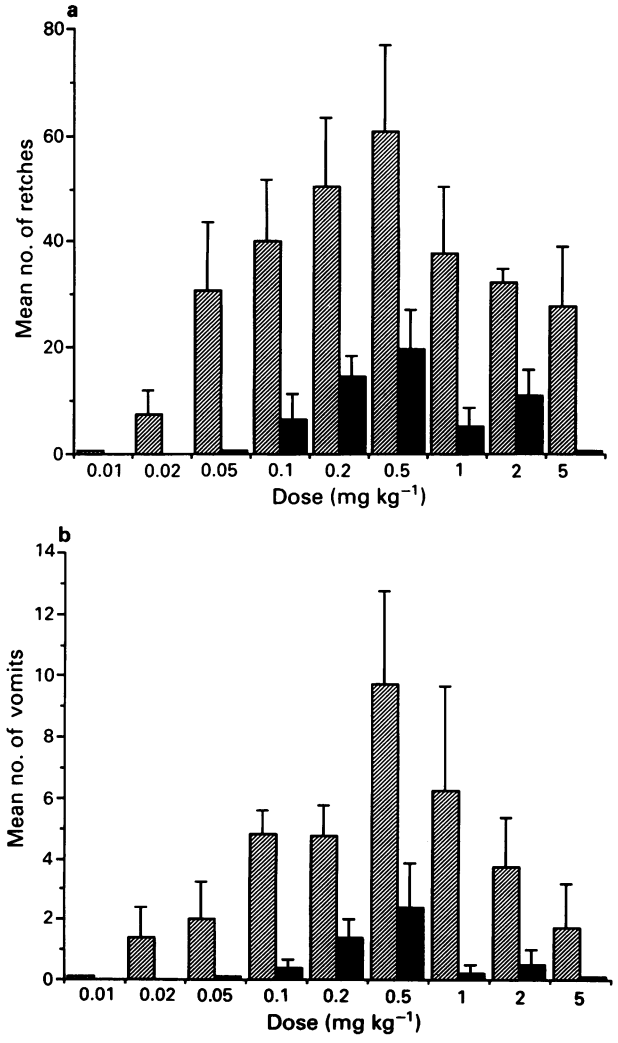

Figure 1 Dose-response relationships for mean, total retches (a) and vomits (b) for morphine (solid columns) and morphine 6-glucuronide (hatched columns) given subcutaneously. For *n* values, see Table 1; s.e.mean shown by vertical bars.

The severity of the emetic response at each dose as measured by numbers of retches was significantly greater ($P < 0.05$) following M6G than after morphine. When the mean number of retches to morphine was compared to a four to five fold lower dose of M6G (to compare approximate antinociceptive potencies) there was still a trend to increased response to M6G but this was only significant ($P < 0.05$) at 0.2 mg kg^{-1} morphine-6-glucuronide and 1 mg kg^{-1} morphine. The lack of significance at other doses may reflect the small sample size since there were only 4 or 5 animals at each dose level for each drug. There is a similar, but not so marked trend, when comparing the mean number of vomits at each dose.

There was a trend for the duration of the emetic response to be longer after M6G compared to morphine. Most of the retching and vomiting tended to occur within the first 20 min of the observation period. The pattern and duration of retching for morphine 0.2 mg kg^{-1} (ED_{100}) and M6G 0.05 mg kg^{-1} (ED_{100}) is shown in Figure 2a and b respectively and for vomiting in Figure 2c and d respectively.

Antagonism of the emetic response to morphine and morphine 6-glucuronide

Naloxone The prior administration of the opioid receptor antagonist naloxone (0.5 mg kg^{-1}) completely abolished the emetic response to both M6G 0.05 mg kg^{-1} (ED_{100}) and morphine 0.2 mg kg^{-1} (ED_{100}).

Granisetron and ondansetron Granisetron (1 mg kg^{-1}) failed to attenuate the magnitude of the emetic response to morphine 0.2 mg kg^{-1} and M6G 0.05 mg kg^{-1} as determined by the total number of retches and vomits. The mean number of retches following morphine in the control animals and granisetron-treated animals was 15.9 (± 2.9) and 31.3 (± 6.4) respectively ($P < 0.05$) and following M6G 30.6 (± 12.7) and 69.8 (± 9.2) respectively ($P < 0.05$). The mean number of vomits following morphine in the control animals and granisetron-treated animals was 1.6 (± 0.7) and 1.5 (± 0.08) respectively and following M6G 2.2 (± 1.4) and 6.8 (± 1.3) respectively (not significant). A second 5-HT$_3$ receptor antagonist, ondansetron, was tested against morphine only and also failed to abolish emesis. Again there was a trend for the mean number of retches to be increased (29.7 ± 7.2) compared to control (15.9 ± 2.9) but this was not significant ($P = 0.1$).

Anti-emetic effects of a high-dose of morphine

Morphine (5 mg kg^{-1}) which had previously been shown to have no appreciable emetic effects, completely abolished the emetic response to cyclophosphamide. All 4 animals showed marked sedation whereas only one animal of the 4 animals given morphine 5 mg kg^{-1} alone had such marked sedation. M6G was not investigated as at the highest dose of M6G tested (5 mg kg^{-1}) there was still significant emesis induced.

Other behavioural effects

There was no noticeable difference in either defaecatory pattern or stool consistency following administration of morphine or M6G. No excess salivation was observed. A tremor was noticed during the observation period in some animals receiving either compound but there appeard to be no dose- or drug-relationship. Mild sedation distinguished by a general reduction in locomotor activity was also noted in some animals at the highest doses, particularly with M6G.

Metabolism and pharmacokinetics

Figure 3a shows the plasma concentrations of morphine, morphine 3-glucuronide (M3G) and M6G after 5 mg kg^{-1} intravenous morphine. It also shows the plasma profile of

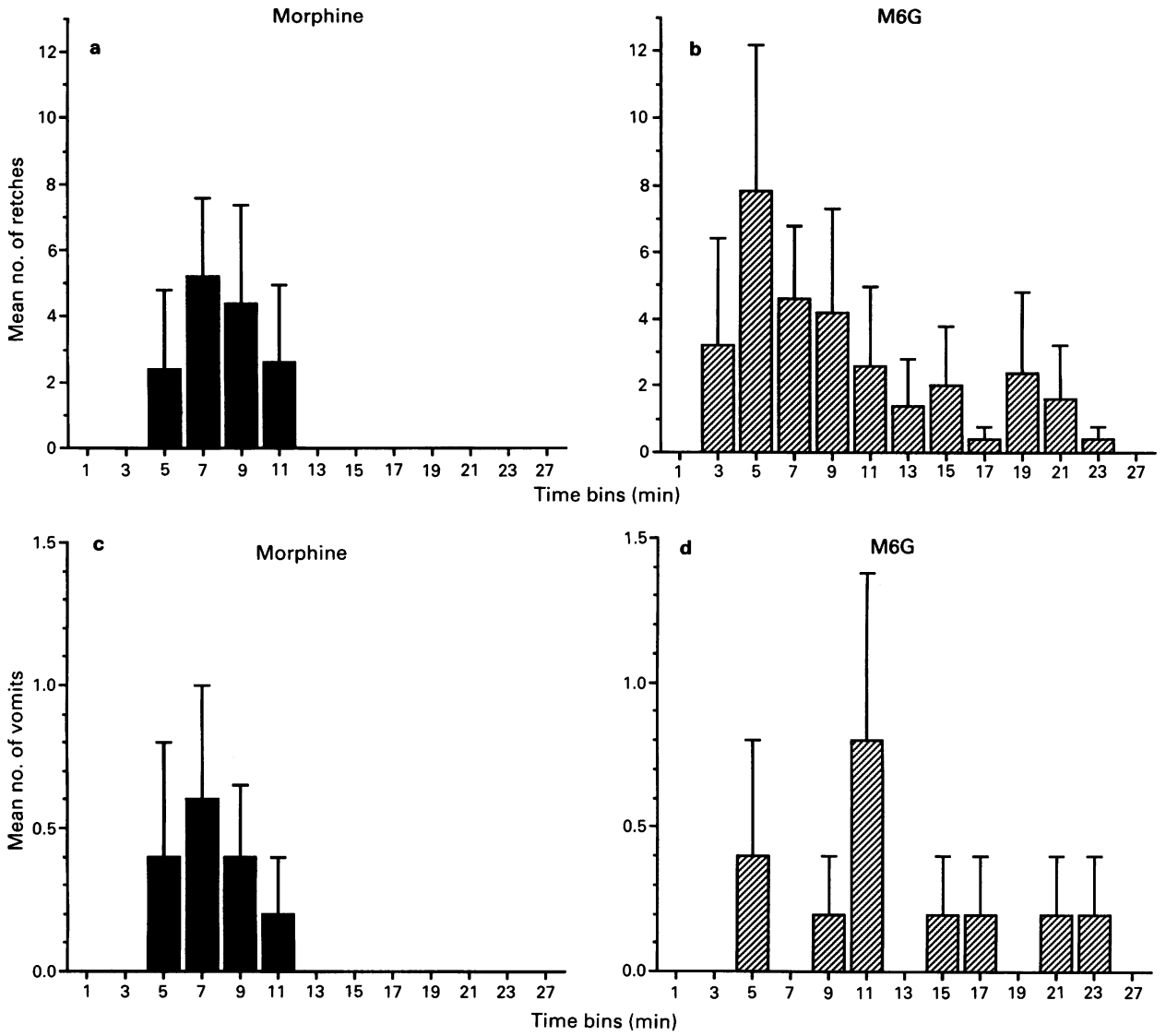

Figure 2 The profile of the emetic response to morphine and morphine 6-glucuronide (M6G). Mean number of retches (a and b) and vomits (c and d) in 2 min time bins for morphine 0.2 mg kg^{-1} and morphine 6-glucuronide 0.05 mg kg^{-1} respectively; s.e.mean shown by vertical bars. Both drugs given at the lowest dose which induces an emetic response in all animals tested (defined here as ED_{100}).

morphine after subcutaneous morphine. Figure 3b shows the plasma M6G levels after either intravenous or subcutaneous administration of 1.67 mg kg^{-1} M6H. Table 2 summarises the pharmacokinetic parameters obtained after the various administrations of morphine and M6G. Peak plasma concentrations of either drug after subcutaneous injection were reached rapidly with levels within 10% of the peak achieved by 7.5 min. Metabolism and or excretion is rapid with the elimination half-life ($t_{\frac{1}{2}}$) of morphine between 45 to 50 min by either route and similarly for M6G. It can be seen that morphine undergoes rapid and extensive metabolism to M3G with the peak level seen at 1 h and the area under the curve (AUC[0−∞]) approximately 9 times that of morphine. In contrast only very low amounts of M6G are formed with the AUC(0−∞) being less than 1% of that of M3G. Following the administration of 0.2 mg kg^{-1} of morphine either intravenously or subcutaneously the plasma pharmacokinetic parameters of morphine were similar to the higher dose with a $t_{\frac{1}{2}}$ of between 35 to 40 min. The plasma levels of M3G and M6G were too low to measure but the bile level of M3G in the gallbladder 140 min after intravenous morphine was 61.5 μmol l^{-1}, 160 times the level of M6G (0.39 μmol l^{-1}). This is similar to the plasma AUC[0−∞] ratios seen with the higher dose of morphine suggesting the relative amounts of M3G and M6G formed are the same following different doses. Following the administration of 0.05 mg kg^{-1} M6G the principle pharmacokinetic parameters were also similar to those obtained after a higher dose with a $t_{\frac{1}{2}}$ of 30 to 55 min.

Discussion

This study has shown M6G to be a potent emetic compound in the ferret. It causes emesis at a four to five fold lower dose than morphine which is in a similar ratio to the greater antinociceptive potency of M6G seen in mice (Shimomura *et al.*, 1971) and rats (Abbott & Palmour, 1988). The severity of the emetic response as assessed by total numbers of retches and vomits at any given dose and duration of emesis also appears greater than with the parent compound morphine, even correcting for an antinociceptive potency advantage of M6G of 3 to 4.

The AUC(0−∞) of M6G in man after an intravenous injection of morphine is 1.5 times higher than that of morphine (Osborne *et al.*, 1990). It is therefore tempting to extrapolate that M6G is responsible for most of the emesis seen in man

after morphine administration. However there are several reasons why this may not be true. Firstly, after an oral dose of morphine to man the AUC(0−∞) of M6G is 9 times higher than that of morphine due to the first pass metabolism of morphine in the liver. Hence one might expect greatly increased emesis in man after an oral morphine dose as compared to an intravenous dose but this is not seen.

Secondly, the present study demonstrates a different metabolic profile in the ferret following morphine administration compared to man. M6G accounts for less than 1% of the metabolic product of morphine with the AUC(0−∞) of M6G being less than 1% that of M3G which is the major metabolite of morphine. Hence the emetic effect seen after morphine in this study is unlikely to be due to the minute amounts of M6G that are present. Previous studies have failed to show M3G having any significant analgesic action or show any significant binding to opioid receptors and it is unlikely that M3G can be implicated as a cause of the emesis seen after morphine despite the high plasma levels seen (Shimomura *et al.*, 1971; Pasternak *et al.*, 1987; Oguri *et al.*, 1987). The emetic effect is most likely to be due to morphine itself.

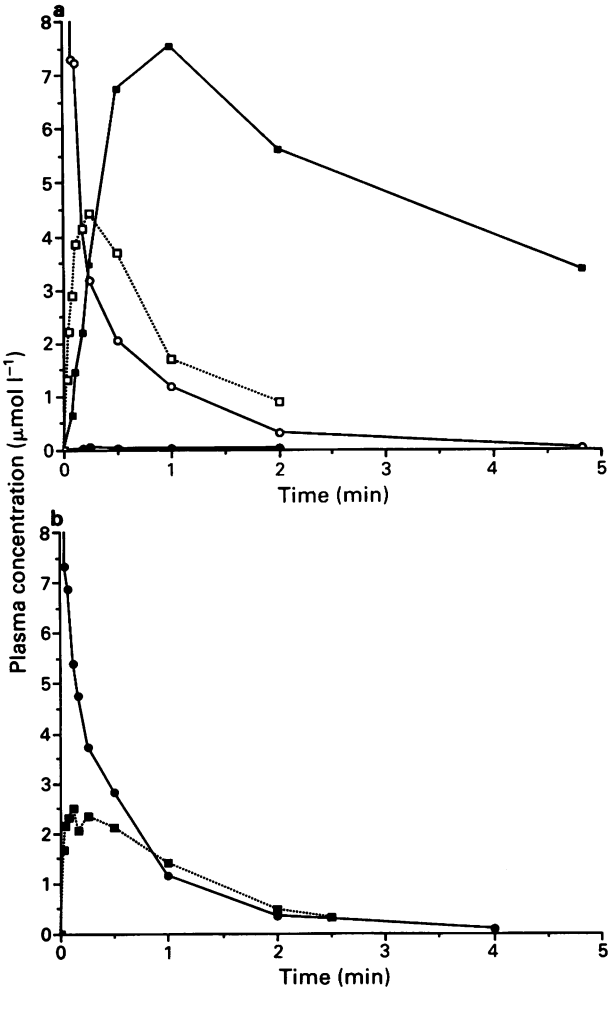

Figure 3 (a) Graph of plasma and metabolite concentrations after intravenous (i.v.) and subcutaneous morphine 5 mg kg^{-1}: (○) morphine levels after i.v. morphine; (■) morphine 3-glucuronide concentration after i.v. morphine; (●) morphine 6-glucuronide concentration after i.v. morphine, and (□) morphine concentration after s.c. morphine. (b) Graph of plasma morphine 6-glucuronide concentrations after i.v. and s.c. morphine 6-glucuronide. Both graphs are from individual animals.

Thirdly, the significant emetic response of ferrets to M6G is in contrast to the results obtained in a phase I study of M6G in human patients with cancer pain (Osborne *et al.*, 1989): 17 patients were treated with single doses of M6G at doses ranging from 0.15 mg kg^{-1} to 0.6 mg kg^{-1} and no patients experienced nausea within this dose-range which produced significant analgesia in 14 of 16 assessable patients. A more controlled study with the same patients or subjects receiving equipotent doses of M6G and morphine is required however to compare formally the compounds in man.

It has previously been demonstrated that opiates may also have antiemetic effects and that these may be mediated via a medullary antiemetic centre (Costello & Borison, 1977; Harris, 1982). The present study has confirmed that not only does morphine fail to induce emesis at a high dose (5 mg kg^{-1}) but in addition it can actually act as an antiemetic against cytotoxic-induced vomiting.

The antinociception and seizures induced by high doses of M6G have been previously found to be antagonized by naloxone (Pasternak *et al.*, 1987). In the present study naloxone completely abolished the emetic response of both morphine and M6G. In contrast the 5-HT$_3$ receptor antagonists, granisetron and ondansetron, so successful in inhibiting the emesis induced by the cytotoxic drug cisplatin (Stables *et al.*, 1987; Bermudez *et al.*, 1988), failed to have any effect on the emetic response to either morphine or M6G, even though the doses used are in excess of those required to block radiation- and cytotoxic-induced emesis in this species (Bermudez *et al.*, 1988). For granisetron the dose used was 20 times that which blocks the emetic response to 200 rads total body irradiation in the ferret (Bhandari & Andrews, 1991). The abdominal visceral innervation plays a major role in the emetic action of cytotoxic agents such as cisplatin as bilateral abdominal vagotomy can totally abolish vomiting to cisplatin in the ferret (Hawthorn *et al.*, 1988). It is thought 5-HT$_3$ receptor antagonists block the emetic action of cisplatin by their action at 5-HT$_3$ receptors on visceral afferent nerves (Andrews *et al.*, 1990) although their action at more central sites cannot be completely excluded. The emesis induced with apomorphine acting on the area postrema is not attenuated by 5-HT$_3$ antagonists (Bermudez *et al.*, 1988) and this together with the data from the present study suggests that the 5-HT$_3$ receptor antagonists do not have their effect on the area postrema.

Although the ferret is thought to be a good model for emesis induced by cytotoxic drugs and radiation in man, it is

Table 2 Pharmacokinetic parameters after intravenous and subcutaneous administration of morphine (5 mg kg^{-1}) and morphine 6-glucuronide (M6G) (1.67 mg kg^{-1}) to individual animals

	Morphine 6-glucuronide		*Morphine i.v.*			*Morphine s.c.*
	i.v.	*s.c.*	*M*	*M3G*	*M6G*	*M*
Elimination $t_{\frac{1}{2}}$ (min)	41	42	46	—	—	47
AUC[0−∞]μmol l.h^{-1}	4.69	3.41	4.73	41.2	0.30	5.37
C_{max} (nmol l^{-1})	10673	2492	17445	7558	58	4442
T_{max} (min)	—	7	—	60	15	15

Elimination $t_{\frac{1}{2}}$ = elimination half-life. AUC[10−∞] = area under the concentration-time curve from zero to infinity. C_{max} = maximum plasma concentration. T_{max} = time to maximal concentration.

possible this is not the case for opioid-like compounds which appear to act via different mechanisms. In addition we have demonstrated that the ferret does not metabolize morphine in the same way as man. Less than 1% of the metabolic product is M6G in the ferret as compared to 10% in man. Hence, as well as demonstrating the different emetic effects of morphine and M6G in varying situations, the present study also demonstrates the importance of studying the drug handling of an animal model used for drug testing, particularly when metabolites are thought to play a role in the clinical effect. Yet another species difference in morphine metabolism has been observed in chickens by Watrous et al. (1970) who found the major metabolite in the urine to be morphine ethereal-sulphate. Species differences have also been shown with respect to the opioid receptor (Paterson et al., 1983). These observations raise the possibility that the actions of morphine and M6G on the opioid receptor may also be different between the ferret and man.

However this study has given us the unique opportunity to observe the emetic effects of morphine alone, as it has insignificant active metabolites in the ferret, whereas in man it is always difficult to determine how much of any effect is due to the morphine administered and how much is due to M6G.

References

ABBOTT, F.V. & PALMOUR, R.M. (1988). Morphine-6-glucuronide: analgesic effects and receptor binding profile in rats. *Life Sci.*, **43**, 1685–1695.

ANDREWS, P.L.R., DAVIS, C.J., BINGHAM, S., DAVIDSON, H.I.M., HAWTHORN, J. & MASKELL, L. (1990). The abdominal visceral innervation and the emetic reflex: pathways, pharmacology and plasticity. *Can. J. Physiol. Pharmacol.*, **68**, 325–345.

BHANDARI, P. & ANDREWS, P.L.R. (1991). Preliminary evidence for an involvement of the putative $5HT_4$ receptor in zacopride and copper sulphate induced vomiting in the ferret. *Eur. J. Pharmacol.*, **204**, 273–280.

BERMUDEZ, J., BOYLE, E.A., MINER, W.D. & SANGER, G.J. (1988). The anti-emetic potential of the 5-hydroxytryptamine$_3$ receptor antagonist BRL43694. *Br. J. Cancer*, **58**, 644–650.

COMROE, J.H. & DRIPPS, R.D. (1948). Reactions to morphine in ambulatory and bed patients. *Surg. Gynecol. Obstet.*, **87**, 221–224.

COSTELLO, D.J. & BORISON, H.L. (1977). Naloxone antagonizes narcotic self-blockade of emesis in the cat. *J. Pharmacol. Exp. Ther.*, **203**, 222–230.

FLORCZYK, A.P., SCHURIG, J.E. & BRADNER, W.T. (1981). Cisplatin induced emesis in the ferret mustela-putorius-furo a new animal model. *Cancer Treat. Rep.*, **66**, 187–194.

HARRIS, A.L. (1982). Cytotoxic-therapy-induced vomiting is mediated via enkephalin pathways. *Lancet*, **i**, 714–716.

HAWTHORN, J., OSTLER, K.J. & ANDREWS, P.L.R. (1988). The role of the abdominal visceral innervation and 5-hydroxytryptamine M-receptors in vomiting induced by the cytotoxic drugs cyclophosphamide and cis-platin in the ferret. *Q. J. Exp. Physiol.*, **73**, 7–21.

JOEL, S.P.L., OSBORNE, R.J. & SLEVIN, M.L. (1988). An improved method for the simultaneous determination of morphine and its principal glucuronide metabolites. *J. Chromatogr.*, **430**, 394–399.

KAMATA, O., WATANABE, S., ISHII, S., UEKI, S., OGURI, K., IDA, S., YOSHIMURA, H. & TSUKAMOTO, H. (1969). Analgesic effects of morphine glucuronides. *Proc. 89th Pharmacol. Soc.* Japan, 443.

MILLER, R.R. (1980). Clinical effects of parenteral narcotics in hospitalized medical patients. *J. Clin. Pharmacol.*, **20**, 165–171.

OGURI, K., IDA, S., YOSHIMURA, H. & TSUKAMOTO, H. (1970). Metabolism of drugs. LXIX. Studies on the urinary metabolites of morphine in several mammalian species. *Chem. Pharmacol. Bull.*, **18**, 2414–2419.

OGURI, K., YAMADA-MORI, I., SHIGEZANE, J., HIRANO, T. & YOSHIMURA, H. (1987). Enhanced binding of morphine and nalorphine to opioid receptor by glucuronate and sulfate conjugations at the 6-position. *Life Sci.*, **41**, 1457–1464.

OSBORNE, R.J., SLEVIN, M.L., JOEL, S.P., TREW, D.M., THOMPSON, P.I. & MALPAS, J.S. (1989). The analgesic activity and pharmacokinetics of morphine-6-glucuronide in man. Proceedings of the association of Cancer Physicians 4th Annual Meeting, Glasgow, Scotland, April 1989. *Br. J. Cancer*, **60**, 451.

OSBORNE, R.J., JOEL, S.P., TREW, D. & SLEVIN, M.L. (1990). Pharmacokinetics of morphine and morphine glucuronides in normal subjects after different routes of morphine administration. *Clin. Pharmacol. Ther.*, **47**, 12–19.

PASTERNAK, G.W., BODNAR, R.J., CLARK, J.A. & INTURRISI, C.E. (1987). Morphine-6-glucuronide, a potent mu agonist. *Life Sci.*, **41**, 2845–2849.

PATERSON, S.J., ROBSON, L.E. & KOSTERLITZ, H.W. (1983). Classification of opioid receptors. *Br. Med. Bull.*, **39**, 31–36.

SHIMOMURA, K., KAMATA, O., UEKI, S., IDA, S., OGURI, K., YOSHIMURA, H. & TSUKAMOTO, H. (1971). Analgesic effects of morphine glucuronides. *Tohoku J. Exp. Med.*, **105**, 45–52.

STABLES, R., ANDREWS, P.L.R., BAILEY, H.E., COSTALL, B. & GUNNING, S.J. (1987). Antiemetic properties of the 5-HT_3-receptor antagonist, GR38032F. *Cancer Treat. Rev.*, **14**, 333–336.

SVENSSON, J.O., RANE, A., SAWE, J. & SJOQVIST, F. (1982). Determination of morphine, morphine-3-glucuronide and (tentatively) morphine-6-glucuronide in plasma and urine using ion-pair high-performance liquid chromatography. *J. Chromatogr.*, **230**, 427–432.

VENTAFRIDDA, V. (1984). Use of systemic analgesic drugs in cancer pain. *Adv. Pain. Res. Ther.*, **7**, 557–575.

WATROUS, W.M., MAY, D.G. & FUJIMOTO, J.M. (1970). Mechanism of the renal tubular transport of morphine and morphine ethereal sulfate in the chicken. *J. Pharmacol. Exp. Ther.*, **172**, 224–229.

YOSHIMURA, H., OGURI, K. & TSUKAMOTO, H. (1969). Metabolism of drugs – LXII. Isolation and identification of morphine glucuronides in urine and bile of rabbits. *Biochem. Pharmacol.*, **18**, 279–286.

(Received May 9, 1990
Revised August 13, 1991
Accepted December 16, 1991)

Br. J. Pharmacol. (1992), **106**, 9–16 © Macmillan Press Ltd, 1992

Comparison of the actions of acetylcholine and BRL 38227 in the guinea-pig coronary artery

D.M. Eckman, J.D. Frankovich & [1]K.D. Keef

Department of Physiology, School of Medicine, University of Nevada, Reno, Nevada 89557, U.S.A.

1 The contractile and electrical responses to acetylcholine (ACh) in isolated segments of guinea-pig and rabbit coronary arteries were compared to those of the putative adenosine 5'-triphosphate (ATP)-dependent K^+ channel opener, BRL 38227.

2 Both ACh and BRL 38227 produced concentration-dependent relaxation of vessel segments contracted with the H_1-receptor agonist, 2-(2-aminoethyl)pyridine.

3 An IC_{90} of either vasodilator also produced 17–20 mV of hyperpolarization of the guinea-pig coronary artery.

4 Glibenclamide (1–35 μM) depolarized the guinea-pig coronary artery by 8–12 mV and antagonized BRL 38227- but not ACh-induced relaxation and hyperpolarization.

5 In the guinea-pig coronary artery, the K^+ channel blockers phencyclidine (PCP, 100 μM), tetraethylammonium (TEA, 10 mM) and scorpion venom (8.7 $\mu g\,ml^{-1}$) all significantly reduced ACh-induced relaxation and hyperpolarization whereas only PCP was an effective antagonist of both relaxation and hyperpolarization with BRL 38227.

6 Similar effects of glibenclamide and scorpion venom on ACh- and BRL 38227-induced relaxation were observed in the rabbit coronary artery.

7 Apamin (3.5 μM) was without effect on either the ACh- or BRL 38227-induced relaxation in the guinea-pig coronary artery.

8 In conclusion, the actions of BRL 38227 in coronary artery are compatible with its proposed effects on ATP-dependent K^+ channels. In contrast, the results with ACh suggest that some step between the initial binding of ACh to endothelial muscarinic receptors and the final relaxation of the smooth muscle depends upon the opening of Ca^{2+}-activated K^+ channels.

Keywords: Vascular smooth muscle; electrophysiology; potassium channel openers; membrane potential; endothelium; vasodilators; cromakalim; acetylcholine; scorpion venom; phencyclidine; apamin; tetraethylammonium; glibenclamide; BRL 38227

Introduction

Acetylcholine (ACh) releases a factor from the endothelium of some blood vessels which hyperpolarizes the smooth muscle. This has given rise to the acronym EDHF or 'endothelium-derived hyperpolarizing factor' (Chen *et al.*, 1988). There is evidence that this factor is independent of the more well known and widely studied relaxing factor EDRF (Chen *et al.*, 1988; Feletou *et al.*, 1988; Huang *et al.*, 1988; Komori *et al.*, 1988). EDRF is widely believed to be nitric oxide (see Furchgott & VanHoutte, 1989). The separation between these two factors has become more complicated, however, with the recent reports of nitric oxide-induced hyperpolarization in some blood vessels (Tare *et al.*, 1990; 1991).

Studies of the rabbit middle cerebral artery have suggested that endothelium-dependent hyperpolarization may involve the opening of an adenosine 5'-triphosphate (ATP)-dependent K^+ channel since the hyperpolarization produced with ACh is reversed by glibenclamide (Standen *et al.*, 1989; Brayden, 1990). This agent blocks ATP-dependent K^+ channels in pancreatic β cells (Sturgess *et al.*, 1985; Schmid-Antomarchi *et al.*, 1987a,b) and cardiac muscle (Fosset *et al.*, 1988). On the other hand, studies of the rat mesenteric artery suggest that the ACh-induced hyperpolarization and relaxation in this vessel are unaffected by glibenclamide so that different hyperpolarizing factors may be involved in the actions of ACh in different blood vessels (McPherson & Angus, 1991).

Another agent which hyperpolarizes vascular smooth muscle by stimulation of K^+ channels is cromakalim (Hamilton *et al.*, 1986; Weir & Weston, 1986b). Unlike ACh which requires release of EDHF, hyperpolarization with cromakalim occurs by direct stimulation of K^+ channels in the smooth muscle membrane e.g., in isolated patches of membrane from the rabbit mesenteric artery, cromakalim has been shown to open K^+ channels (Standen *et al.*, 1989) and in recordings from isolated cells of the rabbit portal vein, addition of cromakalim leads to hyperpolarization (Beech & Bolton, 1989). The K^+ channels stimulated by cromakalim appear to be modulated by ATP since channel activity is reduced in the presence of 1 mM ATP and enhanced in its absence (Standen *et al.*, 1989). In addition it has been reported that glibenclamide: (1) blocks cromakalim-stimulated K^+ currents in isolated patches (Standen *et al.*, 1989); (2) blocks whole-cell cromakalim currents in single portal vein cells (Beech & Bolton, 1989) and (3) blocks the cromakalim-induced reduction in coronary perfusion pressure in guinea-pig isolated heart (Daut *et al.*, 1990) and fall in blood pressure in the rat (Buckingham *et al.*, 1989). Recent studies suggest that the channel opened by cromakalim may also be modulated by calcium (Gelband *et al.*, 1989; Klöckner *et al.*, 1989; Hu *et al.*, 1990; Okabe *et al.*, 1990). We studied the relaxant and hyperpolarizing properties of BRL 38227 which is the active enantiomer present in the racemic mixture known as cromakalim (see Buckingham *et al.*, 1986; Weston, 1989).

In the present study the nature of the ACh-induced hyperpolarization in the guinea-pig coronary artery has been investigated. In this vessel, ACh initiates a large hyper-

[1] Author for correspondence.

polarization (Kitamura & Kuriyama, 1979; Keef & Kreulen, 1988) which is blocked by removal of the endothelium (Keef & Bowen, 1989; Chen *et al.*, 1991). Since there is evidence from studies of the cerebral artery that cromakalim and ACh produce hyperpolarization by activation of the same smooth muscle K^+ channel (Standen *et al.*, 1989; Brayden, 1990) we have compared the relaxant and hyperpolarizing actions of ACh and BRL 38227 in the presence and absence of glibenclamide. To investigate further the mechanism by which these agonists produce hyperpolarization and relaxation we also tested the effects of several other K^+ channel blockers including phencyclidine (PCP), tetraethylammonium (TEA), apamin and scorpion venom. These data have been published in part in abstract form (Eckman & Keef, 1991).

Methods

Contractile experiments

Male guinea-pigs (400–600 g) were killed by CO_2 inhalation followed by exsanguination and the heart removed and placed in cold (10 to 15°C) oxygenated Krebs solution. A 1 to 1.5 cm segment of the left circumflex coronary artery was carefully dissected out and cleaned of all adhering fat and cardiac tissue. Ring segments (3 mm long) were mounted onto two triangular tungsten wires (89 μm diameter). The preparation was mounted vertically in an isolated tissue bath. The upper triangle was attached to a Gould strain gauge and the lower to a stable mount. The tissue bath was maintained at 37°C in Krebs solution of the following composition mM: NaCl 118.5, KCl 4.7, $MgCl_2$ 1.2, $NaHCO_3$ 23.8, KH_2PO_4 1.2, dextrose 11, $CaCl_2$ 2.5 aerated with 95% O_2/5% CO_2.

A resting force of 0.3 g was applied to the guinea-pig coronary artery. In preliminary experiments this was found to stretch vessels to near the optimal length for tension development (i.e. L_0). Vessels were initially equilibrated for 2 h with alternating 4 min exposures to the histamine H_1-receptor agonist, 2-(2-aminoethyl)pyridine (AEP 10^{-3} M, Durant *et al.*, 1975) and to 55 mM KCl (3 M KCl stock solution). The stimulants were added at 10–15 min intervals. Maximum contraction was determined in some experiments by exposing vessel segments to a combination of 10^{-3} M AEP and 100 mM KCl.

Rabbits (1.5–2.5 kg) were killed with an overdose of pentobarbitone injected into the ear vein. The rabbit does not have a true circumflex coronary artery but rather the coronary artery courses down the middle of the left ventricle. This was the vessel used for these studies. A resting force of 0.5 g was applied to 3 mm long segments of vessel. Artery segments were otherwise treated as described above for the guinea-pig. In a few experiments the endothelium of vessel segments was removed to study the direct contractile effects of ACh on the smooth muscle. This was accomplished by gentle scraping of the lumen with a stainless steel rod. The successful removal of endothelium was judged by a lack of relaxant response to application of ACh between 0.1 and 10 μM when tissues were contracted with AEP (10^{-4} M).

Intracellular measurements

For experiments measuring membrane potential, a 0.5 to 0.7 cm segment of the guinea-pig circumflex coronary artery or the rabbit left ventricular artery was used. Vessels were carefully cut open along their longitudinal axis and pinned down in the bath, adventitial side up. Microelectrodes filled with 3 M KCl and having resistances between 70 and 100 MΩ were used. All intracellular measurements were made through the adventitia into the media. Intracellular measurements were made in the absence of the contractile stimulus AEP since it is easier to obtain long term impalements under these conditions. In a previous study we have shown that the magnitude of hyperpolarization with ACh is greater in the presence of AEP than in its absence presumably since the depolarization which occurs upon exposure to AEP brings the membrane farther away from E_K (Keef & Bowen, 1989). Impalements were judged on the basis of a rapid drop in potential upon entering the cell, a low noise level and minimal change in electrode resistance and zero potential before and after impalement. Signals were viewed on a digital oscilloscope (Nicolet) and stored on tape with a Vetter PCM Recording Adapter attached to a Panasonic Video Cassette Recorder.

Statistics

Statistical significance was determined by two-tailed paired or unpaired Student's t test and where appropriate analysis of variance was performed. Changes were considered significant at $P < 0.05$. Data are expressed as mean ± s.e.mean. IC_{50} values were calculated by use of a computer programme entitled 'Analysis of the Regression Line' which is based upon *Manual of Pharmacologic Calculations with Computer Programs* (Tallarida & Murray, 1987).

Drugs used

Acetylcholine HCl (ACh, Sigma), 2-(2-aminoethyl)pyridine, (AEP, Aldrich), glibenclamide (Sigma), scorpion venom (*Leiurus quinquestriatus hebraeus*, Sigma), phencyclidine (PCP, Sigma). ACh, AEP and PCP were made up in concentrated stock solution in distilled water. Scorpion venom was made fresh daily in distilled water. Glibenclamide was dissolved in polyethylene glycol and BRL 38227 (levrocromakalim) was dissolved in either 50% polyethylene glycol and 50% distilled water or dimethyl sulphoxide. All stock solutions were kept in the dark at 2° C during use and stored between days in the freezer. Neither polyethylene glycol nor dimethyl sulphoxide produced direct effects in the concentrations used in this study.

Results

Comparison of acetylcholine- and BRL 38227-induced relaxation

The time course and magnitude of relaxation with various concentrations of acetylcholine (ACh, 10 nM–1 μM) and BRL 38227 (10 nM–1 μM) were compared. Segments of guinea-pig coronary artery were contracted with 2-(2-aminoethyl)pyridine (AEP, 1 mM). This concentration of AEP produced a contraction which was 48.6 ± 2.9% of that produced by combined AEP and 100 mM KCl ($n = 11$). The various concentrations of ACh or BRL 38227 were added sequentially so that the time course of response could be measured. Relaxation with each concentration of ACh was more rapid in onset and reached a maximum faster than with BRL 38227. For example, relaxation with a 90% maximal inhibitory concentration of ACh (i.e., IC_{90}, 0.35 μM) relaxed the tissue in 0.64 ± 0.07 min ($n = 15$) whereas with an IC_{90} of BRL 38227 (1 μM) maximal relaxation was reached after 2.47 ± 0.27 min ($n = 17$). An example of the time course of relaxation with various concentrations of ACh and BRL 38227 is shown in Figure 1a. The IC_{50} for ACh-induced relaxation was 0.022 μM ($n = 17–24$, Figure 1b) whereas for BRL 38227 it was 0.029 μM ($n = 13–22$, Figure 1b).

Effect of glibenclamide on acetylcholine- and BRL 38227-induced relaxation

The concentration-response relationship for ACh was measured in the presence and absence of 1 and 35 μM glibenclamide in segments of guinea-pig coronary artery. Vessels were contracted with AEP and increasing concentrations of ACh (0.01 μM to 1 μM) were subsequently added in a cumulative manner. In 6 of the 17 tissues, addition of 35 μM

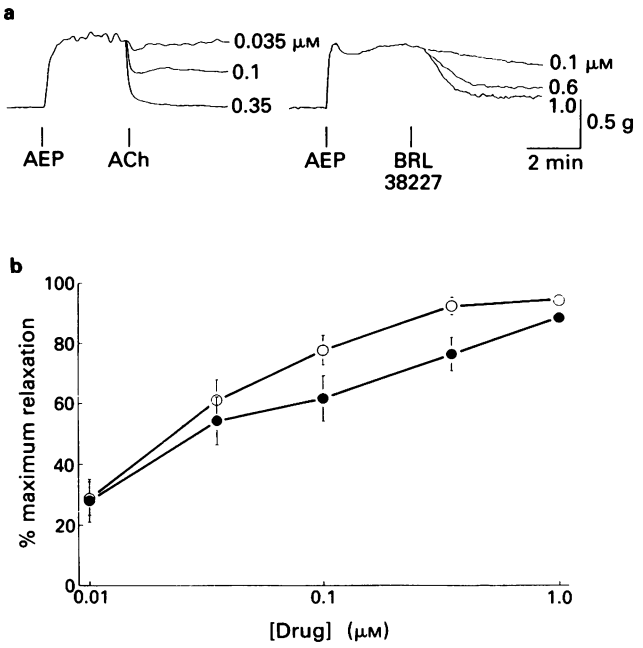

Figure 1 Comparison of the vasodilator properties of acetylcholine (ACh) and BRL 38227 in coronary artery segments contracted with 2-(2-aminoethyl)pyridine (AEP). (a) Typical examples of the relaxations observed with various concentrations of ACh (top left) and BRL 38227 (top right) in two vessel segments from the same animal. The entire contractile record for the lowest concentration of either vasodilator is shown. The relaxations obtained at higher concentrations of vasodilators have been superimposed at the arrows so that the time course of relaxations can be compared. The concentrations of vasodilator used are noted to the right of both contractile records. Note that both the onset of relaxation and the time to peak relaxation are slower for BRL 38227 than for ACh. (b) Concentration-response relationships for acetylcholine (○, $n = 8-10$)- and BRL 38227 (●, $n = 5-15$)-induced relaxations in the guinea-pig coronary artery in segments contracted with AEP. Shown are mean values with s.e. mean indicated by vertical bars.

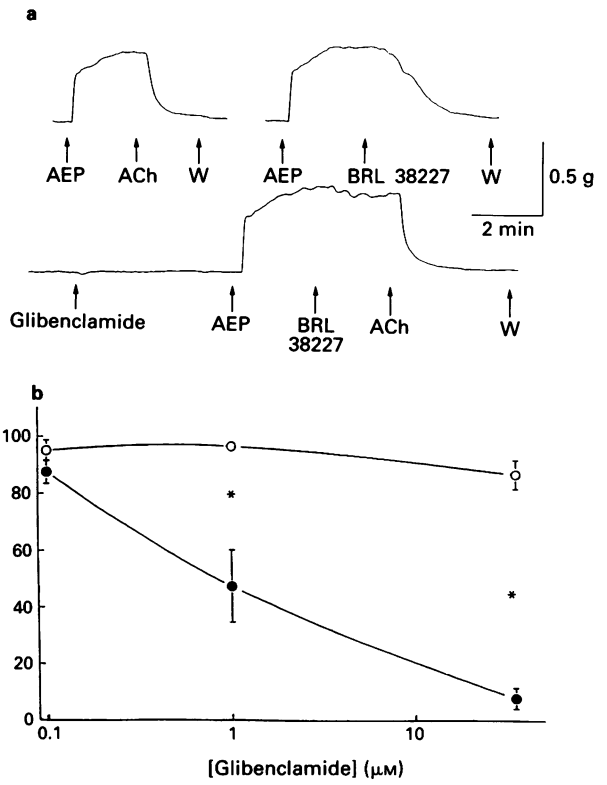

Figure 2 Comparison of the effects of glibenclamide on the relaxation initiated with either acetylcholine (ACh) or BRL 38227 in vessel segments contracted with 2-(2-aminoethyl)pyridine (AEP). (a) Example of the selective antagonism of the BRL 38227 (1 μM)- but not the ACh (0.35 μM)-induced relaxation with glibenclamide (35 μM) in a single vessel segment. Removal of drug from the bath is indicated with a W. Upper contractile recordings; control responses to application of either ACh or BRL 38227. Lower contractile record; in the presence of glibenclamide, BRL 38227 no longer relaxed the vessel whereas the response to ACh was still intact. (Note: the mean values shown in (b) of this figure for ACh-induced relaxations in the presence of glibenclamide were obtained in the absence of BRL 38227). (b) Concentration-response relationships for the effects of glibenclamide (0.1–35 μM) on relaxations induced with either ACh (○, 0.35 μM, $n = 3-8$) or BRL 38227 (●, 1 μM, $n = 6-8$). Note that 1 to 35 μM glibenclamide led to significant ($^*P < 0.05$) inhibition of the response to BRL 38227 whereas the responses to ACh were unaffected. Shown are mean values with s.e.mean indicated by vertical bars.

glibenclamide produced a contraction which was 1.6 ± 0.7% of that elicited with AEP. Neither 1 nor 35 μM glibenclamide significantly shifted the concentration-response relationship for ACh-induced relaxation (IC_{50} for ACh in control solution = 0.022 μM, $n = 8-10$; in 1 μM glibenclamide = 0.07 μM, $n = 5-9$; in 35 μM glibenclamide = 0.054 μM, $n = 5-10$). The effects of 0.1, 1 and 35 μM glibenclamide were also tested on relaxations produced with an IC_{90} of either BRL 38227 (1 μM) or ACh (0.35 μM). Glibenclamide addition produced a concentration-dependent inhibition of BRL 38227-induced relaxations whereas responses to ACh were unchanged. These data are summarized in Figure 2.

Comparison of acetylcholine- and BRL 38227-induced hyperpolarization

The time course and magnitude of changes in membrane potential with a 6–7 min exposure to ACh (0.35 μM) and BRL 38227 (1 μM) were compared in segments of guinea-pig coronary artery. The mean resting membrane potential in this preparation was − 52.4 ± 1.5 mV ($n = 31$). There was no significant difference between the magnitude of the hyperpolarization produced to ACh (17.7 ± 1.1, $n = 28$) or BRL 38227 (19.2 ± 1.6, $n = 21$). The time to peak hyperpolarization with ACh (1.64 ± 0.13 min, $n = 8$) was significantly faster than with BRL 38227 (3.28 ± 0.41 min, $n = 8$). Examples of the hyperpolarization produced with these agents are included in Figure 3.

Effect of glibenclamide on acetylcholine- and BRL 38227-induced hyperpolarization

In these experiments we examined the effects of glibenclamide on the hyperpolarization produced with both ACh and BRL 38227 in segments of guinea-pig coronary artery. Addition of glibenclamide alone led to a concentration-dependent depolarization of the membrane (10 μM glibenclamide: 8.8 ± 1.8 mV, $n = 10$; 35 μM glibenclamide: 12.3 ± 1.8 mV, $n = 8$; Figure 3a). In one experiment, an 8 mV depolarization was also observed upon exposure to 1 μM glibenclamide. In the presence of this agent the peak hyperpolarization elicited with ACh (0.35 μM) was not sigificantly reduced (control: 17.7 ± 1.1 mV, $n = 28$; 10 μM glibenclamide: 17.2 ± 2.6 mV, $n = 4$; 35 μM glibenclamide: 17.3 ± 1.7, $n = 4$). Glibenclamide (10 μM) prevented the BRL 38227 (1 μM)-induced hyperpolarization ($n = 4$). An example of the differential effects of glibenclamide on hyperpolarization with BRL 38227 versus ACh is shown in Figure 3b.

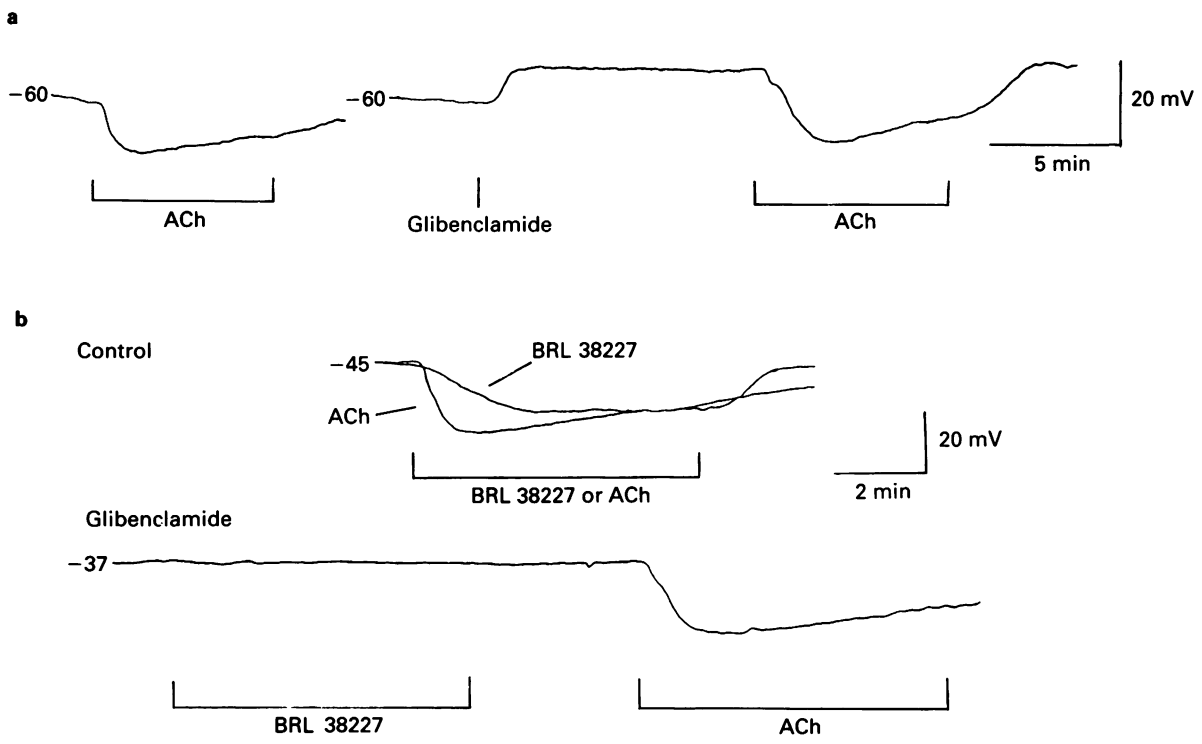

Figure 3 Effect of glibenclamide (35 μM) on resting membrane potential and the hyperpolarization produced with acetylcholine (ACh) or BRL 38227. (a) Effect of glibenclamide on resting membrane potential and the response to ACh (1 μM). Intracellular recording obtained from a single cell. Initial exposure to ACh resulted in a 15 mV hyperpolarization. Thirteen min after removal of ACh, glibenclamide was added to the bath leading to an 11 mV depolarization. Subsequent addition of ACh 10 min later induced a hyperpolarization of 27 mV. (b) Comparison of the effects of glibenclamide on the hyperpolarization produced with BRL 38227 (1 μM) versus ACh (0.35 μM). Control responses to these two agonists in the same cell are superimposed in the upper trace. Note that the onset of hyperpolarization as well as the rate of repolarization are more rapid for ACh than for BRL 38227. In the lower trace a later portion of the membrane potential recording in the same cell is shown following 10 min of exposure to glibenclamide. (Not shown: glibenclamide depolarized the tissue by 8 mV). Subsequent addition of BRL 38227 in the continued presence of glibenclamide did not hyperpolarize the tissue whereas hyperpolarization with ACh was still obtained.

Comparison of the effects of potassium channel blockers on the BRL 38227- and ACh-induced relaxation

In these experiments we examined the effects of PCP, TEA, scorpion venom and apamin to provide additional evidence for the involvement of K^+ channels in the actions of ACh and to differentiate further the BRL 38227- and ACh-induced hyperpolarization-relaxation pathways.

The concentration-response relationships for ACh- and BRL 38227-induced relaxation were measured in the presence and absence of either 100 μM PCP or 10 mM TEA in segments of guinea-pig coronary artery. Vessels were contracted with AEP and increasing concentrations (0.01 μM to 1 μM) of either ACh or BRL 38227 were added in a cumulative manner. The modifying agents were then added 10 min before addition of AEP and the concentration-response relationship for ACh or BRL 38227 repeated. In all tissues, PCP addition alone caused a contraction (12 ± 3% of the AEP response, $n = 6$). Likewise, in all tisssues, TEA addition alone caused contraction (5 ± 2% of the AEP response, $n = 5$). Both PCP (100 μM) and TEA (10 mM) significantly shifted the concentration-response relationship for ACh to the right whereas with BRL 38227 only PCP produced a significant shift (Figure 4). The actions of PCP on the shape of the concentration-response relationship for BRL 38227 and ACh differed, i.e., PCP produced a greater decrease in the steepness of the concentration-response relationship for BRL 38227 than for ACh. Thus, in the absence of PCP, both 1 μM ACh and 1 μM BRL 38227 produced near maximal relaxation. However, in the presence of PCP, ACh (1 μM) still elicited approximately 68% ($n = 6$) maximum relaxation whereas BRL 38227 (1 μM) elicited only 30% ($n = 6$) maximum relaxation (Figure 4).

In contrast to the effects of PCP and TEA on ACh-induced responses, apamin (3.5 μM, $n = 7$) did not significantly reduce relaxations with either ACh ($n = 4$) or BRL 38227 ($n = 3$).

Crude scorpion venom is known to contain several different compounds which block K^+ channels (Strong, 1990) and thus the effects of scorpion venom (8.7 μl ml^{-1}) on the relaxant responses to ACh (0.35 μM) and BRL 38227 (1 μM) were compared. Application of scorpion venom 30 min before AEP elicited a transient contraction (i.e., 3.4 ± 0.8% of the AEP response, $n = 8$). Scorpion venom significantly reduced the ACh relaxation to 24 ± 6% ($n = 4$) of control whereas BRL 38227 relaxations were unchanged ($n = 4$). Thus whereas glibenclamide preferentially blocked BRL 38227 responses, scorpion venom preferentially reduced ACh-induced relaxations (see Figure 5).

Comparison of the effects of potassium channel blockers on the BRL 38227- and ACh-induced hyperpolarization

Membrane potential measurements were undertaken in segments of guinea-pig coronary artery to determine whether the relative ability of PCP (35 μM) and TEA (10 mM) to block hyperpolarization was similar to their ability to block relaxation. Addition of TEA led to a 10.5 ± 0.9 mV ($n = 6$) depolarization (Table 1). In the presence of TEA, ACh-induced hyperpolarization was reduced to 22.5% ($n = 3$) of control whereas the BRL 38227-induced hyperpolarization ($n = 3$) was greater than control, presumably because the

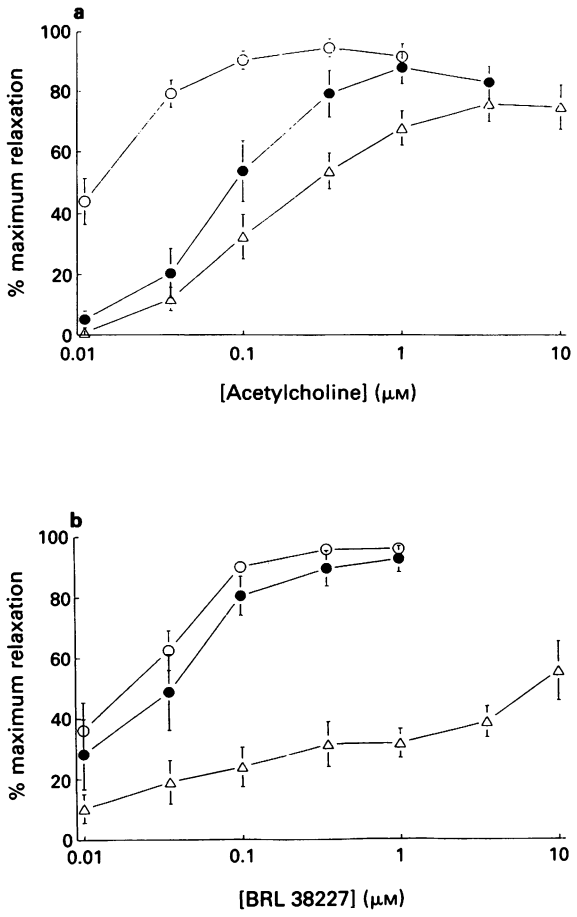

Figure 4 Comparison of the effects of control (○), phencyclidine (PCP, △, 100 μM, a, $n = 5-6$; b, $n = 3-6$) and tetraethylammonium (TEA, (●, 10 mM, a, $n = 3-5$; b, $n = 3-5$) on the concentration-dependent relaxation produced with either ACh (a) or BRL 38227 (b) in guinea-pig vessel segments (control responses, ○) contracted with 2-(2-aminoethyl) pyridine (AEP). PCP significantly shifted the concentration-response relationships for both ACh and BRL 38227 to the right. With TEA a significant shift was only observed for ACh responses. Shown are mean values with s.e.mean indicated by vertical bars.

membrane potential was further away from the potassium equilibrium potential (Table 1). Addition of PCP also depolarized the tissue (8.4 ± 1.7 mV, $n = 7$). Both the BRL 38227- ($n = 3$) and ACh ($n = 4$)-induced hyperpolarization were significantly reduced in the presence of 35 μM PCP (Table 1). These observations indicated that concentrations of PCP and TEA which reduced relaxation also significantly attenuated the associated hyperpolarization.

Scorpion venom elicited a transient depolarization of the tissue (5.5 ± 1.8 mV, $n = 4$). After 15 min exposure to scorpion venom the ACh-induced hyperpolarization was almost completely blocked (6.2% of control, $n = 4$) whereas that induced by BRL 38227 was still 53.6% of control amplitude ($n = 4$, Table 1).

Effects of glibenclamide and scorpion venom in the rabbit coronary artery

Since the effects of glibenclamide on membrane potential responses in the guinea-pig coronary artery (present study) differed from the actions of this drug in the cerebral artery (Brayden, 1990) we also performed several experiments in the rabbit coronary artery to determine whether the insensitivity to glibenclamide was a more general characteristic of ACh-induced responses in the coronary vasculature. Glibenclamide (35 μM) did not block either the ACh (10 μM)-induced relaxation ($n = 3$) or hyperpolarization ($n = 3$) in the rabbit coronary artery, suggesting that this may be a general characteristic of the actions of ACh in coronary vessels (Figure 5a). As observed in the guinea-pig coronary artery, scorpion venom (8.7 μg ml^{-1}) blocked the ACh (10 μM) but not the BRL 38227 (1 μM)-induced relaxation in the rabbit coronary vessel (Figure 5b, $n = 3$).

To ensure that the actions of scorpion venom on ACh-induced relaxation were not due to antagonism of muscarinic receptors we also tested the efffects of scorpion venom (8.7 μg ml^{-1}) on the ACh (10 μM)-induced contraction which can be evoked in this tissue. ACh (10 μM) initiated a 1.2 ± 1.19 g ($n = 3$) contraction when added to endothelium-denuded vessels in the absence of AEP. The response to ACh following a 30 min exposure to scorpion venom (8.7 μg ml^{-1}) was not reduced in magnitude ($n = 3$) suggesting that scorpion venom does not block muscarinic receptors at this concentration. In 1 of 3 vessels, scorpion venom elicited a transient contraction (0.2 g).

Table 1 Effect of K^+ channel blockers on the hyperpolarization induced by acetylcholine and BRL 38227

	Resting E_m (mV)	*Acetylcholine* (0.35 μM) *hyperpolarization* (mV)	*BRL 38227* (1 μM) *hyperpolarization* (mV)
Control	52.4 ± 1.5	17.7 ± 1.1	19.2 ± 1.6
	Amplitude depolarization (mV)	*Acetylcholine hyperpolarization* (mV) {% of control}	*BRL 38227 hyperpolarization* (mV) {% of control}
Phencyclidine (35 μM)	8.4 ± 1.7	5.7 ± 2.6 {32.2}	3.0 ± 1.0 {15.6}
Tetraethylammonium (10 mM)	10.5 ± 0.9	4.0 ± 0.5 {22.5}	20.7 ± 2.3 {107.8}
Glibenclamide (10 μM)	8.8 ± 1.8	17.2 ± 2.6 {97.1}	0 ± 0 {0}
Scorpion venom (8.7 μM)	5.5 ± 1.8	1.1 ± 0.8 {6.2}	10.3 ± 4.2 {53.6}

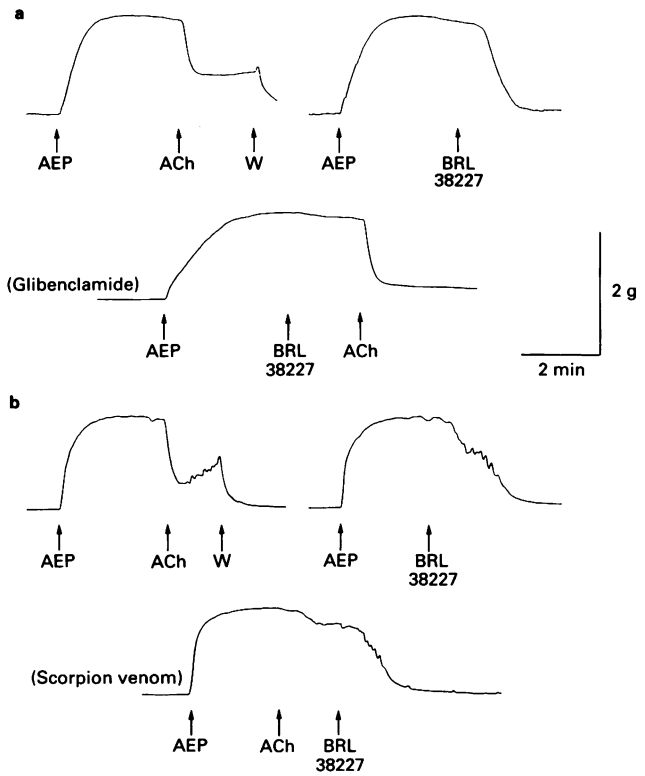

Figure 5 Comparison of the effects of (a) glibenclamide (35 μM) and scorpion venom (8.7 μg ml^{-1}) on either acetylcholine (ACh, 10 μM)- or BRL 38227 (1 μM)-induced relaxations in isolated segments of the rabbit coronary artery. Glibenclamide significantly reduced the BRL 38227-induced relaxation whereas the ACh-induced relaxation was unchanged. The opposite effect was observed with scorpion venom, i.e., scorpion venom inhibited the relaxation elicited with ACh, but was without significant effect on the response to BRL 38227.

Discussion

The present study has shown that both ACh and BRL 38227 can produce complete relaxation of isolated segments of the guinea-pig coronary artery when contracted with the histamine H_1-receptor agonist, AEP and that both are capable of eliciting a large hyperpolarization. Although the responses to ACh and BRL 38227 superficially resemble one another, the differential inhibitory effects of several different K^+ channel blockers on these vasodilators suggests that the mechanism by which they elicit relaxation and hyperpolarization differs in important ways.

The results of the present study indicate that the ACh (0.35 μM)-induced hyperpolarization occurs by a glibenclamide (10 μM)-insensitive mechanism in both the guinea-pig and rabbit coronary artery. These data are in agreement with some studies (McPherson & Angus, 1991; Chen *et al.*, 1991) but differ from the results in rabbit middle cerebral artery (Standen *et al.*, 1989; Brayden, 1990). There are several possible reasons for the differences including: (1) a different hyperpolarizing factor released from the two kinds of blood vessels; (2) the same hyperpolarizing factor affecting different K^+ channels on the smooth muscle cells or (3) a glibenclamide-sensitive release mechanism in the endothelial cells of the cerebral artery. Further research is required to determine which of these possibilities is correct. In contrast to ACh responses, glibenclamide was very effective in blocking both the relaxation and hyperpolarization produced with BRL 38227. Such data indicate that glibenclamide-sensitive channels are present in coronary artery even though this pathway is not affected by factors which ACh releases from the endothelium.

Much evidence links the relaxant actions of ACh in other blood vessels to the release of endothelium-derived relaxing factor (EDRF) which stimulates guanylate cyclase activity leading to a reduction in free intracellular calcium concentration (see Furchgott & VanHoutte, 1989). However, in tissues in which ACh also initiates hyperpolarization, an additional mechanism which must be considered is a decrease in the open probability of voltage-dependent L-type Ca^{2+} channels. This mechanism has been proposed by others for a variety of different vasodilators (e.g., Weir & Weston, 1986b; Meisheri *et al.*, 1988; Standen *et al.*, 1989; Brayden *et al.*, 1991). L-type Ca^{2+} channels have recently been characterized in single cells of the guinea-pig and rabbit coronary arteries (Ganitkevich & Isenberg, 1990; Matsuda *et al.*, 1990). Relaxation with ACh may therefore involve two concurrent mechanisms i.e., stimulation of guanylate cyclase activity and a decrease in the open probability of voltage-dependent Ca^{2+} channels. Evidence for this hypothesis has recently been reported in studies of rat femoral veins (Nagao & VanHoutte, 1991).

Unlike ACh, BRL 38227 does not stimulate guanylate cyclase activity in vascular smooth muscle (Coldwell & Howlett, 1987; Taylor *et al.*, 1988). Thus the hyperpolarization produced by BRL 38227 suggests that the associated relaxation involves a reduction in the open probability of voltage-dependent Ca^{2+} channels. The fact that glibenclamide and PCP block not only the hyperpolarization but also the relaxation initiated with BRL 38227 also suggests that the former event is causally related to the latter one.

An interesting observation made in this study is that addition of glibenclamide alone (1–35 μM) led to depolarization (8–12 mV) of the guinea-pig coronary artery. This result is in agreement with studies of rat mesenteric arteries in which glibenclamide produced a concentration-dependent (0.1–3.5 μM) depolarization (1–9 mV) of the tissue (McPherson & Angus, 1991) but differs from the rabbit cerebral artery where depolarization was not observed with glibenclamide at concentrations up to 5 μM (Brayden, 1990). In the rat mesenteric arteries, glibenclamide-induced depolarization was obtained both in the presence and absence of the endothelium. Glibenclamide may depolarize the coronary and mesenteric vessels because K^+ channels sensitive to this agent are open at the resting membrane potential. In pancreatic β cells, much lower concentrations of glibenclamide (i.e., 0.1 to 10 nM) are required to antagonize ATP-dependent K^+ channels (Sturgess, 1985; Schmid-Antomarchi *et al.*, 1987a,b) than are required in vascular smooth muscle to block the actions of cromakalim (Beech & Bolton, 1989; Buckingham *et al.*, 1989; Winquist *et al.*, 1989; Standen *et al.*, 1989), BRL 38227 (Wilson *et al.*, 1989) or diazoxide (Winquist *et al.*, 1989). It is possible that the higher concentrations of glibenclamide needed to antagonize the BRL 38227 response in blood vessels might also affect other K^+ channels in some way. However, if such a mechanism were occurring it could not be entirely nonspecific because glibenclamide apparently does not affect the K^+ channels involved in ACh-induced hyperpolarization.

The ability of other K^+ channel blockers to inhibit relaxation and hyperpolarization with BRL 38227 and ACh also differed. TEA (10 mM), for example, significantly reduced the relaxation and hyperpolarization initiated with ACh in the coronary artery but was without effect on BRL 38227 responses. The relative insensitivity of BRL 38227 responses to TEA is compatible with the proposed actions of cromakalim on either ATP-dependent K^+ channels (Standen *et al.*, 1989; Nelson *et al.*, 1990) or delayed rectifier K^+ channels (Beech & Bolton, 1989) both of which are relatively insensitive to TEA as opposed to Ca^{2+} activated K^+ channels which are very sensitive to this agent (Beech & Bolton, 1989). The greater effectiveness of TEA in inhibiting the actions of ACh suggest that large conductance Ca^{2+} activated K^+ channels may be involved in the pathways by which ACh produces relaxation in this vessel. This hypothesis was also suggested by Chen *et al.* (1991).

While PCP antagonized both ACh and BRL 38227 responses, its action was greater on BRL 38227 than on ACh. The ability of PCP (100 μM) to almost completely block the BRL 38227-induced hyperpolarization is commensurate with its reported effects on outward currents in single cells of the portal vein (Beech & Bolton, 1989). In their study, 100 μM PCP produced complete abolition of the cromakalim currents but only a 25% reduction in Ca^{2+} activated K^+ channel activity. The effects of PCP on the ACh-induced relaxation and hyperpolarization on the other hand are more difficult to interpret since PCP has also been reported to act as a partial antagonist of muscarinic receptors (Albuquerque *et al.*, 1983). In spite of this additional action of PCP on muscarinic receptors, PCP produced greater antagonism of BRL 38227 responses than of ACh responses.

Apamin has been reported to block small conductance Ca^{2+} activated K^+ channels. These channels are coupled to activation of both purinoceptors and adrenoceptors in the gastrointestinal tract of some species (Hugues *et al.*, 1982; Weir & Weston, 1986a; Strong, 1990). In our studies we found that a large concentration of apamin (i.e., 3.5 μM) was without effect on the relaxant actions of either ACh or BRL 38227 suggesting that this channel is not involved in the pathway by which either vasodilator produces relaxation.

Scorpion venom selectively antagonized ACh- but not BRL 38227-induced relaxations in both the guinea-pig and rabbit coronary artery. These data are similar to the differential effects of scorpion venom on ACh but not BRL 34915 in rat mesenteric arteries (Adeagbo & Malik, 1990). The actions of scorpion venom were not due to antagonism of muscarinic receptors since scorpion venom did not block ACh-induced contractions in segments of endothelium-denuded rabbit coronary artery. Charybdotoxin, a relatively specific blocker of large conductance Ca^{2+} activated K^+ channels (Miller *et al.*, 1985) is present in crude scorpion venom (see Strong, 1990). The actions of scorpion venom may therefore have been related to this component of the crude mixture. However, the concentration of charybdotoxin estimated to be present in our studies (i.e., 2–4 nM assuming 0.1–0.2% of total protein content, Strong, 1990) is somewhat less than the K_d reported for the inhibition of Ca^{2+} channels in patch clamp studies (e.g., 10 nM, Miller *et al.*, 1985). Since other K^+ channel blockers are also present in crude scorpion venom (see Strong, 1990), it is entirely possible that inhibition was due to a component of the crude extract other than charybdotoxin.

The present study has shown that BRL 38227 and ACh produce equivalent hyperpolarization at concentrations which elicit equivalent relaxation making it likely that membrane potential-dependent mechanisms contribute equally to the relaxations which are observed. In contrast to this similarity, the results suggest that these agonists initiate hyperpolarization by different mechanisms. Whereas the inhibitory effects of glibenclamide on the BRL 38227-induced hyperpolarization are compatible with the activation of ATP-dependent K^+ channels, the actions of ACh do not appear to include this channel. The effects of various K^+ channel blockers on responses to ACh suggest instead that some step in the sequence of events occurring between the initial binding of ACh to endothelial muscarinic receptors and the final relaxation of the smooth muscle depends upon the opening of Ca^{2+} activated K^+ channels.

Our appreciation to Drs J.R. Hume, C.H. Gelband and J.M. Post for reading this manuscript and offering helpful advice and to Dr J. Kenyon for many informative talks on K^+ channel blockers. We would also like to express our sincere gratitude to the Reno Eagles club for helping to make this study possible. This research was supported with NIH grant no. HL40399, a grant-in-aid from the AHA Nevada Affiliate and an award from the Reno Eagles club. Our appreciation to SmithKline Beecham for their generous donation of BRL 38227.

References

ADEAGBO, A.S.O. & MALIK, K.U. (1990). Endothelium-dependent and BRL 34915-induced vasodilatation in rat isolated perfused mesenteric arteries: role of G-proteins, K^+ and calcium channels. *Br. J. Pharmacol.*, **100**, 427–434.

ALBUQUERQUE, E.X., AGUAYO, L.G., WARNICK, J.E., ICKOWICZ, R.K. & BLAUSTEIN, M.P. (1983). Interactions of phencyclidine with ion channels of nerve and muscle: behavioral implications. *Fed. Proc.*, **42**, 2584–2589.

BEECH, D.J. & BOLTON, T.B. (1989). Properties of the cromakalim-induced potassium conductance in smooth muscle cells isolated from the rabbit portal vein. *Br. J. Pharmacol.*, **98**, 851–864.

BRAYDEN, J.E. (1990). Membrane hyperpolarization is a mechanism of endothelium-dependent cerebral vasodilation. *Am. J. Physiol.*, **259** (*Heart. Circ. Physiol.* **28**), H668–H673.

BRAYDEN, J.E., QUALE, J.M., STANDEN, N.B. & NELSON, M.T. (1991). Role of potassium channels in the vascular response to endogenous and pharmacological vasodilators. *Blood Vessels*, **28**, 147–153.

BUCKINGHAM, R.E., CLAPHAM, J.C., COLDWELL, M.C., HAMILTON, T.C. & HOWLETT, D.R. (1986). Stereospecific mechanism of action of the novel antihypertensive agent, BRL 34915. *Br. J. Pharmacol.*, **87**, 78P.

BUCKINGHAM, R.E., HAMILTON, T.C., HOWLETT, F.R., MOOTOO, S. & WILSON, C. (1989). Inhibition by glibenclamide of the vasorelaxant action of cromakalim in the rat. *Br. J. Pharmacol.*, **97**, 57–64.

CHEN, G., SUZUKI, H. & WESTON, A.H. (1988). Acetylcholine releases endothelium-derived hyperpolarizing factor and EDRF from rat blood vessels. *Br.. J. Pharmacol.*, **95**, 1165–1174.

CHEN, G., YAMAMOTO, Y., MIWA, K. & SUZUKI, H. (1991). Hyperpolarization of arterial smooth muscle induced by endothelial humoral substances. *Am. J. Physiol.*, **260**, (*Heart Circ. Physiol*, **29**), H1888–H1892.

COLDWELL, M.C. & HOWLETT, D.R. (1987). Specificity of action of the novel anti-hypertensive agent, BRL 34915, as a potassium channel activator; comparison with nicorandil. *Biochem. Pharmacol.*, **36**, 3663–3669.

DAUT, J., MAIER-RUDOLPH, W., VON BECKERATH, N., MEHRKE, G., GUNTHER, K. & GOEDEL-MEINEN, L. (1990). Hypoxic dilation of coronary arteries is mediated by ATP-sensitive potassium channels. *Science*, **247**, 1341–1344.

DURANT, G.J., GANELLIN, C.R. & PARSONS, M.E. (1975). Chemical differentiation of histamine H_1 and H_2-receptor agonists. *J. Med. Chem.*, **18**, 905–909.

ECKMAN, D.M. & KEEF, K.D. (1991). Comparison of the actions of acetylcholine and BRL 38227 in the guinea pig coronary artery. *Biophys. J.*, **59** (2 part 2), 75a.

FELETOU, M. & VANHOUTTE, P.M. (1988). Nitric oxide, ACh and electrical and mechanical properties of canine arterial smooth muscle. *Am. J. Physiol.*, **255**, H207–H212.

FOSSET, M., DE WEILLE, J.R., GREEN, R.D., SCHMID-ANTOMARCHI, H. & LAZDUNSKI, M. (1988). Antidiabetic sulfonylureas control action potential properties in heart cells via high affinity receptors that are linked to ATP-dependent K^+ channels. *J. Biol. Chem.*, **263**, 7933–7936.

FURCHGOTT, R.F. & VANHOUTTE, P.M. (1989). Endothelium-derived relaxing and contracting factors. *FASEB J.*, **3**, 2007–2018.

GANITKEVICH, V. & ISENBERG, G. (1990). Isolated guinea pig coronary smooth muscle cells: acetylcholine induces hyperpolarization due to sarcoplasmic reticulum calcium release activating potassium channels. *Circ. Res.*, **67**, 525–528.

GELBAND, C.H., LODGE, N.J. & VAN BREEMEN, C. (1989). A Ca^{++}-activated K^+ channel from rabbit aorta: modulation by. *Eur. J. Pharmacol.*, **167**, 201–210.

HAMILTON, T.C., WEIR, S.W. & WESTON, A.H. (1986). Comparison of the effects of BRL 34915 and verapamil on electrical and mechanical activity in rat portal vein. *Br. J. Pharmacol.*, **88**, 103–111.

HU, S., KIM, H.S., OKOLIE, P. & WEISS, G.B. (1990). Alterations by glyburide of effects of BRL 34915 and P 1060 on contraction, ^{86}Rb efflux and the maxi-K^+ channel in rat portal vein. *J. Pharmacol. Exp. Ther.*, **253**, 771–777.

HUANG, A.H., BUSSE, R. & BASSENGE, E. (1988). Endothelium-dependent hyperpolarization of smooth muscle cells in rabbit femoral arteries is not mediated by EDRF (nitric oxide). *Naunyn-Schmiedbergs Arch. Pharmacol.*, **338**, 438–442.

HUGUES, M., DUVAL, D., SCHMID, H., KITABGI, P., LAZDUNSKI, M. & VINCENT, J.P. (1982). Specific and pharmacological interactions of apamin, the neurotoxin from bee venom with guinea pig colon. *Life Sci.*, **31**, 437–443.

KEEF, K.D. & KREULEN, D.L. (1988). Electrical responses of the guinea pig coronary artery to transmural stimulation. *Circ. Res.*, **62**, 585–595.

KEEF, K.D. & BOWEN, S.M. (1989). Effect of ACh on electrical and mechanical activity in guinea pig coronary arteries. *Am. J. Physiol.*, **257** (*Heart Circ. Physiol.*, **26**), H1096–H1103.

KITAMURA, K. & KURIYAMA, H. (1979). Effect of acetylcholine on the smooth muscle cell of isolated main coronary artery of the guinea pig. *J. Physiol.*, **293**, 119–133.

KLÖCKNER, U., TRIESCHMANN, U. & ISENBERG, G. (1988). Pharmacological modulation of calcium and potassium channels in isolated vascular smooth muscle cells. *Drug Res.*, **39**, 120–126.

KOMORI, K.R., LORENZ, R.R. & VANHOUTTE, P.M. (1988). Nitric oxide, ACh and electrical and mechanical properties of canine arterial smooth muscle. *Am. J. Physiol.*, **255** (*Heart Circ. Physiol.*, **24**), H207–H212.

MATSUDA, J.J., VOLK, K.A. & SHIBATA, E.F. (1990). Calcium currents in isolated rabbit coronary arterial smooth muscle myocytes. *J. Physiol.*, **427**, 657–680.

MCPHERSON, G.A. & ANGUS, J.A. (1991). Evidence that acetylcholine-mediated hyperpolarization of the rat small mesenteric artery does not involve the K^+ channel opened by cromakalim. *Br. J. Pharmacol.*, **103**, 1184–1190.

MEISHERI, K.D., CIPKUS, L.A. & TAYLOR, C.J. (1988). Mechanism of action of minoxidil sulfate-induced vasodilation: a role for increased K^+ permeability. *J. Pharmacol. Exp. Ther.*, **245**, 751–760.

MILLER, C., MOCZYDLOWSKI, E., LATORRE, R. & PHILLIPS, M. (1985). Charybdotoxin, a protein inhibitor of single Ca^{2+} activated K^+ channels from mammalian skeletal muscle. *Nature*, **313**, 316–318.

NAGAO, T. & VANHOUTTE, P.M. (1991). Hyperpolarization contributes to endothelium-dependent relaxations to acetylcholine in femoral veins of rats. *Am. J. Physiol.*, **261** (*Heart Circ. Physiol.*, **30**), H1034–H1037.

NELSON, M.T., PATLAK, J.B., WORLSEY, J.F. & STANDEN, N.B. (1990). Calcium channels, potassium channels, and voltage dependence of arterial smooth muscle tone. *Am. J. Physiol.*, **259** (*Cell Physiol.*, **28**), C3–C18.

OKABE, K., KAJIOKA, S., NAKAO, K., KITAMURA, K., KURIYAMA, H. & WESTON, A.H. (1990). Actions of cromakalim on ionic currents recorded from single smooth muscle cells of the rat portal vein. *J. Pharmacol. Exp. Ther.*, **252**, 832–839.

SCHMID-ANTOMARCHI, H., DE WEILLIE, J.R., FOSSET, M. & LAZDUNSKI, M. (1987a). The receptor for antidiabetic sulfonylureas controls the activity of the ATP-modulated K^+ channel in insulin-secreting cells. *J. Biol. Chem.*, **262**, 15840–15844.

SCHMID-ANTOMARCHI, H., DE WEILLE, J.R., FOSSET, M. & LAZDUNSKI, M. (1987b). The antidiabetic sulfonylurea glibenclamide is a potent blocker of the ATP-modulated K^+ channel in insulin secretin cells. *Biochem. Biophys. Res. Commun.*, **146**, 21–25.

STANDEN, N.B., QUAYLE, J.M., DAVIES, N.W., BRAYDEN, J.E., HUANG, Y. & NELSON, M.T. (1989). Hyperpolarizing vasodilators activate ATP-sensitive K^+ channels in arterial smooth muscle. *Science*, **245**, 177–180.

STRONG, P.N. (1990). Potassium channel toxins. *Pharmacol. Ther.*, **46**, 137–162.

STURGESS, N.C., ASHFORD, M.L.J., COOK, D.L. & HALES, C.N. (1985). The sulfonylurea receptor may be an ATP-sensitive potassium channel. *Lancet*, **ii**, 474–475.

TALLARIDA, R.J. & MURRAY, R.B. (1987). Procedure 5, Analysis of the regression line. In *Manual of of Pharmacologic Calculations with Computer Programs*. pp. 16–18. New York: Springer-Verlag.

TARE, M., PARKINGTON, H.C., COLEMAN, H.A., NEILD, T.O. & DUSTING, G.J. (1990). Hyperpolarization and relaxation of arterial smooth muscle caused by nitric oxide derived from the endothelium. *Nature*, **346**, 69–71.

TARE, M., PARKINGTON, H.C., COLEMAN, H.A., NEILD, T.O. & DUSTING, G.J. (1991). Nitric oxide hyperpolarization arterial smooth muscle. *J. Cardiovasc. Pharmacol.*, **17** (Suppl. 3), S108–S112.

TAYLOR, S.G., SOUTHERTON, J.S., WESTON, A.H. & BAKER, J.R.L. (1988). Endothelium-dependent effects of acetylcholine in rat aorta: a comparison with sodium nitroprusside and cromakalim. *Br. J. Pharmacol.*, **94**, 853–863.

WEIR, S.W. & WESTON, A.H. (1986a). Effect of apamin on responses to BRL 34915, nicorandil and other relaxants in the guinea pig taenia caeci. *Br. J. Pharmacol.*, **88**, 113–120.

WEIR, S.W. & WESTON, A.H. (1986b). The effects of BRL 34915 and nicorandil on electrical and mechanical activity and on ^{86}Rb efflux in rat blood vessels. *Br. J. Pharmacol.*, **88**, 121–128.

WESTON, A.H. (1989). Smooth muscle K^+ openers; their pharmacology and clinical potential. *Pflügers Arch.*, **414** (Suppl. 1), S99–S105.

WILSON, C., HAMILTON, T.C. & CAWTHORNE, M.A. (1989). Antagonism of vasorelaxation to BRL 38227 by non-sulfonylurea hypoglycemic agents. *Br. J. Pharmacol.*, **98**, 723P.

WINQUIST, R.J., HEANEY, L.A., WALLACE, A.A., BASKIN, E.P., STEIN, R.B., GARCIA, M.L. & KACZOROWSKI, G.J. (1989). Glyburide blocks the relaxation response to BRL 34915 (cromakalim), minoxidil sulfate and diazoxide in vascular smooth muscle. *J. Pharmacol. Exp. Ther.*, **248**, 149–156.

(Received August 2, 1991
Revised December 12, 1991
Accepted January 7, 1992)

Br. J. Pharmacol. (1992), **106**, 17–24 © Macmillan Press Ltd, 1992

The involvement of potassium channels in the action of ciclazindol in rat portal vein

†Th. Noack, G. Edwards, †P. Deitmer, *P. Greengrass, T. Morita, *P-O. Andersson, D. Criddle, *M. G. Wyllie & [1] A.H. Weston

Smooth Muscle Research Group, Department of Physiological Sciences, University of Manchester, Manchester, M13 9PT; †Department of Physiology, University of Marburg, Deutschhausstrasse 2, W-3550 Marburg, Germany and *Pfizer Central Research, Sandwich, Kent CT13 9NJ

1 In whole portal veins, ciclazindol (0.3–10 μM) increased the amplitude and duration, but decreased the frequency of spontaneous contractions. Glibenclamide (0.3–10 μM) produced a small increase in contraction amplitude and duration with a small reduction in contraction frequency.

2 In whole portal veins, ciclazindol (1–10 μM) antagonized the relaxant effects of BRL 38227 in a non-competitive manner. Under identical conditions, the effects of glibenclamide (0.3–10 μM) appeared to be competitive.

3 In whole portal veins loaded with ^{42}K, ciclazindol itself (up to 3 μM) had no detectable effect on basal ^{42}K exchange. However, the increase in ^{42}K efflux produced by BRL 38227 (5 μM) was antagonized by ciclazindol (3 μM). Similar effects were produced by glibenclamide (up to 3 μM).

4 In freshly-isolated portal vein cells examined by the whole-cell voltage-clamp technique, ciclazindol (1–100 μM) inhibited the slowly-activating and inactivating transient outward current (I_{TO}) which could be generated at potentials more positive than −30 mV. In addition ciclazindol (1–10 μM) inhibited the non-inactivating K-current (I_{KCO}) induced by BRL 38227 (10 μM).

5 In freshly-isolated portal vein cells under current-clamp conditions, the hyperpolarization produced by BRL 38227 (10 μM) was reversed by ciclazindol (1–10 μM).

6 In porcine brain membrane fragments, glibenclamide (0.65 nM) displaced 50% of the binding of [^{3}H]-glibenclamide whereas ciclazindol (up to 10 μM) had no effect.

7 It is concluded that ciclazindol is a K-channel blocker. Its action is not selective for the channel(s) which carry I_{KCO} but also extends to those which carry I_{TO}. Its inability to displace [^{3}H]-glibenclamide from porcine brain fragments may indicate that antagonism of BRL 38227 by ciclazindol in smooth muscle is exerted at a site different from that of glibenclamide.

Keywords: Ciclazindol; rat portal vein; BRL 38227; $^{42}K^+$ efflux; glibenclamide; [^{3}H]-glibenclamide binding; whole-cell K-currents

Introduction

Ciclazindol is an imidazoisoindole derivative which induces weight loss in man (Greenbaum & Harry, 1980) and modifies diet-induced thermogenesis in experimental animals (Rothwell *et al.*, 1981). In a variety of smooth muscles, preliminary studies showed that ciclazindol antagonized the action of BRL 38227, the active component of the potassium (K) channel opener cromakalim. This action of ciclazindol seemed to be associated with K-channel blockade (Morita *et al.*, 1991).

Adenosine 5'-triphosphase (ATP)-sensitive K-channels are found in the ventromedial hypothalamic nucleus (VMHN), a region of the brain closely involved with the control of feeding (see Blundell, 1991). An increase in extracellular glucose concentration excites VMHN cells (Ono *et al.*, 1982), an effect associated with closure of their ATP-sensitive K-channels (Ashford *et al.*, 1990a). This effect of glucose is similar to that exerted on insulin-secreting cells (Dunne, 1990) and in both regions it can be mimicked by the sulphonylurea tolbutamide (Ashford *et al.*, 1990b; Dunne, 1990). Sulphonylureas also antagonize both the *in vivo* hypotensive effects and the *in vitro* vasorelaxant action of K-channel openers like cromakalim (Buckingham *et al.*, 1989; Cavero *et al.*, 1989; Quast & Cook, 1989a). This has led to the suggestion that ATP-sensitive K-channels form the major site of action for these agents (Quast & Cook, 1989b) and data supporting such a view have recently been published (Standen *et al.*, 1989; Kovacs & Nelson, 1991). However, recent studies in portal vein indicate that cromakalim and BRL 38227 interact with more than one glibenclamide-sensitive K-channel type (rabbit: Beech & Bolton, 1989a; rat: Noack *et al.*, 1991). Furthermore, the ATP-sensitivity of the K-channel modulated by cromakalim has been questioned (Nakao & Bolton, 1991).

The objective of the present experiments was to investigate the effects of ciclazindol on rat portal vein under a variety of conditions. By use of both whole tissues and freshly-isolated single cells it was hoped that such an investigation would clarify any interaction between ciclazindol and K-channels in portal vein and indicate whether this agent would be a useful tool with which to characterize the site of action of agents like BRL 38227. A preliminary account of some of the results of this study has already been published (Morita *et al.*, 1991).

Methods

The majority of experiments were performed on portal veins, isolated from male Sprague-Dawley rats which were killed by stunning and bleeding.

Tissue bath experiments

Whole portal veins were mounted under 10 mN tension for isometric recording. The tissues were allowed to equilibrate

[1] Author for correspondence.

in Krebs solution (see Drugs and solutions) for 1 h before they were exposed at 6 min intervals to increasing concentrations of BRL 38227 added cumulatively. Antagonism by glibenclamide or ciclazindol was established by incubating the portal vein for 30 min with increasing concentrations of either ciclazindol or glibenclamide before the subsequent concentration-effect curves to BRL 38227 were constructed in the continuing presence of one of these modifying agents.

Mechanical responses of the portal vein were recorded and the activity integrated with respect to time by use of an Apple Macintosh Plus computer in conjunction with MacLab hardware (MacLab 8) and software (Chart, version 2.5) (Analog Digital Instruments).

Whole-cell current recordings

The fat and connective tissue were carefully removed from individual portal veins and the smooth muscle cells were freshly dispersed with a mixture of purified collagenase (Sigma, type VII) and papain (Lammel *et al.*, 1991). The resulting single cells were stored in KB-medium (Klöckner & Isenberg, 1985). They remained viable for up to 40 h and all experiments were carried out at 26°C. Patch pipettes were made from borosilicate glass and had a resistance of 2–4 MOhm.

In these experiments, the composition (mM) of the solutions was as follows: pipette (internal) Na^+ 5, K^+ 122.4, Mg^{2+} 1.2, Cl^- 129.8, $H_2PO^-_4$ 1.2, glucose 11, HEPES 10, EGTA 1.2, oxalacetic acid 5, sodium pyruvate 2, sodium succinate 5, pH 7.3; bath (external) Na^+ 125, K^+ 6, Mg^{2+} 3.7, $H_2PO^-_4$ 1.2, Cl^- 137.2, glucose 11, HEPES 10, EGTA 1, pH 7.3 aerated with O_2.

Experiments were performed in the 'whole-cell mode' of the patch clamp technique (Hamill *et al.*, 1981) using an Axopatch-1C amplifier (Axon Instruments) or the clamp system designed in our laboratory and which was functionally similar to the commerically-available unit EPC7 (List). The settling time of both systems was less than 500 μs.

Voltage commands and data acquisition were performed on-line with an AT-compatible computer equipped with an appropriate interface (Axolab 1100 or Axon TL-1). For cell stimulation and for recording and analyzing data the pClamp 5.5 programme was used (Axon Instruments). Data were stored on either a digital audio tape recorder or a video recorder in conjunction with a pulse code modulator. Voltage protocols and the evoked membrane currents were monitored continuously on a chart pen recorder (Gould 2400). Unless indicated, the data described were not corrected by linear leak subtraction.

The effects of BRL 38227 and ciclazindol were investigated by adding the appropriate amount of each agent to the main reservoir containing the external solution to ensure that responses were obtained under steady-state conditions. The bath was continuously perfused with fresh external solution by use of a pump (LKB Microperpex); a second identical pump was used to remove excess solution from the recording chamber.

To determine the effects of ciclazindol and of BRL 38227 on membrane potential, a series of measurements was performed with a voltage-clamp amplifier which permitted fast (< 1 ms) switching to current-clamp conditions. The properties of this combined voltage/current-clamp amplifier were similar to those described by Clark & Giles (1987).

[^{3}H]-glibenclamide binding

Frozen pigs brains were homogenized for 20 s in 10 volumes of ice-cold Tris buffer, pH 7.4 at 5°C. The homogenates were pooled and then centrifuged for 20 min at 50,000 *g*. After centrifugation, the supernatant was discarded and the residual pellet was homogenized (10 strokes of a Teflon-pestle glass homogenizer) in 10 volumes of fresh ice-cold buffer. This procedure was repeated and the resulting final pellet was resuspended in fresh buffer solution to give a final concentration of 0.5 mg protein ml^{-1} and stored at −70°C until required.

Experiments were carried out at 26°C and were initiated by dispersing the stored homogenate for 20 s to ensure uniformity; 400 μl of the homogenate (200 μg protein) was then incubated with 1 nM [^{3}H]-glibenclamide (in 50 μl) with the addition of 50 μl of either buffer (total binding), or glibenclamide (final concentration 100 μM) (non-specific binding) or of the appropriate concentration of competing ligand (either ciclazindol or glibenclamide, 1 pM to 100 pM). Unbound ligand was separated from bound by vacuum filtration (Brandel Harvester) through GF/B filters which had been presoaked for 2 h in polyethyleneimine (0.5% in Tris buffer) to prevent [^{3}H]-glibenclamide binding to the filter. Non-specific binding was subtracted from total binding to membranes and filters to obtain specific binding. Filters were transferred to counting vials containing 4 ml Ecoscint (Packard) and monitored for tritium in a scintillation counter. The data were analysed by a nonlinear regression curve-fitting routine.

^{42}K efflux studies

Portal veins were removed as already described and each was allocated to a separate treatment group as follows: (1) vehicle control, (2) BRL 38227 (5 μM) + glibenclamide (3 μM), (4) BRL 38227 (5 μM) + ciclazindol (3 μM). The veins were then impaled on syringe needles, attached to a gassing manifold, and allowed to equilibrate for about 1 h in normal Krebs at 37°C. They were then incubated for 3 h in Krebs solution in which the potassium was derived from $^{42}K_2CO_3$. Following this loading period, each tissue was passed at 4 min intervals through a series of tubes containing 3 ml normal Krebs solution or normal Krebs solution containing either ciclazindol (3 μM) or glibenclamide (3 μM) as appropriate for the treatment group. Tissues were exposed to BRL 38227 (5 μM) or vehicle (ethanol 0.035% v/v) between the 28th and 48th min of the efflux experiment. The tissues were then blotted and the radioactive content of the tissues and of the efflux samples corresponding to each collection period was determined in a γ-counter. The fractional loss of ^{42}K from each tissue was standardized for a 1 min period and expressed as a rate coefficient (% per min).

Drugs and solutions

The following substances were used: ciclazindol (Pfizer), collagenase, type VII (Sigma), glibenclamide (Sigma), [^{3}H]-glibenclamide (50.9 Ci per mmol: Dupont), BRL 38227 (SmithKline Beecham), papain (Sigma), $^{42}K_2CO_3$ (University of Manchester Reactor Facilities). Glibenclamide was made up as a 1 mM stock solution in 100% ethanol or as a 10 mM solution in dimethylsulphoxide (DMSO) (whole-cell clamp). BRL 38227 was prepared as a 10 mM stock solution in 70% ethanol or as a 250 mM solution in DMSO (whole-cell clamp). Ciclazindol was made up as a 50 mM solution in ethanol. Dilutions of ethanol or DMSO-based stocks were made with twice-distilled water.

The Krebs solution used in the organ bath and ion flux experiments had the following composition (mM): Na^+ 142.7, K^+ 5.9, Ca^{2+} 2.6, Mg^{2+} 1.2, Cl^- 127.6, $H_2PO_4^-$ 1.2, HCO_3^- 25, SO_4^{2-} 1.2 and glucose 11.1. It had a pH of 7.4 at 37°C when bubbled with 95% O_2, 5% CO_2.

The Tris buffer used in the [^{3}H]-glibenclamide binding studies had the following composition (mM): Na^+ 136, K^+ 5, Ca^{2+} 2.5, Mg^{2+} 1.2, Cl^- 148.4, Tris 50 and was adjusted with HCl to pH 7.5 at 25°C.

Data presentation

Numerical values are given as mean ± s.e.mean with the number of observations in parentheses.

Results

Effect of ciclazindol on spontaneous mechanical activity and membrane currents

Spontaneous mechanical activity In the concentration-range 0.3–10 μM, ciclazindol produced an increase in the integrated spontaneous mechanical activity of portal veins. At the lower end of this concentration-range, this consisted of a slight increase in the height of each wave with an occasional complex contraction of increased duration. In the presence of ciclazindol 10 μM, there was a slight reduction in wave frequency, but the amplitude and duration of each wave increased giving rise to a complex pattern of activity (Figure 1).

Whole-cell voltage clamp experiments To investigate further the interaction of ciclazindol with membrane potassium channels, the modulation of K-currents by ciclazindol was studied under whole-cell clamp conditions. To prevent contamination with calcium influx and associated current components, these experiments were carried out with bathing and pipette solutions to which no calcium was added and which contained 1 mM EGTA (Amédée *et al.*, 1990).

In such a 'calcium free' bathing solution, depolarization of rat portal vein cells from a holding potential of −90 mV to potentials up to −40 mV elicited an outward current with fast activation kinetics. The current inactivated to a steady current level within a few milliseconds (Figure 2Ab). With depolarizations positive to −30 mV (Figure 2Bb and 2Cb) an additional outward current component was detected. This component also inactivated but exhibited slower kinetics than the very rapidly-activating and -inactivating current just described. Both these time-dependent outward current components declined to a steady current level (complete inactivation of the slowly-inactivating component is not shown in Figure 2 due to the relatively short test pulse duration). This steady current could be also achieved when the membrane potential was stepped to the same range of test potentials from a holding potential of −10 mV. The difference between the peak slowly activating outward current elicited from a holding potential of −90 mV and the steady current elicited from a holding potential of −10 mV was termed the transient outward current (I_{TO}) and described the amplitude of this slowly-inactivating current component. I_{TO} had characteristics similar to the K-current I_{dK} or I_{TO} previously described in rabbit and guinea-pig portal veins respectively (Beech & Bolton, 1989b; Noack *et al.*, 1990). The difference between the non-inactivating current and zero current (dashed line in Figure 2A-C) was designated I_{NI}. The initial rapidly-activating and -inactivating current component was similar to the K-current known as the A-current previously described in neurones, cardiac and smooth muscle. In the present study, the effects of ciclazindol on the slowly-inactivating current component I_{TO} and the non-inactivating current component I_{NI} were investigated.

When the peak current level of I_{TO} was plotted against the test potentials at which it was activated, the current-voltage (*I*-V) relationship shown in Figure 2D was obtained. This relationship shows two of the characteristics of this current component. Firstly, I_{TO} was activated at potentials positive to −30 mV and secondly it exhibited marked outward rectification. In contrast, the *I*-V relationship of the component I_{NI} showed quite different characteristics. I_{NI} crossed the abscissa scale near −30 mV (zero current potential), indicating that it was a mixed ionic current. Furthermore, outward rectification was less pronounced than for I_{TO}, and the magnitude of I_{NI} was approximately one tenth that of I_{TO} at potentials between 0 and +30 mV (Figure 2D).

The current traces in Figure 2A-C and the associated current-voltage relationship in Figure 2D show data which were not corrected by subtraction of the portion of linear leak current between pipette and membrane which was represented by a resistance of about 4 GOhm. A subtraction of the leakage current produced by that leak resistance yielded a real zero current potential of about −50 mV.

When ciclazindol (10 μM) was added to the bathing solu-

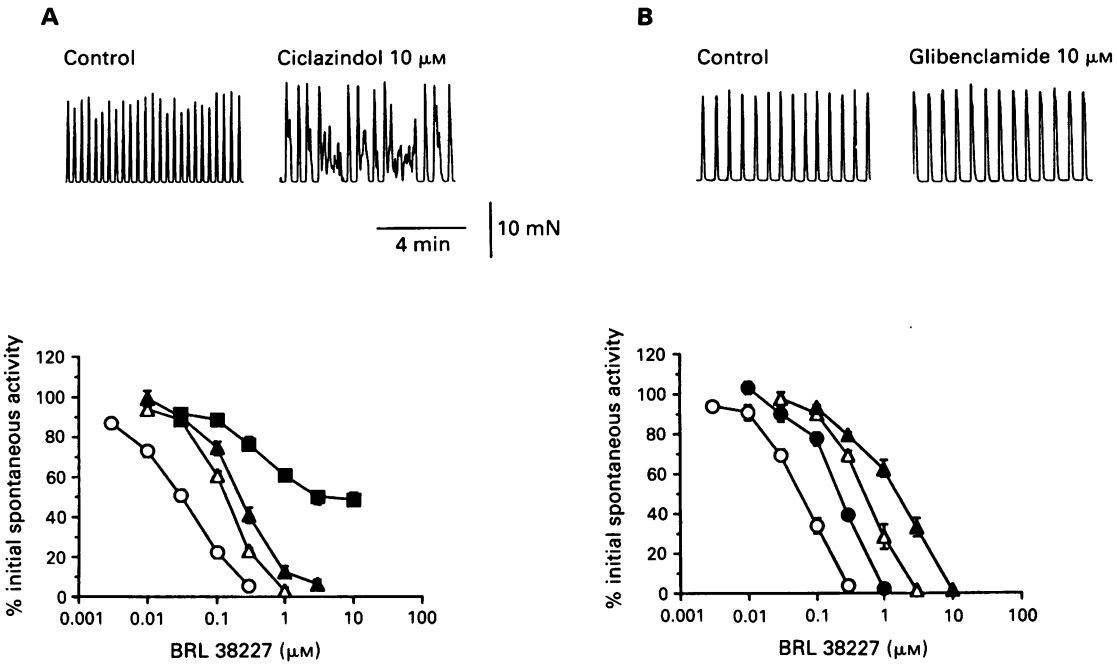

Figure 1 Effect of (A) ciclazindol and (B) glibenclamide on spontaneous mechanical activity (upper panels) and BRL 38227-induced inhibition of this activity (lower panels) in rat portal vein. (A) Upper panel: typical spontaneous mechanical activity in a single preparation 5 min after exposure to ethanol vehicle (control) and 5 min after exposure of ciclazindol (10 μM); lower panel: effect of ciclazindol (1 μM, △; 3 μM, ▲, 10 μM, ■) on the inhibition of mechanical activity produced by BRL 38227 (control, ○). (B) Upper panel: effect of glibenclamide (10 μM) on spontaneous mechanical activity; lower panel: effect of glibenclamide (0.3 μM, ●; 1 μM, △; 3 μM, ▲) on responses to BRL 38227 (control, ○). Other details as described in (A). In the lower panels, each point is the mean derived from 6 experiments ± s.e.mean (vertical lines).

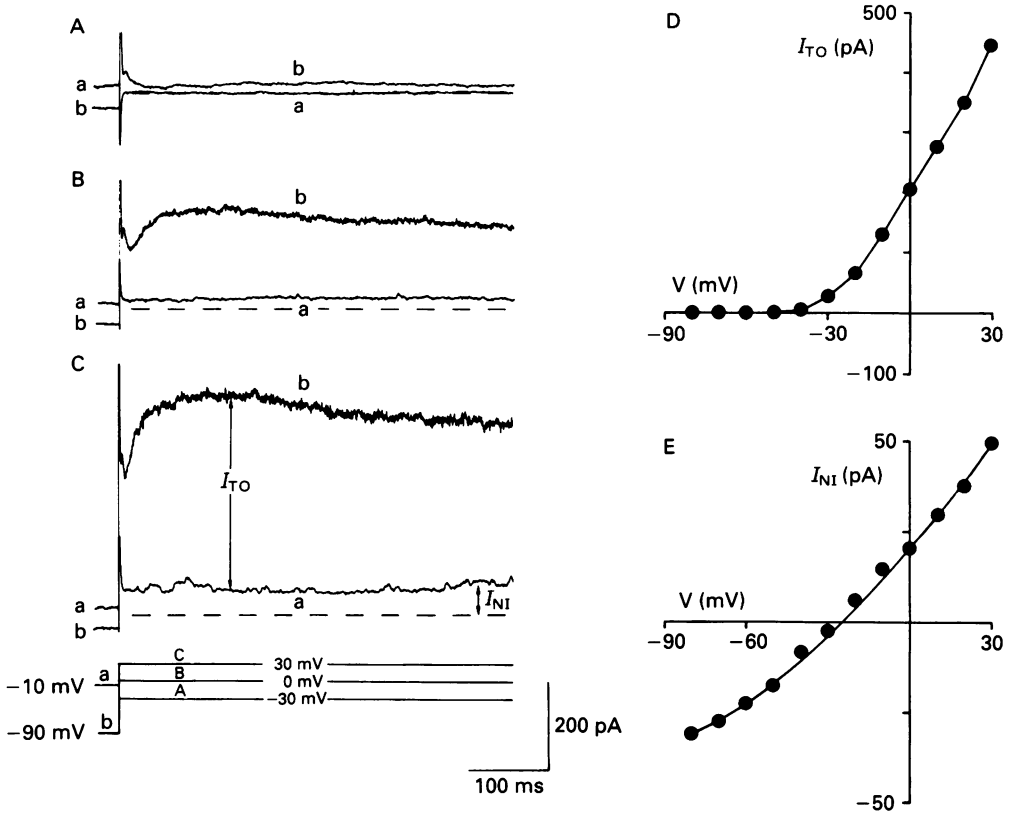

Figure 2 Typical characteristics of the slowly-inactivating transient outward current (I_{TO}) and of the non-inactivating current (I_{NI}) elicited from a single rat portal vein cell. The membrane potential was stepped either from a holding potential (HP) of −10 mV (a) or −90 mV (b) to the different test potentials (A-C). (D-E) Current-voltage relationships derived from two families of test potentials (HP −90 mV or −10 mV) of I_{TO} (D) and I_{NI} (E) obtained from the same cell as shown in A-C. Note that I_{TO} (in contrast to I_{NI}) is only available at potentials more positive than about −30 mV (Ab, D) and that I_{TO} is inactivated at a holding potential of −10 mV (Aa, Ba, Ca). The dashed line in A-C indicates the zero current. In (A), this line is obscured by the lower current trace (a).

tion, the amplitude of the fast-inactivating, A-type current component elicited by stepping from a holding potential of −90 mV to −40 mV was slightly decreased. The current at the end of the 500 ms test pulse was not changed. When the membrane potential was stepped to more positive potentials at which I_{TO} was activated (Figure 3C,D), a reduction in the magnitude of this major current component in rat portal vein was observed. In contrast, the size of I_{NI} was unchanged (Figure 3). Further evidence that ciclazindol (10 μM) inhibited I_{TO} but not I_{NI} was gained from experiments in which currents were elicited from a holding potential of −10 mV. In the five cells investigated, ciclazindol (10 μM) reduced I_{NI} at each test potential by less than 5 pA (data not shown). However, in these five cells, the control value of I_{TO} was 588 pA ± 60 pA at +30 mV, while in the presence of ciclazindol (10 μM), I_{TO} was suppressed to 388 pA ± 45 pA, a reduction of 33.1 ± 7.4%. Over the concentration range 1–100 μM, ciclazindol inhibited I_{TO} in a concentration-dependent manner (Figure 3F), with an IC_{50} value of approximately 20 μM. In the presence of ciclazindol (100 μM) the inhibition of I_{TO} was nearly complete, although at this concentration significant inhibition of I_{NI} was also observed (data not shown).

Antagonism of BRL 38227 by ciclazindol

Preliminary experiments (Morita *et al.*, 1991) had indicated that ciclazindol exhibited K-channel blocking properties and in the present study the ability of this agent to stimulate spontaneous mechanical activity in the portal vein and to inhibit I_{TO} (see above) is consistent with this view. To determine whether the inhibition of I_{TO} constituted the major K-channel blocking property of ciclazindol, the ability of this agent to antagonize the effects of BRL 38227 was also investigated. In organ bath and ^{42}K efflux experiments, the changes produced by ciclazindol were compared with those induced by glibenclamide, the agent which has become the standard antagonist of agents like BRL 38227 (Buckingham *et al.*, 1989).

Organ bath experiments In the organ bath, ciclazindol (1–10 μM) produced a concentration-dependent reversal of the inhibitory effect of BRL 38227 on spontaneous mechanical activity (Figure 1). At the lower end of this concentration-range, the BRL 38227 dose-response curve was shifted to the right in parallel fashion. However, at a concentration of 10 μM, BRL 38227 was unable to inhibit completely the spontaneous tension waves giving the appearance of non-competitive antagonism by ciclazindol (Figure 1). Glibenclamide (0.3–3 μM) produced a small, but significant increase in the integrated mechanical activity of portal veins and over this concentration-range, the effects of BRL 38227 were antagonized in a competitive-like manner (Figure 1).

Changes in ^{42}K efflux To determine whether the ability of ciclazindol to reverse the effects of BRL 38227 was due to K-channel blockade, portal veins were loaded with ^{42}K and the effects of ciclazindol on ^{42}K exchange were investigated. At concentrations up to 3 μM, ciclazindol itself had no significant effect on ^{42}K efflux. However, at this concentration, ciclazindol antagonized the increase in ^{42}K efflux produced by exposure to BRL 38227 (5 μM) (Figure 4). Similarly, glibenclamide (up to 3 μM) had no detectable effect on ^{42}K efflux but antagonized the ^{42}K efflux-enhancing effects of BRL 38227 (Figure 4).

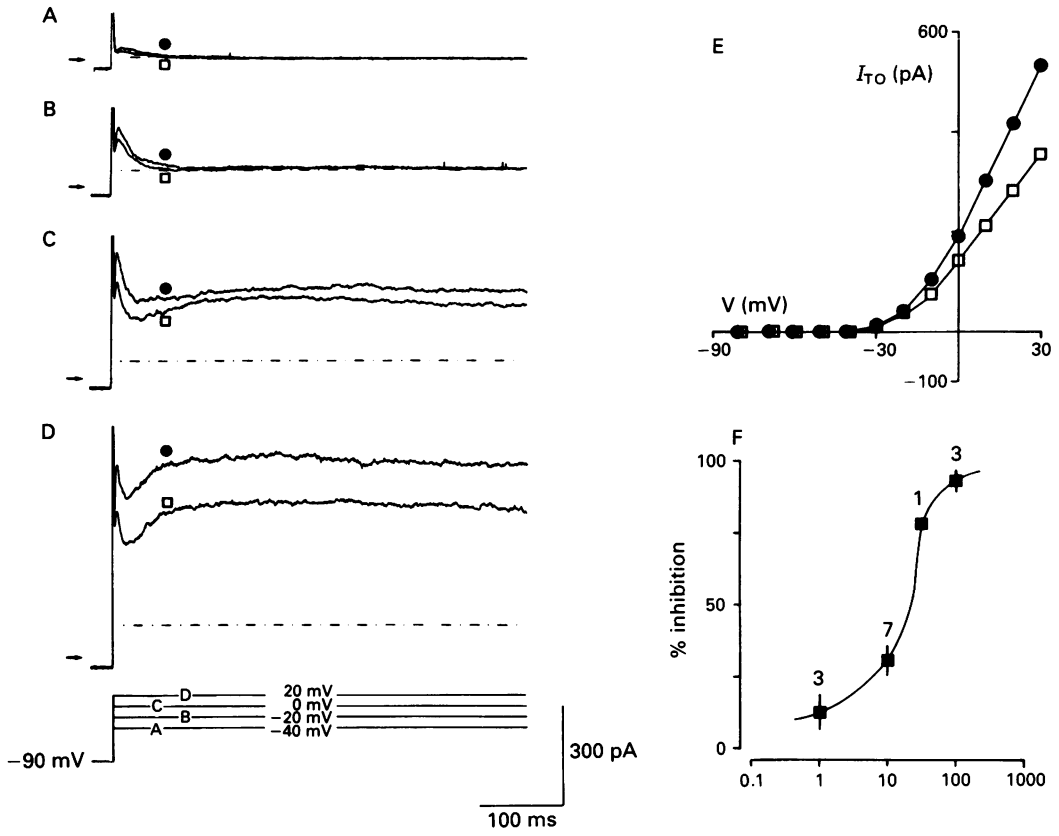

Figure 3 Effect of ciclazindol on membrane currents in rat portal vein. The membrane potential was stepped from a holding potential (HP) of −90 mV to different test potentials as indicated (A-D). Note that ciclazindol (□: 10 μM) had no effect on the non-inactivating current (I_{NI}; A,B) but that it inhibited the slowly-inactivating transient outward current I_{TO} (C,D). (E) Current-voltage relationships of I_{TO} under control conditions (●) and in the presence of ciclazindol (□: 10 μM) in the bathing solution (mean values derived from 5 cells, the s.e.mean values are obscured by the symbols). (F) Concentration-response curve for ciclazindol on the peak value of I_{TO}. The inhibition was calculated from currents elicited at a test potential of 0 mV (numbers indicate the number of cells).

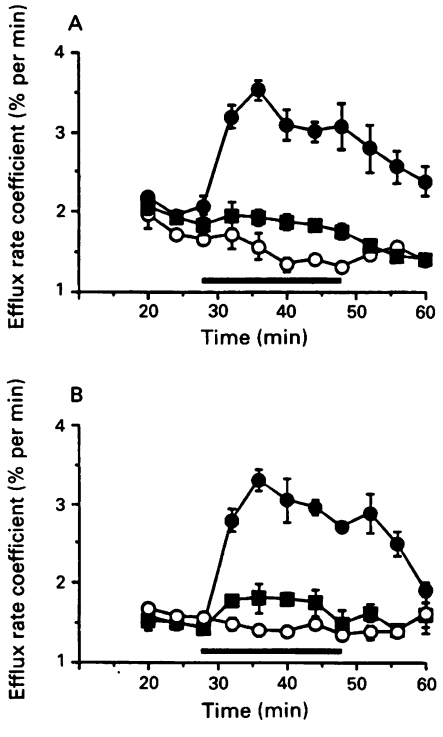

Whole cell voltage- and current-clamp experiments To clarify further the effects of ciclazindol on K-currents in rat portal vein, the effects of this agent on the K-current induced by BRL 38227 were evaluated. In this tissue, BRL 38227 induces a non-inactivating potassium current (I_{KCO}), an effect antagonized by glibenclamide (Noack *et al.*, 1991; 1992). In the present study, experiments were performed with an amplifier which allowed rapid switching from the conventional voltage-clamp to the current-clamp mode to provide membrane potential measurements (see Methods).

When a portal vein cell was kept under voltage-clamp at a holding potential of −50 mV and the membrane potential was stepped to 0 mV, I_{TO} and I_{NI} were observed (Figure 5A). After current recording for 600 ms, the system was switched for 3 s into the current-clamp mode and the membrane potential was measured. The mean of ten such episodes of current and voltage recording from a single cell is shown in Figure 5A. The addition of BRL 38227 (10 μM) to the bath-

Figure 4 Effects of (A) ciclazindol and (B) glibenclamide on ^{42}K exchange in rat portal vein. (A) Basal efflux (○); BRL 38227, 5 μM (●); BRL 38227, 5 μM in PSS containing ciclazindol 3 μM (■). (B) Basal efflux (○); BRL 38227, 5 μM (●); BRL 38227, 5 μM in PSS containing glibenclamide 3 μM (■). In the experiments involving ciclazindol or glibenclamide, the PSS contained one of these modifying agents throughout the efflux experiment. Tissues were exposed to BRL 38227 or ethanol (solvent control) for 20 min between the 28th and 48th min of the efflux experiment (▬). Neither ciclazindol nor glibenclamide (each up to 3 μM) had any significant effect on ^{42}K exchange. Each point is the mean derived from 5 experiments ± s.e.mean (vertical bars).

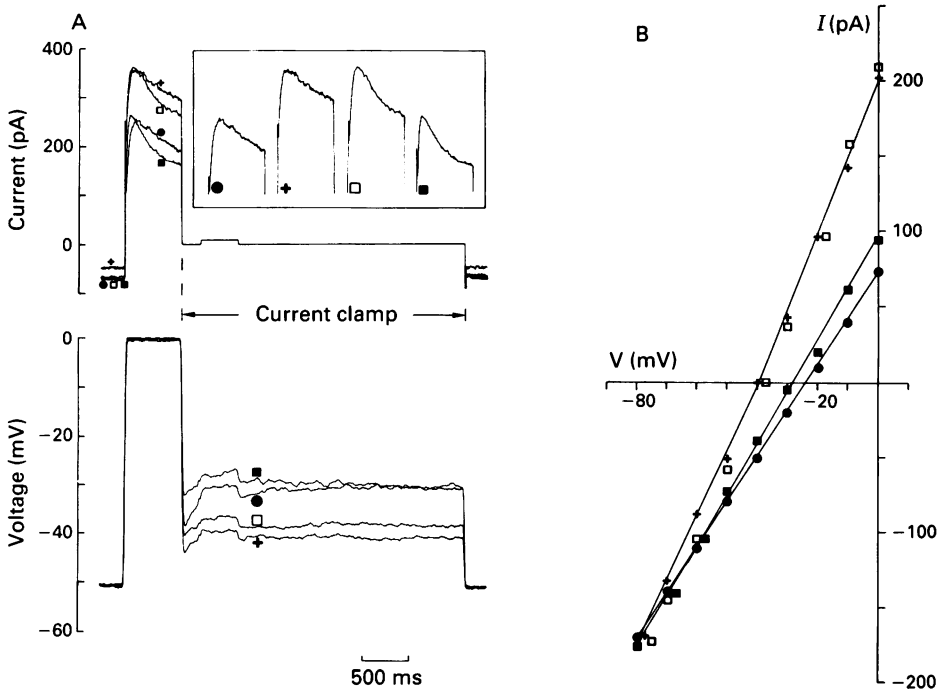

Figure 5 Voltage-clamp/current-clamp protocol and the typical interaction between ciclazindol and BRL 38227 in a single cell from rat portal vein. (A) Initially, in voltage-clamp mode the membrane potential was stepped from −50 mV to 0 mV for 600 ms (lower panel) which elicited both the slowly-inactivating and non-inactivating currents I_{TO} and I_{NI}, respectively (upper panel). After 600 ms, during the inactivation of I_{TO}, the system was switched into the current clamp mode, allowing measurement of membrane potential. During the initial phase of current clamp, a current of +10 pA was injected to give an indication of membrane input resistance. Current measured under control conditions (●) was markedly enhanced by BRL 38227 (+: 10 μM) (inset upper panel) and the membrane potential moved approximately 15 mV towards E_K (−83 mV) (lower panel). Exposure to ciclazindol (1 and 10 μM) in the continuing presence of BRL 38227 (□ and ■, respectively) modified the outward current (inset, upper panel) and the membrane potential returned towards control values. Each current and voltage trace is the average derived from 10 identical successive voltage/ current clamp protocols. Note the different time-courses of I_{TO} and the corresponding membrane potentials immediately after stepping to current clamp in the four conditions of the experiment. (B) Current-voltage relationship of I_{NI} from the same cell as shown in (A). Currents were elicited from a holding potential of −10 mV (to inactivate I_{TO}) and the end currents measured after each 600 ms test pulse were plotted against the test potential under the four conditions. The marked increase of outward current in the presence of BRL 38227 (+) compared to controls (●) reflects the presence of I_{KCO}. I_{KCO} was inhibited in a concentration-dependent manner by ciclazindol (□, 1 μM; ■, 10 μM). The lines were fitted by eye; all intersect near the potassium equilibrium potential (E_K = −83 mV) indicating that I_{KCO} is a potassium current.

ing solution increased the outward current (see insert in Figure 5A) and the membrane potential hyperpolarized from −30 mV to −42 mV. The electrotonic potential following current injection of 10 pA (400 ms in duration) was little affected. When ciclazindol (1 μM) was added to the bathing solution in the continuing presence of BRL 38227, the membrane potential depolarized (current-clamp), indicating inhibition of I_{KCO} by ciclazindol (Figure 5A). Additionally a slight change of the inactivation kinetics of I_{TO} under ciclazindol (1 μM) was visible under voltage-clamp. When the bath concentration of ciclazindol was increased from 1 to 10 μM, a marked reduction of outward current was detected under voltage-clamp conditions (Figure 5A, insert) and in the current clamp mode the membrane potential measured 3 s after the changeover from voltage-clamp had returned to its control level.

Under voltage-clamp, the current-voltage relationship of the non-inactivating current generated from a holding potential of −10 mV was evaluated and the effect of BRL 38227 on outward current was then determined (Figure 5B). The current induced by BRL 38227 (10 μM) crossed the control curve near the actual potassium equilibrium potential (E_K = −83 mV) indicating that a pure potassium current (I_{KCO}) was enhanced by BRL 38227. As expected from the voltage traces obtained under current clamp conditions, ciclazindol inhibited I_{KCO} in a concentration-dependent manner. The shift of the zero current potential induced by BRL 38227 (Figure 5B) was of similar size to the hyperpolarization detected under current clamp conditions.

The concentration-dependent effects of ciclazindol on I_{KCO} and membrane potential were derived from experiments in which the 'switched clamp' protocol was used to obtain paired data. Under these conditions the magnitude of I_{KCO} produced by BRL 38227 (10 μM) was 97.8 pA ± 38.0 pA at −25 mV (n = 3) and ciclazindol inhibited I_{KCO} in a concentration-dependent manner with an IC_{50} of 2.5 μM. The hyperpolarization induced by BRL 38227 (10 μM) was 21.6 mV ± 5.3 mV (n = 3). The concentration-response curve for the inhibitory effect of ciclazindol on BRL 38227-induced hyperpolarization showed a slope similar to that obtained from membrane currents with an IC_{50} of 2 μM.

Ligand binding studies

To obtain information about the site of action of ciclazindol, the ability of this agent to displace [^{3}H]-glibenclamide from binding sites in porcine brain membrane fragments was investigated. In these experiments the concentration of glibenclamide required to displace 50% of bound [^{3}H]-glibenclamide was 0.65 ± 0.08 nM (n = 8). In contrast, ciclazindol (up to 10 μM) was unable to displace [^{3}H]-glibenclamide from these sites. These data are summarized in Figure 6.

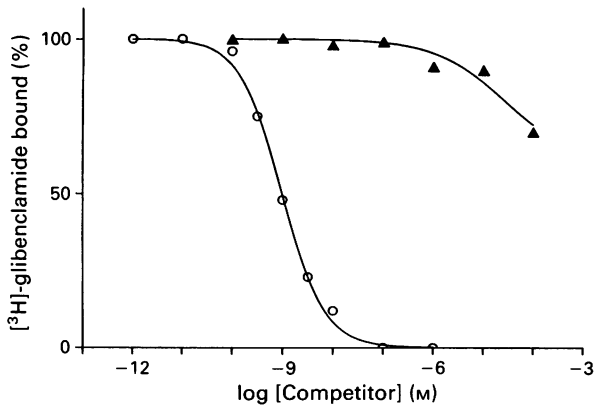

Figure 6 Ability of ciclazindol (▲) and glibenclamide (○) to displace [^{3}H]-glibenclamide from binding sites in porcine brain membranes. In contrast to glibenclamide, ciclazindol (up to 10 μM) failed to displace [^{3}H]-glibenclamide from its binding site. Each point is the mean derived from 8 experiments.

Discussion

The results of the present study provide a detailed account of the mode of action of ciclazindol. Previously described from *in vivo* studies as an anorectic agent (Greenbaum & Harry, 1980; Rothwell *et al.*, 1981) and identified as a monoamine uptake blocker from *in vitro* studies (Becket *et al.*, 1973), ciclazindol has now been clearly identified as a K-channel blocking agent.

In organ bath studies, ciclazindol antagonized the mechano-inhibitory effects of BRL 38227 with a potency similar to that of glibenclamide. However, in contrast to this sulphonylurea which behaved like a competitive antagonist of BRL 38227, relatively high concentrations of ciclazindol showed some features of non-competitive antagonism against this K-channel opener. In further contrast to glibenclamide, which had little stimulatory effect on the spontaneous pattern of mechanical activity in portal vein, ciclazindol produced a characteristic enhancement of tension waves. This consisted of an increase in the duration and complexity of mechanical changes, especially at the upper end of its tested concentration-range.

The ^{42}K efflux experiments performed in the present study confirmed that the antagonism of BRL 38227 by ciclazindol was associated with K-channel blockade. In the concentration range effective as a competitive-type antagonist in the organ bath, ciclazindol inhibited the increase in ^{42}K efflux produced by BRL 38227. Similar effects were produced by glibenclamide and no qualitative difference between ciclazindol and glibenclamide could be detected in these experiments. Neither ciclazindol nor glibenclamide produced a detectable change in basal ^{42}K exchange.

Further confirmation of the K-channel blocking effects of ciclazindol was obtained from the single cell electrophysiological studies. Under the conditions employed (calcium omitted from the bath and pipette solutions both of which contained EGTA, $\geqslant$ 1 mM, Amédée *et al.*, 1990), three essentially calcium-independent current types were identified. These comprised a rapidly-inactivating, transient K-current, a slowly-inactivating, transient outward K-current (I_{TO}) and a complex of non-inactivating background currents (I_{NI}). Further details of these currents have been described (Noack *et al.*, 1991) and will form the subject of another paper. However, preliminary experiments showed that ciclazindol exerted relatively little effect on the rapidly-inactivating transient outward K-current and experiments were thus restricted to those involving I_{TO} and I_{NI}.

When I_{TO} was evoked by depolarizing the membrane to voltages more positive than −30 mV, ciclazindol produced a concentration-dependent inhibition of this current. Although the extent to which an individual current contributes to the characteristic pattern of electrical and mechanical activity in a whole tissue is uncertain, such an inhibitory effect on I_{TO} could explain the characteristic excitatory action of ciclazindol on spontaneous mechanical activity in rat portal vein. In such a spontaneously active, spiking tissue, membrane potentials more positive than −30 mV are achieved during each multispike electrical complex measured using sharp microelectrodes (Jetley & Weston, 1980). Thus, inhibition of I_{TO} would prolong each complex and increase the duration and complexity of tension waves.

Inhibition of I_{TO} was not reflected in the efflux experiments in which basal ^{42}K exchange was unaffected by ciclazindol. It thus seems probable that any reduction in ^{42}K efflux due to inhibition of I_{TO} was negated by increased flux through other K-channels. These could include Ca-sensitive K-channels which make a significant contribution to portal vein total K-conductance in normal PSS (Winquist *et al.*, 1989) together with other voltage-sensitive K-conductances. These would all be activated by the prolonged multispike complexes which apparently develop on exposure to ciclazindol following inhibition of I_{TO}.

When individual cells were exposed to BRL 38227, this agent evoked a non-inactivating K-current (I_{KCO}) which was inhibited by ciclazindol. Such an action clearly contributes to the ability of ciclazindol to antagonize the effects of BRL 38227 in both the mechanical and ^{42}K studies in whole portal veins. If ciclazindol interacts directly with the K-channel responsible for carrying I_{KCO}, such an effect could manifest itself as competitive-type antagonism of BRL 38227 in whole portal veins. In addition in such a spiking tissue, the ciclazindol-induced inhibition of I_{TO} could also contribute functionally to the observed antagonism in whole tissues. Indeed, it is tempting to speculate that the non-competitive component of ciclazindol antagonism of BRL 38227 in the organ bath results from functional antagonism by ciclazindol as a result of ciclazindol-induced inhibition of I_{TO}. Such a non-competitive component was not seen in the organ bath with glibenclamide which does not inhibit I_{TO} (Weston, unpublished observations).

Collectively, the results from the tissue bath, ^{42}K efflux and whole-cell clamp experiments indicate that the ability of ciclazindol and glibenclamide to antagonize BRL 38227 is exerted at a common K-channel. To obtain further information about the site of action of ciclazindol, binding experiments were conducted in porcine brain with [^{3}H]-glibenclamide. The results of these clearly identified a glibenclamide binding site, but no interaction between this location and ciclazindol was detected. One explanation could be that ciclazindol binds directly to a location on a K-channel to which, in contrast, the glibenclamide binding site is indirectly coupled. Recent experiments on the VMHN have shown that the tolbutamide binding site is indeed indirectly coupled to its target K-channel (Ashford *et al.*, 1990b). However, it is always possible that the binding data obtained in the present study together with those of Ashford *et al.* (1990b) cannot be extrapolated to smooth muscle. Nevertheless, these results at least suggest that ciclazindol and glibenclamide may not share a common site in respect of their ability to inhibit I_{KCO} in rat portal vein.

The present investigation has clearly identified that ciclazindol is capable of blocking K-currents in smooth muscle. Its action in this respect is not restricted to the portal vein, but also extends to other non-vascular smooth muscles (Morita *et al.*, 1991). The K-channel blocking action of ciclazindol in portal vein was exerted on both I_{TO} and I_{KCO} with an IC_{50} value against I_{KCO} approximately ten times lower than that against I_{TO}. In the absence of a potassium channel opener, ciclazindol was a relatively selective inhibitor of I_{TO} which can be regarded as the delayed rectifier in this tissue. Such inhibition occurred at concentrations lower than those of other delayed rectifier blockers and thus ciclazindol

is one of the most potent blockers of the smooth muscle delayed rectifier yet described.

It is not possible from the present study to say whether blockade of K-channels similar to those which carry I_{TO} and I_{KCO} in smooth muscle is responsible for the anorectic and amine uptake-blocking properties of this agent identified in previous studies (Becket *et al.*, 1973; Greenbaum & Harry, 1980; Rothwell *et al.*, 1981). However, the VMHN does contain tolbutamide-sensitive K-channels (Ashford *et al.*, 1990b) and blockade of these may indeed form the basis of the anorectic effects of ciclazindol.

This study was supported by the Deutsche Forschungsgemeinschaft (Th.N. and P.D.) and by Pfizer Central Research (G.E.) and by SmithKline Beecham (D.C.).

References

AMÉDÉE, T., LARGE, W.A. & WANG, Q. (1990). Characteristics of chloride currents activated by noradrenaline in rabbit ear artery cells. *J. Physiol.*, **428**, 501–516.

ASHFORD, M.L.J., BODEN, P.R. & TREHERNE, J.M. (1990a). Glucose-induced excitation of hypothalamic neurones is mediated by ATP-sensitive K^+ channels. *Pflügers Arch.*, **415**, 479–483.

ASHFORD, M.L.J., BODEN, P.R. & TREHERNE, J.M. (1990b). Tolbutamide excites rat glucoreceptive ventromedial hypothalamic neurones by indirect inhibition of ATP-K^+ channels. *Br. J. Pharmacol.*, **101**, 531–540.

BECKET, P.R., SOUTHGATE, P.J. & SUGDEN, R.F. (1973). The pharmacology of Wy 23409, a new antidepressant. *Naunyn-Schmiedebergs Arch. Pharmacol.*, **279**, R27.

BEECH, D.J. & BOLTON, T.B. (1989a). Properties of the cromakalim-induced potassium conductance in smooth muscle cells isolated from the rabbit portal vein. *Br. J. Pharmacol.*, **98**, 852–863.

BEECH, D.J. & BOLTON, T.B. (1989b). Two components of potassium current activated by depolarization of single smooth muscle cells from the rabbit portal vein. *J. Physiol.*, **418**, 293–309.

BLUNDELL, J. (1991). Pharmacological approaches to appetite suppression. *Trends Pharmacol. Sci.*, **12**, 147–157.

BUCKINGHAM, R.E., HAMILTON, T.C., HOWLETT, D.R., MOOTOO, S. & WILSON, C. (1989). Inhibition by glibenclamide of the vasorelaxant action of cromakalim in the rat. *Br. J. Pharmacol.*, **97**, 57–64.

CAVERO, I., MONDOT, S. & MESTRE, M. (1989). Vasorelaxant effects of cromakalim in rats are mediated by glibenclamide-sensitive potassium channels. *J. Pharmacol. Exp. Ther.*, **248**, 1261–1268.

CLARK, R.B. & GILES, W.R. (1987). Sodium current in single cells from bullfrog atrium: voltage dependence and ion transport properties. *J. Physiol.*, **391**, 235–265.

DUNNE, M.J. (1990). Nutrient and pharmacological stimulation of insulin-secreting cells – marked differences in the onset of electrical activity. *Exp. Physiol.*, **75**, 771–777.

GREENBAUM, R. & HARRY, T.V.A. (1980). Ciclazindol as an adjunct to weight control. *J. Pharmacother.*, **3**, 82–83.

HAMILL, O.P., MARTY, A., SAKMANN, B. & SIGWORTH, F.J. (1981). Improved patch clamp techniques for high-resolution current recording from cells and cell-free membrane patches. *Pflügers Arch.*, **391**, 85–100.

JETLEY, M. & WESTON, A.H. (1980). Some effects of sodium nitroprusside, D 600 and nifedipine on rat portal vein. *Br. J. Pharmacol.*, **68**, 311–319.

KLÖCKNER, U. & ISENBERG, G. (1985). Action potentials and net membrane currents of isolated smooth muscle cells (urinary bladder of the guinea-pig). *Pflügers Arch.*, **405**, 329–339.

KOVACS, R.J. & NELSON, M.T. (1991). ATP-sensitive K^+ channels from aortic smooth muscle incorporated into planar lipid bilayers. *Am. J. Physiol.*, **261**, H604–H609.

LAMMEL, E., DEITMER, P. & NOACK, Th. (1991). Suppression of steady membrane currents by acetylcholine in single smooth muscle cells of the guinea-pig gastric fundus. *J. Physiol.*, **432**, 259–282.

MORITA, T., EDWARDS, G., ANDERSSON, P., GREENGRASS, P., IBOTTSON, T., NEWGREEN, D.T., WESTON, A.H. & WYLLIE, M.G. (1991). Ciclazindol, a novel antagonist of the action of potassium channel openers in smooth muscle. *J. Physiol.*, **446**, 365P.

NAKAO, K. & BOLTON, T.B. (1991). Cromakalim-induced potassium currents in single dispersed smooth muscle cells of rabbit artery and vein. *Br. J. Pharmacol.*, **102**, 155P.

NOACK, Th., DEITMER, P. & GOLENHOFEN, K. (1990). Features of a calcium independent, caffeine sensitive outward current in single smooth muscle cells from guinea pig portal vein. *Pflügers Arch.*, **416**, 467–469.

NOACK, Th., DEITMER, P., EDWARDS, G., WESTON, A.H. & GOLENHOFEN, K. (1991). Effects of BRL 38227 on whole cell currents in vascular smooth muscle. *Pflügers Arch.*, **419**, R85.

NOACK, Th., DEITMER, P., EDWARDS, G. & WESTON, A.H. (1992). Characterization of potassium currents modulated by BRL 38227 in rat portal vein. *Br. J. Pharmacol.*, (in press).

ONO, T., NISHINO, H., FUKUDA, M., SASAKI, K., MURAMOTO, K.I. & OOMURA, Y. (1982). Glucoresponsive neurones in rat ventromedial hypothalamic tissue slices in vitro. *Brain Res.*, **232**, 494–499.

QUAST, U. & COOK, N.S. (1989a). *In vitro* and *in vivo* comparison of two K^+ channel openers, diazoxide and cromakalim, and their inhibition by glibenclamide. *J. Pharmacol. Exp. Ther.*, **250**, 261–270.

QUAST, U. & COOK, N.S. (1989b). Moving together: K^+ channel openers and ATP sensitive K^+ channels. *Trends Pharmacol. Sci.*, **10**, 431–435.

ROTHWELL, N.J., STOCK, M.J. & WYLLIE, M.G. (1981). Sympathetic mechanisms in diet-induced thermogenesis: modification by ciclazindol and anorectic drugs. *Br. J. Pharmacol.*, **74**, 539–546.

STANDEN, N.B., QUAYLE, J.M., DAVIES, N.W., BRAYDEN, J.E., HUANG, Y. & NELSON, M.T. (1989). Hyperpolarizing vasodilators activate ATP-sensitive K^+ channels in arterial smooth muscle. *Science*, **245**, 177–180.

WINQUIST, R.J., HEANEY, L.A., WALLACE, A.A., BASKIN, E.P., STEIN, R.B., GARCIA, M.L. & KACZOROWSKI, G.J. (1989). Glyburide blocks the relaxation response to BRL 34915 (cromakalim), minoxidil sulphate and diazoxide in vascular smooth muscle. *J. Pharmacol. Exp. Ther.*, **248**, 149–156.

(Received December 16, 1991
Accepted January 7, 1992)

Br. J. Pharmacol. (1992), **106**, 25–32 © Macmillan Press Ltd, 1992

Adenosine modulation of calcium currents in postganglionic neurones of avian cultured ciliary ganglia

[1]Max R. Bennett, R. Kerr & G. Khurana

The Neurobiology Research Centre, University of Sydney, N.S.W. 2006, Australia

1 Calcium currents in postganglionic neurones of cultured 7- to 10-day embryonic avian ciliary ganglia were analyzed under whole-cell voltage-clamp and their modulation by 2-chloroadenosine determined.

2 In the presence of tetrodotoxin (200 nM) in the medium to block the Na^+ current and CsCl (105 mM) in the patch-clamp electrode to block the K^+ current, two different components of the calcium currents (transient and sustained) were identified on the basis of their voltage-dependent kinetics as well as their sensitivity to the dihydropyridine agonist Bay K 8644 and antagonist nifedipine.

3 The sustained current inactivated very slowly ($\tau > 1000$ ms; for test potentials from -20 mV to $+40$ mV) but was reactivated at a holding potential (Vh) of -40 mV. The current was increased on average over 50% by 1 μM of Bay K 8644 at a test potential of 0 mV and decreased over 35% by 1 μM of nifedipine.

4 The transient current inactivated slowly ($\tau < 200$ ms; for test potentials from -20 mV to $+40$ mV), and could be completely reactivated at a Vh of -80 mV. This current was unaffected by Bay K 8644 (1 μM) but reduced on average by 8% with nifedipine (1 μM).

5 The sustained and transient currents were decreased more than 70% by 5 μM of ω-conotoxin and decreased more than 50% by 250 μM verapamil.

6 2-Chloroadenosine (1 μM) decreased the transient current by over 50% and the sustained current by less than 10%. In the presence of nifedipine (1 μM), 2-chloroadenosine decreased the transient current by over 30% and the remaining sustained current by 35%. In the presence of 8-phenyltheophylline (10 μM), 2-chloroadenosine no longer decreased either the transient or sustained currents but did have a slight potentiating effect on both the transient and sustained currents.

7 These observations of the effects of 2-chloroadenosine on the transient and sustained currents are discussed in relation to the different calcium channel types at preganglionic nerve terminals.

Keywords: Synapse; calcium current; ciliary neurones; adenosine

Introduction

Endogenous adenosine modulates transmission at preganglionic nerve terminals in avian ciliary ganglia, where it acts to depress the secretion of acetylcholine quanta (Bennett & Ho, 1991). This purine nucleoside also reduces the duration of plateau-type action potentials generated in both ciliary neurones and their preganglionic calyciform nerve terminals following exposure to tetraethylammonium ions (Bennett & Ho, 1991). These observations suggest that adenosine acts to reduce the inward calcium current associated with such plateau-type action potentials. Adenosine reduces the duration of plateau-type action potentials generated in sympathetic neurones (Henon & McAfee, 1983) and dorsal root ganglion neurones (MacDonald *et al.*, 1986; Dolphin *et al.*, 1986). Voltage-clamp studies of this action of adenosine on dorsal-root ganglion neurones have shown that it is mediated by an A_1-type adenosine receptor (Ribeiro & Sebastiao, 1986; Dolphin *et al.*, 1986) which acts through calcium channels (Gross *et al.*, 1989; Kasai & Aosaki, 1989).

Distinct types of high-threshold calcium channels have been proposed (Fox *et al.*, 1987) but their existence and function is a matter of controversy (for reviews see Carbone & Swandulla, 1989; Swandulla *et al.*, 1991). The calcium current in most neurones consists of a rapidly-inactivating component followed by a slowly-inactivating component (Sher & Clementi, 1991). Recently the rapid component has been referred to as 'transient' whilst the slow component has been termed 'sustained' (Schroeder *et al.*, 1990). The dihydropyridines used to characterize the L-type calcium channel in muscle can affect both the transient and sustained calcium current in neurones (Slesinger & Lansman, 1991), whilst ω-conotoxin from the venom of *Conus Geographus* can affect both the transient and sustained calcium currents (Sher & Clementi, 1991). However, substantial calcium current remains in some neurones when both dihydropyridine antagonists and ω-conotoxin are applied together (Regan *et al.*, 1991). In the present work transient and sustained currents have been recorded from 7- to 10-day old chick embryo ciliary neurones and their relative sensitivity to dihydropyridines and ω-conotoxin determined. The action of the adenosine analogue 2-chloroadenosine on the dihydropyridine-sensitive and insensitive macroscopic calcium currents is then described.

[1]Author for correspondence.

Methods

Ciliary ganglion cell preparation

White leghorn chicks were used for all experiments. Ciliary ganglia from 7–10 day old chick embryos were dissected free in Ca^{2+}, Mg^{2+}-free Hanks Balanced Salt Solution containing 0.3% bovine serum albumin (BSA), and incubated at 37°C for 30 min. No proteolytic enzymes were used. The supernatant was removed and 1 ml of Dulbecco's Modified Eagles Media (DMEM, Flow, Sydney) supplemented with 2 mM glutamine, 1.0 μ ml^{-1} penicillin, 50 μg ml^{-1} streptomycin, 10% heat-inactivated horse serum (CSL) and 2% chick embryo extract was added. The ganglia were then mechanically

dissociated by repeated trituration through a Pasteur pipette. The resultant single cell suspension was plated onto 13 mm glass coverslips previously coated with poly-L-lysine in 24-well plates (Corning) and maintained at 37°C in a 5% CO_2 in air water-saturated atmosphere until required. Neurones were used for whole-cell recording within 12 to 24 h after plating, when they have few processes. These cells were chosen to minimize difficulties involving spatial non-uniformities of membrane potential arising from inadequate space clamp; if these occurred the results were excluded.

Solutions

Electrodes for forming gigaohm seals with the cell membranes of ciliary neurones were made from boro-silicate capillary tubing and had resistances of 0.5 to 4.0 MΩ when filled with internal solution (Hamill *et al.*, 1981). For the whole-cell recording presented in this work, the pipette solution consisted of (mM): CsCl 105, CsEGTA 10, $MgCl_2$ 1, HEPES 40, ATP 2, and GTP 1, pH adjusted to 7.3 with CsOH. The bathing solution consisted of (mM): $CaCl_2$ 5, TEACl 135, glucose 10, HEPES 10, and tetrodotoxin (TTX), 200 nM, pH adjusted to 7.3 with TEAOH. Variations on these solutions involved elevating the concentration of $CaCl_2$ and the substitution of $BaCl_2$ for $CaCl_2$. Such changes are noted in the appropriate legends. All experiments were at room temperature, about 21°C.

Recording

Whole-cell patch-clamp techniques were used (Fenwick *et al.*, 1982) to voltage-clamp ciliary neurones. Prior to forming seals the pipette current due to liquid junction potentials within the electrode and bath was nulled and the pipette capacitance compensated. After establishing a seal, the patch membrane was broken under slight negative pressure by a short (0.5 ms) 1.5 V pulse. This negative pressure, which prevented electrode blockage, was maintained throughout the course of the experiment. Ion currents were recorded via an Axopatch-IC amplifier and a labmaster interface on an IBM-AT using pClamp (Axon Instruments) software. Currents filtered at 5 kHz, were sampled at 3 kHz. Cells were held at the holding potentials for 4 s before test pulses were applied.

Current records presented in the figures have had periods of less than 2 ms at the onset and offset of the command pulses removed to eliminate spurious points due to incomplete capacitance compensation. These current records have been subjected to leak subtraction. Voltage-clamp control was determined according to several criteria: firstly, smooth voltage-dependent current activation; secondly, lack of excessive delay in onset of current; thirdly, onset and offset kinetics that were dependent on voltage but not on the amplitude of the current. Isopotentiality of the neuronal membrane was determined by testing the exponentiality of the capacitive transient.

Drugs

2-Chloroadenosine, ω-conotoxin, Bay K 8644, (methyl 1, 4-dihydro-2,6-dimethyl-3-nitro-4-(2-trifluoromethylphenyl)-pyridine-5-carboxylate), nifedipine, 8-phenyltheophylline and verapamil (all from SIGMA Chemical Co.) were dissolved in recording medium and applied by pressure ejection (2 to 7 kPa) from micropipettes with tip diameters of about 10 μM. These pipettes were positioned about 20 μM to 50 μM from the neurone cell body during a puff application and then removed as described by Bennett & Ho (1991).

Statistics

Data are expressed as mean ± s.e.mean and n represents the number of experiments. The significance of the difference between the n pairs of observations made before and after application of a drug was calculated by Student's t test. P values of 0.05 or less were considered to represent significant differences.

Results

High-voltage threshold calcium currents with transient and sustained components were present in all ciliary neurones studied ($n = 150$); the description of these components given below, together with their sensitivities to different drugs, is not to imply that they are due to separate channel subtypes (see Discussion). These neurones rarely possessed low-voltage threshold currents indicating the presence of T-type channels (Fox *et al.*, 1987) so that these were not studied in detail. Only very small T-type currents can be observed in somatic motoneurones from similar-aged embryos to those used in the present work (McCobb *et al.*, 1989). The usual current-voltage (I–V) relation, observed when a holding potential (Vh) of −100 mV was used and $BaCl_2$ was substituted for $CaCl_2$, is shown in Figure 1d; the current increases for more depolarized test voltages up to about +10 mV then decreases monotonically to zero at about +60 mV. If, however, a smaller Vh of −50 mV was used much smaller currents were generated at each test voltage, although the $I-V$ curve was the same shape, as shown in Figure 1b. The transient current is not present at relatively positive holding potentials (see Figure 3) so that the smaller current in Figure 1b only contains the sustained component. The failure of the cell to generate currents at relatively negative test potentials in Figure 1d suggests that T-type channels are not present. In order to obtain some idea of the time course of the transient and sustained currents, double exponential curves were fitted to the total current generated from a Vh = −80 mV over a wide range of test potentials as shown in Figure 2a. These show that the transient current inactivates relatively slowly ($\tau < 200$ ms; Figure 2b) and the sustained current inactivates very slowly ($\tau > 1000$ ms; Figure 2b). The time constants of decay for the transient currents (176 ± 28 ms) and sustained currents (2341 ± 208 ms) were well separated in all 10 neurones studied (Figure 2b).

The voltage-dependence of the inactivation of the transient and sustained currents was determined in 39 neurones for which no T current was detectable. The sustained current was taken as the total current present at the end of a 600 ms test pulse and the transient current calculated as the difference between the peak current and the sustained current (see Figure 2a). Test pulses to +20 mV for 600 ms were used to detect the sustained and transient components of the currents generated from different holding potentials (Figure 3b). Figures 3c and 3d show the amplitude of the sustained and transient currents respectively during the test pulse plotted against the holding potential to give typical inactivation curves for sustained and transient currents observed in these neurones. The voltage-range for inactivation of the sustained current is different from that of the transient current (compare filled circles in Figures 3c and d) as inactivation of the sustained current is small at −49mV whereas it is relatively large for the transient current. Fitting the Boltzman relation to the data by the method of least squares yields for the sustained current a $V_{\frac{1}{2}}$ of −25.3 ± 1.9 mV ($n = 39$) and a V* of 17.5 ± 0.6 mV; the results for the transient current were a $V_{\frac{1}{2}}$ of −49.4 ± 1.3 mV ($n = 39$) and a V* of 13.1 ± 0.4 mV. Activation of sustained and transient currents was determined from a holding potential of −80 mV to test potentials between −50 and +10 mV (Figure 3a). Figures 3c and 3d (open circles) give the activation curves obtained for the sustained and transient currents respectively: both the sustained and transient current components increase steeply between −20 mV and +10 mV and there is very little quantitative difference between their activation curves.

The actions of the dihydropyridine agonist Bay K 8644 and the antagonist nifedipine on the sustained and transient

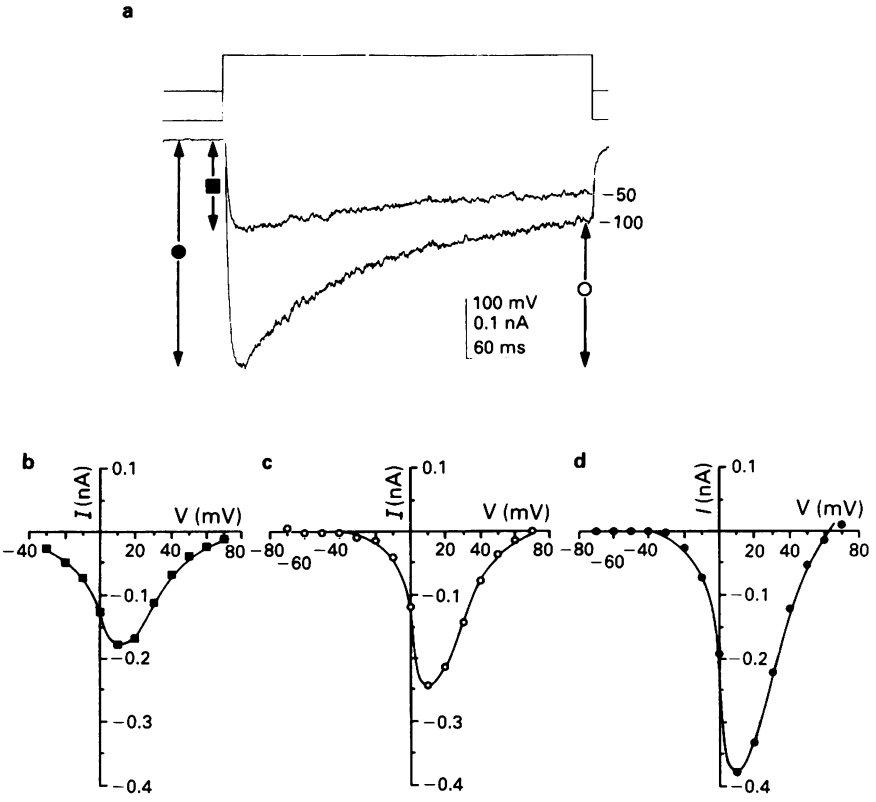

Figure 1 Different components of the inward current, during whole-cell voltage-clamp, separated by use of different holding potentials. In (a) are shown the currents evoked by a test potential of +10 mV from a Vh = −100 mV or Vh = −50 mV. In (b) are shown the peak currents (*I*) for different test potentials (V) from a Vh = −50 mV (■ in a). (c) Gives the magnitude of the transient current (*I*) for different test potentials (V) from a Vh = −100 mV (○ in a); (d) shows the peak currents (*I*) for different test potentials (V) from a Vh = −100 mV (● in a). $BaCl_2$ 5 mM was substituted for $CaCl_2$ 5 mM in the bath.

currents were determined (Figure 4 and 5). Bay K 8644 (1 μM) increased the sustained current (Figure 4a) and this occurred for positive command voltages from a holding potential of −50 mV (Figures 4b and c). For depolarizations to 0 mV ($n = 5$) the sustained current was increased from −376 ± 64 pA to −531 ± 67 pA and this increase was significant. The effect of Bay K 8644 (1 μM) on the transient current was to shift its current-voltage relation about −10 mV without changing the shape of the relation (Figure 4b); for depolarizations to 0 mV ($n = 5$) the transient current increased from −398 ± 33 pA to −423 ± 44 pA and this result was not significant. Nifedipine (1 μM) decreased the sustained current in six neurones by over 35% but decreased the transient current by less than 10% (Figure 5a); this decrease occurred for positive command voltages (Figure 5b and c). For depolarizations to 20 mV ($n = 6$) the sustained current was reduced from −276 ± 36 pA to −180 ± 30 pA and the transient current from −317 ± 69 pA to −294 ± 66 pA; both of these reductions were significant.

The actions of the calcium channel blockers, ω-conotoxin and verapamil, on the transient and sustained currents were determined (Figure 6a and Figure 7a). The toxin (5 μM) decreased both currents (Figure 6b and c) and this occurred over the entire range of command voltages examined from a holding potential of −100 mV (Figure 6b and c). For depolarizations to +20 mV ($n = 3$) the transient current was reduced from −307 ± 96 pA to −48 ± 39 pA and the sustained current was reduced from −375 ± 56 pA to −63 ± 22 pA; the reduction in both of these currents was significant. Verapamil (250 μM) also decreased both currents in four neurones from these ganglia (Figure 7a); this also occurred over the entire range of command voltages (Figure 7b and c). For depolarizations to +20 mV ($n = 4$) the transient current was reduced from −414 ± 83 pA to −128 ± 22 pA and the sustained current reduced from −343 ± 36 pA to −164 ± 60 pA; the reduction of both of these currents was significant.

2-Chloroadenosine (1 μM) decreased the transient current in all eight neurones studied, but left the sustained current unaffected (Figure 8). For depolarizations to +30 mV ($n = 11$) the transient current was significantly reduced from −388 ± 80 pA to −198 ± 48 pA; the sustained current changed from −422 ± 67 pA to −395 ± 50 pA, and this was not a significant reduction. This effect on the transient current occurred over the complete range of command voltages used (Figure 8b). There were no significant changes in either the transient or sustained current due to the action of 2-chloroadenosine in the presence of 8-phenyltheophylline (10 μM, $n = 6$): the transient and sustained currents were −396 ± 85 pA and −640 ± 35 pA respectively in the control, and −355 ± 80 pA and −637 ± 33 pA respectively in the presence of 2-chloroadenosine plus 8-phenyltheophylline. However in the presence of 40 μM 8-phenyltheophylline, 2 μM 2-chloroadenosine had a slight potentiating effect on both the transient and sustained currents (Figure 9a). For depolarizations to +20 mV ($n = 3$) the transient current was increased from −110 ± 26 pA to −133 ± 28 pA and the sustained current from −106 ± 34 pA to −119 ± 37 pA (Figure 9b and c); however, these changes were not significant.

It was of interest to know whether the nifedipine-resistant sustained current (see Figure 5a) was sensitive to 2-chloroadenosine as it is possible that such dihydropyridine-insensitive currents may represent a tail of the transient current component (Plummer & Hess, 1991). 2-Chloroadenosine (2 μM) reduced the transient component in the usual way but also reduced the nifedipine (1 μM)-resistant sustained current (Figure 10a). At depolarizations to +20 mV ($n = 4$) the transient current was reduced from −345 ± 92 pA to −231 ± 63 pA and the sustained current from −214 ± 35 pA to

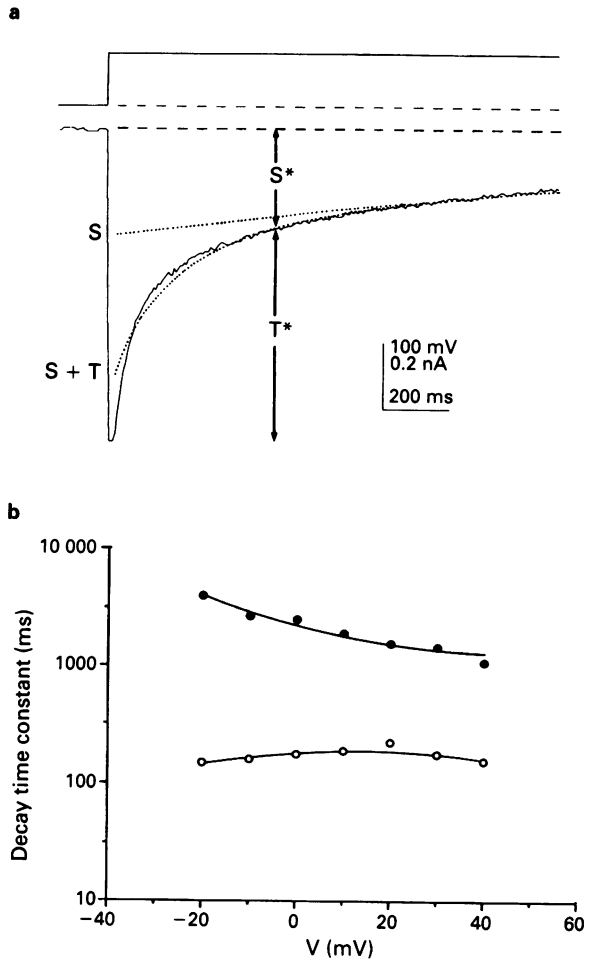

Figure 2 Transient and sustained components of the whole-cell calcium current. In (a) is shown the start of a voltage-clamp record of a test potential of 0 mV from a Vh = −80 mV and of 10 s duration; indicated on the current record is a double-exponential curve fit (dotted lines) to the sustained current (S) and to the sustained plus transient current (S + T). In (b) is shown the voltage-dependence of the time constants of current decay for the sustained current (●) and the transient current (○) derived from the double-exponential curve fits given in (a). The bath contained 5 mM $CaCl_2$ in (a) and (b). Also shown in (a) is the method used for calculating the sustained current (S*) and transient current (T*) for the I/V curves given in later figures: S* was the total current at the end of 600 ms and this was subtracted from the peak current to give T*.

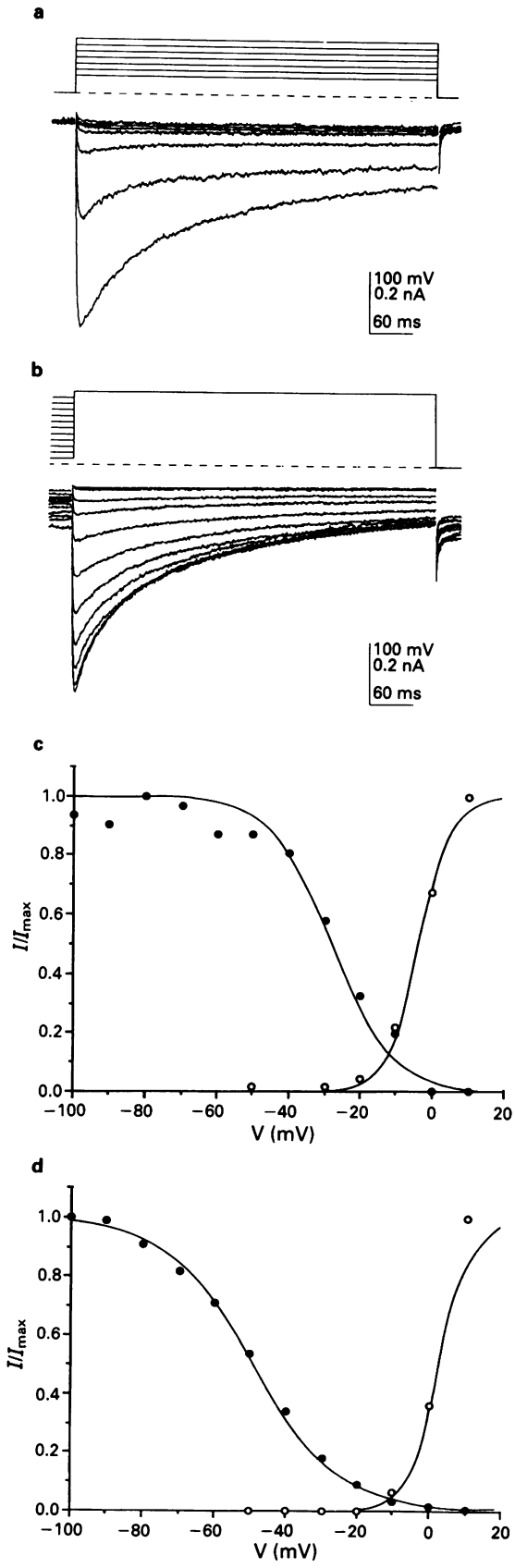

Figure 3 Voltage-dependence of activation and inactivation of the calcium current: (a) shows the currents elicited by depolarizing pulses from a Vh of −80 mV to the different test potentials from −50 mV to +10 mV indicated; (b) shows the currents that were evoked by a test depolarization to +20 mV from the various holding potentials (Vh) indicated between −90 mV to +10 mV. In (c) (●) give the sustained current amplitudes (I), normalized to the maximal sustained current amplitude (I_{max}), obtained at Vh = −80 mV, plotted against the holding potential, using the data in (b). (○) Give the sustained current amplitudes (I) normalized to the maximal sustained current amplitude (I_{max} at +10 mV), plotted against the test potential, using the data in (a). The smooth curves are drawn according to the Boltzmann relations $I/I_{max} = [1 + \exp(V - V½)/V^*]^{-1}$ where $V½ = -28$ mV and $V^* = 8.5$ mV for closed circles and, $I/I_{max} = \{1 + \exp(V½ - V)/V^*\}^{-1}$ where $V½ = 4$ mV and $V^* = 4.5$ mV for open circles. In (d) a similar analysis is presented for the transient current component, in which for (●), I_{max} was obtained at $V_h = -100$ mV, $V½ = -49$ mV and $V^* = 12$ mV; for (○), I_{max} was obtained at a test potential of 10 mV, $V½ = 3$ and $V^* = 4.5$. The bath contained 5 mM $CaCl_2$.

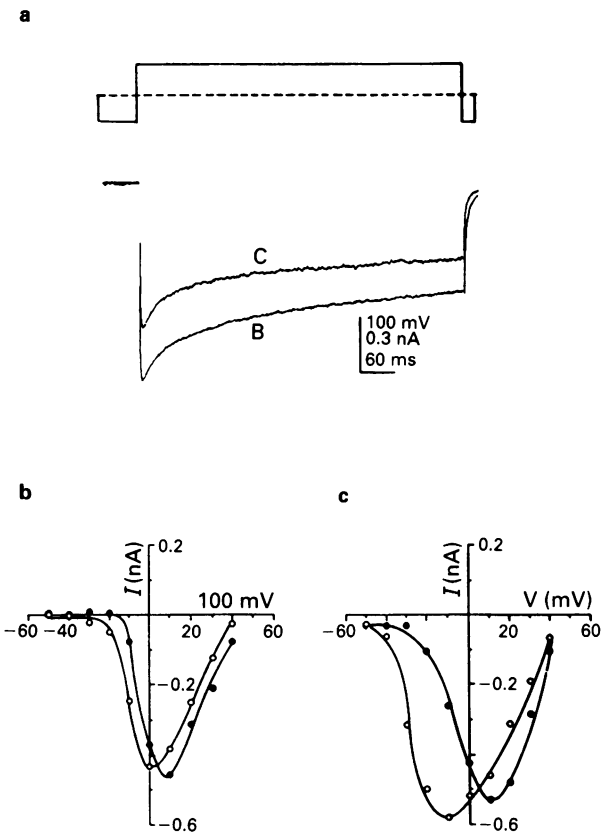

Figure 4 Effect of Bay K 8644 (1 μM) on the transient and sustained currents. In (a) is shown the currents evoked with a Vh = −50 mV to a test potential of +10 mV both before (C) and after (B) exposure to Bay K 8644. In (b) a graph is given of the transient current before (●) and after (○) Bay K 8644. In (c) a graph is given of the sustained current before (●) and after (○) Bay K 8644. In (b) and (c) the voltages are the test potentials. The bath contained 5 mM $CaCl_2$.

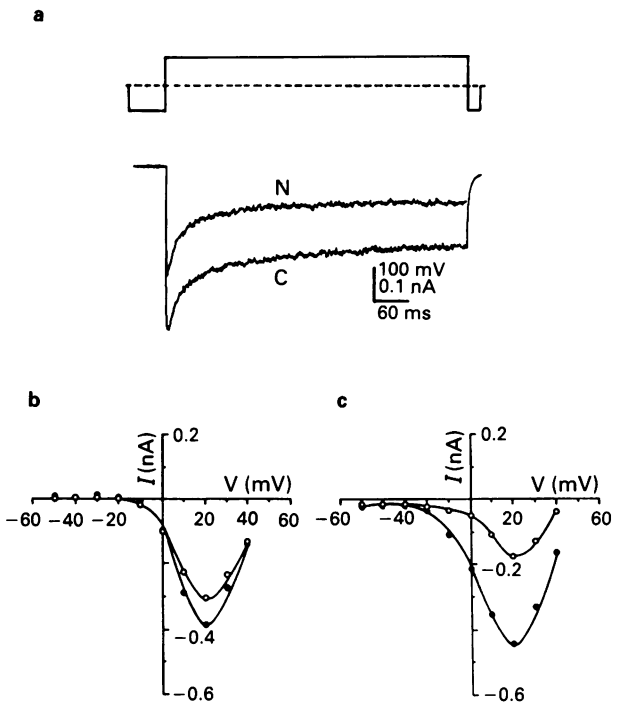

Figure 5 Effect of nifedipine (1 μM) on the transient and sustained currents. In (a) is shown the currents evoked with a Vh = −50 mV to a test potential of +10 mV both before (C) and after (N) exposure to nifedipine. In (b) a graph is given of the transient current before (●) and after (○) nifedipine. In (c) a graph is given of the sustained current before (●) and after (○) nifedipine. In (b) and (c) the voltages are the test potentials. The bath contained 5 mM $CaCl_2$.

−144 ± 32 pA (Figure 10b and c). The decrease in both of these currents was significant.

Discussion

The separation of high-voltage activated calcium currents into two types generated by different channels, termed L and N by Tsien and his colleagues (Fox *et al.*, 1987; Tsien *et al.*, 1987; 1988) is at present a matter of considerable debate (see for example Swandulla *et al.*, 1991), and so has not been followed in the present work. It was originally thought that the sustained current was due to the dihydropyridine-sensitive L-channel, but more recent observations show that the putative N-channel also contributes a sustained current (Aosaki & Kasai, 1989; Plummer *et al.*, 1989; Plummer & Hess, 1991). The possibility exists that the pharmacological agents used at present to distinguish between high-voltage activated calcium channel types are actually working on essentially equivalent calcium channels with different drug sensitivities (Swandulla *et al.*, 1991). Until this is resolved it is best to describe the macroscopic calcium current as transient or sustained and to consider their relative sensitivity to dihydropyridines and ω-conotoxin in each neuronal preparation. In the ciliary neurone a component of the sustained current was blocked by nifedipine and enhanced with Bay K 8644 which is consistent with a contribution from an L-type channel. Synaptic transmission in the ganglion and calcium current in the nerve terminal is not blocked by nifedipine

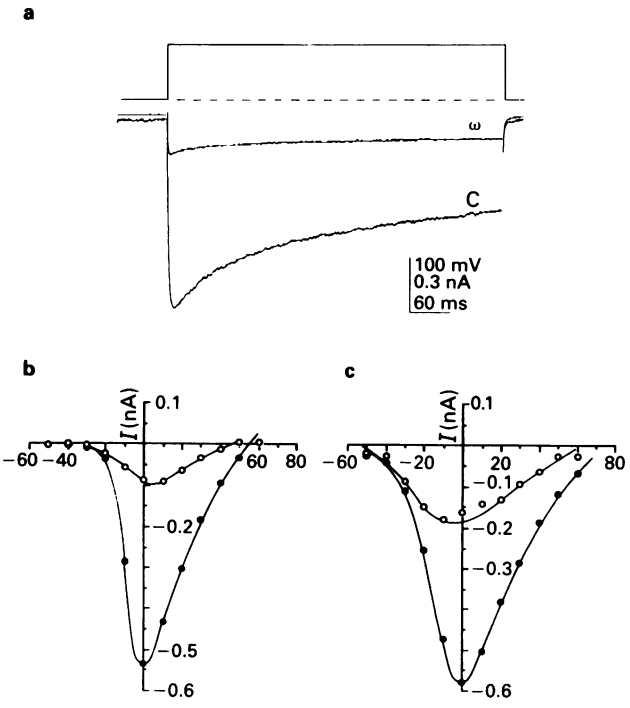

Figure 6 Effect of ω-conotoxin (5 μM) on the transient and sustained currents. In (a) is shown the currents evoked with a Vh = −100 mV to a test potential of 0 mV both before (C) and after (ω) exposure to ω-conotoxin. In (b) a graph is given of the transient current before (●) and after (○) ω-conotoxin. In (c) a graph is given of the sustained current before (●) and after (○) ω-conotoxin. In (b) and (c) the voltages are the test potentials. The bath contained 5 mM $CaCl_2$.

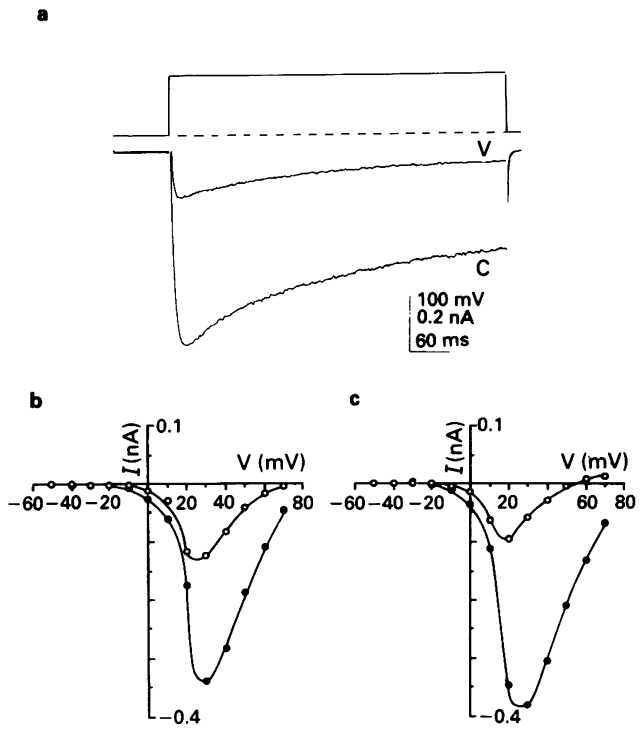

Figure 7 Effect of verapamil (250 μM) on the transient and sustained currents. In (a) is shown the currents evoked with a Vh = −80 mV to a test potential of +30 mV both before (C) and after (V) exposure to verapamil. In (b) a graph is given of the transient current before (●) and after (○) verapamil. In (c) a graph is given of the sustained current before (●) and after (○) verapamil. In (b) and (c) the voltages are the test potentials. The bath contained 20 mM $CaCl_2$.

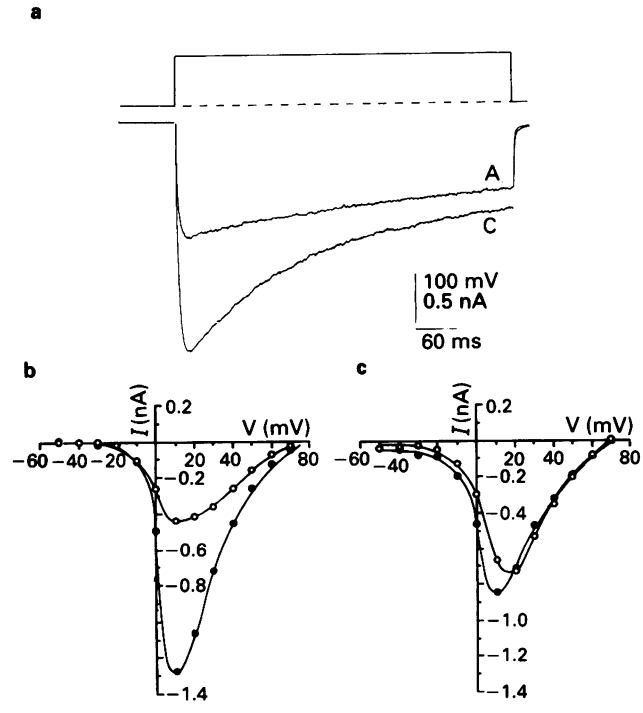

Figure 8 Effect of 2-chloroadenosine (1 μM) on the transient and sustained currents. In (a) is shown the currents evoked with a Vh = −80 mV to a test potential of +10 mV during the control (C) and after (A) 2-chloroadenosine. In (b) a graph is given of the transient current before (●) and after (○) 2-chloroadenosine. In (c) a graph is given of the sustained current before (●) and after (○) 2-chloroadenosine. In (b) and (c) the voltages are the test potentials. The bath contained 10 mM $CaCl_2$.

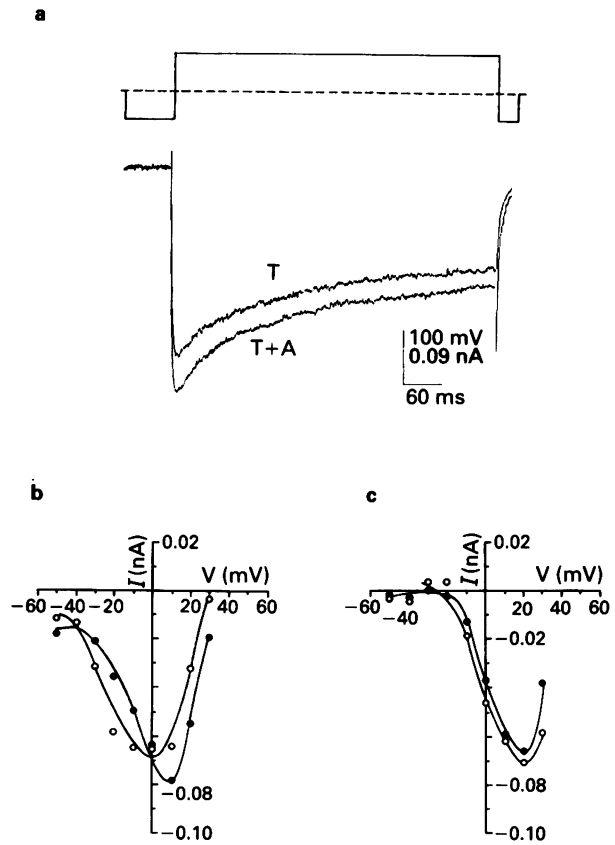

Figure 9 Effect of 2-chloroadenosine (2 μM) on the transient and sustained currents in the presence of 8-phenyltheophylline (40 μM). In (a) is shown the currents evoked with a Vh = −50 mV to a test potential of +10 mV in the presence of 8-phenyltheophylline alone (T) and after (T + A) exposure to 2-chloroadenosine in the presence of 8-phenyltheophylline. In (b) a graph is given of the transient current in the presence of 8-phenyltheophylline alone (●) and after (○) exposure to 2-chloroadenosine plus 8-phenyltheophylline. In (c) a graph is given of the sustained current in the presence of 8-phenyltheophylline alone (●) and after (○) exposure to 2-chloroadenosine plus 8-phenyltheophylline. In (b) and (c) the voltages are the test potentials. The bath contained 15 mM $CaCl_2$.

(Stanley & Atrakchi, 1990) so that this L-type current is unlikely to play a role in transmission. However ω-conotoxin blocks synaptic transmission and the calcium current in ciliary nerve terminals (Stanley & Atrakchi, 1990; Stanley & Goping, 1991). This toxin eliminates most of the transient and sustained current in the ganglion, so it does not help in distinguishing which of these plays the predominant role in transmission. It is not known if verapamil blocks transmission in the ganglion although it substantially depresses both the transient and sustained currents as it does in cultured chick-embryo motorneurones (McCobb *et al.*, 1989).

The transient current was substantially depressed by 2-chloroadenosine, with only a slight effect on the sustained current. This analague of adenosine has a similar effect on the transient calcium currents in dorsal root ganglion (Dolphin *et al.*, 1986; MacDonald *et al.*, 1986; Scott & Dolphin, 1987) where it acts through a pertussis-toxin sensitive G protein (Holz *et al.*, 1986; Gross *et al.*, 1989; Kasai & Oasaki, 1989). Transient calcium currents, with a voltage-dependent inactivation different from that observed in the present work, have been identified in avian preganglionic nerve terminals (Stanley, 1989; Brosius *et al.*, 1990; Yawo, 1990); the modulation of these by adenosine is not known. Given the present uncertainty concerning the identity of different calcium-channel subtypes it is even possible that a single high-voltage activated calcium current exists which is

carried by fundamentally equivalent calcium channels with different drug sensitivities that are turned-on only slowly in the presence of adenosine due to a time- and voltage-dependent uncoupling of G-proteins from the channels at depolarized membrane potentials (Swandulla *et al.*, 1991).

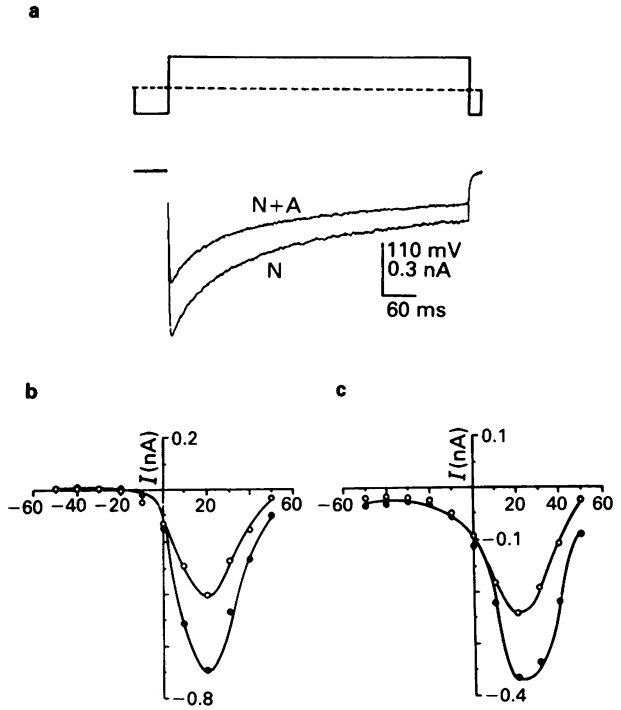

Figure 10 Effect of 2-chloroadenosine (1 μM) on the transient and sustained currents in the presence of nifedipine (1 μM). In (a) is shown the currents evoked with a Vh = −50 mV to a test potential of +10 mV in the presence of nifedipine alone (N) and after (N + A) exposure to 2-chloroadenosine in the presence of nifedipine. In (b) a graph is given of the transient current in the presence of nifedipine alone (●) and after (○) exposure to 2-chloroadenosine plus nifedipine. In (c) a graph is given of the sustained current in the presence of nifedipine alone (●) and after (○) exposure to 2-chloroadenosine plus nifedipine. In (b) and (c) the voltages are the test potentials. The bath contained 15 mM $CaCl_2$.

References

AOSAKI, T. & KASAI, H. (1989). Characterization of two kinds of high-voltage-activated Ca-channel currents in chick sensory neurons. *Eur. J. Physiol.*, **414**, 150–156.

BECHEM, M. & SCHRAMM, M. (1988). Electrophysiology of dihydropyridine calcium agonist. In *'The Calcium Channel: Structure, Function and Implications'*. ed. Morad, M., Nayler, W., Kazda, S. & Schramm, M. pp. 63–70. London: Springer-Verlag.

BENNETT, M.R. & HO, S. (1991). Probabilistic secretion of quanta from nerve terminals in avian ciliary ganglia modulated by adenosine. *J. Physiol.*, **440**, 513–527.

BROSIUS, D.C., HACKETT, J.T. & TUTTLE, J.B. (1990). Presynaptic calcium currents evoking quantal transmission from avian ciliary ganglion neurones. *Synapse*, **5**, 313–323.

CARBONE, E. & SWANDULLA, D. (1989). Neuronal calcium channels: kinetics blockade and modulation. *Prog. Biophys. Molec. Biol.*, **54**, 31–58.

DOLPHIN, A.C., FORDA, S.R. & SCOTT, R.M. (1986). Calcium-dependent currents in cultured rat dorsal root ganglion neurons are inhibited by an adenosine analogue. *J. Physiol.*, **373**, 47–61.

FENWICK, E.M., MARTY, A. & NEHER, E. (1982). A patch clamp study of bovine chromaffin cells and of their sensitivity to acetylcholine. *J. Physiol.*, **331**, 577–597.

FOX, A.P., NOWYCKY, M.C. & TSIEN, R.W. (1987). Kinetic and pharmacological properties distinguishing three types of calcium currents in chick sensory neurones. *J. Physiol.*, **394**, 149–172.

GROSS, R.A. & MACDONALD, R.L. & RYAN-JASTROW, T. (1989). 2-chloroadenosine reduces the N calcium current of cultured mouse sensory neurones in a pertussis toxin-sensitive manner. *J. Physiol.*, **411**, 585–595.

HAMILL, O.P., MARTY, A., NEHER, E., SAKMANN, G. & SIGWORTH, F.J. (1981). Improved patch-clamp techniques for high-resolution current recording from cells and cell-free membrane patches. *Pflügers Arch.*, **391**, 85–100.

HENON, B.K. & MCAFEE, D.A. (1983). The ionic basis of adenosine receptor actions on post-ganglionic neurones in the rat. *J. Physiol.*, **336**, 607–620.

HOLZ IV, G.G., RANE, S.G. & DUNLAP, K. (1986). GTP-binding proteins mediate transmitter inhibition of voltage-dependent calcium channels. *Nature*, **319**, 670–672.

KASAI, H. & OASAKI, T. (1989). Modulation of Ca-channel current by an adenosine analog mediated by a GTP-binding protein in chick sensory neurons. *Eur. J. Physiol.*, **414**, 145–149.

MACDONALD, R.L., SKERRITT, J.H. & WERZ, M.A. (1986). Adenosine agonists reduce voltage-dependent calcium conductance of mouse sensory neurones in cell culture. *J. Physiol.*, **370**, 75–90.

MCCOBB, D.P., BEST, P.M. & BEAM, K.G. (1989). Development alters the expression of calcium currents in chick limb motoneurones. *Neuron*, **2**, 1633–1643.

PLUMMER, M.R. & HESS, P. (1991). Reversible uncoupling of inactivation in N-type calcium channels. *Nature*, **351**, 657–659.

PLUMMER, M.R., LOGOTHETIS, D.E. & HESS, P. (1989). Elementary properties and pharmacological sensitivities of calcium channels in mammalian peripheral neurones. *Neuron*, **2**, 1453–1463.

REGAN, L.J., SAH, D.W.Y. & BEAN, B.P. (1991). Ca^{2+} channels in rat central and peripheral neurons: high-threshold current resistant to dihydropyridine blockers and ω-conotoxin. *Neuron*, **6**, 269–280.

RIBEIRO, J.A. & SEBASTIAO, A.M. (1986). Adenosine receptors and calcium: basis for proposing a third (A3) adenosine receptor. *Prog. Neurobiol.*, **26**, 179–209.

SCHROEDER, J.E., FISCHBACH, P.S., MAMO, M. & MCCLESKEY, E.W. (1990). Two components of high-threshold Ca^{2+} current inactivate by different mechanisms. *Neuron*, **5**, 445–452.

SCOTT, R.H. & DOLPHIN, A.C. (1987). Inhibition of calcium currents by an adenosine analogue 2-chloroadenosine. In *Topics and Perspectives in Adenosine Research*. ed. Gerlach, E. & Becker, B.F., pp. 549–558. Berlin: Springer-Verlag.

SHER, E. & CLEMENTI, F. (1991). ω-conotoxin-sensitive voltage-operated calcium channels in vertebrate cells. *Neurosci.*, **42**, 301–307.

SLESINGER, P.A. & LANSMAN, J.B. (1991). Inactivating and non-inactivating dihydropyridine-sensitive calcium channels in mouse cerebellar granule cells. *J. Physiol.*, **439**, 301–323.

STANLEY, E.F. (1989). Calcium currents in a vertebrate presynaptic nerve terminal: the chick ciliary ganglion calyx. *Brain Res.*, **505**, 341–345.

STANLEY, E.F. & ATRAKCHI, A.H. (1990). Calcium currents recorded from a vertebrate presynaptic nerve terminal are resistant to the dihydropyridine nifedifine. *Proc. Natl. Acad. Sci. U.S.A.*, **87**, 9683–9687.

STANLEY, E.F. & GOPING, G. (1991). Characterization of a calcium current in a vertebrate cholinergic presynaptic nerve terminal. *J. Neurosci.*, **11**, 985–993.

SWANDULLA, D., CARBONE, E. & LUX, H.D. (1991). Do calcium channel classifications account for neuronal calcium channel diversity? *Trends Neurosci.*, **14**, 46–51.

TSIEN, R.W., HESS, P., MCCLOSKEY, E.W. & ROSENBERG, R.L. (1987). Calcium channels: mechanisms of selectivity, permeation and block. *Annu. Rev. Biophys. Biophys. Chem.*, **6**, 265–290.

TSIEN, R.W., LIPSCOMBE, D., MADISON, D.V., BLEY, K.R. & FOX, A.P. (1988). Multiple types of neuronal calcium channels and their selective modulation. *Trends Neurosci.*, **11**, 431–437.

YAWO, H. (1990). Voltage-activated calcium currents in presynaptic nerve terminals of the chicken ciliary ganglion. *J. Physiol.*, **428**, 199–213.

(Received December 9, 1991
Accepted January 7, 1992)

Br. J. Pharmacol. (1992), **106**, 33–38 © Macmillan Press Ltd, 1992

Modulation by peripheral opioids of basal and distension-stimulated gastric acid secretion in the rat

[1]J.V. Esplugues, M[a].D. Barrachina & J. Esplugues

Departamento de Farmacología, Facultad de Medicina, Universidad de Valencia, 46010 Valencia, Spain.

1 The influence of opioids in modulating gastric acid secretory responses has been investigated in the continuously perfused stomach of the anaesthetized rat.

2 Intravenous administration of morphine (0.75–3 mg kg^{-1}) or the peripherally acting enkephalin analogue, BW443C (0.75–3 mg kg^{-1}), substantially augmented acid secretion in basal conditions. These effects were significantly inhibited by the opioid antagonists naloxone (1 mg kg^{-1}) and the peripherally acting N-methylnalorphine (2 mg kg^{-1}). When administered alone, neither opioid antagonist influenced basal acid output.

3 Acid secretory responses to different levels of gastric distension (5–20 cmH_2O) were significantly and dose-dependently reduced in rats pretreated with morphine (3 mg kg^{-1}) or BW443C (1.5 mg kg^{-1}). Previous administration of either naloxone or N-methyl nalorphine reversed the inhibitory effects of opioids on gastric acid secretion stimulated by distension. Likewise, blockade of opioid receptors with naloxone or N-methylnalorphine significantly increased acid output induced by distension.

4 Levels of serum gastrin in control animals were not increased after intragastric distension (20 cmH_2O). Pretreatment with BW443C (1.5 mg kg^{-1}) did not modify the levels of gastrin present during basal or distension stimulated conditions.

5 Pretreatment with morphine or BW443C did not influence the acid responses to i.v. injection of pentagastrin (100 μg kg^{-1}), histamine (5 mg kg^{-1}) or carbachol (4 μg kg^{-1}). Acid secretion induced by i.v. administration of 2-deoxy-D-glucose (150 mg kg^{-1}) was reduced in rats pretreated with morphine but not with BW443C. Gastric secretory responses to insulin (0.3 i.u. kg^{-1}) were not modified by i.v. morphine.

6 These observations support a role for peripherally acting opioids in the regulation of gastric acid secretion during basal and distension-stimulated conditions.

Keywords: Gastric acid; gastric distension; pentagastrin; histamine; carbachol; insulin; 2-deoxy-D-glucose; morphine; peripheral opioids; capsaicin; sensory neurones.

Introduction

Distension of the stomach wall is one of the main stimulants of H^+ production during the gastric phase of acid secretion (Debas, 1987). Although the processes involved in this secretory response are not fully clarified, two types of mechanisms have been proposed. Gastric distension is generally coupled with changes in the release of peptides, such as gastrin and somatostatin (Walsh, 1988) with profound influences on acid production. Furthermore, recent studies (Esplugues *et al.*, 1990; Raybould & Taché, 1989) have confirmed earlier evidence (Debas, 1987) that distension of the gastric wall activates a nervous reflex of acid secretion, in which both efferent and afferent fibres take part.

Opioids have been shown to modulate a great number of gastrointestinal functions in both physiological and pathophysiological circumstances. In the rat stomach, endogenous opioids play an important role in the control of motility (Kromer, 1988), blood flow (Piqué *et al.*, 1990) and the ability of the mucosa to withstand challenge (Esplugues *et al.*, 1989; Esplugues & Whittle, 1990). However, their role in the control of gastric acid secretion is still controversial (Kromer, 1988). Opioids have been shown to influence nervous functions affecting the gastric mucosa and the release of peptides (Walsh, 1988), including gastrin (Nishi *et al.*, 1987), and it is therefore feasible that they could modulate acid responses to distension. To evaluate this possibility the effects of low doses of morphine, and the peripherally acting enkephalin analogue, BW443C (Adcock *et al.*, 1988; Follenfant *et al.*, 1988) have been investigated and characterized by use of opioid antagonists in a model of distension-stimulated acid secretion in the anaesthetized rat. To confirm the specificity and the central or peripheral location of such effects, the actions of opioids have also been analyzed on the production of acid induced by direct stimuli of the oxyntic cell (pentagastrin, histamine and carbachol) or through stimulation of the CNS (insulin or 2-deoxy-D-glucose).

[1]Author for correspondence at: Departamento de Farmacología, Facultad de Medicina, Avd. Blasco Ibañez 15, 46010 Valencia, Spain.

Methods

General

Wistar rats of either sex, weighing 200–250 g, were fasted for 24 h before the experiments but received drinking water *ad libitum*. The procedure used for the measurement of gastric acid secretion was that described by Ghosh & Schild (1958). In brief, animals were anaesthetized with urethane (1.5 g kg^{-1}, i.p.) and the trachea intubated. A soft catheter was inserted into the stomach through an incision in the cervical oesophagus and held in place by a ligature. After a laparotomy, a second polyethylene cannula was inserted into the stomach via an incision in the duodenum, held in place by two ligatures, and led outside the abdominal wall. The jugular vein was cannulated for administration of saline or drugs. At the beginning of the experiment, the stomach was flushed with 50–100 ml of saline to remove any solid content. Once the surgical preparation had been completed, a period of 1 h was allowed for stabilization. Thereafter, the

stomach lumen was perfused continuously (0.9 ml min^{-1}) via the oesophageal catheter with saline at room temperature. The gastric effluent was collected every 30 min and H^+ output determined by automatic titration (Radiometer Copenhagen, Denmark) of aliquots (4 ml) of the perfusate to pH 7 with 0.01 N NaOH. In some experiments mean systemic arterial blood pressure (BP) was measured from a cannula in a carotid artery connected to a pressure transducer (Hewlett Packard HP-1280).

Once the gastric acid output had remained constant for 60 min it was considered as basal acid secretion. Thereafter, morphine (0.75–3 mg kg^{-1}), the peripheral opioid agonist BW443C (0.75–3 mg kg^{-1}) or saline were administered i.v. and acid output recorded for a further period of 30 min before stimulating acid secretion. To investigate the effects of opioid antagonists, rats were pretreated (i.v.) 10 min before morphine or BW443C with naloxone (1 mg kg^{-1}) or N-methylnalorphine (2 mg kg^{-1}). Various types of experiments were performed according to the stimulus of gastric acid secretion. In the first series of studies, gastric distension was used to promote acid output. Distension of the stomach was obtained by placing the tip of the antroduodenal cannula 5, 10 or 20 cm above the perfused stomach, where it was maintained for the remainder of the experimental period. To evaluate the possible influence of opioids on gastrin levels, in some animals blood samples were obtained from the carotid artery during the basal period and 120 min after starting the intragastric distension (20 cmH_20), an interval of time at which maximal levels of acid secretion were registered. Gastrin concentrations in serum were measured by radioimmunoassay (CIS biointernational, detection limit 10 pg ml^{-1}) and results expressed as fmol ml^{-1}.

In a second series of experiments gastric acid secretion was stimulated, 30 min after administration of opioids, by a bolus injection (i.v.) of histamine (5 mg kg^{-1}), pentagastrin (100 μg kg^{-1}), carbachol (4 μg kg^{-1}), insulin (0.3 iu kg^{-1}) or 2-deoxy-D-glucose (2DG, 150 mg kg^{-1}). To analyze the possibility that some differential effects attributed to opioids could be consequence of discrepancies in the time elapsed from the time of their administration till the maximal secretory response had been elicited by the various stimulants of acid production, in one experiment morphine (3 mg kg^{-1}, i.v.) was injected 120 min before pentagastrin (100 μg kg^{-1}).

In all cases each preparation was used for a single response only, with treatment being allocated randomly between preparations. Values of acid production during stimulation were obtained in each animal as the difference between the absolute production of acid after stimulation of H^+ and the basal levels of acid secretion in an equivalent period of time and expressed as μEq H^+ 100 g^{-1} 30/60/180 min^{-1}.

Drugs

Histamine, carbachol, 2-deoxy-D-glucose and naloxone were purchased from Sigma Chemical Co. Morphine hydrochloride (Palex), pentagastrin (Peptavlon, ICI), and insulin (Humulina NPH, Lilly) were obtained as clinically available preparations. BW443C (H-Tyr-D-Arg-Gly-Phe[4-NO_2]-Pro-NH_2) and N-methylnalorphine were a gift from Dr S. Moncada and Dr B.J.R. Whittle (Wellcome Research Laboratories). All drugs were dissolved in saline immediately before use and administered in a volume of 2 ml kg^{-1}.

Statistical analysis

All data are expressed as mean ± s.e.mean. Comparisons between groups were made by Student's *t* test for unpaired data, and *P* values of 0.05 or less were taken as significant.

Results

Effects of opioids on basal acid secretion

As shown in Table 1, the i.v. administration of saline (2 ml kg^{-1}) did not modify the level of acid production in nonstimulated conditions. However, the basal level of gastric secretion was dose-dependently augmented by 38%, 50% ($P<0.001$) and 95% ($P<0.01$) following i.v. administration of 0.75, 1.5 and 3 mg kg^{-1} of morphine, respectively. Administration of the peripherally acting opioid agonist, BW443C likewise dose-dependently enhanced the output of acid in basal conditions by 147% ($P<0.01$), 255% ($P<0.001$) and 203% ($P<0.001$) after 0.75, 1.5 and 3 mg kg^{-1}, i.v., respectively. Pretreatment (i.v.) with either the opioid antagonist naloxone (1 mg kg^{-1}), which acts on both central and peripheral opioid receptors, or N-methylnalorphine (2 mg kg^{-1}), a peripherally acting quaternary opioid receptor antagonist (Smith *et al.*, 1982), prevented the increased production of acid induced by both morphine (3 mg kg^{-1}) and BW443C (3 mg kg^{-1}). However if administered alone neither naloxone nor N-methylnalorphine produced any significant change in the rate of basal acid production.

Inhibition by opioids of acid responses to gastric distension

Distension of the rat stomach *in vivo* produced a progressive increase in acid secretion, which peaked 120–150 min after application of an intragastric pressure of 20 cmH_2O with a H^+ production of 8.8 ± 1.5 μEq 100 g^{-1} 30 min^{-1}. The total

Table 1 Effects of the i.v. administration of opioid agonists (morphine and BW443C) and antagonists (naloxone and N-methylnalorphine) on resting levels of acid secretion (μEq H^+100 g^{-1} 30 min^{-1}) in the perfused stomach of the anaesthetized rat

Treatment (mg kg^{-1})	n	*Resting*	*Treated*	Δ
Saline	74	3.0 ± 0.8	2.5 ± 0.3	0.1 ± 0.2
Morphine				
(0.75)	5	2.4 ± 0.8	3.3 ± 1.0	0.9 ± 0.5
(1.5)	7	4.6 ± 0.9	6.9 ± 1.1	2.6 ± 1.0***
(3)	45	1.9 ± 0.4	3.7 ± 0.6	2.0 ± 0.6**
(3) + Naloxone (1)	5	1.6 ± 0.7	1.3 ± 0.5	0.3 ± 0.8
(3) + N-Me Nalorph (2)	5	0.1 ± 0.1	0.1 ± 0.1	0.0 ± 0.0
BW433C				
(0.75)	4	1.7 ± 0.2	4.2 ± 0.9	2.5 ± 0.8**
(1.5)	32	1.1 ± 0.4	3.9 ± 0.8	2.8 ± 0.7***
(3)	3	3.3 ± 1.6	10 ± 1.7	6.8 ± 3.3***
(3) + Naloxone (1)	6	3.0 ± 1.5	3.3 ± 1.4	0.3 ± 0.3
(3) + N-Me Nalorph (2)	3	0.1 ± 0.1	0.8 ± 0.5	0.8 ± 0.5
Naloxone (1)	3	2.7 ± 0.5	2.8 ± 0.3	0.1 ± 0.1
N-Me Nalorph (2)	3	3.0 ± 0.5	3.3 ± 0.6	0.3 ± 0.5

Values are means ± s.e.; *n*, number of experiments. Abbreviations: N-Me Nalorph = N-methylnalorphine. Statistical difference from the saline control group is shown by $^{**}P<0.01$ and $^{***}P<0.001$.

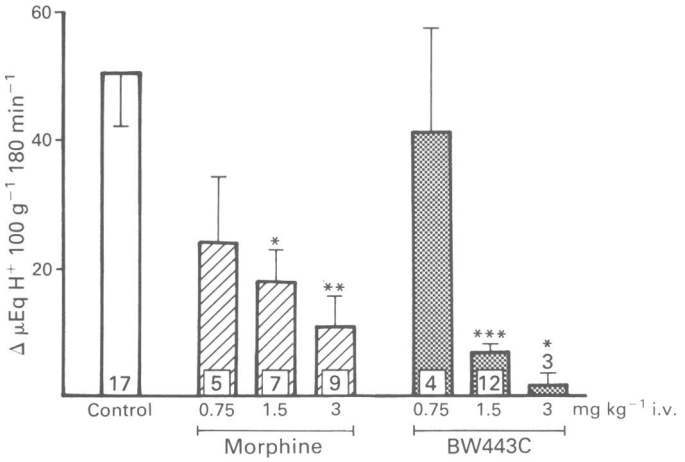

Figure 1 Inhibition by morphine and the peripheral opioid agonist BW443C (0.75–3 mg kg^{-1}, i.v.) of acid secretion induced by gastric distension with 20 cmH_2O. Results, expressed as the difference between basal and stimulated H^+ output, are means (columns) ± s.e. mean (vertical bar), and the level of statistical difference from the control group is shown by $*P<0.05$, $**P<0.01$ and $***P<0.001$. Numbers inside the columns represent the animals used per experimental group.

acid output during these experiments was 50.3 ± 8.3 μEq 100 g^{-1} 180 min^{-1} ($n = 17$). Intravenous pretreatment (30 min) with 0.75, 1.5 and 3 mg kg^{-1} of morphine (Figure 1) dose-dependently decreases the acid response to 20 cmH_2O distension by 52 ± 21% ($n = 5$), 65 ± 10% ($P<0.05$, $n = 7$) and 78 ± 8% ($P<0.01$, $n = 9$) respectively. Likewise, H^+ output caused by gastric distension (20 cmH_2O) was reduced by 18 ± 33% ($n = 4$), 87 ± 3% ($P<0.001$, $n = 12$) and 96 ± 4% ($P<0.05$, $n = 3$) following the i.v. injection of BW443C at the doses of 0.75, 1.5 and 3 mg kg^{-1} respectively. As shown in Figure 2, pretreatment with morphine (3 mg kg^{-1}) or BW443C (1.5 mg kg^{-1}) significantly ($P<0.05$) decreased gastric acid responses induced by intragastric distension with 5 cmH_2O by 84 ± 15% ($n = 6$) and 85 ± 10% ($n = 7$) and those produced by an intragastric pressure of 10 cmH_2O by 65 ± 13% ($n = 7$) and 56 ± 13% ($n = 9$) respectively. In control animals, basal plasma levels of gastrin (22.7 ± 2.4 fmol ml^{-1}, $n = 16$) were not significantly modified after 120 min of intragastric distension with 20 cmH_2O (24 ± 3.4 fmol ml^{-1}). Likewise, they were not significantly different from those of rats undergoing similar experimental conditions and pretreated with 1.5 mg kg^{-1} of BW443C, respectively 20.1 ± 0.9 and 19.8 ± 0.7 fmol ml^{-1} ($n = 8$). Administration of morphine (3 mg kg^{-1}) or BW443C (1.5 mg kg^{-1} each) did not significantly modify BP ($n = 4$ in both) which remained between 100–120 mmHg during the duration of the experiments.

In further experiments shown in Figure 3, the inhibitory effects of morphine (3 mg kg^{-1}) and BW443C (1.5 mg kg^{-1}) on the acid response to 20 cmH_2O distension were prevented by 5 min i.v. pretreatment with the opioid receptor antagonist naloxone (1 mg kg^{-1}) or the peripherally acting opioid antagonist N-methylnalorphine (2 mg kg^{-1}). Furthermore, administration of naloxone (1 mg kg^{-1}, $n = 7$) or N-methylnalorphine (2 mg kg^{-1}, $n = 6$) alone significantly increased the acid output stimulated by 20 cmH_2O gastric distension by 73 ± 18% and 64 ± 15% respectively.

Effects of opioids on acid secretion stimulated by other secretagogues

The i.v. injection of histamine (5 mg kg^{-1}), pentagastrin (100 μg kg^{-1}) or carbachol (4 μg kg^{-1}) induced rapid increases in acid output by the stomach which peaked 40 min later. Pretreatment with morphine (3 mg kg^{-1}) 30 min before did not modify the secretory responses elicited by these three agents (Figure 4). The values of total acid output in control and morphine-treated rats were, respectively, 48.7 ± 7.1 ($n = 7$) and 46.8 ± 5.5 ($n = 3$) μEq H^+ 100 g^{-1} 60 min^{-1} for histamine, 22.8 ± 2.7 ($n = 7$) and 18.3 ± 3.2 ($n = 3$) μEq H^+ 100 g^{-1} 60 min^{-1} for pentagastrin, or 72.9 ± 6.7 ($n = 11$) and 64.1 ± 10.1 ($n = 4$) μEq H^+ 100 g^{-1} 60 min^{-1} for carbachol. The administration of morphine (3 mg kg^{-1}) 120 min before pentagastrin (100 μg^{-1}, i.v.) induced a rapid and sustained increase in basal acid output, with values comparable to those of Table 1, without modifying the secretory response elicited by pentagastrin (20.7 ± 2.8 μEq H^+ 100 g^{-1} 60 min^{-1}, $n = 4$) which was similar to that of control animals (17 ± 3.5 μEq H^+ 100 g^{-1} 60 min^{-1}, $n = 4$).

Administration (i.v.) of 2-deoxy-D-glucose ($n = 8$) or insulin ($n = 8$) induced a progressive increase in acid secretion, which peaked 140 min later with a H^+ production of

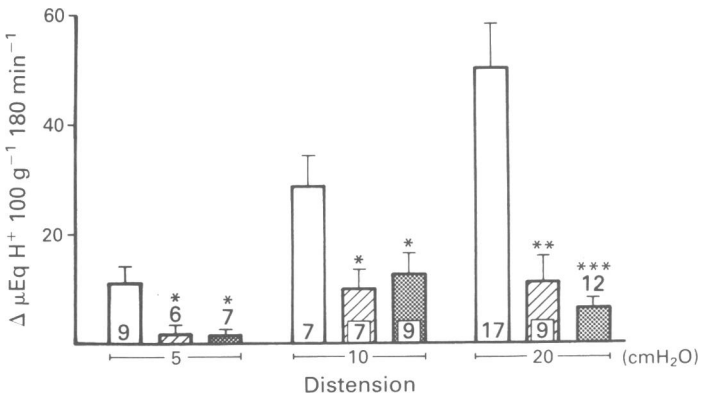

Figure 2 Inhibition by morphine (3 mg kg^{-1}, i.v., hatched column) and the peripheral opioid agonist BW443C (1.5 mg kg^{-1}, i.v., stippled column) of acid secretion induced by various levels of gastric distension (5, 10 and 20 cmH_2O). Results, expressed as the difference between basal and stimulated H^+ output, are means (columns) ± s.e.mean (vertical bars), and the level of statistical difference from the corresponding control group is shown by $*P<0.05$, $**P<0.01$ and $***P<0.001$. Numbers inside the columns represent the animals used per experimental group.

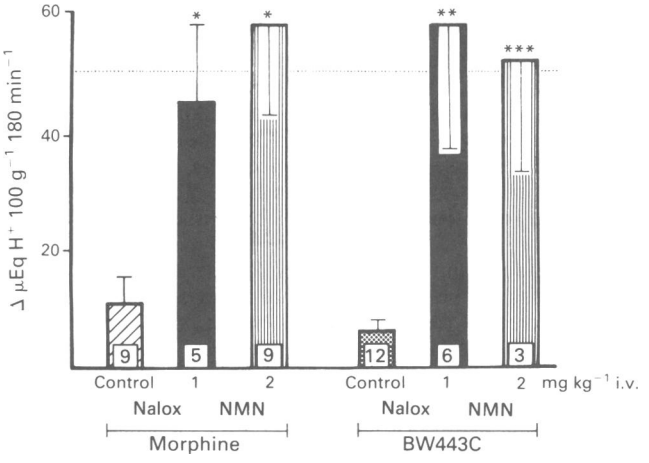

Figure 3 Effects of pretreatment with the opioid antagonists naloxone (1 mg kg^{-1}, i.v.) and the peripherally acting antagonist N-methylnalorphine (NMN, 2 mg kg^{-1}, i.v.) on the inhibition by morphine (3 mg kg^{-1}, i.v.) and BW443C (1.5 mg kg^{-1}, i.v.) of acid secretion induced by gastric distension (20 cmH_2O). Results, expressed as the difference between basal and stimulated H^+ output, are means (columns) ± s.e.mean (vertical bars), and the level of statistical difference from the group treated with morphine or BW443C is shown by $*P<0.05$, $**P<0.01$, $***P<0.001$. The dotted line represents the level of acid output in control rats. Numbers inside the columns represent the animals used per experimental group.

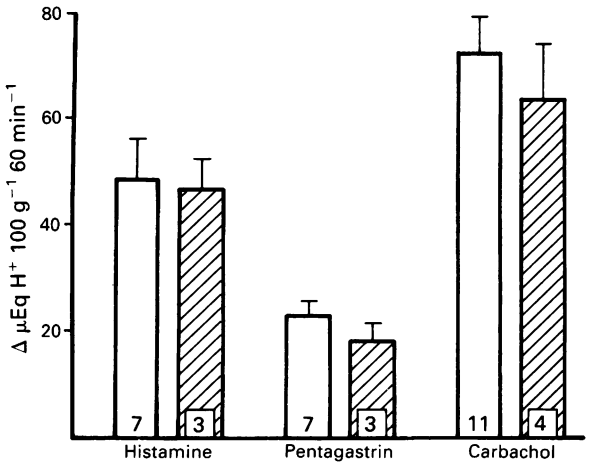

Figure 4 Acid production induced by a i.v. bolus injection of histamine (5 mg kg^{-1}), pentagastrin (100 μg kg^{-1}) or carbachol (4 μg kg^{-1}) in the continuously perfused stomach of rats control (open columns) and pretreated with morphine (3 mg kg^{-1}, i.v., hat ched columns). Results, expressed as the difference between basal and stimulated H^+ output, are means (columns) ± s.e. (vertical bars). Numbers inside the columns represent animals used per experimental group.

23 ± 8 and 36 ± 9 μEq 100 g^{-1} 30 min^{-1} and a total acid output 110 ± 35 and 137 ± 31 μEq 100 g^{-1} 180 min^{-1}, respectively ($n = 8$ in both) (Figure 5). Acid responses to 2-deoxy-D-glucose were significantly ($P<0.05$) reduced by 85.6 ± 8.2% in animals pretreated with morphine (3 mg kg^{-1}, $n = 6$) but not after administration of BW443C (1.5 mg kg^{-1}). Pretreatment with morphine (3 mg kg^{-1}) did not modify acid responses to insulin (0.3 iu kg^{-1}).

Discussion

Our results have shown that opioids can modulate the acid secretory responses stimulated by gastric distension in the rat. Thus, i.v. administration of morphine induced a significant and dose-dependent reduction in acid production following different levels of gastric distension. This effect appears to be exerted at peripherally-located opioid receptors because BW443C, a polar enkephalin analogue which does not cross the blood brain barrier (Adcock *et al.*, 1988; Follenfant *et al.*, 1988) likewise substantially inhibited acid responses to distension of the stomach. An inhibitory, non-specific action by opioids on acid secretion has been ruled out, since response to stimulation of the oxyntic cell with pentagastrin, histamine or the synthetic muscarinic agonist, carbachol, were not influenced by either morphine or BW443C.

Intravenous administration of the opiate antagonist, naloxone, abolished the actions of morphine and BW443C on gastric secretory responses to distension, thus implying an interaction with classical opiate receptors. The peripherally acting quaternary antagonist, N-methylnalorphine (Smith *et al.*, 1982) likewise reversed the inhibitory effects of both opioid agonists on gastric acid secretion induced by distension, giving further support to a peripheral site of action of opioids in this model. The finding that naloxone and N-methylnalorphine by themselves significantly increased acid responses to distension points to a physiological regulatory role for peripherally-acting endogenous opioids in responses to this stimulant of acid secretion. Although the opioid receptors involved have not been fully characterized, the low doses employed in the present study and the specificity of morphine, BW443C, naloxone and N-methyl nalorphine implicate μ receptors in this mechanism.

Insulin administration decreases the level of glucose in blood which, once identified by the brain, leads to a vagally-mediated increase in acid output. The actions of 2DG on gastric acid production have been classically compared with those of insulin, since this analogue of glucose cannot be metabolized and causes the release of endogenous insulin by the pancreas (Debas, 1987). However, the effects of 2DG are more complex and a direct action on various hypothalamic, diencephalic and medullary sites in the CNS, as well as hepatic sites in the periphery have also been described (Debas, 1987). In the rat, Watanabe *et al.* (1987) and Ho *et al.* (1987) have previously shown that intravenous infusion of morphine decreased acid production stimulated by 2DG, but not that evoked by electrical stimulation of the vagus. Our results with a bolus injection of morphine confirm its inhibitory effect on secretory responses induced by this glucose analogue. However, acid responses by insulin were not influenced suggesting that effects of 2DG on gastric acid output are the consequence of actions other than insulin release. Furthermore, the fact that BW443C did not influence responses to 2DG, at doses that abolished responses to gastric distension, implies that both activation of acid output by 2DG and the inhibitory effects of morphine on this model are CNS-mediated events.

When other procedures have been used to stimulate gastric secretion in the rat, administration of morphine and related compounds have reproduced the actions shown here, i.e. either lacked any effect or decreased acid responses. Thus, in the rat isolated stomach, submaximal acid stimulation with pentagastrin, histamine, bethanechol or isoprenaline was not modified by high concentrations of morphine (Canfield & Spencer, 1981). Furthermore, i.v. or i.c.v. pretreatment with morphine *in vivo* reduced responses to pyloric occlusion (Glavin *et al.*, 1986; Ho *et al.*, 1986; Fox & Burks, 1988), TRH administration (Morley *et al.*, 1981) or electrical vagal stimulation (Rozé *et al.*, 1982). In contrast, in the present study administration of morphine in basal, non-stimulated conditions brought about a significant increase in acid secretion which was reversed by concomitant administration of naloxone. Such stimulatory effect has been previously described in the dog (Kromer, 1988), and in our experiments it seems the result of activation of opioid receptors located in

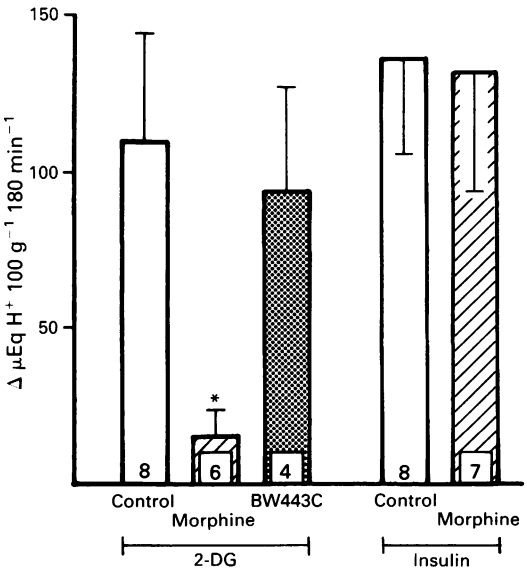

Figure 5 Acid production induced by a i.v. bolus injection of 2-deoxy-D-glucose (2-DG 150 mg kg^{-1}) and insulin (0.3 iu kg^{-1}) in the continuously perfused stomach of rats control and pretreated with morphine (3 mg kg^{-1}, i.v.) or the peripheral opioid agonist BW443C (1.5 mg kg^{-1}, i.v.). Results, expressed as the difference between basal and stimulated H^+ output, are means (columns) ± s.e.mean (vertical bars), and the level of statistical difference from the respective control group is shown by $*P<0.05$. Numbers inside the columns represent the animals used per experimental group.

the periphery since administration of BW443C enhanced basal acid secretion, whereas N-methylnalorphine reversed the effects of both morphine and BW443C. The failure of opioid antagonist naloxone by itself to affect the level of the basal acid secretion suggests that endogenous opioids do not modulate this process. However, the present observations also imply that the release of high levels of enkephalins, possibly during different stress situations, may lead to increased levels of resting acid secretion in the fasting stomach, a circumstance that could partially account for changes in the susceptibility of the gastric mucosa to damage appearing in such conditions.

The mechanisms responsible for the changes in the rate of acid production brought about by the administration of opioids have not been fully evaluated in the present study and only an hypothesis can be suggested. In the anaesthetized rat, systemic ablation of sensory nerves after pretreatment with the neurotoxin capsaicin (Holzer, 1988) induces effects similar to those of morphine on stimulated acid secretion. Thus responses to gastric distension (Raybould & Taché, 1989; Esplugues *et al.*, 1990), 2DG (Evangelista *et al.*, 1989) and TRH (Raybould *et al.*, 1990) were reduced, whereas those to insulin, pentagastrin, histamine, carbachol (Esplugues *et al.*, 1990) or vagal electrical stimulation (Evangelista *et al.*, 1990) were not influenced by this treatment. The comparability of the effects of morphine to those of capsaicin pretreatment suggest a common mechanism of action. Opioid receptors have been located on sensory fibres, both in the periphery and the CNS, where they modulate the release of various neuropeptides including substance P and calcitonin gene-related peptide (Russell *et al.*, 1987; Holzer, 1988). In the stomach the inhibitory effects of opioids on this population of neurones has been suggested as one of the factors implicated in the regulation of blood flow and mucosal defense (Esplugues & Whittle, 1990; Pique *et al.*, 1990; Holzer *et al.*, 1991). Thus there is good circumstantial evidence to suggest that opioids may inhibit distension- or 2DG-stimulated acid secretion by actions on sensory neurones. This explanation would not cover their stimulatory effect on basal output, since this is not affected by pretreatment with capsaicin (Esplugues *et al.*, 1990), and implies the existence of other mechanisms. Opioids influence the release in the gastric tissue of neurohormonal mediators of acid secretion such as gastrin (Nishi *et al.*, 1987). However, the finding that BW443C did not modify gastrin levels rules out the possibility that this action could be responsible for the changes induced by opioids on basal acid secretion. Furthermore, gastrin levels were not modified after 120 min of gastric distension confirming the previous suggestion (Debas, 1987) that this peptide plays a limited role in the secretory response induced by this stimulant of acid production. The effect of opioids on the release of other modulators of acid secretion like somatostatin (Chiba *et al.*, 1980), acetylcholine (Kromer, 1988) or histamine (Garrison, 1990) has also been shown and new studies will be necessary for analyzing the possible involvement of such actions in this model of acid secretion. In conclusion, administration of opioids seems to induce a complex picture of superimposed stimulatory and inhibitory actions, affecting both the CNS and the periphery, the overall outcome of which would be manifested as increases or decreases in acid production depending on the stimuli of acid secretion and, possibly, the different mediators involved.

The authors would like to thank Mrs Amparo Canet for her technical help and Mrs Dora Martí for valuable assistance in the preparation of the figures. The present study has been supported by a grant from 'Programa Nacional de Investigación y Desarrollo Farmaceutico' (FAR No 89-0432). M^a.D.B. is the recipient of the 'Schering-Plough' fellowship for Gastrointestinal Research.

References

ADCOCK, J.J., SCHNEIDER, C. & SMITH, T.W. (1988). Effects of codeine, morphine a novel opioid pentapeptide BW443C, on cough, nociception and ventilation in the unanaesthetized guinea-pig. *Br. J. Pharmacol.*, **93**, 93–100.

CANFIELD, S.P. & SPENCER, J. (1981). The actions of morphine and naloxone on acid secretion by the rat isolated stomach. *Eur. J. Pharmacol.*, **71**, 135–138.

CHIBA, T., TAMINATO, T., KADOWAKI, S., INOUE, Y., MORI, K., SEINO, Y., ABE, H., CHIHARA, K., MATSUKURA, S., FUJITA, T. & GOTO, Y. (1980). Effects of various gastrointestinal peptides on gastric somatostatin release. *Endocrinology*, **106**, 145–149.

DEBAS, H.T. (1987). Peripheral regulation of gastric acid secretion. In *Physiology of the Gastrointestinal Tract*, 2nd Ed, ed. Jonhson, L.R. pp. 931–945. New York: Raven Press.

ESPLUGUES, J.V., RAMOS, E.G., GIL, L. & ESPLUGUES, J. (1990). Influence of capsaicin-sensitive afferent neurones on the secretory responses of the rat stomach *in vivo*. *Br. J. Pharmacol.*, **100**, 491–496.

ESPLUGUES, J.V., WHITTLE, B.J.R. & MONCADA, S. (1989). Local opioid-sensitive afferent sensory neurones in the modulation of gastric damage induced by Paf. *Br. J. Pharmacol.*, **97**, 579–85.

ESPLUGUES, J.V. & WHITTLE, B.J.R. (1990). Morphine potentiation of ethanol-induced gastric mucosal damage in the rat: Role of local sensory afferent neurons. *Gastroenterology*, **98**, 82–89.

EVANGELISTA, S., SANTICIOLI, P., MAGGI, C.A. & MELI, A. (1989). Increase in gastric acid secretion induced by 2-deoxy-D-glucose is impaired in capsaicin pretreated rats. *Br. J. Pharmacol.*, **98**, 35–37.

FOLLENFANT, R.L., HARDY, G.W., LOWE, L.A., SCHNEIDER, C. & SMITH, T.W. (1988). Antinociceptive effects of the opioid peptide BW443C compared with classical opiates; peripheral versus central actions. *Br. J. Pharmacol.*, **93**, 85–92.

FOX, D.A. & BURKS, T.F. (1988). Roles of central and peripheral Mu, Delta and Kappa opioid receptors in the mediation of gastric acid secretory effects in the rat. *J. Pharmacol. Exp. Ther.*, **244**, 456–462.

GARRISON, J.C. (1990). Histamine, bradykinin, 5-hydroxytryptamine, and their antagonists. In *Goodman and Gilman's The Pharmacological Basis of Therapeutics*, 8th Ed. ed. Goodman Gilman, A.F., Rall, T.W., Nies, A.S. & Taylor, P., pp. 575–599. New York: Pergamon Press.

GHOSH, M.N. & SCHILD, H.O. (1958). Continuous recording of acid gastric secretion in the rat. *Br. J. Pharmacol. Chemother.*, **13**, 54–61.

GLAVIN, G.B., KIERNAN, K., HNATOWICH, M.R. & LABELLA, F.S. (1986). Effects of morphine and naloxone on stress ulcer formation and gastric acid secretion. *Eur. J. Pharmacol.*, **124**, 121–127.

HO, M.M., DAI, S. & OGLE, C.W. (1987). Morphine reduces vagal-stimulated gastric acid secretion through a central action. *Eur. J. Pharmacol.*, **139**, 251–257.

HO, M.M., OGLE, C.W. & DAI, S. (1986). Effects of morphine, hypoxaemia and hypercapnia on the rat stomach. *Eur. J. Pharmacol.*, **126**, 103–109.

HOLZER, P. (1988). Local effector functions of capsaicin-sensitive sensory nerve endings: involvement of tachykinins, calcitonin gene-related peptide and other neuropeptides. *Neuroscience*, **24**, 739–768.

HOLZER, P., LIVINGSTON, E.H. & GUTH, P.H. (1991). Sensory neurons signal for an increase in rat gastric mucosal blood flow in the face of pending acid injury. *Gastroenterology*, **101**, 416–423.

KROMER, W. (1988). Endogenous and exogenous opioids in the control of gastrointestinal motility and secretion. *Pharmacol. Rev.*, **40**, 121–162.

MORLEY, J., LEVINE, A. & SILVIS, S. (1981). Endogenous opiates inhibit gastric acid secretion induced by central administration of thyrotropin-releasing hormone (TRH). *Life Sci.*, **29**, 293–297.

NISHI, S., SEINO, Y., KITANO, N., SENO, M., TSUJI, K., KUROSE, T., TAMINATO, T., TSUDA, K., YANAIHARA, C., YANAIHARA, N. & IMURA, H. (1987). Effects of naloxone on basal and vagus nerve-induced secretions of GRP, gastrin and somatostatin from the isolated perfused rat stomach. *Life Sci.*, **41**, 1787–1793.

PIQUE, J.M., ESPLUGUES, J.V. & WHITTLE, B.J.R. (1990). Influence of morphine or capsaicin pretreatment on rat gastric microcirculatory response to PAF. *Am. J. Physiol.*, **258,** G352–G357.

RAYBOULD, H.E. & TACHÉ, Y. (1989). Capsaicin-sensitive vagal afferent fibres and stimulation of gastric acid secretion in anaesthetized rats. *Eur. J. Pharmacol.*, **167,** 237–243.

RAYBOULD, H.E., HOLZER, P., REDDY, N., YANG, H. & TACHÉ, Y. (1990). Capsaicin-sensitive vagal afferents contribute to gastric acid and vascular responses to intracisternal TRH. *Peptides*, **11,** 789–795.

ROZÉ, C., DUBRASQUET, M., CHARIOT, J. & VAILLE, C. (1982). Methadone inhibition of vagally induced pancreatic and gastric secretions in rats: central and peripheral sites of action. *Eur. J. Pharmacol.*, **78,** 271–278.

RUSSELL, N.J.W., SCHAIBLE, H-G. & SCHMIDT, R.F. (1987). Opiates inhibit the discharges of fine afferent units from inflamed knee joint of the cat. *Neurosci. Lett.*, **76,** 107–112.

SMITH, T.W., BUCHAN, P., PARSONS, D.N. & WILKINSON, S. (1982). Peripheral antinociceptive effects of N-methylmorphine. *Life Sci.*, **31,** 1205–1208.

WALSH, J.H. (1988). Peptides as regulators of gastric acid secretion. *Annu. Rev. Physiol.*, **50,** 41–63.

WATANABE, K., YANO, S. & MINIKAWA, Y. (1987). Morphine inhibits the gastric acid secretion stimulated by 2-deoxy-D-glucose via a central mechanism in the anesthetized rats. *Eur. J. Pharmacol.*, **143,** 293–298.

(Received September 30, 1991
Revised December 19, 1991
Accepted January 7, 1992)

Br. J. Pharmacol. (1992), **106**, 39–44 © Macmillan Press Ltd, 1992

Manifestations of acute opiate withdrawal contracture in rabbit jejunum after μ-, κ- and δ-receptor agonist exposure

Pacifico Valeri, Luigi A. Morrone & Luca Romanelli

Institute of Pharmacology and Pharmacognosy, University of Rome 'La Sapienza' 00185 Rome, Italy

1 Following a 5 min *in vitro* exposure to morphine (1.3×10^{-7} M), U-50,488H (2.5×10^{-8} M) and deltorphin (1.6×10^{-8}–6.5×10^{-9} M), the rabbit isolated jejunum exhibited a precipitated contracture after the addition of naloxone (2.75×10^{-7} M).

2 The precipitated responses to U-50,488H and deltorphin but not to morphine were reproducible in the same tissue.

3 The precipitated contractures were blocked completely by tetrodotoxin (3×10^{-7} M), partially by atropine (1.5×10^{-7} M) and not affected by hexamethonium (1.4×10^{-5} M).

4 Naloxone administration (2.75×10^{-7} M) before the agonist prevented the development of the adaptive response to morphine and U-50,488H but not to deltorphin.

5 The selective antagonists norbinaltorphimine (2.7×10^{-8}–2.7×10^{-9} M) and naltrindole (1.1×10^{-7} M) prevented the adaptive response development only to the respective agonists.

6 The opioid agonists partially inhibited the spontaneous activity of the tissue. This study has shown that independent activation of μ-, κ- and δ-opioid receptors can induce dependence in this isolated tissue. Rabbit jejunum is a suitable tissue for studying the acute effects of opioids on the adaptative processes determined by their administration.

Keywords: Opiate withdrawal; morphine; U-50,488H; rabbit jejunum; deltorphin

Introduction

The enteric nervous system has become one of the most investigated tissues in the field of neuroscience because it is easily accessible and has similarities to the central nervous system; this makes it a suitable model for the study of the cellular biology of neurones (Wood, 1987). The guinea-pig isolated ileum has been extensively and successfully used to study not only the acute effects of opioids, but also the long-term effects of tolerance and dependence. The responses obtained from this tissue share many features in common with those observed in the central nervous system (Kosterlitz & Waterfield, 1975; Schulz & Herz, 1976; Leslie *et al.*, 1980; Szerb, 1982).

The observation that a strong naloxone-induced contracture could be obtained not only from the ilea of morphine-treated animals but also from untreated animals after a brief *in vitro* exposure to opioids has led to significant advances in understanding the dependence phenomena (Lujan & Rodriguez, 1981; Collier *et al.*, 1981; Chahl, 1983; 1986; Valeri *et al.*, 1990a,b; Morrone *et al.*, 1990). In fact, these results indicate that the cellular mechanisms of dependence may be initiated very rapidly following occupation of receptors and that these mechanisms are operating within the myenteric plexus. The characteristics of dependence development and its precipitation with naloxone in the guinea-pig ileum are similar to those of acute dependence in experimental animals and man (Kosersky *et al.*, 1974; Eisenberg, 1982; Krystal & Redmond, 1983; Bickel *et al.*, 1988; Valeri *et al.*, 1989; 1990a).

Although separate populations of opioid receptors are present in many peripheral tissues of different animal species, only the guinea-pig ileum has been used as a suitable preparation for the study of the biochemical mechanisms involved in the development of dependence and its manifestation.

Attempts to obtain a naloxone-precipitated contracture in mouse vas deferens after exposure of the tissue to morphine have been unsuccessful (Gillan *et al.*, 1979; Vargas *et al.*, 1987), probably because of the low basal activity of this tissue as compared to that of guinea-pig ileum (Johnson & Fleming, 1989). In this context, the rabbit intestine might be particularly well-suited since its spontaneous activity is more pronounced than that of guinea-pig ileum and it contains enkephalins with neuromodulator functions (Oka, 1980; Huidobro-Toro & Yoshimura, 1983; Pairet & Ruckebusch, 1984). The marked spontaneous activity of the rabbit jejunum might reflect either that the neuronal circuits involved are different from those of guinea-pig ileum, or that the same circuits are involved but they interact in a different way in the two tissues. Little is known of the opioid system, the inhibitory action of which on intestinal motility is well known, in the rabbit jejunum. From our preliminary observations we presume this tissue to be particularly sensitive to opioids and to the characteristic homeostatic changes induced by these substances.

The aim of the present investigation was to study the characteristics of the response to naloxone of the rabbit jejunum after a brief *in vitro* exposure to μ-, κ- and δ-opioid receptor antagonists; the results are compared with those obtained in the guinea-pig ileum. This comparison may give information on the respective roles of the different receptor subtypes in the development and expression of dependence. A comparative study of rabbit jejunum and guinea-pig ileum might also provide information on a possible diversity in the organization of the opioid system in both tissues and the physiological role of this system.

Methods

New Zealand White male rabbits, weighing 2–2.5 kg, were killed by a blow on the neck and exsanguination. The abdomen was opened by midline incision and three or four segments of jejunum 3 cm long were removed from the same animal and placed in 10 ml tissue baths containing Tyrode solution of the following composition (mM): NaCl 137, KCl 2.7, $CaCl_2$ 1.8, $MgCl_2$ 1.05, NaH_2PO_4 0.4, $NaHCO_3$ 11.9 and

glucose 5, gassed with 95% O_2 and 5% CO_2 and maintained at 37°C. The tissues were connected to an isotonic transducer (Ugo Basile, Italy) counterbalanced by 1 g loading and allowed to equilibrate for 45 min; during this period regular spontaneous activity was recorded without washing.

Effects of naloxone after 5 min exposure to the opioid agonists

Morphine (1.3×10^{-7} M), U-50,488H (2.5×10^{-8} M) and deltorphin (1.6×10^{-8} M–6.5×10^{-9} M) were used as selective μ-, κ- and δ-opioid receptor agonists respectively. The effect of naloxone (2.75×10^{-7} M) was tested following a 5 min contact of the jejunum with one of the opioid receptor agonists. The same tissue was used for different tests after a resting period of 20–25 min following washing. In the experiments with morphine each segment was tested only once, after the preliminary observation that reproducible responses could not be obtained. All experiments were repeated on at least four separate jejunum preparations obtained from different rabbits.

The sensitivity of tissues to acetylcholine (ACh) (1×10^{-7} M) was tested before and after a 5 min contact with the opioid agonist.

Effects of atropine, hexamethonium, tetrodotoxin and opioid receptor antagonists on naloxone withdrawal responses

Hexamethonium (1.38×10^{-5} M), tetrodotoxin (3×10^{-7} M) and opioid antagonists were injected into the bath 5 min before one of the agonists and atropine (1.5×10^{-7} M) 1 min before naloxone.

Drugs

Morphine hydrochloride and naloxone hydrochloride were purchased from SIFAC (Milan, Italy), hexamethonium, atropine and tetrodotoxin from Sigma Chemical Co. (St. Louis, MO, U.S.A.), nor-binaltorphimine dihydrochloride from Research Biochemicals Inc (Natick, MA, U.S.A.), U-50,488H from Upjohn Co. (Kalamazoo, MICH, U.S.A.). Naltrindole (17-cyclopropylmethyl-6,7 dehydro-3, 14-dihydroxy-6,72,3-indolo-morphnan) and deltorphin ([D-Ala²] deltorphin I) were generous gifts from Prof. V. Erspamer.

Stock solutions were 1 mg ml^{-1} in deionized water and ethanol (1:1), from which further dilutions were prepared freshly before use.

Results

Withdrawal response after morphine

A typical tracing of jejunum contracture response to naloxone (2.75×10^{-7} M) administered after a 5 min exposure of the tissue to morphine (1.3×10^{-7} M) is shown in Figure 1. The first contact with morphine slightly inhibited the rabbit jejunum pendular movements; subsequent administration of naloxone increased the tone by about 20–30% of the normal tissue spontaneous activity. However, after washout, followed by a 25 min interval and a further 5 min exposure to morphine, naloxone did not elicit a response. The response to naloxone after successive applications of morphine could not be obtained again even when the test interval was increased to 2 h or the agonist concentration increased to 6.7×10^{-7} M. The morphine-precipitated response was completely blocked by atropine. In naive tissues, naloxone also caused a response but this was less marked than that obtained from tissues exposed to morphine. Segments rendered tolerant to morphine were not cross-tolerant to the other agonists (not shown).

Withdrawal response after U-50,488H

The addition of the κ opioid agonist U-50,488H ($2–5 \times 10^{-8}$ M) caused a dose-related decrease of the spontaneous activity amplitude (Figure 2). This decrease never exceeded 30–60% and, at times, was associated with a relaxation of the muscle. The application of naloxone to the tissue after 5 min contact with the κ agonist caused a marked contracture, the amplitude of which was 67 ± 13% (mean ± s.d.; $n = 10$) of the amplitude of the maximal response to ACh. This contracture, in many cases, was accompanied by a reduction in spontaneous activity (Figure 2a and b). After washing followed by a 25 min interval, to allow the adaptive response to fade, a further 5 min exposure to U-50,488H followed by naloxone elicited responses of the same intensity which were related to the concentration of the agonist. The direct effects of the κ-agonist on tone and spontaneous activity in some isolated jejunum lessened on repeated administration but the responsiveness to naloxone was unaltered.

The responses of the jejunum to U-50,488H and subsequent injections of naloxone were blocked by the prior administration of a very low concentration (2.7×10^{-9} M) of the specific κ antagonist, nor-binaltorphimine (BNI) (Figure 2c) or by the non-specific antagonist naloxone (2.75×10^{-7} M) (Figure

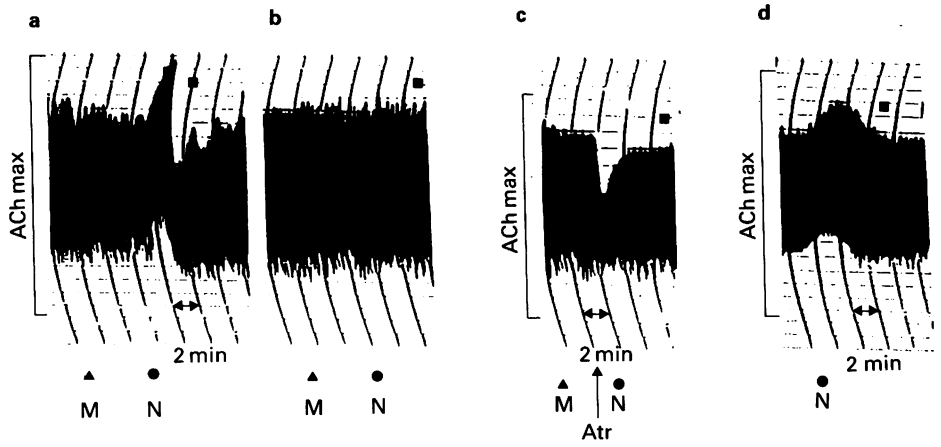

Figure 1 Typical contracture responses to naloxone (N, 2.75×10^{-7} M) in rabbit jejunum after a 5 min exposure of the tissue to morphine (M, 1.3×10^{-7} M) (a); the same tissue after washout (■) followed by a 25 min interval and a further 5 min exposure to M (same dose) (b). Atropine (Atr, 1.5×10^{-7} M), tested in another tissue preparation completely blocked the withdrawal response (c). N (2.75×10^{-7} M), produced a response also in a naive tissue (d).

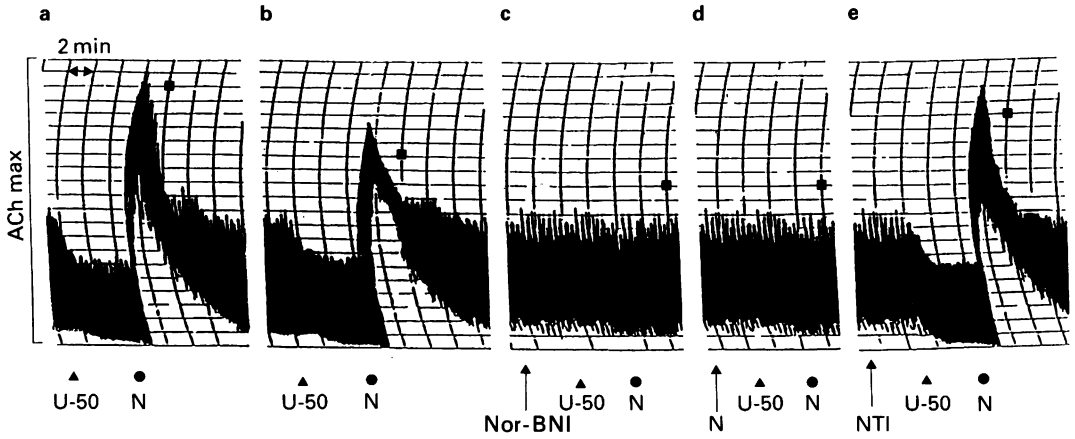

Figure 2 Typical tracings showing the effect of U-50,488H (U-50) on the spontaneous activity of rabbit jejunum and subsequent contracture responses to naloxone (N, 2.75×10^{-7} M) after a 5 min exposure of the tissue to U-50 5×10^{-8} M (a) and 2×10^{-8} M (b). Norbinaltorphimine (Nor-BNI, 2.7×10^{-9} M) and N (2.75×10^{-7} M), administered 5 min before U-50, inhibited the decrease of tone and spontaneous activity induced by U-50 and completely blocked the withdrawal responses (c and d, respectively). Naltrindole (NTI, 1×10^{-7} M) did not affect the responses to the κ-antagonist and to N (e). All tracings shown in figure were recorded from the same tissue preparation with a 25 min interval between tests. (■) Washout.

2d). However, naltrindole (1.1×10^{-7} M), a specific antagonist of δ receptors, had no effect (Figure 2e).

Hexamethonium (1.38×10^{-5} M), injected 5 min before the κ agonist, neither affected the tissue spontaneous activity nor the contraction elicited by naloxone (Figure 3a-b); on the other hand, tetrodotoxin (3×10^{-7} M) inhibited both the direct effect of U-50,488H on tone and spontaneous activity and the naloxone-induced response (Figure 3c). Atropine (1.5×10^{-7} M), applied to the tissue 1 min before naloxone (Figure 3d) drastically reduced the contractile response to naloxone. However, this reduction was never complete even with doses up to 1.5×10^{-6} M. Atropine also reduced the spontaneous activity of the jejunum in the absence of the κ agonist but there seemed to be some seasonal variation in its potency.

Withdrawal response to deltorphin

The addition of deltorphin (1.63×10^{-8} M), a selective δ-opioid receptor agonist strongly decreased the jejunum tone. Injection of naloxone (2.75×10^{-7} M) 5 min after the agonist, elicited a contractile response which was 61 ± 14% (mean ± s.d.; $n = 10$) of ACh maximal response (Figure 4a). As with the κ agonist, after washing and the usual 25 min interval time, the responses elicited by naloxone were reproducible and related to the deltorphin concentration (Figure 4a-b). In most tissues deltorphin reduced the tone without affecting the amplitude of the pendular movements; in some others, both parameters were decreased. In some tissues the direct response to the δ agonist decreased with time, although more slowly than with the κ agonist, but the contracture to naloxone was of the same intensity for several hours. The specific receptor antagonist, naltrindole (1.1×10^{-7} M), administered 1 min before deltorphin, blocked both the direct effect of deltorphin on the spontaneous activity of the tissue and the indirect one caused by naloxone (Figure 4c). Neither naloxone (2.75×10^{-7} M) nor nor-binaltorphimine (1.1×10^{-8} M) decreased these responses (Figure 4d-e). A higher dose of the κ antagonist was not used as concentrations as low as 1×10^{-8} M induced a contraction in many preparations. Administration of a higher concentration (1×10^{-6} M) of naloxone (not shown) prior to deltorphin had no effect on the reduced tissue tone induced by the 5 min exposure to the agonist but decreased by about 50% the

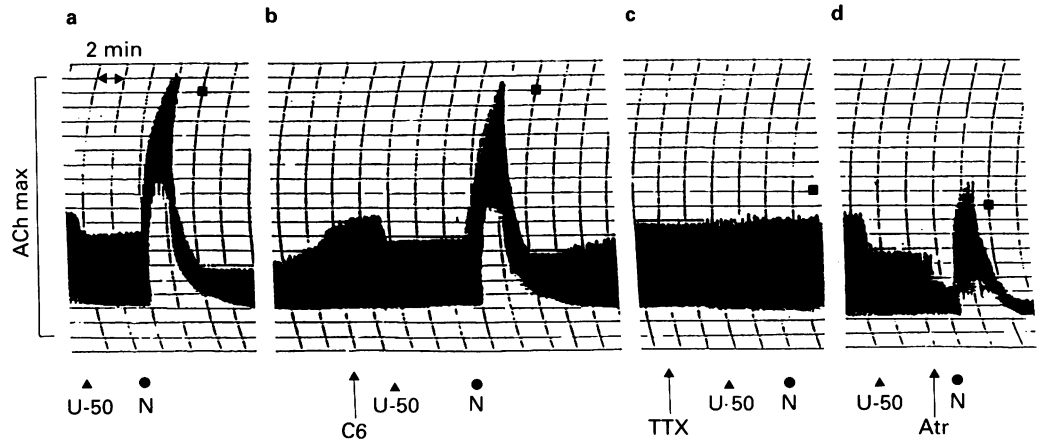

Figure 3 Typical tracings showing that hexamethonium (C6, 1.38×10^{-5} M), injected 5 min before U-50,488H (U-50, 5×10^{-8} M), did not affect either the tissue pendular activity or the contraction elicited by naloxone (N, 2.75×10^{-7} M) after 5 min exposure to the κ-antagonist (a and b). Tetrodotoxin (TTX, 3×10^{-7} M) inhibited both the decrease of tone and spontaneous activity caused by U-50 and the N-induced response (c). Atropine (Atr, 1.5×10^{-7} M), administered 1 min before N, reduced both the tissue activity and the contracture response to N (d). (■) Washout.

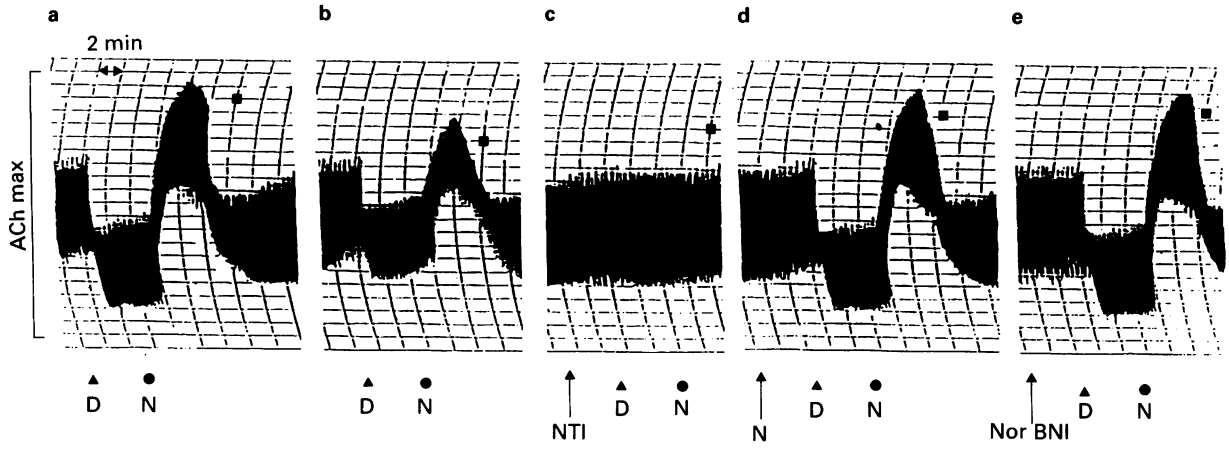

Figure 4 Typical tracings showing the effect of deltorphin (D) on the spontaneous activity of rabbit jejunum and subsequent contracture responses to naloxone (N, 2.75×10^{-7} M), after a 5 min exposure of the tissue to D, 1.63×10^{-8} M (a) and 6.52×10^{-9} M (b). Naltrindole (NTI, 1.1×10^{-7} M), administered 5 min before D, completely blocked both the reduction of spontaneous activity caused by D and the withdrawal response to N (c). N (2.75×10^{-7} M) and nor-binaltorphimine (Nor-BNI, 1.1×10^{-8} M) did not affect either the direct effect of D on the tone or the spontaneous activity of tissue and the contracture to N (d and e, respectively). All tracings shown in figure were recorded from the same tissue preparation with a 25 min interval between tests. (■) Washout.

response elicited by naloxone itself (2.75×10^{-7} M).

Hexamethonium, tetrodotoxin and atropine, administered at the same concentrations as before elicited effects similar to those observed in the experiments with U-50,488H (Figure 5).

Discussion

The present study demonstrates that following a brief period of contact (5 min) with morphine or selective κ- and δ-opioid receptor agonists, the rabbit isolated jejunum exhibited a naloxone-precipitated contracture. This clearly shows that an adaptive response was induced in rabbit isolated jejunum by a brief exposure to an opioid, as observed previously in guinea-pig ileum. The use of morphine and the recently developed selective κ- and δ-opioid receptor agonists, U-50,488H and deltorphin (VonVoigtlander *et al.*, 1983; Erspamer *et al.*, 1989) and their respective selective antagonists, nor-binaltorphimine and naltrindole (Portoghese *et al.*, 1987; 1988), has demonstrated the presence of μ-, κ- and δ-opioid receptors in the rabbit jejunum and of their respective roles in the development of this adaptive response. The finding that rabbit jejunum which had not been exposed to opioids also responded to naloxone, albeit with a slight but significant contractile response, was not completely unexpected since opioid peptides are present in this tissue and a similar effect has been described by some authors in guinea-pig ileum (Frederickson *et al.*, 1976; Lujan & Rodriguez, 1981; Collier *et al.*, 1981). Responses to naloxone have also been described in opiate-naive rats and mice (Collier *et al.*, 1972; Francis *et al.*, 1975).

In the experimental conditions used in the present study only the first challenge with morphine followed by naloxone elicited a contractile response of the tissue. In contrast, responses induced by the agonists selective for κ- and δ-opioid receptors were reproducible for several hours. The fact that only one response to naloxone was obtained after morphine could indicate that in the rabbit jejunum there is a small population of μ-receptors and, therefore, a relatively low receptor reserve. In this respect, the rabbit jejunum appears

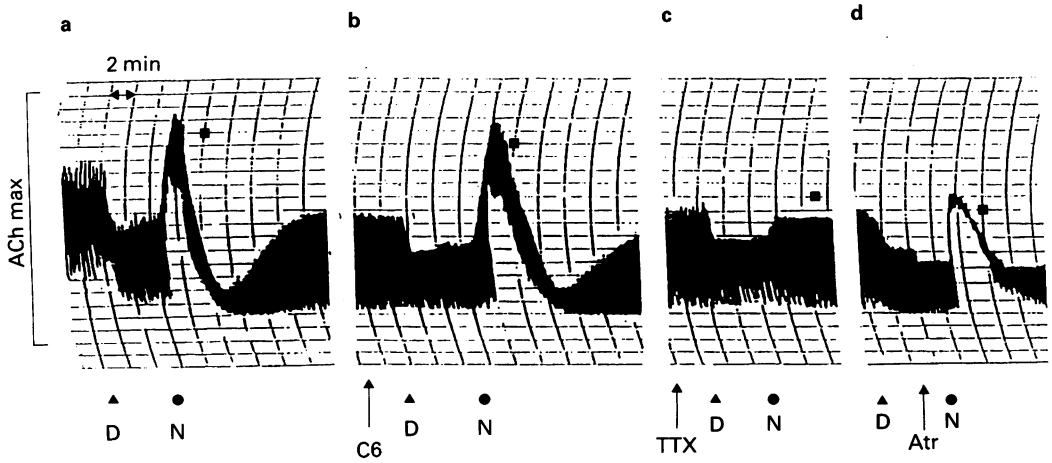

Figure 5 Typical tracings showing that hexamethonium (C6, 1.38×10^{-5} M), injected 5 min before deltorphin (D, 1.63×10^{-9} M), did not affect either the tissue pendular activity or the contraction elicited by naloxone (N, 2.75×10^{-7} M) after 5 min exposure to D. Tetrodotoxin (TTX, 3×10^{-7} M) prevented the withdrawal response to N but not the direct effect of D on the spontaneous activity. (c) Atropine (Atr, 1.5×10^{-7} M), administered 1 min before N, reduced both the tissue activity and the contracture response to N (d). (■) Washout.

to differ from the guinea-pig ileum in which reproducible naloxone-precipitated contractures to morphine/naloxone (Valeri *et al.*, 1990a) have been obtained. More detailed studies on the rabbit jejunum should be carried out, for example with lower agonist and antagonist concentrations to fully characterize the role of μ-opioid receptors in this response. The recent development of the selective κ-opioid antagonist, NBI, will also help to establish the respective roles of μ- and κ-opioid receptors in these phenomena in the guinea-pig ileum (Coupar & Quinn, 1987). Irrespective of the subtype of opioid receptor involved, the naloxone-induced contractures were neuronally mediated since they were completely blocked by tetrodotoxin. These responses, particularly to morphine, were also reduced by atropine, suggesting that they were mediated by parasympathetic cholinergic neurones in the myenteric plexus. The addition of hexamethonium, which prevents the action of ACh at the nicotinic receptors within the myenteric plexus did not significantly alter the withdrawal responses, suggesting that the excitation of myenteric neurones was not a consequence of activity in the preganglionic cholinergic neurone.

The observation that the sensitivity of the preparation to ACh was not changed by any of the opioid agonists (not shown) and that naloxone administered before the agonist prevented the adaptive response development, is consistent with the notion that the responses were presynaptically mediated via opioid receptors.

Naloxone (2.75×10^{-7} M) when administered before the agonist, prevented the development of the adaptive response to morphine and U-50,488H but not to deltorphin, i.e. the contractile response to naloxone administered after a 5 min exposure to deltorphin was the same whether or not naloxone itself ($2.75-5.5 \times 10^{-7}$ M) had been administered before the δ-receptor agonist. These observations may suggest that this concentration of naloxone blocked only a fraction of the δ receptors which was insufficient to antagonize the agonist action of deltorphin but was sufficient to precipitate a contracture. A rather similar effect was observed in the guinea-pig ileum, with regard to μ-receptors (Schulz *et al.*, 1985; Cherubini, 1988).

If the assumption is made that the naloxone-precipitated contracture is an indicator of dependence, then all three opioid receptor agonists have the potential of inducing dependence by acting on their respective receptors. In fact, the selective κ- and δ-opioid antagonists blocked only the development of dependence induced by their respective agonists, suggesting that μ-, δ- and κ-receptor types may act independently in producing the adaptive changes which lead to the establishment of dependence.

These observations may not apply to the opioid effects in the whole animal: it has recently been demonstrated that the selective blockade of δ-opioid receptors prevents the development of morphine-dependence in acutely and chronically treated mice (Abdelhamid *et al.*, 1991).

The finding of the present study that acute dependence can be induced in rabbit jejunum is an important result. Although it appears that the expression of dependence concerns mainly the excitation of the cholinergic neuron, as in the guinea-pig ileum, the activity of this neuron may be modulated by different neuronal systems in the two tissues. Preliminary results obtained with drugs that antagonize both *in vivo* and *in vitro* the withdrawal syndrome and with peptides known to be involved in dependence seem to be consistent with this concept (unpublished).

In this study we were particularly interested in establishing if, in a tissue which possesses opioid receptors and a high spontaneous activity, the expression of dependence could be revealed *in vitro* and if opioid agonists acting on different subtype receptors acted independently. This working procedure is a simple and versatile tool as constant comparable responses can be elicited in a short time in the same preparation, which is particularly useful in pharmacological studies. Moreover, the spontaneous motility of this tissue, which appears to be regulated by the opioid system, enables us to study the system itself and its interactions with other systems without electrical or chemical stimulation.

References

ABDELHAMID, E.E., SULTANA, M., PORTOGHESE, R.S. & TAKEMORI, A.E. (1991). Selective blockage of delta opioid receptors prevents the development of morphine tolerance and dependence in mice. *J. Pharmacol. Exp. Ther.*, **258**, 299–303.

BICKEL, W.K., STITZER, M.L., LIEBSON, I.A. & BIGELOW, G.E. (1988). Acute physical dependence in man: effects of naloxone after brief morphine exposure. *J. Pharmacol. Exp. Ther.*, **244**, 126–132.

CHAHL, L.A. (1983). Contracture of guinea-pig ileum on withdrawal of methionine^5-enkephalin is mediated by substance P. *Br. J. Pharmacol.*, **80**, 741–749.

CHAHL, L.A. (1986). Withdrawal responses of guinea-pig isolated ileum following brief exposure to opiates and opioid peptides. *Naunyn-Schmiedebergs Arch. Pharmacol.*, **333**, 387–392.

CHERUBINI, E., NORTH, R.A. & TOKIMASA, T. (1988). Action of naloxone on myenteric neurons removed from morphine treated guinea pigs. *J. Pharmacol. Exp. Ther.*, **247**, 830–838.

COLLIER, H.O.J., FRANCIS, D.L. & SCHNEIDER, C. (1972). Modification of morphine withdrawal by drugs interacting with humoral mechanisms: some contradictions and their interpretation. *Nature*, **237**, 220–223.

COLLIER, H.O.J., CUTHBERT, N.J. & FRANCIS, D.L. (1981). Model of opiate dependence in the isolated ileum. *Br. J. Pharmacol.*, **73**, 921–932.

COUPAR, I.M. & QUINN, M.J. (1988). The effects of the selective κ-opioid agonist MR 2034 on the guinea-pig ileum. *J. Pharm. Pharmacol.*, **40**, 378–380.

EISENBERG, R.M. (1982). Further studies on the acute dependence produced by morphine in opiate naive rats. *Life Sci.*, **31**, 1531–1540.

ERSPAMER, V., MELCHIORRI, P., FALCONIERI-ERSPARMER, G., NEGRI, L., CORSI, R., SEVERINI, C., BARRA, D., SIMMACO, M. & KREIL, G. (1989). Deltorphins: A family of naturally occurring peptides with high affinity and selectivity for opioid binding sites. *Proc. Natl. Acad. Sci. U.S.A.*, **86**, 5188–5192.

FRANCIS, D.L., ROY, A.C. & COLLIER, H.O.J. (1975). Morphine abstinence and quasi-abstinence effects after phosphodiesterase inhibition and naloxone. *Life Sci.*, **16**, 1901–1906.

FREDERICKSON, R.C.A., HEWES, C.R. & AIKEN, J.W. (1976). Correlation between the in vivo and in vitro expression of opiate withdrawal precipitated by naloxone: their antagonism by 1-(Δ)^9-tetrahydrocannabinol. *J. Pharmacol. Exp. Ther.*, **199**, 375–384.

GILLAN, M.G.C., KOSTERLITZ, H.W., ROBSON, L.E. & WATERFIELD, A.A. (1979). The inhibitory effects of presynaptic α-adrenoceptor agonists on contractions of guinea-pig ileum and mouse vas deferens in the morphine-dependent and withdrawn states produced *in vitro*. *Br. J. Pharmacol.*, **66**, 601–608.

HUIDOBRO-TORO, J.P. & YOSHIMURA, K. (1983). Pharmacological characterization of the inhibitory effects of neurotensin on the rabbit ileum myenteric plexus preparation. *Br. J. Pharmacol.*, **80**, 645–653.

JOHNSON, S.M. & FLEMING, W.W. (1989). Mechanisms of cellular adaptive sensitivity changes: applications to opioid tolerance and dependence. *Pharmacol. Rev.*, **41**, 435–488.

KOSERSKY, D.S., HARRIS, R.A. & HARRIS, L.S. (1974). Naloxone precipitated jumping activity in mice following the acute administration of morphine. *Eur. J. Pharmacol.*, **26**, 122–144.

KOSTERLITZ, H.W. & WATERFIELD, A.A. (1975). In vitro models in the study of structure-activity relationships of narcotic analgesic. *Annu. Rev. Pharmacol.*, **15**, 29–47.

KRYSTAL, J.H. & REDMOND, D.E. (1983). A preliminary description of acute physical dependence on morphine in the vervet monkey. *Pharmacol. Biochem. Behav.*, **18**, 289–291.

LESLIE, F.M., CHAVKIN, C. & COX, B.M. (1980). Opioid binding properties of brain and peripheral tissues: evidence for eterogeneity in opioid ligand binding sites. *J. Pharmacol. Exp. Ther.*, **214**, 395–402.

LUJAN, M. & RODRIGUEZ, R. (1981). Pharmacological characterization of opiate physical dependence in the isolated ileum of guinea-pig. *Br. J. Pharmacol.*, **73**, 859–866.

MORRONE, L.A., PIMPINELLA, G., ROMANELLI, L., PICCINELLI, D. & VALERI, P. (1990). Clonidine and nifedipine inhibit the abstinence but not the development of dependence in isolated guinea-pig ileum. *Pharmacol. Res.*, **22**, Suppl., 1, 19–20.

OKA, T. (1980). Enkephalin receptor in the rabbit ileum. *Br. J. Pharmacol.*, **68**, 193–195.

PAIRET, P. & RUCKEBUSCH, Y. (1984). Opioid receptor agonists in the rabbit colon: comparison of in vivo and in vitro studies. *Life Sci.*, **35**, 1653–1658.

PORTOGHESE, P.S., LIPKOWSKI, A.W. & TAKEMORI, A.E. (1987). Binaltorphimine and nor-binaltorphimine, potent and selective k-opioid receptor antagonists. *Life Sci.*, **40**, 1287–1292.

PORTOGHESE, P.S., SULTANA, M. & TAKEMORI, A.E. (1988). Naltrindole, a highly selective and potent non-peptide opioid receptor antagonist. *Eur. J. Pharmacol.*, **146**, 185–186.

SCHULZ, R. & HERZ, A. (1976). Aspects of opiate dependence in myenteric plexus of guinea-pig. *Life Sci.*, **19**, 1117–1128.

SCHULZ, R., SEIDL, E. & HERZ, A. (1985). Opioid dependence in the guinea-pig myenteric plexus is controlled by non-tolerant and tolerant opioid receptors. *Eur. J. Pharmacol.*, **110**, 335–341.

SZERB, J.C. (1982). Correlation between acetylcholine release and neuronal activity in the guinea-pig ileum myenteric plexus: effect of morphine. *Neuroscience*, **7**, 327–340.

VALERI, P., MARTINELLI, B., MORRONE, L.A. & SEVERINI, C. (1990a). Reproducible withdrawal contractions of isolated guinea-pig ileum after brief morphine exposure: effects of clonidine and nifedipine. *J. Pharm. Pharmacol.*, **42**, 115–120.

VALERI, P., MARTINELLI, B., PIMPINELLA, G. & SEVERINI, C. (1989). Effect of dapiprazole, a selective alpha$_1$ blocking drug on development of morphine dependence and withdrawal behaviour in mice. *Drug Alcohol Dependence*, **23**, 73–77.

VALERI, P., MORRONE, L.A., PIMPINELLA, G. & ROMANELLI, L. (1990b). Some pharmacological characteristics of the guinea-pig ileum opioid system activated by cholecystokinin. *Neuropharmacology*, **29**, 231–236.

VARGAS, M.L., MUSACCHIO, J.M., BANSINATH, M., TURNDORF, H. & PUIG, M.M. (1987). Naloxone elicits an excitatory response in the morphine-tolerant mouse vas deferens. *Neuropharmacology*, **26**, 1815–1818.

VONVOIGTLANDER, P.F., LAHTI, R.A. & LUDENS, J.H. (1983). U-50,488: a selective and structurally novel non-Mu (Kappa) opioid agonist. *J. Pharmacol. Exp. Ther.*, **224**, 7–12.

WOOD, J.D. (1987). Physiology of the enteric nervous system. In *Physiology of the Gastrointestinal Tract*. 2nd edition, ed. Johnson, L.R. pp. 67–109. New York: Raven Press.

(Received July 8, 1991
Revised November 29, 1991
Accepted January 7, 1992)

Br. J. Pharmacol. (1992), **106**, 45–48 © Macmillan Press Ltd, 1992

Mechanism of the vasodilator action of calcitonin gene-related peptide in conscious rats

Aly Abdelrahman, Yong-Xiang Wang, Sylvia Diana Chang & [1]Catherine C.Y. Pang

Department of Pharmacology & Therapeutics, Faculty of Medicine, The University of British Columbia, 2176 Health Sciences Mall, Vancouver, B.C., V6T 1Z3, Canada

1 The aim of this study was to investigate whether the hypotensive effect of rat α-calcitonin gene-related peptide (αCGRP) in conscious rats is mediated by endothelium-derived nitric oxide (NO) or the opening of adenosine 5′-triphosphate (ATP)-sensitive potassium (K_{ATP}) channels.

2 Dose-mean arterial pressure (MAP)-response curves of αCGRP were examined in the presence of vehicle, phenylephrine, K_{ATP} channel antagonist glibenclamide or NO synthase inhibitors, N^G-nitro-L-arginine methyl ester (L-NAME) and N^G-nitro-D-arginine methyl ester (D-NAME). Dose-MAP-response curves for sodium nitroprusside were also constructed in the presence and absence of L-NAME and D-NAME.

3 αCGRP and nitroprusside produced dose-dependent reductions in MAP which were potentiated by phenylephrine. Both L-NAME and D-NAME attenuated the depressor response to αCGRP but not nitroprusside.

4 Dose-MAP-response curves for pinacidil, a K_{ATP}-channel activator, were also examined in the presence of glibenclamide or vehicle. Glibenclamide attenuated pinacidil- but not αCGRP-induced reductions in MAP.

5 It is concluded that the hypotensive effects of αCGRP are partially mediated via endothelium-derived NO but not via the opening of K_{ATP} channels.

Keywords: Calcitonin gene-related peptide (CGRP); N^G-nitro-L-arginine methyl ester (L-NAME); N^G-nitro-D-arginine methyl ester (D-NAME); glibenclamide; pinacidil; nitroprusside; nitric oxide synthase inhibitor; K_{ATP} channel

Introduction

Calcitonin gene-related peptide (CGRP) is a potent vasodilator in isolated arterial smooth muscle and perfused vascular beds (Brain *et al.*, 1985; Grace *et al.*, 1987; Nelson *et al.*, 1990; Kawasaki *et al.*, 1990; Han *et al.*, 1990). In conscious rats, CGRP decreases blood pressure (Dipette *et al.*, 1987). The mechanism of the vasodilator effect of CGRP is not clear. The hypotensive effect of CGRP is not affected by pretreatment with propranolol, atropine, pyrilamine, cimetidine or indomethacin (Siren & Feuerstein, 1988).

There are regional differences in the dependence on the presence of endothelium for the vasodilator effects of CGRP. The relaxant effect of CGRP is attenuated by the removal of the endothelium in rat isolated aortic rings (Brain *et al.*, 1985; Grace *et al.*, 1987). However, the removal of the endothelium from human pulmonary arteries and veins (McCormack *et al.*, 1989), human skeletal muscle arteries and pig splenic arteries (Pernow, 1989) or bovine coronary artery (Greenberg *et al.*, 1987) does not affect the vasodilator effect of CGRP. Prieto *et al.* (1991) showed that that the removal of the endothelium attenuates CGRP-induced relaxation in the rat proximal epicardial but not intramyocardial coronary arteries. The role of ATP-sensitive potassium (K_{ATP}) channels in *in vitro* relaxation effects of CGRP is also unclear. The results of Nelson *et al.* (1990) suggest that CGRP hyperpolarizes arterial smooth muscle by the activation of K^+ channels. In contrast, the K_{ATP}-channel antagonist, glibenclamide, was found to be ineffective in inhibiting CGRP-induced relaxation in rat isolated coronary arteries (Prieto *et al.*, 1991) and human mammary artery (Boyle & Brown, 1991).

The aim of the present study was to examine whether the mechanism of the vasodepressor effect of CGRP in conscious rats involves the opening of K_{ATP} channels and/or nitric oxide (NO) formation. Dose-mean arterial pressure (MAP)-response curves were constructed for rat αCGRP in the absence and presence of glibenclamide, a K_{ATP} channel antagonist (Standen *et al.*, 1989; Winquist *et al.*, 1989), N^G-nitro-L-arginine methyl ester (L-NAME), an inhibitor of NO synthase (Rees *et al.*, 1990), and its D-enantiomer (D-NAME).

Methods

Surgical preparation

Male Sprague-Dawley rats (300–400 g) were anaesthetized with halothane (4% in air for induction, 1.5% in air for maintenance). Cannulae were inserted into the femoral artery for the measurement of MAP by a pressure transducer (P23DB, Gould Statham, CA) and into both femoral veins for the administration of drugs. All cannulae were filled with heparinized normal saline (25 iu ml^{-1} in 0.9% NaCl) and tunnelled s.c. to the back of the neck, exteriorized and secured. The rats were allowed to recover from the effects of anaesthesia for 4 h before use.

Effects of L-NAME and D-NAME on αCGRP- and nitroprusside-induced hypotension

Rats were randomly divided into four groups ($n = 6$ each). Normal saline (1 ml kg^{-1}), phenylephrine (5 μg kg^{-1} min^{-1}), L-NAME (13 mg kg^{-1}), D-NAME (320 mg kg^{-1}) were each injected as an i.v. bolus or continuously infused into groups I, II, III and IV, respectively. The doses of L-NAME and D-NAME used were two times those which produced maximum pressor responses which were stable and long-lasting (> 2 h). Ten min (40 min for D-NAME) later, αCGRP

[1] Author for correspondence.

(0.1–1.6 μg kg^{-1} min^{-1}, 4 min each dose) was infused into each group. In groups III and IV, after MAP had returned to the levels immediately prior to the infusion of αCGRP, sodium nitroprusside (10–100 μg kg^{-1} min^{-1}, 4 min each dose) was also infused into the rats.

Effects of glibenclamide on hypotensive response of αCGRP and pinacidil

Rats were divided into four groups ($n = 4$–6 each). Glibenclamide (20 mg kg^{-1}) was injected into groups V and VII followed 20 min later by the infusion of αCGRP (0.1–1.6 μg kg^{-1} min^{-1}, 4 min each dose) or pinacidil (10–160 μg kg^{-1} min^{-1}, 4 min each dose), respectively. In group VI and VIII, dimethylsulphoxide (DMSO, 0.25 ml kg^{-1}) was given in place of glibenclamide.

Drugs

Rat αCGRP, L-NAME (Sigma Chemical Co., St Louis, MO, U.S.A.), D-NAME (Bachem Bioscience Inc., PA, U.S.A.) and sodium nitroprusside (Fisher Scientific Co., NJ, U.S.A.) were dissolved in normal saline. Pinacidil (Eli Lilly and Co., IN, U.S.A.) was dissolved in 20% ethanol. Glibenclamide (Glyburide Micronized, Quebec, Canada) was dissolved in 95% DMSO (Sigma Chemical Co., MO, U.S.A.).

Statistics

Data were analysed by analysis of variance (ANOVA). Duncan's multiple range test was used for comparisons of group means. A probability of error $P < 0.05$ was preselected as the criterion for statistical significance.

Results

Table 1 shows baseline MAP prior to and after treatments with the vehicle or antagonists. There were no differences in baseline MAP among any groups. Phenylephrine, L-NAME and D-NAME caused similar increases in MAP. Glibenclamide increased MAP in both groups V and VII but only the increase in group V reached statistical significance. Neither saline (group I) nor DMSO (groups VI, VIII) increased MAP.

Figure 1 shows that αCGRP and nitroprusside both caused dose-dependent decreases in MAP (group I) which was potentiated by phenylephrine-induced hypertension (group II). L-NAME (group III) and D-NAME (group IV) attenuated the depressor responses of αCGRP (Figure 1a) but not those of nitroprusside (Figure 1b) compared to the corresponding responses in the phenylephrine group.

αCGRP and pinacidil produced similar reductions in MAP in DMSO-treated groups VI and VIII, respectively (Figure 2a,b). Glibenclamide did not affect the depressor responses of αCGRP (group V, Figure 2a) but attenuated those of pinacidil (group VII, Figure 2b) which reached statistical significance at the second, fourth and last doses.

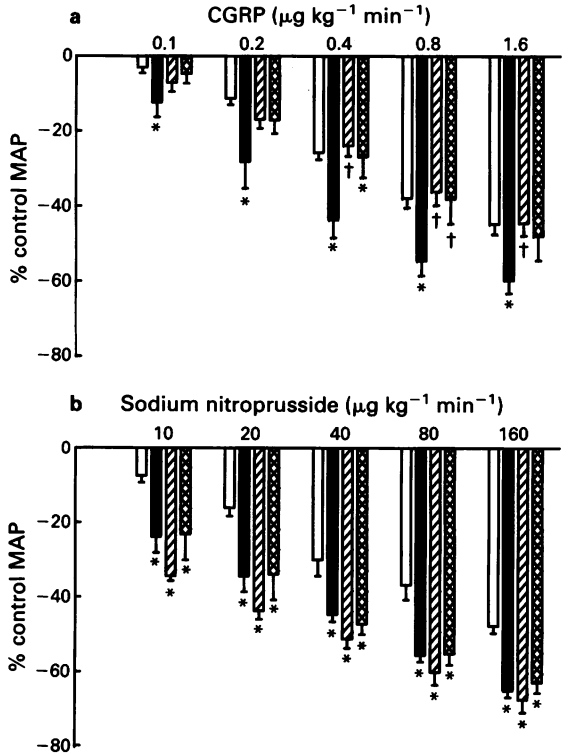

Figure 1 Effects of α-calcitonin gene-related peptide (αCGRP) (a) and sodium nitroprusside (b) on mean arterial pressure (MAP, means with s.e.mean shown by vertical bars, represented as % control) in four groups of conscious rats ($n = 6$ each) in the presence of saline (1 ml kg^{-1}, open columns), phenylphrine (5 μg kg^{-1} min^{-1}, closed columns), N^G nitro-L-arginine methyl ester (L-NAME, 13 mg kg^{-1}, hatched columns) or D-NAME (320 mg kg^{-1}, cross hatched columns). *Significantly ($P < 0.05$) different from saline treatment; †Significantly different from phenylephrine group.

Discussion

In the present study, both L-NAME and D-NAME raised MAP. L-NAME has been shown to produce pressor responses in anaesthetized (Rees *et al.*, 1990) and conscious rats (Gardiner *et al.*, 1991). D-NAME, on the other hand, was reported to have no pressor effect (Rees *et al.*, 1990). How-

Table 1 Mean arterial pressure (MAP, means ± s.e.mean) prior to and following treatments with drugs or vehicle in 8 groups of conscious rats

Groups		n	*MAP* (mmHg) *Control*	*Treatment*
I	Saline (1 ml kg^{-1})	6	126 ± 6	126 ± 7
II	Phenylephrine (5 μg kg^{-1} min^{-1})	6	109 ± 4	159 ± 4[a]
III	L-NAME (13 mg kg^{-1})	6	112 ± 6	155 ± 6[a]
IV	D-NAME (320 mg kg^{-1})	6	115 ± 5	152 ± 8[a]
V	Glibenclamide (20 mg kg^{-1})	6	115 ± 3	127 ± 3[a]
VI	DMSO (0.25 ml kg^{-1})	6	112 ± 3	113 ± 4
VII	Glibenclamide (20 mg kg^{-1})	4	118 ± 10	131 ± 12
VIII	DMSO (0.25 ml kg^{-1})	4	121 ± 4	129 ± 5

[a]Significantly different from control ($P < 0.05$).
L-NAME = N^G-nitro-L-arginine methyl ester; D-NAME = N^G-nitro-D-arginine methyl ester; DMSO = dimethylsulphoxide.

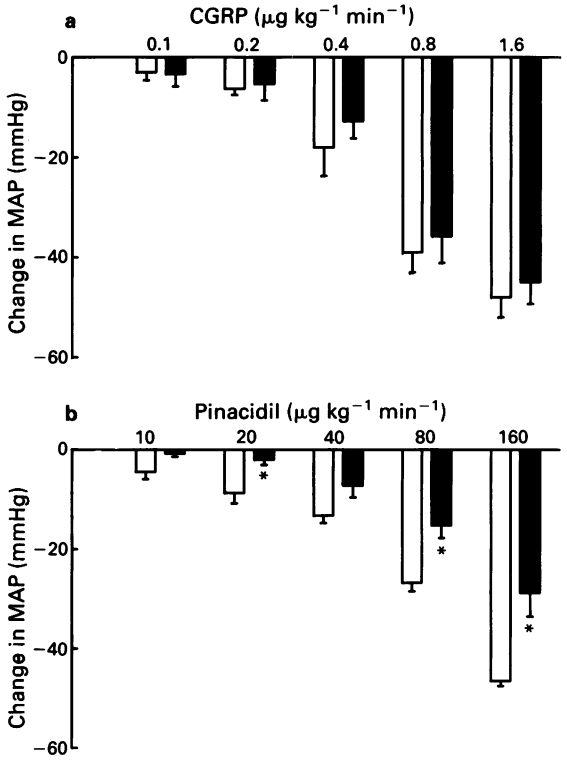

Figure 2 Effects of α-calcitonin gene-related peptide (αCGRP) ($n = 6$ per group, a) or pinacidil ($n = 4$ per group, b) on mean arterial pressure (MAP, means with s.e.mean shown by vertical bars) in four groups of conscious rats 20 min after treatment with glibenclamide (20 mg kg^{-1}, closed columns) or its solvent dimethylsulphoxide (DMSO, 0.25 ml kg^{-1}, open columns). *Significantly different from DMSO-treatment group ($P < 0.05$).

ever, the dose of D-NAME used in the present study is at least three times higher than those used in the study by Rees and co-workers (1990). We have also reported that injections of both the L- and D-enantiomers of another N^G-substituted arginine analogue, N^G-nitro-arginine (NNA), also raise MAP in conscious rats; the pressor responses of both L-NNA and D-NNA are antagonized by L-arginine but not D-arginine suggesting that the effects involve the inhibition of L-arginine/NO pathway (Wang *et al.*, 1991).

The hypotensive effects of αCGRP in the absence and presence of L-NAME and D-NAME were compared with those of the endothelium-independent vasodilator, nitroprusside. It is well-known that vasodilator drugs cause greater depressor response when MAP is elevated. Therefore, phenylephrine was used to raise MAP in another group of rats which served as a control for L-NAME and D-NAME. αCGRP and nitroprusside dose-dependently decreased MAP; the depressor effects of both were potentiated by phenylephrine. L-NAME and D-NAME both inhibited the depressor responses of αCGRP but not those of nitroprusside. This suggests that the reduced hypotensive effect of αCGRP caused by L-NAME and D-NAME is due to the inhibition of endothelial NO synthase. Gray & Marshall (1990) showed that N^G-monomethyl-L-arginine (L-NMMA) attenuates CGRP-induced relaxation in noradrenaline-contracted rat aortic rings and that this attenuation is inhibited by L-arginine. These investigators also show that CGRP increases guanosine 3′:5′-cyclic monophosphate (cyclic GMP) levels in the rat aorta and that the relaxant effects of CGRP and acetylcholine but not that of nitroprusside are attenuated by methylene blue. These *in vitro* results suggest that vasodilatation by CGRP involves the NO pathway (Gray & Marshall, 1991). *In vivo* studies show that although CGRP causes similar depressor responses in rats pretreated with endothelin-1 or L-NAME, there is less vasodilatation in the hindlimb of rats given L-NAME, suggesting that NO contributes to the vasodilator effect of CGRP in the hindquarters (Gardiner *et al.*, 1991).

It has also been reported that CGRP increases adenosine 3′:5′-cyclic monophosphate (cyclic AMP) but not cyclic GMP levels in rat aortic smooth muscle cells (Kubota *et al.*, 1985). In isolated rat aortic rings, nitroprusside increases cyclic GMP in both intact and endothelium-denuded preparations, acetylcholine increases cyclic GMP only in rings with intact endothelium while CGRP does not increase cyclic GMP in either condition (Grace *et al.*, 1987). In the rat coronary arteries, methylene blue does not affect CGRP-induced relaxation suggesting that the relaxation does not involve NO (Prieto *et al.*, 1991). Therefore, although our results show that NO is involved in CGRP-induced vasodilatation, it does not exclude the possibility that CGRP can directly relax arteries by increasing cyclic AMP.

Our results also show that glibenclamide attenuated the depressor response of pinacidil but not that of αCGRP suggesting that the vasodilator effect of αCGRP does not involve the opening of K_{ATP} channels. There are inconsistent reports on the role of K_{ATP} channels in the vasorelaxation effect of CGRP. Nelson *et al.* (1990) showed that CGRP opens single K^+ channels on rabbit mesenteric arterial smooth muscle cells and that the CGRP-induced vasodilator effect is partially reversed by glibenclamide. In contrast, glibenclamide does not affect CGRP-induced relaxation in rat isolated coronary arteries (Prieto *et al.*, 1991). Boyle & Brown (1991) showed that glibenclamide reverses the vasodilator effect of diazoxide (a K_{ATP}-channel activator) but not that of CGRP in the human mammary artery. One should be cautious in the extrapolation of results from *in vitro* to *in vivo* studies since they involve responses in large arteries and arterioles, respectively.

In conclusion, this study shows that the hypotensive effect of αCGRP in conscious rats is attenuated by L-NAME and D-NAME suggesting that it is mediated via the NO pathway. Since the depressor response of αCGRP is not affected by glibenclamide at a dose which blocked K_{ATP} channels, αCGRP does not produce vasodilatation by the opening of K_{ATP} channels.

This work was supported by the Heart and Stroke Foundation of British Columbia and Yukon. A.A. was a recipient of the University of British Columbia Graduate Fellowship. S.D.C. was a recipient of the Pharmaceutical Manufacturer's Association Summer Research Scholarship.

References

BOYLE, J.J. & BROWN, M.J. (1991). Glibenclamide fails to reverse relaxations induced by calcitonin gene related peptide (CGRP) in human mammary artery and saphenous vein. *Br. J. Pharmacol.*, **102**, 200P.

BRAIN, S.D., WILLIAMS, T.J., TIPPINS, J.R., MORRIS, H.R. & MACINTYRE, I. (1985). Calcitonin gene-related peptide is a potent vasodilator. *Nature*, **313**, 54–56.

DIPETTE, D.J., SCHWARZENBERGER, K., KERR, N. & HOLLAND, O. (1987). Systemic and regional haemodynamic effects of calcitonin gene-related peptide. *Hypertension*, **9** (suppl. III), 142–146.

GARDINER, S.M., COMPTON, A.M., KEMP, P.A., BENNETT, T., FOULKES, R. & HUGHES, B. (1991). Haemodynamic effects of human α-calcitonin gene-related peptide following administration of endothelin-1 or N^G-nitro-L-arginine methyl ester in conscious rats. *Br. J. Pharmacol.*, **105**, 1256–1262.

GRACE, G.C., DUSTING, G.J., KEMP, B.E. & MARTIN, T.J. (1987). Endothelium and the vasodilator action of rat calcitonin gene-related peptide (CGRP). *Br. J. Pharmacol.*, **91**, 729–933.

GRAY, D.W. & MARSHALL, I. (1990). Calcitonin gene-related peptide (CGRP) endothelium dependent relaxation in rat aorta is inhibited by L-NMMA. *Br. J. Pharmacol.*, **99,** 104P.

GRAY, D.W. & MARSHALL, I. (1991). Human α-calcitonin gene-related peptide (CGRP) relaxes rat thoracic aorta by releasing nitric oxide and raises cyclic AMP and cyclic GMP. *Br. J. Pharmacol.*, **102,** 126P.

GREENBERG, B., RHODEN, K. & BARNES, P. (1987). Calcitonin gene-related peptide (CGRP) is a potent non-endothelium-dependent inhibitor of coronary vasomotor tone. *Br. J. Pharmacol.*, **92,** 789–794.

HAN, S., NAES, L. & WESTFALL, T.C. (1990). Calcitonin gene-related peptide is the endogenous mediator of nonadrenergic-noncholinergic vasodilation in rat mesentry. *J. Pharmacol. Exp. Ther.*, **255,** 423–428.

KAWASAKI, H., NUKI, C., SAITO, A. & TAKASAKI, K. (1990). Role of calcitonin gene related peptide containing nerves in the vascular adrenergic neurotransmission. *J. Pharmacol. Exp. Ther.*, **252,** 403–409.

KUBOTA, M., MOSELEY, J.M., BUTERA, L., DUSTING, G.J., MACDONALD, P.S. & MARTIN, T.J. (1985). Calcitonin gene-related peptide stimulates cyclic AMP formaton in rat aortic smooth muscle cells. *Biochem. Biophys. Res. Commun.*, **132,** 88–94.

MCCORMACK, D.G., MAK, J.C.W., COUPE, M.O. & BARNES, P.J. (1989). Calcitonin gene-related peptide vasodilation of human pulmonary vessels. *J. Appl. Physiol.*, **67,** 1265–1270.

NELSON, M.T., HUANG, Y., BRAYDEN, J.E., HESCHELER, J. & STANDEN, N.B. (1990). Arterial dilations in response to calcitonin gene-related peptide involve activation of K^+ channels. *Nature*, **344,** 771–773.

PERNOW, J. (1989). Actions of constrictor (NPY and endothelin) and dilator (substance P, CGRP and VIP) peptides on pig splenic and human skeletal muscle arteries: involvement of endothelium. *Br. J. Pharmacol.*, **97,** 983–989.

PRIETO, D., BENEDITO, S. & NYBORG, N.C.B. (1991). Heterogeneous involvement of endothelium in calcitonin gene-related peptide-induced relaxation in coronary arteries from rat. *Br. J. Pharmacol.*, **103,** 1764–1768.

REES, D.D., PALMER, R.M.J., SCHULZ, R., HODSEN, H.F. & MONCADA, S. (1990). Characterization of three inhibitors of endothelial nitric oxide synthase *in vitro* and *in vivo*. *Br. J. Pharmacol.*, **101,** 746–752.

SIREN, A. & FEUERSTEIN, G. (1988). Cardiovascular effects of rat calcitonin gene-related peptide in the conscious rat. *J. Pharmacol. Exp. Ther.*, **247,** 69–78.

STANDEN, N.B., QUAYLE, J.M., DAVIES, N.W., BRAYDEN, J.E., HUANG, Y. & NELSON, M.T. (1989). Hyperpolarizing vasodilators activate ATP-sensitive K^+ channels in arterial smooth muscle. *Science*, **245,** 177–180.

WANG, X.-Y., ZHOU, T. & PANG, C.C.Y. (1991). Pressor effects of L and D enantiomers of N^G-nitro-arginine in conscious rats are antagonized by L- but not D-arginine. *Eur. J. Pharmacol.*, **200,** 77–81.

WINQUIST, R.J., HEANEY, L.A., WALLACE, A.A., BASKIN, E.P., STEIN, R.B., GARCIA, M.L. & KACZOROWSKI, G.J. (1989). Glyburide blocks the relaxation response to BRL 34915 (cromakalim), minoxidil sulfate and diazoxide in vascular smooth muscle. *J. Pharmacol. Exp. Ther.*, **248,** 149–156.

(Received December 10, 1991
Accepted January 7, 1992)

Br. J. Pharmacol. (1992), **106**, 49–54 © Macmillan Press Ltd, 1992

Comparison of pyrrolidinyl and piperidinyl benzamides for their anticonvulsant activity and inhibitory action on sodium channel

Yu Zhu, [1]Wha Bin Im, Richard A. Lewis & Philip F. VonVoigtlander

CNS Diseases Research, The Upjohn Company, Kalamazoo, MI 49001, U.S.A.

1 A pair of benzamide analogues containing a pyrrolidinyl or piperidinyl group was examined for their anticonvulsant activity against the electroshock-induced seizures in mice and the ability to block the voltage-gated Na channel in N1E-115 cells, in comparison with the prototype compound, U-54494A, (±)-*cis*-3,4-dichloro-N-methyl-N-[2-(1-pyrrolidinyl)-cyclohexyl]-benzamide, a potent anticonvulsant and a Na channel blocker.

2 The pyrrolidinyl benzamide (U-49524E) was found to be effective against the electroshock-induced seizures ($ED_{50} = 35$ mg kg^{-1}, i.p.) whereas the benzamide with a piperidinyl moiety (U-49132E) was inactive ($ED_{50} > 100$ mg kg^{-1}).

3 Using whole-cell patch clamp techniques we found that U-49132E was several times less potent, with an IC_{50} of 396 μM as compared to 118 μM for U-49524E at the holding potential of −80 mV, and was much slower in blocking Na channels with a half-time of 10.7 ± 1.1 min vs. 2.2 ± 0.4 min for its counterpart.

4 Qualitatively, their general modes of interaction with Na channels were similar to each other and to that of U-54494A in that they interacted with the resting and slowly-inactivated states of the channels and exhibited a use-dependent inhibition because of a slow recovery from the inactivated state in the presence of the drugs.

5 Comparison of their physicochemical properties, shows the less potent and slowly acting U-49132E is more hydrophobic and bulkier than U-49524E, but has the same pK_a. This suggests that the drugs approach the Na channel through a narrow and hydrophilic pathway.

6 Overall, this study underscores the importance of inhibiting the Na channel to the anticonvulsant activity of the benzamide compounds.

Keywords: Anticonvulsant; patch clamp; sodium channel; U-49132E; U-49524E; U-54494A

Introduction

Voltage-dependent Na channels are primarily responsible for the depolarizing phase of action potentials in neurones. Various compounds block the Na currents and are used as local anaesthetics or anticonvulsants. In particular, phenytoin and carbamazepine are known to interact with the slowly-inactivated Na channels. The slow recovery rate of the drug-bound channels from inactivation leads to a use-dependent block and is responsible for their anticonvulsant activity (Schwarz & Grigat, 1989; Rogawski & Porter, 1990). Recently, we have shown that U-54494A, (±)-*cis*-3,4-dichloro-N-methyl-N-[2-(1-pyrrolidinyl)-cyclohexyl]-benzamide, is a potent anticonvulsant (VonVoigtlander *et al.*, 1987) and blocks the Na current in N1E-115 neuroblastoma cells (Zhu & Im, 1991). The drug has been shown to interact with the slowly-inactivated state of the Na channel and to retard the recovery process like phenytoin, in addition to its interaction with the resting state of the Na channel. In the course of our studies on the structure-activity relationship for benzamide compounds, we discovered a pair of U-54494A analogues which differ slightly in their structures, but vary widely in their anticonvulsant activities. They are U-49524E (*trans*-α,α,α,-trifluoro-N-methyl-N-[2-pyrrolidinyl-cyclohexyl]-*p*-toluamide) and U-49132E (*trans*-α,α,α,-trifluoro-N-methyl-N-[2-piperidino-cyclohexyl-*p*-toluamide) (Figure 1). U-49524E containing a pyrrolidinyl group was a potent anticonvulsant whereas U-49132E containing a piperidinyl group was not. In this study, we also found that U-49132E was less potent and much slower in blocking the Na channel than U-49524E. Their interactions with the Na channels were further characterized.

[1]Author for correspondence

Methods

Electroshock-induced seizures in mice

Charles River CF-1 (18–22 g) male mice were dosed intraperitoneally in the range of 6.25 to 200 mg kg^{-1} (drugs dissolved in 0.9% saline). Anticonvulsant activity, 1 h after the drug administration, was assessed by determination of electroshock-induced seizure thresholds as previously described (VonVoigtlander *et al.*, 1987). Generally, 10 mice were used to establish a threshold (mA) of the electroshock convulsions in the control which was typically 25 mA for a period of 0.2 s. The ED_{50} represents the dose of the drugs which enhance the threshold of the electroshock seizures to 100 mA for a 0.2 s stimulus.

Cell culture

Mouse neuroblastoma cells (NIE-115) were grown in Dulbecco's modified Eagle's medium (Sigma Chemical Co., USA) supplemented with 5% foetal calf serum, 20 mM HEPES, penicillin (100 u ml^{-1}) and streptomycin (100 μg ml^{-1}) at 37°C under humidified air containing 10% CO_2 (Quandt & Narahashi, 1984). The cells were differentiated by reducing

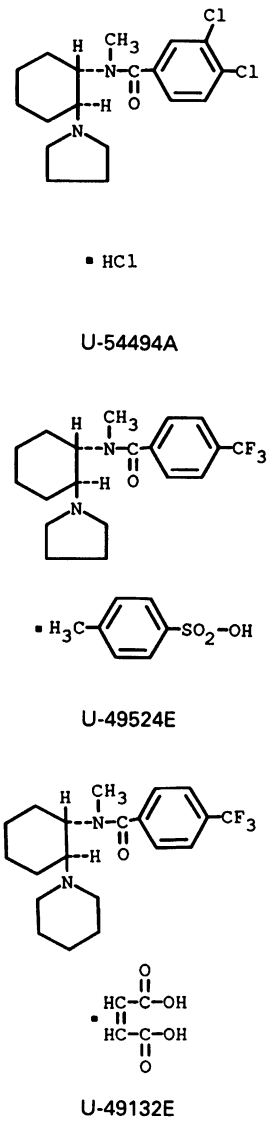

Figure 1 Structures of U-54494A, U-49524E and U-49132E.

foetal calf serum to 1% and adding 2% of dimethylsulphoxide in the medium for 6–9 days before use.

Voltage-clamp recording

The whole-cell configuration of the patch clamp technique (Hamill *et al.*, 1981) was used to record the Na channel current. Patch pipettes were made of borosilicate glass capillary tubes (Kimax-51, Kimble Products, U.S.A.) on a Flaming/Brown Micropipette Puller (P-80/PC, Sutter Instrument Co. U.S.A.). After fire polishing, the pipette tip had a resistance of 0.5 to 2 MΩ in solutions described below. Cells grown on the cover slip were transferred to a small chamber (1 ml volume) on the stage of an inverted light microscope and superfused by gravity with the external solution at a rate of 1.5 to 2 ml min^{-1}. The membrane current through the pipette was recorded by a current-voltage converter consisting of an Axopatch-1D amplifier and a CV-4 headstage (Axon Instrument Co., U.S.A.) and stored on diskettes by use of 'Pclamp 5.5' acquisition software (Axon Instrument Co.). Signal was filtered at 5 kHz. Linear leakage current was subtracted by a P/N procedure provided by the 'Pclamp 5.5' programme. The capacitive transient current and the series resistance were compensated for using the features of the Axopatch-1D amplifier. Each test pulse was applied at an interval of 20 s which is sufficiently long to avoid the use-dependent effect of the drug.

Solutions

Pipette solution contained (in mM): CsCl 100, CsF 50, Na-HEPES 10 and glucose 5, pH 7.0. The external solution contained (mM): NaCl 125, KCl 5.5, $CaCl_2$ 3, $MgCl_2$ 0.8, glucose 20 and Na-HEPES 20 (pH 7.4). Stocks of drugs were first made with water and later added to the external solution. All experiments were performed at room temperature. (22 ± 1°C).

Data analysis

In most cases, data were normalized to their appropriate maximal values under various conditions. When two drugs were tested on the same cell, a paired Student's t test was used. Otherwise, an unpaired t test was used to determine the significance of differences (Dudewicz & Mishra, 1988). $P<0.05$ was considered significantly different. Data are presented as mean ± standard error in most cases.

Results

U-49132E and U-49524E, despite the minor structural difference, display widely different potency in anticonvulsant activity. Figure 2 shows that in mice treated intraperitoneally with the drugs, U-49524E enhanced the electroshock threshold from 25 to 100 mA with an ED_{50} value of 35 mg kg^{-1}, but U-49132E was not effective up to the dose of 100 mg kg^{-1}. In similar experiments, U-54494A, the prototype compound in the benzamide series, was effective with an ED_{50} value of 25 mg kg^{-1}.

Because the anticonvulsant activity of U-54494A has been ascribed to its block of the voltage-dependent Na channel currents (Zhu & Im, 1991), we compared in this study the interactions of its analogues with the Na channel in N1E 115 cells. Figure 3a shows typical recordings of the inward Na currents with and without drugs. U-49524E and U-49132E (at 50 μM) reduced the peak Na current at all the depolarizing potentials. The drug effect was recorded after a steady-state effect of the drug was reached, typically 5 to 10 min for U-49524E and 20 min or more for U-49132E (see below). Figure 3b illustrates the current-voltage (I–V) relationships of the Na channels with and without 50 μM U-49524E and U-49132E. The drugs showed no considerable effect on the shape of the I–V relationship and the apparent reversal potential. Figure 3c shows a superimposition of the control current trace to the drug-treated one obtained at the same depolarizing voltage as the control and multiplied by an appropriate factor. No noticeable deviations are observed

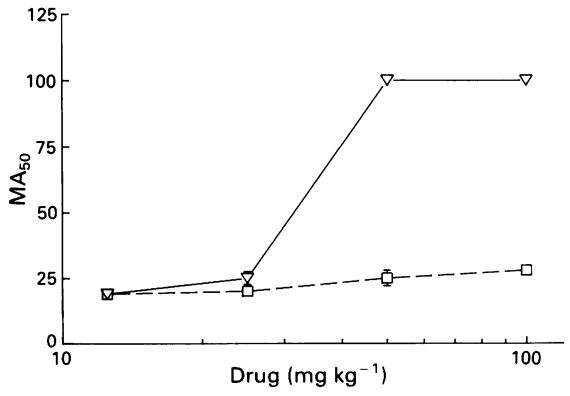

Figure 2 Dose-response of U-49524E (▽) and U-49132E (□) to the maximal electroshock seizures. The increase in the threshold of electroshock convulsion (MA_{50}) was determined 60 min after mice were injected intraperitoneally.

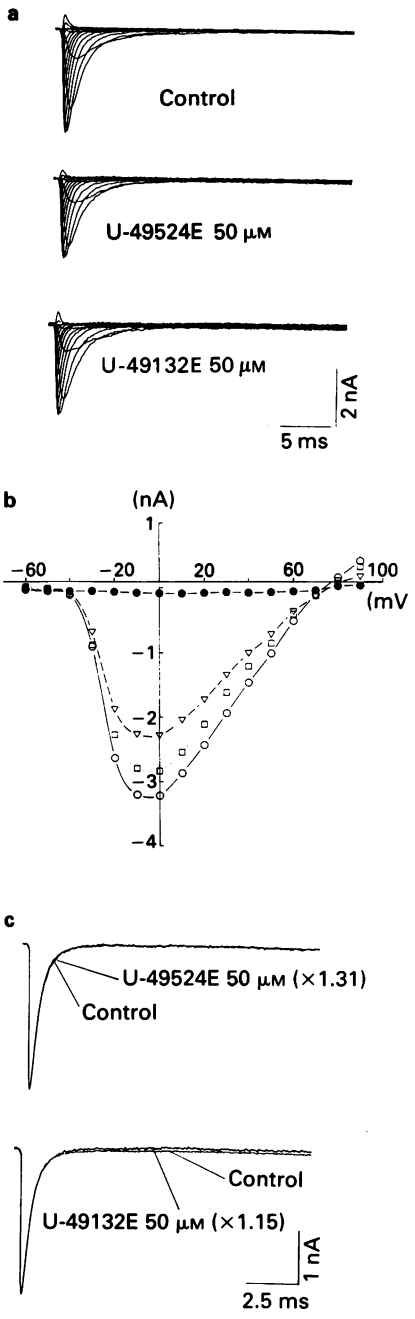

Figure 3 Effects of U-49524E and U-49132E on the current-voltage relationship of the Na channel. (a) Tracings of the whole-cell patch clamp recording of the Na currents generated upon a series of depolarizations from holding potential − 80 mV to various potentials for 30 ms with and without drugs. (b) The peak amplitudes of the Na currents with and without drugs are plotted as a function of depolarizing potentials: (○) control; (●) 1 μM tetrodotoxin; (▽) 50 μM U-49524E; (□) 50 μM U-49132E. (c) Superimposition of control traces and those in the presence of drugs (from a) generated upon depolarization to 0 mV. Traces with drugs have been multiplied.

between the two traces superimposed, indicating that the two compounds like U-54494A exert no effect on the kinetics of the channel activation or inactivation and have no apparent time-dependent block.

Figure 4 shows the time-course profiles for inhibition by U-49132E and U-49524E of the peak Na currents. The inhibitory action of U-49524E (50 μM) rapidly reached a plateau with a half time of 2.2 ± 0.4 min ($n = 10$) (the same $t_{\frac{1}{2}}$ for U-54494A), but that of U-49132E at 50 μM was much slower, its half time being 10.7 ± 1.1 min ($n = 12$, $P < 0.01$, unpaired t test). The values of the half time were not altered noticeably as the concentration of the drugs increased to 100 μM (data not shown). All the current measurements in the presence of the drugs in this study, therefore, were performed as their inhibitory effects reached a plateau.

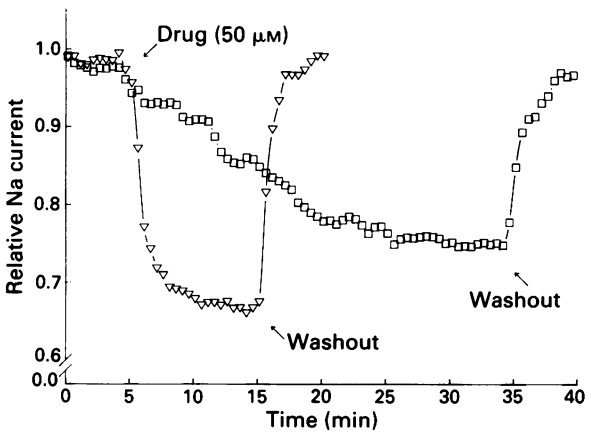

Figure 4 Time-course of resting block of Na channel by U-49524E (▽) and U-49132E (□). The peak Na current was measured after a depolarizing pulse from − 80 mV to 0 mV at an interval of 10 s. The drugs were superfused and washed out at a rate of 1.5 to 2 ml min^{-1}.

The general patterns of blocking the Na currents by two compounds were qualitatively similar. A quantitative difference, however, was observed in their potency to block the currents. Figure 5 shows dose-response profiles of the drugs at the holding potentials of − 80 or − 120 mV . The dose-response profiles were analyzed using the equation:

$$I_{Na} = 1/[1 + (C/IC_{50})^k]$$

where C is the concentration of drugs, IC_{50} is the half maximal inhibitory dose, and k is the slope of the curve. U-49524E was 3 to 5 times more potent than U-49132E in blocking the Na currents; the IC_{50}s were 118.2 and 396.1 μM for U-49524E and U-49132E, respectively, at the holding potential of − 80 mV, and 281 and 1435 μM at − 120 mV, respectively. The corresponding values for the parent compound, U-54494A, were 72.1 and 228.7 μM at − 80 and − 120 mV, respectively. It should be mentioned that the inhibition of the Na current occurred at − 120 mV is a true

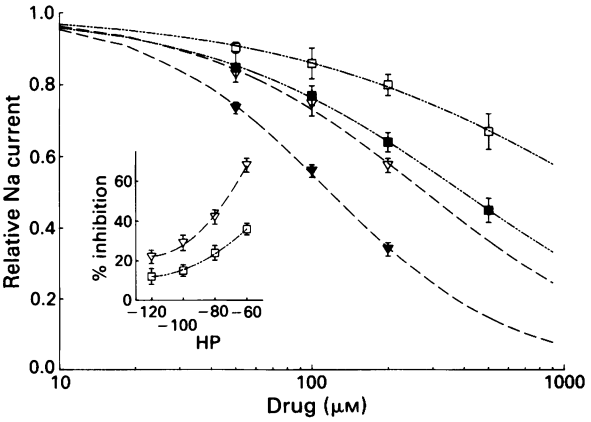

Figure 5 Dose-response of the Na current to U-49524E (▽) and U-49132E (□). The peak Na current was measured after depolarization to 0 mV for 30 ms from holding potentials of either − 120 (open symbols) or − 80 mV (filled symbols) and normalized to the control values in the absence of drugs ($n = 3$–7). Curves were drawn with the function expressed in Results. Inset: holding potential (HP) dependent block of the Na channel by U-49524E (▽) and U-49132E (□) at 100 μM.

'resting block' since a further hyperpolarization (to − 140 mV, data not shown) did not relieve the block. The Hill coefficients of the curve (k) for U-49524E were 0.969 at − 120 mV and 1.22 at − 80 mV, suggesting the possibility of more than one binding site for U-49524E at a holding potential more positive than − 120 mV. The Hill coefficients for U-49132E are less than unity, 0.684 and 0.851 at − 120 mV and − 80 mV, respectively, suggesting a limited access of the drug to the channel.

The inset of Figure 5 illustrates that with a fixed concentration of drugs at 100 μM, the percentage inhibition is a function of the holding potential. This indicates the block of the Na channel by those two agents is voltage-dependent; the more depolarized potential, the more inhibition.

The steady-state inactivation of the Na channel was examined (see Figure 6) by fitting the data to the function (Matsuki *et al.*, 1984):

$$h_\infty(\text{or } S_\infty) = 1/(1 + \exp[E_m - E_{\frac{1}{2}})/k])$$

where h_∞ or S_∞ is the fast and slow inactivation, respectively, E_m is the conditioning potential, $E_{\frac{1}{2}}$ is the conditioning potential at which 50% of the Na channel is inactivated and k is the slope of the curve. The fast inactivation was produced with a short conditioning pulse (100 ms) and a 2 ms gap between the conditioning and test pulses while the slow inactivation was produced with a long conditioning pulse (2 s) and a long hyperpolarizing gap (50 ms) between the conditioning and test pulses to relieve the fast inactivation. The drugs did not alter the parameters for the fast inactivation (data not shown), but brought about hyperpolarizing shifts in the slow inactivation. The shift was − 9.7 ± 1.0 mV ($n = 5$) and − 6.4 ± 1.3 mV ($n = 5$) for U-49524E and U-49132E, respectively, at 100 μM from the control $E_{\frac{1}{2}}$ of − 39.4 ± 2.0 mV ($P < 0.01$ for both compounds, paired t test). U-49524E induced a larger shift than U-49132E ($P < 0.05$, paired), but brought about the same shift as U-54494A.

The recovery from the inactivated state of the Na channels was examined with a double exponential function (Chernoff & Strichartz, 1989):

$$I/I_{max} = 1\text{-}A_1{*}\exp(-t/\tau_1)\text{-}A_2{*}\exp(-t/\tau_2)$$

where A_1, A_2 are proportional constants and τ_1, τ_2 are the time constants of two phases of the recovery. Table 1 shows the results from the analysis of the recovery processes for the inactivated Na channels in the presence of 50 and 100 μM of U-49132E and U-49524E. The drugs at the two concentrations had a marginal effect on the fast phase of recovery, both the amplitude (A_1) and time constants (τ_1). The fraction associated with the fast phase (A_1) accounts for 84 ± 7% of the recovery processes in the control as well as in the presence of the drugs at 50 μM, but for 80 ± 6% with the drugs at 100 μM. τ_1 was 5.9 ± 0.3 ms for the control, 6.9 ± 0.3 ms for both U-49132E and U-49524E at 50 μM, and 7.1 ± 0.5 and 8.4 ± 0.8 ms for the respective drugs at 100 μM. As the drug concentration was raised to 100 μM, the fraction associated with the slow recovery phase (A_2) marginally increased from 16 ± 3 to 20 ± 4%. On the other hand, the time constant for the slow recovery (τ_2) changed as a function of the drug concentrations. τ_2 increased from 225 ± 28 ms to 914 ± 96 ms with U-49524E and to 582 ± 63 ms with U-49132E at the concentration of 50 μM, and further increased to 5744 ± 620 and to 722 ± 110 with the respective drug at a concentration of 100 μM (Figure 7). This indicates that the dissociation of the drug from the inactivated channels is very slow, particularly with the U-49524E. The marked dependence of the slow recovery rate for 49524E on its concentration suggests that the drug stabilizes the channel in the slow inactivated state and leads to an increase in the apparent time constant for recovery. With U-49132E, on the other hand, its apparent recovery rate was much less dependent on the concentration, implying that U-49132E has a limited ability to stabilize the channel in the inactivated state.

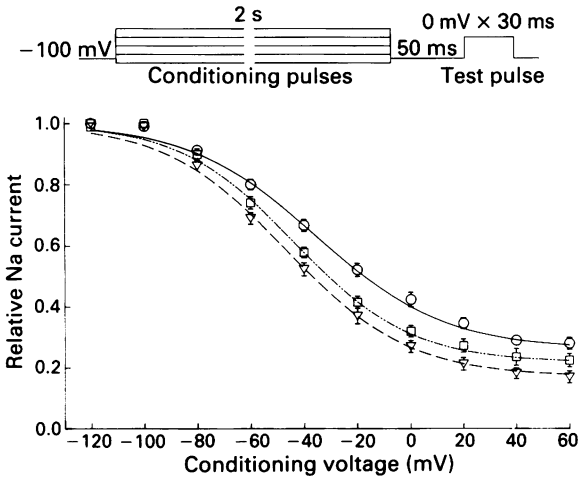

Figure 6 Effects of U-49524E (▽) and U-49132E (□) on the steady-state slow inactivation of the Na channel (○, control). A 2 s conditioning pulse to various potentials followed by a 50 ms rest at − 100 mV was applied. The peak Na current was normalized to its maximal value (the first peak current in this case) in the absence or presence of drugs (100 μM).

The recovery rate of Na channels from the slow inactivation in the presence of the drugs appears also to be responsible for the drug-induced use-dependent block. To examine the use-dependency arising solely from the slow inactivation, we have eliminated the accumulation of block from the resting and the fast inactivation block of Na channels by using a long gap, 300 ms at − 100 mV, between pulses. Under these conditions, the control show no accumulation of block during the 9 consecutive pulses. This is consistent with our analysis that the slow inactivated state of the channel in the absence of the drugs recover with a time constant of 225 ± 28 ms, which is too short to survive the 300 ms gap. We have compared the degree of the use-dependent block at the 9th pulse at the two concentrations of the drug. At 50 μM, the use-dependent block was 10 ± 3% for U-49132E and 16 ± 4% for U-49524E. At a concentration of 100 μM, the extent of block by U-49132E was not measurably altered

Table 1 Kinetic parameters for the recovery of Na channels from inactivation states

		U-49132E		*U-49524E*	
Parameters	*Control*	50 μM	100 μM	50 μM	100 μM
A_1	0.85 ± 0.07	0.89 ± 0.05	0.76 ± 0.05	0.85 ± 0.07	0.76 ± 0.06
A_2	0.17 ± 0.03	0.19 ± 0.03	0.18 ± 0.04	0.18 ± 0.03	0.19 ± 0.03
τ_1 (ms)	5.9 ± 0.3	6.9 ± 0.3	7.1 ± 0.5	6.9 ± 0.3	8.4 ± 0.8
τ_2 (ms)	225.0 ± 28	582.0 ± 63	722.0 ± 110	914.0 ± 96	5744.0 ± 620

Na channels in N1E 115 cells were inactivated by use of the pulse protocol in Figure 7. The time courses for the recovery of Na channels from inactivated states in the presence of U-49132E and U-49524E at concentrations of 50 and 100 μM were analyzed with a double exponential equation: $I/I_{max} = 1\text{-}A_1{*}\exp(-t/\tau_1)\text{-}A_2{*}\exp(-t/\tau_2)$ where A_1, A_2 are proportional constants and τ_1, τ_2 are the time constants of two phases of the recovery. The data represent the mean of three to nine separate experiments with a standard error.

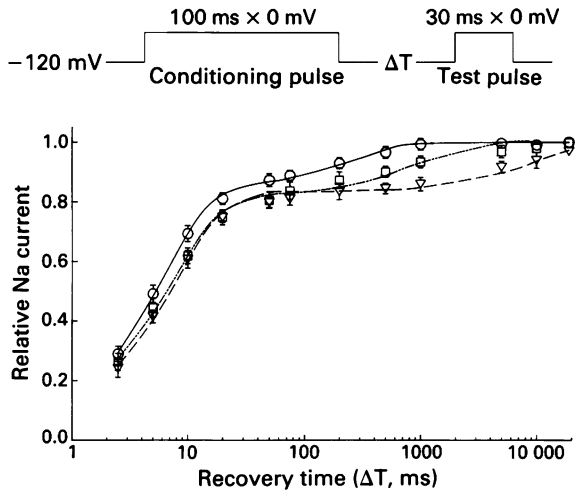

Figure 7 Effects of U-49524E (▽) and U-49132E (□) on the recovery from the inactivated channel (○, control). Cells were first depolarized from − 120 mV to 0 mV for 100 ms, then were allowed various durations at − 120 mV to recover before a test pulse. The peak current was normalized to a maximal value (which was not treated with any conditioning pulse) in the absence or presence of 100 μM drugs.

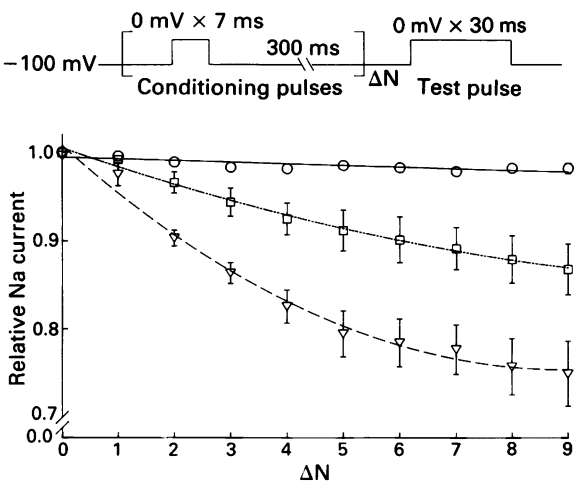

Figure 8 Use-dependent block of the Na channel by U-49524E (▽) and U-49132E (□). Cell was treated with trains (varied from 0 to 9) of conditioning pulses from − 100 to 0 mV before the test pulse. The interval between each conditioning pulse was 300 ms. The peak Na current was normalized to the first one in the absence (○) or presence of drugs (100 μM).

but that by U-49524E increased to 25 ± 4% (Figure 8). These results indicate the importance of the slow recovery rates (τ_2) in the extent of the use-dependent block: the marginal dependence of τ_2 for U-49132E on its concentration may account for the unnoticeable change in the use-dependent block as its concentration was raised from 50 to 100 μM whereas the large increase in the τ_2 for U-49524E (from 914 ± 96 to 5744 ± 620 ms) with the same change in its concentration appears to be responsible to the enhanced use-dependent block.

Discussion

In this study, we have shown that the two benzamide analogues containing either pyrrolidinyl (U-49524E) or piperidinyl (U-49132E) substituent at C2 of the cyclohexyl ring displayed remarkable differences in the anticonvulsant activity against electric shock in mice and their interactions with the voltage-dependent Na channel in neuroblastoma (N1E-115) cells. It appears that U-49524E has a very similar profile to its prototype compound U-54494A in both anticonvulsant activity and Na channel blocking actions whereas U-49132E lacks anticonvulsant activity and has a very weak Na channel blocking action. The determining factors for anticonvulsant activity of a drug *in vivo* are its intrinsic activity and pharmacokinetic parameters. Considering similar physicochemical properties between the two compounds (see below), the lack of anticonvulsant activity *in vivo* by U-49132E could be attributed to a combination of its low potency in the resting block of the Na channel, slow onset of action, and the poor use-dependent block. It appears, therefore, that blocking the Na channel (probably a rapid onset of block) is an important mechanism for the anticonvulsant activity of U-54494A and its active analogues.

The modes of the interaction of two benzamides with the Na channel, nevertheless, were qualitatively similar to each other. The drugs interact with the resting and slowly-inactivated states of the Na channel without affecting activation and inactivation kinetics and the shape of the *I*-V curve. The two agents induce a slow recovery from the inactivated state and lead to use-dependent block which is thought to be crucial for anticonvulsants like phenytoin and carbamazepine (Matsuki *et al.*,1984; Willow *et al.*, 1985).

It is of interest to explore why the piperidinyl group in place of the pyrrolidinyl in the benzamide series markedly delayed the onset of inhibition and reduced the inhibitory potency on the Na channel. It has been suggested that potency in blocking the Na channel may be dependent upon several factors such as molecular weight, hydrophobicity, pK_a, or spacial configuration (Yeh & Ten Eick, 1987; Courtney, 1990). We compared the physicochemical properties of the two compounds. The pK_a values of U-49132E and U-49524E are not expected to be different from that of U-54494A which was 8.4. For instance, the pK_a of piperidine, 11.28, is the same as that of pyrrolidine, 11.27, and the sigma value for the CF3 group, 0.46, is also identical to the sum of *para* and *meta* chloro groups (Perrin *et al.*, 1981). Their hydrophobicity as estimated by Hansch-Leo Fragment Approach in octanol/water system are somewhat different, log p being 4.23 for U-49524E and 4.79 for U-49132E. Given the same pK_a for the both compounds, U-49132E, the more hydrophobic one, would penetrate hydrophobic phase more readily than U-49524E. In fact, however, U-49524E, the more hydrophilic drug, shows the faster rate of action on the Na channels. This suggests that the interaction between the drug and channel is not all hydrophobic but includes a critical hydrophilic action. Another explanation for the different drug effects would be the size effect as suggested by Courtney (1988) for cardiac Na channel blockers. The spacial configuration of a piperidinyl group is considerably more nonplanar and bigger than the pyrrolidinyl group, about 30% larger in a spacial computational model. It appears that drugs reach the receptors through somewhat sterically restricted pathways and that the passage may be more limited for the more hydrophobic and bulkier U-49132E. It is conceivable that the active species of the drugs is the protonated form.

In conclusion, our results support the importance of the ability of benzamide analogues to block the Na channel for their anticonvulsant activity and are in agreement with the steric restriction proposal for Na channel blockers to reach the inactivated state (Courtney, 1988).

The authors are indebted to Dr F.N. Quandt for kindly providing N1E-115 neuroblastoma cells and very helpful consultations during this work and Dr W. Morozowich for his help in obtaining the physicochemical properties of benzamide compounds.

References

CHERNOFF, D.M. & STRICHARTZ, G.R. (1989). Tonic and phasic block of neuronal sodium currents by 5-hydroxyhexano-2',6'-xylide, a neutral lidocaine homologue. *J. Gen. Physiol.*, **93,** 1075–1090.

COURTNEY, K.R. (1988). Why do some drugs preferentially block open sodium channels. *J. Mol. Cell Cardiol.*, **20,** 461–464.

COURTNEY, K.R. (1990). Sodium channel blockers: the size/solubility hypothesis revisited. *Mol. Pharmacol.*, **37,** 855–859.

DUDEWICZ, E.J. & MISHRA, S.N. (1988). *Modern Mathematical Statistics.* New York: Wiley.

HAMILL, O.P., MARTY, A., NEHER, E., SAKMANN, B. & SIGWORTH, F.J. (1981). Improved patch-clamp techniques for high-resolution current recording from cells and cell-free membrane patches. *Pflügers. Arch.*, **391,** 85–100.

MATSUKI, N., QUANDT, F.N., TEN EICK, R.E. & YEH, J.Z. (1984). Characterization of the block of sodium channels by phenytoin in mouse neuroblastoma cells. *J. Pharmacol. Exp. Ther.*, **228,** 523–530.

PERRIN, D.D., DEMPSEY, B. & SERJEANT, E.P. (1981). *pKa Prediction for Organic Acids and Bases.* London: Chapman & Hall.

QUANDT, F.N. & NARAHASHI, T. (1984). Isolation and kinetic analysis of inward currents in neuroblastoma cells. *Neuroscience,* **13,** 249–262.

ROGAWSKI, M.A. & PORTER, R.J. (1990). Antiepileptic drugs: pharmacological mechanisms and clinical efficacy with consideration of promising developmental stage compounds. *Pharmacol. Rev.*, **42,** 223–286.

SCHWARZ, J.R. & GRIGAT, G. (1989). Phenytoin and carbamazepine: potential- and frequency-dependent block of Na currents in mammalian myelinated nerve fibers. *Epilepsia,* **30,** 286–294.

VON VOIGTLANDER, P.F., HALL, E.D., OCHOA, M.C., LEWIS, R.A. & TRIZENBERG, H.J. (1987). U-54494A: a unique anticonvulsant related to kappa opioid agonists. *J. Pharmacol. Exp. Ther.*, **243,** 542–547.

WILLOW, M., GONOI, T. & CATTERALL, W.A. (1985). Voltage clamp analysis of the inhibitory actions of diphenylhydantoin and carbamazepine on voltage-sensitive sodium channels in neuroblastoma cells. *Mol. Pharmacol.*, **27,** 549–558.

YEH, J.Z. & TEN EICK, R.E. (1987). Molecular and structural basis of resting and use-dependent block of sodium current defined using disopyramide analogues. *Biophys. J.*, **51,** 123–135.

ZHU, Y. & IM, W.B. (1991). Block of sodium channel current by anticonvulsant U-54494A in mouse neuroblastoma cells. *J. Pharmacol. Exp. Ther.*, (in press).

(Received October 21, 1991
Revised January 6, 1992
Accepted January 9, 1992)

Br. J. Pharmacol. (1992), **106**, 55–60 © Macmillan Press Ltd, 1992

Studies on curare-like action of 2,2′,2″-tripyridine in the mouse phrenic nerve-diaphragm

*,[1]S.Y. Lin-Shiau, K.S. Hsu & W.M. Fu

Institutes of Pharmacology and *Toxicology, College of Medicine, National Taiwan University, Taipei, Taiwan

1 The curare-like action of 2,2′,2″-tripyridine (a synthetic by-product of the herbicide, paraquat) was studied in mouse phrenic nerve-diaphragm preparation. The inhibition by 2,2′,2″-tripyridine of nerve-evoked twitches was dependent on the concentration, ranging from 1 to 100 μM, which had no significant effect on the twitch amplitudes evoked by direct muscle stimulation.

2 The twitch inhibition by 2,2′,2″-tripyridine was reversible and could be antagonized by anti-cholinesterase agents such as neostigmine, physostigmine as well as ecothiophate.

3 Pretreatment with either 0.7 μM (+)-tubocurarine or 2.2 μM succinylcholine shifted the concentration-inhibition curve of 2,2′,2″-tripyridine to the left.

4 2,2′2″-Tripyridine inhibited not only acetylcholine-induced contracture of the denervated mouse diaphragm but also that of the chick biventer cervicis muscle. Like (+)-tubocurarine, 2,2′,2″-tripyridine protected the twitches from the inhibition by α-bungarotoxin and also specifically inhibited the binding of [^{125}I]-α-bungarotoxin to the mouse diaphragm. All of these findings indicate that 2,2′,2″-tripyridine possesses curare-like action and inhibits the muscle contractions through binding to postsynaptic acetylcholine receptors.

5 The postsynaptic inhibition exhibited by 2,2′,2″-tripyridine was also implicated in the tetanic fade, a decrease in the amplitude of miniature endplate potential (m.e.p.p.) and endplate potential (e.p.p.).

6 The clinical implication of these findings is that 2,2′,2″-tripyridine may be involved in the cause of respiratory failure in paraquat-intoxicated workers since 2,2′,2″-tripyridine is a by-product of paraquat synthesis.

Keywords: 2,2′,2″-Tripyridine; curare-like action; α-bungarotoxin binding; nicotinic acetylcholine receptor

Introduction

2,2′,2″-Tripyridine is a pyridine derivative (Figure 1) which has been found to be a synthetic by-product of the herbicide paraquat. Epidemiological studies showed that the incidence of skin cancer of paraquat manufacturers was much higher than that of the general population in Taiwan (Wang *et al.*, 1987). We have identified 2,2′,2″-tripyridine in the crude products of paraquat and found it to be a strong mutagen (Kuo *et al.*, 1986; Lin *et al.*, 1988). In addition, 2,2′,2″-tripyridine was more potent than paraquat in producing carcinogenic action and DNA damage (Jennette *et al.*, 1974; Lin *et al.*, 1988). Although 2,2′,2″-tripyridine has long been known to be a metal chelating agent derived from 1,10-phenanthroline (Howe-Grant *et al.*, 1976), the pharmacological actions of 2,2′,2″-tripyridine have not been well characterized.

In this paper, we have investigated the effects of 2,2′,2″-tripyridine on muscle contraction and transmitter release in the mouse phrenic nerve-diaphragm preparation. The results show that 2,2′,2″-tripyridine is a specific antagonist of nicotinic acetylcholine receptors comparable to (+)-tubocurarine. The findings suggest the possible involvement of 2,2′,2″-tripyridine in the respiratory failure of paraquat-intoxicated workers.

Methods

Mouse phrenic nerve-diaphragm preparation

Phrenic nerve-hemidiaphragm preparations were isolated from ICR strain mice (20–30 g) according to the method of Bülbring (1946). The muscle preparation was suspended in 10 ml of modified Krebs solution (composition in mM: NaCl 130.6, KCl 4.8, $MgSO_4$ 1.2, $NaHCO_3$ 12.5, $CaCl_2$ 2.5 and glucose 11.1) maintained at 37.0 ± 0.5°C and oxygenated with 95% O_2 and 5% CO_2. The phrenic nerve was stimulated with 0.05 ms rectangular pulses at the frequencies indicated. Muscle contractions were recorded via an isometric transducer (Grass FT.03) on a Grass Model 7 polygraph.

Chick biventer cervicis nerve-muscle preparations

Chicks aged 3–5 days were used in all experiments. The biventer cervicis nerve-muscle preparation was isolated according to the method of Ginsborg & Warriner (1960). The muscle was suspended in 10 ml of modified Krebs solution which was constantly gassed with 95% O_2 + 5% CO_2 at 37.0 ± 0.5°C. The nerve was stimulated through the tendon with supramaximal rectangular pulses of 0.05 ms at a rate of 0.2 Hz. The contraction of the muscle was recorded isometrically with a force-displacement transducer (Grass FT.03) on a Grass Model 7 polygraph.

Intracellular recordings

Conventional microelectrode recording techniques (Fatt & Katz, 1951) were used. Glass microelectrodes filled with 3 M

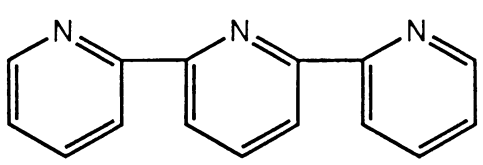

Figure 1 Chemical structure of 2,2′,2″-tripyridine.

[1] Author for correspondence.

KCl had resistances in the range of 3–10 MΩ. The mouse diaphragm was placed in modified Krebs solution at 37.0 ± 0.5°C and oxygenated with 95% O_2 + 5% CO_2. A high impedance amplifier (WPI) and Hitachi V-352 oscilloscope were used for recordings. The amplitude and frequency of miniature endplate potentials (m.e.p.ps) were measured by conventional techniques and recorded with a Data 6100 waveform analyzer. The amplitude of endplate potentials (e.p.ps), elicited at 1 Hz was determined in a modified Krebs solution containing 0.3 mM Ca^{2+} and 1.4–2.2 mM Mg^{2+}.

[^{125}I]-α-bungarotoxin binding studies

The binding of [^{125}I]-α-bungarotoxin was studied in the mouse diaphragm preparations. The preparations were incubated with [^{125}I]-α-bungarotoxin at 37.0 ± 0.5°C for 3.5 h in the presence or absence of various concentrations of 2,2',2''-tripyridine. It was then washed repeatedly with 5 ml modified Krebs solutions for 5 min duration, and with three changes of bathing solution. The treated diaphragms were trimmed, blotted with filter paper and weighed. The level of radioactivity was measured on a gamma counter (LKB 1282).

Drugs

α-Bungarotoxin was isolated from the venom of *Bungarus multicinctus* by the method described by Lee *et al.* (1972). The homogeneity of the purified toxins was verified by disc gel electrophoresis (David, 1964).

All of the chemical compounds listed above for the test experiments were purchased from Sigma Chemical Company, St. Louis, Missouri, U.S.A. [^{125}I]-α-bungarotoxin was obtained from Amersham, Buckinghamshire, England.

Statistics analysis

Results are given as mean ± s.e.means. Numbers of experiments are indicated by *n*. The significance of difference was evaluated by Student's *t* test. When more than one group was compared with one control, significance was evaluated according to ANOVA. Probability values (*P*) of less than 0.05 were considered to be significant.

Results

Twitch inhibition of mouse diaphragm induced by 2,2',2''-tripyridine

2,2',2''-Tripyridine inhibited the nerve evoked twitches of the mouse diaphragm but had no effect on the twitches evoked by direct muscle stimulations (Figure 2). Anticholinesterase agents such as 0.3 μM neostigmine, 0.4 μM physostigmine and 0.5 μM ecothiophate all completely reversed the twitch inhibition by 2,2',2''-tripyridine (Figure 2b). As shown in Figure 3, the concentration-inhibition curve of 2,2',2''-tripyridine was parallel to those of (+)-tubocurarine and succinylcholine respectively. From these curves, the concentrations of (+)-tubocurarine, succinylcholine and 2,2',2''-tripyridine required for 50% inhibition were estimated to be 0.7, 13 and 48 μM respectively. Pretreatment with a low concentration of either 0.7 μM (+)-tubocurarine or 2.2 μM succinylcholine shifted the concentration-inhibition curve of 2,2',2''-tripyridine to the left in a parallel manner (Figure 4).

Antagonistic action of 2,2',2''-tripyridine on nicotinic acetylcholine receptors

As shown on Figures 5a and b, 2,2',2''-tripyridine inhibited acetylcholine contracture of denervated mouse diaphragm and of chick biventer cervicis muscle in a manner similar to (+)-tubocurarine. The concentration-contracture curves for acetylcholine were shifted in a parallel fashion to the right by

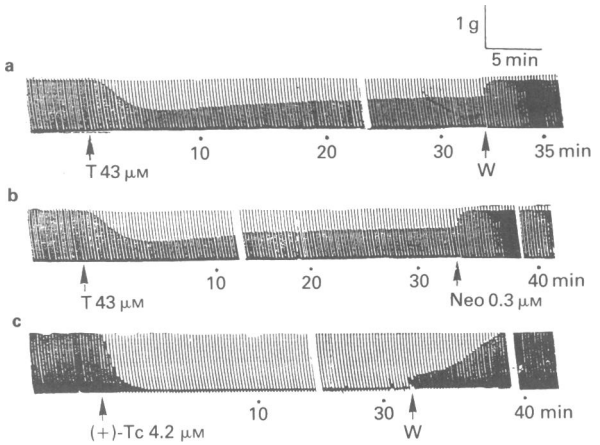

Figure 2 Effects of 2,2',2''-tripyridine and (+)-tubocurarine on twitch responses of mouse diaphragm. (a) Twitch responses to the nerve stimulation were partially inhibited by treatment with 2,2',2''-tripyridine (T, 43 μM), while the twitches to direct muscle stimulation remained unchanged after prolonged incubation of 120 min. The twitches blocked by 2,2',2''-tripyridine could be completely recovered either by washout (W) with modified Krebs solution (a) or (b) by neostigmine (Neo, b). (+)-Tubocurarine ((+)-TC, 4.2 μM) reversibly inhibited the twitches in response to the nerve stimulations (c).

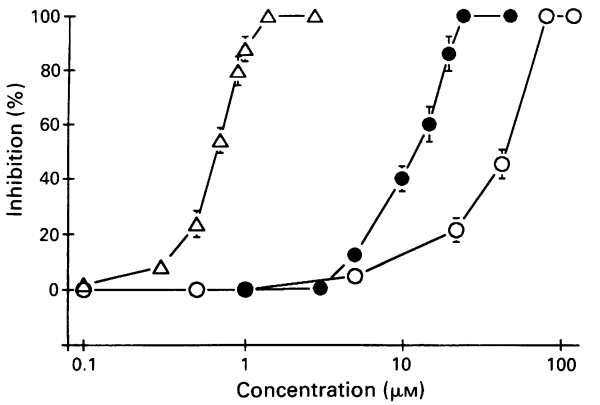

Figure 3 Concentration–dependent inhibition of nerve evoked twitches of the mouse diaphragm induced by 2,2',2''-tripyridine (○, $n = 6–8$), (+)-tubocurarine (△, $n = 6–8$) and succinylcholine (●, $n = 4–6$). The nerve-muscle preparation was suspended in 10 ml of modified Krebs solution and stimulated indirectly. The twitch amplitude was measured 60 min after the addition of various concentrations of inhibitors and caculated as a percentage of the control twitches.

2,2',2''-tripyridine and (+)-tubocurarine (Figure 5b). Furthermore, both 2,2',2''-tripyridine and (+)-tubocurarine protected the muscle contractions of mouse diaphragm from the inhibitory action of α-bungarotoxin (Figure 6). As shown in Table 1, α-bungarotoxin alone inhibited the twitch amplitude by 5.2 ± 2.8%, 23.6 ± 3.7%, 42.8 ± 2.3% and 100% at about 16, 30, 40 and 74 min respectively after the application of the toxin. However, pretreatment with either 22 μM and 43 μM 2,2',2''-tripyridine or 1 μM (+)-tubocurarine enhanced twitch blockade induced by α-bungarotoxin; the time required for complete blockade was found to be 41.7 ± 6.5 min, 33.2 ± 3.7 min and 16.3 ± 3.7 min respectively after addition of the toxin. Although the twitches recovered almost completely by washout immediately after the complete twitch blockade (% twitch restored in Table 1) at the above indicated time, it was considered to be due to an incomplete blockade by α-bungarotoxin. Therefore, some mouse diaphragm preparations

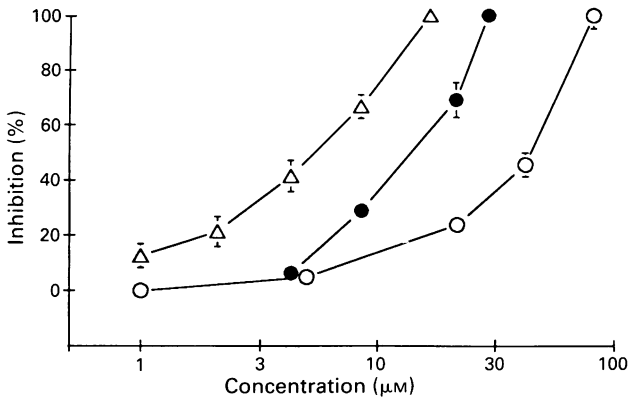

Figure 4 Enhancement by (+)-tubocurarine and succinylcholine of the twitch-inhibitory action of 2,2',2''-tripyridine in the mouse diaphragm. The nerve-muscle preparation was suspended in 10 ml of modified Krebs solution and stimulated indirectly at 0.2 Hz. The preparations were pretreated for 30 min in order to reach a steady twitch amplitude with either 0.7 μM (+)-tubocurarine (Δ, $n = 4-6$) or 2.2 μM succinylcholine (●, $n = 4-6$) prior to the addition of 2,2',2''-tripyridine. Twitch-inhibition by 2,2',2''-tripyridine was estimated as a percentage of the respective control prior to 2,2',2''-tripyridine. 2,2',2''-Tripyridine alone (○, $n = 6-8$).

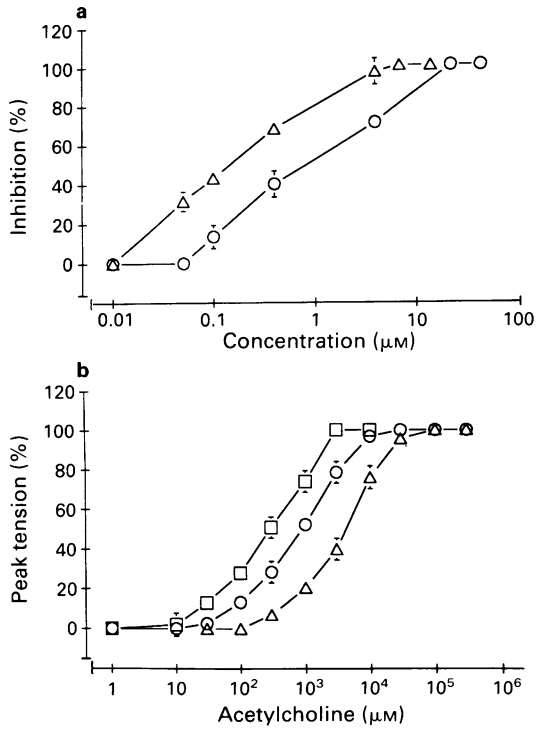

Figure 5 Inhibition by 2,2',2''-tripyridine and (+)-tubocurarine on the dose-response curve of acetylcholine-contracture of denervated mouse diaphragm (a) and the chick biventer cervicis muscle (b). 2,2',2''-Tripyridine (○, $n = 4-6$) and (+)-tubocurarine (Δ, $n = 4-6$) at various concentrations were applied to denervated mouse diaphragm for 30 min. The acetylcholine (0.1 mM)-induced contracture was then recorded and calculated as a percentage inhibition of the contracture prior to the addition of 43 μM 2,2',2''-tripyridine or 7 μM (+)-tubocurarine.

undergoing similar treatments were left in contact with the toxin plus either 2,2',2''-tripyridine or (+)-tubocurarine for 75 min after the application of the toxin (delay twitch recovery as indicated on Table 1). It was clearly shown that the blockade by α-bungarotoxin alone could not be reversed

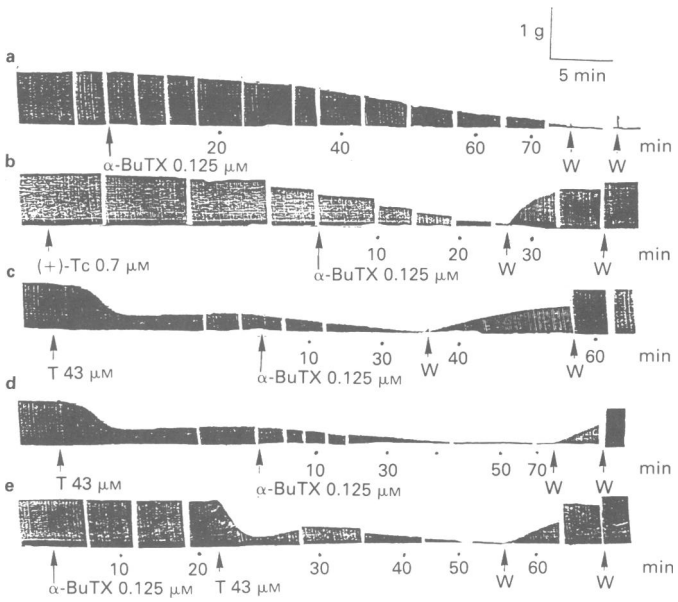

Figure 6 Protection by (+)-tubocurarine and 2,2',2''-tripyridine from the irreversible inhibition on twitches of mouse diaphragm induced by α-bungarotoxin. The phrenic nerve of mouse diaphragm was electrically stimulated and the contraction of the diaphragm was recorded isometrically. The irreversible twitch inhibition was produced by α-bungarotoxin (α-BuTX, 0.125 μM), (a). Pretreatment with either (+)-tubocurarine (b) or 2,2',2''-tripyridine (c) completely restored the twitches inhibited by α-BuTX even when washout is carried out 30 min after complete twitch-inhibition, (d). The reversal of twitch-inhibition is also exhibited by the application of 2,2',2''-tripyridine 20 min after α-bungarotoxin, (e). W denotes washout with modified Krebs solution.

by washout but pretreatment with either 2,2',2''-tripyridine or (+)-tubocurarine allowed delayed twitch recovery by about 40% and 62% respectively (Table 1). The most prominent effect of 2,2',2''-tripyridine was to inhibit the binding of [^{125}I]-α-bungarotoxin to the mouse diaphragm. The concentration of 2,2',2''-tripyridine required for 50% inhibition on the binding of [^{125}I]-α-bungarotoxin was 48 μM which was comparable to that for 50% inhibition of nerve-evoked twitches (Figure 7).

Effects of 2,2',2''-tripyridine on tetanic contraction, m.e.p.ps and e.p.ps

As shown on Figure 8a, 2,2',2''-tripyridine progressively inhibited the tetanic contractions. By contrast, the control tetanic contractions remained sustained without fading. (+)-Tubocurarine produced a similar tetanic fade (Figure 8b). On the other hand, 2,2',2''-tripyridine inhibited the single twitches dependent on the frequency of electrical stimulations; the higher the stimulation frequency was, the greater the inhibition that was produced (Figure 9). Moreover, 2,2',2''-tripyridine reduced the frequency and amplitude of miniature endplate potentials (m.e.p.ps) and endplate potentials (e.p.ps), but did not change the resting membrane potential (Table 2).

Discussion

In this paper, we have shown that 2,2',2''-tripyridine preferentially inhibited the nerve-evoked twitches of the mouse diaphragm and left the muscle-evoked twitches unaffected, indicating that 2,2',2''-tripyridine might either inhibit acetylcholine release from motor nerve terminals or antagonize the postsynaptic acetylcholine receptors. Evidence obtained from this study suggests that 2,2',2''-tripyridine pos-

Table 1 Twitch inhibition by α-bungarotoxin in mouse diaphragm treated with either 2,2',2''-tripyridine or (+)-tubocurarine

Treatment	*Conc.* (μM)	*Time to twitch block* (min)	*Twitch restored* (%)	*Delayed twitch recovery* (%)
α-Bungarotoxin	0.125	74.1 ± 3.6 (48)	—	0
α-Bungarotoxin + 2,2',2''-Tripyridine	0.125 22	41.7 ± 6.5* (21)	94.2 ± 2.3* (10)	38.8 ± 4.7* (11)
	43	33.2 ± 3.7* (38)	97.2 ± 6.5* (28)	39.2 ± 4.1* (10)
α-Bungarotoxin + (+)-tubocurarine	0.125 1	16.3 ± 3.7* (8)	98.2 ± 3.4* (4)	62.3 ± 6.7* (4)

Data are presented as means ± s.e.means.
The twitches of the mouse diaphragm in the modified Krebs solution were evoked by electrical stimulations of the phrenic nerve. 2,2',2''-Tripyridine (43 μM, $n = 34$) and (+)-tubocurarine (1 μM, $n = 6$) alone did not produce neuromuscular blockade after 3 h of treatment and the partial twitch inhibition is reversible after washout. 'Twitch restored' and 'Delayed twitch recovery' are defined as the recovery of twitches by washout of the toxins immediately or 30–60 min after the neuromuscular blockade produced by α-bungarotoxin in the presence or absence of either 2,2',2''-tripyridine or (+)-tubocurarine.
The numbers in parentheses are the number of experiments.
*$P < 0.05$ as compared with control.

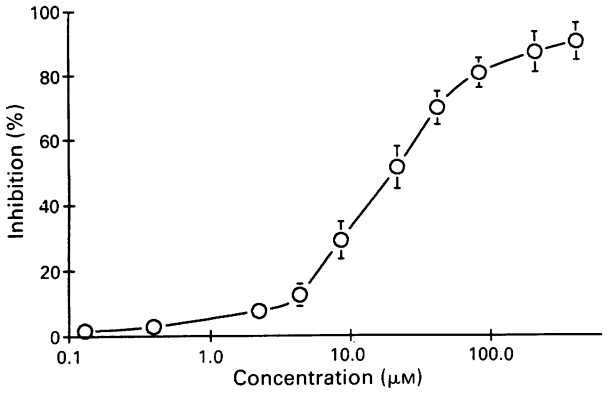

Figure 7 Concentration-inhibition curve of 2,2',2''-tripyridine on [^{125}I]-α-bungarotoxin binding to the mouse diaphragm. Data are presented as mean ± s.e.means (vertical bars, $n = 6–8$). The mouse diaphragm was incubated with [^{125}I]-α-bungarotoxin plus various concentrations of 2,2',2''-tripyridine at 37 ± 0.5°C for 3.5 h. The inhibition was calculated as a percentage of the specific binding of [^{125}I]-α-bungarotoxin in the absence of 2,2',2''-tripyridine.

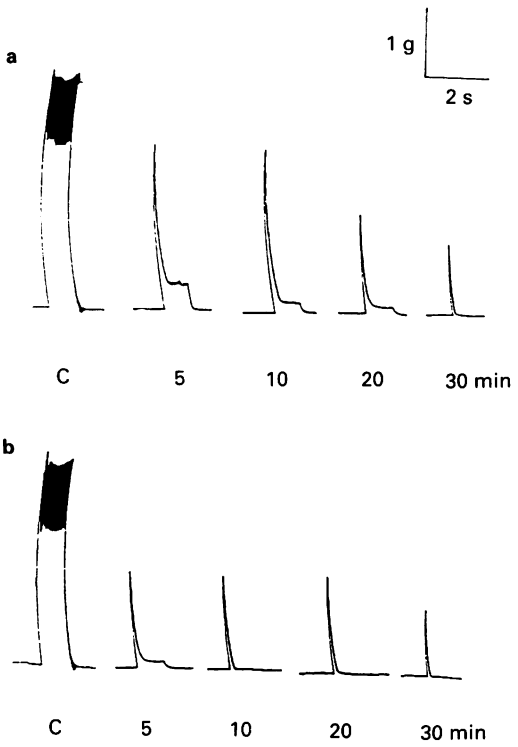

Figure 8 Inhibition by 2,2',2''-tripyridine and (+)-tubocurarine of the tetanic contraction of the mouse diaphragm. The phrenic nerve of the mouse diaphragm was stimulated (50 Hz, 1 s pulse duration) every 30 s in modified Krebs solution. The five successive panels show the tetanic responses of control (C) and those treated with either 43 μM 2,2',2''-tripyridine (a) or 1 μM, (+)-tubocurarine (b) for various time intervals.

sesses a curare-like action: 2,2',2''-tripyridine directly inhibited acetylcholine-contracture of the denervated mouse diaphragm and chick biventer cervicis muscle. Like (+)-tubocurarine, 2,2',2''-tripyridine shifted the concentration-contracture curve of acetylcholine to the right in a parallel manner. Pretreatment with a low concentration of either 0.7 μM (+)-tubocurarine or 2.2 μM succinylcholine potentiated the inhibitory action of 2,2',2''-tripyridine on the nerve-evoked twitches and also shifted its concentration-inhibition to the left in a parallel manner. Based on these findings together with the fact that both (+)-tubocurarine and succinylcholine are known to be an antagonist and an agonist respectively of the nicotinic acetylcholine receptors (Paton & Zaimis, 1952; Liley & North, 1953), it is proposed that 2,2',2''-tripyridine is a competitive inhibitor of nicotinic acetylcholine receptors.

α-Bungarotoxin which was isolated from the venom of *Bungarus multicinctus* is known to be a specific irreversible antagonist of nicotinic acetylcholine receptors (Lee & Chang, 1966). Pretreatment with (+)-tubocurarine protected the nicotinic acetylcholine receptors from the binding of α-bungarotoxin (Miledi *et al.*, 1971). Similarly, we have demonstrated that pretreatment of the mouse diaphragm with 2,2',2''-tripyridine and then subsequent application of α-bungarotoxin reversibly blocks the twitches which were resumed after washout, while the paired control treated with α-bungarotoxin alone irreversibly blocked twitches. This finding indicates that the occupation of 2,2',2''-tripyridine on nicotinic acetylcholine receptors excluded the binding of α-bungarotoxin and the subsequent washout of the reversible binding of 2,2',2''-tripyridine allowed muscle contractions to recover. The reversal effect of 2,2',2''-tripyridine could also be shown even when 2,2',2''-tripyridine was applied 20 min after α-bungarotoxin. More direct evidence was obtained by the

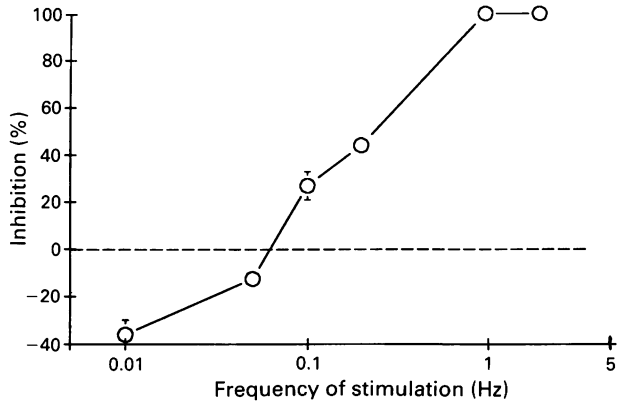

Figure 9 Frequency-dependent inhibition by 2,2',2''-tripyridine of twitch amplitude of mouse diaphragm. The mouse phrenic nerve-diaphragm preparation was suspended in 10 ml of modified Krebs solution and stimulated indirectly on the nerve. Note that the higher the stimulation frequency, the greater was the inhibition by 2,2',2''-tripyridine (43 μM) ($n = 4-6$).

competitive inhibitory action of 2,2',2''-tripyridine on specific binding of radioactive [^{125}I]-α-bungarotoxin. The concentration (48 μM) of 2,2',2''-tripyridine required for 50% inhibition of the binding of [^{125}I]-α-bungarotoxin was coincidently similar to that for 50% inhibition of nerve-evoked twitches as well as that of acetylcholine contractures respectively. All of these results support the theory that the neuromuscular blocking action of 2,2',2''-tripyridine was mainly due to the antagonistic action on nicotinic acetylcholine receptors.

The chemical structures of an antagonist required for binding to nicotinic acetylcholine receptors were claimed to be a mono-quaternary or bistertiary amines (Kitz *et al.*, 1969; Kharkevich & Skoldinov, 1980). The mono-quarternary compounds were claimed to have less stable bonds with acetylcholine receptors of skeletal muscle than the bistertiary compounds. 2,2',2''-Tripyridine posseses three tertiary nitrogen atoms in the pyridine rings so that the bonds between nicotinic acetylcholine receptors and 2,2',2''-tripyridine may be less stable than compounds (e.g. (+)-tubocurarine, succinylcholine) with one or two quaternary nitrogen atoms. The fact that IC_{50} values (concentrations for 50% inhibition on the twitch amplitude) of (+)-tubocurarine, succinylcholine and 2,2',2''-tripyridine were 0.7, 13 and 48 μM respectively supports the contention of a weaker but specific competitive inhibitor of 2,2',2''-tripyridine on nicotinic acetylcholine receptors.

It has been reported that nicotinic acetylcholine receptors were also present on the motor nerve terminals (Miyamato, 1978; Standaert, 1982). The presynaptic acetylcholine receptors were claimed to function as modulators of acetylcholine release from the motor nerve terminals (Bowman, 1980; Bowman *et al.*, 1986; Chang & Hong, 1986). Binding of (+)-tubocurarine to the presynaptic receptors decreased the release of acetylcholine (Wilson, 1982; Chang & Hong, 1986). In this paper, we have found that 2,2',2''-tripyridine decreased not only the frequency and amplitude of m.e.p.ps but also the amplitude of e.p.ps. It was considered that 2,2',2''-tripyridine probably inhibited the presynaptic nicotinic acetylcholine receptors which resulted in the reduction of acetylcholine release. The tetanic fade phenomenon as well as stimulation-frequency dependent inhibition on twitches also implied that 2,2',2''-tripyridine might exert effects on the presynaptic sites. A similar conclusion was reached by Bowman (1980) and Bowman *et al.* (1986) for the presynaptic action of (+)-tubocurarine. This possibility of the presynaptic action of 2,2',2''-tripyridine merits further study.

In conclusion, 2,2',2''-tripyridine inhibited the nerve-evoked twitches of the mouse diaphragm through a curare-like action on postsynaptic nicotinic acetylcholine receptors. This inhibitory action of 2,2',2''-tripyridine on the diaphragm contraction may contribute to the respiratory failure of paraquat intoxicated workers since 2,2',2''-tripyridine was proved to be a synthetic by-product of paraquat from the condensation of a pyridine moiety.

This work was supported by research grants from the National Science Council, Republic of China (NSC79-0421-B002-12Z and NSC80-0421-B002-08Z).

Table 2 Decrease in amplitude of miniature endplate potentials (m.e.p.ps) and endplate potentials (e.p.ps) of the mouse diaphragm induced by 2,2',2''-tripyridine or (+)-tubocurarine

		M.e.p.ps		E.p.ps	
Treatment	*Conc.* (μM)	*Frequency* (event/s^{-1})	*Amplitude* (mV)	*Amplitude* (mV)	*RMP* −mV)
Control		1.21 ± 0.7	1.21 ± 0.5	4.28 ± 0.41	77.8 ± 4.9
2,2',2''-Tripyridine	4.3	0.99 ± 0.08*	0.75 ± 0.04*	2.78 ± 0.19*	76.5 ± 3.7
	22	0.74 ± 0.06*	0.59 ± 0.03*	1.42 ± 0.37*	74.8 ± 3.7
	43	0.49 ± 0.08*	0.47 ± 0.03*	0.73 ± 0.28*	76.8 ± 4.2
(+)-Tubocurarine	0.28	1.20 ± 0.03	0.84 ± 0.07*	3.21 ± 0.13*	75.2 ± 3.7

Data are presented as mean ± s.e.means obtained from 4 preparations, for each preparation: 6–8 endplates were studied.
2,2',2''-Tripyridine and (+)-tubocurarine were added cumulatively and the incubation time was more than 20 min for each concentration added.
The endplate potentials (e.p.ps) were evoked by 1 Hz nerve stimulation on the mouse diaphragm in 0.3 mM Ca^{2+} and 1.4–2.2 mM Mg^{2+} modified Krebs solution.
*$P < 0.05$ as compared with control.

References

BOWMAN, W.C. (1980). Prejunctional and postjunctional cholineceptors at the neuromuscular junction. *Anesth. Analg.*, **59**, 935–943.

BOWMAN, W.C., GIBB, A.J., HARVEY, A.L. & MARSHALL, I.G. (1986). Prejunctional actions of cholinoceptor agonists and antagonists, and of anticholinesterase drugs. In *Handbook Exp. Pharmacol.*, Vol. 79. *New Neuromuscular Blocking Agents. Basic and Applied Aspects.* ed. Kharkevich, D.A., pp. 141–170. Berlin: Springer-Verlag.

BÜLBRING, E. (1946). Observation on the isolated phrenic nerve diaphragm preparation of the rat. *Br. J. Pharmacol. Chemother.*, **1**, 38–61.

CHANG, C.C. & HONG, S.J. (1986). A regenerating release of acetylcholine from mouse nerve terminals treated with anticholinesterase agents. *Neurosci. Lett.*, **69**, 203–207.

DAVID, B.J. (1964). Disc electrophoresis II. Method and application to human serum proteins. *Ann. N.Y. Acad. Sci.*, **121**, 404–459.

FATT, P. & KATZ, B. (1951). An analysis of the endplate potential recorded with an intracellular electrode. *J. Physiol.*, **115,** 320–370.

GINSBORG, B.L. & WARRINER, J. (1960). The isolated chick biventer cervicis nerve muscle preparation. *Br. J. Pharmacol.*, **15,** 410–411.

HOWE-GRANT, M., WU, K.C., BAUER, W.R. & LIPPARD, S.J. (1976). Binding of Platinum and Palladium metallointercalation reagents and antitumour drugs to closed and open DNAs. *Biochemistry*, **15,** 4339–4346.

JENNETTE, K.W., LIPPARD, S.J., VASILIADES, G.A. & BAUER, W.R. (1974). Metallointer-calation reagents. 2-Hydroxyethanethiolato (2,2',2''-tripyridine)- platinum (II) monocation binds strongly to DNA by intercalation. *Proc. Natl. Acad. Sci. U.S.A.*, **71,** 3839–3843.

KHARKEVICH, D.A. & SKOLDINOV, V.P. (1980). On some principles of interaction of curare-like agents with acetylcholine receptors of skeletal muscle. *J. Pharm. Pharmacol.*, **32,** 733–739.

KITZ, R.J., KARIS, J.H. & GINSBARG, S. (1969). A study in vitro of new short-acting nondepolarizing neuromuscular blocking agents. *Biochem. Pharmacol.*, **18,** 871–881.

KUO, M.L., WANG, L.D. & LIN, J.K. (1986). Mutagenicity and cytotoxicity of dipyridyl derivatives and waste water discharged from paraquat manufactory. *J. Chin. Oncol. Soc.*, **2,** 1–8.

LEE, C.Y., CHANG, S.L., KAU, S.T. & LUH, S.Y. (1972). Chromatographic separation of venom of Bungarus multicinctus and characterization of its components. *J. Chromat.*, **72,** 71–81.

LEE, C.Y. & CHANG, C.C. (1966). Modes of actions of purified toxins from elapid venoms on neuromuscular transmission. *Mem. Inst. Butantan Simp.*, **33,** 355–372.

LILEY, A.W. & NORTH, K.A.K. (1953). An electrical investigation of effects of repetitive stimulation on mammalian neuromuscular junction. *J. Neurophysiol.*, **16,** 509–527.

LIN, J.K., KUO, M.L., LEE, K.W. & LIN-SHIAU, S.Y. (1988). DNA cleavage effect and cytotoxicity of the waste water discharged from paraquat manufactory. *J. Chin. Oncol. Soc.*, **4,** 1–2.

MILEDI, M., MOLINOFF, P. & POTTER, L.T. (1971). Isolation of the cholinergic receptor protein from *Torpedo* electric tissue. *Nature*, **233,** 599–603.

MIYAMATO, M.D. (1978). The actions of cholinergic drugs on motor nerve terminals. *Pharmacol. Rev.*, **29,** 221–237.

PATON, W.D.M. & ZAIMIS, E. (1952). The methonium compound. *Pharmacol. Rev.*, **4,** 219–253.

STANDAERT, F.G. (1982). Release of transmitter at the neuromuscular junction. *Br. J. Anaesth.*, **54,** 131–145.

WANG, J.D., LI, W.M., HU, F.C. & HU, K.H. (1987). The occupational risk and the development of premalignant skin lesions among paraquat manufacturers. *Br. J. Indust. Med.*, **44,** 196–200.

WILSON, D.F. (1982). Influence of presynaptic receptors on neuromuscular transmission in rat. *Am. J. Physiol.*, **242,** C366–C372.

(Received November 13, 1991
Revised January 9, 1992
Accepted January 10, 1992)

Br. J. Pharmacol. (1992), **106**, 61–66 © Macmillan Press Ltd, 1992

Combined dose-ratio analysis of cholecystokinin receptor antagonists, devazepide, lorglumide and loxiglumide in the guinea-pig gall bladder

*[1]L.A. Bishop, V.P. Gerskowitch, R.A.D. Hull, N.P. Shankley & J.W. Black

James Black Foundation, 68 Half Moon Lane, London SE24 9JE and *Department of Analytical Pharmacology, King's College School of Medicine & Dentistry, The Rayne Institute, 123 Coldharbour Lane, London SE5 9NU

1 Interactions between cholecystokinin octapeptide (CCK-8) and CCK_A-receptor antagonists derived from benzodiazepines (devazepide) and glutamic acid (lorglumide and loxiglumide) have been examined in an improved bioassay using the guinea-pig, isolated, gall bladder preparation.

2 The presence of CCK_B-receptors in the assay was provisionally-ruled out on the basis of the low potency of pentagastrin in the assay. By applying analyses of both agonism and antagonism, pentagastrin was shown to behave as a partial agonist at the CCK_A-receptor.

3 Devazepide, lorglumide and loxiglumide behaved as simple competitive antagonists of CCK_A-receptors and pK_B values of 9.98, 7.59 and 7.07 were estimated, respectively.

4 Application of a combined dose-ratio analysis to the interactions between CCK-8 and combinations of devazepide/lorglumide and devazepide/loxiglumide indicated that these molecules behave as syntopic, competitive, antagonists at the CCK_A-receptor.

5 We conclude that the guinea-pig gall bladder assay contains a homogeneous population of CCK_A-receptors and offer an explanation for the differences between our results and those obtained recently by Maubach *et al.* (1991) which were taken as preliminary evidence for CCK_A-receptor heterogeneity.

Keywords: Receptor, cholecystokinin; muscle, smooth, gall bladder; pentagastrin; devazepide; lorglumide; loxiglumide

Introduction

The pharmacological classification of cholecystokinin (CCK)/gastrin receptors as CCK_A and CCK_B was proposed on the basis of the behaviour of selective agonists and antagonists in both radioligand binding studies and functionally-intact bioassays (see Woodruff & Hughes, 1991). Among the most frequently-used antagonists for testing and developing this classification are the benzodiazepine derivative, devazepide (Evans *et al.*, 1986) and the glutamic acid derivatives lorglumide (Makovec *et al.*, 1987) and loxiglumide (Setnikar *et al.*, 1987). Devazepide, lorglumide and loxiglumide are reported to be selective, competitive, antagonists for CCK_A-receptors with pK_D values of ~ 10.1, 7.7 and 6.5, respectively as compared with pK_D values at CCK_B-receptors of ~ 6.6, 5.6 and 5.0, respectively (Setnikar *et al.*, 1987; Lotti & Chang, 1989). These pK_B values have been estimated on the assumption that the agonist-antagonist interactions are competitive. If these ligands are to be used to prove the homogeneity of hormone receptors, then the assumption that the competitive behaviour is due to mutual exclusivity at a common site, so called syntopic behaviour, must be made.

However, 'competitive' behaviour can be found for example in bioassays involving high efficacy agonists and functional antagonists and in ligand binding assays involving agonists and allosteric antagonists.

There are marked differences in chemical structure and physico-chemical properties between the benzodiazepine and glutamic acid derivatives and the peptide hormone itself. Consequently, it seemed pertinent to question whether these ligands compete for the same site at the CCK_A-receptor. We have applied a combined dose-ratio analysis (Paton & Rang, 1965; Black *et al.*, 1986; Shankley *et al.*, 1988) which, as far as we are aware, provides the only currently available test for behaviour consistent with a syntopic, competitive mechanism of action. The experiments were performed on the guinea-pig gall bladder assay which has conventionally been considered to contain a single population of CCK_A-receptors. We found that it was necessary to improve the existing assay so that it met the generally-accepted criteria for quantitative analysis (Furchgott, 1972; Black & Shankley, 1985). However, during the course of these studies Maubach *et al.* (1991) presented data which, they concluded, provided preliminary evidence for CCK_A-receptor heterogeneity in the guinea-pig gall bladder. Our findings are discussed in the light of their conclusions.

Methods

Guinea-pig gall bladder assay

The assay was based on the method described by La Morte *et al.* (1981). In brief, four longitudinal strips of smooth muscle were dissected from each gall bladder taken from male Dunkin-Hartley guinea-pigs (250–500 g) and suspended in 20 ml organ baths maintained at 29°C ± 0.5 in modified (low Ca^{2+}) Krebs-Henseleit solution (mM: Na^+ 143, K^+ 5.9, Ca^{2+} 0.5, Mg^{2+} 1.2, Cl^- 128, HPO_4^{2-} 1.2, SO_4^{2+} 1.2, D-glucose 10, HCO_3^- 25) and gassed with 95% O_2 and 5% CO_2. Following the application of a single 1 g load, the tissues were allowed to relax until a stable baseline was produced. Tension, expressed in grams, was continuously recorded with an isometric transducer.

Experimental protocols

A stable baseline was achieved after an initial 20–40 min relaxation period at which time the bathing solution was replaced and tissues incubated for a further 60 min period in

[1] Author for correspondence.

the absence of an antagonist or appropriate vehicle. In preliminary studies it was found, following a primary CCK-8 concentration-effect (E/[A]) curve, that there was a residual degree of CCK_A-receptor stimulation even though the tissue had been subject to multiple washes (6 washes at 5 min intervals). Therefore, only a single, cumulative, agonist E/[A] curve was obtained in each tissue. Experiments were allocated to a randomised block design so that 4–8 replicates were obtained for each treatment group.

Data analysis

Logistic curve-fitting E/[A] data from individual preparations were fitted to a general logistic function to provide estimates of the midpoint slope parameter (p), midpoint location ($\log[A_{50}]$) and upper asymptote (α) of the curves. These parameters, expressed as mean ± s.e.mean, were used for subsequent analysis and display of data (see Black & Shankley, 1985 for details).

Competitive analysis Competitive analysis was performed according to the procedure described previously (Black *et al.*, 1985a). When no significant differences in values of p and α were found by one-way ANOVA, then the $\log[A_{50}]$ values in the absence and presence of antagonist (B) were directly fitted to the following derivation of the Schild equation,

$$\log[A_{50}]_B = \log[A_{50}] + \log\left(1 + \frac{[B]^b}{10^{\log K_B}}\right).$$

When the Schild slope parameter (b) was not significantly different from unity, then the data were re-fitted with b constrained to unity so that the antagonist equilibrium dissociation constant could be estimated as $\log K_B \pm$ s.e. For purposes of display, conventional Schild plots have been constructed with slopes of unity which intersect the abscissa scale at the pK_B calculated by the method above.

Combined dose-ratio analysis This analysis was performed according to the procedure developed by Shankley *et al.* (1988). In brief, when two antagonists act syntopically, that is, at the same site, then their combined dose-ratio is given by:

$$r_{(B+C)} = r_B + r_C - 1$$

where r_B and r_C are the dose-ratios obtained independently in the presence of the antagonists B and C, respectively. This relationship can be re-written in terms of the experimentally-estimated $\log[A_{50}]$ values,

$$S_A = \log[A_{50}]_{B+C} - \log([A_{50}]_B + [A_{50}]_C - [A_{50}]),$$

where S_A is the test statistic for the model which will have a value of zero when the data comply with the model. Similarly, when two antagonists act independently, that is, allotopically, their combined dose ratios multiply,

$$r_{(B+C)} = r_B.r_C$$

This relationship may also be expressed in terms of $\log[A_{50}]$ values,

$$S_M = \log[A_{50}]_{B+C} - \log[A_{50}]_B - \log[A_{50}]_C + \log[A_{50}],$$

so that S_M, the test statistic, will have a value of zero when the data complies with this model.

Analysis of agonism The agonism expressed by pentagastrin was analysed by direct model-fitting of the concentration-effect curve data to the following equation which describes the behaviour of an agonist in a single receptor-effector system (Black & Leff, 1983):

$$E = \frac{E_M[A]^n\tau^n}{(K_A + [A])^n + [A]^n\tau^n}$$

The fit was performed using the BMDP derivative-free, non-linear regression, programme (Dixon, 1990) on a VAX 3200 computer. The parameters for the maximum effect (E_M) and the slope parameter of the transducer function (n) were constrained to numeric values (see Results) and estimates made of the equilibrium dissociation constant (K_A) and the operational efficacy (τ) (for further details see Black *et al.*, 1985b).

Compounds

Compounds were obtained and prepared as follows: the sulphated octapeptide of cholecystokinin (CCK-8) and pentagastrin were obtained from Cambridge Biochemicals Ltd., UK. CCK-8 was dissolved in 10% absolute ethanol to provide a final stock solution of 2 mM concentration. Pentagastrin was dissolved in 100% dimethylformamide (DMF) to give a 100 mM stock. Devazepide, also known as L364718 (a gift from Merck, Sharpe & Dohme Ltd, U.S.A.), was dissolved in DMF to give a 0.12 mM stock concentration. Lorglumide (CR1409) and loxiglumide (CR1505) (Rotta Spa, Milan) were dissolved in an aqueous solution of NaOH (pH = 8) to give a 12 mM stock concentration. All compounds were subsequently diluted in distilled water. The maximum volume of DMF and distilled water added to any one 20 ml organ bath was 20 µl and 500 µl, respectively. Neither the vehicles nor the antagonists were found to produce significant effects on baseline tone.

Results

Analysis of CCK-8 concentration-effect (E/[A]) curve data in guinea-pig gall bladder

Assay problems were encountered when cholecystokinin octapeptide (CCK-8) was used as agonist on the guinea-pig gall bladder assay prepared according to the method of La Morte *et al.* (1981) who used it for studying the effects of histamine. Although concentration-dependent responses were obtained, the assay was prone to agonist-induced spontaneous activity and, as shown previously (Nieber *et al.*, 1988), unstable response profiles (Figure 1a). This behaviour made the determination of precise response levels uncertain. In addition, an unacceptably high variation was found in the shape and location ($\log[A_{50}]$) of the E/[A] curves (Figure 1a).

The spontaneous activity was eliminated by reducing the temperature from 37°C to 29°C and by lowering the $[Ca^{2+}]$ from 2.5 mM to 0.5 mM (Figure 1a). A reduction in variability was obtained by the use of very small (3 × 1 mm) strips cut from the body of the gall bladder (Figure 1a). These changes had the effect of reducing the standard deviation about the mean $\log[A_{50}]$ from 0.79 to 0.39 ($n = 21$, $n = 24$, respectively) and increasing the potency of CCK-8 by almost one log unit. Moreover, under the improved assay conditions the E/log[A] curves were consistently monotonic and symmetrical around the $\log[A_{50}]$. Therefore, it was possible, objectively, to analyse the data by fitting it to the three-parameter logistic function (see Methods) to obtain the parameter values like those shown in Table 1.

Analysis of pentagastrin concentration-effect (E/[A]) curve data in guinea-pig gall bladder

CCK-8 is reported to be a powerful stimulant of not only CCK_A-receptors but also CCK_B-receptors (Lotti *et al.*, 1986). Therefore, it was possible that the analysis of the antagonists could be confounded by the presence of CCK_B-receptors which might also be coupled to smooth muscle contraction in the gall bladder. This was investigated with pentagastrin as agonist because it is a selective agonist with nM potency in those tissues classified as containing CCK_B-receptors (Lotti *et al.*, 1986) but only µM potency in those now classified as

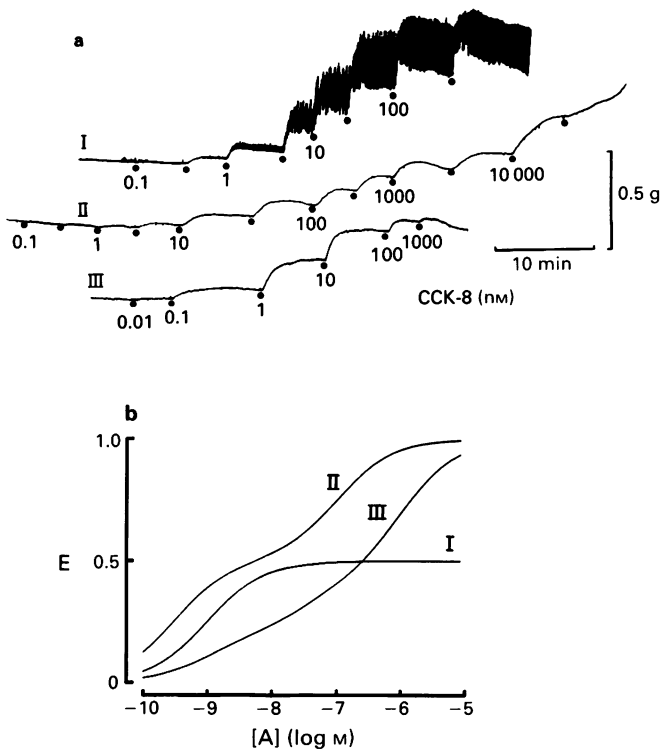

Figure 1 Development of the guinea-pig gall bladder assay. (**a**) Experimental traces showing cholecystokinin octapeptide (CCK-8) E/[A] curves obtained by cumulative dosing. Traces showing, (I) spontaneous activity observed when the assay was prepared according to La Morte *et al.*, 1981, (II) a complex curve following the reduction of both temperature, from 37°C to 29°C, and $[Ca^{2+}]$ from 2.5 mM to 0.5 mM and (III) a monotonic curve following the additional reduction in the size of the preparation (see Results for details) (**b**) Simulations showing theoretical E/[A] curves obtained from a mathematical model which describes the summation of effects from multiple units of tissue within a single bioassay preparation. Each unit is assumed to produce E as a simple rectangular hyperbolic function of [A], so that the total effect is given by,

$$E = \frac{\alpha_1.[A]}{[A_{50}]_1 + [A]} + \frac{\alpha_2.[A]}{[A_{50}]_2 + [A]} + \frac{\alpha_2.[A]}{[A_{50}]_3 + [A]}$$

The potency ($[A_{50}]$) of A and the maximum effect (α) can vary in each unit. In the simulations, assays are assumed to consist of (I) one functional unit ($[A_{50}]_1 = 1$ nM, $\alpha_1 = 0.5$), (II) two functional units with $\log[A_{50}]$ values separated by 2 log units ($[A_{50}]_1 = 0.3$ nM, $[A_{50}]_2 = 100$ nM) and equal contributions to the total effect ($\alpha_1 = \alpha_2 = 0.5$), (III) three functional units with $\log[A_{50}]$ values separated by 1.5 log unit intervals ($[A_{50}]_1 = 1$ nM, $[A_{50}]_2 = 30$ nM, $[A_{50}]_3 = 1$ μM) and unequal contributions to the total effect ($\alpha_1 = 0.20$, $\alpha_2 = 0.20$, $\alpha_3 = 0.60$).

Table 1 Analysis of cholecystokinin octapeptide (CCK-8) and pentagastrin E/[A] curves on the guinea-pig gall bladder assay

		logistic curve-fitting parameters[3]		
	n	$\log[A_{50}]$	p	α (force:g)
CCK-8	4	−8.63 ± 0.13	0.63 ± 0.05	0.42 ± 0.12
Pentagastrin	4	−5.38 ± 0.11	0.87 ± 0.18	0.16 ± 0.05[1]

	Agonism model-fitting[2]	
	pK_A	τ
Pentagastrin	4.86 ± 0.52	0.34 ± 0.24

[1]Significantly different from the value of α for the CCK-8 E/[A] curve, $P < 0.05$. [2]CCK-8 was assumed to be a high efficacy agonist in the assay to permit estimation of pK_A and τ values for pentagastrin (see text for details). [3]See Methods for details.

containing CCK_A-receptors (Williams *et al.*, 1978).

Although pentagastrin produced concentration-dependent increases in tension, it was 10000 fold less potent than CCK-8 and the maximum of the pentagastrin E/[A] curve (α) was significantly less than that obtained with CCK-8 (Figure 2a and Table 1). To determine whether pentagastrin was acting as a partial agonist at CCK_A-receptors, two further experiments were performed. First, pentagastrin E/[A] curves were obtained in the presence of a concentration (0.1 μM) of the selective CCK_A-receptor antagonist, devazepide, which is ~1000 fold higher than its K_B at CCK_A-receptors but ~2.5 fold lower than its reported K_B at CCK_B-receptors. Second, CCK-8 E/[A] curves were obtained in the absence and presence of 100 μM pentagastrin which was pre-incubated for 30 min.

The results (Figure 2b) were consistent with pentagastrin behaving as a partial agonist at CCK_A-receptors; that is, devazepide totally abolished the response to pentagastrin and pentagastrin produced a small (1.13 ± 0.18 log unit) significant shift of the CCK-8 E/log[A] curve in quantitative agreement with expectations for the interaction between a low efficacy and high efficacy agonist competing for a common receptor (Barlow *et al.*, 1967). This conclusion was supported by the results of directly-fitting the individual pentagastrin E/[A] data to the model of agonism described by Black & Leff (1983) (see Methods). A good fit was obtained, as judged-by-eye, and estimates were made of the equilibrium dissociation constant, K_A, and the efficacy parameter, τ, for pentagastrin at the CCK_A-receptor (Table 1 and Figure 2a).

The model fitting was only possible by making the, as yet untestable, assumption that CCK-8 was a high efficacy agonist in the assay. Thus, the value of α for CCK-8 could be taken to be equal to the model parameter for the maximum possible agonist effect in the system (E_M) and the midpoint slope parameter (p) of the CCK-8 concentration-effect curve taken to be equal to the midpoint slope of the transducer function (n). Importantly, the pK_B (5.10 ± 0.18, d.f. = 7), estimated for pentagastrin from the single shift competition experiment using CCK-8 as agonist, was not significantly different from the equilibrium dissociation constant value ($pK_A = 4.86 \pm 0.52$, d.f. = 13) estimated by the analysis of the agonism produced by pentagastrin.

Therefore, the presence of potentially-confounding responses due to activation of CCK_B-receptors could be provisionally ruled-out.

Analysis of competitive antagonism

Devazepide, loxiglumide and lorglumide produced concentration-dependent inhibition of the CCK-8-induced contractions resulting in parallel, rightward, displacement of the E/log[A] curves. Subsequent analysis of the $\log[A_{50}]$ values indicated that the compounds behaved as simple competitive antagonists over the range of concentrations used and pK_B values were estimated (Table 2 and Figure 3).

Combined dose-ratio analysis

The combined dose-ratio analysis experiments were designed to test whether the three antagonists, the glutamic acid derivatives (lorglumide and loxiglumide) and the benzodiazepine derivative (devazepide) acted syntopically at the CCK_A-receptor. The optimum discrimination between the multiplicative and additive models is achieved, theoretically, when large dose-ratios are used in the test. However, in practice, we were restricted to a maximum shift of 2–2.5 log units of the CCK-8 E/[A] curve by the limited solubility of CCK-8 itself. Therefore, antagonist concentrations were chosen which were predicted to produce log dose-ratios of approximately 1.7. Thus, if addition of dose-ratios occurred then the predicted combined log dose-ratio of 2 would have been fully-quantifiable. Clearly, if the dose-ratios multiplied then the CCK-8 E/[A] curves would have been displaced to

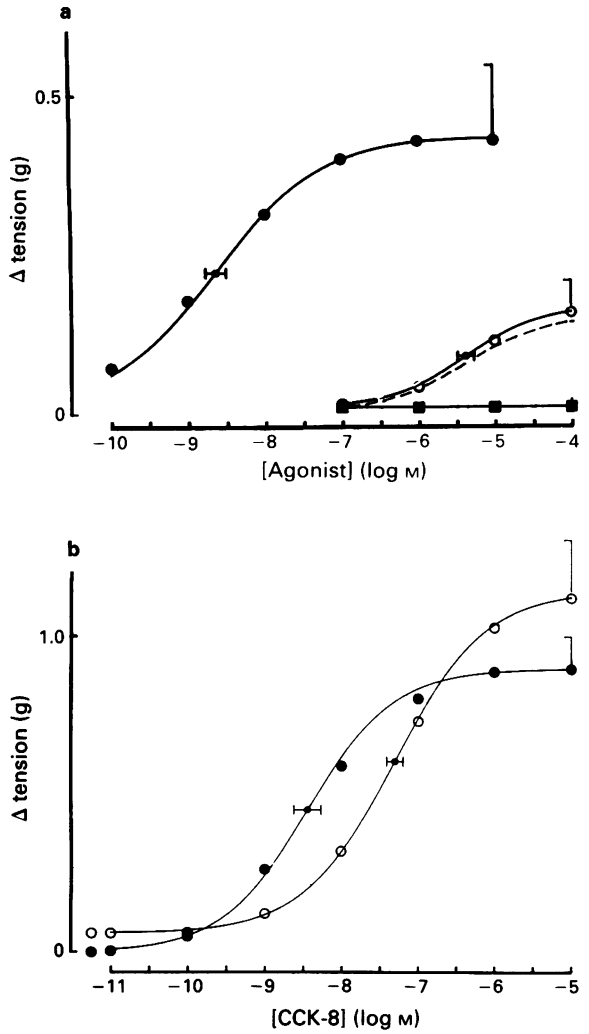

Figure 2 (a) E/[A] curves obtained using cholecystokinin octapeptide (CCK-8) (●), pentagastrin (○) and pentagastrin in the presence of 100 nM L-364718 (■) in the guinea-pig gall bladder assay. Data from individual preparations ($n = 4$) were fitted to a general logistic function and the midpoint slope location ($\log[A_{50}]$) and upper asymptote (α) of the curves expressed as mean ± s.e.mean. The hatched line shown superimposed on the pentagastrin E/[A] data was drawn using the parameters estimated by fitting the Black & Leff (1983) model of agonism (see text for details). (b) CCK-8 E/[A] curves in the absence (●) and presence (○) of 100 μM pentagastrin preincubated for 30 min.

Table 2 Analysis of cholecystokinin octapeptide (CCK-8) antagonist interactions on the guinea-pig gall bladder assay

Compound	*b* (s.e.)	pK_B (s.e.)	*n*
Lorglumide	1.05 (0.23)	7.59 (0.21)	64
Loxiglumide	1.27 (0.16)	7.07 (0.21)	64
Devazepide	1.19 (0.09)	9.98 (0.13)	22

such an extent (log dose-ratio = 3.4) that only threshold CCK-8 responses would have been visible. The data obtained in both experiments were consistent with the additive, syntopic, model and allowed rejection of the multiplicative, allotopic, model (Figure 4 and Table 3). Thus, lorglumide was concluded to be acting syntopically with devazepide which, in turn, was found to act syntopically with loxiglumide.

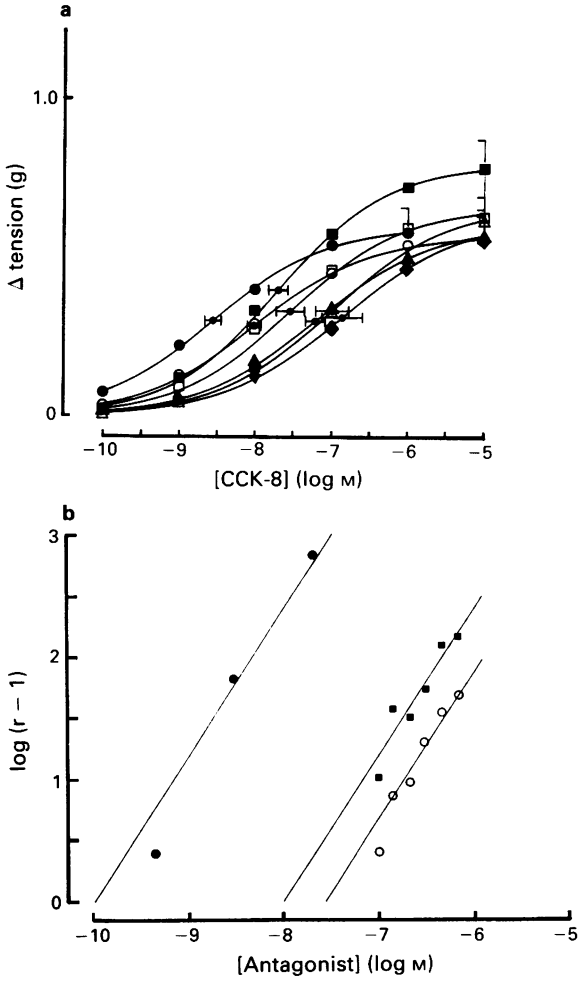

Figure 3 Analysis of competitive antagonism: (a) cholecystokinin octapeptide (CCK-8) E/[A] curves ($n = 6/8$ ± s.e.mean) in the guinea-pig gall bladder assay in the absence (●) and presence of (○) 0.4, (■) 0.6, (□) 1, (▲) 1.5, (△) 2.5, (◆) 4 μM loxiglumide. (b) Schild plots for the interaction between CCK-8 and devazepide (●), loxiglumide (■) and lorglumide (□) on the guinea-pig gall bladder assay.

Discussion

The primary aim of the study was to determine if the benzodiazepine derivative, devazepide, and the glutamic acid derivatives, loxiglumide and lorglumide, act syntopically and competitively at CCK_A-receptors in the guinea-pig gall bladder. Although this preparation has been previously described (La Morte *et al.*, 1981), in practice, we found it was necessary to improve the existing techniques for CCK_A-receptor bioassay. We wanted to apply models of agonism and antagonism, based on the applicability of the Law and Mass Action to the ligand-receptor interactions. These require for simplicity that measurements of effect are made when the agonist response achieves a clearly-defined, sustained plateau. This steady-state condition is usually assumed to indicate an underlying equilibrium condition at the receptors.

In addition to improving the signal-to-noise ratio and reducing spontaneous activity in the tissues to allow accurate, response measurement, the technical changes provided the bonus of increasing the apparent potency of the CCK-8. This allows the behaviour of the antagonists to be studied over a wider range of concentrations, with the E/[A] curves fully-defined, than would have otherwise been possible due to the limited solubility and cost of the peptide agonist, CCK-8.

No evidence for CCK_B-receptors was found in the im-

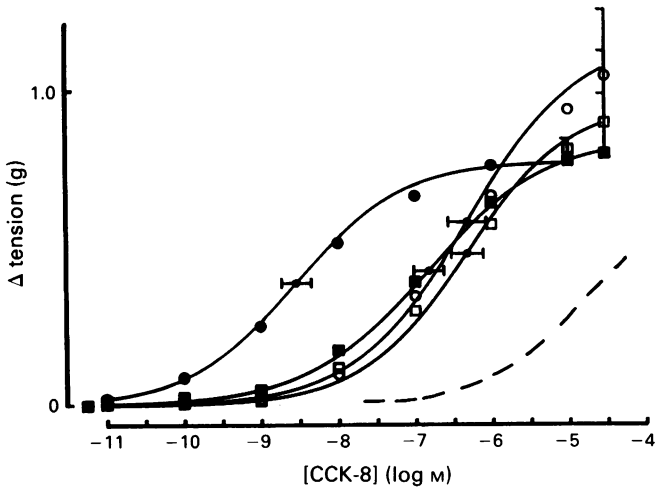

Figure 4 Combined dose-ratio analysis: cholecystokinin octapeptide (CCK-8) E/[A] curves in the absence (●) and presence of 6 nM devazepide (○), 1 μM loxiglumide (■) and a combination of 6 nM devazepide and 1 μM loxiglumide (□). The dashed line shows the location of the CCK-8 E/[A] curve which was predicted by assuming that the antagonists acted independently.

Table 3 Combined dose-ratio analysis

B C (1 μM)	*Devazepide* (6 nM) + *lorglumide* (1 μM)	*Devazepide* (6 nM) + *loxiglumide*
Observed log r_B	1.68	1.20
Observed log r_C	2.18	1.84
Multiplication:		
Expected log $r_{(B+C)}$	3.87	3.04
Addition:		
Expected log $r_{(B+C)}$	2.30	1.92
Observed log $r_{(B+C)}$	2.19	1.99
$S_A \pm$ s.e.	0.11 ± 0.26	0.01 ± 0.21
$S_M \pm$ s.e.	1.68 ± 0.42*	1.14 ± 0.30*

*Significantly different from zero, $P < 0.05$.

proved assay and it was shown that the benzodiazepine derivative, devazepide, and the glutamic acid derivatives, loxiglumide and lorglumide, behaved syntopically and competitively at CCK_A-receptors. From a medicinal chemistry point of view, this result suggests that a molecular model of the CCK_A-receptor requires receptor binding homology for these different chemical structures and the peptide hormone, CCK-8, itself. In addition, we did not find any evidence for CCK_A-receptor heterogeneity as judged by the finding that the CCK-8 E/[A] curves were symmetrical and monotonic in the absence and presence of the antagonists and that the Schild plots were linear over a wide range of antagonist, and, therefore, agonist concentrations.

Recently, Maubach *et al.* (1991) published, in abstract form, data from the analysis of the interactions between, *inter alia*, CCK-8 and two of the antagonists used in this study, devazepide and lorglumide, in an assay also prepared from the guinea-pig gall bladder. In their study, a Schild plot slope significantly greater than unity was obtained with devazepide. The CCK-8 E/[A] curves, in both the absence and presence of the antagonists, were referred to as 'extended' because increases in tension were obtained over 5 log cycles of CCK-8 concentration. Maubach *et al.* (1991) concluded that this was preliminary evidence for CCK_A-receptor heterogeneity. Clearly, our results do not support this view. There are several obvious technical differences between their studies and ours; they incubated antagonists for 30 min rather than 60 min; their experiments were conducted at 37°C whereas we used 29°C; consecutive CCK-8 E/[A] curves were obtained on each preparation rather than a single one; the assay consisted of half gall bladders rather than short, thin strips. Our experience with long strips of tissue suggests that CCK-8 E/[A] curves could be flat with associated high variance if the muscle was taken from a relatively large area of the gall bladder (Figure 1).

We have considered one explanation for these 'extended' curves which may have general applicability to the development and interpretation of other bioassays. Regional variation of hormone receptor concentration is recognised within physiological structures such as the urinary bladder (Taira, 1972). The operational model of agonism (Black & Leff, 1983), in common with other models (Furchgott, 1966), predicts that this variation would have the effect of changing the potency of high efficacy agonists. It was possible to simulate the various profiles of 'extended' CCK E/[A] curves shown in Figure 1 by assuming that the assays prepared from larger pieces of muscle contain several operational units of muscle. Thus, although the receptors in the units are the same, each unit has a different sensitivity to the agonist. The total effect measured in an assay was assumed to be given by the summation of the effects produced by the individual units (Figure 1b). In terms of this model, it is as though, by choosing to use small strips of muscle taken from the central section of the gall bladder, that we have selected a homogeneous muscle unit set with high CCK_A-receptor concentration, so that potent, monotonic CCK-8 E/[A] curves were obtained.

We gratefully acknowledge the skilled technical assistance of Alexander Gerskowitch and Matthew Wilson.

References

BARLOW, R.B., SCOTT, N.C. & STEPHENSON, R.P. (1967). The affinity and efficacy of onium salts on the frog rectus abdominis. *Br. J. Pharmacol.*, **31**, 18–196.

BLACK, J.W., GERSKOWITCH, V.P., LEFF, P. & SHANKLEY, N.P. (1986). Analysis of competitive antagonism when this property occurs as part of a pharmacological resultant. *Br. J. Pharmacol.*, **89**, 547–555.

BLACK, J.W. & LEFF, P. (1983). Operational models of pharmacological agonism. *Proc. R. Soc. B.*, **220**, 141–162.

BLACK, J.W., LEFF, P. & SHANKLEY, N.P. (1985a). Further analysis of anomalous pK_B values for histamine H_2-receptor antagonists on the isolated mouse stomach assay. *Br. J. Pharmacol.*, **86**, 581–587.

BLACK, J.W., LEFF, P., SHANKLEY, N.P. & WOOD, D. (1985b). An operational model of pharmacological agonism: the effect of E/[A] curve shape on agonist dissociation constant estimation. *Br. J. Pharmacol.*, **84**, 561–581.

BLACK, J.W. & SHANKLEY, N.P. (1985). The isolated stomach preparation of the mouse: a physiological unit for pharmacological analysis. *Br. J. Pharmacol.*, **86**, 571–579.

BOCK, M.G., DIPARDO, R.M., EVANS, B.E., RITTLE, K.E., WHITTER, W.L., VEBER, D.F., ANDERSON, P.S. & FREIDINGER, R.M. (1989). Benzodiazepine gastrin and brain cholecystokinin receptor antagonists. *J. Med. Chem.*, **32**, 13–16.

DIXON, W.J. (1990). ed: *BMDP Statistical Software*. Berkeley, Los Angeles & London. University of California Press.

EVANS, E., RITTLE, K.E., BOCK, M.G., DIPARDO, M., WHITTER, W.L., VEBER, D.F., ANDERSON, P.S. & FREIDINGER, R.M. (1986). Design of potent, orally effective nonpeptidal antagonists of the peptide hormone cholecystokinin. *Proc. Natl. Acad. Sci. U.S.A.*, **83,** 4918–4922.

FURCHGOTT, R.F. (1972). The classification of adrenoceptors (adrenergic receptors). An evaluation from the standpoint of receptor theory. *Handb. Exp. Pharmakol.*, **33,** 283–335.

LOTTI, V.J., CHANG, R.S.L., KLING, P.J. & CERINO, D.J. (1986). Evidence that cholecystokinin octapeptide (CCK-8) acts as a potent, full agonist on gastrin receptors for acid secretion in the isolated mouse stomach: lack of antagonism by the specific CCK antagonist asperlicin. *Digestion*, **35,** 170–174.

LOTTI, V.J. & CHANG, R.S.L. (1989). A new potent and selective non-peptide gastrin antagonist and brain cholecystokinin receptor (CCK-B) ligand: L365260. *Eur. J. Pharmacol.*, **162,** 273–280.

MAKOVEC, F., BANI, M., CEREDA, R., CHISTE, R., PACINI, M.A., REVEL, L., ROVATI, L.A. & SETNIKAR, I. (1987). Pharmacological properties of lorglumide as a member of a new class of cholecystokinin antagonists. *Arz.-Forsch.*, **37,** 1265–1268.

MAUBACH, K., PATEL, M. & SPRAGGS, C.F. (1991). Interaction of gastrin/cholecystokinin agonists and antagonists on guinea-pig gall bladder. *Br. J. Pharmacol.*, **104,** 142P.

LA MORTE, W.W., HINGSTON, S.J. & WISE, W.E. (1981). pH-dependent activity of H_1- and H_2-histamine receptors in guinea-pig gall bladder. *J. Pharmacol. Exp. Ther.*, **217,** 638–644.

NIEBER, K., MILENOV, K., RAKOVSKA, A., HENKLEIN, P. & OEHME, P. (1988). Responses of guinea-pig gastric, ileal and gall bladder smooth muscle to desamino-cholecystokinin octapeptide (CCK 7). *Meth. Find. Exp. Clin. Pharmacol.*, **10,** 513–520.

PATON, W.D.M. & RANG, H.P. (1965). The uptake of atropine and related drugs by intestinal smooth muscle of the guinea pig in relation to acetylcholine receptors. *Proc. R. Soc. B.*, **183,** 1–44.

SETNIKAR, I., BANI, M., CEREDA, R., CHISTE, R., MAKOVEC, F., PACINI, M.A., REVEL, L., ROVATI, L.C. & ROVATI, L.A. (1987). Pharmacological characterisation of a new potent and specific nonpolypeptide cholecystokinin antagonist. *Arz.-Forsch.*, **37,** 703–707.

SHANKLEY, N.P., BLACK, J.W., GANELLIN, C.R. & MITCHELL, R.C. (1988). Correlation between log $P_{OCT/H20}$ and pK_B estimates for a series of muscarinic and histamine H_2-receptor antagonists. *Br. J. Pharmacol.*, **94,** 264–274.

TAIRA, N. (1972). The autonomic pharmacology of the bladder. *Annu. Rev. Pharmacol.*, **12,** 197–208.

WILLIAMS, J.A., KORC, M. & DORMER, R.L. (1978). Action of secretagogues on a new preparation of functionally intact, isolated pancreatic acini. *Am. J. Physiol.*, **235,** E517–E524.

WOODRUFF, G.N. & HUGHES, J. (1991). Cholecystokinin antagonists. *Annu. Rev. Pharmacol. Toxicol.*, **31,** 469–501.

(Received November 20, 1991
Revised January 7, 1992
Accepted January 13, 1992)

Br. J. Pharmacol. (1992), **106**, 67–72 © Macmillan Press Ltd, 1992

Stimulation of noradrenaline release in human cerebral cortex mediated by N-methyl-D-aspartate (NMDA) and non-NMDA receptors

Klaus Fink, *Rolf Schultheiß & [1]Manfred Gőthert

Institute of Pharmacology and Toxicology, University of Bonn, Reuterstraße 2 b, D-5300 Bonn 1 and *Clinic of Neurosurgery, University of Bonn, Sigmund-Freud-Str. 25, D-5300 Bonn 1, Germany

1 Human brain cortical slices from patients undergoing neurosurgery for treatment of epilepsy resistant to antiepileptic drugs were used to identify and characterize N-methyl-D-aspartate (NMDA) and non-NMDA receptors mediating stimulation of noradrenaline release. The slices preincubated with [^{3}H]-noradrenaline were superfused with Krebs-Henseleit solution with or without Mg^{2+} (1.2 mmol l^{-1}) and were stimulated by 2-min exposure to NMDA, kainic acid or (**RS**)-α-amino-3-hydroxy-5-methyl-4-isoxazolepropionic acid (AMPA).

2 In slices superfused without Mg^{2+}, NMDA induced a concentration-dependent tritium overflow.

3 The NMDA-evoked tritium overflow was almost abolished by tetrodotoxin (TTX), Mg^{2+} or by omission of Ca^{2+} from the superfusion fluid. 2-Amino-5-phosphonopentanoic acid (AP5; a competitive NMDA receptor antagonist) or dizocilpine (formerly MK-801; an antagonist at the phencyclidine receptor within the NMDA-gated ion channel) inhibited the NMDA-evoked tritium overflow. The stimulatory effect of NMDA was not significantly enhanced by glycine added to the superfusion fluid but was reduced by 7-chlorokynurenic acid (an antagonist at the glycine site coupled to the NMDA receptor).

4 In slices superfused with solution containing Mg^{2+}, kainic acid or AMPA induced a concentration-dependent tritium overflow which was susceptible to blockade by TTX.

5 The kainic acid-evoked tritium overflow was not affected by DL-(E)-2-amino-4-methyl-5-phosphono-3-pentanoic acid (CGP37849; a competitive NMDA receptor antagonist), but was inhibited by 6-cyano-7-nitroquinoxaline-2,3-dione (CNQX; an antagonist at glutamate receptors of the non-NMDA type).

6 The AMPA-evoked tritium overflow was also inhibited by CNQX.

7 It is concluded that NMDA receptors as well as kainate- and AMPA-recognizing non-NMDA receptors stimulate noradrenaline release in the human brain cortex.

Keywords: NMDA receptors; non-NMDA receptors; kainic acid; AMPA, human cerebral cortex; noradrenaline release

Introduction

Previous investigations in rat brain cortical and hippocampal slices provided evidence that the NMDA receptor, i.e. one of the main classes of excitatory amino acid (EAA) receptors at which glutamate is assumed to be the physiological agonist (for reviews see Cotman & Monaghan, 1988; Stone & Burton, 1988; Collingridge & Lester, 1989), mediates a powerful stimulation of noradrenaline release (Jones *et al.*, 1987; Ransom & Deschenes, 1988; Fink *et al.*, 1989; 1990a; Gőthert & Fink, 1989). Furthermore, it has been suggested that noradrenaline release in cortical slices of the rat can also be stimulated via the kainate receptor (Fink & Gőthert, 1990), another EAA receptor class.

EAA receptors, in particular NMDA receptors, seem to be involved in pathological events in the human brain associated with epilepsy, excitotoxic neuronal cell damage after hypoglycaemia or ischaemia, and neurodegenerative disorders such as Huntington's chorea or senile dementia of the Alzheimer type (for review see Meldrum & Garthwaite, 1990). Therefore, the identification of EAA receptors in human cerebral tissue and the elucidation of their functional role are highly desirable. In human *post mortem* neocortical preparations, NMDA receptors have been identified by quantitative autoradiography (Janssen *et al.*, 1989) and by radioligand binding studies (Hubbard *et al.*, 1989; Kornhuber *et al.*, 1989; Ninomija *et al.*, 1990; Procter *et al.*, 1991). In addition, the properties of the NMDA receptors in the human brain have been investigated in few electrophysiological studies on surgically removed cortical tissue (Schwarzkroin *et al.*, 1983; Wuarin *et al.*, 1990). However, *in vitro* studies on EAA-induced transmitter release from human neocortical preparations have not yet been carried out.

In view of the lack of such data, the aim of the present study was to investigate whether NMDA and other EAA receptor agonists stimulate noradrenaline release in the human cerebral cortex and, if so, to determine whether the receptors involved resemble the EAA receptors in the rat brain with respect to their pharmacological properties. A preliminary account of the present data was given at the Autumn Meeting of the German Society of Pharmacology and Toxicology, Berlin 1991 (Fink *et al.*, 1991a).

Methods

Cerebral cortical tissue (temporo-basolateral region) was obtained from 11 male and 19 female patients (age 28.8 ± 2.2 years) who suffered from severe epilepsy resistant to antiepileptic drugs and, hence, underwent neurosurgical treatment. The tissue was plunged into cold (4°C) Krebs-Henseleit solution (composition see below) immediately after resection. The patients, premedicated with flunitrazepam and atropine, had been anaesthetized with thiopentone (for introduction), fentanyl and enflurane or isoflurane (for maintenance). Pancuronium had been injected to achieve muscular relaxation.

[1]Author for correspondence.

The cerebral cortical specimens used for preparation of the slices for the present experiments were part of the tissue which had to be removed for therapeutic reasons. The slices (0.3 mm thick, 12 mm diameter) which were prepared within 40 min after removal of the tissue were incubated for 30 min in Krebs-Henseleit solution (37°C) composed as follows (mmol l^{-1}): NaCl 118, KCl 4.8, $NaHCO_3$ 25, KH_2PO_4 1.2, $CaCl_2$ 1.3, $MgSO_4$ 1.2, glucose 11.1, ascorbic acid 0.06, disodium EDTA 0.03 (equilibrated with 95% O_2 and 5% CO_2). During incubation this solution contained 50 nmol l^{-1} [^{3}H]-noradrenaline (specific activity 43.7 Ci mmol l^{-1}). Subsequently, the slices were superfused for 62 min at a flow rate of 0.6 ml min^{-1} with either Mg^{2+}-free Krebs-Henseleit solution (in most of the experiments in which NMDA was used for stimulation) or 'normal' Krebs-Henseleit solution containing Mg^{2+} 1.2 mmol l^{-1} (in experiments in which kainic acid or AMPA was used for stimulation; for chemical name of AMPA, see below). In a few experiments, Ca^{2+} was omitted from the Mg^{2+}-free solution throughout superfusion. Tritium overflow was stimulated by addition of NMDA, kainic acid or AMPA for 2 min after 40 min of superfusion. When the effects of drugs on stimulation-evoked tritium overflow were investigated, they were present from the 20th min of superfusion onward. The superfusate was continuously collected in 5 min samples. At the end of superfusion the radioactivity in the superfusate samples and slices (solubilized with 0.5 ml Soluene) was determined by liquid scintillation counting.

Tritium efflux was calculated as the fraction of the ^{3}H content in the slice at the beginning of the respective collection period (fractional rate of ^{3}H efflux). To quantify effects of drugs on basal efflux, the fractional rate was determined in the sample collected immediately before stimulation. Basal efflux was assumed to decline linearly from the sample before to that 15–20 min after onset of stimulation. Stimulation-evoked ^{3}H overflow was calculated by subtraction of basal from total efflux during the stimulation period and the following 13 min and was expressed as percentage of the tritium content in the slice at the onset of stimulation.

The concentration-response curve for NMDA was fitted to the data points according to a sigmoidal logistic equation by iterative nonlinear regression analysis (Motulsky & Ransnas, 1987). Results are given as means ± s.e.mean of n experiments. A t test for unpaired data was used to compare mean values.

Drugs

The following drugs were used: (−)-[ring-2,5,6-^{3}H]-noradrenaline ([^{3}H]-NA; NEN, Dreieich, FRG); N-methyl-D-aspartate (NMDA), glycine sodium salt, kainic acid, DL-2-amino-5-phosphonopentanoic acid (AP5), tetrodotoxin (TTX; Sigma Chemical Co., St. Louis, MO, U.S.A.); dizocilpine hydrogen maleate (RBI, Natick, MA, U.S.A.); 7-chlorokynurenic acid (7-Cl-KYNA), (RS)-α-amino-3-hydroxy-5-methyl-4-isoxazolepropionic acid (AMPA), 6-cyano-7-nitroquinoxaline-2,3-dione (CNQX; Tocris Neuramin, Buckhurst Hill, England); DL-(E)-2-amino-4-methyl-5-phosphono-3-pentanoic acid (CGP37849; Ciba Geigy Ltd., Basel, Switzerland).

Results

Basal tritium efflux

In control experiments, basal tritium efflux from slices preincubated with [^{3}H]-noradrenaline and superfused with Krebs-Henseleit solution with or without Mg^{2+} gradually decreased with time (results not shown in detail; for representative control values of basal tritium efflux in the two periods of superfusate sampling before stimulation, see Figure 1). Basal tritium efflux was not modified by any of the ionic conditions or drugs investigated in the present study at the concentrations indicated below (results not shown).

NMDA-evoked tritium overflow

In slices superfused with Mg^{2+}-free solution (unless stated otherwise), exposure to NMDA 1 mmol l^{-1} for 2 min induced an increase in tritium efflux which was reversible within 13 min after removal of NMDA (Figure 1). This NMDA-evoked tritium overflow (above basal efflux) was concentration-dependent, with a maximum (1.87% of tissue tritium, corresponding to 0.25 ± 0.004 nCi) at 3 mmol l^{-1} and an EC_{50} value of 112 μmol l^{-1} (Figure 2). Addition of Mg^{2+} 1.2 mmol l^{-1} or TTX 0.3 μmol l^{-1} to the superfusion fluid, or omission of Ca^{2+} ions, almost abolished the NMDA-evoked tritium overflow (Figure 3).

The tritium overflow evoked by NMDA 1 mmol l^{-1} was reduced by AP5 100 μmol l^{-1} and dizocilpine 100 nmol l^{-1} by 68 and 83%, respectively (Figure 3).

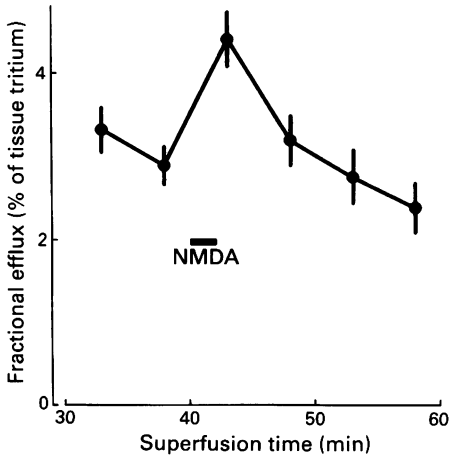

Figure 1 Stimulatory effect of N-methyl-D-aspartate (NMDA) on tritium efflux from human brain cortex slices preincubated with [^{3}H]-noradrenaline and superfused with Mg^{2+}-free medium. Abscissa scale: time after onset of superfusion. Stimulation with NMDA (1 mmol l^{-1}) during the 2 min period indicated by the horizontal bar. Tritium content per slice at the onset of stimulation: 14.5 ± 0.79 nCi. Means with s.e.mean (vertical lines) of 24 experiments.

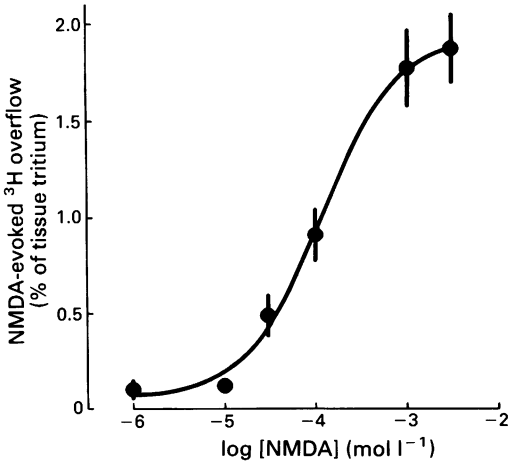

Figure 2 Concentration-response curve for the N-methyl-D-aspartate (NMDA)-evoked tritium overflow from human brain cortex slices preincubated with [^{3}H]-noradrenaline and superfused with Mg^{2+}-free medium. NMDA was added for 2 min after 40 min of superfusion. Means with s.e.mean (vertical lines) of 24 experiments.

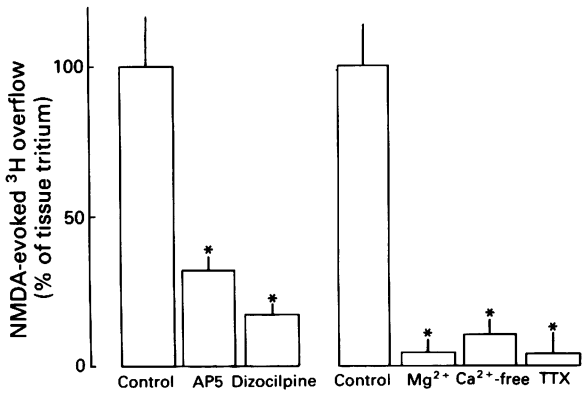

Figure 3 Effect of DL-2-amino-5-phosphonopentanoic acid (AP5), dizocilpine (MK-801), Mg^{2+}, tetrodotoxin (TTX) or omisson of Ca^{2+} on the N-methyl-D-aspartate (NMDA, 1 mmol l^{-1})-evoked tritium overflow from human brain cortex slices preincubated with [^{3}H]-noradrenaline and superfused with Mg^{2+}-free medium. NMDA was added for 2 min after 40 min of superfusion. Mg^{2+} (1.2 mmol l^{-1}) or TTX (0.3 μmol l^{-1}) were added to, and Ca^{2+} was omitted from, the medium throughout superfusion. AP5 (100 μmol l^{-1}) or dizocilpine (100 nmol l^{-1}) was added to the medium from the 20th min of superfusion onward until the end of the experiments. Means with s.e.mean (vertical lines) of 7–13 experiments. *$P<0.01$, compared to the corresponding controls.

Glycine 100 μmol l^{-1} did not significantly modify the NMDA-evoked tritium overflow, whereas 7-Cl-KYNA 100 μmol l^{-1} almost completely inhibited this NMDA-evoked response (Figure 4).

Kainic acid-evoked tritium overflow

In slices superfused with solution containing Mg^{2+} 1.2 mmol l^{-1}, kainic acid concentration-dependently stimulated tritium overflow (Figure 5). The responses induced by kainic acid 0.1 and 1 mmol l^{-1} were considerably lower than those evoked by the same NMDA concentrations (compare Figure 2). CNQX 30 μmol l^{-1} and TTX 0.3 μmol l^{-1} inhibited the kainic acid (1 mmol l^{-1})-evoked tritium overflow by 77 and 72%, respectively, but CGP37849 30 μmol l^{-1} did not alter the response to kainic acid (Figure 6).

AMPA-evoked tritium overflow

The experiments with AMPA were also carried out in slices superfused with solution containing Mg^{2+} 1.2 mmol l^{-1}. AMPA induced a concentration-dependent stimulation of tritium overflow, which was even less pronounced than that induced by kainic acid at equimolar concentration (Figure 7; compare Figure 5). CNQX 30 μmol l^{-1} and TTX 0.3 μmol l^{-1} inhibited the AMPA (1 mmol l^{-1})-evoked tritium overflow by 67 and 83%, respectively (Figure 8).

Discussion

The present study revealed that NMDA, kainic acid and AMPA stimulate tritium overflow from human cerebral cortical slices preincubated with [^{3}H]-noradrenaline. The evoked tritium overflow from cerebral slices preincubated with [^{3}H]-noradrenaline reflects the release of radioactively labelled and unlabelled noradrenaline from the noradrenergic nerve terminals contained in the slices (see Starke, 1977; Chesselet, 1984) and is subsequently referred to as noradrenaline release.

The present study was mainly focussed on release-stimulating NMDA receptors, which have also been investigated more extensively than non-NMDA receptors in rat brain preparations (for references, see Introduction). In one set of experiments with NMDA the ionic composition of the superfusion fluid was modified. The stimulatory effect of NMDA was strongly inhibited when Ca^{2+} was omitted from the superfusion fluid (suggesting a decreased availability of Ca^{2+} ions for stimulus-release coupling) or when the superfusion fluid contained a physiological Mg^{2+} concentration. These results are compatible with the well-known Ca^{2+}-dependence of the NMDA-induced responses (MacDermott *et al.*, 1986) and with the characteristic Mg^{2+}-induced blockade of the NMDA-gated cation channel (Mayer *et al.*, 1984). The Mg^{2+} block is voltage-dependent (Mayer *et al.*, 1984; Nowak *et al.*, 1984). The removal of the Mg^{2+} block by depolarizing agents has been demonstrated for NMDA-induced noradrenaline release in rat brain cortical slices (Fink *et al.*, 1990a).

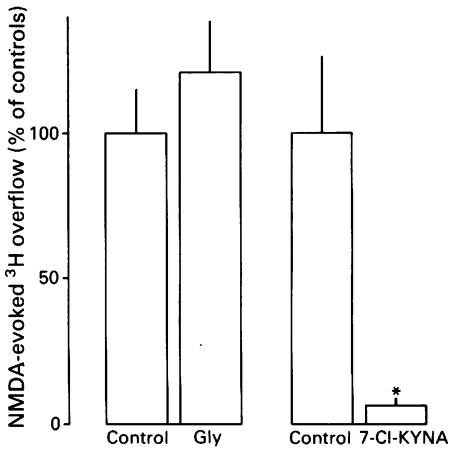

Figure 4 Effect of glycine (Gly, 100 μmol l^{-1}) or of the glycine antagonist 7-chlorokynurenic acid (7-Cl-KYNA; 100 μmol l^{-1}) on the N-methyl-D-aspartate (NMDA, 1 mmol l^{-1})-evoked tritium overflow from human brain cortex slices preincubated with [^{3}H]-noradrenaline and superfused with Mg^{2+}-free medium. Gly or 7-Cl-KYNA was added to the medium from the 20th min of superfusion until the end of the experiments. Means with s.e.mean (vertical lines) of 7–17 experiments. *$P<0.001$, compared to the corresponding controls.

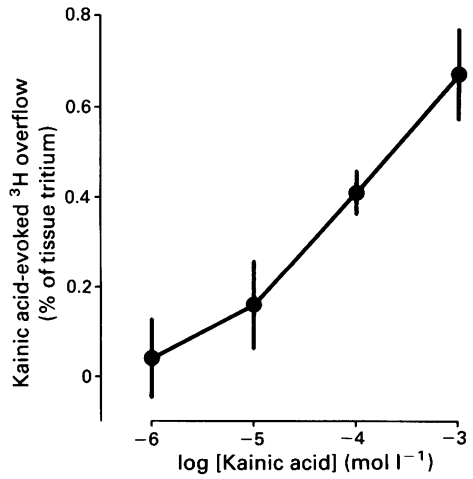

Figure 5 Concentration-response curve for the kainic acid-evoked tritium overflow from human brain cortex slices preincubated with [^{3}H]-noradrenaline and superfused with medium containing Mg^{2+} (1.2 mmol l^{-1}). Kainic acid was added for 2 min after 40 min of superfusion. Means with s.e.mean (vertical lines) of 7–11 experiments.

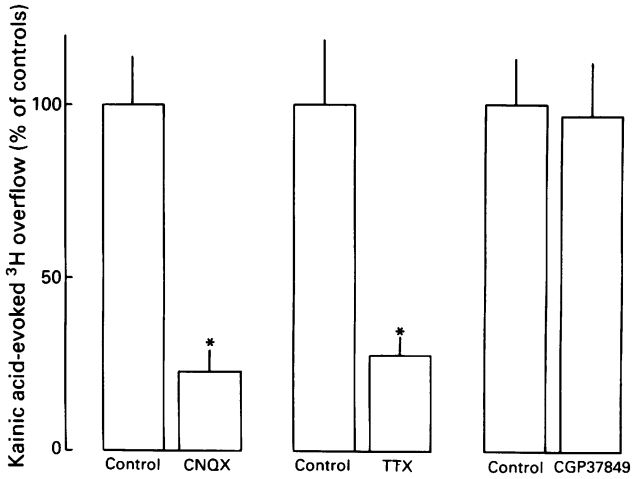

Figure 6 Effect of 6-cyano-7-nitroquinoxaline-2,3-dione (CNQX, 30 μmol l^{-1}), tetrodotoxin (TTX, 0.3 μmol l^{-1}) or DL-(E)-2-amino-4-methyl-5-phosphono-3-pentanoic acid (CGP37849, 30 μmol l^{-1}) on the kainic acid (1 mmol l^{-1})-evoked tritium overflow from human brain cortex slices preincubated with [^{3}H]-noradrenaline and superfused with medium containing Mg^{2+} (1.2 mmol l^{-1}). CNQX, TTX or CGP37849 was added to the medium from the 20th min of superfusion until the end of the experiments. Means with s.e.mean (vertical lines) of 12–16 experiments. *$P<0.01$, compared to the corresponding controls.

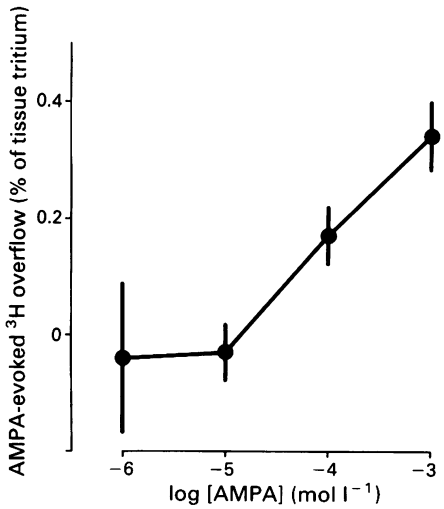

Figure 7 Concentration-response curve for the (RS)-α-amino-3-hydroxy-5-methyl-4-isoxazole propionic acid (AMPA)-evoked tritium overflow from human brain cortex slices preincubated with [^{3}H]-noradrenaline and superfused with medium containing Mg^{2+} (1.2 mmol l^{-1}). AMPA was added for 2 min after 40 min of superfusion. Means with s.e.mean (vertical lines) of 7–8 experiments.

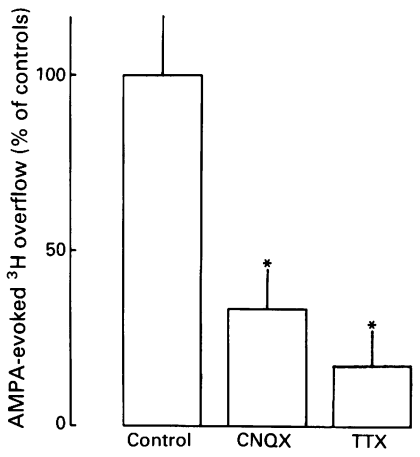

Figure 8 Effect of 6-cyano-7-nitroquinoxaline-2,3-dione (CNQX, 30 μmol l^{-1}) or tetrodotoxin (TTX, 0.3 μmol l^{-1}) on the (RS)-α-amino-3-hydroxy-5-methyl-4-isoxazole propionic acid (AMPA, 1 mmol l^{-1})-evoked tritium overflow from human brain cortex slices preincubated with [^{3}H]-noradrenaline and superfused with medium containing Mg^{2+} (1.2 mmol l^{-1}). CNQX or TTX were added to the medium from the 20th min of superfusion until the end of the experiments. Means with s.e.mean (vertical lines) of 6–11 experiments. *$P<0.05$, compared to the controls.

In the present study, the NMDA recognition site of the NMDA receptor system was characterized by the potency of NMDA in inducing noradrenaline release and by means of AP5, a competitive NMDA receptor antagonist (Watkins *et al.*, 1990). The EC_{50} value of NMDA was almost identical to that previously determined in rat cortical slices and the degree of inhibition by AP5 was also comparable with that in rat cortical slices (Fink *et al.*, 1989). A similar potency of NMDA to that in the present study was also found by other authors who investigated transmitter release in rat brain slices (Gonzales & Woodward, 1990; Woodward & Gonzales, 1990; Sacaan & Johnson, 1990). However, the potency of NMDA in slices was almost 100 times lower than that found in rat cortical synaptosomes (Fink *et al.*, 1990b) and that which corresponds to its K_i value for NMDA binding sites in cerebral membrane preparations (Sills *et al.*, 1991). The possibility had to be considered that this discrepancy may be due to an insufficient equilibration between the superfusion fluid and the slices within the 2 min period of exposure to NMDA. Yet this possibility could be excluded by our previous experiments in rat cortical slices, in which the exposure time was extended to 20 min; the maximum release clearly occurred within the first 2 min followed by a marked continuous decline in the releasing effect in the subsequent 2 min fractions (Fink *et al.*, 1989). Probably the discrepancy in potency of NMDA in slices and synaptosomes is related to additional interacting mechanisms triggered by NMDA in the more complex slice preparation e.g., an attenuation of NMDA-evoked noradrenaline release in slices can be brought about via inhibitory presynaptic receptors on the noradrenergic varicosities. These receptors can be activated by the endogenous agonists released from the corresponding neurones within the slice. Basically it has been shown that the NMDA-evoked noradrenaline release in the rat brain cortex can be inhibited via presynaptic α_2-adrenoceptors and histamine H_3 receptors (Fink *et al.*, 1991b). In contrast, in thin layers of synaptosomes, any released transmitter is washed away so rapidly that it remains subthreshold for presynaptic receptor activation (see Starke *et al.*, 1989).

In the context of comparison between data obtained in human and rat cortical slices it should be noted that in the human slices the maximal tritium overflow, which can be evoked by NMDA, was about 2% of the tritium content in the slice (Figure 2) and, hence, was about 7 times lower than that observed under identical conditions in rat cortical slices (Fink *et al.*, 1989). This discrepancy may reflect species differences and/or it may be related to an impairment of the tissue caused by surgical manipulations and to pathological alterations due to the patient's disease. Quantitatively, such influences have to be considered, but they do not exclude a qualitative analysis of the NMDA receptors (and non-NMDA receptors, see below) in the human cortical tissue.

The NMDA receptor mediating noradrenaline release in human cortical slices also exhibited pharmacological properties which are compatible with the operation of the modulatory phencyclidine (PCP) site within the NMDA gated cation channel. Dizocilpine (MK-801) has high affinity for the PCP site (Lodge & Johnson, 1990). Binding of dizocilpine to this site results in blockade of the cation chan-

nel and, accordingly, in an inhibition of the NMDA-evoked response (Lalies *et al.*, 1988), in the present case of NMDA-evoked noradrenaline release. The degree of inhibition found here with dizocilpine 100 nmol l^{-1} was compatible with its affinity for the PCP site in radioligand binding studies and with its potency in electrophysiological experiments on rat brain cortical slices (Wong *et al.*, 1986).

The glycine site is another well-characterized modulatory site of the NMDA receptor system: presence of endogenous and/or exogenous glycine is an important prerequisite for the manifestation of NMDA-evoked responses (Johnson & Ascher, 1987; Keith *et al.*, 1989; Fink *et al.*, 1990b; Huettner, 1991). When endogenous glycine is present in a given preparation at an amount sufficient to produce a maximal or nearly maximal stimulation of the glycine site, the importance of this site can be disclosed by application of a glycine receptor antagonist which strongly inhibits the response under study, whereas surplus exogenous glycine does not further amplify the NMDA-evoked response (Keith *et al.*, 1989; Craig & White, 1991). In agreement with these findings and considerations, it was observed here that 7-Cl-KYNA, a glycine receptor antagonist (Kemp *et al.*, 1988; Henderson *et al.*, 1990; Huettner, 1991), strongly inhibited the NMDA-evoked noradrenaline release in human cortical slices, whereas exogenous glycine did not significantly increase this NMDA-induced response. In view of the fact that 7-Cl-KYNA has also weak affinity for the NMDA recognition site itself (Kemp *et al.*, 1988), blockade of this site may contribute to the 7-Cl-KYNA-induced inhibition of NMDA-evoked noradrenaline release. However, it is very improbable that such an antagonism at the NMDA recognition site accounts for a major part of this effect, since the 7-Cl-KYNA concentration applied in the present experiments was 1.7 times lower than its IC_{50} in inhibiting [^{3}H]-glutamate binding, but about 200 times higher than its IC_{50} in inhibiting [^{3}H]-glycine binding (Kemp *et al.*, 1988).

Finally we found that TTX almost abolished the stimulatory effect of NMDA on noradrenaline release. The same result was previously obtained in rat brain cortical slices (Fink *et al.*, 1989). The most plausible explanation for this finding is that the NMDA receptor involved is located on an as yet unknown interneurone which releases an excitatory neurotransmitter. The latter, in turn, stimulates noradrenaline release by activating a presynaptic receptor (Fink *et al.*, 1989). However, it should be noted that NMDA receptors were recently also identified on rat brain cortical (Fink *et al.*, 1990b) and hippocampal synaptosomes (Pittaluga & Raiteri, 1990), suggesting that the small tetrodotoxin-resistant component of noradrenaline release in slices corresponds to release evoked by NMDA receptors on the noradrenergic varicosities themselves (Fink *et al.*, 1990b). Analogously, the presence of presynaptic NMDA receptors on the noradrenergic varicosites of the human brain cortex cannot be ruled out by the present experiments on slices; this matter can only be clarified by future experiments on human cortical synaptosomes.

In addition, the present investigation provided evidence that noradrenaline release in the human brain cortex can also be stimulated by non-NMDA receptors. Thus, both kainic acid and AMPA induced noradrenaline release, although Mg^{2+} ions were present in the superfusion fluid at a concentration which almost completely abolished the NMDA-evoked release. Full concentration-response curves for kainic acid and AMPA could not be constructed since these compounds, which were not available to us in sufficient amounts, exhibited a low apparent potency. The involvement of NMDA receptors was further excluded by the inability of CGP37849, a preferential NMDA receptor antagonist (Fagg *et al.*, 1989), to inhibit the kainic acid-evoked noradrenaline release. This antagonist is more potent than AP5 in blocking NMDA receptors (apparent pA_2 in the rat brain cortex 6.25 versus 5.14; unpublished results and Fink *et al.*, 1989, respectively). On the other hand, CNQX, a non-NMDA receptor antagonist (Watkins *et al.*, 1990), inhibited the kainic acid- and AMPA-evoked noradrenaline release, suggesting that non-NMDA receptors mediate the responses by these EAA agonists. However, since CNQX does not discriminate between kainate and AMPA receptors (Watkins *et al.*, 1990), a more exact classification of the receptors involved cannot be given. Concerning their location, the same considerations hold true as for the NMDA receptors (see above): the ability of TTX to attenuate considerably the kainic acid- and AMPA-evoked responses suggests that part of the receptors are located on an as yet unknown interneurone which releases a neurotransmitter with stimulant properties on noradrenaline release.

In conclusion, the present study revealed that noradrenaline release in the human cerebral cortex can be stimulated via NMDA receptors as well as kainic acid- and AMPA-recognizing non-NMDA receptors.

We wish to thank Mrs H. Burisch and Mrs I. Konrad for their skilled technical assistance, Mrs R. Korneli for typing the manuscript and Dr Waldmeier from Ciba Geigy Basel for the generous gift of CGP37849.

References

CHESSELET, M.-F. (1984). Presynaptic regulation of neurotransmitter release in the brain: facts and hypothesis. *Neuroscience*, **12**, 347–375.

COLLINGRIDGE, G.L. & LESTER, R.A.J. (1989). Excitatory amino acid receptors in the vertebrate central nervous system. *Pharmacol. Rev.*, **40**, 143–210.

COTMAN, C.W. & MONAGHAN, D.T. (1988). Excitatory amino acid neurotransmission: NMDA receptors and Hebb-type synaptic plasticity. *Annu. Rev. Neurosci.*, **11**, 61–80.

CRAIG, C.G. & WHITE, T.D. (1991). Endogenous glycine modulates N-methyl-D-aspartate-evoked release of adenosine and [^{3}H]noradrenaline from rat cortical slices. *Eur. J. Pharmacol.*, **197**, 1–7.

FAGG, G.E., POZZA, M.F., OLPE, H.R., BRUGGER, F., BAUMANN, P., BITTIGER, H., SCHMUTZ, M., ANGST, C., BRUNDISH, D., ALLGEIER, H., HECKENDORN, R. & DINGWALL, J.G. (1989). CGP 37849: characterization of a novel and potent competitive N-methyl-D-aspartate (NMDA) receptor antagonist. *Br. J. Pharmacol.*, **97**, 582P.

FINK, K., BÖNISCH, H. & GÖTHERT, M. (1990b). Presynaptic NMDA receptors stimulate noradrenaline release in the cerebral cortex. *Eur. J. Pharmacol.*, **185**, 115–117.

FINK, K. & GÖTHERT, M. (1990). Inhibition of N-methyl-D-aspartate-induced noradrenaline release by alcohols is related to their hydrophobicity. *Eur. J. Pharmacol.*, **191**, 225–229.

FINK, K., GÖTHERT, M., MOLDERINGS, G. & SCHLICKER, E. (1989). N-Methyl-D-aspartate (NMDA) receptor-mediated stimulation of noradrenaline release, but not release of other neurotransmitters, in the rat brain cortex: receptor location, characterization and desensitization. *Naunyn-Schmiedebergs Arch. Pharmacol.*, **339**, 514–521.

FINK, K., GÖTHERT, M. & SCHLICKER, E. (1990a). Veratridine and other depolarizing agents counteract the inhibitory effect of Mg^{2+} ions on N-methyl-D-asparate (NMDA)-induced noradrenaline release in vitro. *Naunyn-Schmiedebergs Arch. Pharmacol.*, **342**, 53–60.

FINK, K., SCHLICKER, E. & GÖTHERT, M. (1991b). Modulation of N-methyl-D-aspartate (NMDA)-stimulated noradrenaline release in rat brain cortex by presynaptic α_2-adrenoceptors and histamine H_3 receptors. In *Advances in the Biosciences – Presynaptic Receptors and Neuronal Transporters*. ed. Langer, S.Z., Galzin, A.M. & Costentin, J. Oxford, New York: Pergamon Press, pp. 125–126.

FINK, K., SCHULTHEIß, R. & GÖTHERT, M. (1991a). Noradrenaline (NA) release in human cerebral cortex is mediated by N-methyl-D-aspartate (NMDA) and non-NMDA receptors. *Naunyn-Schmiedebergs Arch. Pharmacol.*, **344**, (Suppl.), R66.

GONZALES, R.A. & WOODWARD, J.J. (1990). Ethanol inhibits N-methyl-D-aspartate-stimulated [^{3}H]norepinephrine release from rat cortical slices. *J. Pharmacol. Exp. Ther.*, **253**, 1138–1144.

GÖTHERT, M. & FINK, K. (1989). Inhibition of N-methyl-D-aspartate and L-glutamate-induced noradrenaline and acetylcholine release in the rat brain by ethanol. *Naunyn-Schmiedebergs Arch. Pharmacol.*, **340**, 516–521.

HENDERSON, G., JOHNSON, J.W. & ASCHER, P. (1990). Competitive antagonists and partial agonists at the glycine modulatory site of the mouse N-methyl-D-aspartate receptor. *J. Physiol.*, **430**, 189–212.

HUETTNER, J.E. (1991). Competitive antagonism of glycine at the N-methyl-D-aspartate (NMDA) receptor. *Biochem. Pharmacol.*, **41**, 9–16.

HUBBARD, C.M., REDPATH, G.T., MACDONALD, T.L. & VANDENBERG, S.E. (1989). Modulatory effects of aluminium, lithium, magnesium, and zinc ions on [^{3}H]MK-801 binding in human cerebral cortex. *Brain Res.*, **486**, 170–174.

JANSSEN, K.L.R., FAULL, R.L.M. & DRAGUNOW, M. (1989). Excitatory amino acid receptors in the human cerebral cortex: a quantitative autoradiographic study comparing the distribution of [^{3}H]TCP, [^{3}H]glycine, L-[^{3}H]glutamate, [^{3}H]AMPA and [^{3}H]kainic acid binding sites. *Neuroscience*, **32**, 587–607.

JOHNSON, J.W. & ASCHER, P. (1987). Glycine potentiates the NMDA response in cultured mouse brain neurons. *Nature*, **325**, 529–531.

JONES, S.M., SNELL, L.D. & JOHNSON, K.M. (1987). Phencyclidine selectively inhibits N-methyl-D-aspartate-induced hippocampal (^{3}H)-norepinephrine release. *J. Pharmacol. Exp. Ther.*, **240**, 492–497.

KEITH, R.A., MANGANO, T.J., MEINERS, B.A., STUMPO, R.J., KLIKA, A.B., PATEL, J. & SALAMA, A.I. (1989). HA-966 acts at a modulatory glycine site to inhibit N-methyl-D-aspartate-evoked neurotransmitter release. *Eur. J. Pharmacol.*, **166**, 393–400.

KEMP, J.A., FOSTER, A.C., LEESON, P.D., PRIESTLEY, T., TRIDGETT, R., IVERSEN, L.L. & WOODRUFF, G.N. (1988). 7-Chlorokynurenic acid is a selective antagonist at the glycine modulatory site of the N-methyl-D-aspartate receptor complex. *Proc. Natl. Acad. Sci., U.S.A.*, **85**, 6547–6550.

KORNHUBER, J., MACK-BURKHARDT, F., KORNHUBER, M.E. & RIEDERER, P. (1989). [^{3}H]MK-801 binding sites in post-mortem human frontal cortex. *Eur. J. Pharmacol.*, **162**, 483–490.

LALIES, M., MIDDLEMISS, D.N. & RANSOM, R. (1988). Stereoselective antagonism of NMDA-stimulated noradrenaline release from rat hippocampal slices by MK-801. *Neurosci. Lett.*, **91**, 339–342.

LODGE, D. & JOHNSON, K.M. (1990). Noncompetitive excitatory amino acid receptor antagonists. *Trends Pharmacol. Sci.*, **11**, 81–86.

MACDERMOTT, A.B., MAYER, M.L., WESTBROOK, G.L., SMITH, S.J. & BARKER, J.L. (1986). NMDA-receptor activation increases cytoplasmic calcium concentration in cultured spinal cord neurones. *Nature*, **321**, 519–522.

MAYER, M.L., WESTBROOK, G.L. & GUTHRIE, P.B. (1984). Voltage-dependent block by Mg^{2+} of NMDA responses in spinal cord neurones. *Nature*, **309**, 261–263.

MELDRUM, B. & GARTHWAITE, J. (1990). Excitatory amino acid neurotoxocity and neurodegenerative disease. *Trends Pharmacol. Sci.*, **11**, 379–387.

MOTULSKY, H.J. & RANSNAS, L.A. (1987). Fitting curves to data using nonlinear regression: a practical and nonmathematical review. *FASEB*, **1**, 365–374.

NINOMIJA, H., FUKUNAGA, R., TANIGUCHI, T., FUJIWARA, M. & KAMEYAMA, M. (1990). [^{3}H]N-[1-(2-thienyl)cyclohexyl]-3,4-piperidine ([^{3}H]TCP) binding in human frontal cortex: decreases in Alzheimer-type dementia. *J. Neurochem.*, **54**, 526–532.

NOWAK, L., BREGESTOWSKI, P., ASCHER, P., HERBERT, A. & PROCHIANTZ, A. (1984). Magnesium gates glutamate-activated channels in mouse central neurones. *Nature*, **307**, 462–465.

PITTALUGA, A. & RAITERI, M. (1990). Release-enhancing glycine-dependent NMDA receptors exist on noradrenergic terminals of hippocampus. *Eur. J. Pharmacol.*, **191**, 231–234.

PROCTER, A.W., STRATMANN, G.C., FRANCIS, P.T., LOWE, S.L., BERTOLUCCI, P.H.F. & BOWEN, D.M. (1991). Characterisation of the glycine modulatory site of the N-methyl-D-aspartate receptor ionophore complex in human brain. *J. Neurochem.*, **56**, 299–310.

RANSOM, R.W. & DESCHENES, N.L. (1988). NMDA-induced hippocampal ^{3}H norepinephrine release is modulated by glycine. *Eur. J. Pharmacol.*, **156**, 149–155.

SACAAN, A.I. & JOHNSON, K.M. (1990). Spermidine reverses arcaine's inhibition of N-methyl-D-aspartate-induced hippocampal [^{3}H]norepinephrine release. *J. Pharmacol. Exp. Ther.*, **255**, 1060–1063.

SCHWARZKROIN, P.A., TURNER, D.A., KNOWLES, W.D. & WYLER, A.R. (1983). Studies of human and monkey 'epileptic' neocortex in the in vitro slice preparation. *Ann. Neurol.*, **13**, 249–257.

SILLS, M.A., FAGG, G., POZZA, M., ANGST, C., BRUNDISH, D.E., HURT, S.D., WILUSZ, E.J. & WILLIAMS, M. (1991). [^{3}H]CGP 39653: a new N-methyl-D-aspartate antagonist radioligand with low nanomolar affinity in rat brain. *Eur. J. Pharmacol.*, **192**, 19–24.

STARKE, K. (1977). Regulation of noradrenaline release by presynaptic receptor systems. *Rev. Physiol. Biochem. Pharmacol.*, **77**, 1–124.

STARKE, K., GÖTHERT, M. & KILBINGER, H. (1989). Modulation of neurotransmitter release by presynaptic autoreceptors. *Physiol. Rev.*, **69**, 864–989.

STONE, T.W. & BURTON, N.R. (1988). NMDA receptors and ligands in the vertebrate CNS. *Progr. Neurobiol.*, **10**, 333–368.

WATKINS, J.C., KROGSGAARD-LARSEN, P. & HONORÉ, T. (1990). Structure-activity relationships in the development of excitatory amino acid receptor agonists and competitive antagonists. *Trends Pharmacol. Sci.*, **11**, 25–33.

WONG, E.H.F., KEMP, J.A., PRIESTLEY, T., KNIGHT, A.R., WOODRUFF, G.N. & IVERSEN, L.L. (1986). The anticonvulsant MK-801 is a potent N-methyl-D-aspartate antagonist. *Proc. Natl. Acad. Sci. U.S.A.*, **83**, 7104–7108.

WOODWARD, J.J. & GONZALES, R.A. (1990). Ethanol inhibition of N-methyl-D-aspartate-stimulated endogenous dopamine release from rat striatal slices: reversal by glycine. *J. Neurochem.*, **54**, 712–715.

WUARIN, J.P., KIM, Y.I., CEPEDA, C., TASKER, J.G., WALSH, J.P., PEACOCK, W.J., BUCHWALD, N.A. & DUDEK, F.E. (1990). Synaptic transmission in human neocortex removed for treatment of intractable epilepsy in children. *Ann. Neurol.*, **28**, 503–511.

(Received September 30, 1991
Revised January 2, 1992
Accepted January 14, 1992)

Br. J. Pharmacol. (1992), **106**, 73–78 © Macmillan Press Ltd, 1992

Penicillin-induced potentiation of glycine receptor-operated choride current in rat ventro-medial hypothalamic neurones

Naofumi Tokutomi, [2]Nadia Agopyan & [1]Norio Akaike

Department of Neurophysiology, Tohoku University School of Medicine, Sendai 980, Japan

1 Effects of penicillin G (PCN) on glycine (Gly)-evoked Cl^- current (I_{Gly}) were investigated in acutely dissociated rat ventro-medial hypothalamic (VMH) neurones by the whole cell mode of patch clamp technique.

2 When PCN was applied simultaneously with Gly, PCN depressed I_{Gly} like a Cl^- channel blocker.

3 The PCN-induced blocking action was clearly observed at a low PCN concentration (30 u), while the maximal blockade was achieved by 600 u (units per 10 ml) PCN.

4 When tested solution containing both PCN and Gly was quickly substituted with one containing Gly only, a new rebound-like transient current (I_T) which also passed through Cl^- channel, was elicited.

5 The peak amplitude of I_T induced by PCN at concentrations higher than 100 u was greater than that induced by glycine alone. We termed this phenomenon PCN-induced potentiation of I_{Gly}. In all cells tested, PCN potentiated I_{Gly}.

6 At a lower PCN concentration below 30 u, I_T generation was not clear in the presence of 10^{-5} M γ-aminobutyric acid. With PCN a higher concentration than 300 u, I_T amplitude was treater than that of the original peak I_{Gly}. This was observed in 18 neurones out of 21. The maximal amplitude of the I_T was achieved with 600 u PCN.

Keywords: Rat CNS neurone; glycine; Cl^- channel; penicillin; potentiation

Introduction

Glycinergic as well as GABAergic innervation plays an important role in inhibitory regulation of neuronal activity in mammalian CNS (Aprison *et al.*, 1976; Aprison & Daly, 1978; Kita & Oomura, 1982; McGeer *et al.*, 1987). Glycine (Gly) and γ-aminobutyric acid (GABA) generate inhibitory postsynaptic potentials (i.p.s.ps) by enhancing the influx of Cl^- throught the strychnine-sensitive Gly receptor (Young & Synder, 1973; 1974; Zarbin *et al.*, 1981) and the $GABA_A$ receptor (Curtis *et al.*, 1970; Stephenson, 1988), respectively. Amino acid sequences deduced from complementary DNA clones show significant homology in both Gly and $GABA_A$ receptor channel complexes (Betz, 1990). The $GABA_A$ receptor-mediated Cl^- current is known to be down-regulated externally by several antagonists such as bicuculline and picrotoxin (Hori *et al.*, 1978; Akaike *et al.*, 1985; Smart & Constanti, 1986; Yakushiji *et al.*, 1987) and up-regulated by potentiating agents such as benzodiazepines (Suria & Costa, 1975; Macdonald & Barker, 1978; Hattori *et al.*, 1986; Yakushiji *et al.*, 1989) and barbiturates (Higashi & Nishi, 1982; Akaike *et al.*, 1990) though their specific binding sites cooperated with the $GABA_A$ receptor (Olsen, 1982). $GABA_A$ receptor-mediated Cl^- current has also been reported to be regulated intracellularly by (a) Ca^{2+} in frog sensory neurones (Inoue *et al.*, 1986; Maruyama *et al.*, 1988); (b) adenosine 5′-triphosphate (ATP) in mouse cultured hippocampal neurones (Stelzer *et al.*, 1988); (c) adenosine 3′:5′-cyclic monophosphate (cyclic-AMP) dependent kinase in both hippocampal and spinal cord neurones (Harrison & Lambert, 1989; Porter *et al.*, 1991) and (d) protein kinase C (Corradetti *et al.*, 1989; Agopyan & Agopyan, 1991). However, very little is known about the modulation of the Gly receptor-Cl^- channel complex. Several agents such as strychnine, brucine, thebaine, 4-phenyl-4-formyl-N-methyl-piperidine, N,N-dimethyl muscimol and N-methyl-THIP have been known to down-regulate the Gly-receptor mediated Cl^- current via receptor-antagonism (Curtis *et al.*, 1967; Krogsgaard-Larsen *et al.*, 1982). The glycinergic response has been reported to be enhanced directly by an antiepileptic chlormethiazole (Gent & Wacey, 1983; Hales *et al.*, 1990) and a general anaesthetic propofol (Hales *et al.*, 1990; Hales & Lambert, 1991) and indirectly by some glycine uptake-inhibitors (Lopez-Lahoya *et al.*, 1981). Depending on the tissue used, intracellular application of cyclic AMP was recently reported to either augment (Song & Huang, 1990) or attentuate I_{Gly} (Agopyan *et al.*, 1991). Studies on various agents up-regulating the strychnine-sensitive Gly response directly may provide new possibilities of experimental and clinical approaches as the development of barbiturates and benzodiazepines have done for GABA.

We discovered recently that penicillin G, an antibiotic, in addition to blocking the Cl^- channel, potentiates I_{Gly} in acutely dissociated ventromedial hypothalamic (VMH) neurones of Wistar rats. This is the first account of an agent that produces biphasic and reciprocal modulation of the glycinergic Cl^- response externally through a direct effect on Gly receptor Cl^- channel complexes. A detailed analysis of PCN-induced blockade and potentiation of I_{Gly} was performed.

Methods

Preparations

Ventromedial hypothalamic (VMH) neurones were freshly dissociated as described previously (Takahashi *et al.*, 1989) with some modification. Wistar rats (10–15 day old) were decapitated under ether anaesthesia; 400 μm thick slices containing the VMH were obtained with a vibratome tissue slicer (Dosaka, Japan), and incubated in well oxygenated standard solution for 50 min at room temperature (22°C). Thereafter, the brain slices were incubated in the standard solution containing pronase 0.17 mg ml^{-1} (Sigma, U.S.A.) for 20 min at 37°C and successively in another solution containing thermolysine 0.17 mg ml^{-1} (Sigma, U.S.A.) under the same conditions. Following the enzyme treatment slices were rinsed with a Ca^{2+}-free EGTA solution and then kept in the oxygenated

[1] Author for correspondence.
[2] Present address: Max-Planck Institut für Medizinische Forschung, Abteilung Zellphysiologie, D-6900 Heidelberg, Germany.

standard solution at room temperature for 15 min. The VMH region was taken out by micro-punching the enzymatically treated brain slices and triturating gently with fire-polished pasteur pipettes in a cell-culture dish (Falcon, U.S.A.) containing standard solution. Within 20 min after the dissociation, the neurones were well-fixed to the bottom of the dish allowing the start experiments.

Electrical measurement

Low resistance pipettes (3–4 MΩ) filled with the internal solution described in the next section were used; 70–80% of the series resistance (7–8 MΩ) after rupturing of the membrane was compensated. Whole-cell membrane currents were recorded under voltage-clamped conditions at a holding potential (V_H) of −20 mV (except for the study of current-voltage relationships) by use of a patch-clamp amplifier (Nihon Kohden, Japan). The V_H used (−20 mV) coupled with a Cl^- equilibrium potential (E_{Cl}) of −3.8 mV gave a 16 mV driving force for Cl^- and thus prevented Cl^- redistribution (Akaike *et al.*, 1987) during continuous glycine application. The ionic currents were low pass-filtered at a cut off frequency of 10 kHz and monitored simultaneously on a storage oscilloscope (Iwatsu, MS-5100A) and pen recorder (National, VP6621A). Currents were stored on a PCM video recorder (Mitsubishi, F73) for off-line analysis using pClamp software (Axon Instruments, U.S.A.).

Solutions

The ionic composition of the standard external solution was (in mM): NaCl 150, KCl 5, $CaCl_2$ 2, $MgCl_2$ 1, N-2-hydroxyethyl piperazine-N′-ethanesulphonic acid (HEPES) 10, and glucose 10, the internal solution was: N-methyl-D-glucamine chloride (NMG-Cl) 130, 1,2-*bis*(*o*-aminophenoxy)ethane-N, N,N′,N′-tetracetic acid (BAPTA) 10, HEPES 10; $MgCl_2$ 4, ATP 4, and GTP-Na_2 1. The pH of the external solution was adjusted to 7.4 by tris(hydroxymethyl)aminomethane (Tris base) and that of the internal solution was adjusted to 7.25 by HCl (0.1 N). Glycine (Nakarai) and penicillin G (Meiji) were dissolved in the external solution just before use. Drugs were rapidly applied within 5 and 10 ms by a multi-barrelled pipette previously described by Carbone & Lux (1987) positioned close to the neurone (50 to 100 μm in distance).

Results

Penicillin induced potentiation of I_{Gly}

In all rat VMH neurones tested, Gly evoked Cl^- current (I_{Gly}) in a dose-dependent manner. In comparison with I_{GABA} in the same neurones, the I_{Gly} was selectively blocked by 10^{-7} M strychnine (not shown), being consistent with our previous report (Tokutomi *et al.*, 1989). Application of a mixture containing PCN (600 u) and Gly (10^{-5} M) depressed the I_{Gly} evoked by 10^{-5} M Gly at a V_H of −20 mV although PCN in the absence of Gly did not produce any effect in the VMH neurones. However, a rebound-like transient current (I_T) was evoked when the mixture was quickly replaced by an external solution containing only Gly (Figure 1a). The amplitude of I_T was greater than that of the extrapolated control (dashed-trace) evoked by 10^{-5} M Gly alone. We considered this rebound I_T as a PCN-induced potentiation of I_{Gly}. We grouped I_Ts, obtained from 21 cells, according to their amplitudes after normalizing them to the control peak I_{Gly} and observed enhancement of I_{Gly} by PCN in all cells (Figure 1b). Moreover in 18 cells out of 21, the amplitude of I_T was greater than that of the peak I_{Gly}.

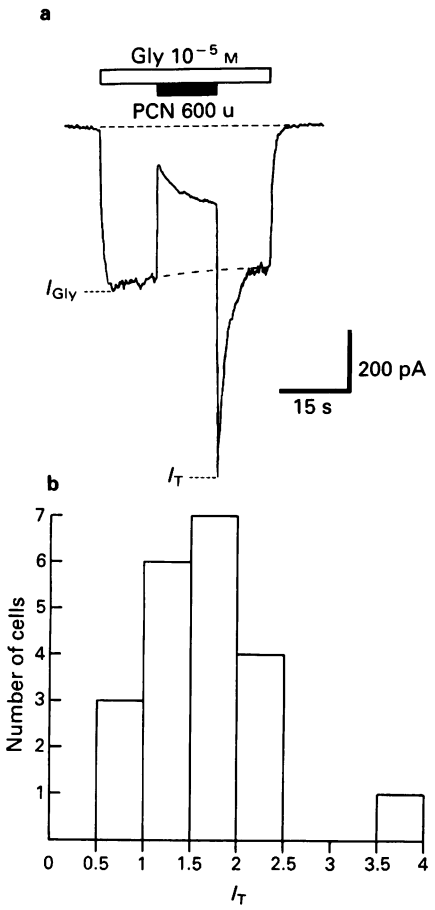

Figure 1 Penicillin (PCN)-induced potentiation of I_{Gly}. (a) Open and closed horizontal bars show the application of glycine (Gly 10^{-5} M) and PCN (600 u, units per 10 ml), respectively. Simultaneously applied PCN blocked I_{Gly} evoked at a V_H of −20 mV, while a rebound-like potentiation of I_{Gly} (I_T) was elicited when the mixture was replaced by a pure Gly solution. The dashed line on the current trace indicates the original time course of the I_{Gly} by extrapolation. (b) Histograms showing the occurrence of the rebound-like I_{Gly}. The amplitude of I_T (abscissa scale) was normalized to the peak amplitude of the control I_{Gly}. The ordinate scale shows the number of cells. In 18 cells out of 21, the potentiation was observed.

Effects of repetitive application of penicillin on I_{Gly}

When simultaneous application of PCN and Gly was interposed, repeatedly, during the densitization phase of I_{Gly}, the amplitude of I_T gradually decreased in accordance with the development of the densensitization of I_{Gly}. Hence, throughout the present study, the external solution containing PCN was applied 11 to 13 s after the Gly application, to minimize the influence of desensitization.

Current-voltage (I-V) relationship of penicillin-induced actions on I_{Gly}

Figure 3a shows the effect of 600 u PCN-induced actions on both the inward and the outward I_{Gly}s evoked by 10^{-5} M Gly at V_Hs of −30 and +30 mV, respectively. We defined the degree of blockade as the minimum current amplitude observed during the blockade, and that of potentiation as the peak amplitude of I_T. Both the I_{Gly} and I_T showed slight inward and outward rectification in *I*-V curves at negative and positive holding potentials, respectively. The *I*-V curve in the presence of PCN was nearly linear; this was observed in all neurones tested ($n = 4$). In two neurones out of four, the inward I_{Gly} showed a little faster desensitization than that of the outward one even though both I_{Gly} had nearly identical amplitude. A representative example of a set of *I*-V curves for the control (●), PCN-blocked I_{Gly} (▲) and potential I_{Gly} (□) is shown in Figure 3b. The reversal potentials estimated from each *I*-V relationship were close to the E_{Cl} of −3.8 mV

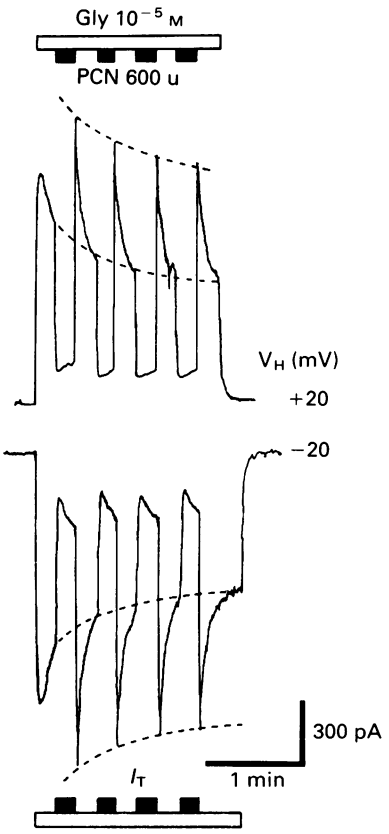

Figure 2 Effect of repetitive application of penicillin (PCN) on I_{Gly}. Open and closed horizontal bars show the application of glycine (Gly 10^{-5} M) and PCN (600 u), respectively. Both the outward and inward I_{Gly} evoked at V_Hs of +20 and −20 mV, respectively are shown. The superimposed desensitization phases were nearly identical in both the I_{Gly} and I_T, as shown by dashed lines.

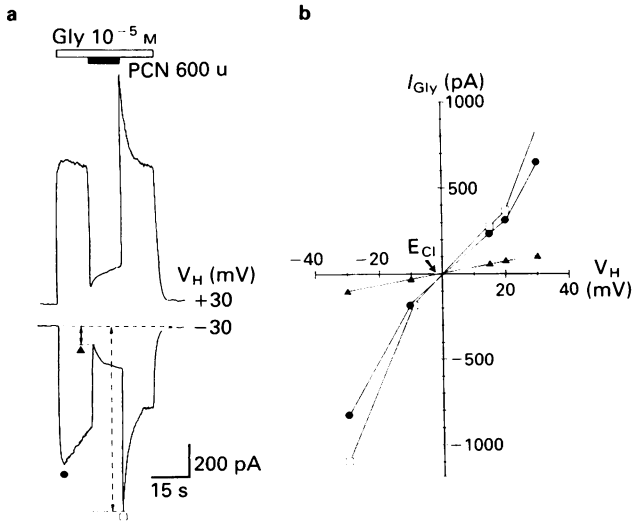

Figure 3 Current-voltage (*I*-V) relationship of penicillin (PCN)-induced actions on I_{Gly}. (a) PCN-induced blockade and potentiation (I_T) of both the outward and inward I_{Gly}s evoked at V_Hs of +30 and −30 mV, respectively. Open and closed horizontal bars show the application of Gly (10^{-5} M) and PCN (600 u). (b) *I*-V curves for the control (●), blocked (▲) and I_T (□). Cl^- equilibrium potential (E_{Cl}) calculated by the Nernst equation is indicated by arrow.

calculated by the Nernst equation using the extra- and intracellular Cl^- concentrations.

Concentration-dependent effects of penicillin on I_{Gly}

Various concentrations of PCN (6 to 2000 u) were tested on the I_{Gly} induced by 10^{-5} M Gly. PCN blocked and potentiated I_{Gly} (I_T) in a concentration-dependent manner (Figure 4a). The amplitudes of both the blocked and potentiated I_{Gly} were normalized to that of control, and summarized in Figure 4b as a function of PCN concentration. At PCN concentrations below 30 u, I_T generation was not clear, while at higher PCN concentrations over 300 u, the amplitude of the I_T was greater than that of the original I_{Gly} estimated by the superimposed dashed-traces of the control I_{Gly} desensitization. The maximal amplitude of I_T was achieved with 600 u PCN and decreased again at 2000 u. The PCN-induced blocking action was clearly observed at a low PCN concentration (30 u), while the maximal blockade was also achieved with 600 u PCN. As shown in Figure 4a, I_{Gly} was slightly restored at higher PCN concentrations over 600 u.

Penicillin induced potentiation of I_{Gly}

Effects of PCN on I_{Gly} evoked by various concentrations of Gly were tested. The effect of 600 u PCN on I_{Gly} evoked by either low (10^{-5} M) or high (3×10^{-4} M) concentrations of Gly is shown in Figure 5a. The I_{Gly} evoked at a V_H of

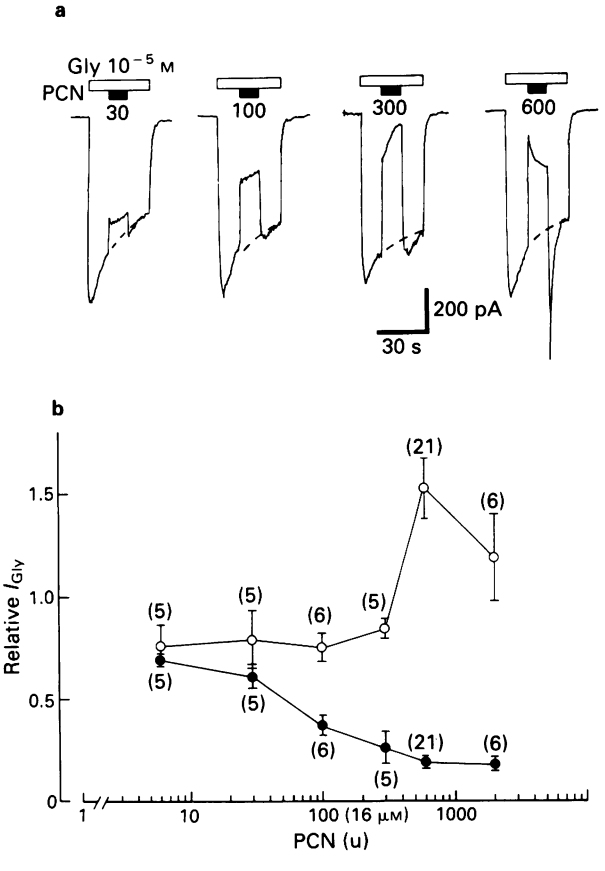

Figure 4 Concentration-dependent biphasic actions of penicillin (PCN) on I_{Gly}. (a) A representative effect of penicillin (PCN) at various concentrations on I_{Gly} evoked at a V_H of −20 mV. Open and closed horizontal bars show the application of glycine (Gly, 10^{-5} M) and PCN (30–600 u), respectively. (b) The relative amplitude (ordinate scale) of both the blocked I_{Gly} (●) and I_T (○) were normalized to that of the control peak I_{Gly}, and plotted versus the concentration of PCN (abscissa scale). Data are shown as mean values with standard error bars. Numbers in parentheses indicate the number of cells tested.

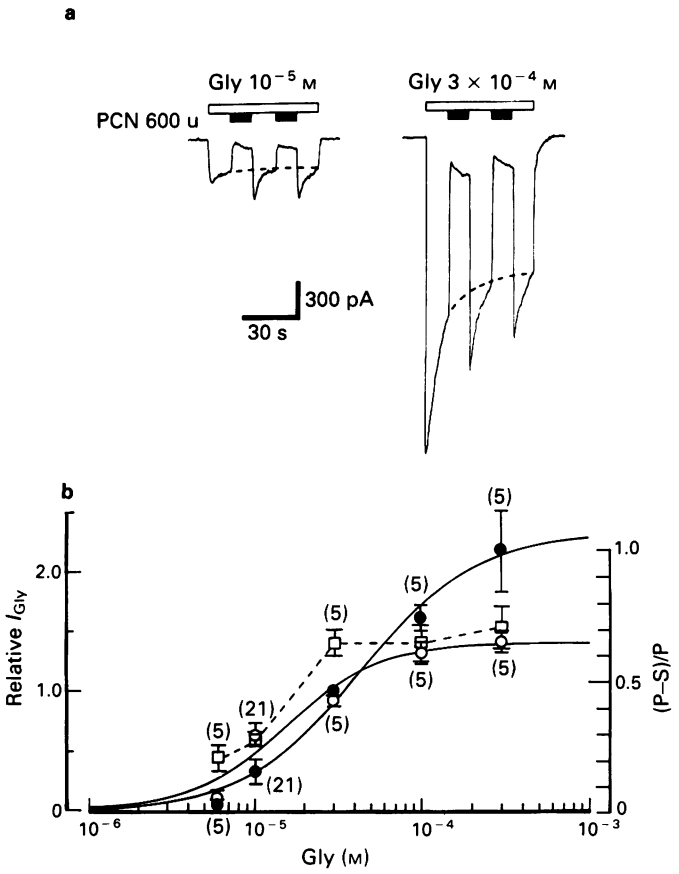

Figure 5 Penicillin (PCN)-induced biphasic action on I_{Gly} evoked by various concentration of glycine (Gly). (a) Effects of 600 u PCN on I_{Gly}s evoked by a low (10^{-5} M) and a high concentration (3×10^{-4} M) Gly at a V_H of -20 mV. Open and closed horizontal bars show the application of Gly and PCN, respectively. (b) Relationship between the relative amplitude (oridinate scale) normalized to that of the peak I_{Gly} evoked by 3×10^{-5} M Gly and the concentration of Gly (abscissa scale): (●) control; (○) I_T and (□) (P-S)/P. Data are shown as mean values with standard error bars. Numbers in parentheses indicate the number of cells tested.

-20 mV had a typical current shape depending on the Gly concentration used. The I_{Gly} induced by low concentrations of Gly showed a slight desensitization whereas that induced by higher concentrations revealed a considerable desensitization. In the presence of a constant concentration (600 u) of PCN, the peak amplitude of I_T was greater than the peak amplitude of the I_{Gly} evoked by Gly of low concentrations (6×10^{-6} and 10^{-5} M). However, at Gly concentrations over 10^{-5} M the amplitude of I_T was smaller than that of the peak I_{Gly} although the I_T amplitude was always greater than that of I_{Gly} shown by the extrapolated dashed lines. The peak amplitude of the first I_T was normalized to that of the peak I_{Gly} and plotted against the concentration of Gly in Figure 5b. To evaluate the influence of the Gly receptor desensitization on the PCN effect, the desensitized part of the current amplitude (P-S), where the current amplitude S was measured 45 s after the application of Gly, was also normalized to the peak amplitude (P) of I_{Gly} evoked by various concentration of Gly and plotted as the function of the Gly concentration. The degree of desensitization and the decrement in the I_T correlated.

Discussion

The antibiotic, penicillin (PCN), is a known channel blocker of the $GABA_A$ receptor-operated Cl^- channel in amphibian peripheral neurones (Yakushiji *et al.*, 1987) and mammalian CNS neurones (Chow & Mathers, 1986; Twyman *et al.*, 1991). Its epileptogenic activities *in vitro* (Raichle *et al.*, 1971; Krnjevic *et al.*, 1977) and the myoclonus and seizures provoked by a high concentration of PCN *in vivo* (Ajimone-Marsen, 1969; Kao & Crill, 1972) have been well described. We show here that PCN modulates the strychnine-sensitive Gly response by potentiating the Cl^- current after blocking it. In this study, PCN-induced attenuation of I_{Gly} appeared to be due to a similar mechanism to that of I_{GABA} studied in frog sensory neurones (Yakushiji *et al.*, 1987; Katayama *et al.*, 1991). The reversal potential of potentiated I_{Gly} (I_T) like that of the control and blocked I_{Gly} was close to the E_{Cl}, indicating that I_T was also carried by Cl^- passing through the Gly receptor-operated Cl^- channel. PCN applied in the absence of Gly produced no conductance change. Faster desensitization of the inward I_{Gly} than that of the outward one which was observed in two neurones (Figure 3a) might be due to some voltage-dependent modulation of the desensitization kinetics of the I_{Gly} although it was not observed in all neurones.

In frog sensory neurones, the presence of kinetically distinct populations of $GABA_A$ receptor Cl^- channel complexes with distinct single channel conductance was suggested, by use of current-fluctuation analysis and the single channel recording with patch-clamp technique (Yasui *et al.*, 1985). This suggestion was supported by the findings that both the activation and desensitization of whole cell $GABA_A$-Cl^- current in the same preparation consisted of two exponential components with a different GABA concentration-dependency (Akaike *et al.*, 1986). Recent molecular biological studies also provided direct evidence for the presence of a variety of $GABA_A$ receptor channels composed of various combinations of subunits (Fuchs & Sieghart, 1989; Pritchett *et al.*, 1989; Shivers *et al.*, 1989; Yemer *et al.*, 1989; Verdoorn *et al.*, 1990). Complementary DNA cloning indicates considerable diversity also for the glycine receptor in the spinal cord and other brain regions (Becker *et al.*, 1988; Akagi & Miledi, 1988; Akagi *et al.*, 1989). It was suggested that tissue-specific modulation of I_{Gly} by cyclic-AMP (Song & Huang, 1990; Agopyan *et al.*, 1991) was due to such a diversity in the Gly receptor channel population. By contrast, PCN seemed to affect all Gly receptor Cl^- channel subtypes included in the VMH neurones since PCN depressed and potentiated I_{Gly} evoked by either a low or a high concentration Gly. When the concentration of PCN was higher than 600 u, gradual restoration of I_{Gly} was observed in the presence of PCN. The restoration during the I_{Gly}-blockade might suggest that the potentiation of I_{Gly} had already started during the blockade. Moreover the smaller amplitude of the I_T in the presence of 2000 u PCN compared with that in the presence of 600 u PCN in Figure 4b might also suggest that the reduced I_T was still influenced by the blocking effect at the high PCN concentration.

The relationship between the PCN effects and the concentration of PCN revealed that both attenuation and potentiation of I_{Gly} by PCN have distinct concentration-dependency. We previously investigated the stoichiometry of the action of PCN on GABA-evoked Cl^- current in frog sensory neurones (Katayama *et al.*, 1991). The effect of PCN on I_{GABA} in the frog DRG neurones was also biphasic, consisting of a blockade and a slight potentiation. In that paper, a model was proposed, where the PCN-induced potentiation of I_{GABA} was attributed to the partially liganded GABA receptor Cl^- channel and the blockade of I_{GABA} to the fully liganded one. A similar difference in PCN-liganding might also underlie the attenuation and potentiation of I_{Gly} in the present study. To determine the distinct liganding of the PCN molecule in producing blockade and potentiation of the I_{Gly}, complete separation of both effects with proper PCN derivatives is necessary since measurement of both PCN actions is difficult at high PCN concentrations because of the mutual interference between the effects.

The physiological significance of glycinergic neurotransmission has not yet been determined mainly due to the shortage of externally potentiating agents of the Gly response. If it were possible to isolate the PCN-induced potentiation of I_{Gly} by modification of the chemical structure of PCN derivatives, it would facilitate the understanding of the physiology, pharmacology and pathology (Muramoto *et al.*, 1981) of glycinergic neurotransmission and might provide new therapeutic possibilities.

This investigation was supported by Grants-in-Aid for Scientific Research (No. 03770037 to N.T. and Nos 02241101, 02304031, 02404022 and 03304026 to N.A.) from The Ministry of Education, Science and Culture, Japan.

References

AGOPYAN, N. & AGOPYAN, I. (1991). Effects of protein kinase C activators and inhibitors on membrane properties, synaptic responses and cholinergic actions in CA1 subfield of rat hippocampus. *Synapse*, **7**, 193–206.

AGOPYAN, N., TOKUTOMI, N. & AKAIKE, N. (1991). Cyclic AMP enhances the run-down of glycine current in acutely dissociated ventromedial hypothalamic neurons. *Proc. of the third IBRO World Congress of Neuroscience* (Montreal, Canada). p. 357. ed. IBRO Secretariat, Paris: Pergamon Press.

AJIMONE-MARSEN, C. (1969). Acute effects of topical epileptogenic agents. In *Basic Mechanisms of the Epilepsies*. ed. Jasper, H.N., Ward, A.A. & Pope, A., pp. 299–319. Boston: Little, Brown & Co.

AKAGI, H. & MILEDI, R. (1988). Heterogeneity of glycine receptors and their messenger RNAs in rat brain and spinal cord. *Science*, **241**, 270–273.

AKAGI, H., PATTON, E. & MILEDI, R. (1989). Discrimination of heterogeneous mRNAs encoding strychnine-sensitive glycine receptors in Xenopus oocytes by antisense oligonucleotides. *Proc. Natl. Acad. Sci. U.S.A.*, **86**, 8103–8107.

AKAIKE, N., HATTORI, K., OOMURA, Y. & CARPENTER, D.O. (1985). Bicuculline and picrotoxon block γ-aminobutyric acid-gated Cl^- conductance by different mechanisms. *Experientia*, **379**, 171–185.

AKAIKE, N., INOUE, M. & KRISHTAL, O.A. (1986). 'Concentration-clamp' study of γ-amino-butyric acid-induced chloride current kinetics in frog sensory neurones. *J. Physiol.*, **379**, 171–185.

AKAIKE, N., INOMATA, N. & TOKUTOMI, N. (1987). Contribution of chloride-shift to the fade of GABA-gated currents in frog. *J. Physiol.*, **394**, 85–98.

AKAIKE, N., TOKUTOMI, N. & IKEMOTO, Y. (1990). Augmentation of GABA-induced current in frog sensory neurons by pentobarbital. *Am. J. Physiol.*, **258**, C452–460.

APRISON, M.H., DALY, E.C., SHANK, R.P. & MCBRIDE, W.J. (1976). Neurochemical evidence for glycine as a transmitter and a model for its intrasynaptosomal compartmentation. In *Metabolic Compartmentation and Neurotransmission*. ed. Berl, S., Clarke, D.D. & Schneider, D. pp. 37–63. New York: Plenum Press.

APRISON, M.H. & DALY, E.C. (1978). Biochemical aspects of transmission at inhibitory synapses: the role of glycine. *Adv. Neurochem.*, **3**, 203–294.

BECKER, C.M., HOCH, W. & BETZ, H. (1988). Glycine receptor heterogeneity in rat spinal cord during postnatal development. *EMBO J.*, **7**, 3717–3726.

BETZ, H. (1990). Ligand-gated ion channels in the brain: the amino acid receptor superfamily. *Neuron*, **5**, 383–392.

CARBONE, E. & LUX, H.D. (1987). Kinetics and selectivity of a low-voltage-activated calcium current in chick and rat sensory neurones. *J. Physiol.*, **386**, 547–570.

CHOW, P. & MATHERS, D. (1986). Convulsant doses of penicillin shorten the lifetime of GABA-induced channels in cultured central neurones. *Br. J. Pharmacol.*, **88**, 541–547.

CORRADETTI, R., PUGLIESE, A.M. & ROPERT, N. (1989). The protein kinase C inhibitor 1-(5-isoquinolinesulphonyl)-2-methylpiperazine (H-7) disinhibits CA1 pyramidal cells in rat hippocampal slices. *Br. J. Pharmacol.*, **98**, 1376–1382.

CURTIS, D.R., HOSLI, L. & JOHNSTON, G.A.R. (1967). Inhibition of spinal neurons by glycine. *Nature*, **215**, 1502–1503.

CURTIS, D.R., DUGGAN, A.W., FELIX, D. & JOHNSTONE, G.A.R. (1970). GABA, bicuculline and central inhibition. *Nature*, **226**, 1222–1224.

FUCHS, K. & SIEGHART, W. (1989). Evidence for the existence of several different α- and β- subunits of the GABA/benzodiazine receptor complex from rat brain. *Neurosci. Lett.*, **97**, 329–333.

GENT, J.P. & WACEY, T.A. (1983). The effects of chlormethiazole on single unit activity in rat brain; interactions with inhibitory and excitatory neurotransmitters. *Br. J. Pharmacol.*, **80**, 439 444.

HALES, T.G., PETERS, J.A., LAMBERT, J.J. & KATS, R.L. (1990). Modulation of the glycine receptor by chlormethiazole (CLM) and 2,6-diisopropylphenol (Propofol). *Soc. Neurosci. Abst.*, **16**, 356.

HALES, T.G. & LAMBERT, J.J. (1991). The actions of propofol on inhibitory amino acid receptors of bovine adrenomedullary chromaffin cells and rodent central neurones. *Br. J. Pharmacol.*, **104**, 619–628.

HARRISON, N.L. & LAMBERT, N.A. (1989). Modification of $GABA_A$ receptor function by an analog of cyclic AMP. *Neuroscience Letts.*, **105**, 137–142.

HATTORI, K., OOMURA, Y. & AKAIKE, N. (1986). Diazepam action on γ-aminobutyric acid-activated chloride currents in internally perfused frog sensory neurons. *Cell. Molec. Neurobiol.*, **6**, 307–323.

HIGASHI, H. & NISHI, S. (1982). Effect of barbiturates on the GABA receptor of cat primary afferent neurones. *J. Physiol.*, **332**, 299–314.

HORI, N., IKEDA, K. & ROVERTS, R. (1978). Muscimol, GABA and picrotoxin: effects on membrane conductance of a crustacean muscle. *Brain Res.*, **141**, 364–370.

INOUE, M., OOMURA, Y., YAKUSHIJI, T. & AKAIKE, N. (1986). Intracellular calcium ions decrease the affinity of the GABA receptor. *Nature*, **324**, 156–158.

KAO, L.L. & CRILL, W.E. (1972). Penicillin induced segmental myoclonus I motor responses and intracellular recording from motoneurons. *Arch. Neurol.*, **26**, 156–161.

KATAYAMA, N., YAMAMOTO, M., TOKUTOMI, N. & AKAIKE, N. (1991). Penicillin-induced modulation of $GABA_A$ receptor operated Cl^- current in frog sensory neurons. *Proc. of the third International Congress of Comparative Physiology and Biochemistry*. (Tokyo, Japan). p. 95. ed. Kawashima, S., Kobayashi, M. & Shimgyoji, C. Tokyo: Heibunsha Inc.

KITA, H. & OOMURA, Y. (1982). Evidence for a glycinergic corticolateral hypothalamic inhibitory pathway in the rat. *Brain Res.*, **235**, 131–136.

KRNJEVIC, K., PUIL, E. & WERMAN, R. (1977). Bicucullin, benzyl penicillin and inhibitory amino acids in the spinal cord of the cat. *Can. J. Physiol.*, **55**, 670–680.

KROGSGAARD-LARSEN, P., HJEDS, H., CURTIS, D.R., LEAH, J.D. & PEET, M.J. (1982). Glycine antagonists structurally related to muscimol, THIP or isoguvacine. *J. Neurochem.*, **39**, 1319–1324.

LOPEZ-LAHOYA, J., GARCIA, M.L., BENAVIDES, J. & UGARTE, M. (1981). Inhibition by methylmalonate of glycine uptake by synaptosomes from rat spinal cord. *J. Neurochem.*, **36**, 325–327.

MACDONALD, R. & BARKER, J.L. (1978). Benzodiazepine specifically modulate GABA-mediated postsynaptic inhibition in cultured mammalian neurones. *Nature*, **271**, 563–564.

MARUYAMA, T., OOMURA, Y., SADOSHIMA, J., TOKUTOMI, N., BEHRENDS, J. & AKAIKE, N. (1988). Modulation of the Gaba- and pentobartial-gated Cl current by intracellular calcium in frog sensory neurons. In *Cellular Mechanisms of Conditioning and Behavioral Plasticity*. ed. Woody, C.G., Alkon, D.L. & McGaugh, J.L., pp. 493–500, New York: Plenum Press.

MCGEER, P.L., ECCLES, J.C. & MCGEER, E.G. (1987). Inhibitory amino acid neurotransmitters. In *Molecular Neurobiology of the Mammalian Brain*. ed McGeer, P.L., Eccles, J.C. & McGeer, E.G., pp. 197–234. New York: Plenum Press.

MURAMOTO, O., KANAZAWA, I. & ANDO, K. (1981). Neurotransmitter abnormality in rolling mouse Nagoya, an ataxic mutant mouse. *Brain Res.*, **215**, 295–304.

OLSEN, R.W. (1982). Drug interactions at the GABA receptor ionophore complex. *Ann. Rev. Pharmacol. Toxicol.*, **22**, 245– 277.

PORTER, N.M., TWYMANN, R.E., UHLER, M.D. & MACDONALD, R.L. (1990). Cyclic AMP-dependent protein kinase decreases $GABA_A$ receptor current in mouse spinal neurons. *Neuron*, **5**, 789–796.

PRITCHETT, D.B., SONTHEIMER, H., SHIVERS, B.D., YMER, S., KETTENMANN, H., SCHOFIELD, P.R. & SEEBURG, P.H. (1989). Importance of a novel $GABA_A$ receptor subunit for benzodiazepine pharmacology. *Nature*, **338**, 582–585.

RAICHLE, M.E., KULT, H., LOUIS, S. & McDOWELL, F. (1971). Neurotoxicity of intravenously administered penicillin G. *Arch Neurol.*, **25**, 232–239.

SHIVERS, B.D., KILLISCH, I., SPRENGEL, R., SONTHEIMER, H., KOHLER, M., SCHOFIELD, P.R. & SEEBURG, P.H. (1989). Two novel $GABA_A$ receptor subunits exist in distinct neuronal subpopulations. *Neuron*, **3**, 327–337.

SMART, T.G. & CONSTANTI, A. (1986). Studies on the mechanism of picrotoxin and other convulsants at the crustacean muscle GABA receptor. *Proc. R. Soc. B*, **227**, 191–216.

SONG, Y. & HUANG, L.M. (1990). Modulation of glycine receptor chloride channels by cAMP dependent protein kinase in spinal trigeminal neurons. *Nature*, **348**, 242–245.

STELZER, A., KAY, A.R. & WONG, R.K.S. (1988). $GABA_A$-receptor function in hippo-campal cells is maintained by phosphorylation factors. *Science*, **241**, 339–341.

STEPHENSON, F.A. (1988). Understanding of the $GABA_A$ receptor: a chemically gated ion channel. *Biochem. J.*, **249**, 21–32.

SURIA, A. & COSTA, E. (1975). Action of diazepam, dibutyryl cGMP on presynaptic nerve terminals in frog sympathetic ganglia. *Brain Res.*, **87**, 102–106.

TAKAHASHI, K., TATEISI, N., KANEDA, M. & AKAIKE, N. (1989). Comparison of low threshold Ca^{2+} currents in the hippocampal CA_1 neurons among the newborn, adult and aged rats. *Neurosci. Lett.*, **103**, 29–33.

TOKUTOMI, N., KANEDA, M. & AKAIKE, N. (1989). What confers specificity on glycine for its receptor site? *Br. J. Pharmacol.*, **97**, 353–360.

TWYMAN, R.E., GREEN, R.M. & MacDONALD, R.L. (1991). Kinetics of open channel block of single $GABA_A$ receptor channels by penicillin. *J. Physiol.* (in press).

VERDOORN, T.A., DRAGUHN, A., YMER, S., SEEBURG, P.H. & SAKMANN, B. (1990). Functional properties of recombinant rat $GABA_A$-receptors depend upon subunit composition. *Neuron*, **4**, 918–928.

YAKUSHIJI, T., TOKUTOMI, N., AKAIKE, N. & CARPENTER, D.O. (1987). Antagonists of GABA responses, studied using internally perfused frog dorsal root ganglion neurons. *Neuroscience*, **22**, 1123–1133.

YAKUSHIJI, T., TOKUTOMI, N. & AKAIKE, N. (1989). Augmentation of GABA-induced chloride current in frog sensory neurons by diazepam. *Neurosci. Res.*, **6**, 309–320.

YASUI, S., ISHIZUKA, S. & AKAIKE, N. (1985). GABA activates different types of chloride conducting receptor-ionophore complexes in a dose-dependent manner. *Brain Res.*, **344**, 176–180.

YEMER, S., SCHOFIELD, P.R., DRAGUHN, A., WERNER, P., KOHLER, M. & SEEBURG, P.H. (1989). GABA-A receptor β subunit heterogeneity: functional expression of cloned cDNAs. *EMBO J.*, **8**, 1665–1670.

YOUNG, A.B. & SNYDER, S.H. (1973). Strychnine binding associated with glycine receptors of the central nervous system. *Proc. Natl. Acad. Sci. U.S.A.*, **70**, 2832–2836.

YOUNG, A.B. & SNYDER, S.H. (1974). Strychnine binding in rat spinal cord membranes associated with the synaptic glycine receptor: cooperativity of glycine interactions. *Mol. Pharmacol.*, **10**, 790–809.

ZARBIN, M.A., WAMSLEY, J.K. & KUHAR, M.J. (1981). Glycine receptor: light microscope autoradiographic localization with [^{3}H]strychnine. *J. Neurosci.*, **1**, 532–547.

(Received September 23, 1991
Revised January 2, 1992
Accepted January 14, 1992)

Br. J. Pharmacol. (1992), **106**, 79–84 © Macmillan Press Ltd, 1992

Haemodynamic effects of a new dihydropyridine calcium entry blocker, S-12968-(−), in a rat model of cardiovascular calcium overload

Touria Makki, Isabelle Lartaud, Laure Bray-des Boscs, Christine Capdeville-Atkinson, Jean-Marc Chillon, *Maurice Hoffman, †Jean-Pierre Nicolas & [1]Jeffrey Atkinson

Laboratoire de Pharmacologie Cardio-vasculaire, Faculté de Pharmacie de l'Université de Nancy I, 5 rue Albert Lebrun, 54000 Nancy; *Laboratoire de Pharmacie Galénique, de Biopharmacie et de Pharmacie Clinique, Faculté de Pharmacie de l'Université de Nancy I, 5 rue Albert Lebrun, 54000 Nancy, and †INSERM U308, 38 rue Lionnois, 54000 Nancy, France

1 The haemodynamic effects of S-12968-(−), a new dihydropyridine calcium entry blocker (enantiomer of S-11568), were compared with those of the stereoisomer, S-12967-(+), nifedipine, and sodium nitroprusside.

2 A first experiment was performed in conscious, young male rats chronically implanted with femoral artery and vein cannula and repeated in rats previously treated with vitamin D_3 and nicotine. Such treatment produces marked vascular calcium overload, especially of the compliance arteries, with no overt sign of toxicity as far as can be judged from the plasma profile.

3 In conscious rats the hypotensive effects of S-12968-(−), nifedipine and sodium nitroprusside were of similar potency. The falls in blood pressure produced by nifedipine and sodium nitroprusside were accompanied by reflex tachycardia which was less marked in the vascular calcium overload model. S-12968-(−) did not induce reflex tachycardia. S-12967-(+) increased blood pressure in both models.

4 A second experiment was performed in open-chest pentobarbitone-anaesthetized rats with electromagnetic flowprobes on the ascending aorta. In controls the falls in blood pressure produced by low doses (0.1 and 0.3 mg kg^{-1}, i.v.) of S-12968-(−) were accompanied by falls in total peripheral resistance. The higher dose (1 mg kg^{-1}, i.v.) of S-12968-(−) produced no change in total peripheral resistance, and in rats pretreated with vitamin D_3 and nicotine, cardiac output fell.

5 In conclusion, S-12968-(−) appears to have a dual action and to lower blood pressure at higher doses at least in part by a cardiac effect. This phenomenon is more pronounced in rats pretreated with vitamin D_3 and nicotine.

6 S-12967-(+) resembles a calcium channel activator in this model.

Keywords: Vascular calcium overload; dihydropyridine calcium entry blockers; haemodynamics

Introduction

Although dihydropyridine calcium entry blockers (CEB) are widely used as first line therapeutic agents, many have a major disadvantage in the treatment of cardiovascular diseases in that they induce reflex tachycardia (Kiowski *et al.*, 1986). Newer, longer acting dihydropyridines may have a certain advantage in this respect and in the present paper we present the cardiovascular effects in the rat of a new dihydropyridine, S-12968-(−), enantiomer of S-11568-([2-(7 amino 2,5-dioxaheptyl) 3-ethoxycarbonyl 4-)2,3-dichlorophenyl) 5-methoxycarbonyl 6-methyl 1,4 dihydropyridine], see Figure 1 and Prieto *et al.*, 1991). Its effects on blood pressure were compared to those produced by the stereoisomer S-12967-(+), nifedipine or sodium nitroprusside. *In vitro* studies show that S-12967-(+) is at least 10 times less potent than S-12968-(−) (Randle *et al.*, 1990). As there are several reasons to support the hypothesis that CEB may be especially effective following vascular calcium overloads such as occur in atherosclerosis (Hof, 1990) and arteriosclerosis (Fleckenstein *et al.*, 1990), we repeated our experiments in a rat model of vascular calcium overload (Henrion *et al.*, 1991). In a second experiment the effects of S-12968-(−) on cardiac output and total peripheral resistance were studied.

Methods

Animals

Male, outbred Wistar rats, 200–240 g, purchased from Iffa-Credo SA, L'Arbresle, France, were housed under standard conditions. They were given a standard rodent diet (UAR, Villemoisson sur Orge, France) and water; body weight (g) was recorded daily.

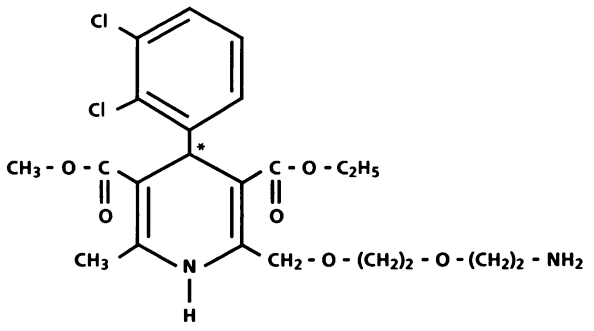

Figure 1 Chemical structure of S-12967-(+) and S-12968-(−) (*indicates asymmetric C-atom in the dihydropyridine ring).

[1] Author for correspondence.

Vitamin D_3 and nicotine treatment

Approximately half of the rats ($n = 72$) were injected with vitamin D_3 (300,000 iu kg^{-1}, i.m.), at 08 h 00 min on day 1. Immediately following the administration of vitamin D_3, rats were given nicotine (25 mg kg^{-1}, p.o.). The nicotine administration was repeated at 18 h 00 min. Rats were allowed 16 days to recover (Henrion *et al.*, 1991). The control group ($n = 89$) followed a similar protocol except that animals were injected on day 1 with 0.15 M NaCl, i.m., and received 2 injections of distilled water (5 ml kg^{-1}, p.o.).

Effects of S-12968-(−), S-12967-(+), nifedipine, sodium nitroprusside or 0.15 M NaCl on blood pressure and heart rate in conscious rats

A polyethylene cannula consisting of an intravascular portion (internal diameter 0.28 mm, external diameter 0.61 mm) welded to an extravascular portion (internal diameter 0.58 mm, external diameter 0.96 mm), was placed in the femoral artery under halothane/oxygen anaesthesia. A second polyethylene cannula consisting of an intravascular portion (internal diameter 0.40 mm, external diameter 0.80 mm) welded to an extravascular portion (internal diameter 0.76 mm, external diameter 1.22 mm), was placed in the femoral vein. Rats were then allowed 24 h to recover from the operation and on day 17 the femoral artery cannula was connected to a low volume pressure transducer for the measurement of arterial pressure (diastolic, systolic, and pulse, mmHg). Mean arterial pressure (mmHg) was obtained by electronic integration of the pulse pressure signal. Heart rate (b.p.m.) was recorded with a ratemeter driven by the pulse pressure signal.

Conscious unrestrained rats were maintained in their home cages for blood pressure recording. On the day of the experiment, the cannula, which passed through the skin behind the neck, was connected to the recording and injection systems but no harness was used. Following 30 min recording of basal values for blood pressure and heart rate, rats were injected i.v. with S-12968-(−) (0.1 to 3 mg kg^{-1}), S-12967-(+) (0.3 to 10 mg kg^{-1}), nifedipine (0.1 to 3 mg kg^{-1}), sodium nitroprusside (0.1 to 3 mg kg^{-1}) or 0.15 M NaCl. Each animal received 4 injections (i.v.) of one drug or of 0.15 M NaCl only. Blood pressure and heart rate were recorded 2, 5, 10, 15 and 30 min after each dose. Doses were administered cumulatively.

Effects of S-12968-(−) on cardiac output and total peripheral resistance in pentobarbitone-anaesthetized rats

Rats ($n = 6$, per group) were anaesthetized with sodium pentobarbitone (50 mg kg^{-1}, i.p.) and cannula introduced into the femoral artery and vein. The thorax was opened and an electromagnetic flowprobe (Narco Biosystems, Houston, Texas, USA) placed on the ascending aorta, S-12968-(−) was injected (0.1, 0.3 and 1 mg kg^{-1}, i.v.) at 30 min intervals. Changes in mean arterial pressure (mmHg), cardiac output (ml min^{-1}), heart rate (beats min^{-1}, b.p.m.), stroke volume (μl $beat^{-1}$) and total peripheral resistance (mmHg ml^{-1} min^{-1}) were measured before and after i.v. injection.

Blood sampling and tissue calcium analysis

Thirty minutes following the final dose of each substance, 1 ml of blood was removed for the determination of sodium, potassium, calcium, magnesium, phosphate, glucose, triglycerides, cholesterol, urea, creatinine, protein, alkaline phosphatase and aspartate aminotransferase activities. An autopsy was carried out and samples of the thoracic aorta, carotid artery, tail artery, left ventricular myocardium, duodenum and right kidney were removed for the analysis of tissue calcium and magnesium content.

Calcium (mM) in plasma samples was determined by reaction with methylthymol blue, and phosphate (mM) by formation of a phosphomolybdate complex with ammonium heptamolybdate. Magnesium (mM) was determined with the calmagite reagent (3-hydroxy-4-2-hydroxy-5-methylphenylazo-1-naphtalene sulphonic acid). Sodium (mM) and potassium (mM) were determined by flame emission photometry. Creatinine (μM) was estimated from the rate of formation of the picrate-creatinine complex, and urea (mM) by incubation with urease. Cholesterol and triglycerides (mM) were determined with cholesterol oxidase and lipase, and glucose concentration (mM) by incubation with glucose oxidase then with peroxidase. Protein concentration (g l^{-1}) was determined by the Lowry method. Aspartate aminotransferase activity (iu ml^{-1}) was estimated by incubation with L-aspartate and alkaline phosphatase activity (iu l^{-1}) by incubation with nitro-4-phenol phosphate.

For tissue calcium and magnesium analysis, tissues were weighed and heated to constant dry weight. Dry tissue samples were dissolved in nitric acid (14 N) and left for 72 h at room temperature. The sample was then centrifuged (2000 *g*, 10 min) and the supernatant removed. Lanthanum chloride was added to the supernatant, the solution was atomized and changes in optical density at 422.7 nm for calcium, and 285.2 nm for magnesium, were measured (atomic absorption spectrophotometer model 2380, Perkin-Elmer, Norwalk, Connecticut, U.S.A.). Tissue calcium and magnesium values are given as μmol g^{-1} tissue dry weight.

Substances used

S-12968-(−) and S-12967-(+) (Figure 1) were kindly provided by I.R.I.S., Paris, France. Vitamin D_3 or cholecalciferol (Vi-Dé), a gift of Sandoz AG, Bern, Switzerland, was dissolved in an aequeous solution of sodium citrate, propylene glycol, butyl alcohol, isobutyl alcohol and emulsifying agent (Mulgofen EL-719, Antara Chemicals, New York, NY, U.S.A.). Ampoules of 7.5 mg (= 300,000 iu) in 1 ml of this solution were opened immediately prior to the intramuscular injection. Nicotine bitartrate, nifedipine and sodium nitroprusside were purchased from Sigma, St. Louis, Missouri, U.S.A. Fresh solutions were prepared each day. Doses are given in terms of the base.

Statistics

Values are given as means ± s.e.mean. Significant differences between means were calculated by ANOVA and the Scheffe test. Linear regression analysis was used for the determination of the statistical significance of the correlation (r) of heart rate (b.p.m., y) with mean arterial pressure (mmHg, x), and pulse pressure (mmHg, y) with diastolic arterial pressure (mmHg, x). Analysis was performed by use of the individual values for each animal at each dose of substance.

Results

Body weight and blood parameters

Treatment with vitamin D_3 and nicotine induced an initial fall in body weight from the first (219 ± 3 g) to the sixth day (182 ± 3 g). From the sixth to the sixteenth day, vitamin D/nicotine-treated animals gained weight at a rate of + 8.3 ± 0.5 g per day. Control rats gained weight from the first (215 ± 2 g) to the sixteenth day (320 ± 3 g), at a rate of + 6.6 ± 0.5 g per day. Following cannulation of the femoral artery and vein growth stopped and body weight on the seventeenth day (263 ± 4 g for vitamin D/nicotine-treated animals and 319 ± 3 g for controls) was not significantly different from that on the sixteenth day.

Only minor differences were observed in the various blood parameters between controls ($n = 89$) and vitamin D/nicotine-treated animals ($n = 72$). Although there were slight falls

in vitamin D/nicotine-treated animals, in magnesium (0.85 ± 0.04, controls 0.98 ± 0.04 mM, $P<0.05$), potassium (3.78 ± 0.08, controls 4.00 ± 0.06 mM, $P<0.05$), and phosphate (1.59 ± 0.07, controls 1.94 ± 0.07 mM, $P<0.05$) levels, and aspartate aminotransferase activity (190 ± 38, controls 326 ± 45 i.u. l^{-1}, $P<0.05$), there were no signs of renal or other toxicity.

Tissue calcium and magnesium

Treatment with vitamin D_3 and nicotine produced large increases in the calcium content of most organs but no significant change in magnesium content apart from a small increase in the carotid artery and kidney (Table 1). The increase in tissue calcium was greatest in the compliance blood vessels, 24 fold for thoracic aorta and 10 fold for the carotid artery.

Basal blood pressure and heart rate values for conscious rats, and changes in blood pressure and heart rate following saline

Treatment with vitamin D_3 and nicotine produced a 12% increased in systolic arterial pressure (145 ± 2, $n = 72$, controls 129 ± 3 mmHg, $n = 89$, $P<0.05$), a 7% decrease in diastolic arterial pressure (87 ± 2, controls 93 ± 3 mmHg, $P<0.05$), a 60% increase in pulse pressure (57 ± 2, controls 36 ± 3 mmHg, $P<0.05$), but no change in mean arterial pressure (106 ± 2, controls 105 ± 2 mmHg) or in heart rate (440 ± 14, controls 454 ± 10 b.p.m.).

Administration of 0.15 M NaCl had no significant effect in either controls ($n = 25$) or vitamin D/nicotine-treated animals ($n = 22$; results not shown).

Effects of S-12968-(−), S-12967-(+), nifedipine or sodium nitroprusside on blood pressure and heart rate in conscious rats

S-12968-(−) produced cumulative, dose-related falls in blood pressure, the maximum effect being observed 5 or more min following each i.v. injection (Figure 2). At the end of the experiments values were lower than at the beginning: controls 79 ± 4/54 ± 3 versus 120 ± 6/85 ± 8 mmHg, vitamin D/nicotine-treated animals 92 ± 4/58 ± 4 versus 133 ± 3/88 ± 6 mmHg. Doses of less than 3 mg kg^{-1} had no significant effect on heart rate. Following a dose of 3 mg kg^{-1} there was a fall in heart rate in controls (from 485 ± 12 b.p.m. to 389 ± 12 b.p.m., $P<0.05$) and vitamin D/nicotine-treated animals (from 462 ± 10 b.p.m. to 361 ± 11 b.p.m., $P<0.05$).

Nifedipine produced similar changes to those observed with S-12968-(−) except that the initial fall in blood pressure was more rapid (Figure 3). At the end of the experiment values were lower than at the beginning: controls, 91 ± 5/

Table Tissue calcium and magnesium levels (μmol g^{-1} dry weight) in rats

	Controls ($n = 89$)	*Vitamin D/ nicotine-treated animals* ($n = 72$)	*Ratio*
Calcium			
Thoracic aorta	10 ± 1	244 ± 43*	24
Carotid artery	26 ± 2	268 ± 39*	10
Tail artery	17 ± 1	52 ± 6*	3
Left ventricular myocardium	3.4 ± 0.5	35 ± 6*	11
Duodenum	3.0 ± 0.5	6.8 ± 1.2*	2
Right kidney	5.0 ± 0.3	83 ± 22*	17
Magnesium			
Thoracic aorta	23 ± 2	33 ± 4	1
Carotid artery	41 ± 4	69 ± 9*	2
Tail artery	32 ± 2	26 ± 2	1
Left ventricular myocardium	42 ± 1	44 ± 1	1
Duodenum	41 ± 3	43 ± 3	1
Right kidney	37 ± 1	81 ± 7*	2

Values are given as means ± s.e.mean. *$P<0.05$.

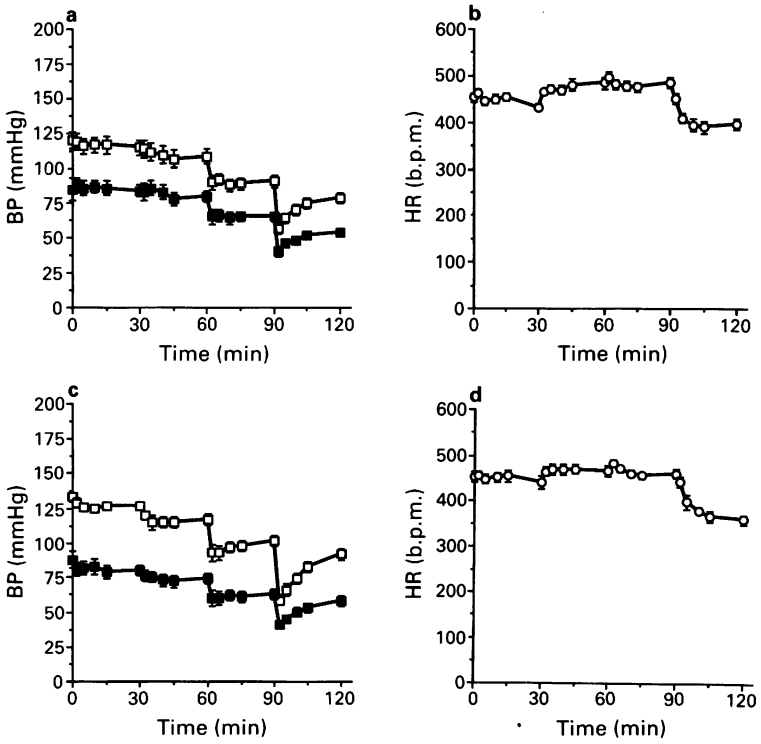

Figure 2 Changes in systolic (□) and diastolic (■) blood pressure (mmHg, a,c), and in heart rate (HR, b.p.m.) (○, b,d) in controls (a,b, $n = 13$) and vitamin D/nicotine-treated rats (c,d, $n = 11$) injected i.v. with S-12968-(−) (0.1, 0.3, 1 and 3 mg kg^{-1} at 0, 30, 60 and 90 min).

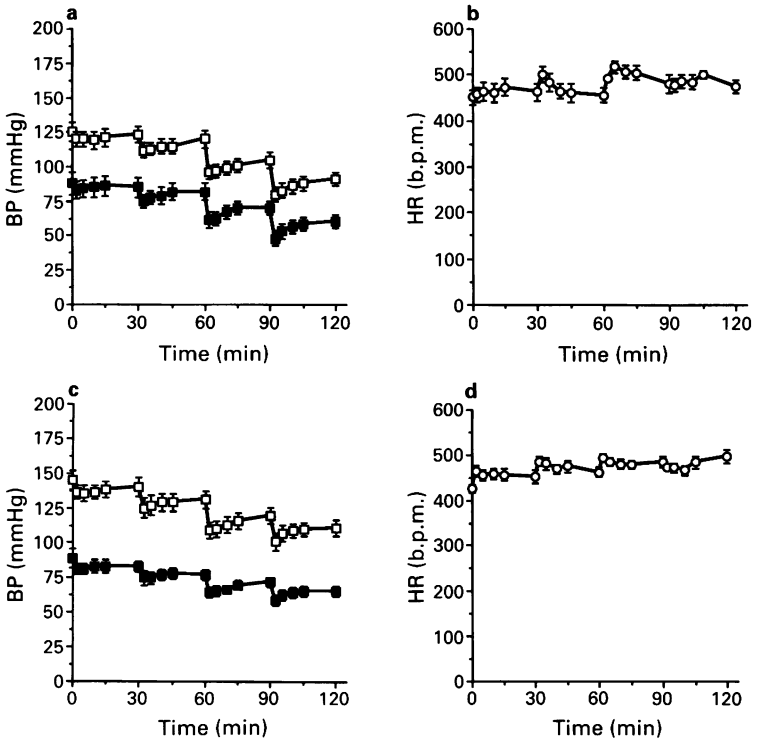

Figure 3 Changes in systolic (□) and diastolic (■) blood pressure (mmHg, a,c), and in heart rate (HR, b.p.m.) (○, b,d) in controls (a,b, $n = 11$) and vitamin D/nicotine-treated rats (c,d, $n = 12$) injected i.v. with nifedipine (0.1, 0.3, 1 and 3 mg kg^{-1} at 0, 30, 60 and 90 min).

60 ± 5 versus 125 ± 7/88 ± 8 mmHg, vitamin D/nicotine-treated animals, 111 ± 6/66 ± 4 versus 145 ± 7/89 ± 7 mmHg. The falls in blood pressure produced by doses of 0.3 and 1 mg kg^{-1} of nifedipine were accompanied by reflex tachycardia which was more pronounced in controls than in vitamin D/nicotine-treated animals. The slope (b) relating the increase in heart rate to the fall in mean arterial pressure, an index of baroreflex sensitivity, had a value of 2.65 b.p.m. mmHg^{-1} in controls ($r = 0.57$, $P < 0.05$) and 0.89 in vitamin D/nicotine-treated animals ($r = 0.37$, $P < 0.05$). Following the highest dose (3 mg kg^{-1}) there was no significant change in heart rate (Figure 3), or in pulse pressure (Figure 4). S-12968-(−) produced a fall in pulse pressure especially in vitamin D/nicotine-treated animals.

Sodium nitroprusside produced rapid falls in blood pressure, which were accompanied by tachycardia (Figure 5). The slope (b) relating the increase in heart rate to the fall in mean arterial pressure had a value of 2.05 b.p.m. mmHg^{-1} in controls ($r = 0.81$, $P < 0.05$) and 0.74 in vitamin D/nicotine-treated animals ($r = 0.37$, $P < 0.05$).

S-12967-(+) produced dose-related increases in blood pressure of short duration, the maximum effect generally being observed 2 min after the i.v. injection (Figure 6). The effects were more pronounced in controls than in vitamin D/nicotine-treated animals. The slope (b) relating the decrease in heart rate to the increase in mean arterial pressure had a value of −3.18 b.p.m. mmHg^{-1} in controls ($r = 0.69$, $P < 0.05$) and −1.60 in vitamin D/nicotine-treated animals ($r = 0.39$, $P < 0.05$).

Effects of S-12968-(−) on cardiac output and total peripheral resistance in pentobarbitone-anaesthetized rats

S-12968-(−) produced dose-related falls in mean arterial pressure in pentobarbitone-anaesthetized rats (Figure 7). At higher doses falls in cardiac output, mainly due to falls in stroke volume, were observed. Such effects were more pronounced in vitamin D/nicotine treated rats, and in such animals the blood pressure lowering effect of the largest dose of S-12968-(−) injected (1 mg kg^{-1}) was accompanied by a large fall in cardiac output with no significant change in total peripheral resistance. The fall in cardiac output resulted from a fall in stroke volume.

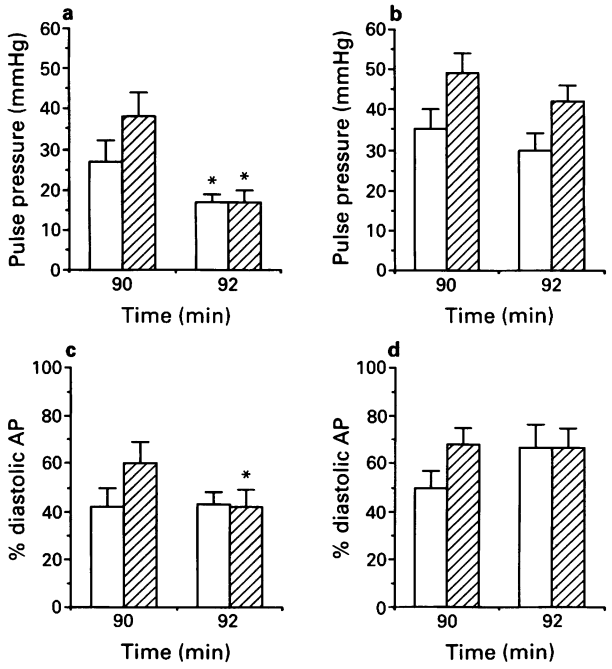

Figure 4 Pulse pressure (mmHg: a, b, percentage of diastolic arterial pressure (AP): c,d) before (90 min) and 2 min following (92 min) an i.v. injection of S-12968-(−) (a,c) or nifedipine (b,d) at a dose of 3 mg kg^{-1} (controls: open columns, vitamin D/nicotine-treated rats: hatched columns).

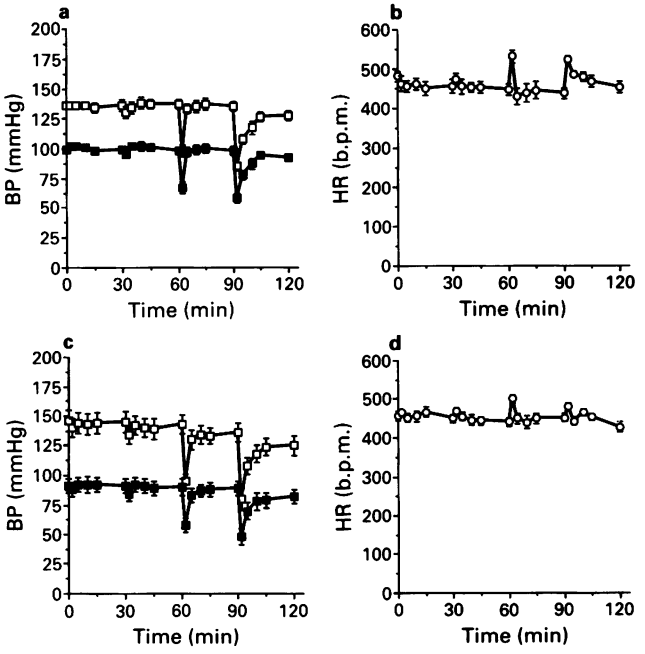

Figure 5 Changes in systolic (□) and diastolic (■) blood pressure (mmHg, a,c), and in heart rate (HR, b.p.m.) (○, b,d) in controls (a,b, $n = 12$) and vitamin D/nicotine-treated rats (c,d, $n = 11$) injected i.v. with sodium nitroprusside (0.1, 0.3, 1 and 3 mg kg^{-1} at 0, 30, 60 and 90 min).

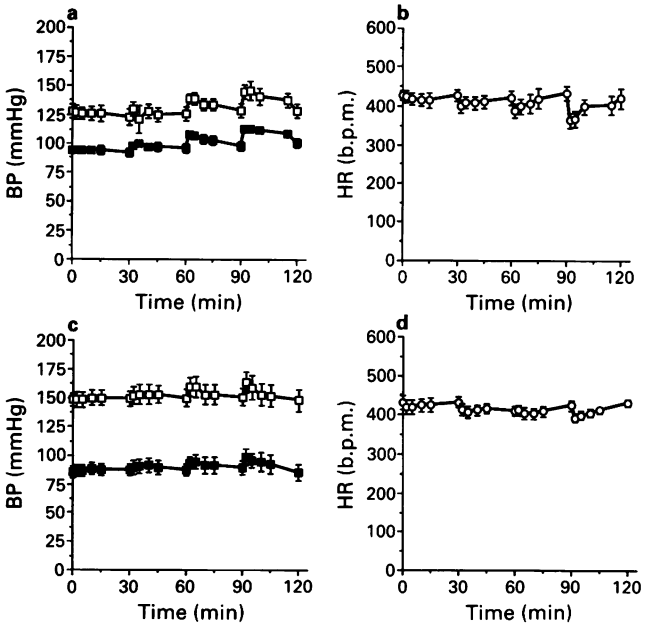

Figure 6 Changes in systolic (□) and diastolic (■) blood pressure (mmHg, a,c), and in heart rate (HR, b.p.m.) (○, b,d) in controls (a,b, $n = 12$) and vitamin D/nicotine-treated rats (c,d, $n = 10$) injected i.v. with S-12967-(+) (0.3, 1, 3 and 10 mg kg^{-1} at 0, 30, 60 and 90 min).

Discussion

In conscious rats the main difference between S-12968-(−) and nifedipine was that the falls in blood pressure provoked by S-12968-(−) were not accompanied by reflex tachycardia. The absence of reflex tachycardia cannot be explained by the fact that S-12968-(−) is longer acting than nifedipine, as this is not the case in this experiment, and nifedipine and sodium

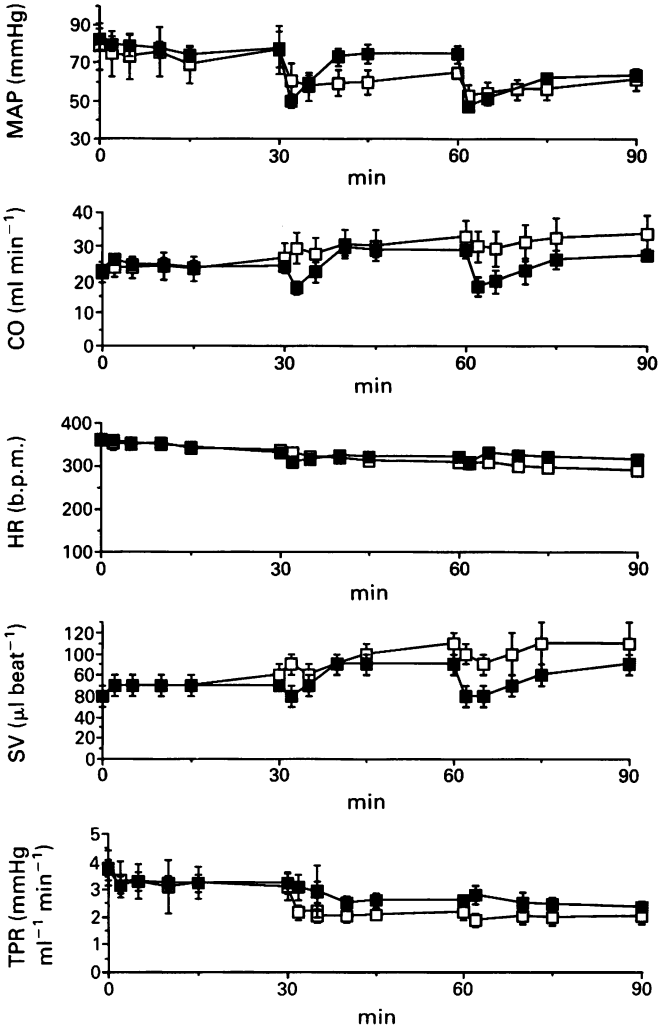

Figure 7 Changes in mean arterial pressure (MAP, mmHg), cardiac output (CO, ml min^{-1}), heart rate (HR, b.p.m.), stroke volume (SV, μl beat^{-1}) and total peripheral resistance (TPR, mmHg ml^{-1} min^{-1}) following i.v. injections of S-12968-(−) (0.1, 0.3 and 1 mg kg^{-1} at 30 min intervals) in controls (□, $n = 6$) and vitamin D/nicotine-treated animals (■, $n = 6$).

nitroprusside which have very different hypotensive profiles provoke similar degrees of reflex tachycardia. Furthermore the long-acting dihydropyridine, amlodipine (which has a chemical structure similar to that of S-12968-(−); Frishman, 1990) does provoke reflex tachycardia.

The *in vitro* calcium channel inhibitory properties of S-12968-(−) appear to be no different from those of other dihydropyridines, such as nifedipine (Randle *et al.*, 1990). *In vivo*, however, S-12968-(−) has a greater selectivity for myocytes than for vascular smooth muscle cells (Sassen *et al.*, 1991). In our study, the absence of reflex tachycardia also suggests that S-12968-(−) has an effect on the heart. Such an action would also explain the effects of S-12968-(−) on pulse pressure in vitamin D/nicotine-treated rats and the bradycardia observed after the highest dose. In these animals, a high dose of S-12968-(−) produced a fall in pulse pressure which was greater than that to be expected from the concomitant fall in diastolic arterial pressure. Such a fall in pulse pressure could be due to an increase in large artery compliance or a fall in cardiac output. Whilst we cannot exclude the possibility of an acute effect of S-12968-(−) on compliance, a decrease in cardiac output is confirmed by our results in pentobarbitone-anaesthetized vitamin D/nicotine-treated rats. In the anaesthetized pig, S-12968-(−) has a negative inotropic effect (Sassen *et al.*, 1991).

The use of the vitamin D/nicotine model revealed the possibility of a cardiac effect of S-12968-(−). Whilst the hypotensive profiles of S-12968-(−) and nifedipine were similar in controls, in vitamin D/nicotine-treated rats, S-12968-(−) had a greater effect on systolic and pulse pressure than did nifedipine. A further sign of cardiac dysfunction in this model is seen in the decrease in baroreflex sensitivity following nifedipine and sodium nitroprusside in the present paper and in our previous results (Lartaud *et al.*, 1991). The effects of S-12968-(−) (and nifedipine and sodium nitroprusside) on diastolic arterial pressure were similar in controls and vitamin D/nicotine-treated rats suggesting that the control of peripheral resistance is not modified in this model.

Finally, S-12967-(+) increased blood pressure in a dose-related way in both controls and vitamin D/nicotine-treated animals suggesting that S-12967-(+) is a calcium channel activator. Electrophysiological studies (Randle *et al.*, 1990) do not confirm this hypothesis, however, so the mechanism of its pressor effect remains to be elucidated. Furthermore *in vitro* studies by Prieto *et al.* (1991) show that in isolated mesenteric resistance arteries the two stereoisomers have both contractile and relaxant properties.

This work was supported by grants from the Urban District Council of Nancy and IRIS, Paris, France. The help and advice of Béatrice Dard-Brunelle of IRIS is gratefully acknowledged by the authors.

References

FLECKENSTEIN, A., FREY, M., ZORN, J. & FLECKENSTEIN-GRÜN, G. (1990). Calcium, a neglected key factor in hypertension and arteriosclerosis. Experimental vasoprotection with calcium antagonists or ACE inhibitors. In *Hypertension: Pathophysiology, Diagnosis and Management*. ed. Laragh, J.H. & Brenner, B.M. pp. 471–509. New York: Raven Press.

FRISHMAN, W.H. (1990). Amlodipine. In *Cardiovascular Drug Therapy*. ed. Messerli, F.H. pp. 1017–1033. Philadelphia: W.B. Saunders.

HENRION, D., CHILLON, J.M., GODEAU, G., MULLER, F., CAPDEVILLE-ATKINSON, C., HOFFMAN, M. & ATKINSON, J. (1991). The consequences of aortic calcium overload following vitamin D_3 plus nicotine treatment in young rats. *J. Hypertension*, **9**, 919–926.

HOF, R.P. (1990). Antiatherogenic properties of calcium antagonists. In *Coronary and Cerebrovascular Effects of Antihypertensive Drugs*. ed. Atkinson, J., Capdeville, C. & Zannad, F. pp. 182–204. Tunbridge Wells: TransMedica.

KIOWSKI, W., ERNE, P., BERTEL, O., BOLLI, P. & BÜHLER, F.R. (1986). Acute and chronic sympathetic reflex activation and antihypertensive response to nifedipine. *J. Am. Coll. Cardiol.*, **7**, 344–348.

LARTAUD, I., HENRION, D., BARRES, C. & ATKINSON, J. (1991). Cardiac baroreflex sensitivity in conscious rats with cardiovascular calcium overload. *Fund. Clin. Pharmacol.*, (abstract) **5**, 418.

PRIETO, D., MULVANY, M.J. & NYBORG, N.C.B. (1991). S-12967-(+) and S-12968-(−): 1,4-dihydropyridine stereoisomers with calcium channel agonistic and antagonistic properties in rat resistance arteries. *Br. J. Pharmacol.*, **103**, 1703–1708.

RANDLE, J.C.R., LOMBET, A., NAGEL, N., ABRAHAM, C., APTEL, H., PEGLION, J.L. & RENAUD, J.F. (1990). Ca^{2+} channel inhibition by a new dihydropyridine derivative, S11568, and its enantiomers S12967 and S12968. *Eur. J. Pharmacol.*, **190**, 85–96.

SASSEN, L.M.A., VAN DER ZANDE, J., MCFALLS, E.O. & VERDOUW, P.D. (1991). Cardiovascular profile of the new dihydropyridine derivative S12968. *Eur. J. Pharmacol.*, **199**, 61–67.

(Received September 30, 1991
Revised January 2, 1992
Accepted January 14, 1992)

Br. J. Pharmacol. (1992), **106**, 85–90 © Macmillan Press Ltd, 1992

Intervascular and stimulus selectivity of nitrendipine and related derivatives in KCl and prostaglandin $F_{2\alpha}$ precontracted porcine arteries

[1]Georg Kojda, Wolfgang Klaus, Günther Werner & [2]Uwe Fricke

Institut für Pharmakologie der Universität zu Köln, Gleueler Straße 24, D-5000 Köln 41, Germany

1 Dihydropyridine-type calcium entry blockers exhibit a different vasodilator potency depending on the arterial tissue (intervascular selectivity) as well as on the precontracting stimulus used (stimulus selectivity). In addition, the structure of their ester side chains seems to influence their activity.

2 Vascular activity of nitrendipine and six related 3-ester side chain derivatives was investigated in isolated coronary, ulnar and basilar arteries of the pig following precontraction with KCl or prostaglandin $F_{2\alpha}$ ($PGF_{2\alpha}$).

3 After depolarization, all dihydropyridines exhibited a weak preferential action on coronary arteries. Bay E 6927 produced the strongest effect in all vessel types. By contrast, precontraction with $PGF_{2\alpha}$ resulted in a marked preferential action in basilar arteries, although higher concentrations of the dihydropyridines were required for half maximal vasorelaxation. In each case, ulnar arteries were less sensitive.

4 Except with Bay O 5572, the most bulky substituted and least active derivative, only moderate differences were observed within the dihydropyridines studied. On the other hand, there was a pronounced increase in the ratios of the half maximal active concentrations required after precontraction of the vessels with $PGF_{2\alpha}$ compared to KCl (stimulus selectivity) following a limited prolongation of the 3-ester side chain up to an isopropyl-group.

5 It is suggested that the observed shift in the intervascular selectivity after precontraction with $PGF_{2\alpha}$ is a consequence of different contractile mechanisms in the three vessel types studied. The degree of the stimulus selectivity may also depend on the structure of the dihydropyridines.

Keywords: Dihydropyridines; nitrendipine; structure; porcine isolated arteries; intervascular selectivity; stimulus selectivity; prostaglandin $F_{2\alpha}$ ($PGF_{2\alpha}$)

Introduction

Calcium entry blockers of the dihydropyridine type are widely used in the treatment of cardiovascular diseases. On the molecular basis, their main target in the body are L-type calcium channels in the smooth muscles of the arterial system, although they also exhibit a definite influence on calcium channels of other tissues e.g. ventricular muscle (Godfraind *et al.*, 1986). In recent years several new dihydropyridines have been introduced with specific indications, that are based on a selective action of these drugs in different parts of the vascular system (intervascular selectivity). Thus nisoldipine has been described as acting preferentially in coronary arteries (Godfraind *et al.*, 1987,a,b). In addition, Kazda & Towart (1981) reported on the cerebrovascular selectivity of nimodipine, a drug with benefit in the management of cerebrovascular disorders following subarachnoidal haemorrhage (Gelmers *et al.*, 1985). On the other hand, Fricke & Ueckert (1988) demonstrated a particular cerebrovascular selectivity for nisoldipine in depolarized arteries, whereas nimodipine exhibited rather a predominant potency in coronary arteries. However, arterial depolarization as a widely used pharmacological model to study the effects of dihydropyridines reflects only in part the mechanisms responsible for arterial contraction (Bolton, 1979). Other mechanisms may be carried by receptor-mediated pathways. Investigations on dihydropyridines in isolated arteries precontracted with vasoactive agonists often revealed a reduced activity compared to that achieved in the same arteries precontracted by depolarization (Cauvin *et al.*, 1983). Such stimulus selective action has also been described for nitrendipine (Altura & Altura, 1984; Scriabine *et al.*, 1984). However, a comprehensive investigation on the intervascular and stimulus selectivity of dihydropyridines in different arteries of the same species is still lacking.

The present study was performed to investigate (1) if and to what degree nitrendipine displays intervascular and stimulus selectivity and (2) whether the intervascular selectivity depends on the stimulus used for precontraction of the different porcine arteries. In addition, we were interested in activity differences due to a modification of the chemical structure of nitrendipine. Therefore, six nitrendipine derivatives with a modified 3-ester side chain (cf. Figure 1) were included. The ester side chains of dihydropyridines have previously been found to have a direct influence on vasodilator activity (Bossert *et al.*, 1979; Fricke *et al.*, 1988).

Methods

Preparation of vascular ring segments

The experiments were performed on arterial vessels from 5–7 month old pigs (70–90 kg) obtained from the local slaughterhouse. The hearts, brains and forelegs were removed 10–30 min after death. Right coronary, ulnar and basilar arteries were rapidly dissected and flushed gently with cold oxygenated (95% O_2 + 5% CO_2) Krebs-Henseleit solution

[1] Present address: Institut für Pharmakologie der Universität Düsseldorf, Moorenstr. 5, D-4000 Düsseldorf 1, Germany.
[2] Author for correspondence.

(pH 7.4) of the following composition: (mmol l^{-1}): Na^+ 123.07, K^+ 5.87, Ca^{2+} 1.6, Mg^{2+} 1.18, Cl^- 124.78, HCO_3^- 5.00, $H_2PO_4^-$ 2.36, SO_4^{2-} 1.18 and glucose 5.05. After carefully removing all loosely adherent tissue, proximal parts of the arteries were cut into ring segments (3–4 mm) and mounted between stainless steel triangles in a 10 ml jacketed organ bath (37°C) as recently described (Fricke *et al.*, 1988). Previous experiments with KCl (60 mmol l^{-1}) revealed an optimal resting tension of 2.0 g for the coronary and ulnar arteries and 0.7 g for the basilar arteries. Destruction of the endothelium was achieved by carefully rubbing the luminal surface of the artery segments with a thin steel needle. To further prevent the influence of endothelium on the vasodilator activity of the dihydropyridines (Kojda *et al.*, 1990), all vessels were incubated with methylene blue (5–10 μmol l^{-1}) prior to the experimental procedure. Changes in arterial diameter were measured with an isotonic transducer (Fleck, Mainz, Germany) and recorded after amplification on a thermorecorder (Hellige Servomed, Freiburg, Germany) or on a digital point printing recorder (Linseis, Typ LPD 12, Selb, Germany). The contractile response of the artery rings was calculated from the observed changes in their diameter using the equation $W = m\ g\ s$, with W = work, m = tension, g = 9.81 m s^{-2}, s = change in diameter and is given in μJ as described previously (Kojda *et al.*, 1990). Mean values of KCl-induced (60 mmol l^{-1}) contractile work were 50.0 ± 1.5 μJ ($n = 53$); 2.6 ± 0.17 μJ ($n = 37$) and 37.7 ± 1.7 μJ ($n = 46$) and of $PGF_{2\alpha}$-induced contractile work were 55.8 ± 1.9 μJ ($n = 56$); 2.3 ± 0.08 μJ ($n = 54$) and 30.9 ± 2.1 μJ ($n = 46$) for coronary, basilar and ulnar arteries, respectively.

Organ bath experiments

After an equilibration period of 1–2 h, reproducible and maximal contractions were induced by addition of KCl (60 mmol l^{-1}) or $PGF_{2\alpha}$ (50 μmol l^{-1}, in the case of basilar arteries 5 μmol l^{-1}). The different concentrations of $PGF_{2\alpha}$ used have been shown to elicit maximal contractions in the specific vessel types (Werner *et al.*, 1988). Nitrendipine and the six related derivatives shown in Figure 1 were added in a cumulative manner (0.1 nmol l^{-1}–100 μmol l^{-1}), in the course of which the volume of the applied drug solutions did not exceed more than 70 μl. The time intervals were chosen such as to allow a steady state of drug action indicated by a stable arterial tension. To prevent photodegradation of the dihydropyridines all experiments were carried out under sodium light. At the end of each concentration-response curve, all drugs were washed out by rinsing the artery segments several times with Krebs-Henseleit solution. In the case of $PGF_{2\alpha}$ precontracted coronary and ulnar arteries, 200 μmol l^{-1} papaverine was added before the washout period to produce complete relaxation. Ulnar arteries in particular responded with a very slow reduction of tension following the washout period, so that baseline value was not achieved within 1 h. Such incomplete relaxation was not observed in $PGF_{2\alpha}$ precontracted basilar arteries or in depolarized vessels.

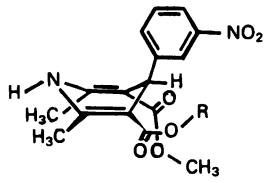

	Substance	R	Mol. wt.	Volume
1	Bay A 4339	$-CH_3$	346.3	20.0
2	Nitrendipine	$-C_2H_5$	360.4	34.7
3	Bay E 6927	$-CH(CH_3)_2$	374.4	62.3
4	Bay N 6391	$-C(CH_3)_3$	388.4	65.3
5	Bay I 1441	$-CH_2-C_6H_5$	422.4	85.1
6	Bay L 3501	$-CH_2-C(CH_3)_3$	402.4	85.7
7	Bay O 5572	$-(CH_2)_7-CH_3$	444.5	171.7

Figure 1 Chemical structure of nitrendipine and related 3-ester side-chain derivatives and their molecular weight (Mol. wt.). The calculated volumes of the 3-ester side-chains (see methods) are given in $Å^3$.

Statistical analysis

Vasorelaxation due to treatment with the drugs is expressed as percentage of the maximal contractile response achieved with the vasoconstrictors used at the beginning of the experiments. The concentrations of the dihydropyridines for half maximal inhibition of KCl and $PGF_{2\alpha}$-induced vasoconstriction (pD_2 values) were calculated from the individual concentration-effect curves as proposed by Hafner *et al.* (1977). All data were analysed by one-way analysis of variance (ANOVA) with subsequent Student-Newman Keuls test (SAS PC Software 6.04, PROC ANOVA) and are expressed as mean values and standard error of the mean (s.e.mean) A P value less than 0.05 was considered significant.

Sterical parameters

The volumes of the different 3-ester side chains of nitrendipine and its derivatives (Figure 1) were approximately estimated by means of calculated data for the widths and length of various chemical substituents published by Verloop *et al.* (1976). These volume data correlated well with the lipophilicity of the dihydropyridines investigated, measured by high performance liquid chromatography (Kojda *et al.*, 1989).

Materials

The chemicals (analytical grade) were purchased from Merck (Darmstadt, Germany) and dissolved in water. The dihydropyridines were generously provided by Bayer AG (Leverkusen, Germany) and dissolved in dimethylsulphoxide, which itself had no effect on the arterial tone up to a concentration in the organ bath of 1%.

Results

KCl-stimulated arteries

The sensitivity to KCl differed in the different vessel types examined. Concentrations for half maximal contractile response were in coronary 32.5 ± 1.3 mmol l^{-1} ($n = 4$) and in ulnar arteries 33.4 ± 0.9 mmol l^{-1} ($n = 5$), whereas in basilar arteries this concentration was significantly reduced to 24.8 ± 0.9 mmol l^{-1} ($n = 4$; $P < 0.01$). Nitrendipine and all related 3-ester-side-chain derivatives inhibited concentration-dependently KCl-induced contractions of the different blood vessels. In coronary arteries Bay E 6927 was significantly more potent than nitrendipine and both compounds exhibited significantly higher pD_2 values than the other dihydropyridines (Table 1, $P < 0.05$). Except for Bay O 5572, which was the weakest drug, the differences in the potency of the compounds studied did not exceed one order of magnitude. A similar situation was observed in basilar and ulnar arteries, though the differences obtained in the potencies were rather more pronounced in basilar arteries (Tables 2 and 3). Contrary to the full relaxation induced by the dihydropyridines in coronary and basilar arteries, the reduction of tension at the end of each concentration-response curve in ulnar arteries

Table 1 The vasodilator potencies of the 1, 4-di-hydropyridines examined (cf. Figure 1, NTD = nitrendipine) on porcine isolated coronary artery rings stimulated with KCl (60 mmol l^{-1}) or prostaglandin $F_{2\alpha}$ ($PGF_{2\alpha}$, 50 μmol l^{-1}) expressed as the concentration producing half maximal response (pD_2) following cumulative drug application

Compound	*pD_2 KCl*	n	*pD_2 $PGF_{2\alpha}$*	n
A 4339	7.49 ± 0.03	6	4.65 ± 0.04*	8
NTD	8.25 ± 0.06	9	4.63 ± 0.10*	11
E 6927	8.53 ± 0.06	11	4.07 ± 0.07*	8
N 6391	7.71 ± 0.09	6	4.10 ± 0.06*	6
I 1441	7.71 ± 0.14	8	4.07 ± 0.07*	8
L 3501	8.02 ± 0.07	7	4.68 ± 0.08*	7
O 5572	5.93 ± 0.11	6	<4.00	8

Mean values and standard error (s.e.mean) of *n* individual experiments are given in − log mol l^{-1}.
Significant differences, $*P<0.00001$.
Because of the very low activity of Bay O 5572 following $PGF_{2\alpha}$-precontraction, this pD_2-value is lacking.

was incomplete (percentage of persisting contraction following the drug sequence given in Figure 1: 26.4 ± 1.5; 12.2 ± 0.6; 16.4 ± 3.3; 31.8 ± 4.1; 17.1 ± 2.0; 16.8 ± 1.1 and 37.1 ± 0.5).

Prostaglandin $F_{2\alpha}$-stimulated arteries

Apart from Bay O 5572, all dihydropyridines produced a distinct vasorelaxation in coronary and basilar arteries. However, compared to KCl-stimulation the calculated pD_2 values were shifted to much higher concentrations (Tables 1 and 2). In addition, treatment with the dihydropyridines did not abolish the contractions of the coronary arteries (percentage of persistent contraction following the drug-sequence given in Figure 1: 15.5 ± 1.7; 25.5 ± 2.7; 44.6 ± 2.7; 41.8 ± 3.4; 40.5 ± 3.9; 30.9 ± 3.5 and 99.6 ± 3.2). In ulnar arteries, only Bay A 4339, nitrendipine and Bay E 6927 produced relaxations of nearly 50% (percentage of persistent contraction following the drug-sequence given in Figure 1: 39.0 ± 2.7; 38.7 ± 2.9; 54.4 ± 3.1; 75.4 ± 2.9; 67.8 ± 4.5; 75.0 ± 4.0 and 82.0 ± 2.4). The corresponding pD_2-values are given in Table 3. As with the results obtained in KCl-stimulated arteries, Bay O 5572 was always the weakest drug tested. By contrast, the strongest potencies were shown by several dihydropyridines, which did not differ significantly from one another ($P<0.05$). Thus, in coronary arteries Bay A 4339, Bay L 3501 and nitrendipine and in basilar and ulnar arteries Bay A 4339 and nitrendipine were the most potent dihydropyridines (Tables 1 to 3).

In contrast to the results obtained after precontraction of the arteries with KCl and to the results with $PGF_{2\alpha}$-stimulated coronary and ulnar arteries, we found a significant linear correlation between the calculated pD_2 values of the dihydropyridines and the volume of their corresponding 3-ester-side-chain in $PGF_{2\alpha}$ precontracted basilar arteries (Figure 2).

Stimulus selectivity

All dihydropyridines exhibited significant differences in potency ($P<0.05$) in coronary and basilar arteries depending on the precontraction method used (Tables 1 and 2). This effect was termed stimulus selectivity. The affinity ratios for each drug plotted in Figure 3 (stimulus selectivity ratios) demonstrate further that the observed reduction of vasodilator potency in $PGF_{2\alpha}$-stimulated arteries was also dependent on the structure of the dihydropyridines. In both arteries Bay E 6927 displayed maximal stimulus selectivity ratios, whereas those of Bay A 4339 were the least. Although it was not possible to consider the whole group of dihydropyridines, a similar tendency could be observed in ulnar arteries (Table 3).

Intervascular selectivity

To quantify approximately the observed differences in potencies in the various vascular beds (intervascular selectivity) for each drug under both experimental conditions, a ratio was obtained between the calculated pD_2-values in coronary arteries and those obtained in basilar compared to ulnar arteries (intervascular ratios). A plot of these ratios (Figure 4) clearly demonstrates that the vasorelaxation induced by the dihydropyridines investigated in the specific vascular beds also depends on the stimulus used for precontraction. In arteries stimulated with KCl the dihydropyridines showed a coronary 'preference' (Figure 4a), whereas after arterial stimulation with $PGF_{2\alpha}$ this 'preference' was markedly shifted to basilar arteries (Figure 4b). In ulnar arteries, the vasodilator action of all the dihydropyridines studied was less pronounced.

Discussion

Calcium entry blockers of the dihydropyridine type reduce the transmembrane calcium flux through distinct ion channels (Godfraind *et al.*, 1986). Voltage operated calcium chan-

Table 2 The vasodilator potencies of the 1, 4-di-hydrophyridines examined (cf. Figure 1, NTD = nitrendipine) on porcine isolated basilar artery rings stimulated with KCl (60 mmol l^{-1}) or prostaglandin $F_{2\alpha}$ ($PGF_{2\alpha}$, 5 μmol l^{-1}) expressed as the concentration producing half maximal response (pD_2) following cumulative drug application

Compound	*pD_2 KCl*	n	*pD_2 $PGF_{2\alpha}$*	n
A 4339	7.29 ± 0.06	4	5.78 ± 0.03*	8
NTD	8.05 ± 0.04	4	5.60 ± 0.07*	12
E 6927	8.42 ± 0.12	6	5.50 ± 0.08*	6
N 6391	7.17 ± 0.10	5	5.31 ± 0.04*	8
I 1441	7.46 ± 0.09	7	5.14 ± 0.06*	8
L 3501	7.48 ± 0.04	6	5.17 ± 0.07*	6
O 5572	5.79 ± 0.08	5	3.89 ± 0.09*	6

Mean values and standard error (s.e.mean) of *n* individual experiments are given in − log mol l^{-1}.
Significant differences, $*P<0.00001$.

Table 3 The vasodilator potencies of the 1, 4-di-hydropyridines examined (cf. Figure 1, NTD = nitrendipine) on porcine isolated ulnar artery rings stimulated with KCl (60 mmol l^{-1}) or prostaglandin $F_{2\alpha}$ ($PGF_{2\alpha}$, 50 μmol l^{-1}) expressed as the concentration producing half maximal response (pD_2) following cumulative drug application

Compound	*pD_2 KCl*	n	*pD_2 $PGF_{2\alpha}$*	n
A 4339	6.35 ± 0.05	7	4.24 ± 0.05*	8
NTD	6.61 ± 0.04	7	4.38 ± 0.12*	6
E 6927	7.20 ± 0.07	7	3.82 ± 0.09*	5
N 6391	6.36 ± 0.05	7	<3.80	9
I 1441	6.53 ± 0.06	7	<3.80	7
L 3501	6.22 ± 0.11	7	<3.80	6
O 5572	4.86 ± 0.12	4	<3.80	5

Mean values and standard error (s.e.mean) of *n* individual experiments are given in − log mol l^{-1}.
Significant difference, $*P<0.0001$).
Because of the very low activity of some drugs following $PGF_{2\alpha}$-precontraction, these pD_2-values are lacking.

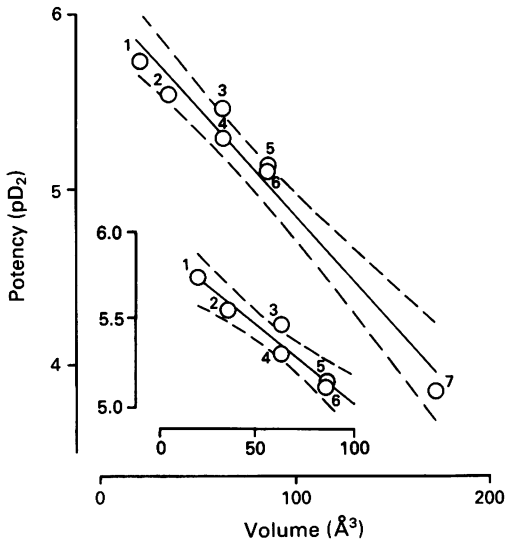

Figure 2 Correlation between the vasodilator potency of the dihydropyridines examined in basilar arteries precontracted with prostaglandin $F_{2\alpha}$ ($PGF_{2\alpha}$, 5 μmol l^{-1}) and the calculated volume of their 3-ester side-chains (for numbers see Figure 1). Volumes are plotted against the pD_2 values ($r = 0.98$; $P < 0.05$). Inset: Same plot without Bay O 5572 (No 7; $r = 0.97$; $P < 0.05$).

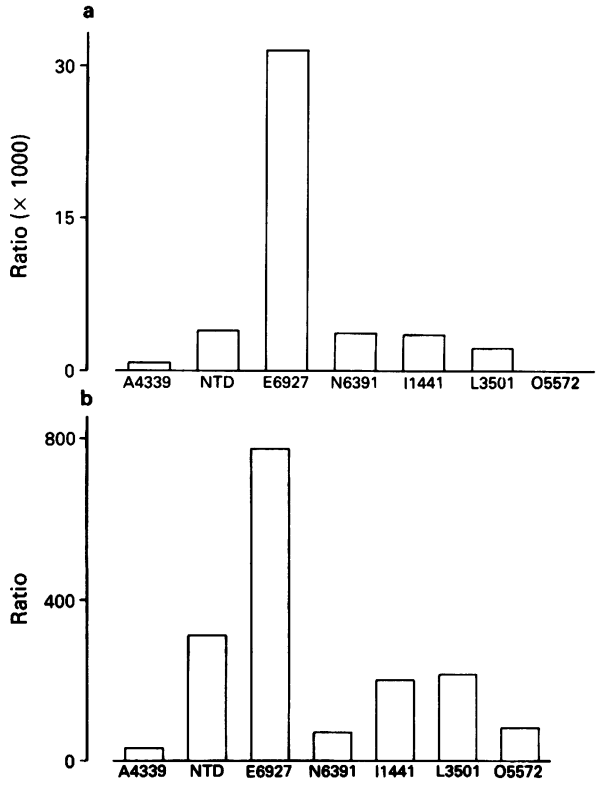

Figure 3 Stimulus selectivity of the 1,4-dihydropyridines examined in porcine (a) coronary and (b) basilar arteries. Plotted are the ratios of half maximal effective molar concentrations (cf. Tables 1 and 2) observed following cumulative drug application in prostaglandin $F_{2\alpha}$ ($PGF_{2\alpha}$) and KCl precontracted vessels. Because of the very low activity of Bay O 5572 in $PGF_{2\alpha}$ precontracted coronary arteries (Table 1) the ratio for this drug is lacking. Note the different ordinate scales.

nels (VOC's), which also exist in vascular smooth muscles (Bolton *et al.*, 1988), are activated by membrane depolarization e.g. by exposure to high potassium. Furthermore, the degree of such depolarization closely parallels the development of contraction e.g. in rat tail artery reaching maximal contraction at a membrane potential of − 20 mV achieved by 60 mmol l^{-1} KCl (Neild & Kotecha, 1987). This concentration of KCl was also sufficient to induce maximal contractions in the different porcine arteries used here.

However, in preliminary experiments we found very similar half-maximal contractile concentrations of KCl in coronary and ulnar arteries, whereas in basilar arteries this concentration was significantly reduced (see Results). On the other hand, we observed only small differences in the pD_2 values of each dihydropyridine investigated in depolarized coronary and basilar arteries, but markedly reduced pD_2 values in depolarized ulnar arteries (Table 1 to 3; Figure 4a). These results indicate that the sensitivity of VOC's in vascular smooth muscles of porcine arteries to KCl may be separated from that to dihydropyridines.

However, Cauvin *et al.* (1983), summarizing the results of various studies on the activity of calcium entry blockers in isolated vessels, suggested a nearly constant sensitivity of

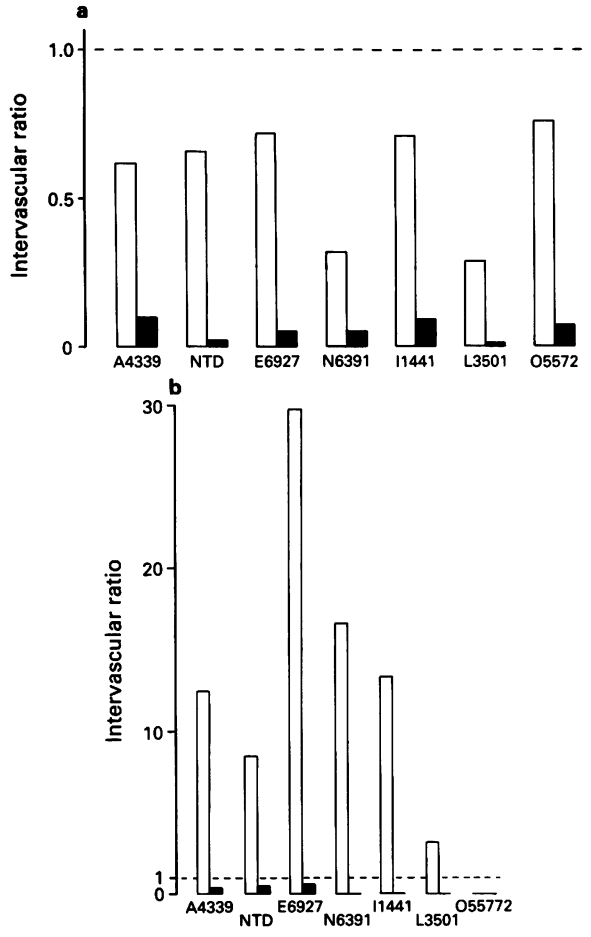

Figure 4 Intervascular selectivity of the 1,4-dihydropyridines examined in porcine arteries precontracted with (a) KCl or with (b) prostaglandin $F_{2\alpha}$ ($PGF_{2\alpha}$). The ratios of the half maximal effective molar concentrations are plotted (cf. Table 1 to 3) following cumulative drug application in coronary arteries which were given a value of 1 (dotted line) relative to those obtained in basilar (open columns) and ulnar (solid columns) arteries. A selectivity for ulnar basilar vessels is expressed by a ratio-value exceeding 1, whereas a selective drug action in coronary arteries is indicated by a ratio-value lower than 1. Because of the very low activity of some drugs in $PGF_{2\alpha}$ precontracted coronary and ulnar arteries, these ratios are lacking.

VOC's to these drugs throughout the arterial system. Although our study supports this concept with respect to coronary and basilar arteries, the 10 fold reduced activity of all dihydropyridines investigated in depolarized ulnar arteries remains to be explained. In addition, 12.2–37.1% of the KCl-induced contractions in ulnar arteries were resistant to the action of nitrendipine and its derivatives even at the highest concentration used (see Results). By contrast, such concentrations completely abolished KCl-induced contractions in coronary and basilar arteries. Therefore we suggest a different distribution of various VOC-types in the arterial tree.

Besides the dihydropyridine-sensitive L-type-VOC's, Benham *et al.* (1987) demonstrated the existence of dihydropyridine-resistant T-type-VOC's in vascular smooth muscle. Furthermore some recent investigations show different vascular L-type-VOC's (Rosenberg *et al.*, 1986; Cruz *et al.*, 1987; Miller, 1987). A different distribution of dihydropyridine-resistant VOC's within the vascular system might also explain the previously described intervascular selectivity of dihydropyridines in various depolarized arteries (Gerthoffer *et al.*, 1987; Joulou-Schaeffer & Freslon, 1987; Fricke & Ueckert, 1988). Interestingly and in accordance with the results presented here, all authors reported a significantly greater vasodilator potency of dihydropyridines in cerebral compared to peripheral vessels.

The intervascular selectivity observed in the present study was not dependent on the different chemical structure of the dihydropyridines. Modification of the 3-ester-side-chain of nitrendipine improved the vasodilator potency only in the case of Bay E 6927, which was the most potent drug in every type of artery after stimulation with KCl (Tables 1 to 3). This result may possibly reflect a more pronounced affinity of Bay E 6927 for dihydropyridine-sensitive L-type-VOC's.

In a second series of experiments we examined the action of nitrendipine and its derivatives in the three vessel types following precontraction with $PGF_{2\alpha}$. This endogeneous prostaglandin has been described as a potent vasoconstrictor of (1) isolated pig (Yamamoto *et al.*, 1987) and human coronary arteries (Förstermann *et al.*, 1988), (2) isolated rat (Godfraind & Miller, 1983) and dog mesenteric arteries (Konishi *et al.*, 1981) and (3) isolated dog (Toda & Onoue, 1988), cat (Uski, 1985) and human cerebral arteries (Rose & Moulds, 1979). In addition, $PGF_{2\alpha}$ seems to be of pathophysiological relevance e.g. in the development of cerebral vasospasms following subarachnoid haemorrhage. Under these conditions the production of prostacyclin is reduced (Brandt *et al.*, 1981), whereas the concentrations in the cerebrospinal fluid of vasoconstrictor prostaglandins including $PGF_{2\alpha}$ increase up to 1 μmol l^{-1} (Walker *et al.*, 1983; Rodriguez y Baena *et al.*, 1985). This concentration of $PGF_{2\alpha}$ is sufficient to elicit strong and stable contractions of human cerebral arteries (White & Robertson, 1987).

In $PGF_{2\alpha}$ precontracted porcine arteries all dihydropyridines investigated exhibited a vasodilator activity, which was strongly reduced compared to that after depolarization. A similar attenuation has been reported with nitrendipine in noradrenaline precontracted rabbit ear arteries (Scriabine *et al.*, 1984) and also in dog coronary and femoral arteries stimulated with 5-hydroxytryptamine or $PGF_{2\alpha}$ (Altura & Altura, 1984). Therefore $PGF_{2\alpha}$-induced vasoconstrictions probably involve mechanisms, which are insensitive to the action of dihydropyridines. Earlier studies revealed that such vasoconstrictions are mediated by a release of intracellular calcium as well as calcium influx from the extracellular space (Takayama, 1986; Santoian *et al.*, 1987). This calcium influx, possibly accompanied by loosely membrane-bound calcium (Uski, 1985), probably occur through both receptor-operated calcium channels (ROC's) and VOC's (Toda & Onoue, 1988). Dihydropyridines inhibit calcium influx through VOC's much more extensively than calcium influx through ROC's, whereas their influence on the release of intracellular stored calcium is a matter of controversy (Bolton, 1979; van Breemen *et al.*, 1979; Meisheri *et al.*, 1981; Godfraind *et al.*, 1986; Hurwitz, 1986). Therefore, the stimulus selectivity (KCl vs. $PGF_{2\alpha}$; Figure 3) of nitrendipine and its derivatives observed in the present study is possibly due to the involvement of calcium influx through ROC's and/or release of intracellular stored calcium following treatment with $PGF_{2\alpha}$.

The very low activity of the drugs studied in $PGF_{2\alpha}$-stimulated porcine coronary and ulnar arteries, which resulted in a high percentage of persisting contractions (see Results) even at the highest drug-concentration used (100 μmol l^{-1}), demonstrates a participation of contractile mechanisms with pronounced insensitivity to dihydropyridines. By contrast, all studied drugs except Bay O 5572, the least active derivative of all, completely abolished $PGF_{2\alpha}$-induced contractions in basilar arteries. Furthermore, the compounds exhibit a significant selective action in such vessels (intervascular selectivity, Figure 4b). Therefore, it seems likely that the enhancement of intracellular calcium concentration required for $PGF_{2\alpha}$-induced contraction in porcine basilar arteries is mainly due to a calcium influx from the extracellular space. In this respect the reduced potency of the dihydropyridines compared to depolarizing conditions points to an involvement of ROC's. The suggestion that different calcium influx pathways participate in $PGF_{2\alpha}$-induced vasoconstriction of basilar arteries is supported by the significant relationship between the chemical structure and the activity of the dihydropyridines (Figure 2), which has not been observed after depolarization. Furthermore, this result raises the question whether or not different calcium influx pathways display a different sensitivity to dihydropyridines depending on the structure of these compounds.

As indicated by the calculated stimulus selectivity ratios plotted in Figure 3, it might be supposed that the stimulus selectivity of dihydropyridines depends on the structure of their 3-ester side chain. Thus a limited prolongation from a methyl (Bay A 4339) to an isopropyl group (Bay E 6927) resulted in strongly increased stimulus selectivity ratios in each vessel type studied. In addition, this increase ensues from both an enhanced activity in depolarized as well as attenuated activity in $PGF_{2\alpha}$ precontracted arteries. These results suggest the possibility of developing dihydropyridines with defined stimulus-selectivity ratios. Such compounds could gain therapeutic value especially in the management of vascular disorders e.g. vasospastic angina or those following subarachnoid haemorrhage.

In brief, our study demonstrates that nitrendipine and six related 3-ester side chain derivatives display intervascular and stimulus selectivity within different arteries of the same species. After depolarization these compounds exhibited a weak preferential action in coronary arteries, whereas after precontraction with $PGF_{2\alpha}$ they predominantly relax basilar arteries. This shift in the intervascular selectivity seems mainly to be a consequence of different mechanisms, by which $PGF_{2\alpha}$-induced contractions are achieved in the different vessels. In addition, the magnitude of the stimulus selectivity, as expressed by the calculated stimulus selectivity ratios, might also be dependent on the chemical structure of the dihydropyridines

The authors wish to thank Dr D. Hafner, Institute of Pharmacology, University of Düsseldorf, for kindly helping in the statistical analysis.

References

ALTURA, B.M. & ALTURA, B.T. (1984). Comparative effects of nitrendipine and verapamil on isolated blood vessels of dogs. In *Nitrendipine*. ed. Scriabine, A., Vanov, S. & Deck, K. pp. 293–309. Baltimore, Muenchen: Urban & Schwarzenberg.

BENHAM, C.D., HESS, P. & TSIEN, R.W. (1987). Two types of calcium channels in single smooth muscle cells from rabbit ear artery studied with whole cell and single channel recording. *Circ. Res.*, **61**(Suppl I), I10–I16.

BOLTON, T.B. (1979). Mechanism of action of transmitters and other substances on smooth muscle. *Physiol. Rev.*, **59**, 606–718.

BOLTON, T.B., MACKENZIE, I. & AARONSON, P.I. (1988). Voltage dependent calcium channels in smooth muscle cells. *J. Cardiovasc. Pharmacol.*, **12**(Suppl. 6), S3–S7.

BOSSERT, F., HORSTMANN, H., MEYER, H. & VATER, W. (1979). Einfluss der Esterfunktion auf die vasodilatierenden Eigenschaften von 1,4-Dihydro-2, 6-dimethyl-4-nitrophenylpyridin-3, 5-dicarbonsaeureestern. *Drug Res.*, **29**, 226–229.

BRANDT, C., LJUNGGREN, B., ANDERSSON, K.E., HINFELT, B. & USKI, T. (1981). Individual variations in response of human cerebral arterioles to vasoactive substances, human plasma and CSF from patients with aneurysmal SAH. *J. Neurosurg.*, **55**, 431–437.

VAN BREEMEN, C., AARONSON, P. & LOUTZENHISER, R. (1979). Beneficial effects of the calcium antagonist PN 200–110 in patients with congestive heart failure. *J. Cardiovasc. Pharmacol.*, **10**, 190–195.

CAUVIN, C., LOUTZENHISER, R. & VAN BREEMEN, C. (1983). Mechanism of calcium antagonist induced vasodilation. *Annu. Rev. Pharmacol. Toxicol.*, **23**, 373–396.

CRUZ, L.J., JOHNSON, D.S. & OLIVERA, B.M. (1987). Characterisation of the ω-conotoxin target. Evidence for tissue specific heterogeneity in calcium channel types. *Biochemistry*, **26**, 820–824.

FÖRSTERMANN, U., MUEGGE, A., ALHEID, U., HAVERICH, A. & FROEHLICH, J.C. (1988). Selective attentuation of endothelium mediated vasodilation in atherosclerotic human coronary arteries. *Circ. Res.*, **26**, 185–190.

FRICKE, U., KLAUS, W. & STEIN, B. (1988). Novel halogenated dihydropyridine derivatives with high vascular selectivity. *Naunyn Schmiedebergs Arch. Pharmacol.*, **338**, 449–454.

FRICKE, U. & UECKERT, M. (1988). Effects of nimodipine, nisoldipine, and halogenated derivatives of nitrendipine in isolated arteries and ventricular muscles of the pig. *Naunyn Schmiedebergs Arch. Pharmacol.*, **338**(Suppl), R36.

GELMERS, H.J., GARTER, K., DE WEERDT, C.J. & WIESNER, H.J.A. (1985). Efficacy of treatment with nimodipine (calcium antagonist) in patients with acute ischemic stroke; a placebo-controlled double-blind, randomized, multicentre trial. *J. Cereb. Blood Flow Metab.*, **5**(Suppl 2), S337–S338.

GERTHOFFER, W.T., SHAFER, P.G. & TAYLOR, S.C. (1987). Selectivity of phenytoin and dihydropyridine calcium channel blockers for relaxation of the basilar artery. *J. Cardiovasc. Pharmacol.*, **10**, 9–15.

GODFRAIND, T. & MILLER, R.C. (1983). Specificity of action of calcium entry blockers, a comparison of their actions in rat arteries and human coronary arteries. *Circ. Res.*, **52**(Suppl 1), 81–91.

GODFRAIND, T., MILLER, R.C. & WIBO, M. (1986). Calcium antagonism and calcium entry blockade. *Pharmacol. Rev.*, **38**, 321–416.

GODFRAIND, T., ENGLEME, C., FINET, M. & JAUMIN, P. (1987a). The actions of nifedipine and nisoldipine on the contractile activity of human coronary arteries and human cardiac tissue in vitro. *Pharmacol. Toxicol.*, **61**, 79–84.

GODFRAIND, T., ENGLEME, C., FINET, M., DEBANDE, B. & JAUMIN, P. (1987b). Comparison of nifedipine and nisoldipine on human arteries and human cardiac tissues in vitro. In *Nisoldipine*. ed. Hugenholtz, P.G. & Meyer, J. pp. 36–44. Berlin: Springer.

HAFNER, D., HEINEN, E. & NOACK, E. (1977). Mathematical analysis of concentration response relationships. *Drug Res.*, **27**, 1871–1873.

HURWITZ, L. (1986). Pharmacology of calcium channels and smooth muscle. *Annu. Rev. Pharmacol. Toxicol.*, **26**, 225–258.

JULOU-SCHAEFFER, G. & FRESLON, J.L. (1987). Compared effects of calcium entry blockers on calcium-induced tension in rat isolated cerebral and peripheral resistance vessels. *Naunyn Schmiedebergs Arch. Pharmacol.*, **336**, 670–676.

KAZDA, S. & TOWART, R. (1981). Differences in the effects of the calcium antagonists nimodipine (Bay E 9736) and benzyclane on cerebral and peripheral smooth muscle. *Br. J. Pharmacol.*, **72**, 582P–583P.

KOJDA, G., FRICKE, U., KLAUS, W. & WERNER, G. (1989). Einfluß der Esterfunktion auf die vaskuläre Selektivität von 4-(3-Nitrophenyl)-1, 4-dihydropyridinen. *Arch. Pharm.*, **322**, 777.

KOJDA, G., KLAUS, W., WERNER, G. & FRICKE, U. (1990). Reduced responses of nitrendipine in $PGF_{2\alpha}$-precontracted porcine isolated arteries after pretreatment with methylene blue. *Basic Res. Cardiol.*, **85**, 461–466.

KONISHI, M., TODA, N. & YAMAMOTO, M. (1981). Different mechanisms of action of histamine in isolated arteries of the dog. *Br. J. Pharmacol.*, **74**, 111–118.

MEISHERI, K.D., HWANG, O. & VAN BREEMEN, C. (1981). Evidence for two separate calcium pathways in smooth muscle plasmalemma. *J. Memb. Biol.*, **59**, 19–25.

MILLER, R.J. (1987). Multiple calcium channels and neuronal function. *Science*, **235**, 46–52.

NEILD, T.O. & KOTECHA, N. (1987). Relation between membrane potential and contractile force in smooth muscle of the rat tail artery during stimulation by norepinephrine, 5-hydroxytryptamine and potassium. *Circ. Res.*, **60**, 791–795.

RODRIGUEZ Y BAENA, R., GAETANI, P., FALCO,. G., BRANZOLI, U. & PAOLETTI, P. (1985). Cisternal and lumbar CSF concentration of arachidonate metabolites in vasospasm following subarachnoidal hemorrhage from ruptured aneurism: biochemical and clinical considerations. *Surg. Neurol.*, **24**, 428–432.

ROSE, G.A. & MOULDS, R.F.W. (1979). Comparison of isolated human cerebral and digital arteries. *Stroke*, **10**, 736–741.

ROSENBERG, R.L., HESS, P., REEVES, J.P., SMILOVITZ, H. & TSIEN, R.W. (1986). Calcium channels in planar lipid bilayers: insights into mechanism of ion permeation and gating. *Science*, **231**, 1564–1567.

SANTOIAN, E.C., ANGERIO, A.D., FITZPATRICK, T.M.,ROSE, J.C., RAMWELL, P.W. & KOT, P.A. (1987). Effects of intracellular and extracellular calcium blockers on the pulmonary vascular response to $PGF_{2\alpha}$ and U46619. *Angiology*, **38**, 51–55.

SCRIABINE, A., JOHNSON, C.E., STEINSLAND, O.S. & ANDERSSON, C.L. (1984). Antagonism of calcium induced constriction of isolated rabbit ear artery by nitrendipine in high potassium and/or norepinephrine containing medium. *J. Cardiovasc. Pharmacol.*, **6**, 944–948.

TAKAYAMA, T. (1986). Effects of prostaglandins on the contractile mechanism especially on an intracellular calcium store in uterine muscle cells. *J. Nippon Heikatsuki Gakkai Zasschi*, **22**, 31–42.

TODA, N. & ONOUE, H. (1988). Prostaglandin $F_{2\alpha}$-induced contraction in isolated dog cerebral, coronary and mesenteric arteries soaked in excess potassium. *Jpn. J. Pharmacol.*, **47**, 204–207.

USKI, T.K. (1985). Cellular calcium and the contraction induced by $PGF_{2\alpha}$ in feline cerebral arteries. *Acta. Pharmacol. Toxicol.*, **56**, 117–125.

VERLOOP, A., HOOGENSTRATEN, W. & TIPKER, J. (1976). Development and application of new steric substituent parameters in drug design. In *Drug Design*, Vol. VIII. ed. Ariens, E.J., pp. 165–207. New York: Raven Press.

WALKER, V., PICKARD, J.D., SANYTHE, P., EASTWOOD, S. & PERRY, S. (1983). Effects of subarachnoid hemorrhage on intracranial prostaglandins. *J. Neurol. Neurosurg. Psychiatry*, **46**, 119–125.

WERNER, G., FRICKE, U., KLAUS, W. & KOJDA, G. (1988). In-vitro Untersuchungen zur lokalen Tonusregulation in verschiedenen Gefäßabschnitten des Hausschweins. *Arch. Pharm.*, **321**, 697.

WHITE, R.P. & ROBERTSON, J.T. (1987). Pharmacodynamic evaluation of human cerebral arteries in the genesis of vasospasm. *Neurosurgery*, **21**, 523–531.

YAMAMOTO, Y., TOKOIKO, H., EGASHIRA, K. & NAKAMURA, M. (1987). Attenuation of endothelium related relaxation and enhanced responsiveness of vascular smooth muscle to histamine in spastic coronary arterial segments from miniature pigs. *Circ. Res.*, **61**, 772–778.

(Received October 8, 1991
Revised January 2, 1992
Accepted January 16, 1992)

Br. J. Pharmacol. (1992), **106**, 91–94 © Macmillan Press Ltd, 1992

Apparent block of K^+ currents in mouse motor nerve terminals by tetrodotoxin, μ-conotoxin and reduced external sodium

M.F.M. Braga, [2]A.J. Anderson, [1]A.L. Harvey & E.G. Rowan

Department of Physiology and Pharmacology, Strathclyde Institute for Drug Research, University of Strathclyde, Glasgow G1 1XW

1 In mouse triangularis sterni nerve-muscle preparations, reduced extracellular Na^+ concentrations and low concentrations of the Na^+ channel blocking toxins tetrodotoxin (TTX, 18–36 nM) and μ-conotoxin GIIIB (0.4–2.0 μM) selectively decreased the amplitude of the component of perineural waveforms associated with nerve terminal K^+ currents, without affecting the main Na^+ spike.

2 Intracellular recording of endplate potentials (e.p.ps) and miniature endplate potentials (m.e.p.ps) from triangularis sterni preparations revealed that TTX and μ-conotoxin GIIIB depressed the evoked quantal release of acetylcholine without significant effects on m.e.p.p. amplitude, frequency or time constant of decay.

3 The apparent block of K^+ current by low concentrations of TTX and μ-conotoxin is probably not a direct effect on K^+ channels but results from a decrease in the passive depolarization of nerve terminals following blockade of a small proportion of axonal Na^+ channels.

Keywords: Tetrodotoxin; μ-conotoxin; K^+ channels; Na^+ channels; neuromuscular junction; neurotransmission; acetylcholine release

Introduction

The use of the perineural recording technique (Mallart, 1985) to monitor the activity of ion channels at or close to motor nerve terminals has enhanced pharmacological studies on motor nerve terminal function. Perineural waveforms, recorded by a microelectrode placed inside the perineural sheaths of mouse motor nerves, are composed mainly of two negative (downward) deflections (Mallart, 1985; Braga *et al.*, 1991). The first negative deflection is associated with Na^+ current at nodes of Ravier in the parent axon. The second negative deflection can be abolished by 3,4-diaminopyridine (3,4-DAP) and tetraethylammonium (TEA) and is associated with outward K^+ current at motor nerve terminals (Brigant & Mallart, 1982; Mallart, 1985). Although the waveforms recorded are closely related to changes in the activity of ion channels at or close to motor nerve terminals (Mallart, 1985), the recordings can be ambiguous because of an overlap in the activities of different classes of ion channels. We have used both perineural and conventional intracellular recording techniques to study the effects of reduced extracellular Na^+ concentrations and two sodium channel blocking toxins, μ-conotoxin and tetrodotoxin (TTX), on motor nerve terminal excitability and acetylcholine release. The results demonstrated that caution is required when using the perineural recording technique to assess the pharmacological actions of compounds on motor nerve terminals: reduction in the driving force for electrotonic depolarization of the terminals can give an apparent block of K^+ channels without noticeable effects on nodal Na^+ current.

Methods

Experiments were performed on the left triangularis sterni nerve-muscle preparation (McArdle *et al.*, 1981) isolated from 15–25 g male mice (Balb C strain). Dissection and experimental conditions are described in detail by Anderson & Harvey (1988). The preparation was pinned thoracic side downwards to the base of a 2–3 ml tissue bath and perfused at a rate of 10–15 ml min^{-1} with the physiological solution of the following composition (mM): NaCl 118.4, KCl 4.7, $MgSO_4$ 1.2, KH_2PO_4 1.2, $CaCl_2$ 2.5, $NaHCO_3$ 25 and glucose 11.1. The solution was maintained at pH 7.3, and bubbled with O_2 containing 5% CO_2, to which 10–12 μM tubocurarine (for extracellular recording) or 2–5 mM Mg^{2+} (for intracellular recording) was added to prevent muscle twitching. In all Mg^{2+}-paralysed experiments, the Ca^{2+} concentration was reduced to 0.5 mM, and a 20 min equilibration period allowed. In some experiments, NaCl was replaced isotonically by choline chloride and when the extracellular Na^+ concentration was 0 mM the preparation was perfused with a solution (aerated with O_2) of the following composition (mM): choline chloride 154.0, KCl 5.0, $MgCl_2$ 1.2, $CaCl_2$ 2.5, glucose 11.1 and HEPES 5.0, the solution was adjusted to pH 7.3 with KOH. The intercostal nerves were stimulated via a suction electrode every 2 s with pulses of 50 μs duration and supramaximal voltage. Experiments were carried out at room temperature (20–25°C).

Intracellular recording

Neuromuscular junctions were identified by the presence of endplate potentials (e.p.ps) and miniature endplate potentials (m.e.p.ps) with rise times of 1 ms or less. E.p.ps and m.e.p.ps were recorded with glass microelectrodes filled with 3 M KCl (resistance 5–20 MΩ), as described previously (Braga *et al.*, 1991); recordings were made continuously from one endplate area before and throughout application of compounds, each endplate area (and hence each preparation) being exposed once to compounds.

Extracellular recording

Presynaptic waveforms were recorded by a glass microelectrode (filled with 2 M NaCl, resistance 5–15 MΩ) placed inside the perineural sheath (near endplate areas) of one of the branches of an intercostal nerve (see Mallart, 1985; Pen-

[1] Author for correspondence.
[2] Present address: Department of Physiology, University of Edinburgh Medical School, Edinburgh EH8 9AG.

ner & Dreyer, 1986; Anderson *et al.*, 1988). The potentials were recorded, amplified and stored as for the intracellular recordings. Usually 20–25 waveforms were recorded at each time period. As the shape of the waveform recorded was very dependent on the electrode position, waveforms were monitored continuously from the same site before and throughout application of drugs. Recording sites were rejected if the signal amplitude fell by more than 10% during the first 20 min before the addition of the compounds. Using this protocol, stable recordings could be obtained over a 180 min period in control solutions or in the presence of drugs.

Materials

All the compounds were obtained from Sigma Chemical Co., Poole, Dorset, except μ-conotoxin GIIIB which was from the Peptide Institute, Inc., Osaka, Japan.

Results

The second negative deflection of perineural waveforms can be selectivity blocked by 3,4-DAP (Figure 1a) and TEA (not shown) and is associated with K^+ current at motor nerve terminals (Mallart, 1985; Braga *et al.*, 1991). Low concentrations of TTX (18–36 nM) and μ-conotoxin GIIIB (0.4–2.0 μM) had little effect on the first negative deflection of the perineural waveform, but produced a concentration-dependent reduction in the amplitude of the second negative deflection (Figures 1b and 1c, respectively). Higher concentrations of TTX and μ-conotoxin GIIIB also reduced the amplitude of the first negative deflection, associated with nodal Na^+ currents (Figures 2a and 3a).

Reduction of the extracellular concentration of Na^+ also induced a graded reduction in the amplitude of the second negative deflection with no apparent effect on the first negative deflection of the perineural waveform (Figure 1d). However, when Na^+ was completely replaced by choline chloride the first negative deflection, which is associated with Na^+ current at nodes of Ranvier in the parent axon, was abolished (Figure 4). Reduced Na^+ concentrations tended to prolong the delay between the stimulus artefact and the perineural waveforms in a concentration-dependent manner (Figure 1d). μ-Conotoxin GIIIB also induced a prolongation in the delay of the perineural waveforms and at 4 μM μ-conotoxin GIIIB, this effect was very marked (Figure 1c).

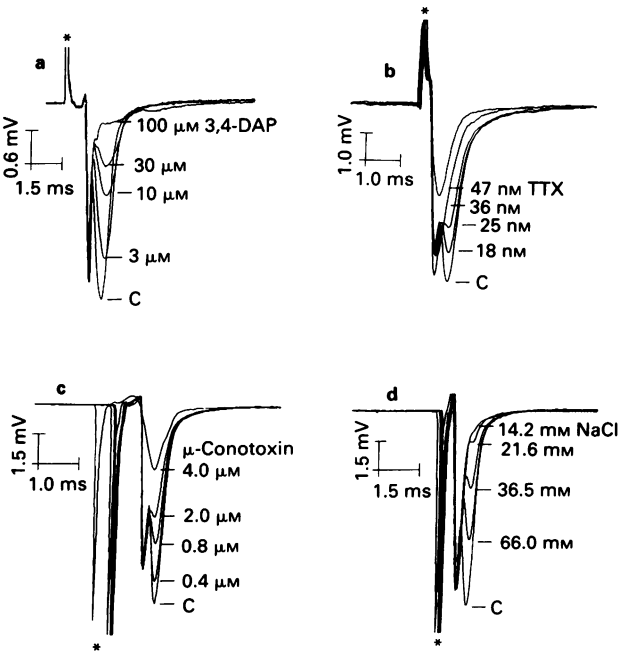

Figure 1 Effects of (a) 3,4-diaminopyridine (3,4-DAP), (b) tetrodotoxin (TTX), (c) μ-conotoxin GIIIB and (d) Na^+ substitution, on perineural waveforms recorded from mouse triangularis sterni preparations. Superimposed recordings from the same site before (C) and after the addition of compounds. Each record is an average of 20–25 waveforms. * = stimulus artefact, which is followed by two downward deflections. The first of these relates to Na^+ currents at the final nodes of Ranvier; the second is associated with outward K^+ currents at the nerve terminals. Note the apparently selective block of K^+ currents by all four treatments.

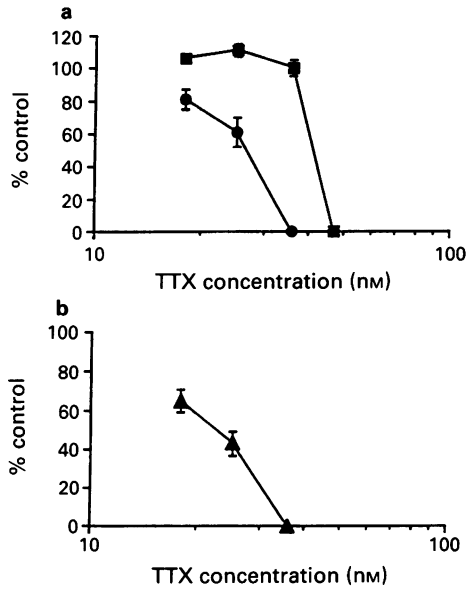

Figure 2 (a) Effects of tetrodotoxin (TTX) on first (■) and second negative deflection (●) of the perineural waveforms. (b) Effects of TTX on quantal content of Mg^{2+} paralysed preparations (▲). Points are means of 3 experiments and s.e. are indicated by the bars unless smaller than symbols.

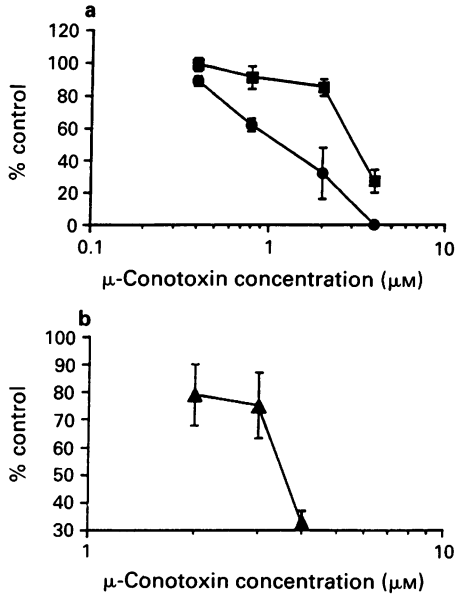

Figure 3 (a) Effects of μ-conotoxin on first (■) and second negative deflection (●) of the perineural waveforms. (b) Effects of μ-conotoxin on quantal content of Mg^{2+} paralysed preparations (▲). Points are means of 3 experiments and s.e. are indicated by the bars unless smaller than symbols.

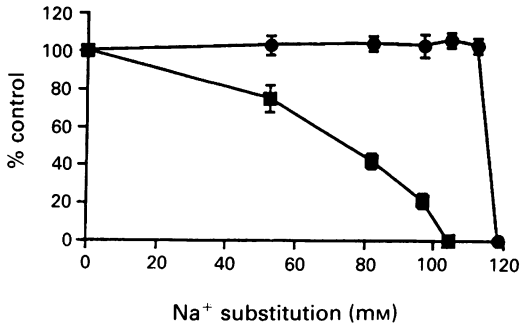

Figure 4 Effects of Na^+ substitution on first (●) and second negative deflection (■) of the perineural waveforms. NaCl was gradually replaced by choline chloride. Points are means of 3 experiments and s.e. are indicated by the bars unless smaller than symbols.

This effect is probably due to a slowing of the propagation of the action potential induced by reduced Na^+ concentrations and the Na^+ channel blocking toxin, μ-conotoxin GIIIB.

The block of K^+ current at motor nerve terminals by 3,4-DAP is accompanied by an increase in the quantal content of e.p.ps (Braga *et al.*, 1991). However, no such increase was observed with TTX or μ-conotoxin GIIIB. In Mg^{2+}-paralysed preparations, control m.e.p.ps were 0.4–0.7 mV in amplitude and had a time constant of decay of 1.0–1.4 ms and the e.p.ps were 2.2–4.0 mV in amplitude and had a time constant of decay of 1.0–1.5 ms at a resting membrane potential of −75 to −85 mV. TTX (18–36 nM) and μ-conotoxin GIIIB (2–4 μM) gradually reduced the amplitude of the evoked e.p.ps in a concentration-dependent manner with no significant change in e.p.p. time constant of decay, or in amplitude, time course of decay or frequency of m.e.p.ps. Therefore, TTX and μ-conotoxin GIIIB reduced quantal content of e.p.ps (Figures 2b and 3b, respectively). Replacement of 52.4 mM of NaCl by choline chloride, which induced a 25 ± 7% ($n = 3$) reduction in the amplitude of the second negative deflection, abolished evoked e.p.ps.

Discussion

Microelectrodes inserted into the perineural sheaths of small motor nerve bundles record a composite of the electrical activity associated with several nerve terminals (Mallart, 1985). The ionic currents underlying the biphasic appearance of perineural waveforms have been well characterized (Mallart, 1985; Penner & Dreyer, 1986). The second negative deflection is associated with the activity of motor nerve terminal K^+ currents (Mallart, 1985; Anderson *et al.*, 1988; Tabti *et al.*, 1989). Pharmacologically, the second component is susceptible to block by 3,4-DAP, TEA and some snake toxins (Rowan & Harvey, 1988; Tabti *et al.*, 1989; Braga *et al.*, 1991). We have now shown that reduced extracellular Na^+ concentrations and low concentrations of the sodium channel blocking toxins μ-conotoxin (Cruz *et al.*, 1985; Hong & Chang, 1989) and TTX also reduced the amplitude of the second component of the perineural waveform. Blockade of K^+ channels, for example by 3,4-DAP, produces an increase in acetylcholine release in triangularis sterni preparations (Braga *et al.*, 1991). However, TTX and μ-conotoxin reduced the quantal content of e.p.ps, suggesting that they were not blocking voltage-dependent or Na^+-activated K^+ currents. The latter current would, in any case, be unlikely to be activated by the amount of Na^+ entering nerve terminals during action potentials (Dryer, 1991). In addition, even partial Na^+ substitution by choline chloride abolished evoked e.p.ps.

The apparent block of K^+ current by low concentrations of μ-conotoxin and TTX can probably be explained by an action of these toxins on Na^+ channels located at the last few nodes of Ranvier and at the heminode. The majority of the unmyelinated length of mammalian motor nerve terminals has a very low density of Na^+ channels (Brigant & Mallart, 1982; Konishi, 1985). Nerve terminal depolarization is mainly achieved by passive spread of electrical activity from the last few nodes. Consequently, blockade of a fraction of the Na^+ current or a reduction in extracellular Na^+ concentration will reduce the spread of depolarization to the nerve terminals. This may result in a reduction in the number of voltage-dependent K^+ channels activated at some of the nerve terminals, and hence a reduction in the amplitude of the second negative deflection of perineural waveforms. The decrease in quantal content induced by TTX and μ-conotoxin is in accordance with this hypothesis, since a reduction of the depolarization of the nerve terminal would be expected to reduce the number of voltage-dependent Ca^{2+} channels activated and therefore reduce quantal content. As expected, complete replacement of Na^+ by choline chloride abolished the perineural waveform as the generation and propagation of the action potential is Na^+-dependent. Moreover, increasing the concentrations of the two Na^+ channel blocking toxins led to a general depression of the perineural waveform, consistent with an effect of the toxins on action potential conduction.

The use of perineural recording techniques to study ion channels at motor nerve terminals is valuable in assessing the pharmacological activity of compounds which alter neuromuscular transmission. However, to help eliminate some of the ambiguity in the interpretation of the recordings, we recommend the use of a range of concentrations of test compounds, and also the use of additional techniques (e.g. intracellular recording) to monitor effects on acetylcholine release.

References

ANDERSON, A.J., & HARVEY, A.L. (1988). Effect of the potassium channel blocking dendrotoxins on acetylcholine release and motor nerve terminal activity. *Br. J. Pharmacol.*, **93**, 215–221.

ANDERSON, A.J., HARVEY, A.L., ROWAN, E.G. & STRONG, P.N. (1988). Effects of charybdotoxin, a blocker of Ca^{2+}-activated K^+ channels on motor nerve terminals. *Br. J. Pharmacol.*, **95**, 1329–1335.

BRAGA, M.F.M., HARVEY, A.L. & ROWAN, E.G. (1991). Effects of tacrine, velnacrine (HP029), suronacrine (HP128) and 3,4-diaminopyridine on skeletal neuromuscular transmission *in vitro*. *Br. J. Pharmacol.*, **102**, 909–915.

BRIGANT, J.L. & MALLART, A. (1982). Presynaptic currents in mouse motor endings. *J. Physiol.*, **333**, 619–636.

CRUZ, L.J., GRAY, W.R., OLIVERA, B.M., ZEIKUS, R.D., KERRY, L., YOSHIKAMI, D. & MOCZYDLOWSKI, E. (1985). *Conus geographus* toxins that discriminate between neuronal and muscle sodium channels. *J. Biol. Chem.*, **260**, 9280–9288.

DRYER, S.E. (1991). Na^+-activated K^+ channels and voltage-evoked ionic currents in brain stem and parasympathetic neurones of the chick. *J. Physiol.*, **435**, 513–532.

HONG, S.J. & CHANG, C.C. (1989). Use of geographutoxin II (μ-conotoxin) for the study of neuromuscular transmission in mouse. *Br. J. Pharmacol.*, **97**, 934–940.

KONISHI, T. (1985). Electrical excitability of motor nerve terminals in the mouse. *J. Physiol.*, **366**, 411–421.

MALLART, A. (1985). Electric current flow inside perineurial sheaths of mouse motor nerves. *J. Physiol.*, **368**, 565–575.

MCARDLE, J.J., ANGAUT-PETIT, D., MALLART, A., BOURNAUD, R., FAILLE, L. & BRIGANT, J.L. (1981). Advantages of the triangularis sterni muscle for investigation of synpatic phenomena. *J. Neurosci. Methods*, **4**, 109–116.

PENNER, R. & DREYER, F. (1986). Two different presynaptic calcium currents in mouse motor nerve terminals. *Pflügers Arch.*, **406,** 190–197.

ROWAN, E.G. & HARVEY, A.L. (1988). Potassium channel blocking actions of β-bungarotoxin and related toxins on mouse and frog motor nerve terminals. *Br. J. Pharmacol.*, **94,** 839–847.

TABTI, N., BOURRET, C. & MALLART, A. (1989). Three potassium currents in mouse motor nerve terminals. *Pflügers Arch.*, **413,** 395–400.

(Received December 18, 1991
Accepted January 16, 1992)

Br. J. Pharmacol. (1992), **106**, 95–100 © Macmillan Press Ltd, 1992

Comparison of the contractile effects of endothelin-1 and sarafotoxin S6b in goat isolated cerebral arteries

*Juan B. Salom, *Germán Torregrosa, *Francisco J. Miranda, *José A. Alabadí & [1]*†Enrique Alborch

*Centro de Investigación, Hospital "La Fe", and †Departamento de Fisiología, Universidad de Valencia, Valencia, Spain

1 The effects of endothelium-derived endothelin-1 and snake venom-derived sarafotoxin S6b, peptides with striking structural and functional similarities, were examined and compared in isolated middle cerebral arteries of goats.

2 Endothelin-1 and sarafotoxin S6b contracted cerebral arteries in a concentration-dependent manner. The potency of endothelin-1 ($EC_{50} = 4.9$ (3.9–6.2) $\times 10^{-10}$ M) was about ten times higher than that of sarafotoxin S6b ($EC_{50} = 5.5$ (4.4–6.9) $\times 10^{-9}$ M). The tension returned to basal values after repeated washings and contraction with endothelin-1 could be reproduced. Endothelin-1 and sarafotoxin S6b induced further contraction in arteries precontracted with prostaglandin $F_{2\alpha}$ (10^{-5} M).

3 Mechanical removal of the endothelium or incubation with indomethacin (10^{-5} M) displaced the concentration-response curves to endothelin-1 and, more pronouncedly, to sarafotoxin S6b to the left. The maximum response to sarafotoxin S6b was also increased by either of these two treatments.

4 Incubation in 'nominally' Ca^{2+}-free medium attenuated the vasoconstrictor response to endothelin-1 but not to sarafotoxin S6b, which was inhibited after incubation in Ca^{2+}-free medium to which EGTA (10^{-4} M) had been added. Pretreatment with caffeine (2×10^{-2} M) in Ca^{2+}-free medium abolished responses to endothelin-1 and sarafotoxin S6b.

5 Bay K 8644 (10^{-10} M, 10^{-8} M) enhanced and nicardipine (10^{-10} M, 10^{-8} M) inhibited in a concentration-dependent manner vasoconstrictor response to endothelin-1. Response to sarafotoxin S6b was only affected by 10^{-8} M Bay K 8644 or nicardipine.

6 It is concluded that endothelin-1 and sarafotoxin S6b are potent vasoconstrictors of goat cerebral arteries, having direct effects on smooth muscle which are counteracted by the endothelium through the release of a vasodilatator substance, probably prostacyclin. Both endothelin-1 and sarafotoxin S6b depend on extracellular Ca^{2+} and on intracellular, caffeine-sensitive Ca^{2+} stores to develop vasoconstriction. However, endothelin-1 depends to a larger extent than sarafotoxin S6b on free extracellular Ca^{2+}.

Keywords: Endothelin-1; sarafotoxin S6b; cerebral arteries; endothelium; Ca^{2+}-entry

Introduction

Endothelin-1 is a 21-amino acid endothelium-derived vasoconstrictor peptide originally isolated from the culture supernatant of porcine aortic endothelial cells (Yanagisawa *et al.*, 1988). Pharmacological activity of endothelin-1 has been described in a wide range of tissues (Yanagisawa & Masaki, 1989). Binding sites of endothelin-1 are widely distributed, which suggests that the peptide can be involved in cardiovascular control and a large variety of organ functions (Koseki *et al.*, 1989). On the other hand, the venom of the burrowing asp, *Atractaspis engaddensis*, contains a group of 21-amino acid peptide toxins (sarafotoxins S6) showing structural and functional similarities with endothelins (Kloog & Sokolovsky, 1989), which are probably due to a common evolutionary origin (Landan *et al.*, 1991).

Endothelins and sarafotoxins compete in their binding to different subtypes of common receptors (Hirata *et al.*, 1989; Kloog *et al.*, 1989). The effects of endothelin-1 and sarafotoxin S6b have been compared in isolated vessels (Han *et al.*, 1990a; Eta & Triggle, 1991), non-vascular smooth muscles (Maggi *et al.*, 1990; Eta & Triggle, 1991), cultured astrocytes (Marsault *et al.*, 1990) and conscious rats (Han *et al.*, 1991), and the results suggest that these two peptides activate different cell signalling systems to different extents through endothelin/sarafotoxin receptors which are not identical.

With regard to the cerebrovascular bed, endothelin-1 contracts isolated cerebral arteries (Asano *et al.*, 1989; Jansen *et al.*, 1989; Martín de Aguilera *et al.*, 1989) and induces *in vivo* diameter reduction of the basilar artery (Asano *et al.*, 1989) and pial arteries (Faraci, 1989). Vasoconstrictor responses to endothelin-1 are greater in the cerebral arteries than in peripheral arteries because cerebral arteries are dependent to a large extent on extracellular Ca^{2+} influx (Tanoi *et al.*, 1991). The presence of endothelin-like immunoreactivity in cerebrovascular endothelial cells suggests that endothelin is a potential endogenous spasmogen (Saito *et al.*, 1991). On the other hand, it has been proposed that sarafotoxin S6b is cardiotoxic as a result of coronary vasospasm (Lee *et al.*, 1986), although it also contracts other arteries (Han *et al.*, 1990a; Eta & Triggle, 1991). However, in contrast to the well characterized effects of endothelin-1, the effects of sarafotoxin S6b in the cerebral arteries are unknown.

In a recent paper we have shown that endothelin-1 reduces cerebral blood flow in conscious goats by inducing contraction of cerebral arteries by a direct action on smooth muscle, which is modulated by the endothelium (Salom *et al.*, 1991). In the present study, we have examined and compared the effects of endothelin-1 and sarafotoxin S6b in goat isolated cerebral arteries. Modulation of these responses by the endothelium, involvement of vasoactive cyclo-oxygenase metabolites and participation of extracellular and intracellular Ca^{2+} sources were also examined and compared.

[1] Author for correspondence at: Centro de Investigación, Hospital "La Fe", E-46009, Valencia, Spain.

Methods

Tissue preparation

Female goats (30–45 kg), previously sedated with 10 mg kg^{-1} ketamine (Ketalar, Parke Davis, intramuscular) and anaesthetized with intravenous 2% sodium thiopentone (Pentothal, Abbot), were killed by intravenous injection of 30 mEq of potassium chloride. The whole brain was rapidly removed, the middle cerebral arteries were dissected free and cut into cylindrical segments measuring 4 mm in length and about 1 mm in outer diameter. Each segment was prepared for isometric tension recording in an organ bath. Two stainless steel L-shaped pins (125 μm in diameter) were introduced through the arterial lumen. One pin was fixed to the organ bath wall, while the other was connected to a strain gauge (Universal Transducing Cell, UC3, Gould Statham) for isometric tension recording (Omniscribe, Houston, D 5237-5). The organ bath contained 5 ml of Ringer-Locke solution, which was bubbled continuously with 95% O_2 and 5% CO_2 to give a pH of 7.3–7.4. The temperature was kept at 37°C. A resting tension of 1 g was applied to the arterial segments and they were allowed to equilibrate for 60–90 min. Tension was readjusted when necessary and the bath fluid was changed every 15 min before starting the experiments.

Procedure

The contractile capacity of the arterial segments was examined by exposure to a high-K^+ (50 mM) Ringer-Locke solution. The effects of endothelin-1 (10^{-12}–3×10^{-8} M) and sarafotoxin S6b (10^{-11}–3×10^{-7} M) were studied by cumulative addition of the peptides to the organ bath. Concentration-response curves were obtained in arteries at resting tension (1 g) and in arteries precontracted with prostaglandin $F_{2\alpha}$ (10^{-5} M). To examine homologous desensitization, two single doses of endothelin-1 (10^{-8} M) with an interval (120 min) for washing were tested.

The role of the endothelium in endothelin-1- and sarafotoxin S6b-elicited responses was checked by rubbing the intimal surface of arterial segments with a scored stainless steel rod. The presence or the absence of endothelium was checked for both by silver staining (Caplan & Schwartz, 1973) and by testing the endothelium-dependent vasodilator response to acetylcholine (10^{-6} M) on prostaglandin $F_{2\alpha}$-precontracted arterial segments (Furchgott *et al.*, 1981). Responses to endothelin-1 and sarafotoxin S6b were obtained in the presence of indomethacin (10^{-5} M, 20 min) to examine the involvement of vasoactive cyclo-oxygenase metabolites.

The influx of extracellular Ca^{2+} upon stimulation with endothelin-1 and sarafotoxin S6b was studied by obtaining responses to the peptides after incubation (20 min) in Ca^{2+}-free medium and Ca^{2+}-free medium to which EGTA (10^{-4} M) had been added. To examine the existence of a caffeine-sensitive intracellular Ca^{2+} store which could contribute to the endothelin-1- and sarafotoxin S6b-elicited responses, some arteries were incubated in Ca^{2+}-free medium and caffeine (2×10^{-2} M) was added before obtaining responses to the peptides. To assess the involvement of dihydropyridine-sensitive Ca^{2+}-channels in the endothelin-1- and sarafotoxin S6b-induced responses, we obtained responses to the peptides after incubation (20 min) with the Ca^{2+}-entry activator, Bay K 8644 (10^{-10} M, 10^{-8} M) and the Ca^{2+}-entry blocker, nicardipine (10^{-10} M, 10^{-8} M, 10^{-6} M).

Statistics

The contractile response to endothelin-1 and to sarafotoxin S6b is expressed as a percentage of the previous contraction induced by 50 mM KCl. The concentration-ratio was calculated for the responses at the level of the EC_{50} (half-maximal effective concentration). The maximum effects (E_{max}) were expressed as means ± s.e.mean and EC_{50} as the geometric mean with its confidence limits (95%) for repeated experiments. Statistical comparisons of E_{max} and $-\log EC_{50}$ (pD_2) values were obtained by analysis of variance (ANOVA) and Newman-Keuls tests. A probability value of less than 5% was considered significant.

Drugs and solutions

Endothelin-1 and sarafotoxin S6b (Peptide Institute Inc.) were dissolved in twice distilled water and diluted in phosphate buffered saline with 0.05% bovine serum albumin (Sigma, fraction V). Prostaglandin $F_{2\alpha}$ (Sigma) was dissolved in ethanol and diluted in saline solution. Acetylcholine (Sigma) was dissolved and diluted in saline. Indomethacin (Sigma) was dissolved and diluted in ethanol. EGTA (Sigma) was directly dissolved in the Ca^{2+}-free medium. Caffeine (Merck) was dissolved in distilled water. Bay K 8644 (methyl 1, 4-dihydro-2, 6-dimethyl-3-nitro-4-2 (-trifluoromethylphenyl)-pyridine-5-carboxylate, Bayer AG) was dissolved in ethanol and diluted in saline. Experiments with Bay K 8644 were carried out under sodium-vapour light to prevent photodegradation. Nicardipine (Ferrer Internacional) was dissolved in twice distilled water and diluted in saline.

The Ringer-Locke solution had the following composition (mM): NaCl 120, KCl 5.4, $CaCl_2$ 2.2, $MgCl_2$ 1.0, $NaHCO_3$ 25 and glucose 5.6. In KCl-depolarizing solution, NaCl was replaced by an equimolar amount of KCl. The Ca^{2+} -free solution was prepared by omitting $CaCl_2$. The phosphate buffered saline had the following composition (mM): NaCl 150, NaH_2PO_4 10.0.

Results

Endothelin-1 (10^{-11}–3×10^{-8} M) produced slowly developing, concentration-dependent contractions of the goat middle cerebral artery (Figure 1a). Repeated washings of the arteries for at least 2 h restored the resting tension. Two consecutive single doses of endothelin-1 (10^{-8} M), separated by an interval of 2 h for washing, induced vasoconstrictor responses that were not significantly different (117 ± 8% vs. 101 ± 6% of the 50 mM KCl-elicited response, $n = 5$). Sarafotoxin S6b (10^{-10}–3×10^{-7} M) also produced concentration-dependent vasoconstrictor responses (Figure 1b). The EC_{50} value for sarafotoxin S6b was about 10 times greater than that for endothelin-1, but the maximum responses were not significantly different (Tables 1 and 2). In arteries precontracted with prostaglandin $F_{2\alpha}$ (10^{-5} M), additional vasoconstrictor responses were elicited by both endothelin-1 and sarafotoxin S6b (Figure 1), with significantly ($P < 0.01$) lower EC_{50} values than at resting tension (Tables 1 and 2).

Mechanical removal of the endothelium did not significantly change the contractile response to 50 mM KCl, while concentration-response curves to endothelin-1 and sarafotoxin S6b were displaced to the left (Figure 1). The decrease in the EC_{50} value produced by rubbing the endothelium was more significant for sarafotoxin S6b ($P < 0.01$) than for endothelin-1 ($P < 0.05$) and was accompanied by a significant ($P < 0.01$) increase in sarafotoxin S6b-induced but not in endothelin-1-induced maximum response (Tables 1 and 2). Incubation with indomethacin (10^{-5} M) produced a displacement to the left of the concentration-response curves to endothelin-1 and sarafotoxin S6b (Figure 1), which was significantly greater than the displacement produced by endothelium removal. Maximum response to sarafotoxin S6b but not to endothelin-1 was significantly ($P < 0.05$) increased by indomethacin (Tables 1 and 2).

After exposure to 'nominally' Ca^{2+}-free medium, the maximum vasocontrictor response to endothelin-1 was significantly ($P < 0.01$) reduced, with no change in the EC_{50} value. The maximum response to endothelin-1 in Ca^{2+}-free medium to which EGTA (10^{-4} M) had been added was significantly ($P < 0.01$) reduced with respect to the control but it was not

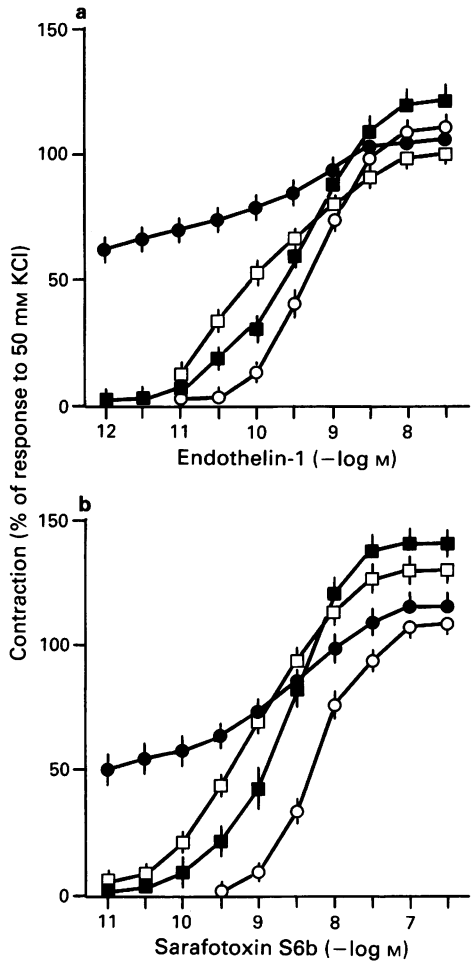

Figure 1 Concentration-response curves to (a) endothelin-1 and (b) sarafotoxin S6b in goat isolated middle cerebral arteries. (○) Control arteries, $n = 23$ in (a) and $n = 21$ in (b); (●) arteries precontracted with 10^{-5} M prostaglandin $F_{2\alpha}$ (54 ± 4% and 45 ± 6% of response to 50 mM KCl in (a) and (b), respectively), $n = 6$ in (a) and $n = 7$ in (b); (■) endothelium-free arteries, $n = 11$ in (a) and $n = 8$ in (b); (□) arteries incubated with 10^{-5} M indomethacin, $n = 9$ in (a) and $n = 7$ in (b). Symbols represent mean values and vertical bars show s.e.mean.

Table 1 EC_{50} and maximum effect (E_{max}) values for endothelin-1 in goat isolated middle cerebral arteries undergoing various treatments

	EC_{50} ($\times 10^{-10}$ M)	E_{max} (% of 50 mM KCl)	n
Control	4.9(3.9–6.2)	110 ± 4	23
Prostaglandin $F_{2\alpha}$, 10^{-5} M	1.1(0.4–3.0)[b]	105 ± 6	6
Without endothelium	3.3(2.8–3.9)[a]	120 ± 6	11
Indomethacin, 10^{-5} M	0.7(0.4–1.3)[b]	99 ± 2	9
Ca^{2+}-free medium, Ca(0)	4.0(2.3–6.9)	57 ± 7[b]	12
Ca(0) + EGTA, 10^{-4} M	3.0(1.4–6.6)	38 ± 11[b]	7
Bay K 8644, 10^{-10} M	2.0(1.4–3.0)[a]	100 ± 4	8
Bay K 8644, 10^{-8} M	0.9(0.4–1.9)[b]	103 ± 4	6
Nicardipine, 10^{-10} M	3.3(2.0–5.5)	68 ± 4[b]	4
Nicardipine, 10^{-8} M	9.5(4.3–21.4)	43 ± 2[b]	4
Nicardipine, 10^{-6} M	8.9(6.2–12.9)	38 ± 2[b]	4

EC_{50} values are geometric mean with 95% confidence interval and E_{max} values are mean ± s.e.mean from n arterial segments.
[a]Significantly different from control ($P < 0.05$).
[b]Significantly different from control ($P < 0.01$).

significantly different from the maximum response in 'nominally' Ca^{2+}-free medium (Figure 2a, Table 1). In contrast, the concentration-response curve to sarafotoxin S6b was not significantly modified in 'nominally' Ca^{2+}-free medium, but it was significantly ($P < 0.01$) inhibited after exposure to Ca^{2+}-free medium to which EGTA (10^{-4} M) had been added (Figure 2b, Table 2). On the other hand, after exposure to Ca^{2+}-free medium, addition of caffeine (2×10^{-2} M) elicited a transient contraction with a peak of 488 ± 61 mg (11 ± 1% of 50 mM KCl-elicited contraction, $n = 8$). Subsequent addition of endothelin-1 or sarafotoxin S6b failed to produce vasoconstriction.

Incubation with Bay K 8644 displaced the concentration-response curve to endothelin-1 to the left (Figure 3a), with significant, concentration-related reductions in the EC_{50} value (10^{-10} M, $P < 0.05$; 10^{-8} M, $P < 0.01$) and no change in the maximum response (Table 1). Nicardipine (10^{-10} M, 10^{-8} M) significantly ($P < 0.01$) reduced the maximum vasoconstrictor response to endothelin-1. Increasing nicardipine concentration to 10^{-6} M failed to produce further inhibition of the endothelin-1-induced vasoconstriction (Table 1). The concentration-response curve to sarafotoxin S6b was less affected by incubation with Bay K 8644 or nicardipine (Figure 3b). Bay K 8644 (10^{-8} M) produced a significant ($P < 0.05$) reduction in the EC_{50} value, and the reduction in the sarafotoxin S6b-induced maximum response was only significant ($P < 0.01$) for 10^{-8} M nicardipine (Table 2).

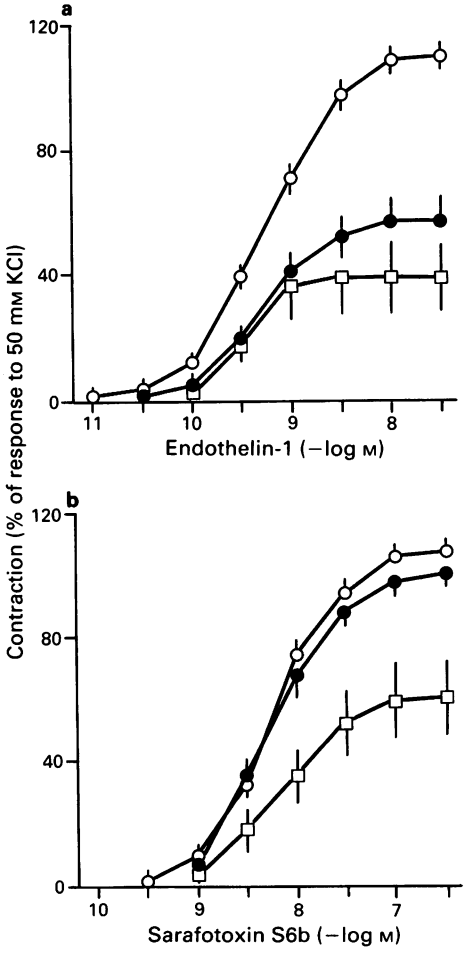

Figure 2 Concentration-response curves to (a) endothelin-1 and (b) sarafotoxin S6b in goat isolated middle cerebral arteries. (○) Control arteries, $n = 23$ in (a) and $n = 21$ in (b); (●) arteries incubated in Ca^{2+}-free medium, $n = 12$ in (a) and $n = 13$ in (b); (□) Ca^{2+}-free medium + 10^{-4} M EGTA, $n = 7$ in (a) and $n = 12$ in (b). Symbols represent mean values and vertical bars show s.e.mean.

Table 2 EC_{50} and maximum effect (E_{max}) values for sarafotoxin S6b in goat isolated middle cerebral arteries undergoing various treatments

	EC_{50} ($\times 10^{-9}$ M)	E_{max} (% of 50 mM KCl)	n
Control	5.5(4.4–6.9)	108 ± 3	21
Prostaglandin $F_{2\alpha}$, 10^{-5} M	1.7(1.4–2.2)[b]	114 ± 5	7
Without endothelium	2.1(1.4–3.1)[b]	140 ± 5[b]	8
Indomethacin, 10^{-5} M	0.8(0.6–1.0)[b]	129 ± 5[a]	7
Ca^{2+}-free medium, Ca(0)	5.1(3.2–8.1)	100 ± 2	13
Ca(0) + EGTA, 10^{-4} M	8.9(4.6–17.4)[a]	61 ± 12[b]	12
Bay K 8644, 10^{-10} M	4.5(3.8–5.2)	116 ± 5	7
Bay K 8644, 10^{-8} M	2.6(1.9–3.5)[a]	113 ± 3	11
Nicardipine, 10^{-10} M	4.9(3.3–7.2)	98 ± 3	8
Nicardipine, 10^{-8} M	5.9(3.5–9.8)	77 ± 3[b]	7

EC_{50} values are geometric mean with 95% confidence interval and E_{max} values are mean ± s.e.mean from n arterial segments.
[a]Significantly different from control ($P<0.05$).
[b]Significantly different from control ($P<0.01$).

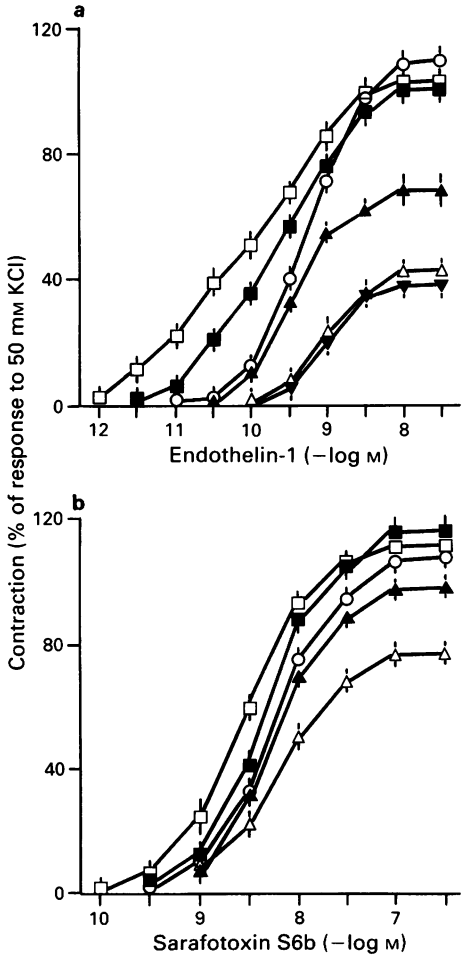

Figure 3 Concentration-response curves to (a) endothelin-1 and (b) sarafotoxin S6b in goat isolated middle cerebral arteries. (○) Control arteries, $n = 23$ in (a) and $n = 21$ in (b); (■) arteries incubated with 10^{-10} M Bay K 8644, $n = 8$ in (a) and $n = 7$ in (b); (□) 10^{-8} M Bay K 8644, $n = 6$ in (a) and $n = 11$ in (b); (▲) 10^{-10} M nicardipine, $n = 4$ in (a) and $n = 8$ in (b); (△) 10^{-8} M nicardipine, $n = 4$ in (a) and $n = 7$ in (b); (▼) 10^{-6} M nicardipine, $n = 4$. Symbols represent mean values and vertical bars show s.e.mean.

Discussion

In spite of the vastly different biological origins of endothelin-1 (mammalian vascular endothelium) and sarafotoxin S6b (reptilian venom), they show a striking structural homology, which is probably due to a common evolutionary origin (Landan *et al.*, 1991). It has been suggested that endothelin-1 and sarafotoxin S6b share common binding sites and mechanisms of action (Kloog & Sokolovsky, 1989). Our results show that endothelin-1 and sarafotoxin S6b are potent vasoconstrictors of goat cerebral arteries, but the vasoconstrictor potency of endothelin-1 was about ten times higher than that of sarafotoxin S6b. The response to endothelin-1 is also greater than to sarafotoxin S6b in the rat mesenteric vascular bed (Han *et al.*, 1990a), aorta (Maggi *et al.*, 1990) and uterus (Bousso-Mittler *et al.*, 1989). However, endothelin/sarafotoxin receptors may exist as subtypes in different tissues, since sarafotoxin S6b is about ten times more potent than endothelin-1 in the guinea-pig isolated bronchus (Maggi *et al.*, 1990). Nevertheless, both peptides are more potent than other vasoconstrictor substances, like 5-hydroxytryptamine (Salom *et al.*, 1989), noradrenaline (Salom *et al.*, 1990) and prostaglandin $F_{2\alpha}$ (Salom *et al.*, 1991) in goat cerebral arteries.

The constrictor activity of endothelin-1 is usually slow in onset, long-lasting, and extremely difficult to wash out (Yanagisawa & Masaki, 1989). Variable persistence of the endothelin-1-induced contraction after removal of the peptide from the bathing solution has been described in cerebral arteries from rat (Edwards & Trizna, 1990), cat (Saito *et al.*, 1989; Jansen *et al.*, 1989), dog (Saito *et al.*, 1991) and man (Hardebo *et al.*, 1989; Papadopoulos *et al.*, 1990). Our results show that complete relaxation of goat cerebral arteries contracted with endothelin-1 can be achieved after repeated washings for at least 2 h. Moreover, the vasoconstrictor response to endothelin-1 can be reproduced in the same arterial segment. By contrast, endothelin-1 shows a high degree of tachyphylaxis in feline cerebral arteries (Jansen *et al.*, 1989) and rat aorta (Auguet *et al.*, 1990). Therefore, binding mechanisms of endothelin-1 seem to vary in different species and vascular beds.

Endothelins evoke endothelium-dependent vasodilatation in isolated aorta (Sakata *et al.*, 1989) and in perfused mesentery of the rat (Warner *et al.*, 1989). Release of endothelium-derived relaxing factor (EDRF) and prostacyclin is induced by endothelins in rat mesenteric arteries (Warner *et al.*, 1989; Rakugi *et al.*, 1989). Sarafotoxin S6b causes vasorelaxation in the isolated mesenteric arterial bed of the rat precontracted with methoxamine (Douglas & Hiley, 1990). Neither endothelin-1 nor sarafotoxin S6b produced vasodilatation of precontracted goat cerebral arteries, but further vasoconstriction was elicited, and this is in agreement with other reports showing that endothelin-1 does not relax precontracted cerebral arteries of cat (Saito *et al.*, 1989), dog (Saito *et al.*, 1991) and man (Hardebo *et al.*, 1989). Therefore, it seems that neither endothelin-1 nor sarafotoxin S6b are able to release enough of any vasodilatator substance from cerebral arteries to overcome vasoconstrictor effects.

The endothelium modulates vascular smooth muscle contraction by interposing a physical barrier, extracting or degrading vasoactive substances, converting precursors into vasoactive products, and releasing inhibitory and excitatory mediators (Vanhoutte *et al.*, 1986). We found that removal of the endothelium increased the sensitivity of goat cerebral arteries to endothelin-1 and even more to sarafotoxin S6b. It has been shown that removal of the endothelium increases the vasoconstrictor response to endothelin-1 in cat cerebral arteries (Saito *et al.*, 1989; Kauser *et al.*, 1990), rat aorta (Eglen *et al.*, 1989; Sakata *et al.*, 1989; Topouzis *et al.*, 1991) and rat superior mesenteric arterial bed (Randall *et al.*, 1989). In contrast, the endothelium does not modulate vasoconstrictor responses to endothelin-1 in canine cerebral arteries (Saito *et al.*, 1991), human cerebral arteries (Hardebo

et al., 1989; Martin de Aguilera *et al.*, 1990), porcine coronary artery (Kasuya *et al.*, 1989a) or rabbit aorta (Ohlstein *et al.*, 1989). With regard to sarafotoxin S6b, its vasoconstrictor responses are enhanced by destruction of the endothelium in the rat superior mesenteric arterial bed (Douglas & Hiley, 1990) but not in rat aorta (Topouzis *et al.*, 1991). Therefore, the endothelium produces a partial inhibition of vasoconstrictor response to endothelin-1 and sarafotoxin S6b to a different extent in goat cerebral arteries, as differences seem to exist between different vascular beds and species. On the other hand, we found that indomethacin enhanced the vasoconstrictor responses to endothelin-1 and sarafotoxin S6b, which indicates that the two peptides induce the release of a vasodilatator cyclo-oxygenase product, probably prostacyclin. This product partially counteracts vasoconstriction in goat cerebral arteries. Endothelin-1-induced vasoconstriction is also modulated by a vasodilator cyclo-oxygenase product in cat cerebral arteries (Kauser *et al.*, 1990) and other vascular beds (Neubauer *et al.*, 1990; Miura *et al.*, 1991).

Early studies on the vasoconstrictor activity of endothelin-1 suggested that the influx of extracellular Ca^{2+} was required because the peptide was an endogenous agonist of the dihydropyridine-sensitive Ca^{2+} channel (Yanagisawa *et al.*, 1988). Subsequent findings showed that the activation of Ca^{2+} channels by endothelin-1 is not direct but is secondary to its interaction with specific receptors outside the channel complex (Auguet *et al.*, 1988; Goto *et al.*, 1989). Extracellular Ca^{2+} influx is involved in the peripheral vasoconstriction produced by both endothelin-1 and sarafotoxin S6b (Han *et al.*, 1990b; Tabrizchi & Triggle, 1990). Our results show that vasoconstriction of goat cerebral arteries produced by both endothelin-1 and sarafotoxin S6b partially depends on the influx of extracellular Ca^{2+}, since they were inhibited after the Ca^{2+} was removed from the medium. However, the nature of the extracellular Ca^{2+} pools mobilized by the two peptides was not the same. Endothelin-1-induced vasoconstriction depended on free extracellular Ca^{2+} and sarafotoxin S6b-induced vasoconstriction depended on externally membrane-bound Ca^{2+}, which withstood washing with 'nominally' Ca^{2+}-free medium but was displaced by EGTA. In addition, our results show the existence of an intracellular Ca^{2+} store sensitive to endothelin-1 and sarafotoxin S6b which overlaps with the caffeine-sensitive store, since caffeine inhibited the vasoconstriction produced by both endothelin-1 and sarafotoxin S6b in Ca^{2+}-free medium. Our results are in agreement with previous reports on porcine coronary artery showing that vasoconstriction induced by endothelin-1 is inhibited by pretreatment with caffeine (Kasuya *et al.*, 1989b; Kodama *et al.*, 1989).

Evidence has been provided that endothelin-1 activates the dihydropyridine-sensitive, voltage-dependent Ca^{2+} channel (Goto *et al.*, 1989), thus accelerating Ca^{2+} influx and producing vasoconstriction but through a binding site that is distinct from that of dihydropyridines (Kasuya *et al.*, 1989a). Our results show that vasoconstrictions produced by endothelin-1 and sarafotoxin S6b in goat cerebral arteries were mediated in part by Ca^{2+} entry through dihydropyridine-sensitive Ca^{2+} channels, since they were potentiated by Bay K 8644 and inhibited by nicardipine. Interestingly, vasoconstriction induced by sarafotoxin S6b was less affected by Ca^{2+} entry modulators because it depends to a lesser extent on free extracellular Ca^{2+}. It has been shown that endothelin-1 produces greater contraction of canine cerebral arteries than peripheral arteries because cerebral arteries depend to a larger extent on extracellular Ca^{2+} (Tanoi *et al.*, 1991). In contrast, the vasoconstrictor effect of endothelin-1 on rat intracerebral arterioles is only slightly attenuated by nicardipine, because it depends mainly on the release of intracellular Ca^{2+} stores (Edwards & Trizna, 1990).

In conclusion, endothelin-1 and sarafotoxin S6b induce potent vasoconstriction in goat cerebral arteries, which is partially inhibited by the endothelium through the release of a vasodilatator substance, probably prostacyclin. The amount of this substance is not sufficient to produce vasodilatation but it does partially counteract vasoconstriction. Both endothelin-1 and sarafotoxin S6b depend on extracellular Ca^{2+} and on intracellular, caffeine-sensitive Ca^{2+} stores to induce vasoconstriction. However, endothelin-1 depends to a larger extent than sarafotoxin S6b on free extracellular Ca^{2+} for its activity as shown by the greater effects of Ca^{2+} entry modulators on endothelin-1-induced vasoconstriction.

We thank Dr S. Lluch for his helpful comments and Ms L. Martínez and Ms M.C. Tirados for technical assistance. J.A.A. holds a F.I.S.S.S. research fellowship.

References

ASANO, T., IKEGAKI, I., SUZUKI, Y., SATOH, S. & SHIBUYA, M. (1989). Endothelin and the production of cerebral vasospasm in dogs. *Biochem. Biophys. Res. Commun.*, **159**, 1345–1351.

AUGUET, M., DELAFLOTTE, S., CHABRIER, P.E., PIROTZKY, E., CLOSTRE, F. & BRAQUET, P. (1988). Endothelin and Ca^{++} agonist Bay K8644: different vasoconstrictive properties. *Biochem. Biophys. Res. Commun.*, **156**, 186–192.

AUGUET, M., DELAFLOTTE, S., GUILLON, J.M., ROUBERT, P., CHABRIER, P.E. & BRAQUET, P. (1990). Endothelin-1, but not sarafotoxin S6b, induces cross-desensitization of rat aorta contraction. *Eur. J. Pharmacol.*, **187**, 293–294.

BOUSSO-MITTLER, D., KLOOG, Y., WOLLBERG, Z., BDOLAH, A., KOCHVA, E. & SOKOLOVSKY, M. (1989). Functional endothelin/sarafotoxin receptors in the rat uterus. *Biochem. Biophys. Res. Commun.*, **162**, 952–957.

CAPLAN, B.A. & SCHWARTZ, C.J. (1973). Increased endothelial cell turnover in areas of *in vivo* Evans Blue uptake in the pig aorta. *Atherosclerosis*, **17**, 401–417.

DOUGLAS, S. & HILEY, C.R. (1990). Endothelium-dependent vascular activities of endothelin-like peptides in the isolated superior mesenteric arterial bed of the rat. *Br. J. Pharmacol.*, **101**, 81–88.

EDWARDS, R. & TRIZNA, W. (1990). Response of isolated intracerebral arterioles to endothelins. *Pharmacology*, **41**, 149–152.

EGLEN, R.M., MICHEL, A.D., SHARIF, N.A., SWANK, S.R. & WHITING, R.L. (1989). The pharmacological properties of the peptide, endothelin. *Br. J. Pharmacol.*, **97**, 1297–1307.

ETA, E. & TRIGGLE, C.R. (1991). A comparative study of endothelin and sarafotoxin action in vascular and non-vascular smooth muscle. *Neurochem. Int.*, **18**, 559–564.

FARACI, F.M. (1989). Effects of endothelin and vasopressin on cerebral blood vessels. *Am. J. Physiol.*, **257**, H799–H803.

FURCHGOTT, R.F., ZAWADZKI, J.V. & CHERRY, P.D. (1981). Role of endothelium in the vasodilator response to acetylcholine. In *Vasodilatation*. ed. Vanhoutte, P.M. & Leusen, I. pp. 49–66. New York: Raven Press.

GOTO, K., KASUYA, Y., MATSUKI, N., TAKUWA, Y., KURIHARA, H., ISHIKAWA, T., KIMURA, S., YANAGISAWA, M. & MASAKI, T. (1989). Endothelin activates the dihydropyridine-sensitive, voltage-dependent Ca^{2+} channel in vascular smooth muscle. *Proc. Natl. Acad. Sci. U.S.A.*, **86**, 3915–3918.

HAN, S.P., KNUEPFER, M.M., TRAPANI, A.J., FOK, K.F. & WESTFALL, T.C. (1990a). Endothelin and sarafotoxin S6b have similar vasoconstrictor effects and postsynaptically mediated mechanisms. *Eur. J. Pharmacol.*, **177**, 29–34.

HAN, S.P., KNUEPFER, M.M., TRAPANI, A.J., FOK, K.F. & WESTFALL, T.C. (1990b). Cardiac and vascular actions of sarafotoxin S6b and endothelin-1. *Life Sci.*, **46**, 767–775.

HAN, S.P., TRAPANI, A., FOK, K.F., WESTFALL, T.C. & KNUEPFER, M.M. (1991). A comparison of the hemodynamic effects of endothelin-1 and sarafotoxin S6b in conscious rats. *J. Pharmacol. Exp. Ther.*, **256**, 183–188.

HARDEBO, J.E., KÅHRSTRÖM, J., OWMAN, C. & SALFORD, L.G. (1989). Endothelin is a potent constrictor of human intracranial arteries and veins. *Blood Vessels*, **26**, 249–253.

HIRATA, Y., YOSHIMI, H., MARUMO, F., WATANABE, T.X., KUMAGAYE, S., NAKAJIMA, K., KIMURA, T. & SAKAKIBARA, S. (1989). Interaction of synthetic sarafotoxin with rat vascular endothelin receptors. *Biochem. Biophys. Res. Commun.*, **162**, 441–447.

JANSEN, I., FALLGREN, B. & EDVINSSON, L. (1989). Mechanisms of action of endothelin on isolated feline cerebral arteries: in vitro pharmacology and electrophysiology. *J. Cereb. Blood Flow Metab.*, **9**, 743–747.

KASUYA, Y., ISHIKAWA, T., YANAGISAWA, M., KIMURA, S., GOTO, K. & MASAKI, T. (1989a). Mechanism of contraction to endothelin in isolated porcine coronary artery. *Am. J. Physiol.*, **257**, H1828–H1835.

KASUYA, Y., TAKUWA, Y., YANAGISAWA, M., KIMURA, S., GOTO, K. & MASAKI, T. (1989b). Endothelin-1 induces vasoconstriction through two functionally distinct pathways in porcine coronary artery: contribution of phosphoinositide turnover. *Biochem. Biophys. Res. Commun.*, **161**, 1049–1055.

KAUSER, K., RUBANYI, M. & HARDER, D.R. (1990). Endothelium-dependent modulation of endothelin-induced vasoconstriction and membrane depolarization in cat cerebral arteries. *J. Pharmacol. Exp. Ther.*, **252**, 93–97.

KLOOG, Y., BOUSSO-MITTLER, D., BDOLAH, A. & SOKOLOVSKY, M. (1989). Three apparent receptor subtypes for the endothelin/sarafotoxin family. *FEBS Lett.*, **253**, 199–202.

KLOOG, Y. & SOKOLOVSKY, M. (1989). Similarities in mode and sites of action of sarafotoxins and endothelins. *Trends Pharmacol Sci.*, **10**, 212–214.

KODAMA, M., KANAIDE, H., ABE, S., HIRANO, K., KAI, H. & NAKAMURA, M. (1989). Endothelin-induced Ca-independent contraction of the porcine coronary artery. *Biochem. Biophys. Res. Commun.*, **160**, 1302–1308.

KOSEKI, C., IMAI, M., HIRATA, Y., YANAGISAWA, M. & MASAKI, T. (1989). Autoradiographic distribution in rat tissues of binding sites for endothelin: a neuropeptide? *Am. J. Physiol.*, **256**, R858–R866.

LANDAN, G., BDOLAH, A., WOLLBERG, Z., KOCHVA, E. & GRAUR, D. (1991). Evolution of the sarafotoxin/endothelin superfamily of proteins. *Toxicon.*, **29**, 237–244.

LEE, S.Y., LEE, C.Y., CHEN, Y.M. & KOCHVA, E. (1986). Coronary vasospasm as the primary cause of death due to the venom of the burrowing asp, *Atractaspis engaddensis*. *Toxicon.*, **24**, 285–291.

MAGGI, C.A., GIULIANI, S., PATACCHINI, R., SANTICIOLI, P., GIACHETTI, A. & MELI, A. (1990). Further studies on the response of guinea-pig isolated bronchus to endothelins and sarafotoxin S6b. *Eur. J. Pharmacol.*, **176**, 1–9.

MARSAULT, R., VIGNE, P., BREITTMAYER, J.P. & FRELIN, C. (1990). Astrocytes are target cells for endothelins and sarafotoxin. *J. Neurochem.*, **54**, 2142–2144.

MARTIN DE AGUILERA, E., IRURZUN, A., VILA, J.M., ALDASORO, M., GALEOTE, M.S. & LLUCH, S. (1990). Role of endothelium and calcium channels in endothelin-induced contraction of human cerebral arteries. *Br. J. Pharmacol.*, **99**, 439–440.

MIURA, K., YUKIMURA, T., YAMASHITA, Y., SHIMMEN, T., OKUMURA, M., YAMANAKA, S., IMANISHI, M. & YAMAMOTO, K. (1991). Renal and femoral vascular responses to endothelin-1 in dogs: role of prostaglandins. *J. Pharmacol. Exp. Ther.*, **256**, 11–17.

NEUBAUER, S., ERTL, G., HAAS, U., PULZER, F. & KOCHSIEK, K. (1990). Effects of endothelin-1 in isolated perfused rat heart. *J. Cardiovasc. Pharmacol.*, **16**, 1–8.

OHLSTEIN, E.H., HOROHONICH, S. & HAY, D.W.P. (1989). Cellular mechanisms of endothelin in rabbit aorta. *J. Pharmacol. Exp. Ther.*, **250**, 548–555.

PAPADOPOULOS, S.M., GILBERT, L.L., WEBB, R.C. & D'AMATO, C.J. (1990). Characterization of contractile responses to endothelin in human cerebral arteries: implications for cerebral vasospasm. *Neurosurgery*, **26**, 810–815.

RAKUGI, H., NAKAMARU, M., TABUCHI, Y., NAGANO, M., MIKAMI, H. & OGIHARA, T. (1989). Endothelin stimulates the release of prostacyclin from rat mesenteric arteries. *Biochem. Biophys. Res. Commun.*, **160**, 924–928.

RANDALL, M.D., DOUGLAS, S.A. & HILEY, C.R. (1989). Vascular activities of endothelin-1 and some alanyl substituted analogues in resistance beds of the rat. *Br. J. Pharmacol.*, **98**, 685–699.

SAITO, A., SHIBA, R., KIMURA, S., YANAGISAWA, M., GOTO, K. & MASAKI, T. (1989). Vasoconstrictor response of large cerebral arteries of cats to endothelin, an endothelium-derived vasoactive peptide. *Eur. J. Pharmacol.*, **162**, 353–358.

SAITO, A., SHIBA, R., YANAGISAWA, M., MASAKI, T., KIMURA, S., YAMADA, K., MIMA, T., SHIGENO, T. & GOTO, K. (1991). Endothelins: vasoconstrictor effects and localization in canine cerebral arteries. *Br. J. Pharmacol.*, **103**, 1129–1135.

SAKATA, K., OZAKI, H., KWON, S.C. & KARAKI, H. (1989). Effects of endothelin on the mechanical activity and cytosolic calcium levels of various types of smooth muscle. *Br. J. Pharmacol.*, **98**, 483–492.

SALOM, J.B., TORREGROSA, G., MIRANDA, F.J., ALABADI, J.A., ALVAREZ, C. & ALBORCH, E. (1990). Effects of Ca^{2+} entry blockers on $CaCl_2$-, KCl- and noradrenaline-induced contractions of goat cerebral arteries. *Eur. J. Pharmacol.*, **177**, 1–8.

SALOM, J.B., TORREGROSA, G., MIRANDA, F.J., ALABADI, J.A., ALVAREZ, C. & ALBORCH, E. (1991). Effects of endothelin-1 on the cerebrovascular bed of the goat. *Eur. J. Pharmacol.*, **192**, 39–45.

SALOM, J.B., TORREGROSA, G., MIRANDA, F.J., ALABADI, J.A., ALVAREZ, C. & ALBORCH, E. (1991). Ca^{2+}-entry blockers inhibit prostanglandin $F_{2\alpha}$-induced cerebrovascular contractile responses in goats. *Eur. J. Pharmacol.*, **203**, 33–39.

SALOM, J.B., TORREGROSA, G., MIRANDA, F.J., ALABADI, J.A., CAMPOS, V. & ALBORCH, E. (1989). Effect of Ca^{2+} entry blockers on contraction of cerebral arteries elicited by 5-HT, $PGF_{2\alpha}$ and hemorrhagic cerebrospinal fluid. In *Pharmacology of Cerebral Ischemia*. ed. Krieglstein, J. pp. 75–79. Stuttgart: Wissenschaftliche Verlagsgesellschaft.

TABRIZCHI, R. & TRIGGLE, C.R. (1990). Effects of nifedipine, Bay K 8644, and pertussis toxin on pressor response to sarafotoxin-b in pithed rats. *J. Cardiovasc. Pharmacol.*, **16**, 495–500.

TANOI, C., SUZUKI, Y., SHIBUYA, M., SUGITA, K., MASUZAWA, K. & ASANO, M. (1991). Mechanisms of the enhanced vasoconstrictor responses to endothelin-1 in canine cerebral arteries. *J. Cereb. Blood Flow Metab.*, **11**, 371–379.

TOPOUZIS, S., HUGGINS, J.P., PELTON, J.T. & MILLER, R.C. (1991). Modulation by endothelium of the responses induced by endothelin-1 and some of its analogues in rat isolated aorta. *Br. J. Pharmacol.*, **102**, 545–549.

VANHOUTTE, P.M., RUBANYI, G.M., MILLER, V.M. & HOUSTON, D.S. (1986). Modulation of vascular smooth muscle contraction by the endothelium. *Annu. Rev. Physiol.*, **48**, 307–320.

WARNER, T.D., DE NUCCI, G. & VANE, J.R. (1989). Rat endothelin is a vasodilator in the isolated perfused mesentery of the rat. *Eur. J. Pharmacol.*, **159**, 325–326.

YANAGISAWA, M., KURIHARA, H., KIMURA, S., TOMOBE, Y., KOBAYASHI, M., MITSUI, Y., YAZAKI, Y., GOTO, K. & MASAKI, T. (1988). A novel potent vasoconstrictor peptide produced by vascular endothelial cells. *Nature*, **332**, 411–415.

YANAGISAWA, M. & MASAKI, T. (1989). Endothelin, a novel endothelium-derived peptide. Pharmacological activities, regulation and possible roles in cardiovascular control. *Biochem. Pharmacol.*, **38**, 1877–1883.

(Received October 29, 1991
Accepted January 20, 1992)

Br. J. Pharmacol. (1992), **106**, 101-108 © Macmillan Press Ltd, 1992

Imidazoline binding sites in human placenta: evidence for heterogeneity and a search for physiological function

Sophia Diamant, Talia Eldar-Geva & [1]Daphne Atlas

Department of Biological Chemistry, The Hebrew University of Jerusalem, Jerusalem 91904, Israel

1 An α_2-adrenoceptor antagonist, idazoxan, that binds to both α_2-adrenoceptors and to imidazoline sites (IR), has been used to characterize human placental IR. Human placenta is shown to be the richest source of IR (1800 ± 100 fmol mg^{-1} protein; K_d 38.9 ± 3.4 nM).

2 Primary cells derived from human placenta and grown in monolayers, also displayed a high density of receptors (3209 ± 136 fmol mg^{-1} in cytotrophoblasts and 3642 ± 144 fmol mg^{-1} protein in syncytiotrophoblast enriched cell culture).

3 [^{3}H]-idazoxan did not show binding characteristics of α_2-adrenoceptors in human placental membranes or human trophoblastic cells, thus making it a ligand of choice to study the imidazoline site. The tissue appeared to be lacking α_2-adrenoceptors in that other α_2-adrenoceptor ligands, [^{3}H]-rauwolscine and [^{3}H]-clonidine, do not bind to α_2-adrenoceptors in human placenta.

4 IRs are localized on the cell surface, as determined by the release of bound [^{3}H]-idazoxan from cells, when washed with high ionic/acidic medium.

5 Imidazoline receptors of human placenta display high affinity for amiloride (72 ± 27 nM). The high affinity was used as a criterion to classify IR to IR_a subtype (placenta, rabbit kidney, rabbit liver and rabbit adipose cells) as opposed to the IR_b subtype which display low affinity for amiloride (>2 μM, in all the other tissues).

6 Several novel ligands comprising a guanido functional group attached to an aromatic residue (e.g. benziliden-amino-guanidine (BAG), guanido pyrole) display pronounced selectivity for IR over the α_2-adrenoceptors as the affinity of BAG is about 40 fold higher ($K_d = 18.9 \pm 13.8$ nM in human placenta), than the affinity for α_2-adrenoceptors ($K_d = 768 \pm 299$ nM in human platelets). Imidazoline sites bind selectively BAG and other guanido ligands thus indicating a distinct structural requirement at its site of binding.

7 K^+ channel blockers and monovalent ions (e.g. Cs^+ and NH_4^+) interfere with idazoxan binding to IR, indicating a possible involvement of IR in K^+ transport.

Keywords: Human placenta; imidazoline sites; CDS-clonidine displacing substance

Introduction

Imidazoline binding sites were recently described as pharmacologically distinct from α_2-adrenoceptors. These sites were identified and characterized in rabbit kidney cells (Coupry *et al.*, 1987; 1989; Hamilton *et al.*, 1988), pig kidney (Vigne *et al.*, 1989), fat cells (Langin & Lafontan, 1989), rat liver and lung, human platelets (Zonnenschein *et al.*, 1990), rat medulla oblongata (Ernsberger *et al.*, 1987) and guinea-pig ileum (Kupitz, Diamant & Atlas, unpublished observations).

These sites are not a subtype of adrenoceptors since (a) they can be separated from the α_2-adrenoceptors on lectin-affinity column (Parini *et al.*, 1989), (b) they do not recognize adrenaline nor the specific α_1- or α_2-adrenoceptor antagonists such as prazosin and yohimbine (see Atlas, 1991). However, the site binds, with very high affinity, α_2-adrenoceptor ligands which have guanidine and imidazoline structures (Coupry *et al.*, 1987; Langin & Lafontan, 1988; Michel *et al.*, 1989; Wikberg, 1989; Zonnenschein *et al.*, 1990). The density of the imidazoline sites dramatically exceeds the density of α_2-adrenoceptors in most of the cells where both are present, and appear in high density in cells which lack α_2-adrenoceptors such as rat liver (Zonnenschein *et al.*, 1990). Although a large variety of ligands bind with high affinity to the imidazoline sites and the sites are found in many cells, so far no function has been attributed to them.

A possible interaction of the imidazoline receptors with K^+-channels was suggested, based on the reduction in [^{3}H]-idazoxan specific binding produced by a high K^+ concentration in kidney cells (Coupry *et al.*, 1987) and by K^+-channel blockers in liver cells (Zonnenschein *et al.*, 1990).

Furthermore, in rat isolated kidney cells, structures with the imidazoline moiety induce inhibition of ^{22}Na uptake and changes in intracellular pH (Bidet *et al.*, 1990). Since the effects correlate with the binding order potency of imidazoline ligands, it was suggested that they are mediated by imidazoline receptors.

In this paper we have characterized imidazoline binding sites in human placenta, where their density is the highest reported so far. In addition, in human placental membranes, no α_2-adrenoceptors were detected with the radiolabelled specific α_2-adrenoceptor antagonist, [^{3}H]-rauwolscine, or the α_2-adrenoceptor agonist, [^{3}H]-clonidine. Furthermore no specific binding to α_2-adrenoceptors was observed with [^{3}H]-idazoxan.

We have used (a) placental membrane preparation, (b) freshly isolated cytotrophoblasts and (c) cultured cytotrophoblasts (which fuse to form syncytia *in vitro*) for the pharmacological characterization of imidazoline receptors and for exploring the physiological function of these sites.

Methods

Placental membrane preparation

Placental membranes were prepared from human full term placentas obtained from normal pregnancies immediately

[1] Author for correspondence.

after vaginal delivery, and processed as previously described (Gradey-Levassort *et al.*, 1984).

Isolation of trophoblast

Cytotrophoblast cells were prepared from human term placentas and cultured as previously described (Kliman *et al.*, 1986; Gileadi *et al.*, 1988). The cells, plated in multiwell dishes (0.5 to 1.0 million cells per well), gradually fused to form syncytia over a period of 24 to 72 h and were grown in culture up to 4 days.

Preparation of brush border membrane vesicles

Microvillous membranes were isolated from human term placentas as previously described (Johnson & Smith, 1988).

Platelet membrane preparation

Platelet membranes were prepared as previously described (Diamant *et al.*, 1987).

Protein determination

Protein was determined according to the method of Lowry *et al.* (1951), with bovine serum albumin used as a standard.

Binding of radioligands to placental membranes

The binding assay was carried out essentially as described for liver membranes (Zonnenschein *et al.*, 1990). Imidazoline receptor and α_2-adrenoceptors were characterized using cirazoline and noradrenaline respectively, for determining non specific binding. In saturation experiments the K_d and B_{max} values were analyzed with Enzfitter, a non linear regression data analysis programme (Leatherbarrow, 1987). Affinities of various ligands, were determined in displacement assays, using 3–4 nM [^{3}H]-idazoxan. The K_i values were calculated using EBDA- LIGAND computerized programme (Munson & Rodbard, 1980).

Binding of [^{3}H]-idazoxan to trophoblast cells

Freshly prepared trophoblast cells in suspension or plated in a 24 multiwell dish (NUNC) (5×10^5 cells/well) were washed with isotonic KRH buffer pH 7.4 (composition, mM): NaCl 108, KCl 5, $MgCl_2$ 1.2, $CaCl_2$ 1.8, HEPES-Tris 20, glucose 10, and incubated with increasing concentrations (2 to 30 nM) of [^{3}H]-idazoxan in the presence and in the absence of 20 μM cirazoline. Incubation of the cells was carried out for 4 h at 4°C. The suspended cells were filtered through GF/C filters, washed with cold isotonic buffer and processed as described for membranes (Zonnenschein *et al.*, 1990). Plated cells were washed 3 times with cold isotonic buffer, dissolved in 0.1% SDS and counted in a scintillation counter.

Displacement of [^{3}H]-rauwolscine from human platelet membranes

The assay was performed as previously described (Diamant *et al.*, 1987); 4–5 nM [^{3}H]-rauwolscine, and 50 μM adrenaline were used for evaluation of non specific binding.

Binding of [^{3}H]-idazoxan and [^{3}H]-dihydroalprenolol to membrane vesicles

[^{3}H]-idazoxan binding to vesicle membranes was carried out in 50 mM Tris-HCl buffer containing 2 mM $MgCl_2$, at 4°C for 4 h as described for cytotrophoblast cells. Specific binding to IR and α_2-adrenoceptors was determined with 20 μM cirazoline and 50 μM adrenaline respectively. [^{3}H]-dihydroalprenolol binding was determined at 30°C for 40 min using 10 μM propranolol for evaluation of non specific binding.

Alkaline phosphatase activity

Placental alkaline phosphatase activity was determined at pH 10.5 with p-nitrophenyl phosphate as the substrate according to Galski *et al.* (1981).

ATPase activity

ATPase activity was determined by colorimetric measurement of inorganic phosphate (Pi) released from ATP during incubation at 37°C (Fiske & Subbarow, 1925). The assay conditions were according to Post & Sen (1967).

Na^+/K^+ ATPase activity was dependent on Na^+ and K^+ ions and inhibited by ouabain (0.1 mM). Mg-ATPase activity was absolutely dependent on Mg^{2+} ions.

Purification of clonidine displacing substance (CDS)

CDS was purified according to a procedure previously described (Atlas & Burstein, 1984; Atlas *et al.*, 1987).

Materials

[^{3}H]-idazoxan and [^{3}H]-rauwolscine were obtained from the Radiochemical Centre, Amersham (England); [^{3}H]-clonidine and [^{14}C]-aminoisobutyric acid ([^{14}C]-AIB) from NEN Research Products (U.S.A.). Clonidine and amiloride were purchased from Sigma (U.S.A.). The following were gifts: rilmenidine (53341) from Servier, France; naphazoline and UK-14,304 (5-bromo-6-[2-imidazolin-2-ylamino]-quinoxaline) from Lilly Research Laboratories (U.S.A.); guanoxan and 94/2007.B ([4-(chloromethyl)-2-thiazolyl]guanidine) from Dr A.L. Green, SmithKline & Beecham (England); cirazoline from Synthelabo (France); amiloride analogues (5-(N-ethyl-N-isopropyl) amiloride (EIPA); 5-(N,N-hexamethylene) amiloride (HMA); 5-[N-methyl-N-(guanidinocarbonylmethyl)] amiloride-(MGCMA) from E.J. Cragoe; idazoxan (RX 781094) from Reckitt & Colman (U.K.); guanabenz was synthesized by D.A. (Diamant & Atlas, 1986); guanidopyrol and guanidotyramine were synthesized by D.A. and benzyliden-aminoguanidine (BAG) was from A. Dagan (Makor Chemicals, Israel).

Results

Binding of [^{3}H]-idazoxan to placental membrane

[^{3}H]-idazoxan was added in increasing concentrations (0.4 to 30 nM) to placental membranes in the absence and presence of cirazoline (20 μM) and incubated at 4°C for 4 h. Saturation binding isotherms obtained for [^{3}H]-idazoxan (Figure 1) gave a $B_{max} = 1800$ fmol mg^{-1} protein whereas non-specific binding was 10% to 15% of the total binding, and a $K_d = 38.9 \pm 3.4$ nM. The dissociation constant value is higher than the K_d values reported for liver or kidney membranes (10 and 1.5 nM respectively, Zonnenschein *et al.*, 1990). The K_d value for idazoxan was obtained by extrapolation from a non-linear regression data analysis using the computerized Enzfitter programme (Leatherbarrow, 1987). The time course of [^{3}H]-idazoxan (4 nM) binding to placental membrane at 4°C and at 30°C shows different saturation values (155 and 60 fmol mg^{-1} protein respectively) but equilibrium is reached after 30 min at both temperatures (Figure 2). Interestingly, in liver membranes, maximal binding (at 4 nM [^{3}H]-idazoxan) is similar at 4°C and 30°C but equilibrium is reached faster at 30°C compared to 4°C (Figure 3). [^{3}H]-idazoxan was not displaced by 100 μM adrenaline (or noradrenaline) indicating that it does not label α_2-adrenoceptors in placental membranes (Figure 4). Furthermore, binding of [^{3}H]-rauwolscine (0.3 to 14 nM) or [^{3}H]-clonidine (0.5 to 20 nM) to human placental membrane in the absence and in the presence of

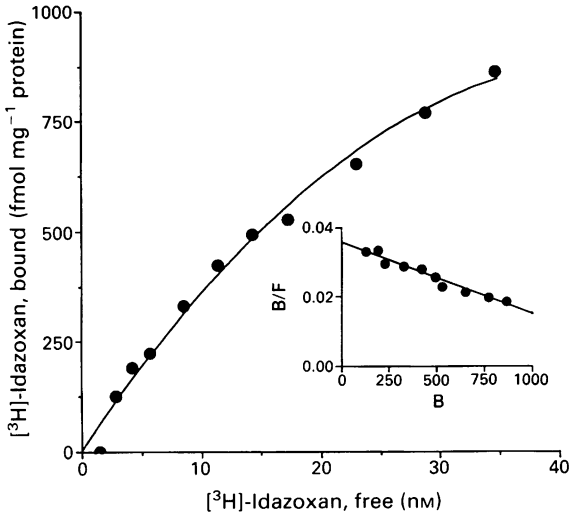

Figure 1 Specific binding of [^{3}H]-idazoxan to human placental membranes. The assay was carried out at 4°C for 4 h and non specific binding was determined in the presence of 20 μM cirazoline. A Scatchard plot (presented in insert) was derived from non-linear analysis of the data, using the Enzfitter computer curve fitting programme (Leatherbarrow, 1987). B represents specific bound [^{3}H]-idazoxan in fmol mg^{-1} protein; F free [^{3}H]-idazoxan concentration in nM. The data presented are a representative experiment, which was repeated 8 times with similar results (see Table 4).

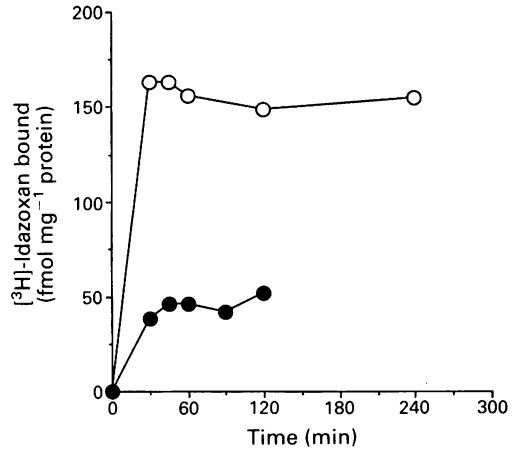

Figure 2 Effect of temperature on [^{3}H]-idazoxan specific binding to human placental membranes. Binding assay was carried out using 4 nM [^{3}H]-idazoxan in 250 μl of 50 mM Tris-HCl buffer, pH 7.4, containing 2 mM $MgCl_2$ and 150 μg membranal protein at 4°C (○) and 30°C (●). For each time interval non specific binding was determined using 20 μM cirazoline. The data represent a typical experiment ($n = 7$).

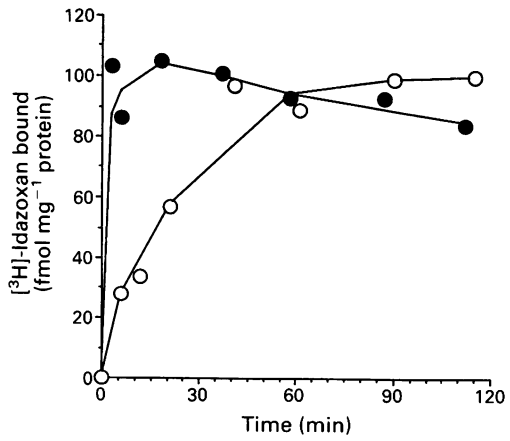

Figure 3 Effect of temperature on [^{3}H]-idazoxan specific binding to rat liver membranes. The assay conditions were as indicated in Figure 2: incubations at 4°C (○) and 30°C (●). The data represent a typical experiment ($n = 2$).

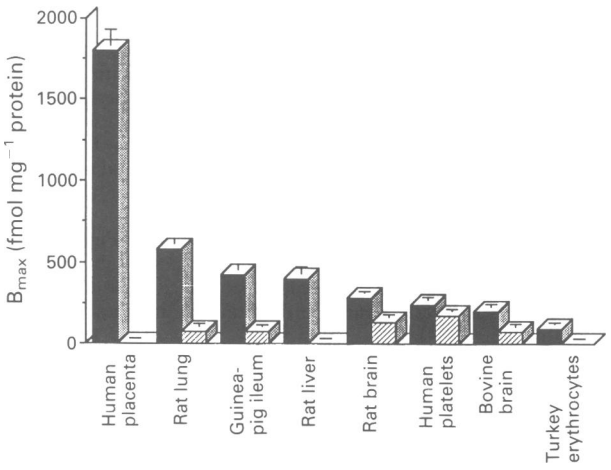

Figure 4 Specific binding of [^{3}H]-idazoxan to membranes of different tissues. Human placenta and platelet membranes were prepared as described in the methods section; rat lung and liver (Zonnenschein *et al.*, 1990) rat and bovine brain membranes (Atlas & Burstein, 1984); the guinea-pig ileum membranes (Kupitz, Diamant & Atlas, unpublished), turkey erythrocytes membrane according to Feder *et al.* (1986). Membranes (150 to 250 μg protein) were incubated with increasing concentrations (0.5 to 30 nM) of [^{3}H]-idazoxan in 250 μl of 50 mM Tris-HCl buffer containing 2 mM $MgCl_2$. The incubation was carried out at 30°C for 40 min except for human placental membranes which were incubated at 4°C for 4 h. Non specific binding was determined with 20 to 100 μM cirazoline (solid columns) and adrenaline 100 μM (hatched columns). B_{max} values were analyzed using the Enzfitter computer programme (Leatherbarrow, 1987).

100 μM adrenaline failed to show any specific binding, thus indicating either the absence of α_2-adrenoceptors or a very low affinity of these ligands for α_2-adrenoceptors compared with other tissues (data not shown). As shown in Figure 4, human placental membranes display the highest number of IR receptors compared to IR sites in different tissues. Like rat liver membranes, placental membranes do not express α_2-adrenoceptors (see above).

Displacement of the [^{3}H]-idazoxan bound to membranes by various imidazoline and guanidine ligands and CDS

Displacement experiments were carried out with crude placental membranes. The guanidine and the imidazoline ligands, some of which are used as antihypertensive drugs, have a common structural feature; namely, a guanidine or an imidazoline group. As shown in Table 1, the guanidine-type ligands displayed high affinity towards the imidazole receptor, with guanoxan, BAG (analogue of guanabenz lacking two substituted chloride on the benzyl ring) and guanidopyrol being most effective (K_is 3.55, 18.9 and 11.2 nM respectively). Both guanidopyrol and BAG have been shown to bind with relatively low affinity to α_2-adrenoceptors (see Table 1), thus making them selective drugs for IR. Of the imidazoline type ligands, cirazoline displayed the highest affinity for IR whereas UK 14,304 and clonidine displayed poor affinity for IR with higher affinity for α_2-adrenoceptors which makes them specific α_2-adrenoceptor ligands. Clonidine displacing substance (CDS), extracted from bovine brain and purified according to Atlas & Burstein (1984) and Atlas *et al.* (1987), displaced [^{3}H]-idazoxan specifically bound to placental membranes with an apparent K_d of 2.32 units (Table 1).

Table 1 Affinity of different ligands to imidazoline sites (IR) and α_2-adrenoceptors (α_2 AR) in placental and platelet membranes

	K_i (nM)		
Ligand	*IR placenta*	*α_2AR platelets*	*IR/α_2AR affinity*
Guanoxan	3.55 ± 2.91	85.0 ± 11.0	23.94
Guanidopyrol	11.2 ± 6.3	10100 ± 1515	905.00
BAG	18.9 ± 13.8	768.0 ± 299	40.63
Cirazoline	38.6 ± 12.2	142.1 ± 24.5	3.68
Idazoxan*	38.9 ± 3.4	3.94 ± 0.25	0.10
Guanabenz	48.9 ± 13.7	23.9 ± 8.2	0.49
Guanidotyramine	105.0 ± 38.0	4640 ± 2366	44.19
Naphazoline	128.0 ± 57.1	38.85 ± 22.8	0.30
94/2007B	673 ± 114	81500 ± 65200	121.10
UK-14304	1747 ± 227	18.8 ± 4.7	0.01
Clonidine	7390 ± 4367	36.1 ± 8.0	0.005
Rilmenidine	11470 ± 2010	144.6 ± 37.3	0.013
Amiloride	72.2 ± 26.6	35037 ± 13384	486.6
Benzamil	> 10,000	2268 ± 1295	> 0.3
CDS**	2.32 Unit	1.28 Unit	0.55

Membranes (150 to 250 µg protein per assay) were incubated with 3–4 nM [^{3}H]-idazoxan or with 4–5 nM [^{3}H]-rauwolscine, in 250 µl of 50 mM Tris HCl buffer, pH 7.4, containing 2 mM $MgCl_2$ and appropriate concentration of ligands. For placenta the incubation was performed at 4°C for 2 h and non specific binding was determined with 20 µM cirazoline. For platelet membranes, the assay was performed for 40 min at 30°C and 50 µM adrenaline was used for non-specific binding. K_i values were calculated by EBDA-LIGAND analysis using: K_d of idazoxan in placental membranes = 39 nM, and K_d of rauwolscine = 4.3 nM for platelet membranes.
*The value represents K_d (see Scatchard analysis in Figure 1).
**A unit of amount of CDS (clonidine displacing substance) was defined as the activity needed to displace 50% of [^{3}H]-clonidine specifically bound to rat brain membranes (Atlas & Burstein, 1984).

Table 2 Effect of K^+-channel blockers and monovalent cations on [^{3}H]-idazoxan binding in placental membranes

	IC_{50} (mM)
4-Aminopyridine	0.025 ± 0.01
CsCl	2.63 ± 0.76
NH_4HCO_3	3.03 ± 2.86
NaCl	29.6 ± 11.70
KCl	39.5 ± 0.20

The assay was performed as described in Table 1 for placental membranes.

Table 3 Binding of [^{3}H]-idazoxan to human placental membranes and to trophoblast cells

	B_{max} (fmol mg^{-1} protein)	*K_d (nM)*
Term placental membranes	1800 ± 100	38.9 ± 3.4 (n = 8)
Cytotrophoblasts	3209 ± 136	15.8 ± 1.4 (n = 5)
Cultured trophoblasts	3642 ± 144	36.3 ± 3.0 (n = 5)

Freshly prepared cytotrophoblast cells in suspension or plated in monolayer and grown in culture for 24 to 96 h, were incubated with 2 to 30 nM [^{3}H]-idazoxan (in presence and absence of 100 µM cirazoline) for 4 h at 4°C. The binding assay was terminated by rapid filtration through GF/C filters (for suspended cells) or by washes with cold isotonic buffer (for plated cells). B_{max} and K_d values were calculated using Enzfitter-non linear regression data analysis programme (Leatherbarrow, 1987). The data are average ± s.e.mean of 8 experiments for placental membranes, of 3 experiments for cytotrophoblasts and of 5 experiments – for cultured trophoblasts.

Displacement of [^{3}H]-idazoxan by amiloride and its analogues

Amiloride, an inhibitor of the Na^+/H^+ antiporter, which has a guanido structure, binds with high affinity to IR, K_i = 72 ± 27 nM (as determined by displacement of [^{3}H]-idazoxan from crude placental membranes), and very poorly to human platelet membranes, K_i = 35 µM (Table 1). Amiloride analogues, substituted on the 5-amino nitrogen of the pyrazine nucleus, displayed lower affinity towards imidazoline sites but slightly higher affinity towards α_2-adrenoceptors (data not shown). Benzamil, an amiloride analogue, with a benzyl group substituted on the nitrogen of the guanido group (Kleyman & Cragoe, 1988) displayed no affinity toward IR receptors, indicating the importance of an intact guanidino group for recognition (Table 1).

Effect of monovalent ions and K^+-channel blockers on binding of [^{3}H]-idazoxan to placental membranes

The order of potency of the various ions in displacing [^{3}H]-idazoxan was $Cs^+ > NH_4^+ > Na^+ > K^+$. 4-Amino-pyridine (4-AP), a K^+ channel blocker, was very effective in displacing idazoxan from placental membranes (IC_{50} = 25 µM, Table 2), as compared to its potency in inhibiting K^+ channels in neuronal cells.

Binding of [^{3}H]-idazoxan to trophoblasts in suspension or grown in culture

Binding to cells in suspension or grown in monolayers was carried out for 4 h at 4°C. As shown in Table 3, freshly prepared cytotrophoblast cells show a higher number of IR sites (B_{max} = 3209 ± 136 fmol mg^{-1} protein) than that observed for human placental membranes and the K_d value for idazoxan was lower (K_d = 15.8 ± 1.3 nM, Figure 5).

B_{max} values were similar when trophoblasts were kept in culture for different time intervals (24 to 96 h). The affinity for idazoxan in cultured cells was similar to the affinity observed for placental membranes.

Binding of [^{3}H]-idazoxan to plasma membrane or to intracellular compartments

To examine the possibility that [^{3}H]-idazoxan binds intracellularly (Tesson *et al.*, 1991), the cells were washed with 0.2 M acetic acid/0.5 M NaCl at the end of the binding assay and cell viability was verified by Trypan blue staining (Haigler *et al.*, 1980; Mahan *et al.*, 1985). The acidic-hypertonic wash of the cells was shown to remove all the ligand bound at the cell surface leaving the cells with the ligand inside, intact. As shown in Table 4, 86.5% of the specific binding was released from the cells under these conditions, indicating that it was associated with the cell surface.

Effect of temperature on [^{3}H]-idazoxan binding to placental cells

In trophoblast cells, as in placental membranes, the number of [^{3}H]-idazoxan (2.5 nM) sites labelled at 4°C are twice the sites labelled at 30°C (Figure 6). Possible internalization and binding to inner organelle membranes at 30°C was examined by applying the method of Haigler *et al.* (1990). At the end of 2 h binding, the cells were washed with 0.2 M acetic acid/0.5 M NaCl. The wash out and the washed cells were counted. As shown in Figure 6 (insert) binding was washed out completely, and no binding was found inside the cells.

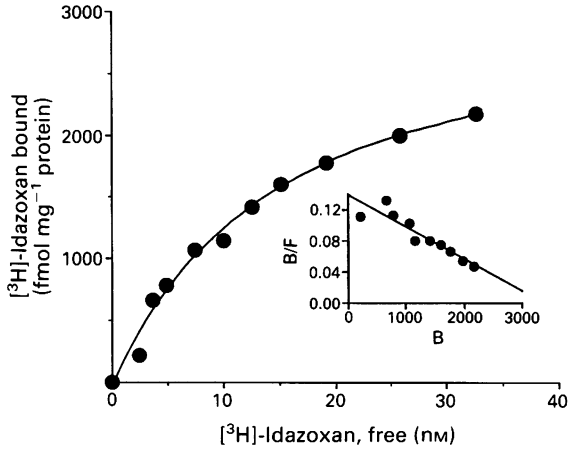

Figure 5 Specific binding of [^{3}H]-idazoxan to human cytotrophoblast cells. Binding assay was performed on cells, suspended in isotonic KRH buffer (see Methods), containing 2–30 nM [^{3}H]-idazoxan, in the presence and in the absence of 20 μM cirazoline. The assay was carried out for 4 h at 4°C. A Scatchard plot (presented in insert) was derived from non linear analysis of the data using Enzfitter computer programme (Leatherbarrow, 1987). The data presented are of a representative experiment which was repeated 3 times.

Table 4 Distribution of [^{3}H]-idazoxan binding in trophoblast cells

	B_{max} (fmol mg^{-1} protein)	B_{max} (%)	K_d (nM)
Surface	4135 ± 785	86.5	38.5 ± 11.3
Inside	647 ± 146	13.5	27.7 ± 9.7

Trophoblast cells, grown for 24 h in culture, were incubated with 1–22 nM [^{3}H]-idazoxan at 4°C. At the end of 4 h incubation, the cells were washed with acidic high salt buffer (0.5 M NaCl/0.2 M acetic acid, pH 2.5) and the radioactivity in the washout and the cells was measured.

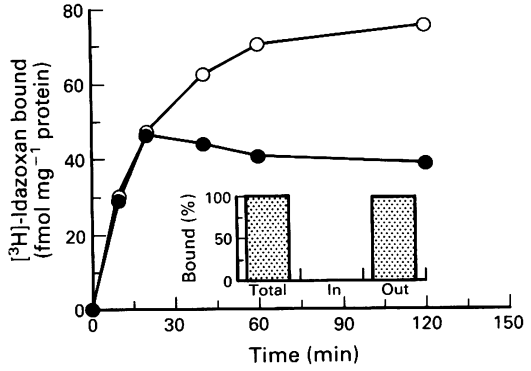

Figure 6 Effect of temperature on [^{3}H]-idazoxan specific binding to human trophoblast cells. Trophoblast cells, grown in culture for 24 h, were incubated with 2.5 nM [^{3}H]-idazoxan at 4°C (○) and 30°C (●) in the absence and in the presence of 20 μM cirazoline. At the end of incubation period the cells were washed with isotonic buffer, solubilized in 0.1 N NaOH and counted. Insert: cells were incubated for 2 h with [^{3}H]-idazoxan at 30°C (in the presence and in the absence of 20 μM cirazoline), then incubated with 0.2 M acetic acid/0.5 M NaCl pH 2.5 for 15 min, the medium removed and counted ('Out') and the remaining radioactivity of the cells was counted ('In'). 'Total' = the radioactivity observed with regular isotonic buffer wash (100%).

Localization of imidazoline receptor

Determination of [^{3}H]-idazoxan binding activity in brush border membranes and crude membranes (enriched in basolateral membranes as determined by distribution of the activity of alkaline phosphatase and Mg-ATPase), revealed that only 8% of the binding sites were present in the brush border membrane and 92% of the idazoxan binding sites were localized in the basal membrane and other cellular membrane structures (Table 5). Imidazoline receptors co-localized with β-adrenoceptors in that 85% of [^{3}H]-dihydroalprenolol binding sites were found in basolateral membrane enriched vesicles and only 15% in brush border membranes. On the other hand α_2-adrenoceptors were present in a very small number in the brush border membrane fraction (63 fmol mg^{-1} protein) and were absent from the crude membranes preparation.

ATPase activity

The driving force for many transport processes in placenta is generated by ATPase activities. We determined various ATPase activities in crude placental membranes enriched with basolateral membranes and in isolated brush border membranes. High activity of Mg-ATPase was found in brush border membranes, two times higher than in basolateral membranes enriched preparation (as expected from asymmetric transporting epithelial cells Table 5). This activity was not affected by any of the high affinity guanido and imidazoline ligands (Table 6). No Na^+/K^+ dependent ouabain-sensitive ATPase activity could be detected, most likely due to the very high Mg-ATPase activity.

In bovine brain, where Na^+/K^+ ATPase activity could be measured, none of the imidazoline/guanido-ligands tested had a significant effect on Na^+/K^+ ATPase activity (Table 6).

Discussion

A new population of binding sites labelled with [^{3}H]-idazoxan, which is pharmacologically distinct from α_2-adrenoceptors, have been recently characterized in many tissues (Doxey *et al.*, 1983). In this study, we characterized the imidazoline receptor in human placenta membranes and attempted to determine its function in trophoblasts. Screening of various tissues for the abundance of IR showed that human placenta is the richest in these sites (1800 ± 100 fmol mg^{-1} protein; K_d = 38,9 ± 3.4 nM). Since human placenta varies from donor to donor, we noticed a heterogeneity in receptor numbers but the most common was around 2000 fmol mg^{-1} protein. The choice of human placenta for studies on IR is also based on the finding that [^{3}H]-idazoxan as well as [^{3}H]-rauwolscine and [^{3}H]-clonidine do not label α_2-adrenoceptors in crude membranes and trophoblast cells. As previously reported by Gradey-Levassort *et al.* (1984), we were not able to identify α_2-adrenoceptors in human placenta.

The pharmacological profile of the placental imidazoline sites is similar to that observed for imidazoline sites in liver and other tissues. A few guanido ligands display a remarkable selectivity for placental imidazoline receptors with high affinity for IR and low affinity for α_2-adrenoceptors (e.g. guanido-pyrol K_i = 11.2 ± 6 nM and > 10 μM respectively). The 40 to 900 fold difference in affinity indicates that the imidazoline site represents a new site with a unique structural requirement. Unlike most other tissues, the placental imidazoline sites display high affinity for amiloride, a Na^+/H^+ antiporter blocker. The difference in affinity of IR for amiloride and its analogue, in different tissues might help in subdividing imidazoline sites into two subtypes: IR_1, which displays high affinity for amiloride (Table 7) and includes sites from human placenta, rabbit kidney, adipocytes and

Table 5 Distribution of imidazoline binding sites (IR), α_2- (α_2 AR) and β-adrenoceptors (βAR) in relation to alkaline phosphatase and Mg-ATPase activities in placental vesicles

	IR	*α_2AR*	*βAR*	*Alkaline phosphatase*	*Mg-ATPase*
	(fmol mg^{-1} protein)			*(μmol min^{-1} mg^{-1} protein)*	*(μgPi min^{-1} mg^{-1} protein)*
Crude membranes	2045 ± 75	0	567 ± 85	141	12.4
Brush-border membranes	233 ± 69	63 ± 30	99 ± 10	628	20.6

Steady state binding of [^{3}H]-idazoxan to IR sites was measured at 4°C after 4 h incubation, binding of [^{3}H]-idazoxan to α_2AR and [^{3}H]-dihydroalprenolol to βAR was determined after 40 min incubation at 30°C. B_{max} values were obtained from Scatchard analysis using the Enzfitter programme.

Table 6 The effect of imidazoline ligands on ATPase activity in placental and brain membranes

Ligand	*Mg^{2+}-ATPase*	*Na^+/K^+ ATPase*
	(μgPi min^{-1} mg^{-1} protein)	
Control	12.9	27.4
Idazoxan	12.5	30.8
Cirazoline	12.9	36.5
Guanabenz	12.1	28.5
Clonidine	12.8	28.5
UK 14304	12.9	—
Naphazoline	12.0	—

Mg-ATPase activity in placental membranes was determined with 150–200 μg protein. The membranes are preincubated in presence of 100 μM ligand for 10 min at 37°C, following the incubation in the presence of 3 mM ATP. The activity obtained in the absence of 5 mM Mg^{2+} was similar to blank value (without enzyme) and was subtracted as a background.
Na/K-ATPase activity in bovine brain membranes (prepared as described by Atlas & Sabol, 1981) was determined using 100–130 μg protein in presence of 100 μM Na^+, 20 μM K^+ and 5 mM Mg^{2+}. The activity was sensitive to ouabain (60% inhibition by 1 mM ouabain).

Table 7 Subdivision of imidazoline receptors (IR) into two subtypes according to their affinity for amiloride

IR subtype	*Tissue*	*Affinity for amiloride K_i (nM)*	*Reference*
IR_a	Human placenta	72	This work
	Rabbit kidney	30	Coupry *et al.* (1989)
	Rabbit fat cells	48	Langin & Lafontan (1989)
	Rabbit liver	160	Tesson *et al.* (1990)
IR_b	Human kidney	1109	Michel & Insel (1989)
	Guinea-pig ileum	2850	Kupitz, Diamant & Atlas unpublished
	Pig kidney	3000	Vigne *et al.* (1989)
	Human fat cells	3873	Langin *et al.* (1990)
	Rat liver	4809	Zonnenschein *et al.* (1990)
	Rat kidney	7760	Michel *et al.* (1989)
	Human liver	10,000	Tesson *et al.* (1990)

liver tissue, as opposed to IR_b, which binds amiloride poorly and is found in a variety of tissues where IR have been described (e.g. rat liver, guinea-pig ileum and rat brain, Table 6). This classification which is based almost entirely on the relative potency of amiloride, is still preliminary and calls for functional responses for confirmation. Similar suggestions were made by Michel & Insel (1989) and Wikberg & Uhlen (1990).

Amiloride competition with [^{3}H]-idazoxan binding to placental membranes, suggests an involvement of imidazoline receptors in Na^+ movement. Indeed in rat kidney cells ^{22}Na influx was inhibited by cirazoline, idazoxan, UK-14304 and rilmenidine, not via α_2-adrenoceptors (Bidet *et al.*, 1990). A comparison of binding constants of amiloride and its analogues with IC_{50} values for Na^+ channel (Cuthbert & Fanelli, 1978), Na^+/H^+ antiporter (Simchowitz & Cragoe, 1986) and Na^+/Ca^{2+} exchangers (Kaczorowski *et al.*, 1985) indicate that IR may be coupled to a Na^+ channel but not to an antiporter or an exchanger. On the other hand, the renal apical Na^+ channel, which was recently cloned, sequenced and expressed in transfected mammalian cells, displays high affinity for benzamil (Barbry *et al.*, 1990), which binds poorly to placental imidazoline receptors ($K_i > 10{,}000$ nM), indicating that IR is also distinct in structure from the amiloride-sensitive Na^+ channel (Table 1). An intact guanido group appears to be essential for recognition at the imidazoline sites. Further studies are needed to verify the possible involvement of Na^+ channel in IR signalling system.

Preparation of placental brush border membranes (defined by enrichment of alkaline phosphatase activity) enabled the localization of IR in assymetrical placental membrane of syncytiotrophoblasts. We found that 90% of IR are located in the basolateral membrane enriched fraction (facing foetal circulation). α_2-Adrenoceptors labelled with [^{3}H]-idazoxan, are absent from the epical-membrane-enriched-fraction but are present in small concentrations in brush border membranes. This finding provides additional distinction between IR and α_2-adrenoceptors according to their anatomical localization. Coupry *et al.* (1989) have also reported asymmetric distribution of IR in the renal proximal tubule.

Recent studies by Gileadi *et al.* (1988) have shown that cytotrophoblasts isolated from term placenta can be grown in monolayers and can be kept for up to 5 days in culture. We found that freshly prepared cytotrophoblasts as well as cells grown in culture (which differentiate to form syncytia *in vitro*) are rich in imidazoline sites. Their cellular location, was evaluated by washing of the extracellularly bound ligand in a low pH/high salt buffer. As shown, these receptors are present on the cell surface and less than 15% of labelled idazoxan is trapped inside the cells. Similar results were published for rat isolated hepatocytes (Zonnenschein *et al.*, 1990).

The trophoblast cells grown in culture were also used to examine possible functions for IR. The unique anatomical and physiological position of placenta between maternal and foetal circulations, determines its function as a mediator in transport of nutrients, ions and oxygen to foetal blood, and waste products from foetal to the maternal circulation. The abundance of IR in tissues such as human placenta, guinea-pig ileum (Kupitz *et al.*, 1991) and rabbit kidney (Coupry *et al.*, 1987) might suggest a role for IR in the mediation of transport.

Since in liver and in placental membranes, binding of [^{3}H]-idazoxan is reduced in the presence of K^+ channel blockers, we postulated that IR might exert effects through a direct interaction with K^+-channel.

However, membrane potential in vesicles derived from brush border and crude membrane of human placenta

(Breuer, 1989) was not affected by any of the guanido or imidazolidine ligands (data not shown). Amino acid transport through human placenta is one of its vital functions. This process is dependent on external Na^+, and Na^+/K^+ ATPase activity serves as its driving force (Shennan & Boyd, 1987). We measured amino acid ([^{3}H]-aminoisobutyric acid) transport into trophoblasts (Johnson & Smith, 1988) assuming that this process may be directly or indirectly (through the effect of Na gating) regulated by the IR receptor. Our preliminary results (not shown) indicate that Na^+-dependent [^{14}C]-aminoisobutyric acid influx into trophoblasts is slightly (up to 40%) affected by guanidine ligands (e.g. guanabenz, guanoxan). However, since the effective concentration was very high (10 to 100 μM), it cast doubt on the aminoisobutyric acid influx being regulated by IR. Further studies are now being undertaken to measure K^+ gating into intact cells with ^{86}RbCl. The transport of other ions and nutrients are also being studied in an attempt to correlate activity to the activation of the IR receptor.

We thank Ms Batia Gilad for excellent technical assistance. The work was supported by a research grant from Servier, France, and by the H.L. Lauterbach fund.

References

ATLAS, D. (1991). Clonidine-displacing substance (CDS) and its putative imidazoline receptor. *Biochem. Pharmacol.*, **41**, 1541–1549.

ATLAS, D. & BURSTEIN, Y. (1984). Isolation and partial purification of a clonidine displacing substance. *Eur. J. Biochem.*, **144**, 287–293.

ATLAS, D., DIAMANT, S., FALES, H.M. & PANNELL, L. (1987). The brain's own clonidine: purification and characterization of endogenous clonidine displacing substance from brain. *J. Cardiovasc. Pharmacol.*, **10** (Suppl 12), S122–S127.

ATLAS, D. & SABOL, S. (1981). Interaction of clonidine and clonidine analogues with α-adrenergic receptors of Neuroblastoma × Glioma hybrid cells and rat brain. *Eur. J. Biochem.*, **113**, 521–529.

BARBRY, P., CHAMPE, M., CHASSAND, O., MUNEMITSU, S., CHAMPIGNY, G., LINGUELIA, E., MAES, P., FRELIN, C., TARTAR, A., ULLRICH, A. & LAZDUNSKI, M. (1990). Human kidney amiloride-binding protein: cDNA structure and functional expression. *Proc. Natl. Acad. Sci. U.S.A.*, **87**, 7347–7351.

BIDET, M., POUJEOL, P. & PARINI, A. (1990). Effect of imidazolines on Na^+ transport and intracellular pH in renal proximal tubule cells. *Biochem. Biophys. Acta*, **1024**, 173–178.

BREUER, W. (1989). Characterization of chloride channels in membrane vesicles from the kidney outer medulla. *J. Memb. Biol.*, **107**, 35–42.

COUPRY, I., ATLAS, D., PODEVIN, R.A., UZIELLI, I. & PARINI, A. (1989). Imidazoline guanidinium receptic site (IGRS) in renal proximal tubule asymmetric distribution, regulation by cations, and interaction with an endogenous clonidine displacing substance. *J. Pharmacol. Exp. Ther.*, **252**, 293–299.

COUPRY, I., PODEVIN, R.A., DAUSSE, J.P. & PARINI, A. (1987). Evidence for imidazoline binding sites in basolateral membranes from rabbit kidney. *Biochem. Biophys. Res. Commun.*, **147**, 1055–1060.

CUTHBERT, A.W. & FANELLI, G.M. (1978). Effects of some pyrazinecarboxamids on sodium transport in frog skin. *Br. J. Pharmacol.*, **63**, 139–143.

DIAMANT, S., AGRANAT, I., GOLDBLUM, A., COHEN, S. & ATLAS, D. (1985). β-Adrenergic activity and conformation of the antihypertensive specific α_2-agonist drug, guanabenz. *Biochem. Pharmacol.*, **34**, 491–498.

DIAMANT, S. & ATLAS, D. (1986). An endogenous brain substance, CDS, (clonidine displacing substance), inhibits the twitch response of rat vas deferens. *Biochem. Biophys. Res. Commun.*, **134**, 184–190.

DIAMANT, S., ELDOR, A. & ATLAS, D. (1987). A low molecular weight brain substance interacts, similarly to clonidine, with α_2 adrenoceptors of human platelets. *Eur. J. Pharmacol.*, **144**, 247–255.

DOXEY, J.C., ROACH, A.G. & SMITH, C.F.C. (1983). Studies on RX 781094: a selective potent and specific antagonist of α_2-adrenoceptors. *Br. J. Pharmacol.*, **78**, 489–505.

ERNSBERGER, P.A., MEELEY, M.P. & REIS, D.J. (1988). An endogenous substance with clonidine like properties: selective binding to imidazole sites in the ventro lateral medulla. *Brain Res.*, **441**, 309–318.

FEDER, D., IM, M.J., KLEIN, H.W., HEKMAN, M., HOLZHOFER, A., DEES, C., LEVITZKI, A., HELMREICH, E.J.M. & PFEUFFER, T. (1986). Reconstitution of β_1-adrenoceptor-dependent adenylate cyclase from purified components. *EMBO J.*, **5**, 1509–1514.

FISKE, C.H. & SUBBAROW, Y. (1925). The colorimetric determination of phosphorus. *J. Biol. Chem.*, **66**, 375–380.

GALSKI, H., FRIDOVICH, S.E., WEINSTEIN, D., DE GROOT, N., SEGAL, S., FOLMAN, R. & HOCHBERG, A. (1981). Synthesis and secretion of alkaline phosphatase in vitro from first trimester and term human placentas. *Biochem. J.*, **194**, 857–866.

GILEADI, O., SCHNEIDER, T., CHEBATH, J., DE GROOT, N. & HOCHBERG, A. (1988). The expression of protooncogenes and 2'-5' aligoadenylate synthetase in differentiating human trophoblastic cells in vitro. In *Placental Protein Hormones*, ed. Mochizuki, M. & Hussa, R. Amsterdam, New York, Oxford: Excerpta Medica.

GRADEY-LEVASSORT, C., VENTURA, M.A., THIROUX, G. & OLIVE, G. (1984). An attempt to identify α-adrenoceptors in the human placenta. *Dev. Pharmacol. Ther.*, **7**, (Suppl 1), 85–88.

HAIGLER, H.T., MAXFIELD, F.R., WILLINGHAM, M.C. & PASTAN, I. (1980). Dansylcadaverine inhibits internalization of ^{125}I-epidermal growth factor in BALB 3T3 cells. *J. Biol. Chem.*, **255**, 1239–1241.

HAMILTON, C.A., REID, J.L. & YAKUBU, M.A. (1988). [^{3}H]Yohimbine and [^{3}H]idazoxan bind to different sites on rabbit forebrain and kidney membranes. *Eur. J. Pharmacol.*, **146**, 345–348.

JOHNSON, L.W. & SMITH, C.H. (1988). Neutral amino acid transport systems in microvillous membrane of human placenta. *Am. J. Physiol.*, **254**, C773–C780.

KACZOROWSKI, G.J., BARROWS, G.J., DETHMERS, J.K. & TRUMBLE, M.J. (1985). Inhibition of Na^+/Ca^{2+} exchange in pituitary plasma membrane vesicles by analogues of amiloride. *Biochemistry*, **24**, 1394–1399.

KLEYMAN, T.R. & CRAGOE, E.J. Jr. (1988) Amiloride and analogues as a tool in the study of ion transport. *J. Membr. Biol.*, **105**, 1–21..

KLIMAN, H.J., NESTLER, J.E., SERMASI, E., SANGER, J.M. & STRAUSS, J.F. III (1986). Purification, characterization and in vitro differentiation of cytotrophoblast from human term placentae. *Endocrinology*, **118**, 1567.

LANGIN, D. & LAFONTAN, M. (1989). [^{3}H]Idazoxan binding at non-α_2-adrenoceptors in rabbit adipocyte membranes. *Eur. J. Pharmacol.*, **159**, 199–203.

LANGIN, D., PARIS, H. & LAFONTAN, M. (1990). Binding of [^{3}H]adizoxan and of its methoxy derivative [^{3}H]RX821002 in human fat cells: [^{3}H]idazoxan but not [^{3}H]RX 821002 labels additional non $\alpha_2$adrenergic binding sites. *Mol. Pharmacol.*, **37**, 527–531.

LEATHERBARROW, R.J. (1987). *Enzfitter*. Amsterdam, Netherlands: Elsevier Science Publishers B.V.

LOWRY, O.H., ROSEBROUGH, N.Y., FARR, A.L. & RANDALL, R.J. (1951). Protein measurement with the Folin-phenol reagent. *J. Biol. Chem.*, **193**, 265–275.

MAHAN, L.C., MOTULSKY, H.J. & INSEL, P.A. (1985). Do agonists promote rapid internalization of β-adrenergic receptors? *Proc. Natl. Acad. Sci. U.S.A.*, **82**, 6566–6570.

MICHEL, M.C., BRODDE, O.E., SEHNEPEL, B., BEHRENDT, J., TSHADA, R., MOTULSKY, H.J. & INSEL, P.A. (1989). [^{3}H]idazoxan and some other α_2-adrenergic drugs also bind with high affinity to a non-adrenergic site. *Molec. Pharmacol.*, **35**, 324–330.

MICHEL, M.C. & INSEL, P.A. (1989). Are there multiple imidazoline binding sites? *Trends Pharmacol. Sci.*, **10**, 342–330.

MORRISS, F.H. Jr & BOYD, C.A.R. (1988). Placental transport. *The Physiology of Reproduction*. ed. Knobil, E. & Neill, J. pp. 2043–2083. New York: Raven Press Ltd.

MUNSON, P.J. & RODBARD, D. (1980). LIGAND, a versatile computerized approach for characterization of ligand binding system. *Anal. Biochem.*, **107**, 220–239.

PARINI, A., COUPRY, I., GRAHAM, R.M., UZIELLI, I., ATLAS, D. & LANIER, S.M. (1989). Characterization of an imidazoline/guanidinium receptive site distinct from the α_2-adrenergic receptor. *J. Biol. Chem.*, **264**, 11874–11878.

POST, R.L. & SEN, A.K. (1967). *Methods in Enzymology* Vol. X. ed. Estabrook, R.W. & Pullman, M.E. New York and London: Academic Press.

SHENNAN, D.B. & BOYD, C.A.R. (1987). Ion transport by the placenta: a review of membrane transport systems. *Biochem. Biophys. Acta*, **906**, 437–457.

SIMCHOWITZ, L. & CRAGOE, E.J. Jr (1986). Inhibition of chemotactic factor-activated Na^+/H^+ exchange in human neutrophils by analogues of amiloride: structure-activity relationships to the amiloride series. *Mol. Pharmacol.*, **30**, 112–117.

TESSON, F., LEMOINE, A., JOHANN, M. & PARINI, A. (1990). Identification of a non-adrenergic [^{3}H]idazoxan binding site in rabbit and human liver. *Eur. J. Pharmacol.*, **183**, 736–741.

TESSON, F., DRIP-BUUS, C., LEMONINE, A., PEGORIER, J.P. & PARINI, S.A. (1991). Subcellular distribution of imidazoline-guanidinium-receptive sites in human and rabbit liver. *J. Biol. Chem.*, **266**, 155–160.

VIGNE, P., LAZDUNSKI, M. & FRELIN, C. (1989). Guanabenz, guanochlor, guanoxan and idazoxan bind with high affinity to non-adrenergic sites in pig kidney membranes. *Eur. J. Pharmacol.*, **160**, 295–298.

WIKBERG, J.E.S. (1989). High affinity binding of idazoxan to non-catecholaminergic binding site in central nervous system: description of putative idazoxan receptor. *Pharmacol. Toxicol.*, **64**, 151–152.

WIKBERG, J.E.S. & UHLEN, S. (1990). Further characterization of the guinea pig cerebral cortex Idazoxan receptor: solubilization, distinction from the imidazole site, and demonstration of cirazoline as an idazoxan receptor-selective drug. *J. Neurochem.*, **55**, 192–203.

ZONNENSCHEIN, R., DIAMANT, S. & ATLAS, D. (1990). Imidazoline receptors in rat liver cells: a novel receptor or a subtype of α_2-adrenergic receptors? *Eur. J. Pharmacol.*, **190**, 203–215.

(Received September 27, 1991
Revised December 20, 1991
Accepted January 20, 1992)

Br. J. Pharmacol. (1992), **106**, 109–114 © Macmillan Press Ltd, 1992

Chloride channels and anion fluxes in a human colonic epithelium (HCA-7)

R.M. Henderson, M.L.J. Ashford, L.J. MacVinish & [1]A.W. Cuthbert

Department of Pharmacology, University of Cambridge, Tennis Court Road, Cambridge CB2 1QJ

1 Colonic epithelial cells, derived from a human adenocarcinoma (HCA-7), were examined by the patch clamp technique.

2 Outwardly rectifying anion (Cl^-) channels were identified in the apical membrane. The conductance was $g_{in} \approx 26$ pS, $g_{out} \approx 40$ pS. The open state probability of the channels increased with depolarization and the selectivity for Cl^- over K^+ (P_{Cl}/P_K) was ≈ 7.5.

3 The channels were sensitive to intracellular adenosine 3':5'-cyclic monophosphate (cyclic AMP, 0.1 mM), but not to Ca^{2+} (at concentrations up to 1 mM). At depolarized potentials the channels were blocked by pirentanide (1–5 μM) applied intracellularly.

4 HCA-7 monolayers loaded with $^{125}I^-$ (as a marker for Cl^-) were used to measure I^- efflux and converted to instantaneous rate constants.

5 The rate constant for I^- efflux was increased by forskolin and lysylbradykinin (LBK). The effects of forskolin were not effected by BAPTA (an intracellular calcium chelator). The effects of LBK were inhibited by BAPTA and by Ba^{2+}, indicating that LBK raised intracellular Ca^{2+} (Ca_i) which activates Ca^{2+}-sensitive K-channels, the latter being blocked by Ba^{2+}.

6 Although it cannot be conclusively proved that the outwardly rectifying chloride channels described here are solely or partially responsible for the increased anion efflux or transepithelial chloride secretion, the channels are likely to be more relevant for cyclic AMP-requiring rather than Ca^{2+}-requiring secretagogues.

Keywords: Ion channels; chloride; piretanide; cyclic AMP; lysylbradykinin; forskolin

Introduction

A number of cell lines derived from human adenocarcinomata are important for the study of transepithelial ion transport. This is so because in culture the cells can form polarized epithelial monolayers mimicking a sheet of intact epithelium. Examples are the T84 cell line (Dharmsathaphorn *et al.*, 1984), HT_{29} cell line (Augerson & Laboisse, 1984) and the HCA-7 cell line, originally described by Kirkland (1985) and used to study chloride secretion (Cuthbert *et al.*, 1985; 1987; Brayden *et al.*, 1989). Thus far, however, evidence for presumed apical chloride channels has been indirect and no direct evidence for increased apical chloride fluxes has been obtained after application of chloride secretagogues. Direct evidence for both of these is provided by the present study.

Methods

Cell culture

HCA-7 cells, derived from a human colonic adenocarcinoma (Kirkland, 1985) were prepared and grown to confluence as described in detail previously (Cuthbert *et al.*, 1985; 1987). Briefly, cells were seeded onto 10 cm^2 Petri dishes or 6 well (35 mm diameter) plates (Cell Cult, Sterilin Ltd., Hounslow, England) in Dulbecco's Modified Eagle's Medium (Gibco-Europe, Paisley, Scotland) supplemented with glucose (25 mmol l^{-1}) and 10% foetal calf serum (Gibco), kanamycin (100 μg ml^{-1}; Bristol Laboratories, Langley, Slough, England) and amphotericin B (2.5 μg ml^{-1}; E.R. Squibb, Morton, Cheshire, England). Cells were grown at 37°C in an atmosphere of 95% O_2/5% CO_2 for 5–10 days after seeding.

Patch clamp experiments

Cells grown in the 10 cm^2 diameter dishes were used. Generally it was easier to patch cells at the edge of confluent areas. If difficulty was experienced in forming seals, cells were 'rounded up' by exposure for 3–5 min at room temperature to a solution containing (mM): NaCl 135, KCl 5, ethylene diamine tetra-acetic acid, disodium salt (EDTA), 0.6 and 0.5 g l^{-1} trypsin. Patch clamp experiments were conducted using the inside-out configuration of single channel current recording (Hamill *et al.*, 1981). Patch pipettes were made from borosilicate, filamented capillary tubing (1.2 mm o.d., 0.6 mm i.d. (GC120-F10), Clark Electromedical Instruments, Pangbourne, England) and fire-polished to give a pipette resistance of 10–25 MΩ. Solutions were filtered immediately before use with 0.22 μm Acrodisc filters (Gelman Sciences, Ann Arbor, Michigan, U.S.A.). The resistance of the seals was between 50 and 300 GΩ.

Recordings were made with either a List L/M-EPC7 patch clamp amplifier (List Medical, Darmstadt, Germany) or a Dagan 8900 amplifier (Dagan Corporation, Minneapolis, Minnesota, U.S.A.) as described previously (Henderson & Cuthbert, 1991).

Single channel data were analysed on IBM AT-compatible computers using either the pClamp system (Version 5.5.1; Axon Instruments, Inc., Foster City, California, U.S.A.) in combination with a Tecmar Labmaster A/D D/A board, or using the single channel analysis programme PAT (V 6.2) (Dempster, 1988) in combination with a Data Translation DT 2801A A/D D/A board (Data Translation, Inc., Marlborough, Massachusetts, U.S.A.). Current amplitudes were determined from single-point histograms and single channel conductances derived from current-voltage relationships obtained by recording amplitude histograms at a number of different holding potential (V_h) values. The open-state probability was calculated from peak areas of amplitude histog-

[1]Author for correspondence.

rams using the areas of Gaussian distributions fitted to the data (Colquhoun & Sigworth, 1983). Open and closed time distributions of single channel records were determined off-line using analysis programmes incorporating a 50% threshold crossing parameter to detect events. Stretches of data were replayed at the recorded speed, filtered at a bandwidth of 1 kHz (-3 dB) and digitally sampled at 20 μS intervals. Data are represented as mean ± standard error of mean (s.e.mean).

To check the selectivity of chloride channels two approaches were used to change the Cl^- concentration bathing the patch. In the first, the pipette solution contained (mM): HEPES-Na (pH 7.4) 10, KCl 145, EGTA (ethyleneglycol-*bis*-(β aminoethyl ether) N,N,N',N'-tetra-acetic acid) 1 and $CaCl_2$ (adjusted to give 1 μM free Ca^{2+} activity). Free Ca^{2+} activity was calculated from the binding constants for EGTA given by Fabiato & Fabiato (1979). The bath (in contact with the cytosolic face of the patch) contained (mM): NaCl 140, KCl 5, HEPES-Na (pH 7.4) 10, EGTA 1 and Ca^{2+} 1 μM. To reduce the Cl^- concentration the bath solution was replaced with one containing (mM): sucrose 200, NaCl 47, KCl 1.7, HEPES-Na (pH 7.4) 10, EGTA 1 and Ca^{2+} 1 μM. For the second, selectivity for anions was determined with non-iso-osmotic solutions of NaCl and KCl in the pipette and bath, with gradients for either KCl or NaCl. Solutions containing either 70, 140 or 210 mM NaCl or KCl were used to provide ion gradients across the membrane. The solutions also contained (mM): Na-HEPES (pH 7.4) 10, EGTA 1 and Ca^{2+}at 1 mM or 1 μM. Full details of specific experimental conditions are given in the Results section. Both approaches provided gradients across the membrane for K^+, Na^+ and Cl^-. To prevent junction potentials distorting the data when the bath Cl^- composition was changed, the amplifier head stage indifferent electrode was connected to the bath via a 1.5% agar bridge having the same ionic composition as the pipette solution (but without Ca^{2+}).

^{125}Iodide efflux from HCA-7 monolayers

HCA-7 cells were plated out into 6 well (35 mm diameter) plates and incubated at 37°C with the same medium and conditions as used for the patch clamp experiments. The plates were used at 5–6 days when the epithelia were 50–70% confluent.

To load the cells with $^{125}I^-$ the monolayers were washed, three times with efflux buffer and then exposed to the buffer containing 2.5 μ Ci ml^{-1} for 90 min at 37°C. At the end of the loading period the monolayers were again washed, three times, with efflux buffer ($t = 0$). Efflux of $^{125}I^-$ was measured every 30 s by rapidly removing efflux buffer (3 ml) and adding a further aliquot for a total period of 10 min. At the end of 10 min, 3 ml 0.1 N HNO_3 was added and left for 30 min, to remove the remaining tracer. To determine the effect of a secretagogue this was added to the efflux buffer at $t = 3.5$ min until the end of the experiment. The efflux buffer had the following composition (mM): NaCl 135, $CaCl_2$ 1.2, $MgCl_2$ 1.2, K_2HPO_4 2.4, KH_2PO_4 0.6, glucose 10 and HEPES 10 (pH 7.2). The method used is essentially similar to that described by Venglarik *et al.* (1990) and Clancy *et al.* (1990). After counting the samples, with allowance for background, the data were processed to give instantaneous rate constants. Briefly, this was achieved as follows. The total counts released were summed with the residual counts left in the tissue. Thus the fraction of counts remaining in the tissue after $t = 0$ could be plotted with respect to time. If no drug treatment was applied washout was exponential. If a drug increasing or reducing efflux was added, the washout profile changed to one with a greater or lesser slope. Calculation of instantaneous rate constants assumes that the fractional content of isotope between any two adjacent time points represents a segment of an exponential decay curve. The rate constant is then, simply, the reciprocal of the time for the content to fall to 1/e of the value obtaining at the beginning of time segment. A computer programme requiring only the counts released in each interval and the residual counts was devised to process the data.

BAPTA-AM was used to chelate intracellular Ca^{2+} ions in some experiments. To do this the acetoxymethyl ester was dissolved in dimethylsulphoxide (DMSO), diluted in buffer and incubated with the epithelial monolayers for 90 min at a final concentration of 5 μM. Subsequent washing removed excess BAPTA-AM while the intracellularly released BAPTA was trapped in the cells. Cells were loaded with $^{125}I^-$ at the same time as being exposed to BAPTA-AM.

When the effects of Ba^{2+} (1 mM) were investigated, this ion was included in both the loading and efflux solution. However, the composition of the solutions was changed to prevent precipitation as follows. Phosphates were replaced with KCl, 3 mM, and the HEPES concentration was increased to 15 mM.

Both BAPTA-AM and Fura2-AM were purchased from Molecular Probes, Eugene, Oregon, U.S.A.

Results

We have recorded single channel currents from inside-out patches of HCA-7 cells. Several different channel types were seen, but the predominant anion-selective channel was characterized by having an outwardly-rectifying current/voltage relationship. The channel was not evident at a V_h of 0 mV immediately upon excision of the patch, but became active once the membrane had been depolarized to ≈ + 40 mV. Figure 1 shows the current/voltage relationship, pooled for ten patches where [Cl^-] was altered iso-osmotically by replacement with sucrose.

With symmetrical high Cl^- in bath and pipette the inward conductance (g_{in}; measured at the point on the plot corresponding to − 39.2 mV) was 26.8 ± 5.8 pS ($n = 7$), and the outward conductance (g_{out}; measured at + 32 mV) was 40.1 ± 5.1 pS ($n = 10$). Little effect was seen on the outward current (representing Cl^- movement into the cell) when the bath [Cl^-] was reduced by one third, but the inward current

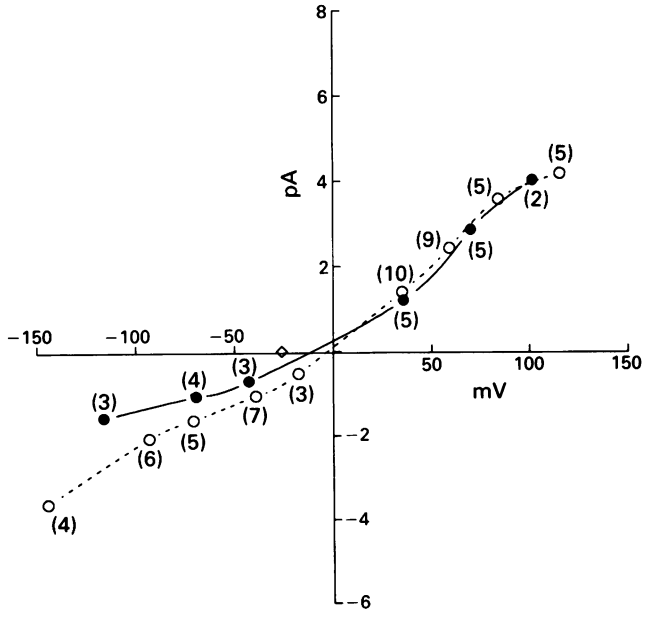

Figure 1 Current-voltage relationship produced from ten separate channels in ten different patches. The numbers adjacent to the points show the number of observations at each point. Cl^- was iso-osmotically replaced with sucrose. (○), Symmetrical solutions containing 145 mM Cl^-; (●), bath solution containing 48.7 mM Cl^-; (◇), represents the equilibrium potential for Cl^-. For full details of the composition of the solutions see Methods.

diminished as one would expect for a channel showing selectivity for Cl^-. The reversal potential (V_{rev}) of $\approx +20$ mV also moved towards the equilibrium potential for Cl^- ≈ -26 mV (Table 1). The selectivity for Cl^- over K^+ can be calculated using the equation:

$$E_{rev} = -\frac{RT}{F} \cdot \ln \frac{P_K + [K^+]_o + P_{Cl^-}[Cl^-]_i}{P_K + [K^+]_i + P_{Cl^-}[Cl^-]_o}$$

Using the value for E_{rev} of ≈ -20 mV obtained from Figure 1 gives a selectivity for Cl^- over K^+ (P_{Cl}/P_K) of ≈ 7.5.

Figure 2 shows single channel recordings made in symmetrical high [Cl^-] solutions and the relationship between single channel open-state probability (P_o) and V_h. There were two channels present in this patch and P_o increases with depolarizing potentials (Figure 2a). As reflected in Figure 2b the channels show rapid openings and closures. This was reinforced by the single channel open and closed dwell time histograms (data not shown). The open events could be fitted with a single exponential, while the closed events were best fitted by two exponentials. Raising the bath (intracellular) calcium concentration from 1 μM to 1 mM produced no significant change in P_o over the range of potentials studied.

The channel exhibited similar properties when the chloride gradient was imposed in the opposite way, i.e. from the bath to pipette, the direction in which chloride ions will flow during transepithelial ion secretion. The results from a series of experiments with different gradients, but with no correction for tonicity, are given in Table 1. The current-voltage curve is shifted in the opposite direction towards E_{Cl} when the gradient is reversed, and the shape of the curve is altered to produce a more linear relationship, reflecting Goldman rectification produced by the Cl^- gradient (Figure 3). Again the relationship of P_o to V_h with symmetrical solutions is as seen earlier with P_o increasing at depolarizing potentials.

The loop diuretic, piretanide, at high concentration (0.2 mM) inhibits chloride secretion on application to the basolateral side of intact epithelial monolayers (Cuthbert *et al.*, 1985). Similarly, it blocks secretion both apically and basolaterally in HCA-7 Colony 1 monolayers (Cuthbert *et al.*, 1987). It was surprising to find that piretanide could block chloride channels in patches from HCA-7 cells when applied to the cytosolic face in low concentrations (1–5 μM).

Figure 4 illustrates one of three similar experiments and shows the effects of piretanide at 1 and 3 μM, on an inside-out patch in symmetrical high chloride solutions. Channel inhibition is shown and was analysed by measuring open and closed dwell time histograms (data not shown). Before piretanide the data were best fitted by one exponential for the open times and two for the closed times. After piretanide, 1 μM, the open time histogram was now best fitted with two exponentials, both with time constants shorter than during the control period. The closed time histogram remained virtually unchanged in the presence of piretanide and furthermore the open state probability (P_o) was reduced by 48%

Table 1 Data for channels recorded with differing Cl^- and cation gradients

Pipette solution	*Bath solution*	*Symmetrical bath and pipette solutions*		*[Cl^-] gradient*	
		g_{in}	g_{out}	E_{Cl}	E_{rev}
70 NaCl	140 NaCl	–	–	+18	+18
210 NaCl	140 NaCl	–	–	−10	− 8
140 NaCl	210 NaCl	31	55	+10	+ 8
140 NaCl	70 NaCl	23	57	−18	−10
140 NaCl	140 KCl *	24 ± 2	40 ± 1	–	–
140 NaCl	37 NaCl**	27 ± 6	40 ± 5	−26	−20

For the symmetrical condition the bath solution was adjusted to be the same as in the pipette. All the solutions given above contained 1 mM EGTA, 1 μM Ca^{2+} and 10 mM HEPES buffered to pH 7.4. The data are for single patches unless otherwise stated (*$n = 7$, **$n = 10$).

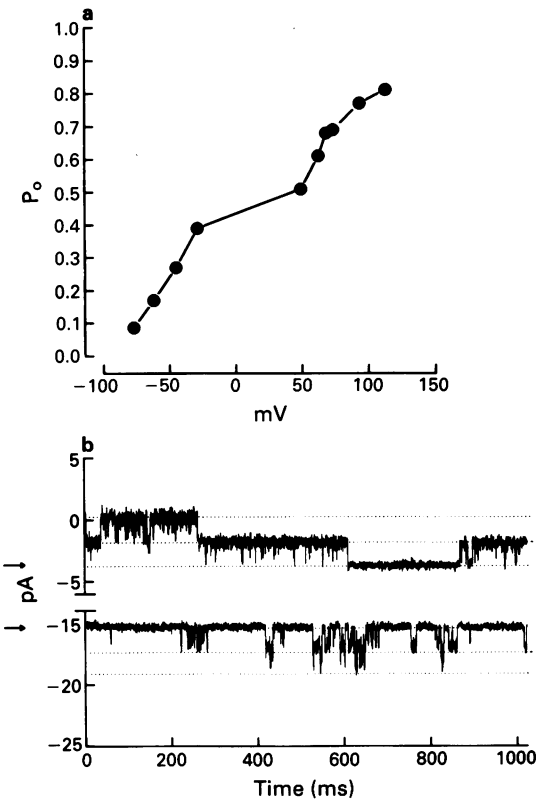

Figure 2 (a), Relationship between single channel open probability (P_o) and holding potential (V_h) for single channel. (b), Single channel records obtained at V_h values of +40 mV (upper) and −50 mV (lower), reflecting the P_o shown in (a). There were two channels active in the patch and the closed levels are shown by the arrows.

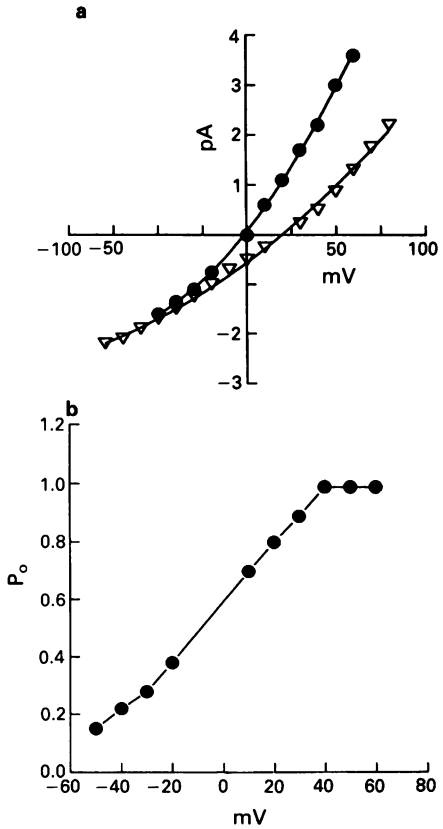

Figure 3 (a) Current-voltage relationship for a single channel, with gradient causing positive reversal potential: (●) symmetrical 140 mM NaCl in bath and pipette; (▽) a different patch with 70 mM NaCl in the pipette. (b), Relationship between P_o and V_h for symmetrical solutions shown in (a).

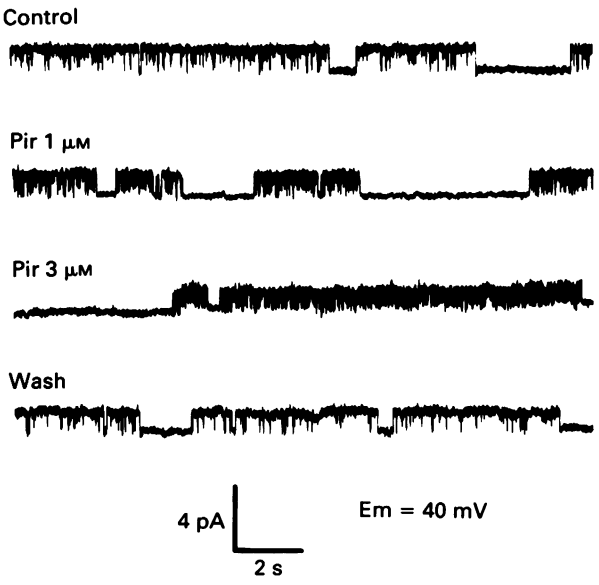

Figure 4 Effect of piretanide (Pir) on single channel behaviour. V_h + 40 mV. An upward deflection indicates channel opening.

(Table 2). With 3 μM piretanide the amplitude of the single channel events was reduced during periods of high frequency flicker block, due to frequency limitation of recording (Figure 4). Note, too, the effects of piretanide were easily reversible. Changing the potential from + 40 mV to − 40 mV in the presence of piretanide removed the high frequency flicker block, which was restored on returning to + 40 mV.

When piretanide at concentrations of 3–5 μM was applied to patches there were long periods of no activity between the high frequency bursts, so that recordings many minutes long were required for analysis. This was achieved in another experiment in which 3 μM piretanide was used (Table 2). One open time and two closed times were evident before piretanide and the closed times were little changed by its addition. The blocker reduced the open time by over 80%, but it was not possible to resolve the very brief open time. P_o was reduced 61% in this instance. It is noted that the control open times were variable over a fourfold range in different patches. Analysis of these data was made during periods of channel activity. In the presence of piretanide it is theoretically possible to measure a third closed time representing long periods of inactivity occurring between the bursts. However, hours of recording in a single patch would be required to collect sufficient events for exponential fitting.

In some isolated inside-out patches in which single chloride channels had been activated by depolarization, after a period of time (10–20 min), the single channel activity ceased and could not be re-elicited by repeated depolarization. To examine if the quiescent channels could be reactivated by adenosine 3':5'-cyclic monophosphate (cyclic AMP) the nucleotide was applied to the cytosolic face. After a delay due to diffusion, cyclic AMP (0.1 mM) in the presence of Ca^{2+}, 1 μM produced a rapid activation of the chloride channel. The result shown in Figure 5 is typical of four experiments. In this example the mean open time before the patch became quiescent was 11.19 ms and the mean closed times were 0.35 and 3.18 ms. These closed times are close to those given in Table 2, while the open time lies between the previously given values. P_o was 0.86 before the patch became quiescent. P_o was, of course, zero during the quiescent phase but cyclic AMP was able to restore the pattern of channel activity to values almost identical to those seen initially (open time, 12.93 ms; closed times 0.28 and 2.05 ms; P_o = 0.87).

Thus far we have shown that the apical membranes of HCA-7 cells have outwardly rectifying chloride channels, sensitive to cyclic AMP and blocked by piretanide applied to the cytosolic face. To examine the question whether the flux of chloride across the apical face was increased by agents which increase intracellular cyclic AMP we used the radioiodide efflux method described under Methods.

Forskolin, an activator of adenylate cylase increases chloride secretion in HCA-7 monolayers and also increases tissue cyclic AMP (Cuthbert *et al.*, 1987). Forskolin (10 μM) increased the rate constant for I^- efflux from HCA-7 cells (Figure 6). The presence of BAPTA within the cell did not reduce the effect of forskolin on increased I^- efflux.

In contrast to the sustained secretory response to forskolin, lysylbradykinin (LBK) produces a transient, rapidly desensitizing chloride secretory response which is Ca^{2+}-dependent (Cuthbert *et al.*, 1987; Pickles & Cuthbert, 1991). LBK, applied apically, also produced a transient increase in I^- efflux in HCA-7 monolayers (Figure 7). However, preincubation with Ba^{2-} or with BAPTA-AM abolished the response to the kinin.

Figure 5 Effect of 100 μM cyclic AMP on channel activity. V_h + 40 mV. Cyclic AMP was added at the point indicated by the arrow resulting in activation of the channel.

Table 2 Effect of piretanide on time constants for channel opening and closing by fitting dwell times

Conditions	*Open times τ (ms)*	*Closed times τ (ms)*	P_o	*Number of events*
Control V_h = + 40 mV Symmetrical Cl^-, 140 mM	14.92	0.480, 2.37	0.61	1500
Pirentanide, 1 μM, V_h = + 40 mV Symmetrical Cl^-, 140 mM	0.85, 3.93	0.95, 2.49	0.32	1459
Control V_h = + 40 mV Symmetrical Cl^-, 140 mM	4.31	0.42, 1.17	0.49	4051
Piretanide, 3 μM V_h = + 40 mV Symmetrical Cl^-, 140 mM	NR, 0.7	0.51, 1.92	0.19	3500

Time constants derived from best-fit exponentials to histograms obtained from the number of events indicated at a bin-width of 0.75 ms. NR indicates not resolved due to frequency limitation of the recording. Open time, closed times and P_o values were measured during periods of channel activity.

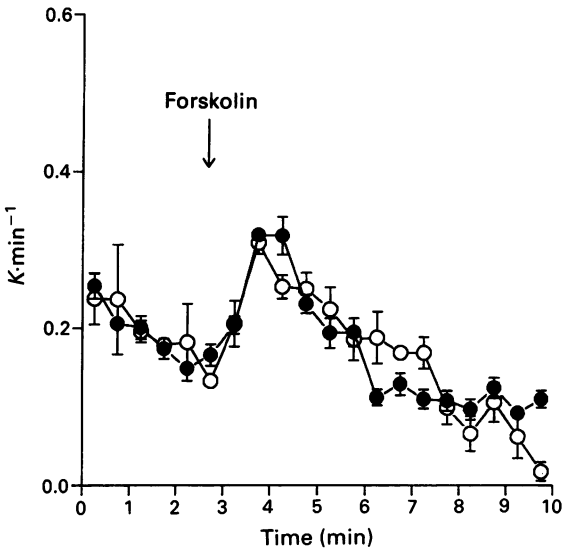

Figure 6 Effects of forskolin, 10 μM, on the rate constant for efflux from HCA-7 monolayers. Each point shows mean for 6 measurements with s.e.mean indicated by vertical bars; (●) data from cells incubated with BAPTA-AM during the $^{125}I^-$-loading period.

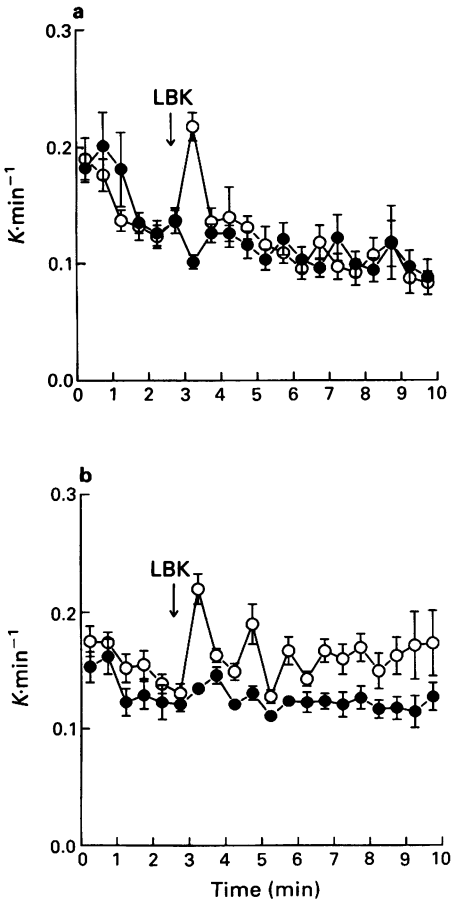

Figure 7 (a) As for Figure 6 except lysylbradykinin LBK, (0.1 μM) was applied as indicated. (●) Results with tissues preincubated with BAPTA-AM. (b) Effect of LBK (0.1 μM) on I^- efflux in the absence (○), and presence (●), of Ba^{2+}, 1 mM. Each point shows mean for 12 measurements; s.e.mean indicated by vertical bars.

Discussion

The outwardly rectifying anion-selective channels found in HCA-7 colonic epithelial cells are similar to outward-rectifying channels described in other epithelia, for example, *Necturus* enterocytes (Giraldez *et al.*, 1989), primary cultures and a cell line derived from the human pancreas (Gray *et al.*, 1989; Hanrahan & Tabcharani, 1990), canine tracheal epithelium (Welsh, 1986) and the apical membrane of the HT_{29} and T84 lines (Hayslett *et al.*, 1987; Halm *et al.*, 1988) also, like HCA-7, derived from human adenocarcinomata. The conductance values of the present study ($g_{in} \approx 25$ pS; $g_{out} \approx 40$ pS) (Table 1) accord well with those seen in HT_{29} and T84 cells (g_{in} and g_{out} approximately 32 and 50 pS, and 24 and 45 pS respectively for the two cell types). The relation of V_h to P_o is also similar in all three cell types, depolarization increasing the open probability. It is most likely that the anion-selective channels are in the apical membranes of the epithelial cells since in culture they grow with the apical surface uppermost and the basolateral face applied closely to the substrate.

As has been shown with other outward rectifying chloride channels (Schoumacher *et al.*, 1987; Li *et al.*, 1988) the channels in HCA-7 cells were cyclic AMP-selective. However, in T84 cells activated by cyclic AMP and with whole cell recording a linear current-voltage relationship is seen, while an outwardly rectifying current results from an increase in Ca_i (Cliff & Frizzell, 1990). This means that chloride secretion in T84 epithelia, and presumably HCA-7 tissues, is complex and that the outwardly rectifying channel may be only one type involved in chloride secretion. For example, low conductance (~10 pS) Cl^- channels with different properties have been seen in other epithelial tissues (Gray *et al.*, 1988).

In HCA-7 epithelia, forskolin or vasoactive intestinal peptide, both of which increase cyclic AMP, also cause chloride secretion (Cuthbert *et al.*, 1987). Here we show that forskolin also increases the rate of I^- efflux, as a marker of Cl^-, from the epithelium. The question which cannot be answered by the present experiments is whether the increased efflux is exclusively or only partially through the outward rectifying channels. By use of short circuit current measurements in HCA-7 epithelia it was shown that the calcium ionophore A23187 and lysylbradykinin (LBK) also increased chloride secretion (Cuthbert *et al.*, 1987). Since LBK does not stimulate prostaglandin formation in HCA-7 cells it was considered that the peptide acted through an increase in Ca_i. Here, we have seen no evidence of channel activation when the cytosolic face of patches were exposed to Ca^{2+}. We have shown elsewhere that LBK is unlikely to raise the Ca_i value to above 1 μM in these colonic epithelia (Pickles & Cuthbert, 1991). It must be concluded that agents which increase Ca_i must act indirectly to increase secretion, most likely by activation of Ca^{2+}-sensitive maxi-K channels in the basolateral membrane. These channels are blocked by Ba^{2+}, which was shown to inhibit the effects of LBK on I^- efflux.

The consequence of activation of basolateral K^+ channels would be to hyperpolarize both the basolateral and apical membranes of the cells; a situation which greatly reduces the open state probability of the Cl^- channels. Thus in HCA-7 monolayers it is likely that the channels we have described are more important for cyclic AMP-mediated secretion than for Ca_i-mediated secretion.

It is of interest that the classical loop diuretic, piretanide, an inhibitor of NaK 2 Cl cotransport, is able to block chloride channels when applied to the cytosolic face at low concentration. Concentrations in the millimolar range are required to inhibit chloride secretion when applied to the basolateral NaK2Cl transporter (Cuthbert *et al.*, 1985). However in intact epithelia with the apical membrane at ≈ -40 mV it is unlikely that piretanide would affect the channels even if it could penetrate the cells, since the block was most apparent at depolarized potentials. Another loop

diuretic, furosemide, has also been shown to inhibit Ca^{2+}-dependent chloride currents in rat lacrimal gland cells (Evans *et al.*, 1986) and more recently both furosemide and bumetanide were shown to inhibit chloride channel fluxes in vesicles prepared from kidney cortex (Pope *et al.*, 1991).

Support from the Wellcome Trust is gratefully acknowledged.

References

AUGERSON, C. & LABOISSE, C.L. (1984). Emergence of permanently differentiated cell clones in a human colonic cancer cell line in culture after treatment with sodium butyrate. *Cancer Res.*, **44**, 3961–3969.

BRAYDEN, D.J., HANLEY, M.R., THASTRUP, O. & CUTHBERT, A.W. (1989). Thapsigargin, a new calcium-dependent epithelial anion secretagogue. *Br. J. Pharmacol.*, **98**, 809–816.

CLANCY, J.P., MCCANN, J.D., LI, M. & WELSH, M.J. (1990). Calcium-dependent regulation of airway epithelial chloride channels. *Am. J. Physiol.*, **258**, L25–L32.

CLIFF, W.H. & FRIZZELL, R.A. (1990). Separate Cl^- conductances activated by cAMP and Ca^{2+} in Cl^--secreting epithelial cells. *Proc. Natl. Acad. Sci. U.S.A.*, **87**, 4956–4960.

COLQUHOUN, D. & SIGWORTH, F.J. (1983). Fitting and statistical analysis of single-channel records. In *Single-channel Recording*. ed. Sakmann, B. & Neher, E. pp.191–263. New York: Plenum Press.

CUTHBERT, A.W., KIRKLAND, S.C. & MACVINISH, L.J. (1985). Kinin effects on ion transport in monolayers of HCA-7 cells, a line from a human colonic adenocarcinoma. *Br. J. Pharmacol.*, **86**, 3–5.

CUTHBERT, A.W., EGLÉME, C., GREENWOOD, H., HICKMAN, M.E., KIRKLAND, S.C. & MACVINISH, L.J. (1987). Calcium- and cyclic AMP-dependent chloride secretion in human colonic epithelia. *Br. J. Pharmacol.*, **91**, 503–515.

DEMPSTER, J. (1988). Computer analysis of electrophysiological signals. In *Microcomputers in Physiology: a Practical Approach*. ed. Fraser, P.J. pp.51–93. Oxford: IRL.

DHARMSATHAPHORN, K., MCROBERTS, J.A., MANDEL, L., TISDALE, D. & MATSUI, H. (1984). A human colonic tumor cell line that maintains vectorial electrolyte transport. *Am. J. Physiol.*, **246**, G204–G208.

EVANS, M.G., MARTY, A., TAN, Y.P. & TRAUTMANN, A. (1986). Blockage of Ca-activated Cl conductance by furosemide in rat lacrimal glands. *Pflügers Arch.*, **406**, 65–68.

FABIATO, A. & FABIATO, F. (1979). Calculator programs for computing the composition of the solutions containing multiple metals and ligands used for experiments in skinned muscle cells. *J. Physiol. Paris*, **75**, 463–505.

GIRALDEZ, F., MURRAY, K.J., SEPULVEDA, F.V. & SHEPPARD, D.N. (1989). Characterization of a phosphorylation-activated Cl^--selective channel in isolated *Necturus* enterocytes. *J. Physiol.*, **416**, 517–537.

GRAY, M.A., GREENWELL, J.R. & ARGENT, B.E. (1988). Secretin-regulated chloride channel on the apical plasma membrane of pancreatic duct cell. *J. Memb. Biol.*, **105**, 131–142.

GRAY, M.A., HARRIS, A., COLEMAN, L., GREENWELL, J.R. & ARGENT, B.E. (1989). Two types of chloride channel on duct cells cultured from human fetal pancreas. *Am. J. Physiol.*, **257**, C240–C251.

HALM, D.R., RECHKEMMER, G.R., SCHOUMACHER, R.A. & FRIZZELL, R.A. (1988). Apical membrane chloride channels in a colonic cell line activated by secretory agonists. *Am. J. Physiol.*, **254**, C505–C511.

HAMILL, O.P., MARTY, A., NEHER, E., SAKMANN, B. & SIGWORTH, F.J. (1981). Improved patch-clamp techniques for high-resolution current recording from cells and cell-free membrane patches. *Pflügers Arch.*, **391**, 85–100.

HANRAHAN, J.W. & TABCHARANI, J.A. (1990). Inhibition of an outwardly-rectifying anion channel by HEPES and related buffers. *J. Memb. Biol.*, **116**, 65–77.

HAYSLETT, J.P., GÖGELEIN, H., KUNZELMANN, K. & GREGER, R. (1987). Characteristics of apical chloride channels in human colon cells (HT_{29}). *Pflügers Arch.*, **410**, 487–494.

HENDERSON, R.M. & CUTHBERT, A.W. (1991). A high-conductance Ca^{2+}-activated K^+ channel in cultured eccrine sweat gland cells. *Pflügers Arch.*, **418**, 271–275.

KIRKLAND, S.C. (1985). Dome formation by a human colonic adenocarcinoma cell line (HCA-7). *Cancer Res.*, **45**, 3790–3795.

LI, M., MCCANN, J.D., LIEDTKE, C.M., NAIRN, A.C., GREENGARD, P. & WELSH, M.J. (1988). Cyclic AMP dependent protein kinase opens chloride channels in normal but not cystic fibrosis airway epithelium. *Nature*, **331**, 358–360.

PICKLES, R.J. & CUTHBERT, A.W. (1991). Relation of anion secretory activity to intracellular Ca^{2+} in response to lysylbradykinin and histamine in a cultured human colonic epithelium. *Eur. J. Pharmacol.*, **199**, 77–91.

POPE, A.J., RICHARDSON, S.K., IFE, R.J. & KEELING, D.J. (1991). Characterisation of the effects of anthranilic and (indanyloxy) acetic acid derivatives on chloride transport in membrane vesicles. *Biochim. Biophys. Acta*, **1067**, 51–63.

SCHOUMACHER, R.A., SHOEMAKER, R.L., HALM, D.R., TALLANT, E.A., WALLACE, R.W. & FRIZZELL, R.A. (1987). Phosphorylation fails to activate chloride channels from cystic fibrosis airway cells. *Nature*, **330**, 752–754.

WELSH, M. (1986). Single apical membrane anion channels in primary cultures of canine tracheal epithelium. *Pflügers Arch.*, **407**, S116–S122.

VENGLARIK, C.J., BRIDGES, R.J. & FRIZZELL, R.A. (1990). A simple assay for agonist regulated Cl and K conductances in salt-secreting epithelial cells. *Am. J. Physiol.*, **259**, C358–C364.

(Received October 23, 1991
Revised January 14, 1992
Accepted January 20, 1992)

Br. J. Pharmacol. (1992), **106**, 115–122 © Macmillan Press Ltd, 1992

The effect of pertussis toxin on β-adrenoceptor responses in isolated cardiac myocytes from noradrenaline-treated guinea-pigs and patients with cardiac failure

L.A. Brown & [1]S.E. Harding

Department of Cardiac Medicine, National Heart & Lung Institute, Dovehouse St, London SW3 6LY

1 A decreased responsiveness to the positive inotropic effects of β-adrenoceptor agonists is a characteristic of human heart failure. We have investigated the involvement of inhibitory guanine nucleotide binding proteins (G-proteins) in this process using pertussis toxin treatment of isolated cardiac myocytes.

2 Myocytes isolated from failing human myocardium had a reduced maximum contractile response to isoprenaline relative to that for maximally stimulating concentrations of calcium, giving an isoprenaline/calcium ratio of 0.71 ± 0.06 ($n = 7$ patients). This was significantly lower than in myocytes from non-failing myocardium, where the isoprenaline/calcium ratio was 1.16 ± 0.07 ($n = 6$, $P < 0.001$). Responses to high calcium were unchanged.

3 Myocytes were treated with pertussis toxin for 3–5 h at 35°C. Successful inactivation of inhibitory G-proteins by pertussis toxin treatment was indicated by a loss of responsiveness to 10 μM adenosine (in the presence of submaximal isoprenaline).

4 Following pertussis toxin treatment of the myocytes from failing human heart the isoprenaline/calcium ratio increased to 1.43 ± 0.27 ($n = 7$, $P < 0.05$). Pertussis toxin treatment had no effect upon the maximum calcium contraction. The isoprenaline/calcium ratio in myocytes from non-failing human ventricle was not affected by the toxin treatment ($n = 3$). These observations support the hypothesis that increased inhibitory G-protein levels or activities contribute to β-adrenoceptor desensitization in human heart failure.

5 β-Adrenoceptor desensitization in human heart failure is thought to be secondary to raised noradrenaline levels in these patients. Experiments were repeated on myocytes isolated from hearts of guinea-pigs which had been chronically infused with noradrenaline. The isoprenaline/calcium ratio of these myocytes was reduced below that of myocytes from sham-operated animals (0.65 ± 0.04, $n = 6$ compared with 0.88 ± 0.02, $n = 7$, $P < 0.001$).

6 Pertussis toxin treatment (2 h at 35°C) increased the isoprenaline/calcium ratio to 1.02 ± 0.02 ($n = 6$, $P < 0.01$) in myocytes from noradrenaline-treated guinea-pigs. This effect of pertussis toxin treatment was not seen in myocytes from sham-operated guinea-pig hearts.

7 Incubation at 35°C for similar periods in the absence of pertussis toxin also restored the isoprenaline/calcium ratio towards normal in the myocytes from both failing human and noradrenaline-treated guinea-pig hearts, although the effect was significantly smaller than that produced by the toxin. Myocytes kept at room temperature (22°C) showed no such evidence of resensitization over periods up to 6 h.

8 These observations are consistent with the hypothesis that raised catecholamine levels result in increased inhibitory G-protein levels and functional β-adrenoceptor desensitization in heart failure.

Keywords: Guanine nucleotide-binding proteins; pertussis toxin; cardiomyocyte; β-adrenoceptor; desensitization; catecholamine; human; osmotic mini-pump; adenosine

Introduction

In human ventricular myocardium it is well established that heart failure produces changes in the β-adrenoceptor pathway that have the collective effect of reducing the contractile responses to β-adrenoceptor agonists, such as isoprenaline (Brown *et al.*, 1986; Fowler *et al.*, 1986; Schwinger *et al.*, 1990). The contractile potential of the muscle is not affected as the maximal response to calcium, which acts independently of the β-adrenoceptor pathway, has been shown to be similar in non-failing and failing human myocardium (Fowler *et al.*, 1986; Schwinger *et al.*, 1990). We have shown that the β-adrenoceptor desensitization observed in intact tissue from failing human hearts is detectable in single myocytes, enzymatically isolated from the myocardium. There is a correlation between the severity of heart failure and the depression of the maximum response to isoprenaline relative to that for calcium (the isoprenaline/calcium ratio) in isolated myocytes (Harding *et al.*, 1989; 1990a, b; 1991).

In cardiac membranes prepared from patients with heart failure there has been a reported increase in the level of myocardial inhibitory guanine nucleotide binding proteins (G-proteins, mainly Gi (Neuman *et al.*, 1988; Feldman *et al.*, 1988)) detected by use of pertussis toxin, which inactivates inhibitory G-proteins by ADP-ribosylation (Sunyer *et al.*, 1989). This could mean an increase in the number of Giα subunits in the failing heart, an increase in the ADP-ribosylation sites on the Giα subunit or an increase in the ribosylation enzymatic activity per unit of Gi. Gi mediates the action of inhibitory hormones and neurotransmitters on the adenylate cyclase system hence an altered activity of Gi could affect the transduction of transmembrane signals in the failing heart. To investigate whether altered activities of the inhibitory G-proteins contribute to the β-receptor desensitiza-

[1]Author for correspondence

tion seen in heart failure, ventricular myocytes were isolated from non-failing and failing human myocardium and the effect of inactivation of inhibitory G-proteins, by treatment with pertussis toxin, on the contractile responses of the myocytes was observed. Myocytes are well suited to this type of experiment, since there are fewer barriers to penetration of the toxin than in intact tissue. Purkinje fibres from dog heart have been successfully treated with pertussis toxin, but required 24 h exposure (Rosen *et al.*, 1988). Treatment of human muscle may well take longer because first, human papillaries are generally thicker than Purkinje fibres and second, human myocytes required longer exposure to higher concentrations than animal myocytes for complete inactivation of Gi function (Brown *et al.*, 1990). Even for the animal experiments described in this study, the use of myocytes has advantages. Although the whole animal can be treated with pertussis toxin, we (Hopwood *et al.*, 1987) and others (Bohm *et al.*, 1988) have shown that the myocardium can be damaged by the procedure. There is also significant mortality associated with toxin treatment of whole animals, which might be increased by prior exposure to noradrenaline (see below).

Adenosine attenuates the contractile response to isoprenaline, this is known as the 'anti-adrenergic effect' (anti-adrenoceptor effect) and can be demonstrated in ventricular myocytes (Brown *et al.*, 1990). We have previously shown that this anti-adrenoceptor effect of adenosine can be blocked with pertussis toxin (by Gi inactivation) in myocytes from human and guinea-pig hearts (Brown *et al.*, 1990). In this study the blockade of the anti-adrenoceptor effect of adenosine (Brown *et al.*, 1990) was used as a marker to indicate successful inactivation of the inhibitory G-proteins.

It is thought that the functional β-adrenoceptor desensitization is the result of the increased catecholamine levels in heart failure patients. Studies have been carried out in which exposure of animals to high circulating catecholamine levels led to a reduced sensitivity to β-agonists (Chang *et al.*, 1982; Vescovo *et al.*, 1989b; Jones *et al.*, 1990a). In this study we have used a similar animal model, the noradrenaline-treated guinea-pig, to produce β-receptor desensitization of ventricular myocytes comparable to that which we see in myocytes isolated from failing human hearts. Pertussis toxin treatment of these myocytes was also carried out.

Methods

Male Dunkin-Hartley guinea-pigs (weight 400–500 g) were subcutaneously implanted with Alzet mini-pumps (model 2002, Alzet, U.S.A.) at the neck after anaesthesia by intraperitoneal injection of Hypnorm (0.16 mg kg^{-1} fentanyl citrate and 5 mg kg^{-1} fluanisone) and a local injection of lignocaine hydrochloride (2 ml kg^{-1} of 10 mg ml^{-1}). The mini-pumps were filled with (−)-noradrenaline hydrochloride dissolved in sterile isotonic saline containing 1 mM ascorbate and preincubated in sterile isotonic saline at 37°C for 4 h before implantation. The rate of infusion of fluid from the mini-pumps was 0.55 μl h^{-1}, delivering 900 μg kg^{-1} h^{-1} noradrenaline for 7 days. Sham-operated animals had the same anaesthetic and incision but no pump was implanted. Myocytes were isolated from guinea-pig hearts as previously described (Brown *et al.*, 1990).

Non-failing human myocardium was obtained in 6 cases. Two were from heart/lung retransplant operations where the rejection was directed towards the lungs. The hearts were originally from donors age 7 and 37 (female and male respectively). Two hearts were from normal donors; in one case (a 50 year-old-female), the heart could not be used for transplantation due to problems with compatibility, in the other (a 35-year-old man) the coronary vessels were found to have too great a degree of atherosclerosis. Another heart was from a patient (age 28, female) with angiosarcoma, who was transplanted before heart failure became established. The sixth sample was obtained from a surgical exision performed on a subject (age 20, male) with Wolff-Parkinson-White syndrome. Failing human ventricular tissue was obtained from explanted hearts at the time of heart transplantation, the patients (7 male, mean age 52 years, range 25–65) were all in end stage heart failure, five due to ischaemic and two due to dilated cardiomyopathy. Informed consent was obtained before the operations. Ventricular myocytes were enzymatically isolated from the left or right ventricular free wall as previously described (Brown *et al.*, 1990; Moody *et al.*, 1990; Harding *et al.*, 1990a,c). Pieces of ventricle (100 mg–3 g) were chopped quickly into chunks of approximately 1 mm^3 using an array of razor blades. The chunks were incubated for a total of 12 min at 35°C in 25 to 50 ml of a low calcium medium (LC) of the following composition: (in mM): NaCl 120, KCl 5.4, $MgSO_4$ 5, pyruvate 5, glucose 20, taurine 20, HEPES 10, nitrilotriacetic acid 5, pH 6.96, containing 1–2 μM calcium. The medium was changed three times during this period. The chunks were stirred by bubbling with 100% O_2. The low calcium medium was removed by straining with 300 μm gauze. The chunks were then incubated at 35°C for 45 min in the above solution with nitrilotriacetic acid omitted and 4 u ml^{-1} type XXIV protease (pronase) and 30 μM calcium added, followed by two 45 min periods with the protease omitted and 400 iu ml^{-1} collagenase added. The medium was shaken gently throughout the incubation, and kept under an atmosphere of 100% O_2. At the end of the second and third 45 min periods the solution containing the dispersed cells was filtered through a 300 μm gauze and centrifuged at 40 *g* for 1 to 2 min. No difference was noted between non-failing and failing human heart with respect to time of digestion.

Myocytes were incubated with pertussis toxin immediately after digestion. The incubation time period and the concentration of the toxin required to inactivate the inhibitory G-proteins ranged from 1–2 h and 1 μg ml^{-1} (guinea-pig) to 3–5 h and 5 μg ml^{-1} (human) (Brown *et al.*, 1990). The incubation of the cells with the pertussis toxin was carried out in the low calcium medium (without nitriotriacetic acid) detailed above, and at 35°C in order to accelerate the reaction. Contractile experiments were then performed at 32°C, as previously described (Harding *et al.*, 1988). Comparisons were made with myocytes which had been kept at room temperature (22°C) and myocytes which had been preincubated at 35°C in the absence of pertussis toxin for an equal time or longer time than those pretreated with pertussis toxin. Calcium concentration-response curves were constructed in an incremental fashion. A maximum was judged to have been reached, for either calcium or isoprenaline, when there was no increase in contraction amplitude with increasing concentrations, or when toxic signs such as phasic contractions or decreases in diastolic length occurred. Following washout, a cumulative concentration-response curve to isoprenaline was constructed and the blockade of the anti-adrenoceptor effect of adenosine by pertussis toxin tested. Only myocytes in which the anti-adrenoceptor effect had been successfully blocked were used to represent pertussis toxin treated cells. Figure 1 shows representative traces of the contraction of single myocytes isolated from the hearts of noradrenaline-treated guinea-pigs. The isoprenaline/calcium ratio (the maximum response to isoprenaline relative to that produced by the maximally stimulating concentration of calcium) and the EC_{50} value (concentration for half-maximal effect) for isoprenaline were calculated for each cell. These were used to determine the extent of β-receptor desensitization and any effects of inhibitory G-protein inactivation.

Isoprenaline hydrochloride, noradrenaline hydrochloride, adenosine and pronase were obtained from Sigma Chemicals, and collagenase from Boehringer Mannheim. All solutions were made in AnalaR water from BDH.

Results were assessed by one-way analysis of variance followed by Student's *t* test where appropriate; these were carried out on paired data whenever possible. For EC_{50}

values, t tests were performed on log transformed values (pD_2). Statistical values quoted throughout are mean ± s.e.mean and n values are for numbers of animals or patients, with results being pooled from 1–4 cells for each heart.

Results

Myocytes isolated from non-failing human myocardium

Myocytes isolated from non-failing human myocardium had approximately equal contraction amplitudes in the presence of maximally activating isoprenaline or calcium (see Table 1) thus giving an isoprenaline/calcium ratio of 1.16 ± 0.07 ($n = 6$). The pD_2 value for isoprenaline averaged 8.89 ± 0.30 ($n = 6$). Figure 2 displays the isoprenaline/calcium ratio and the averaged isoprenaline concentration-response curves from myocytes isolated from non-failing human myocardium following treatment with pertussis toxin or preincubation at 35°C alone. The isoprenaline/calcium ratio decreased slightly following treatment at 35°C with ($n = 3$) or without pertussis toxin ($n = 4$). One-way analysis of variance (ANOVA) was used to compare three conditions: myocytes kept at 22°C (room temperature) or preincubated at 35°C in the absence of pertussis toxin and those pretreated with pertussis toxin at 35°C. This analysis showed no significant differences between isoprenaline/calcium ratios in the three groups. The concentration-response curve to isoprenaline was shifted to the left by toxin, but not 35°C treatment, although the difference in the EC_{50} was not statistically significant ($0.1 > P > 0.05$).

Myocytes isolated from failing human myocardium

In myocytes which have been isolated from failing human ventricle the maximum isoprenaline contractile response was significantly reduced below that for maximally stimulating concentrations of calcium ($P < 0.01$, see Table 1). The isoprenaline/calcium ratio was significantly lower than in the myocytes isolated from non-failing human myocardium ($P < 0.001$). The normalisation of the isoprenaline response to that of calcium in a given cell (the isoprenaline/calcium ratio) has been found to be a more reliable indicator of β-receptor desensitization than either the maximum effect of isoprenaline or its pD_2 (Harding *et al.*, 1989; 1990b; 1991). Isoprenaline/calcium ratios were found to decrease with four indicators of the severity of heart failure (Harding *et al.*, 1989; 1990b; 1991). The pD_2 values for isoprenaline were lower than those obtained from the 'normal' myocardial tissue (8.13 ± 0.23, $n = 7$), further indicating a desensitization of the β-adrenoceptor response. Figure 3 shows the isoprenaline/calcium ratio and the averaged concentration-

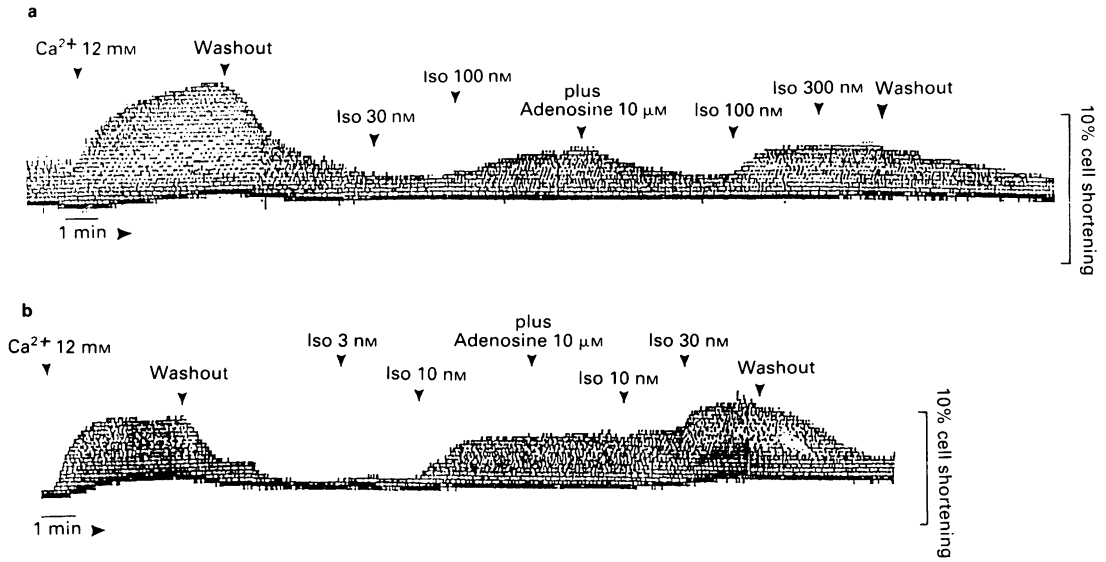

Figure 1 Representative traces of the contraction of single cardiac myocytes isolated from the heart of a noradrenaline-treated guinea-pig. An upward deflection indicates cell shortening. (a) A control myocyte challenged with a maximally activating concentration of calcium, followed (after washout) by increasing concentrations of isoprenaline (Iso). During the isoprenaline concentration-response curve, adenosine is added. Adenosine attenuates the increase in contraction amplitude caused by isoprenaline, this effect is reversed on removal of adenosine. (b) A cell from the same animal following treatment with pertussis toxin. Adenosine has no effect on the contraction amplitude in the presence of isoprenaline.

Table 1 Maximum contraction amplitudes with calcium and isoprenaline of ventricular myocytes isolated from human myocardium

	Preincubation at 22°C		*Preincubation at 35°C*		*Preincubation with pertussis toxin at 35°C*	
	Isoprenaline	*Calcium*	*Isoprenaline*	*Calcium*	*Isoprenaline*	*Calcium*
Non-failing myocardium	10.6 ± 1.3 (6)	9.5 ± 0.9 (6)	9.4 ± 1.1 (4)	10.3 ± 1.0 (4)	11.6 ± 2.6 (3)	12.1 ± 0.9 (3)
Failing myocardium	7.8 ± 0.8 (7)*	10.9 ± 0.6 (7)	10.1 ± 0.4 (5)#	10.1 ± 1.3 (5)	10.5 ± 0.8 (7)##	8.6 ± 1.0 (7)

Values are % cell shortening, mean ± s.e.mean, n = number of patients.
*$P < 0.01$ compared with maximum calcium, failing myocardium, 22°C.
#$P < 0.05$ and ##$P < 0.01$ compared with maximum isoprenaline for failing myocardium at 22°C.

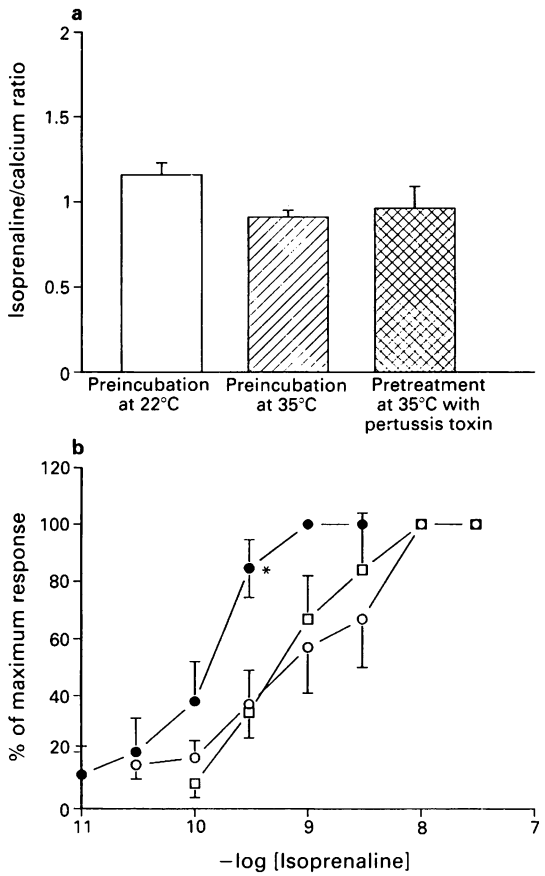

Figure 2 (a) Chart displaying the isoprenaline/calcium ratio calculated for ventricular myocytes isolated from non-failing human myocardium following treatment with pertussis toxin at 35°C ($n = 3$, cross hatched column) or preincubation at 22°C ($n = 6$, open column) or at 35°C ($n = 4$, hatched column) alone. Values are mean with standard error of the mean shown by vertical bars. (b) Mean isoprenaline concentration-response curves in ventricular myocytes isolated from non-failing human myocardium following treatment with pertussis toxin at 35°C ($n = 3$, ●) or preincubation at 22°C ($n = 6$, □) or 35°C ($n = 4$, ○) alone. Values are expressed as a percentage of the maximum isoprenaline response and are mean with standard error of the mean shown by vertical bars. *$P<0.02$ compared with the response given by myocytes preincubated at 22°C alone at the corresponding concentration of isoprenaline.

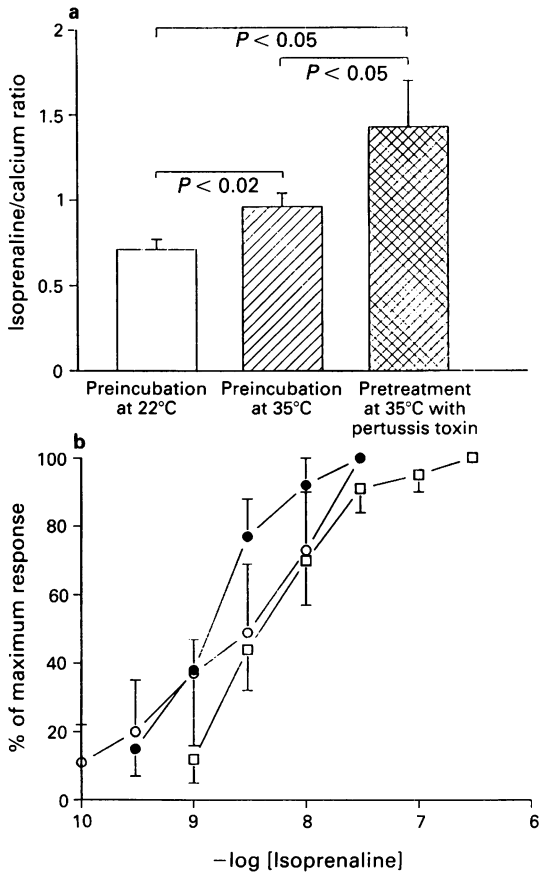

Figure 3 (a) Chart displaying the isoprenaline/calcium ratio calculated for ventricular myocytes isolated from failing human myocardium following treatment with pertussis toxin at 35°C ($n = 7$, cross hatched column) or preincubation at 22°C ($n = 7$, open column) or 35°C ($n = 5$, hatched column) alone. Values are mean with standard error of the mean shown by vertical bars. (b) Mean isoprenaline concentration-response curves in ventricular myocytes isolated from failing human myocardium following treatment with pertussis toxin at 35°C ($n = 6$, ●) or preincubation at 22°C ($n = 7$, □) or 35°C ($n = 5$, ○) alone. Values are expressed as a percentage of the maximum isoprenaline response and are mean with standard error of the mean shown by vertical bars.

response curves for isoprenaline in myocytes isolated from failing myocardium for the three different treatment groups. ANOVA indicated a significant variation between the treatment groups for the maximum isoprenaline contractile response ($P<0.05$). The maximum isoprenaline contraction was significantly increased ($P<0.05$, see Table 1) following preincubation of the myocytes at 35°C in the absence of pertussis toxin. The maximum isoprenaline contraction was also significantly increased ($P<0.01$, see Table 1) following pertussis toxin treatment at 35°C. For the isoprenaline/calcium ratio, ANOVA indicated that there was a significant variation between the three treatment groups ($P<0.05$). The isoprenaline/calcium ratio was significantly increased following preincubation of the cells at 35°C, when compared with those myocytes which were preincubated at room temperature ($n = 7$, $P<0.01$). However, following pertussis toxin pretreatment the isoprenaline/calcium ratio was increased still further. When ANOVA was carried out using the pD_2 values for isoprenaline there was no significant difference between the myocytes in the treatment groups. However, there was a tendency for the sensitivity to isoprenaline to increase following treatment with pertussis toxin at 35°C.

Myocytes isolated from sham-operated guinea-pigs

The isoprenaline/calcium ratio and the pD_2 value for isoprenaline of left ventricular myocytes isolated from sham-operated guinea-pigs were not significantly different from ventricular myocytes isolated from normal guinea-pig hearts ($n = 6$, data not shown). Table 2 shows the maximum contraction amplitudes to isoprenaline and calcium for myocytes isolated from sham-operated guinea-pig hearts. Figure 4 contains the isoprenaline/calcium ratio and the averaged concentration-response curves for isoprenaline in myocytes isolated from sham-operated guinea-pig hearts. There was no significant difference in the isoprenaline/calcium ratio between the treatment groups. The pertussis toxin or 35°C pretreatment had no effect upon the isoprenaline/calcium ratio in these myocytes. However, ANOVA of the pD_2 values for isoprenaline showed significant variation between the treatment groups ($n = 6$, $P<0.01$), with toxin treatment increasing the sensitivity to isoprenaline.

Myocytes isolated from noradrenaline-treated guinea-pig hearts

Table 2 shows the maximum contraction amplitude to isoprenaline and calcium for left ventricular myocytes

Table 2 Maximum contraction amplitudes with calcium and isoprenaline of ventricular myocytes isolated from guinea-pig hearts

	Preincubation at 22°C		*Preincubation at 35°C*		*Preincubation with pertussis toxin at 35°C*	
	Isoprenaline	*Calcium*	*Isoprenaline*	*Calcium*	*Isoprenaline*	*Calcium*
Sham-operated animals	9.3 ± 1.3 (6)	10.7 ± 1.5 (6)	9.1 ± 1.0 (6)	9.7 ± 0.9 (6)	7.4 ± 1.2 (6)	8.7 ± 1.4 (6)
Noradrenaline-treated animals	8.4 ± 1.6 (6)*	11.9 ± 1.3 (6)	8.1 ± 1.4 (6)	10.2 ± 1.4 (6)	10.0 ± 1.6 (6)	10.0 ± 1.5 (6)

Values are % cell shortening, mean ± s.e.mean, n = number of animals.
*$P<0.001$ compared with maximum calcium, noradrenaline-treated myocardium, 22°C.

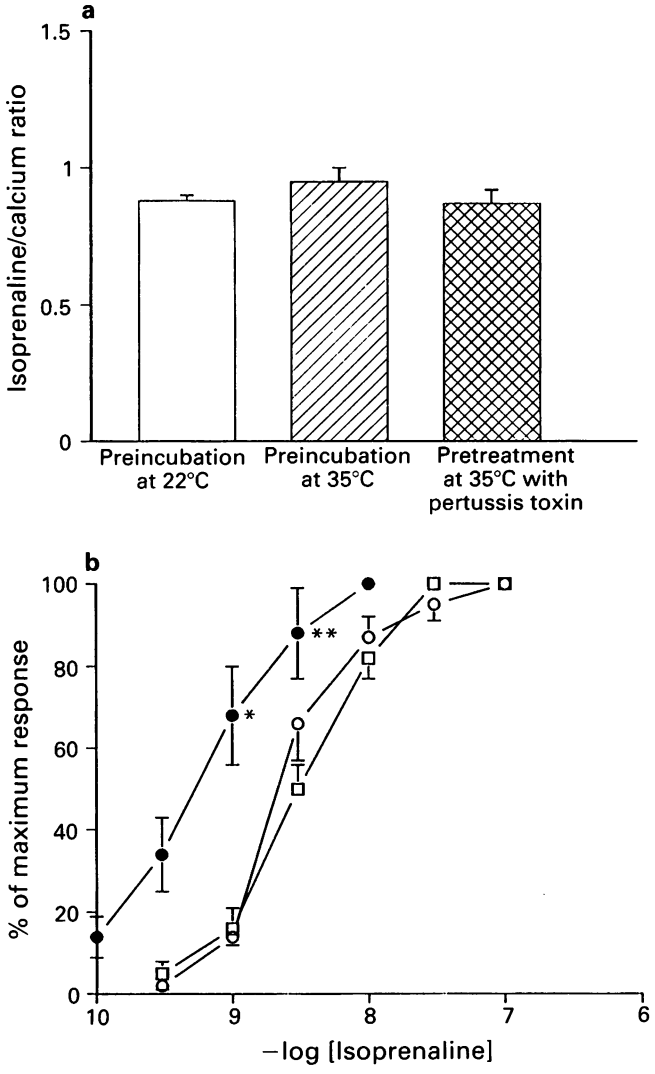

Figure 4 (a) Chart displaying the isoprenaline/calcium ratio calculated for ventricular myocytes isolated from sham-operated guinea-pig hearts following treatment with pertussis toxin at 35°C ($n = 6$, cross hatched column) or preincubation at 22°C ($n = 6$, open column) or 35°C ($n = 6$, hatched column) alone. Values are mean with standard error of the mean shown by vertical bars. (b) Mean isoprenaline concentration-response curves in ventricular myocytes isolated from sham-operated guinea-pig hearts following treatments with pertussis toxin at 35°C ($n = 6$, ●) or preincubation at 22°C ($n = 6$, □) or 35°C ($n = 6$, ○) alone. Values are expressed as a percentage of the maximum isoprenaline response and are mean with standard error of the mean shown by vertical bars. *$P<0.02$, **$P<0.01$ compared with the response given by myocytes preincubated at 22°C alone at the corresponding concentration of isoprenaline.

isolated from noradrenaline-treated guinea-pig hearts. The maximum calcium contraction remained unchanged following noradrenaline treatment. The maximum contractile response to isoprenaline showed a trend towards reduction following noradrenaline treatment but this was not significant. However, the isoprenaline/calcium ratio was significantly reduced in left ventricular myocytes from noradrenaline-treated guinea-pigs when compared with those from sham-operated animals. The pD_2 value for isoprenaline concentration-response curves was also significantly reduced in the left ventricular myocytes following noradrenaline treatment (7.27 ± 0.14 compared with 8.36 ± 0.11, $n = 7$, $P<0.001$), further indicating a β-adrenoceptor desensitization.

Figure 5 displays the isoprenaline/calcium ratio and pD_2 value for isoprenaline calculated from left ventricular myocytes isolated from noradrenaline-treated guinea-pig hearts for the three different treatment groups. ANOVA indicated that there was no significant difference between the treatment groups for the maximum calcium or isoprenaline contractile response (see Table 2). ANOVA indicated that there was however a significant difference between the groups for the isoprenaline/calcium ratio ($n = 6$, $P<0.001$). Following preincubation of the myocytes at 35°C in the absence of pertussis toxin there was a significant increase in the isoprenaline/calcium ratio compared with those myocytes which had been preincubated at room temperature ($P<0.02$, see Figure 5). However, there was a further significant rise in the isoprenaline/calcium ratio following pertussis toxin pretreatment of the myocytes when compared with those kept at 35°C alone. This ratio is significantly higher than that for myocytes isolated from sham-operated guinea-pigs following pertussis toxin treatment. Figure 1 shows representative traces of the contraction amplitude of a left ventricular myocyte isolated from a noradrenaline-treated guinea-pig heart in which the effect of pertussis toxin can be clearly seen. In the pertussis toxin treated cell, sensitivity to isoprenaline is increased over the control. This is evident from the greater maximum effect of isoprenaline relative to that of calcium, and the lower concentration required for threshold inotropic effect. One-way analysis of the pD_2 values for isoprenaline indicated that there was a significant difference between the myocytes in the treatment groups ($n = 6$, $P<0.01$). Following pertussis toxin pretreatment, but not 35°C incubation alone, the pD_2 value for isoprenaline was significantly increased to 8.12 ± 0.18 ($n = 6$, $P<0.02$, see Figure 5).

Discussion

A β-adrenoceptor desensitization was observed in the myocytes which had been isolated from failing human myocardium. This was indicated by a reduced maximum contractile response to the β-agonist, isoprenaline, when compared with the contractile response to maximally stimulating concentrations of calcium. This is consistent with work carried out on isolated ventricular tissue from failing human

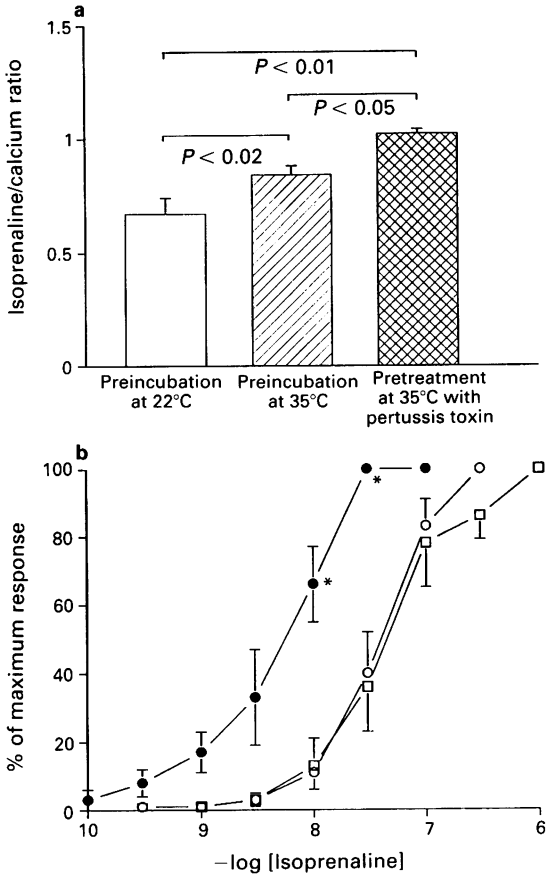

Figure 5 (a) Chart displaying the isoprenaline/calcium ratio calculated for ventricular myocytes isolated from noradrenaline-treated guinea-pig hearts following treatment with pertussis toxin at 35°C ($n = 6$, cross hatched column) or preincubation at 22°C ($n = 6$, open column) or 35°C ($n = 6$, hatched column) alone. Values are mean with standard error of the mean shown by vertical bars. (b) Mean isoprenaline concentration-response curves in ventricular myocytes isolated from noradrenaline-treated guinea-pig hearts following treatment with pertussis toxin at 35°C ($n = 6$, ●) or preincubation at 22°C ($n = 6$, □) or 35°C ($n = 6$, ○) alone. Values are expressed as a percentage of the maximum isoprenaline response and are mean with standard error of the mean shown by vertical bars. *$P<0.01$ compared with the response given by myocytes preincubated at 22°C alone at the corresponding concentration of isoprenaline.

myocardium (Fowler *et al.*, 1986; Schwinger *et al.*, 1990). In comparison, the myocytes which had been isolated from non-failing human myocardium had approximately equal contraction amplitudes in response to maximally stimulating concentrations of isoprenaline and calcium. Following treatment of the myocytes from failing myocardium with pertussis toxin the reduced maximum contractile response to isoprenaline was restored, increasing the isoprenaline/calcium ratio to levels at or above those in the myocytes from non-failing human myocardium. The maximum calcium contractile response of these myocytes was unaffected by the pertussis toxin treatment. The pertussis toxin treatment had no significant effect upon the contractile responses of the myocytes which had been isolated from non-failing human myocardium. These observations with the myocytes from both failing and non-failing human myocardium support the hypothesis that increased Gi levels reported in patients with heart failure (Neumann *et al.*, 1988; Feldman *et al.*, 1988) contribute to the observed β-adrenoceptor desensitization.

How representative are the individual myocytes selected for these studies with respect to whole heart function? It might be argued that we have also selected cells which are desensitized to a different degree from the majority in the heart. Both our animal and human studies give us confidence that this is unlikely to be the case. We have compared myocytes and intact muscle from rabbits which had been chronically infused with isoprenaline (Jones *et al.*, 1989; 1990b). The initial EC_{50} for isoprenaline, as well as the extent of depression of maximum and increase in EC_{50} following treatment, was the same for myocytes and whole muscle. The variability within and between animals was also similar for cells and intact muscle. In another study using β-adrenoceptor desensitized rats, the depression in response of single myocytes to isoprenaline was similar to the decrease in response of the heart rate *in vivo* (Vescovo *et al.*, 1989b). The desensitization of the response to isoprenaline in both atrial and ventricular myocytes from human heart correlated well with several indicators of severity of disease including NYHA class, left ventricular ejection fraction and left ventricular end diastolic pressure (Harding *et al.*, 1989; 1990a,b; 1991). In both animal and human studies on β-adrenoceptor desensitization we have shown by ANOVA that the within-subject variability for isolated cells is much less than the between-subject (Jones *et al.*, 1990a,b; Harding *et al.*, 1990a). In two animal models of heart failure we have observed changes in either biochemical parameters or receptor response which closely parallel those seen in the whole ventricle (Vescovo *et al.*, 1989a; Jones *et al.*, 1990b).

Heart failure is believed to be associated with an increased activation of the sympathetic nervous system (Packer, 1990) which leads to the observed high circulating levels of noradrenaline in patients (Thomas & Marks, 1978). The high levels of noradrenaline are thought to result in increased myocardial β-adrenoceptor occupation and a resultant β-adrenoceptor desensitization. In order to test this hypothesis ventricular myocytes isolated from the hearts of noradrenaline-treated guinea-pigs were compared with those which had been isolated from failing human ventricle. Left ventricular myocytes from noradrenaline infused guinea-pig hearts showed a reduced maximum contractile response to isoprenaline compared with the response for maximally stimulating calcium concentrations. This is consistent with previous studies of prolonged noradrenaline treatment of rat (Jones *et al.*, 1990a) and chick heart cells (Reithmann & Werdan, 1988) and is also in agreement with the results using myocytes that had been isolated from failing human myocardium. Pertussis toxin treatment of myocytes from the hearts of noradrenaline-treated animals once again restored the maximum isoprenaline contractile response, raising the isoprenaline/calcium ratio to levels at or above those in the myocytes isolated from the myocardium of sham-operated animals. This is in agreement with previous studies by Reithmann and Werdan (Reithmann *et al.*, 1989) in which noradrenaline treatment of rat heart cells led to a β-adrenoceptor desensitization and an increase in levels of the inhibitory G-protein, Gi. The pertussis toxin treatment had no significant effect upon the maximum calcium contraction in the myocytes used for this study. There was a slight trend for the maximum calcium response to fall following treatment with pertussis toxin; this was also seen in the myocytes isolated from failing human myocardium. This generalised reduction in contraction amplitude is likely to be a consequence of the prolonged incubation at 35°C, since the 35°C control myocytes show a similar decline. The use of the isoprenaline/calcium ratio throughout the study compensates for any effect of 'fatigue' upon the contractile response of the myocytes. Pertussis toxin treatment had no significant effect on the contractile responses to isoprenaline or calcium of the myocytes isolated from sham-operated guinea-pig myocardium. The observations obtained following pertussis toxin studies with the myocytes isolated from noradrenaline-treated guinea-pig hearts support the hypothesis that raised circulating catecholamine levels lead to an increased level or activity of Gi in heart failure.

The sensitivity of a biological system to β-adrenoceptor stimulation may also be assessed by the pD_2 value calculated

for the agonist ($-\log EC_{50}$). The ventricular myocytes isolated from failing human myocardium and noradrenaline-treated guinea-pig hearts produced pD_2 values for isoprenaline which were lower than those from myocytes isolated from normal or non-failing myocardium. This is indicative of a β-adrenoceptor desensitization. Following pertussis toxin treatment an increase in the pD_2 value for isoprenaline was seen in the myocytes isolated from failing human and noradrenaline-treated guinea-pig hearts. However, we have previously shown that pertussis toxin treatment of myocytes from normal myocardium also increases the pD_2 value and hence the sensitivity for isoprenaline (Brown *et al.*, 1990). This observation was confirmed in the present study, with the sham-operated animals. An increase in the pD_2 value for isoprenaline in the myocytes from failing or noradrenaline-treated myocardium following pertussis toxin treatment cannot therefore be used as evidence for increased Gi levels in heart failure. Gi may have some tonic effect in normal cardiac muscle. Alternatively, it may be that the β-adrenoceptor response which is seen in myocytes from normal or non-failing myocardium is not at its maximum possible level. This could be due to some slight 'desensitization' in the normal heart brought about by resting noradrenaline release. The observation that β-adrenoceptor antagonists can produce supersensitivity of the β-adrenoceptor response in untreated rats supports this hypothesis (Manning *et al.*, 1981). Pertussis toxin would then increase the pD_2 value for isoprenaline in myocytes from normal myocardium by reversing this slight desensitization.

One unexpected result of this study was that preincubation of the myocytes showing β-adrenoceptor desensitization, both from humans and animals, at 35°C in the absence of pertussis toxin appeared to increase the isoprenaline/calcium ratio to above that measured for cells incubated at room temperature. No significant increase in sensitivity to isoprenaline is seen with time after the preparation of myocytes when they are maintained at 22°C for up to 6 h (isoprenaline/calcium ratio increased by $6 \pm 6\%$, $n = 20$). Precisely how incubation at 35°C can restore the isoprenaline contraction and hence the ratio is unclear but one theory may be that the absence of external influences which bought about the desensitization (e.g. high catecholamine levels) allows the myocytes to resensitize and 'up-regulate' their β-adrenoceptors from internal sources. It is known that β-adrenoceptor desensitization will reverse when the concentration of agonist at the receptor is reduced (Doss *et al.*, 1981). This up-regulation process may be accelerated when the myocytes are kept at 35°C as opposed to 22°C. These findings are consistent with the proposed role of increased catecholamines in heart failure.

A further interesting point is that treatment with pertussis toxin at 35°C of the myocytes isolated from noradrenaline-treated guinea-pig myocardium significantly increased the isoprenaline/calcium ratio until it was above that of the isoprenaline/calcium ratio in myocytes from sham-operated guinea-pig hearts. This could be a consequence of an up-regulation of some system which normally opposes the effect of Gi. Removal of the influences of Gi by toxin treatment then leaves this system unopposed, and raises the isoprenaline/calcium ratio. A similar tendency was seen in the human cells, where the isoprenaline/calcium ratio in pertussis toxin treated myocytes from failing human myocardium appeared to be higher than that in myocytes from non-failing human myocardium.

We found it surprising that isoprenaline could produce a higher maximum contraction amplitude than calcium in human myocytes. This was seen in all the toxin-treated myocytes from failing heart, and a large number of the 22°C controls from normal heart. Isoprenaline/calcium ratios greater than one are seldom seen in normal guinea-pig, rabbit or rat hearts (Harding *et al.*, 1988). It is unlikely that the calcium levels were submaximal, since concentrations of up to 25 mM were used, and care was taken to ensure that the responses did not increase further with increasing concentration. It appears that human myocytes are unusual, in that maximal contractile activation is not attainable with high calcium alone. In support of this observation, it has been shown in studies using intact muscle that, even with the marked decrease in β-adrenoceptor responsiveness that accompanies β-receptor desensitization in the failing human ventricle, the response to selective β-agonists is still better than the well preserved calcium response (Fowler *et al.*, 1986).

The observations from this study are consistent with the hypothesis that increased levels of noradrenaline reported in heart failure lead to raised levels of the inhibitory G-protein, Gi, and that this contributes to the observed β-adrenoceptor desensitization in patients with moderate or end-stage heart failure.

We are extremely grateful for the technical assistance of Peter O'Gara and Dylan Wynne. We would like to thank Professor P.A. Poole-Wilson for his help and advice. We also thank Mr John Pepper and Professor Magdi Yacoub for their continuing valuable contributions to our work. This study was supported by the British Heart Foundation.

References

BOHM, M., BRUCKNER, R., SCHAFER, H., SCHMITZ, W. & SCHOLZ, H. (1988). Inhibition of the effects of adenosine on force of contraction and the slow calcium inward current by pertussis toxin is associated with myocardial lesions. *Cardiovasc. Res.*, **22**, 87–94.

BROWN, L., LORENZ, B. & ERDMANN, E. (1986). Reduced positive inotropic effects in diseased human ventricular myocardium. *Cardiovasc. Res.*, **20**, 516–520.

BROWN, L.A., HUMPHREY, S.M. & HARDING, S.E. (1990). The antiadrenergic effect of adenosine and its blockade by pertussis toxin. A comparative study in myocytes isolated from guinea-pig, rat and failing human hearts. *Br. J. Pharmacol.*, **101**, 484–488.

CHANG, H.Y., KLEIN, R.M. & KUNOS, G. (1982). Selective desensitisation of cardiac beta adrenoceptors by prolonged in vivo infusion of catecholamines in rats. *J. Pharmacol. Exp. Ther.*, **221**, 784–789.

DOSS, R.C., PERKINS, J.P. & HARDEN, T.K. (1981). Recovery of beta-adrenergic receptors following long term exposure of astrocytoma cells to catecholamines: role of protein synthesis. *J. Biol. Chem.*, **256**, 12281–12286.

FELDMAN, A.M., CATES, A.E., VEAZEY, W.B., HERSHBERGER, R.E., BRISTOW, M.R., BAUGHMAN, K.L., BAUMGARTNER, W.A. & VAN DOP, C. (1988). Increase of the 40,000-mol wt pertussis toxin substrate (G protein) in the failing human heart. *J. Clin. Invest.*, **82**, 189–197.

FOWLER, M.B., LASER, J.A., HOPKINS, G.L., MINOBE, W. & BRISTOW, M.R. (1986). Assessment of the B-adrenergic receptor pathway in the intact failing human heart: progressive receptor down-regulation and subsensitivity to agonist response *Circulation*, **74**, 1290–1302.

HARDING, S.E., JONES, S.M., VESCOVO, G., O'GARA, P. & POOLE-WILSON, P.A. (1989). Beta-adrenoceptor desensitisation in single ventricular cells isolated from failing human hearts. *Circulation*, **80**, 1748. (Abstract)

HARDING, S.E., JONES, S.M., O'GARA, P., VESCOVO, G. & POOLE-WILSON, P.A. (1990a). Reduced beta-agonist sensitivity in single atrial cells from failing human hearts. *Am. J. Physiol.*, **259**, H1009–H1014.

HARDING, S.E., JONES, S.M., O'GARA, P., VESCOVO, G. & POOLE-WILSON, P.A. (1990b). Decreased response to isoproterenol in single ventricular myocytes from failing human hearts: variation with etiology of disease. *Eur. Heart J.*, **11**, 404. (Abstract)

HARDING, S.E., JONES, S.M., O'GARA, P., DEL MONTE, F., VESCOVO, G. & POOLE-WILSON, P.A. (1992). Isolated ventricular myocytes from failing and non-failing human heart; the relation of age and clinical status of patients to isoproterenol response. *J. Mol. Cell. Cardiol.*, (in press).

HARDING, S.E., O'GARA, P., JONES, S.M., BROWN, L.A., VESCOVO, G. & POOLE-WILSON, P.A. (1990c). Species dependence of contraction velocity in single isolated cardiac myocytes. *Cardiosci.*, **1**, 49–53.

HARDING, S.E., VESCOVO, G., KIRBY, M., JONES, S.M., GURDEN, J. & POOLE-WILSON, P.A. (1988). Contractile responses of isolated rat and rabbit myocytes to isoproterenol and calcium. *J. Mol. Cell. Cardiol.*, **20**, 635–647.

HOPWOOD, A.M., HARDING, S.E. & HARRIS, P. (1987). Pertussis toxin reduces the antiadrenergic effect of 2-chloroadenosine on papillary muscle and the direct negative inotropic effect of 2-chloroadenosine on atrium. *Eur. J. Pharmacol.*, **141**, 423–428.

JONES, S.M., GURDEN, J., HARDING, S.E. & POOLE-WILSON, P.A. (1989). Beta-adrenoceptor desensitisation in papillary muscles and myocytes from the hearts of isoprenaline-treated rabbits. *J. Mol. Cell. Cardiol.*, **21**, suppl II, 199. (Abstract)

JONES, S.M., HUNT, N.A., DEL MONTE, F. & HARDING, S.E. (1990a). Contraction of cardiac myocytes from noradrenaline-treated rats in response to isoprenaline, forskolin and dibutyryl cAMP. *Eur. J. Pharmacol.*, **191**, 129–140.

JONES, S.M., KIRBY, M.S., HARDING, S.E., VESCOVO, G., WANLESS, R.B., DALA LIBERA, L. & POOLE-WILSON, P.A. (1990b). Adriamycin cardiomyopathy in the rabbit: alterations in contractile proteins and myocyte function. *Cardiovasc. Res.*, **24**, 834–842.

MANNING, A.S., YELLON, D.M., COLTART, D.J. & HEARSE, D.J. (1981). Abrupt withdrawal of chronic beta-blockade: adaptive changes in cyclic AMP and contractility. *J. Mol. Cell. Cardiol.*, **13**, 999–1009.

MOODY, C.J., DASHWOOD, M.R., SYKES, R.M., CHESTER, M., JONES, S.M., YACOUB, M.H. & HARDING, S.E. (1990). Functional and autoradiographic evidence for endothelin receptors on human and rat myocytes: comparison with smooth muscle cells. *Circ. Res.*, **67**, 764–769.

NEUMANN, J., SCHMITZ, W., SCHOLZ, H., VON MEYERINCK, L., DORING, V. & KALMAR, P. (1988). Increase in myocardial Gi-proteins in heart failure. *Lancet*, **ii**, 936–937.

PACKER, M. (1990). Role of the sympathetic nervous system in chronic heart failure. *Circulation*, **82**, I-1–I-6.

REITHMANN, C., GIERSCHIK, P., SIDIROPOULOS, D., WERDAN, K. & JAKOBS, K.H. (1989). Mechanism of noradrenaline-induced heterologous desensitisation of adenylate cyclase stimulation in rat heart muscle cells: increase in the level of inhibitory G-protein alpha-subunits. *Eur. J. Pharmacol.*, **172**, 211–221.

REITHMANN, C. & WERDAN, K. (1988). Homologous vs. heterologous desensitization of the adenylate cyclase system in heart cells. *Eur. J. Pharmacol.*, **154**, 99–104.

ROSEN, M.R., STEINBERG, S.F., CHOW, Y.K., BILEZIKIAN, J.P. & DANILO, P., JR. (1988). Role of a pertussis toxin-sensitive protein in the modulation of canine Purkinje fiber automaticity. *Circ. Res.*, **62**, 315–323.

SCHWINGER, R.H., BOHM, M. & ERDMANN, E. (1990). Evidence against spare or uncoupled beta-adrenoceptors in the human heart. *Am. Heart J.*, **119**, 899–904.

SUNYER, T., MONASTIRSKY, B., CODINA, J. & BIRNBAUMER, L. (1989). Studies on nucleotide and receptor regulation of Gi proteins: effects of pertussis toxin. *Mol. Endocrinol.*, **3**, 1115–1124.

THOMAS, J.A. & MARKS, B.H. (1978). Plasma norepinephrine in congestive heart failure. *Am. J. Cardiol.*, **41**, 233–243.

VESCOVO, G., HARDING, S.E., JONES, S.M., DALLA LIBERA, L., PESSINA, A.C. & POOLE-WILSON, P.A. (1989a). Comparison between isomyosin pattern and contractility of right ventricular myocytes isolated from rats with right cardiac hypertrophy. *Basic Res. Cardiol.*, **84**, 536–543.

VESCOVO, G., JONES, S.M., HARDING, S.E. & POOLE-WILSON, P.A. (1989b). Isoproterenol sensitivity of isolated cardiac myocytes from rats with monocrotaline-induced right-sided hypertrophy and heart failure. *J. Mol. Cell. Cardiol.*, **21**, 1047–1061.

(Received November 26, 1991
Revised January 14, 1992
Accepted January 21, 1992)

Br. J. Pharmacol. (1992), **106**, 123–126 © Macmillan Press Ltd, 1992

FR 113680: a novel tripeptide substance P antagonist with NK_1 receptor selectivity

[1]Hiroshi Morimoto, Masako Murai, Yasue Maeda, *Daijiro Hagiwara, *Hiroshi Miyake, *Masaaki Matsuo & Takashi Fujii

Department of Pharmacology, and *Department of Chemistry, New Drug Research Laboratories, Fujisawa Pharmaceutical Co. Ltd., 1-6, 2-chome, Kashima, Yodogawa-ku, Osaka, 532, Japan

1 We have discovered a novel tripeptide substance P (SP) antagonist, FR 113680 [N^{α}-[N^{α}-(N^{α}-acetyl-L-threonyl)-N'-formyl-D-tryptophyl]-N-methyl-N-phenylmethyl-L-phenylalaninamide]. In binding experiments, FR 113680 inhibited [^{3}H]-SP binding to guinea-pig lung membranes (NK_1) in a competitive manner but had not effect on [^{3}H]-SP binding to rat cerebral cortical membranes (NK_1), [^{3}H]-neurokinin A ([^{3}H]-NKA) binding to rat duodenum smooth muscle membranes (NK_2) and [^{3}H]-eledoisin (Ele) binding to rat cerebral cortical membranes (NK_3).

2 In bioassay experiments, FR 113680 dose-dependently inhibited SP-induced guinea-pig ileum contraction (NK_1), but did not inhibit either NKA-induced rat vas deferens contraction (NK_2) or neurokinin B (NKB)-induced contraction of rat portal vein (NK_3). According to Schild plot analysis, the inhibitory effect of FR 113680 on SP-induced guinea-pig ileum contraction is competitive and the pA_2 value is 7.53.

3 The inactivity of FR 113680 on NK_1 receptors in rat compared to guinea-pig may represent species-specific forms of the NK_1 receptor.

4 These findings suggest that FR 113680 interacts selectively with the NK_1 neurokinin receptor.

Keywords: Neurokinin antagonists; NK_1 receptor; tripeptide; FR 113680

Introduction

Substance P(SP), a member of the neurokinin family of related neuropeptides, exerts various biological activities in the central nervous system and in peripheral organs (Pernow, 1983). In airway tissues, it has been suggested that SP is the transmitter of the afferent sensory nerves (C-fibres) which respond to various irritants (Castairs & Barnes, 1986) and may be involved in asthmatic reactions (Lundberg & Saria, 1983; Morimoto *et al.*, 1989). However, direct evidence for the involvement of SP in asthma is still unavailable because of the lack of specific SP receptor antagonists.

We have tried to discover a SP antagonist which blocks the activity of C-fibres and inhibits asthmatic reactions. We recently identified a low molecular weight SP antagonist, FR 113680 [N^{α}-[N^{α}-(N^{α}-acetyl-L-threonyl-)-N'-formyl-D-tryptophyl]-N-methyl-N-phenylmethyl-L-phenylalaninamide], using a [^{3}H]-SP binding assay with guinea-pig lung membranes. Figure 1 shows the chemical structure of FR 113680. This compound was designed from (D-Pro^4, D-Trp^{7,9,10}, Phe^{11}) SP_{4-11} (Octapeptide), which had been reported to exhibit SP-antagonistic activity in guinea-pig trachea (Mizrahi *et al.*, 1984).

Evidence suggests that neurokinins elicit biological responses in mammalian tissues by acting on three distinct receptors, termed NK_1, NK_2 and NK_3, at which SP, neurokinin A (NKA) and neurokinin B (NKB) are respectively the most potent natural ligands (Lee *et al.*, 1986; Regoli *et al.*, 1988).

The involvement of one or more neurokinin receptors in certain biological responses has been suggested (Maggi *et al.*, 1987). The interaction of neurokinins with these receptors can be demonstrated by use of binding techniques and *in vitro* bioassays.

In this paper, we have examined the effects of FR 113680 on [^{3}H]-SP binding to guinea-pig lung membranes and clarified the receptor subtype selectivity of FR 113680 using binding techniques; (NK_1: [^{3}H]-SP binding to rat cerebral cortical synaptic membranes (Lee *et al.*, 1986); NK_2: [^{3}H]-NKA binding to rat duodenum smooth muscle membranes (Bergstrom *et al.*, 1987a); NK_3: [^{3}H]-eledoisin ([^{3}H]-Ele) binding to rat cerebral cortical synaptic membranes (Bergstom *et al.*, 1987b)) and bioassays (NK_1: SP-induced guinea-pig ileum contraction (Regoli *et al.*, 1988); NK_2: NKA-induced rat vas deferens contraction (Dion *et al.*, 1987); NK_3: NKB-induced rat portal vein contraction (Mastrangelo *et al.*, 1986)).

Methods

Preparation of guinea-pig lung and rat duodenum smooth muscle membranes

Membranes were prepared according to Norman *et al.* (1987) with the following modification. Male Hartley guinea-pigs (300–400 g) and Sprague-Dawley rats (250–300 g) were killed, and guinea-pig lung and rat duodenum smooth muscle tissues were homogenized in 10 volumes of ice cold 0.25 M sucrose containing 10 mM Tris-HCl and 0.1 mM EDTA (pH 7.5) with a polytron PT-10 for 1 min. The homogenate was centrifuged at 1000 *g* for 10 min, the pellet was discarded and the supernatant fluid was then centrifuged at 35000 *g* for 20 min. The pellet was washed twice with 9 volumes of 5 mM Tris-HCl (pH 7.5). The final pellet was resuspended in 50 mM Tris-HCl (pH 7.5) and used in binding experiments immediately.

Preparation of rat cerebral cortical synaptic membranes

Membranes were prepared according to Zukin *et al.* (1974). Male Sprague-Dawley rats (250–300 g) were killed and the cerebral cortex was rapidly removed and homogenized in 9 volumes of ice cold 0.32 M sucrose containing 1 mM K_2HPO_4 and 0.1 mM EDTA (pH 7.5) in a glass homogenizer fitted

[1] Author for correspondence.

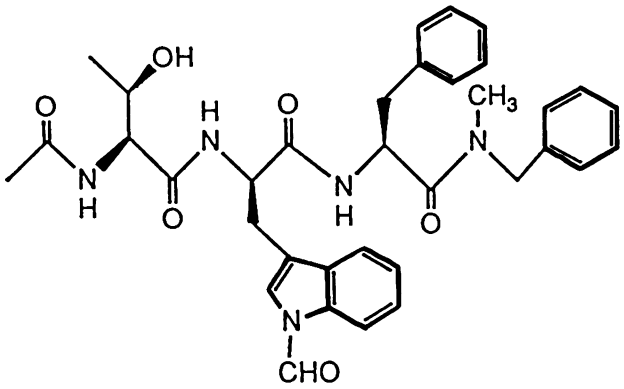

Figure 1 Chemical structure of FR 113680.

with a Teflon pestle. The homogenate was centrifuged at 1000 *g* for 10 min, the pellet was discarded and the supernatant fluid was centrifuged at 20000 *g* for 20 min. The crude synaptosomal pellet was resuspended in distilled water and dispersed. The suspension was centrifuged at 8000 *g* for 20 min. The supernatant was collected and the pellet, a bilayer with a soft, buffy uppercoat, was rinsed carefully with the supernatant fluid to collect the upper layer. The combined supernatant fraction and buffy coat layer was then centrifuged at 35000 *g* for 20 min and the pellet was washed with 9 volumes of 5 mM Tris-HCl (pH 7.5) twice. The final pellet was resuspended in 50 mM Tris-HCl (pH 7.5) and used in binding experiments immediately.

Radioligand binding experiments

The procedure of Lee *et al.* (1983) was used with certain modifications. Binding was initiated by adding 100 µl of the membrane preparation (final concentration; 0.6 mg protein/tube) in duplicate to the radiolabelled ligands ([^{3}H]-SP 1 nM, [^{3}H]-NKA 10 nM, [^{3}H]-Ele 1 nM) at 25°C for either 30 min ([^{3}H]-SP, [^{3}H]-NKA) or 60 min ([^{3}H]-Ele) in a final volume of 500 µl buffer containing 50 mM Tris-HCl (pH 7.5), 0.1 mM $MnCl_2$, bovine serum albumin 200 µg ml^{-1}, chymostatin 5 µg ml^{-1}, leupeptin 4 µg ml^{-1}, bacitracin 40 µg ml^{-1} and various doses of FR 113680. At the end of the incubation period, 5 ml of ice-cold 50 mM Tris-HCl was added to each tube and its content was filtered immediately under reduced pressure through Whatman GF/B glass filters (pretreated with 0.1% polyethyleneimine in water over 3 h before use). Each of the filters was then washed three times with 5 ml of ice-cold 50 mM Tris-HCl and radioactivity was measured by liquid scintillation spectrometry. Non-specific binding was defined as binding in the presence of 5 µM SP, NKA or Ele. Specific binding was calculated by subtracting non-specific binding from total binding. Specific binding corresponded to 85–95% of total binding in all cases. The protein concentration was determined by the method of Lowry *et al.* (1951) with bovine serum albumin used as standard.

Bioassays

The experiments were performed on tissues taken from male guinea-pigs (Hartley, 300–400 *g*) and rats (Sprague-Dawley, 300–400 *g*). Animals were killed and the following organs were rapidly removed: guinea-pig ileum (GPI), rat vas deferens (RVD) and rat portal vein (RPV). Strips of RVD and RPV were suspended in 10 ml organ baths containing warm (37°C), oxygenated (95% O_2, 5% CO_2) Tyrode solution containing (mM): NaCl 137.0, KCl 2.7, $CaCl_2$ 1.8, $MgCl_2$ 1.05, $NaHPO_4$ 0.4, dextrose 5.6 and $NaHCO_3$ 11.9 (pH 7.5). Strips of GPI were incubated in Tyrode solution containing 5.2 µM atropine sulphate and 4.1 µM indomethacin. The tissues were placed under a resting tension of 0.3 g (RVD) and 0.5 g (GPI and RPV). Tension changes were recorded isometrically with a force-displacement transducer and a polygraph system. The preparations were allowed to equilibrate for 60 min and were then stimulated with 1 nM SP (GPI), 100 nM NKA (RVD) or 100 nM NKB (RPV), respectively.

FR 113680 was applied 5 min before agonists. The pA_2 value was obtained according to Arunlakshana & Schild (1959).

Data analysis

All results are given as mean ± s.e.mean and subsequently paired Student's *t* test was used to determined significance of differences between the groups of treatments.

Materials

Tris, bovine serum albumin, chymostatin, leupeptin and bacitracin were purchased from Sigma Chemical Company (St. Louis, MO, U.S.A). Polyethyleneimine was obtained from Nakarai Tesque Chemical Company (Kyoto, Japan). Phosphoramidon was from Peptide Institute Inc. (Osaka, Japan). [^{3}H]-SP (1.65 TBq mmol^{-1}), [^{3}H]-NKA (2.1 TBq mmol^{-1}) and [^{3}H]-Ele (1.20 TBq mmol^{-1}) were purchased from Amersham Int. Ltd., CEA Biology Department and New England Nuclear Corp., respectively.

Results

Inhibition of substance P binding by FR 113680 in guinea-pig lung membranes

FR 113680 dose-dependently inhibited [^{3}H]-SP binding to guinea-pig lung membranes (Figure 2). The affinity constant (K_i) and pseudo Hill coefficient (n_H) of FR 113680 were 15.7 nM and 0.97, respectively. Natural neurokinins were also tested (Figure 2). SP and NKA showed significant inhibitory effects on [^{3}H]-SP binding. NKB caused a small displacement of the binding of [^{3}H]-SP in guinea-pig lung at a concentration of 10 µM. The rank order of affinities of neurokinins was SP ≫ NKA ≫ NKB. The binding site for [^{3}H]-SP in guinea-pig lung membranes was characterized as the NK_1 type. Figure 3 shows Scatchard analysis of [^{3}H]-SP binding in the

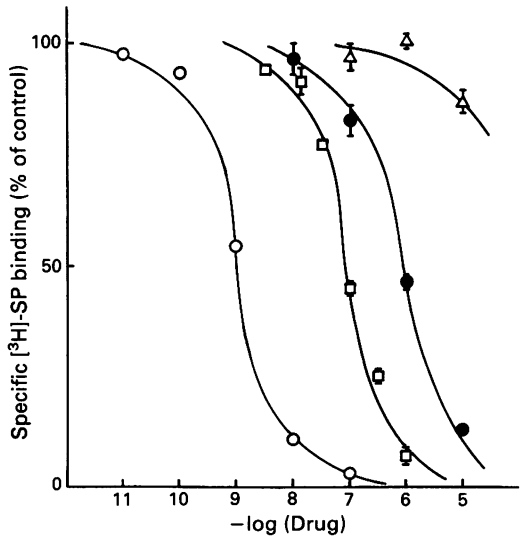

Figure 2 Displacement of [^{3}H]-substance P ([^{3}H]-SP) binding to guinea-pig lung membranes by FR 113680 (□), SP (○), neurokinin A (NKA) (●) and NKB (△). Values are given as a percentage of control [^{3}H]-SP binding and are the mean of three experiments performed in duplicate; s.e.mean shown by vertical bars. Nonspecific binding corresponded to 5–15% of total binding.

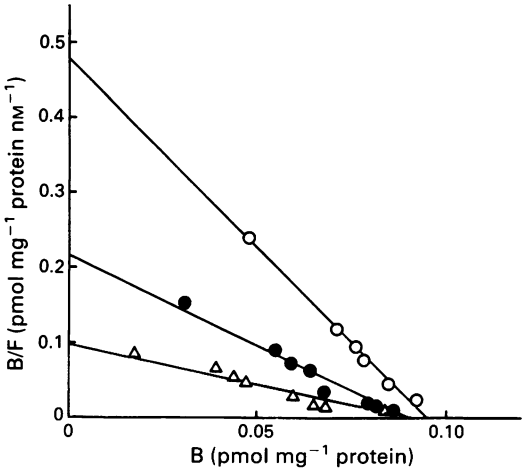

Figure 3 Scatchard analysis of specific [^{3}H]-substance P ([^{3}H]-SP) binding to guinea-pig lung membranes in the absence (○) and in the presence of FR 113680 at 32 nM (●) and 100 nM (△). Data represent a typical experiment that was performed in duplicate and repeated three times with similar results.

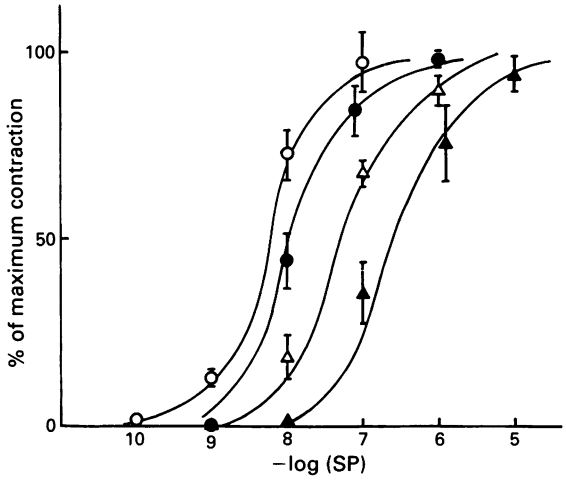

Figure 4 Concentration-response curves for substance P (SP)-induced guinea-pig ileum contractions in the absence (○) and in the presence of FR 113680 at 0.1 μM (●), 1 μM (△) and 10 μM (▲). Each point indicates the mean of four experiments at each concentration, s.e.mean shown by vertical bars.

absence and prescence of FR 113680; the control data is linear indicating that only one type of binding site is present. The decrease in [^{3}H]-SP binding by FR 113680 was due to the increase in receptor affinity (K_D: control, 0.27 ± 0.01 nM; 32 nM FR 113680, 3.80 ± 0.03 nM; 100 nM FR 113680, 9.23 ± 0.06 nM) without a change in B_{max}. FR 113680 (10 μM) did not reduce [^{3}H]-quinuclidinyl benzilate binding (muscarinic receptor ligand) and [^{3}H]-bradykinin binding to guinea-pig lung membranes (data not shown).

Clarification of FR 113680 receptor subtype selectivity

In binding assays, FR 113680 (0.1–10 μM) did not antagonize [^{3}H]-SP binding to rat cerebral cortical synaptic membranes (NK_1), [^{3}H]-NKA binding to rat duodenum smooth muscle membranes (NK_2) or [^{3}H]-Ele binding to rat cerebral cortical synaptic membranes (NK_3) (Table 1).

In bioassay experiments, FR 113680 (10 μM) inhibited completely SP-induced contractions of the guinea-pig ileum (NK_1), but not NKA-induced contraction of the rat vas deferens (NK_2) or NKB-induced contraction of the rat portal vein (NK_3) (data not shown). Figure 4 shows the effect of FR 113680 on the cumulative SP dose-response curves in guinea-pig ileum. Curves were shifted to the right in parallel without the maximal contraction being depressed. The data were analysed by Schild analysis; the slope of the regression lines was not significantly different from 1 and the pA_2 value was 7.53. This indicates that FR 113680 is a competitive antagonist . FR 113680 (10 μM) did not inhibit acetylcholine- and histamine-induced guinea-pig ileum contraction (data not shown).

Discussion

Our present results demonstrate that FR 113680 dose-dependently inhibits [^{3}H]-SP binding to guinea-pig lung membranes. The rank order of affinities of natural neurokinins in this binding assay was SP ≫ NKA ≫ NKB. This suggests that the binding site in guinea-pig lung is of the NK_1 type. According to Scatchard analysis, FR 113680 is a competitive inhibitor at the NK_1 receptor in guinea-pig lung. FR 113680 also significantly inhibited SP-induced contraction of guinea-pig ileum which is also mediated through the NK_1 receptor. However, FR 113680 did not antagonize [^{3}H]-SP on NK_1 receptors in rat cerebral cortex. Two hypotheses can be proposed to explain these differences.

Differences in the affinity of FR 113680 in rat cerebral cortex and guinea-pig ileum or lung may reflect the existence of subtypes of NK_1 receptor. Other antagonists also distinguish between rat and guinea-pig receptors (Snider *et al.*, 1991; Gitter *et al.*, 1991; Fardin & Garrett, 1991). However, these differences have not been observed in a single species and the existence of NK_1 receptor subtypes is therefore not proven.

The simplest explanation of these results could be a variation in the structure of the NK_1 receptor between species. Snider *et al.* (1991) reported a low molecular weight, non-peptide antagonist, CP-96,345, which is selective for NK_1 receptor. This compound is potent in displacing [^{3}H]-SP from bovine brain, but it is about 80 times less potent in rat forebrain. In rat and mouse CP-96,345 binds with reduced potency to the NK_1 receptor compared to many other species (Beresford *et al.*, 1991). Fardin & Garret (1991) also sug-

Table 1 Effects of FR 113680 on neurokinin receptor bindings

	Specific binding (fmol mg^{-1} protein)			
Treatment (μM)	NK_1	NK_2	NK_3	GP lung
Control	25.9 ± 3.0	24.8 ± 4.4	5.22 ± 0.56	36.6 ± 4.4
FR 113680 (0.1)	25.1 ± 2.9	20.5 ± 5.2	5.88 ± 0.85	16.2 ± 2.1**
FR 113680 (1.0)	24.5 ± 2.0	30.2 ± 4.7	5.70 ± 0.74	3.2 ± 1.0**
FR 113680 (10.0)	19.7 ± 2.3	24.0 ± 5.6	4.09 ± 0.46	ND

Each value indicates mean ± s.e.mean of three experiments.
NK_1: [^{3}H]-substance P (1 nM) binding to rat cerebral cortical synaptic membranes.
NK_2: [^{3}H]-neurokinin A (10 nM) binding to rat duodenum smooth muscle membranes.
NK_3: [^{3}H]-eledoisin (1 nM) binding to rat cerebral cortical synaptic membranes.
ND: not determined.
**$P < 0.01$.

gested species differences between [^{3}H]-SP binding sites in rat and guinea-pig. SP was found to possess approximately the same affinity in rat brain, guinea-pig brain and guinea-pig ileum, while peptide antagonists had higher affinities in the guinea-pig. Gitter *et al.* (1991) also showed that CP-96,345 and its analogues were more potent in guinea-pig and rabbit brain than in rat, mouse and chicken brain. FR 113680 is also more potent in guinea-pig (ileum and lung) than in rat. This may be due to differences in NK_1 receptors between rat and guinea-pig.

Most of the neurokinin receptor antagonists reported to date are peptides, with high molecular weights and poor selectivity for the neurokinin receptor subtypes. But, recently several antagonists with improved selectivity for the neurokinin receptors have been reported. CP-96,345, studied by Snider *et al.* (1991), is selective for the NK_1 receptor. This compound was discovered through a chemical file-screening approach. On the other hand FR 113680 was designed from the compound (D-Pro^4, D-Trp^{7,9,10}, Phe^{11})SP_{4-11}. This tripeptide antagonist is the smallest example of a peptide antagonist at the NK_1 receptor.

Neurokinins, particularly SP and NKA, are present in primary afferent sensory nerves (C-fibres) innervating the guinea-pig airway (Lungberg & Saria, 1983). Neurokinins released from sensory nerves by various stimuli are known to produce a powerful constriction of the airway (Maggi *et al.*, 1990; Barnes, 1991). Contractile effects of neurokinins on airway tissues may be of pathogenic relevance in human airway asthma or bronchial-hyperreactivity, and FR 113680 may be clinically useful in the treatment of asthmatic reactions.

References

ARUNLAKSHANA, O. & SCHILD, H.O. (1959). Some quantitative uses of drug antagonists. *Br. J. Pharmacol. Chemother.*, **14**, 48–58.

BARNES, P.J. (1991). Neuropeptides and asthma. *Am. Rev. Respir. Dis.*, **143**, S28–S32.

BERESFORD, I.J.M., BIRCH, P.J., HAGAN, R.M. & IRELAND, S.J. (1991). Investigation into species variants in tachykinin NK_1 receptors by use of the non-peptide antagonist, CP-96,345. *Br. J. Pharmacol.*, **104**, 292–293.

BERGSTROM, L., BEAUJOUAN, J.C, TORRENS, Y., SAFFROY, M., GROWINSKI, J., LAVIELLE, S., CHASSAING, G., MARQUET, A., D'ORLEANS-JUSTE, P., DION, S. & REGOLI, D. (1987a). ^{3}H-neurokinin A labels a specific tachykinin-binding site in the rat duodenal smooth muscle. *Mol. Pharmacol.*, **32**, 764–771.

BERGSTROM, L., TORRENS, Y., SAFFROY, M., BEAUJOUAN, J.C., LAVIELLE, S., CHASSING, G., MORGAT, J.L., GLOWINSKI, J. & MARQUET, A. (1987b). [^{3}H]Neurokinin B and [^{125}I]-Bolton Hunter eledoisin label identical tachykinin binding sites in the rat brain. *Int. Soc. Neurochem.*, **48**, 125–133.

CASTAIRS, J.R. & BARNES, P.J. (1986). Autoradiographic mapping of substance P receptors in lung. *Eur. J. Pharmacol.*, **127**, 295–296.

DION, S., D'ORLEANS-JUSTE, P., DRAPEAU, G., RHALEB, N.E., ROUISSI, N., TOUSIGNANT, C. & REGOLI, D. (1987). Characterization of neurokinin receptors in various isolated organs by the use of selective agonists. *Life Sci.*, **41**, 2269–2278.

FARDIN, V. & GARRET, C. (1991). Species differences between [^{3}H] substance P binding in rat and guinea-pig shown by the use of peptide agonists and antagonists. *Eur. J. Pharmacol.*, **201**, 231–234.

GITTER, B.D., WATERS, D.C., BRUNS, R.F., MASON, N.R., NIXON, J.A. & HOWBERT, J.J. (1991). Species differences in affinities of non-peptide antagonists for substance P receptors. *Eur. J. Pharmacol.*, **197**, 237–238.

LEE, C.-M., CAMPBELL, N.J., WILLIAMS, B.J. & IVERSEN, L.L. (1986). Multiple tachykinin binding sites in peripheral tissues and in brain. *Eur. J. Pharmacol.*, **130**, 209–217.

LEE, C.-M., JAVITCH, J.A. & SNYDER, S.H. (1983). ^{3}H-substance P binding to salivary gland membranes. Regulation by guanyl nucleotides and divalent cations. *Mol. Pharmacol.*, **23**, 563–569.

LOWRY, O.H., ROSEBROUGH, N.J., FARR, A.L. & RANDALL, R.J. (1951). Protein measurement with the Folin phenol reagent. *J. Biol. Chem.*, **197**, 265–275.

LUNDBERG, J.M. & SARIA, A. (1983). Capsaicin-induced desensitization of airway mucosa to cigarette smoke, mechanical and chemical irritants. *Nature*, **302**, 251–253.

MAGGI, C.A., GUILIANI, S., SANTICIOLI, P., REGOLI, D. & MELI, A. (1987). Peripheral effects of neurokinins; functional evidence for the existence of multiple receptors. *J. Autonom. Pharmacol.*, **7**, 11–32.

MASTRANGELO, D., MATHISON, R., HUGGEL, H.J., DION, S., D'ORLEANS-JUSTE, P., RHALEB, N.E., DRAPEAU, G., ROVERO, P. & REGOLI, D. (1986). The rat isolated portal vein: a preparation selective to neurokinins, particularly neurokinin B. *Eur. J. Pharmacol.*, **134**, 321–326.

MIZRAHI, J., ESCHER, E., DORLEANS-JUSTE, P. & REGOLI, D. (1984). Undeca- and octapeptide antagonists for substance P, a study of the guinea-pig trachea. *Eur. J. Pharmacol.*, **99**, 193–202.

MORIMOTO, H., FUJII, T. & SENOH, H. (1989). Plasma extravasation by chemical mediators in rat skin and trachea: a role of neurogenic agents of tracheal edema formation. *Jpn. J. Pharmacol.*, **49**, 389–395.

NORMAN, P., ABRAM, T.S., KLUENDER, H.C., GARDINAR, P.J. & CUTHBERT, N.J. (1987). The binding of [^{3}H]leukotriene C_4 to guinea-pig lung membranes. The lack of correlation of LTC_4 functional activity with binding affinity. *Eur. J. Pharmacol.*, **143**, 323–334.

PERNOW, B. (1983). Substance P. *Pharmacol. Rev.*, **35**, 85–141.

REGOLI, D., DRAPEAU, G., DION, S. & COUTUR, R. (1988). New selective agonists for neurokinin receptors: pharmacological tools for receptor characterization. *Trends Pharmacol. Sci.*, **9**, 290–295.

SNIDER, R.M., CONSTANTINE, J.W., LOWE III, J.A., LONGO, K.P., LABEL, W.S., WOODY, H.A., DROZDA, S.E., DESAI, M.C., VINICK, F.J., SPENCER, R.W. & HESS, H.-J. (1991). A potent nonpeptide antagonist of the substance P (NK_1) receptor. *Science*, **251**, 435–437.

ZUKIN, S.R., YOUNG, A.B. & SNYDER, S.H. (1974). Gamma-aminobutyric acid binding to receptor sites in the rat central nervous system. *Proc. Natl. Acad. Sci. U.S.A.*, **71**, 4802–4807.

(Received September 9, 1991
Revised January 20, 1992
Accepted January 22, 1992)

Br. J. Pharmacol. (1992), **106**, 127–132 © Macmillan Press Ltd, 1992

Modulation of vascular tone by endothelin-1: role of preload, endothelial integrity and concentration of endothelin-1

[1]J.L. Mehta, D.L. Lawson, B.C. Yang, P. Mehta & W.W. Nichols

Departments of Medicine and Pediatrics, College of Medicine, University of Florida and the VA Medical Center, Gainesville, FL, U.S.A.

1 Endothelin-1 (ET-1) has been shown to exert both arterial relaxant and constrictor effects. To examine the mechanisms of these divergent effects, rat aortic rings were suspended in an organ bath (baseline preload, 5 g) and exposed to ET-1 (10^{-11} to 10^{-7} M). ET-1 contracted these rings in a concentration-dependent fashion.

2 When aortic rings were contracted with noradrenaline (NA) to 1 g of tension, ET-1 caused further contraction of these rings. In rings precontracted to 2 to 4 g of tension, low concentrations of ET-1 (10^{-11} to 10^{-9} M) caused a significant relaxation, but high concentrations ($\geqslant 5 \times 10^{-9}$ M) caused a marked contraction, indicating both relaxant and contractile effects of ET-1 depending on the preload and ET-1 concentration.

3 To determine the mechanism of ET-1-induced relaxation, aortic rings were pretreated with the cyclo-oxygenase inhibitor indomethacin, N^G-monomethyl-L-arginine (L-NMMA) an inihibitor of synthesis of endothelium-derived relaxing factor (EDRF), or oxyhaemoglobin (Hb) which decreases the activity of EDRF, prior to their exposure to ET-1. Both indomethacin and L-NMMA markedly ($P<0.01$) attenuated ET-1-induced relaxation, whereas Hb totally abolished it. Removal of the endothelium from aortic rings also abolished ET-1-mediated relaxation.

4 The relaxant effect of ET-1 in NA-precontracted rings was associated with marked accumulation of guanosine 3':5'-cyclic monophosphate (cyclic GMP), whereas ET-1-induced contraction of quiescent rings was not.

5 In manually stretched rings (4 g of tension), ET-1 caused only concentration-dependent contraction, but no cyclic GMP accumulation.

6 Thus, ET-1 contracts rat aortic rings with intact endothelium and those which are passively stretched. However, stimulation of rat aortic rings with NA to modest tension alters the contractile effect of ET-1 to a potent relaxant effect. The ET-1-mediated relaxation in this setting appears to be endothelium-dependent and is related to release of both cyclo-oxygenase products and EDRF.

Keywords: Endothelium; endothelium-derived relaxing factor; endothelium-1; oxyhaemoglobin

Introduction

Endothelin-1 (ET-1), characterized as a 21-amino acid peptide released from cultured porcine endothelial cells (Yanagisawa *et al.*, 1988) exerts potent vasoconstrictor effect in a variety of mammalian blood vessels. Its levels in plasma are increased in myocardial ischaemia and renal insufficiency (Miyauchi *et al.*, 1989; Salminen *et al.*, 1989; Tomita *et al.*, 1989), and it has been suggested that it may exert a vasoconstrictor influence in these disease states (Salminen *et al.*, 1989; Stewart *et al.*, 1991). There is also evidence that ET-1 exerts a vasorelaxant effect, especially when the intravascular pressure is high or when the concentrations of ET-1 are large (de Nucci *et al.*, 1988; Bradley *et al.*, 1990; Perreault & de Marte, 1991).

ET-1 has been shown to induce release of endothelium-derived relaxing factor (EDRF) in intact blood vessels (Lipptton *et al.*, 1988; Warner *et al.*, 1989). EDRF relaxes vascular smooth muscle via stimulation of guanylate cyclase (Furchgott & Zawadski, 1980). Similar release of EDRF from blood vessels has been reported in response to several other vascular smooth muscle agonists, and the vasoconstrictor effects of these agonists are enhanced in the absence of endothelium (Cocks & Angus, 1983; Griffith *et al.*, 1984; Sakuma *et al.*, 1987). The release of EDRF in response to these agonists becomes apparent when the tension in the vascular beds is relatively high (Lawson *et al.*, 1989). ET-1 has also been shown to release eicosanoids from rabbit isolated perfused kidney and spleen (Rae *et al.*, 1989).

We have examined the effects of ET-1 on rat aortic contraction. Since the overall effects of agonists my be dependent on preload as suggested by de Nucci *et al.* (1988), Bradley *et al.* (1990) and Lawson *et al.* (1989), we studied the effects of ET-1 on rat aortic rings exposed to a wide range of preloads.

Methods

Preparation of rat aortic rings

Sprague-Dawley rats (average body weight 225 g) were anaesthetized with halothane and killed. The thoracic aortae were quickly removed and placed into aerated (95% O_2, 5% CO_2) Krebs-Ringer buffer (composition in mM: NaCl 118, KCl 4.7, KH_2PO_4 1.2, $MgCl_2$ 1.2, $CaCl_2$ 2.5, $NaHCO_3$ 12.5, Na-EDTA 0.01 and dextrose 11.1 pH 7.4). Excess adventitious tissue was carefully removed and the vessels were cut into 3–4 mm rings. The vessels were washed with buffer, mounted on wire stirrups, suspended in tissue baths filled with buffer at 37°C and connected to force transducers (Grass Instruments, Quincey, MA) to record changes in isometric force (Lawson *et al.*, 1989).

The rings were stretched to a preload of 5 g and allowed to equilibrate for approximately 2 h. This preload was observed to be appropriate to determine dose-response curves to a

[1] Author for correspondence at: Box J-277, JHMHC, University of Florida, Gainesville, FL 32610, U.S.A.

variety of agonists, including noradrenaline (NA). During the period of equilibration, the buffer was changed every 15 min, and 95% O_2 and 5% CO_2 continuously bubbled. Followng equilibration, the vascular rings were tested for viability by addition of 20 mM KCl. Endothelial integrity was determined in these rings by the presence of characteristic 60 to 80% relaxation in response to acetylcholine (ACh, 10^{-6} M). In some rings, endothelium was removed by gently passing a cotton-tipped swab through the lumen; these rings failed to relax in response to ACh (Lawson *et al.*, 1989), but relaxed promptly in response to nitroglycerin (10^{-6} M) indicating intact vascular smooth muscle function.

Experimental protocol

Aortic rings were exposed to gradually increasing concentrations of ET-1 (10^{-11} to 10^{-7} M). Following stable contraction, rings were exposed to ACh (10^{-6} M). Parallel sets of aortic rings were precontracted with NA (10^{-10} to 10^{-7} M) to achieve varying degrees of tension (1, 2 and 4 g). These NA-precontracted rings were then exposed to ET-1 (10^{-11} to 10^{-7} M). Following sustained effects of ET-1, ACh was added to the organ bath to determine the presence or absence of vascular endothelium.

In parallel experiments, aortic rings were treated with the cyclo-oxygenase inhibitor indomethacin (10^{-5} M) or the competitive inhibitor of EDRF synthesis, N^G-monomethyl L-arginine (L-NMMA, 5×10^{-5} M) (Dinerman *et al.*, 1991). Other aortic rings were treated with oxyhaemoglobin (10^{-5} M), which binds EDRF (Martin *et al.*, 1985). These concentrations of inhibitors were selected based on previous studies (Dinerman *et al.*, 1991), which showed that 10^{-5} M indomethacin decreases prostaglandin synthesis by about 80%, 5×10^{-5} M L-NMMA decreases ACh-mediated relaxation by about 75%, and 10^{-5} M oxyhaemoglobin abolishes the ACh-mediated relaxation. In all these rings, 3 to 4 g of tension was achieved with NA. Following sustained contraction, these rings were exposed to ET-1. Other aortic rings, from which the endothelium had been removed, were also contracted with NA to achieve approximately 3–4 g of force and then exposed to ET-1.

To examine if the effects of ET-1 on NA-precontracted rings were due to increased tension, other aortic rings were stretched manually to a tension of 4 g. After the tension was stable, the rings were exposed to ET-1.

Measurement of cyclic GMP

Manually stretched, NA or ET-1- contracted rings, and other rings exposed to low ET-1 concentrations (5×10^{-9} M) following contraction with NA or manual stretch were flash-frozen in 1 ml of 0.5 mM isobutylmethylxanthine (IBMX) and 10% trichloroacetic acid and stored at − 70°C. These rings were homogenized and sonicated. After centrifugation (2500 *g* for 15 min at 4°C), the resulting supernatants were extracted 4 times in water-saturated ethyl ether (volume 5 ml) and dried under a stream of air. Acetylated guanosine 3′:5′-cyclic monophosphate (cyclic GMP) was measured by radioimmunoassay with an ^{125}I-kit (New England Nuclear, Boston, MA, U.S.A.). The minimum detectable limit of cyclic GMP assay was 2.5 fmol/0.1 ml. The extraction efficiency using [^{3}H]-cyclic GMP was over 95%. All measurements were made in duplicate (variation $< 10\%$). The cyclic GMP levels were expressed in fmol mg^{-1} tissue.

Reagents

L-NMMA was a gift of Dr S. Moncada, Beckenham, UK. Indomethacin was a gift from Merck, Sharp and Dohme, West Point, PA, U.S.A. ET-1 was purchased from Peninsula Laboratories, Belmont, CA, U.S.A. Oxyhaemoglobin was prepared as described previously (Dinerman *et al.*, 1991). All other supplies were purchased from Sigma Chemical, St. Louis, MO, U.S.A.

Statistical analysis

Aortic ring tension was divided by the wet weight of the ring to obtain the isometric tension in g mg^{-1} tissue. All data are expressed as mean ± s.e. and are based on a minimum of four experiments from four separate rats. Statistical analysis was performed with Student's *t* test for paired and unpaired observations, as appropriate. A *P* value of < 0.05 was considered significant. The effects of various interventions on aortic ring contraction or relaxation are expressed as percentage change from baseline contraction.

Results

Effects of endothelin-1 on rat aortic ring contraction

ET-1 induced a slow, concentration-dependent contraction of all aortic rings. The contraction was greater in rings without endothelium than in those with intact endothelium. The increased sensitivity of rings without endothelium to ET-1 is in keeping with previous observations (Miller *et al.*, 1989; Folger *et al.*, 1991), which indicated increased contraction in response to a variety of agonists, including ET-1, in the absence of intact endothelium.

Endothelin-1 and noradrenaline-precontracted rings

The effects of ET-1 varied markedly when the tension of the rat aortic rings was changed with NA (Figures 1 and 2). When the rings were contracted with NA to approximately 1 g of tension, ET-1 caused an additional contraction. The overall contraction was equal to the sum of the contractile actions of NA and ET-1. When the tension with NA was maintained at approximately 2 g, low concentrations of ET-1 evoked gradual relaxation, but higher concentrations caused contraction of the aortic rings. When the aortic rings were precontracted with NA to approximately 3 to 4 g tension, very low concentrations of ET-1 (10^{-11} to 10^{-9} M) caused a potent and rapid relaxation; high concentrations ($\geq 5 \times 10^{-9}$ M), however, evoked a potent contraction. All these vascular rings relaxed in response to ACh.

In parallel experiments, aortic rings contracted with NA to different tensions were observed for 20 min. However, no spontaneous relaxation or contraction was observed, indicating that the effects of ET-1 were indeed caused by ET-1 and were not spontaneous occurrences.

Endothelin-1 and manual stretch

When aortic rings were manually stretched to 1, 2 or 4 g of tension (above the baseline preload of 4 g), ET-1 caused a concentration-dependent contraction (Table 1). This was in marked contrast to NA-precontracted rings which relaxed in response to low concentrations of ET-1. In these rings, ACh also failed to cause any relaxation.

Mechanism of endothelin-1 mediated rat aortic ring relaxation

To determine the mechanism of ET-1-mediated vascular relaxation, parallel sets of rat aortic rings were contracted with NA to a preload of 3–4 g and then exposed to ET-1, while other rings were treated with indomethacin, L-NMMA or oxyhaemoglobin, or endothelium was removed from the rings. Similar tension was achieved in all rings by adding different amounts of NA (Figure 3).

Both L-NMMA and oxyhaemoglobin caused contraction of NA-contracted rings (Figure 3), presumably because both these agents inhibit the vasorelaxant effect of EDRF. Indo-

methacin slightly decreased the rat aortic ring contraction in response to NA. However, the peak tension in the rings prior to addition of ET-1 was similar in all rings.

Indomethacin significantly decreased the vasorelaxant effect of ET-1, but did not abolish it. L-NMMA also markedly decreased the vasorelaxant effect of ET-1, but like indomethacin did not abolish it. Treatment of vascular rings with oxyhaemoglobin on the other hand totally abolished the vasorelaxant effects of ET-1 (Figure 3, Table 2). The relaxant effect of ACh was present in the indomethacin-treated rings, attenuated in the L-NMMA-treated rings, and absent in the oxyhaemoglobin-treated rings (Figure 3). In the NA-precontracted rings, without endothelium, ET-1 failed to cause relaxation at any concentration (Figure 3, Table 2).

Cyclic GMP accumulation

Levels of cyclic GMP increased markedly in NA-precontracted rings from the quiescent state, and further increased upon their exposure to ACh (10^{-6} M) indicating EDRF release. ET-1 alone (10^{-8} M) which caused marked contraction of aortic rings had no effect on accumulation of cyclic GMP. However, treatment of NA-precontracted rings with ET-1 (5×10^{-9} M) resulted in a marked increase in cyclic GMP content ($P<0.02$ *vs* ET-1 alone or NA alone-precontracted rings), indicating that ET-1 caused EDRF release in NA-treated rings. This increase in ET-1 was minimal in rings that were exposed to ET-1 after manual increase in tension (Table 3).

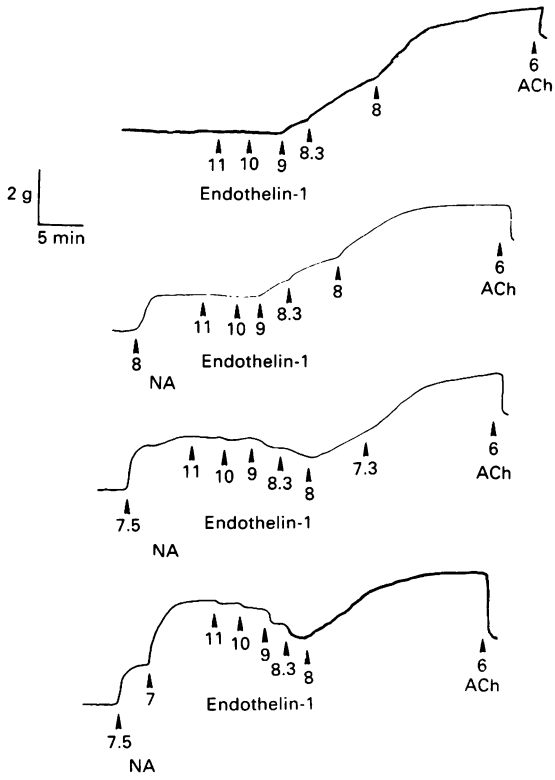

Figure 1 Effect of endothelin-1 (ET-1) on rat aortic rings with intact endothelium contracted to different preloads with noradrenaline (NA). With no prior exposure to NA, ET-1 caused slow but sustained contraction. When another aortic ring from the same aorta was contracted to 1 g preload, ET-1 caused additional concentration-dependent contraction. In other aortic rings precontracted to higher preloads (2 to 4 g), low concentrations of ET-1 caused relaxation, whereas higher concentrations induced contraction. The relaxation is very rapid as the preload is increased (bottom panel).

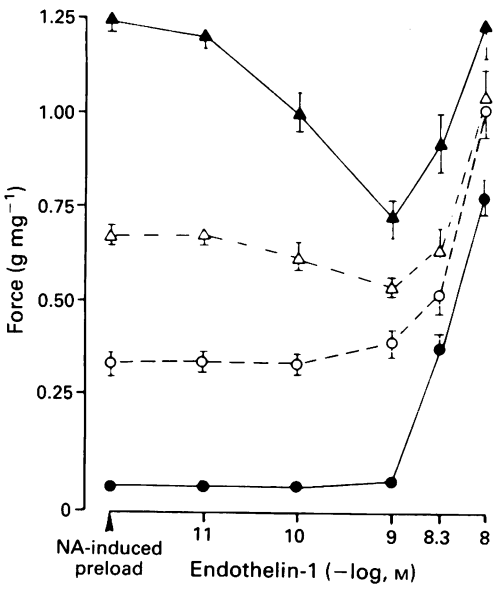

Figure 2 Dual vasoconstrictor and relaxant effects of endothelin-1 (ET-1) on rat aortic rings exposed to various preloads. Data from 4 to 8 experients are presented as mean with s.e. shown by vertical bars.

Discussion

The observations of variable effects of ET-1 on rat aortic rings precontracted to different tensions with NA *in vitro* are novel. At low tension, ET-1 caused an additional contraction of rat aortic rings and the overall effect seemed to represent cumulative interaction between NA and ET-1. Tabuchi *et al.* (1989) also demonstrated potentiation of the vasoconstrictor effects of catecholamines by ET-1. At higher NA-induced tensions, low concentrations of ET-1 ($\leqslant 5 \times 10^{-9}$ M) relaxed the vascular rings, whereas high concentrations ($\geqslant 10^{-8}$ M) induced marked contraction. These dual effects were particularly striking in rings exposed to a tension of 3 to 4 g above the baseline preload when the lowest concentration of ET-1-induced a consistent and prompt relaxation (Figure 2). In contrast to the relaxant effect of ET-1 in NA-precontracted rings is the total absence of ET-1-mediated relaxation in manually stretched rings (Table 1). These observations imply

Table 1 Effect of endothelin-1 (ET-1) on manually stretched rings

	Tension (g mg^{-1})				
Manual stretch		*ET-1* (− log M)			ACh (− log M)
(g)	11	10	9	8	6
1	0.3 ± 0.1	0.4 ± 0.1	0.5 ± 0.2	1.3 ± 0.3	1.3 ± 0.4
2	0.7 ± 0.1	0.8 ± 0.2	1.0 ± 0.2	1.5 ± 0.3	1.4 ± 0.3
4	1.4 ± 0.2	1.5 ± 0.3	1.5 ± 0.3	2.0 ± 0.3	1.9 ± 0.3

Data from 4 experiments as mean ± s.e. Manually stretched rings were exposed to cumulative doses of ET-1 followed by a single dose of acetylcholine. ET-1 did not cause relaxation in any of the rings.

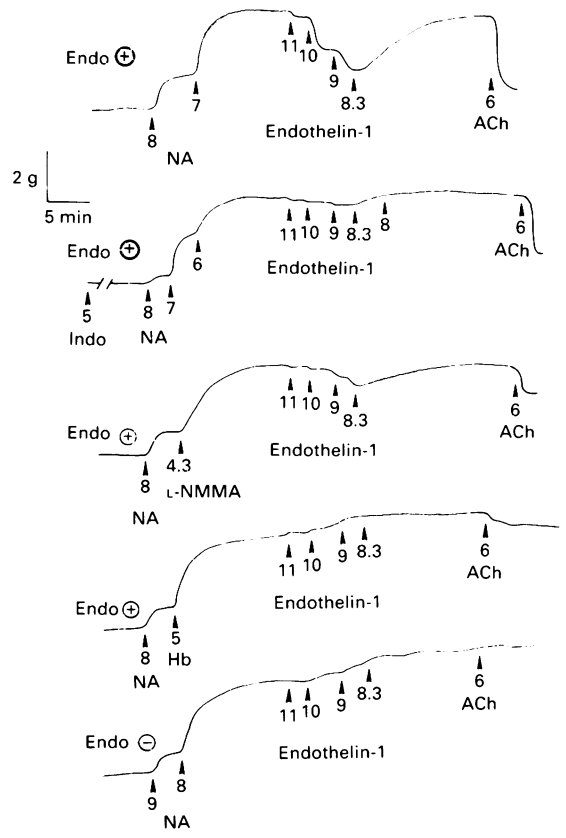

Figure 3 Representative experiments showing mechanism of endothelin-1 (ET-1)-mediated relaxation. Both indomethacin (Indo) and the EDRF synthesis inhibitor N^G-monomethyl-L-arginine (L-NMMA) attentuated the relaxant effect of ET-1, whereas oxyhaemoglobin (Hb) and removal of endothelium (Endo-) abolished the vasorelaxation.

that vascular stretch caused by pharmacological means alters the vascular response to ET-1 in a fashion that is not observed in manually stretched rings.

With respect to the mechanism of ET-1-induced relaxation of NA-precontracted rat aortic rings, it appears that both cyclo-oxygenase products and EDRF are important mediators, since both indomethacin and L-NMMA (competitive inhibitor of EFRF synthesis) decreased the ET-1-mediated relaxation. In contrast to inhibition of relaxation by indomethacin and L-NMMA, oxyhaemoglobin, which binds to EDRF (Martin *et al.*, 1985; Dinerman *et al.*, 1991) and stimulates synthesis of vascular smooth muscle constrictor

Table 3 Guanosine 3':5'-cyclic monophosphate (cyclic GMP) accumulation in rat aortic rings

	Cyclic GMP (fmol mg^{-1})
Quiescent tissues	39 ± 10
NA-precontracted rings	69 ± 15†
NA + ACh	301 ± 71¶
ET-1 (10^{-8} M)-contracted rings	52 ± 5
NA + ET-1 (10^{-8} M)	137 ± 43*
Manual stretch + ET-1 (10^{-8} M)	78 ± 40

Data from 4 experiments as mean ± s.e. Noradrenaline (NA) was used in a concentration required to achieve 4 g of tension. In other experiments, rings were manually stretched to 4 g of tension. ACh-acetylcholine.
†$P<0.02$ vs quiescent rings.
¶$P<0.02$ vs control NA-precontracted rings.
*$P<0.02$ vs NA-or endothelin-1 (ET-1) precontracted or manually stretched rings.

prostaglandins (Toda, 1990), abolished ET-1-mediated relaxation. Particularly noteworthy is the observation that ET-1 failed to cause any relaxation of de-endothelialised rings, indicating that ET-1 induced relaxation is dependent on intact endothelium.

The importance of EDRF release became apparent from cyclic GMP measurements which increased in NA-precontracted rings exposed to ET-1. A similar increase in cyclic GMP in response to ET-1 in rat aortic segments with intact endothelium has recently been shown by Topouzis *et al.* (1991). Importantly, NA induced contraction was associated with almost a doubling of cyclic GMP accumulation. It may be proposed that ET-1 at low concentrations augments NA-mediated cyclic GMP accumulation, whereas high concentrations of ET-1 overcome the release of EDRF.

Previous studies in a variety of blood vessels from different animals (Cocks & Angus, 1983; Griffith *et al.*, 1984; Sakuma *et al.*, 1987; Lawson *et al.*, 1989) show that EDRF is released from endothelium in response to high concentrations of agonists. This release of EDRF may not be antagonized by specific receptor blockers (Lawson *et al.*, 1989), suggesting that EDRF is released from endothelium when vascular tension increases in response to a pharmacological stimulus. Increase in blood flow in human coronary arteries with intact and functional endothelium is also associated with release of EDRF; and this release of EDRF is diminished when endothelium is dysfunctional (Nabel *et al.*, 1990). The present observations of ET-1-mediated aortic ring relaxation when the tension was increased pharmacologically and the inhibition of relaxation by L-NMMA or oxyhaemoglobin are in accordance with this concept.

Rae *et al.* (1989) documented release of eicosanoids,

Table 2 Effect of indomethacin, N^G-monomethyl-L-arginine (L-NMMA), oxyhaemoglobin and removal of endothelium on endothelin-1 (ET-1)-mediated rat aortic ring relaxation

	Tension (g mg^{-1}) *Endothelin-1* (− log M)					
Treatment	*0*	*11*	*10*	*9*	*8.3*	*8*
Buffer alone ($n=8$)	1.24 ± 0.04	1.21 ± 0.03	1.03 ± 0.04	0.73 ± 0.06	0.93 ± 0.12	1.23 ± 0.10
Indomethacin ($n=4$)	1.21 ± 0.05	1.21 ± 0.05	1.20 ± 0.06†	1.10 ± 0.10†	1.20 ± 0.10*	1.22 ± 0.10
L-NMMA ($n=4$)	1.23 ± 0.05	1.23 ± 0.06	1.21 ± 0.08†	1.05 ± 0.07†	1.20 ± 0.08*	1.24 ± 0.07
Oxyhaemoglobin ($n=4$)	1.22 ± 0.04	1.24 ± 0.06	1.27 ± 0.10†	1.29 ± 0.08†	1.31 ± 0.06*	1.32 ± 0.07
Removal of endothelium ($n=4$)	1.23 ± 0.06	1.23 ± 0.07	1.28 ± 0.11†	1.30 ± 0.06†	1.33 ± 0.07*	1.38 ± 0.08

Data are expressed as mean ± s.e.
Tension before endothelin-1 was same in all rings.
†$P<0.01$ and *$P<0.05$, both as compared to endothelin-1-mediated relaxation in buffer alone-treated vascular rings.

mainly prostaglandin E_2 (PGE_2) and to a lesser extent PGI_2 and thromboxane A_2 (TxA_2) from perfused kidney and spleen of rabbits in response to ET-1. Mehta *et al.* (1984) showed that administration of TxA_2-cyclic endoperoxide analog U46,619 in intact dogs is associated with release of eicosanoids, PGI_2 and TxA_2. These observations of eicosanoid release in response to different and unrelated vasoconstrictors suggest that cyclo-oxygenase products are released from endothelium in an attempt to autoregulate vascular tone, when intraluminal stress increases. Our observation of blunting of vasorelaxant effect of low concentrations of ET-1 by indomethacin may be a manifestation of NA-induced release of arachidonate metabolites. Some other investigators, however, have not identified attenuation of the vasodepressor effects of ET-1 in rats, cats or piglets by indomethacin (Bradley *et al.*, 1990; de Nucci *et al.*, 1988; Hasunuma *et al.*, 1990; Lippton *et al.*, 1989; Perreault & De Marte, 1991). The precise reasons for this disparity are not known, but the *in vitro* nature of the present studies (vs. the *in vivo* studies by others) may relate to these differences.

The importance of the dual actions of ET-1 depending on its concentration is exemplified by some recent studies. de Nucci *et al.* (1988) observed ET-1-mediated rise in arterial pressure in rats with low blood pressure (low preload) and a decrease in arterial pressure in rats with high blood pressure (high preload). In studies in newborn piglets (Bradley *et al.*, 1990), low doses of ET-1 increased coronary blood flow, whereas high doses of ET-1 had the opposite effect. Perreault & De Marte (1991) have recently shown ET-1-induced concentration-dependent contraction of pulmonary vasculature of the newborn pig where the baseline pressure was low; however, in accordance with our studies they observed relaxation of pulmonary vasculature by low concentrations of ET-1 when the baseline pressure was high.

An important aspect of the present study relates to the effect of ET-1 on manually stretched rings. These rings were stretched to the same tension as the pharmacologically-treated rings which demonstrated relaxation and cyclic GMP accumulation in response to low concentrations of ET-1. ET-1 caused a concentration-dependent contraction in these rings without any evidence for relaxation or cyclic GMP accumulation. ACh also did not relax the manually stretched rings. These observations suggest that NA treatment results in active tension of the vessel wall and primes or modulates the endothelium in a fashion that ET-1 and ACh become inducers of EDRF release. Vascular ring contraction in response to the thromboxane A_2 receptor agonist, U46,619, has also been associated with EDRF release from rat aortic rings with intact endothelium, and the contractile response to this agonist is enhanced in the presence of EDRF inhibitors or when the endothelium has been removed (Dinerman & Mehta, 1990; Folger *et al.*, 1991). It is possible that low concentrations of ET-1 potentiate EDRF release by NA in rat aortic rings and other vascular tissues with intact endothelium. On the other hand, manual fixed stretch of the rat aortic rings will not permit their tension to decrease in response to ET-1 or ACh. However, when the manually stretched rings are further contracted with NA to an additional 2–3 g of tension, both ET-1 and ACh promptly induce vasodilatation (data not shown). In this regard, high vascular tension in the *in vivo* settings represents pharmacological tension in the tissues, and ET-1 promptly decreases arterial tone. However, high concentrations of ET-1 will consistently override the effect of EDRF and cause contraction of the vascular tissues both *in vitro* and *in vivo*.

In summary, this study shows concentration-dependent arterial relaxant and constrictor effects of ET-1. This substance may serve to regulate vascular tone by inducing release of EDRF and cyclo-oxygenase products in physiological states, but exert potent vasoconstrictor influence on the vascular smooth muscle when endothelial function is not intact. In conditions of endothelial dysfunction, such as acute myocardial ischaemia and renal insufficiency, high circulating levels of ET-1 (Miyauchi *et al.*, 1989; Salminen *et al.*, 1989; Tomita *et al.*, 1989; Stewart *et al.*, 1991) may have a role in the genesis and perpetuation of tissue ischaemia.

These studies were supported by a Merit Review Award from the Veterans Affairs Medical Center and a grant-in-aid from the American Heart Association, Florida Affiliate, St. Petersburg, FL, U.S.A.

References

BRADLEY, L.M., CZAJA, J.F. & GOLDSTEIN, R.E. (1990). Circulatory effects of endothelin in newborn piglets. *Am. J. Physiol.*, **259,** H1613–H1617.

COCKS, T.M. & ANGUS, J.A. (1983). Endothelium-dependent relaxation of coronary arteries by noradrenaline and serotonin. *Nature*, **305,** 627–630.

DE NUCCI, G., THOMAS, R., D'ORLEANS-JUSTE, P., ANTUNES, E., WALDER, C., WARNER, T.D. & VANE, J.R. (1988). Pressor effects of circulating endothelin are limited by its removal in the pulmonary circulation and by the release of prostacyclin and endothelium-derived relaxing factor. *Proc. Natl. Acad. Sci. U.S.A.*, **85,** 9797–9800.

DINERMAN, J.L. & MEHTA, J.L. (1990). Endothelial, platelet and leukocyte interaction in ischemic heart disease: Insights into potential mechanisms and clinical relevance. *J. Am. Coll. Cardiol.*, **16,** 207–222.

DINERMAN, J.L., LAWSON, D.L. & MEHTA, J.L. (1991). Interaction between nitroglycerin and endothelium in vascular smooth muscle relaxation. *Am. J. Physiol.*, **260,** H698–H701.

FOLGER, W.H., LAWSON, D.L., WILCOX, C.S. & MEHTA, J.L. (1991). Response of rat thoracic aortic rings to thromboxane mimetic U-46, 619: roles of EDRF and TxA_2 release. *J. Pharmacol. Exp. Ther.*, **258,** 669–675.

FURCHGOTT, R.F. & ZAWADSKI, J. (1980). The obligatory role of endothelial cells in the relaxation of arterial smooth muscle by acetylcholine. *Nature*, **288,** 373–376.

GRIFFITH, T.M., EDWARDS, D.H., LEWIS, M.J. & HENDERSON, A.H. (1984). Ergonovine-induced arterial dilatation: an endothelium-mediated effect. *J. Mol. Cell. Cardiol.*, **16,** 479–482.

HASUNUMA, K., RODMAN, D.M., O'BRIEN, R.F. & MCMURTRY, I.F. (1990). Endothelin-1 causes pulmonary vasodilatation in rats. *Am. J. Physiol.*, **259,** H48–H54.

LAWSON, D.L., MEHTA, J.L., MEHTA, P. & NICHOLS, W.W. (1989). Endothelium-dependent relaxation of rat aorta rings by leukotriene D_4: Importance of the magnitude of preload. *Eicosanoids*, **2,** 175–181.

LIPPTON, H., GOFF, J. & HYMAN, A. (1988). Effects of endothelin in the systemic and renal vascular beds *in vivo*. *Eur. J. Pharmacol.*, **155,** 197–199.

LIPPTON, H., MCMURTRY, I.F. & HYMAN, A. (1989). Pulmonary vasodilation by endothelin is mediated by potassium channels. *FASEB. J.* **4,** A813.

MARTIN, W., VILLANI, G.M., JOTHIANANDAN, D. & FURCHGOTT, R.F. (1985). Selective blockade of endothelium-dependent and glyceryl trinitrate-induced relaxation by hemoglobin and by methylene blue in the rabbit aorta. *J. Pharmacol. Exp. Ther*, **232,** 7081–7161.

MEHTA, J.L., NICHOLS, W.W. & GOLDMAN, R. (1984). Prostacyclin release following endoperoxide analog infusion in the intact dog. *Am. J. Physiol.*, **246,** R205–R210.

MILLER, V.M., KOMORI, K., BURNETT, J.C, Jr, & VANHOUTTE, P.M. (1989). Differential sensitivity to endothelin in canine arteries and veins. *Am. J. Physiol.*, **257,** H1127–H1131.

MIYAUCHI, T., YANAGISAWA, M., TOMIZAWA, T., SUGISHITA, Y., SUZUKI, N., FUJINO, M., AJISAKA, R., GOTO, K. & MASAKI, T. (1989). Increased plasma concentrations of endothelin-1 and big endothelin-1 in acute myocardial infarction. *Lancet*, **i,** 53–54.

NABEL, E.G., SELWYN, A.P. & GANZ, P. (1990). Large coronary arteries in humans are responsive to changing blood flow: an endothelium-dependent mechanism that fails in patients with atherosclerosis. *J. Am. Coll. Cardiol.*, **16,** 349–356.

PERREAULT, T. & DE MARTE, J. (1991). Endothelin-I has a dilator effect on neonatal pig pulmonary vasculature. *J. Cardiovasc. Pharmacol.*, **18,** 3–50.

RAE, G.A., TRYBULEC, M., DE NUCCI, G. & VANE, J.R. (1989). Endothelin-1 releases eicosanoids from rabbit isolated perfused kidney and spleen. *J. Cardiovasc. Pharmacol.*, **13,** (Suppl. 5), 89–92.

SAKUMA, T., GROSS, S.S. & LEVI, R. (1987). Peptidoleukotrienes induce an endothelium-dependent relaxation of guinea pig main pulmonary artery and thoracic aorta. *Prostaglandins*, **34,** 685–695.

SALMINEN, K., TIKKANEN, I., SAIJONMAA, O., NIEMINEN, M., FYHRQUIST, F. & FRICK, M.H. (1989). Modulaton of coronary tone in acute myocardial infarction by endothelin. *Lancet*, **ii,** 747.

STEWART, D.J., KUBAC, G., COSTELLO, K.B. & CERNACEK, P. (1991). Increased plasma endothelin-1 levels in the early hours of acute myocardial infarction. *J. Am. Coll. Cardiol.*, **18,** 38–43.

TABUCHI, Y., NAKAMARU, M., RAKUGI, H., NAGANO, M. & OGIHARA, T. 1989). Endothelin enhances adrenergic vasoconstriction in perfused rat mesenteric arteries. *Biochem. Biophys. Res. Commun.*, **159,** 1304–1308.

TODA, N. (1990). Mechanism of contracting action of oxyhemoglobin in isolated monkey and dog cerebral arteries. *Am. J. Physiol.*, **258,** H57–H63.

TOMITA, K., OJILE, K., NAKANISHI, T., TOMURA, S., MATSUDA, O. ANDO, K., SHICHIRI, M., HIRATA, Y. & MARUNO, F. (1989). Plamsa endothelin levels in patients with acute renal failure. *N. Engl. J. Med.*, **321,** 1127.

TOPOUZIS, S., HUGGINS, J.P., PELTON, J.T. & MILLER, R.C. (1991). Modulation by endothelium of the responses induced by endothelin-1 and by some of its analogues in rat isolated aorta. *Br. J. Pharmacol.*, **102,** 545–549.

WARNER, T.D., MITCHELL, J.A., DE NUCCI, G. & VANE, J.R. (1989). Endothelin-1 and endothelin-3 release EDRF from isolated perfused arterial vessels of the rat and rabbit. *J. Cardiovasc. Pharmacol.*, **13**(Suppl. 5), 85–88.

YANAGISAWA, M., KURIHARA, H., KIMURA, S., TOMOBE, M., KOBAYASHI, M., MITSUI, Y., YAZAKI, Y., GOTO, K. & MASAKI, T. (1988). A novel potent vasoconstrictor peptide produced by vascular endothelial cells. *Nature*, **332,** 411–415.

(Received August 1, 1991
Revised January 18, 1992
Accepted January 23, 1992)

Br. J. Pharmacol. (1992), **106**, 133–138 © Macmillan Press Ltd, 1992

The pharmacological modulation of thrombin-induced cerebral thromboembolism in the rabbit

[1]G.R. May, W. Paul, P. Crook, *K.D. Butler & [2]C.P. Page

Department of Pharmacology, King's College, University of London, Manresa Road, London SW3 6LX and *Ciba-Geigy Pharmaceuticals Ltd., Wimblehurst Road, Horsham, West Sussex

1 Intracarotid (i.c.) administration of thrombin induced a marked accumulation of ^{111}indium-labelled platelets and ^{125}I-labelled fibrinogen within the cranial vasculature of anaesthetized rabbits.

2 Thrombin (100 iu kg^{-1}, i.c.) – induced platelet accumulation was completely abolished by pretreatment with desulphatohirudin (CGP 39393; 1 mg kg^{-1} i.c., 1 min prior to thrombin). Administration of CGP 39393 1 or 20 min after thrombin produced a significant reduction in platelet accumulation.

3 Intravenous (i.v.) administration of the platelet activating factor (PAF) receptor antagonist BN 52021 (10 mg kg^{-1}) 5 min prior to thrombin (100 iu kg^{-1}, i.c.) had no effect on platelet accumulation.

4 An inhibitor of NO biosynthesis, L-N^G-nitro arginine methyl ester (L-NAME; 100 mg kg^{-1}, i.c.), had no significant effect on the cranial platelet accumulation response to thrombin (10 iu kg^{-1}, i.c.) when administered 5 min prior to thrombin.

5 Defibrotide (32 or 64 mg kg^{-1} bolus i.c. followed by 32 or 64 mg kg^{-1} h^{-1}, i.c., infusion for 45 min) treatment begun 20 min after thrombin (100 iu kg^{-1}, i.c.) did not significantly modify the cranial platelet accumulation response.

6 Cranial platelet accumulation induced by thrombin (100 iu kg^{-1}, i.c.) was significantly reversed by the fibrinolytic drugs urokinase (20 iu kg^{-1}, i.c., infusion for 45 min), anisoylated plasminogen streptokinase activator complex (APSAC) (200 μg kg^{-1}, i.v. bolus) or recombinant tissue plasminogen activator (rt-PA; 100 μg kg^{-1}, i.c. bolus followed by 20 μg kg^{-1} min^{-1}, i.c., infusion for 45 min) administered 20 min after thrombin. APSAC had no significant effect when administered 3 h after thrombin.

7 APSAC (200 μg kg^{-1}, i.v. bolus) significantly reversed thrombin (100 iu kg^{-1}, i.c.) – induced intracranial accumulation of ^{125}I-fibrinogen when administered 20 min after thrombin.

8 These results suggest that neither endogenous PAF nor NO modulate thrombin-induced intracranial platelet accumulation in the rabbit. However, fibrin deposition appears to play an important role as shown by the ability of fibrinolytic agents to reverse platelet and fibrinogen accumulation induced by i.c. thrombin.

Keywords: Platelets; cerebral vasculature; thromboembolism in rabbit

Introduction

Tissue damage, resulting from ischaemia, is a common causative factor in producing the pathological changes associated with clinical conditions such as stroke and occlusive heart disease. Our understanding of the precise mechanisms involved in eliciting ischaemia or the appropriate pharmacological intervention is far from complete. A limiting factor to our understanding of the condition is the availability of convenient and reliable animal models.

Approximately 80% of strokes are thromboembolic in origin (Mohr *et al.*, 1978), the remainder being due to cerebral haemorrhage. Several attempts have been made to develop suitable models of ischaemic stroke either by reducing blood oxygen supply to the whole animal or by ligating vessels to reduce the blood supply to the whole brain or selected areas of the brain. Models of global ischaemia (Levine & Klein, 1960; Levine & Sohn, 1969) are attractive due to their simplicity but bear little relation to the clinical condition, whereas models of focal ischaemia (Anthony *et al.*, 1963; Sundt & Waltz, 1966; Bederson *et al.*, 1986) require invasive surgery. The production of ischaemia by the injection of microspheres (Hegedus *et al.*, 1985) or homologous blood clots (Kaneko *et al.*, 1985; Penar, 1987) reduces invasiveness, but at the expense of reproducibility of the size and location of the infarct created. Such models are useful for studying post-ischaemic events in brain tissue. However, they provide no information regarding the development of the thrombotic event(s) responsible for the ischaemia. This is thought to involve the interaction of blood elements such as platelets, fibrin and possibly neutrophils with the vessel wall.

We have recently described a model for investigating platelet function in the rabbit *in vivo*. In this system, platelet accumulation in the cranium can be induced by intracarotid administration of thrombin (May *et al.*, 1990). This response is not produced by intravenous injection of thrombin or by intracarotid injection of other platelet agonists such as ADP, PAF or collagen (May *et al.*, 1990). The precise mechanism of this thrombin-induced platelet accumulation in the cranial vasculature remains to be determined. The present study has investigated the action of a PAF antagonist (BN 52021), a thrombin inhibitor (hirudin) and an inhibitor of NO synthase (L-N^G-nitroarginine methyl ester, L-NAME) on thrombin-induced platelet accumulation in order to ascertain the involvement of endogenously generated PAF, NO and thrombin in these processes. Furthermore, we have investigated the ability of various fibrinolytic drugs to reverse the established thrombosis in order to elucidate the role of generated fibrin in these thrombotic events.

[1] Present address: Syntex Research Centre, Department of Pharmacology, Herriot Watt Research Park, Riccarton, Edinburgh EH14 4AP.

[2] Author for correspondence.

Methods

Experimental animals

The study was carried out on rabbits (New Zealand White, Froxfield, Petersfield, Hampshire, U.K.) of either sex weighing 2.5 to 3.5 kg. Animals received a standard diet and water *ad libitum*.

Preparation of animals

The rabbits were anaesthetized with a combination of diazepam (5 mg kg^{-1}, i.p.) followed 10 min later by fentanyl citrate 0.315 mg ml^{-1} and fluanisone 10 mg ml^{-1} (Hypnorm, 0.4 ml kg^{-1}, i.m.). Anaesthesia was maintained by i.m. injections of Hypnorm (0.1 ml kg^{-1}) as necessary (approximately 30 min intervals). The left common carotid artery was cannulated in the direction of blood flow for the administration of thrombin and drugs. Intravenous administrations were made into a marginal ear vein.

^{111}Indium-labelling of platelets

Full details of the protocol for isolation and radiolabelling of rabbit platelets have been described elsewhere (May *et al.*, 1990; Thiemermann *et al.*, 1990). Briefly, blood (9 ml) obtained from a marginal ear vein was collected into 1 ml of 3.8% (w/v) trisodium citrate and centrifuged (200 *g*, 10 min) to obtain platelet-rich plasma (PRP). The platelets were then washed by centrifugation (640 *g*, 15 min) in a calcium-free Tyrode solution containing prostaglandin E_1 (PGE_1, 300 ng ml^{-1}) (CFTP). After removal of the supernatant, the surface of the platelet pellet was carefully rinsed with 1 ml CFTP. The platelets were gently resuspended in 1 ml of CFTP and incubated for 1.5 min at 37°C with ^{111}indium oxine (25–50 μCi). After a further centrifugation (640 *g*, 15 min) to remove any excess, unbound ^{111}indium, the platelet pellet was resuspended in CFTP (1 ml/recipient rabbit). The labelled platelets were administered to anaesthetized recipient rabbits via a marginal ear vein.

^{125}Iodine-labelled fibrinogen

^{125}Iodine-labelled human fibrinogen, purchased from Amersham International plc., was reconstituted in sterile saline; 100 μCi of label was injected intravenously into each recipient animal.

Monitoring of radiolabelled blood elements within the circulation

Radioactivity associated with ^{111}indium-labelled platelets or ^{125}I-labelled human fibrinogen was continuously monitored by means of one inch crystal scintillation detectors placed over the thorax (to measure changes in the pulmonary circulation) and head (to measure changes in the cerebral circulation). Counts were estimated with a multi-channel spectrometer (Nuclear Enterprises NE 461) and logged with the aid of a special application interface (AIMS 8000, Mumed Ltd.) by a microcomputer (Dell System 200).

Responses to intracarotid administration of thrombin were measured as changes in radioactivity from baseline values and expressed as % increase in counts. The area under the curve of the agonist-induced % increase in counts was then calculated by computer-assisted planimetry, to give a measure of the response over the monitored time course.

Pharmacological modulation of cerebral thromboembolism

Animals were prepared for experimentation as described above. Radiolabelled platelets or fibrinogen, administered in a volume of 1 ml into a marginal ear vein, were allowed to equilibrate with the endogenous blood elements for at least 1 h.

Each animal received a bolus dose of adenosine diphosphate (ADP, 100 μg kg^{-1}, i.c.) in order to determine whether the platelets were functioning normally and also to eliminate any platelets that might have been damaged during the labelling procedure (May *et al.*, 1990).

After a further 30 min, a bolus dose of thrombin (100 iu kg^{-1}, i.c.) was administered, except for the experiments with D- and L-NAME where 10 iu kg^{-1} was given (to assess possible potentiation). The response to the bolus dose of thrombin was then monitored continuously for 3–6 h, according to the investigation being carried out.

Separate groups of animals were used for each drug treatment and for controls. All controls received either saline or vehicle administration in identical fashion to the treated groups.

A variety of pharmacological agents were studied:

Recombinant desulphatohirudin (CGP 39393)

CGP 39393 (specific activity 11,600 anti-thrombin units mg^{-1}) was prepared in saline and administered as a bolus dose of 1 mg kg^{-1} i.c. to animals with ^{111}indium-labelled platelets. One group ($n = 3$) was pretreated with CGP 39393 1 min before the administration of thrombin while second and third groups received the CGP 39393 1 ($n = 5$) and 20 ($n = 7$) min, respectively, after the administration of thrombin.

BN 52021

BN 52021 was prepared in the supplied vehicle and administered as a bolus dose of 10 mg kg^{-1} i.v. to animals with ^{111}indium-labelled platelets 5 min before the intracarotid injection of thrombin.

Urokinase

Urokinase (from human kidney cells) was prepared in saline and administered as an infusion (20 i.u., i.c.) to animals with ^{111}indium-labelled platelets. The infusion was started 20 min after the administration of thrombin and was continued for 45 min at a rate of 0.1 ml min^{-1}.

APSAC

APSAC (batch number 046, manufactured 9/2/88) was prepared in saline and administered as a bolus dose of 200 μg kg^{-1} i.v. Since deacylation of this compound begins immediately upon reconstitution (Smith *et al.*, 1982), the drug was reconstituted not more than 10 min before injection.

In animals with ^{111}indium-labelled platelets, APSAC was administered 20 min or 3 h after thrombin administration.

In another group of animals with circulating ^{125}I-fibrinogen, APSAC was administered 20 min after intracarotid thrombin administration.

L and D-N^G-nitroarginine methyl ester

L-NAME and D-NAME were prepared in saline. Separate groups of animals with circulating ^{111}In-labelled platelets received a bolus dose of 100 mg kg^{-1}, i.c., of each substance. The injections were made 5 min before injection of thrombin (10 iu kg^{-1}, i.c.).

Recombinant tissue-plasminogen activator (rt-PA)

Lyophilised rt-PA prepared in Chinese hamster ovary cells was dissolved in sterile saline. Animals with circulating ^{111}In-platelets were treated with rt-PA 20 min after injection of thrombin (100 iu kg^{-1}, i.c.). Each animal received a bolus injection of 100 μg kg^{-1}, i.c. followed by an intracarotid

infusion of 20 μg kg^{-1} min^{-1} for 45 min, at a rate of 0.06 ml min^{-1}.

Defibrotide

Defibrotide was prepared in sterile saline. One group of animals received a bolus dose of 32 mg kg^{-1}, i.c., followed by an intracarotid infusion of 32 mg kg^{-1} h^{-1} for 45 min. A second group was treated in a similar fashion with a higher dose of 64 mg kg^{-1}, i.c., bolus plus 64 mg kg^{-1}h^{-1} intracarotid infusion for 45 min. All treatments were begun 20 min after injection of thrombin (100 iu kg^{-1}, i.c.). The infusion rate was 0.06 ml min^{-1}.

Drugs

Drugs used in this study were obtained from the following sources: diazepam (Valium) (Roche, Welwyn Garden City); Hypnorm (Janssen Pharmaceuticals); thrombin, L-NAME, prostaglandin E_1 (PGE_1), urokinase and ADP (Sigma Chemicals); D-NAME (Bachem); recombinant desulphatohirudin (CGP 39393) (a gift from Ciba Geigy Pharmaceuticals, Horsham); APSAC (a gift from Smith Kline Beecham Pharmaceuticals, Great Burgh); defibrotide (a gift from Dr G. Bianchi, Crinos SpA, Villa Guardia, Como, Italy); rt-PA (a gift from Dr Karl Thomae GmbH, Biberach-an-der-Riss, Germany); BN 52021 ([3-(1,1-dimethylethyl)hexahydro-1,4, 47B- trihydroxy- 8-methyl-9H-1,7 (epoxymethanol) -14,6αH_2-cyclopenta(c)furo[2,3b]furo[3',2'3,4]cyclopenta[1,2-d]furah-5,-9, 12(4H)-trione]; a gift from Dr P. Braquet, Institute Henri Beaufort, Le Plessis Robinson, France).

Statistics

Results are presented as mean values ± standard errors of the means (s.e.mean). Following an analysis of variance, the significance of differences between means was assessed by Student's *t* test (unpaired), a Mann Whitney U test or Wilcoxon test as appropriate.

Results

Recombinant desulphatohirudin

Pretreatment of animals with the thrombin inhibitor CGP 39393 (1 mg kg^{-1}, i.c.) 1 min prior to thrombin 100 iu kg^{-1}, i.c., completely abolished the accumulation of radiolabelled platelets in the cranial vasculature (Figure 1a). Treatment of the rabbits with the same dose (1 mg kg^{-1}, i.c.) 1 min (Figure 1a) or 20 min (Figure 1b) after thrombin administration produced smaller but significant ($P<0.05$) reductions (41 and 35% respectively) in the accumulation of platelet-associated radioactivity seen in response to thrombin.

BN 52021

Pretreatment of the rabbits with the PAF antagonist BN 52021 (10 mg kg^{-1}, i.v.) 5 min before the administration of thrombin (100 iu kg^{-1}, i.c.) had no significant effect on the accumulation of radiolabelled platelets in the cranial vasculature (Table 1).

Fibrinolytic agents

Administration of the fibrinolytic agents urokinase (20 u, i.c. infusion) (Figure 2a), rt-PA (100 μg kg^{-1} bolus, 20 μg kg^{-1} min^{-1} infusion, i.c.) (Figure 2b) or APSAC (200 μg kg^{-1} bolus, i.v.) (Figure 3a) 20 min after thrombin administration produced significant ($P<0.05$) reversal of the thrombin-induced platelet accumulation in the cranial vasculature. In addition, APSAC administered 20 min after the administration of thrombin was found to reverse significantly ($P<0.05$, Mann Whitney U test) the accumulation of fibrin(ogen) associated radioactivity in the cranial vasculature (Figure 3b). When administered 3 h after the initiation of the cerebral thromboembolism induced by thrombin, APSAC failed to produce a significant reversal of the accumulation of radiolabelled platelets (Figure 3c).

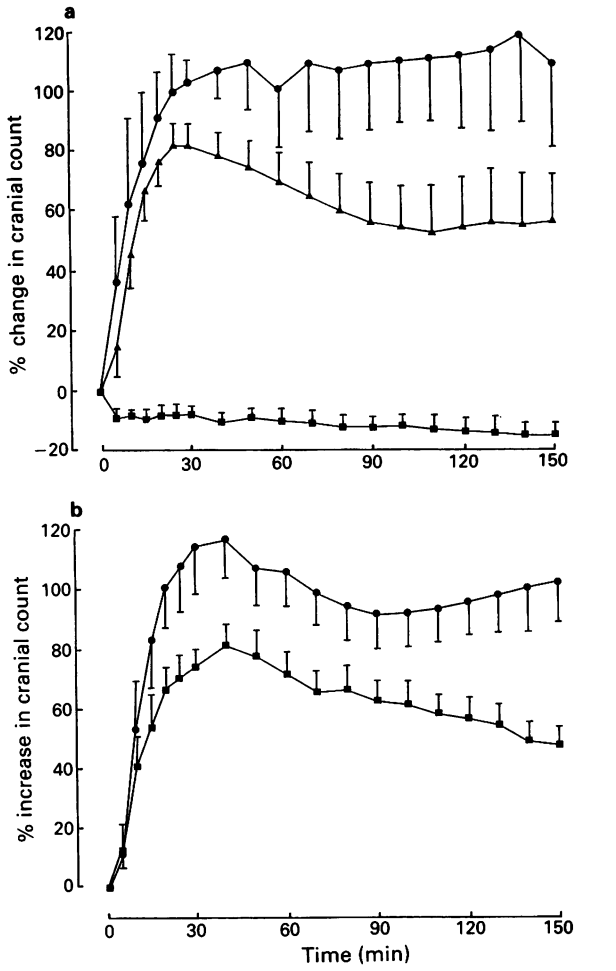

Figure 1 Percentage change in cranial counts plotted against time in rabbits with circulating ^{111}In-labelled platelets. Thrombin (100 iu kg^{-1}, i.c.) was injected at time 0 in all animals. In (a), groups of animals were treated i.c. with saline ($n=4$), 1 min after thrombin (●) or with CGP 39393 (1 mg kg^{-1}) ($n=3$) 1 min before (■) or ($n=5$) 1 min post (▲) thrombin. In (b), groups of animals were treated i.c. with saline ($n=7$) (●) or CGP 39393 ($n=5$) (■) 20 min post thrombin. Values shown are mean with s.e.mean indicated by vertical bars.

Defibrotide

Addition of defibrotide (32 mg kg^{-1} bolus plus 32 mg kg^{-1} h^{-1}, i.c., infusion or 64 mg kg^{-1} bolus plus 64 mg kg^{-1} h^{-1}, i.c., infusion) did not alter significantly the ability of intracartid thrombin to induce platelet accumulation in the cerebral vasculature (Table 1). There was a tendency for the maximal response to thrombin, at 30 min, to be reduced following treatment with the highest dose of defibrotide, but this did not achieve statistical significance (Table 1).

L and D-N^G-nitroarginine methyl ester

Intracarotid administration of L-NAME (100 mg kg^{-1}) or D-NAME (100 mg kg^{-1}) 5 min prior to thrombin failed to alter significantly the magnitude or duration of thrombin-induced platelet accumulation within the cranial vasculature (Table 1).

Table 1 Effect of some pharmacological agents on intracranial platelet accumulation in response to intracarotid thrombin

Treatment	*Max. response* (% increase)	*Area under curve* (over 150 min)	n
Thrombin 100 iu kg^{-1}, i.c.			
Saline	91 ± 23	118 ± 29	5
BN 52021 10 mg kg^{-1}, i.v.	99 ± 8	120 ± 15	5
Thrombin 100 iu kg^{-1}, i.c.			
Saline	100 ± 20	127 ± 33	4
DEF 32 mg kg^{-1}, i.c.*	66 ± 10	102 ± 17	4
Thrombin 100 iu kg^{-1}, i.c.			
Saline	99 ± 16	121 ± 11	4
DEF 64 mg kg^{-1}, i.c.*	87 ± 4	132 ± 7	4
Thrombin 10 iu kg^{-1}, i.c.			
Saline	38 ± 2	29 ± 4	4
D-NAME 100 mg kg^{-1}, i.c.	31 ± 4	27 ± 4	4
L-NAME 100 mg kg^{-1}, i.c.	28 ± 3	36 ± 5	4

Results expressed as mean ± s.e.mean percentage increase (above baseline) in ^{111}indium counts in the head.
*DEF = defibrotide. Dose shown is bolus dose which was followed by an i.c. infusion of the same dose in mg kg^{-1} h^{-1} for 45 min.

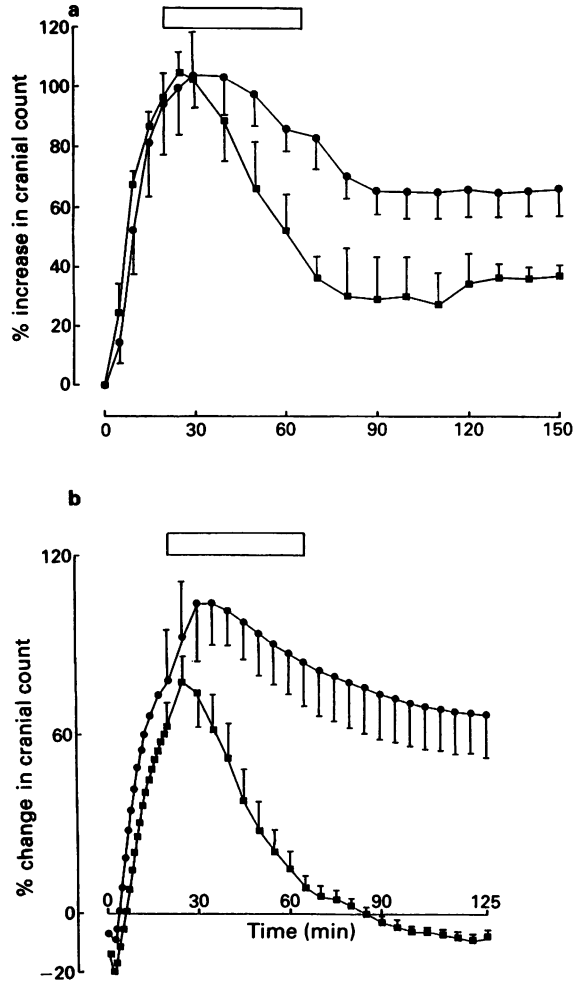

Figure 2 Percentage change in cranial counts plotted against time in rabbits with circulating ^{111}In-labelled platelets. Thrombin (100 iu kg^{-1}, i.c.) was injected at time 0 in all animals. In (a), groups of animals received an i.c. infusion of saline ($n = 5$) (●) or urokinase (20 i.u., $n = 5$) (■) over the time (45 min) dipicted by the bar. In (b), groups of animals received an i.c. bolus then infusion of saline ($n = 4$) (●) or recombinant tissue plasminogen activator (rt-PA, bolus 100 μg kg^{-1}, infusion 20 μg kg^{-1} min^{-1}) ($n = 4$) (■) over the time (45 min) depicted by the bar. Values shown are mean with s.e.mean indicated by vertical bars.

Discussion

Intracarotid thrombin induces a marked, sustained accumulation of labelled fibrin(ogen) and platelets within the cerebral vasculature. The precise nature of the platelet accumulation is not known. It is not likely to be due to simple passive trapping of platelet aggregates since, if this were the case, it would be expected that other platelet agonists such as ADP, collagen and PAF would produce the same effect (May *et al.*, 1990).

Thrombin has two main functions that are important in thrombosis, the conversion of fibrinogen into fibrin and the stimulation of platelet aggregation. It is becoming clear that thrombin plays a central role in thrombotic events (see Hemker & Beguin, 1986), being potent with respect to platelet aggregation and secretion in comparison to other endogenous platelet agonists. Thrombin is also capable of amplifying its own production through the activation of Factors V and VIII (Nesheim & Mann, 1979) and by the expression of phospholipids at the platelet surface (Tracy, 1988). In addition, thrombin can limit its formation via the activation of Protein C. It is, therefore, possible that although the administration of thrombin into the carotid artery acts as a trigger for the subsequent platelet accumulation seen in the cerebral vasculature, there is also further thrombin generation which is important for the overall extent and duration of the observed platelet response. In order to investigate this, use was made of the potent and selective thrombin inhibitor, hirudin. Recombinant desulphatohirudin (CGP 39393) achieves thrombin inhibition by the formation of a stable non-covalent 1:1 complex with thrombin, the formation of which is independent of other plasma factors. It has been shown to have effective anticoagulant and antithrombotic properties not only in venous thrombosis models but also in extracorporeal shunt models and models of arterial thrombosis (Markwardt *et al.*, 1982; Heras *et al.*, 1989; Talbot *et al.*, 1989). It is, therefore, potentially useful as a tool for determining the role of thrombin in thrombotic events.

The present results demonstrate that CGP 39393 administered 1 min before i.c. thrombin completely abolished the response, indicating that the accumulation of platelet-associated radioactivity in the cerebral vasculature was specifically initiated by thrombin. When CGP 39393 was administered after the intracarotid thrombin there was a reduced response, suggesting that there was some thrombin generation following the initial administration. However, this thrombin generation is not likely to be solely responsible for the maintenance of the response since the administration of CGP 39393 at 20 min was not capable of completely reversing the platelet accumulation. However, it is not known whether the

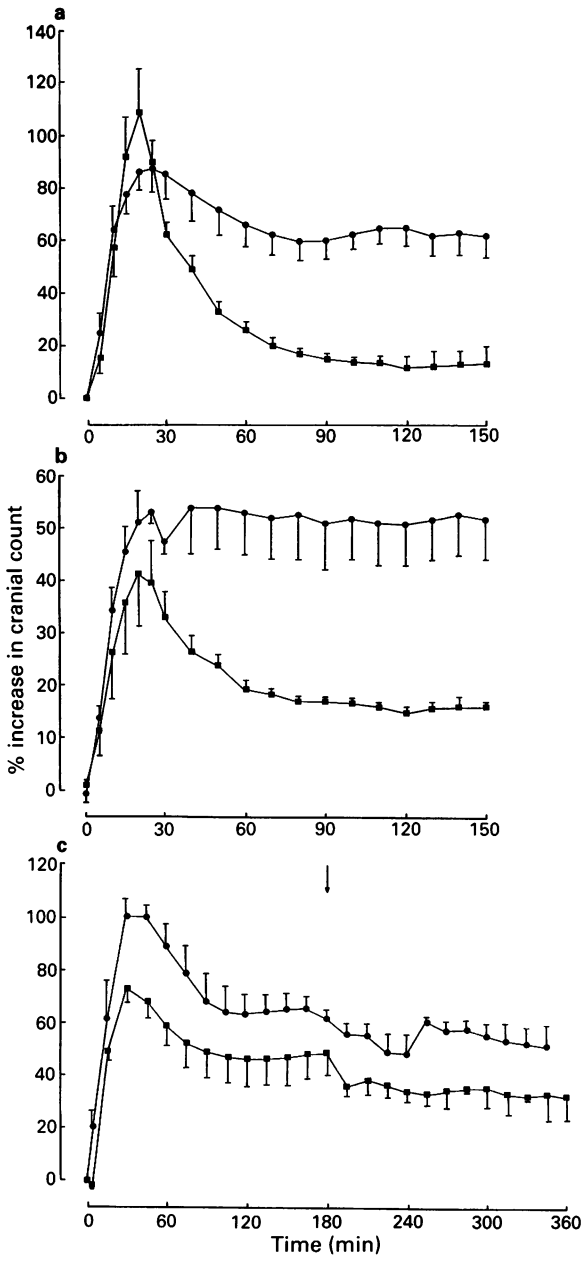

Figure 3 Percentage change in cranial counts plotted against time in rabbits with circulating ^{111}In-labelled platelets (a and c) or ^{125}I-human fibrinogen (b). Thrombin (100 iu kg^{-1}, i.c.) was injected at time 0 in all animals. In (a) and (b) groups of animals received an i.v. bolus injection of saline (●) or anisoylated plasminogen streptokinase activator complex (APSAC, 200 μg kg^{-1}) (■) 20 min after thrombin. In (c), groups of animals received an i.v. bolus injection of saline (●) or APSAC (200 μg kg^{-1}) (■) 3 h post thrombin. Values shown are the mean (s.e.mean shown by vertical bars) for (a) $n = 5$, (b) $n = 4$ or 5, (c) $n = 4$ or 5.

thrombin generation results from prothrombinase complex formation on the activated platelet membrane or by tissue factor expression at the vessel wall or to what extent the CGP 39393 is able to gain access to the site of thrombin generation.

Thrombin is a potent stimulus to platelet activation but in addition it is known to elicit vascular wall injury (Malik, 1983) and to release a variety of biologically active materials from the vascular endothelium eg PAF and endothelium derived relaxing factor (EDRF) (Shuman, 1986). PAF produced in response to stimuli such as thrombin may not necessarily be released but may remain associated with the endothelial cell (McIntyre *et al.*, 1985; Lynch & Henson, 1986) and may even be expressed on the outer surface of the endothelial cell (Zimmerman *et al.*, 1990) such that it may act as a signal to activate circulating blood cells (Kimani *et al.*, 1988; Lamas *et al.*, 1988; Zimmerman *et al.*, 1990) and thus participate in the thrombin-induced platelet accumulation within the cerebral vasculature. However, the naturally occurring PAF receptor antagonist, BN 52021, at a dose which is known to be selective for PAF receptors in the rabbit (Hellewell & Williams, 1989; Coyle *et al.*, 1989), failed to inhibit the accumulation of radiolabelled platelets in the cerebral vasculature. These results suggest that the endogenous generation of PAF is not playing a role in initiating or sustaining the platelet accumulation within the cerebral circulation induced by intracarotid thrombin.

Endothelial cells are now recognised as being important modulators of many aspects of haemostasis, including the activation of blood elements. One product of the vascular endothelium that may play a role in limiting platelet aggregation *in vivo* is EDRF or nitric oxide (NO). This mediator has been shown to be capable of inhibiting platelet adhesion (Radomski *et al.*, 1987; Ignarro *et al.*, 1988) and aggregation *in vitro* (Azuma *et al.*, 1986; Alheid *et al.*, 1987; Furlong *et al.*, 1987; Bhardwaj *et al.*, 1988) and also reducing platelet aggregation *in vivo* (Bhardwaj *et al.*, 1988; Hogan *et al.*, 1988). Recently, inhibitors of NO biosynthesis from L-arginine have been described, and one such inhibitor is L-NAME (Moore *et al.*, 1990). L-NAME has been shown to augment thrombin-induced platelet accumulation within the pulmonary vascular bed of the rabbit (May *et al.*, 1991), suggesting that NO may play a role in modulating the extent of platelet aggregation induced by thrombin and the disaggregation of platelets and neutrophils within the pulmonary vasculature. However, L-NAME at a dose which produced a significant effect on pulmonary platelet accumulation induced by intravenous thrombin and at a 10 fold higher dose, failed to have any significant effect compared to the biologically inactive enantiomer, D-NAME. It would therefore seem that endogenous generation of NO is not important in modulating the cerebral platelet accumulation induced by intracarotid thrombin in the rabbit.

An important function of thrombin is the cleavage of fibrinogen to form fibrin. Intracarotid thrombin appears to elicit fibrin deposition as shown by the accumulation of ^{125}I-labelled fibrinogen over the same concentration-range as platelet accumulation. The deposition of fibrin seems to be an important factor with respect to the platelet trapping observed in response to intracarotid thrombin since the fibrinolytic agents urokinase, APSAC or rt-PA all reverse the accumulation of platelet-associated radioactivity. In addition, APSAC reverses some of the thrombin-induced accumulation of ^{125}I-labelled fibrin(ogen) in the cerebral vasculature.

The fibrinolytic agents used in this study were used as pharmacological tools to gain some insight into the importance of fibrin deposition in the response to intracarotid thrombin. The use of fibrinolytic agents in thrombotic disorders such as myocardial infarction and venous thrombosis is known to produce beneficial effects. The situation regarding the use of fibrinolytics in the management of stroke is less clear due to the dangers of haemorrhagic transformation of infarcted tissue both with respect to the optimal therapeutic regimen and degree of risk involved. An animal model such as this may help to answer these questions. Administration of APSAC 3 h after the intracarotid administration of thrombin did not appear to be effective in reversing the platelet accumulation, supporting previous studies (Reimer *et al.*, 1977) that once the thrombus becomes established it is more difficult to resolve. Defibrotide, another drug suggested to have fibrinolytic activity failed to alter significantly the duration of thrombin-induced platelet accumulation in the cerebral vasculature. Nonetheless, this drug has been shown to possess anti-ischaemic activity in a variety of organs (Thiemermann *et al.*, 1989) and so it will be of interest to

determine whether this drug alters ischaemia resulting from thrombin-induced platelet embolisation within the cerebral circulation.

Intracarotid thrombin induces a marked, sustained accumulation of fibrin and platelets within the cerebral vasculature of the rabbit. The exact mechanisms by which this occurs are not clear but it is, initially, specifically mediated by thrombin and there appears to be some degree of ongoing thrombin generation as shown by the results with CGP 39393. Neither PAF nor NO seem to play a role in modulating this thrombin-induced platelet accumulation, as shown by a specific receptor antagonist and a specific biosynthesis inhibitor respectively. However, it is likely to represent a thrombotic event in which fibrin deposition plays an important role, as shown by the ability of fibrinolytic agents to reverse the accumulation of radiolabelled platelets. Care must be taken when comparing this to existing models of stroke since no formal evaluation of ischaemia or ischaemic tissue damage has been made. This is an aspect that warrants further investigation and this model has the potential to be of use in evaluating the effects of various thrombolytic agents and for investigating the interactions of platelets with the cerebral endothelium.

References

ALHEID, U., FROLICH, J.C. & FORSTERMANN, U. (1987). Endothelium-derived relaxing factor from cultured human endothelial cells inhibits aggregation of human platelets. *Thromb. Res.*, **47**, 561–571.

ANTHONY, L.U., GOLDRING, S., O'LEARY, J.L. & SCHWARTZ, H.G. (1963). Experimental cerebrovascular occlusion in dog. *Arch. Neurol.*, **8**, 515–527.

AZUMA, H., ISHIKAWA, M. & SEKIZAKI, S. (1986). Endothelium-dependent inhibition of platelet aggregation. *Br. J. Pharmacol.*, **88**, 411–415.

BEDERSON, J.B., PITTS, L.H., TSUJI, M., NISHIMURA, M.C., DAVIS, R.L. & BARTKOWSKI, H. (1986). Rat middle cerebral artery occlusion: evaulation of the model and development of a neurological examination. *Stroke*, **17**, 472–476.

BHARDWAJ, R., PAGE, C.P., MAY, G.R. & MOORE, P.K. (1988). Endothelium derived relaxing factor inhibits platelet aggregation in human whole blood and in the rat in vivo. *Eur. J. Pharmacol.*, **157**, 83–92.

COYLE, A.J., PAGE, C.P., ATKINSON, L., SJOERDSMA, K., TOUVAY, C. & METZGER, W.J. (1989). Modification of allergen-induced airway obstruction and airway hyperresponsiveness in an allergic rabbit model by the selective platelet-activating factor antagonist, BN 52021. *J. Allergy Clin. Immunol.*, **84**, 960–967.

FURLONG, B., HENDERSON, A.H., LEWIS, M.J. & SMITH, J.A. (1987). Endothelium-derived relaxing factor inhibits *in vitro* platelet aggregation. *Br. J. Pharmacol.*, **90**, 687–692.

HEGEDUS, K., TURY, F. & MOLNAR, L. (1985). Experimental focal cerebral ischaemia in rabbits. *J. Neurol.*, **232**, 223–230.

HELLEWELL, P.G. & WILLIAMS, T.J. (1989). Antagonism of Paf-induced oedema formation in rabbit skin: a comparison of different antagonists. *Br. J. Pharmacol.*, **97**, 171–180.

HEMKER, H.C. & BEGUIN, S. (1986). Thrombosis and thrombin. In *Biology and Pathology of Platelet-Vessel Wall Interactions*, ed Jolles, G., Legrand, Y. & Nurden, A. pp. 219–226. London: Academic Press.

HERAS, M., CHESEBRO, J.H., PENNY, W.J., BAILEY, K.R., BADIMON, L. & FUSTER, V. (1989). Effects of thrombin inhibition on the development of acute platelet-thrombus deposition during angioplasty in pigs. *Circulation*, **79**, 657–665.

HOGAN, J.C., LEWIS, M.J. & HENDERSON, A.H. (1988). *In vivo* EDRF activity influences platelet function. *Br. J. Pharmacol.*, **94**, 1020–1022.

IGNARRO, L.J., BUGA, G.M., BYRNS, R.E., WOOD, K.S. & GHAUDHURI, G. (1988). Endothelium-derived relaxing factor and nitric oxide possess identical pharmacological properties as relaxants of bovine arterial and venous smooth muscle. *J. Pharmacol. Exp. Ther.*, **246**, 218–226.

KANEKO, D., NAKAMURA, N. & OGAWA, T. (1985). Cerebral infarction in rats using homologous blood emboli: development of a new experimental model. *Stroke*, **16**, 76–84.

KIMANI, G., TONNESEN, M.G. & HENSON, P.M. (1988). Stimulation of eosinophil adherence to human vascular endothelial cells in vitro by platelet-activating factor. *J. Immunol.*, **140**, 3161–3166.

LAMAS, A.M., MULRONEY, C.M. & SCHLEIMER, R.P. (1988). Studies on the adhesive interaction between purified human eosinophils and cultured vascular endothelial cells. *J. Immunol.*, **140**, 1500–1505.

LEVINE, S. & KLEIN, M. (1960). Ischemic infarction and swelling in the rat brain. *Arch. Pathol.*, **69**, 544–553.

LEVINE, S. & SOHN, D. (1969). Cerebral ischemia in infant and adult gerbils. *Arch. Pathol.*, **87**, 315–317.

LYNCH, J.M. & HENSON, P.M. (1987). The intracellular retention of newly synthesized platelet activating factor. *J. Immunol.*, **137**, 2653–2661.

MALIK, A.B. (1983). Pulmonary microembolism. *Physiol. Rev.*, **63**, 1115–1207.

MARKWARDT, F., HAUPTMANN, J., NOWAK, G., KLESSEN, C. & WALSMANN, P. (1982). Pharmacological studies on the antithrombotic action of hirudin in experimental animals. *Thromb. Haemostas.*, **47**, 226–229.

MAY, G.R., CROOK, P., MOORE, P.K. & PAGE, C.P. (1991). The role of nitric oxide as an endogenous regulator of platelet and neutrophil activation within the pulmonary circulation of the rabbit. *Br. J. Pharmacol.*, **102**, 759–763.

MAY, G.R., HERD, C.M., BUTLER, K.D. & PAGE, C.P. (1990). Radioisotopic model for investigating thromboembolism in the rabbit. *J. Pharmacol. Meth.*, **24**, 19–35.

MCINTYRE, T.M., ZIMMERMAN, G.A., SATOH, K. & PRESCOTT, S.M. (1985). Cultured endothelial cells synthesize both platelet-activating factor and prostacyclin in response to histamine, bradykinin, and adenosine triphosphate. *J. Clin. Invest.*, **76**, 271–280.

MOHR, J.P., CAPLAN, L.R., MELSKI, J.W. & et al. (1978). The Harvard co-operative stroke registry: a prospective registry. *Neurology*, **28**, 754–762.

MOORE, P.K., AL-SWAYEH, O.A., CHONG, N.W.S., EVANS, R.A. & GIBSON, A. (1990). L-N^G-nitro arginine (L-NOARG), a novel L-arginine-reversible inhibitor of endothelium-dependent vasodilatation *in vitro*. *Br. J. Pharmacol.*, **99**, 408–412.

NESHEIM, M.E. & MANN, K.G. (1979). Thrombin-catalyzed activation of single chain bovine factor V. *J. Biol. Chem.*, **254**, 1326–1334.

PENAR, P.L. (1987). A model of embolic cerebral ischemia in the rat. *Exp. Neurol.*, **96**, 393–405.

RADOMSKI, M.W., PALMER, R.M.J. & MONCADA, S. (1987). Endogenous nitric oxide inhibits human platelet adhesion to vascular endothelium. *Lancet*, **ii**, 1057–1058.

REIMER, K.A., LOWE, J.E., RASMUSSEN, M.M. & JENNINGS, R.B. (1977). The wavefront phenomenon of ischemic cell death. 1. Myocardial infarct size vs duration of coronary occlusion in dogs. *Circulation*, **56**, 786–794.

SHUMAN, M.A. (1986). Thrombin-cellular interactions. *Ann. N.Y. Acad. Sci.*, **485**, 228–239.

SMITH, R.A.G., DUPE, R.J., ENGLISH, P.D. & GREEN, J. (1982). Acylenzymes as thrombolytic agents in a rabbit model of venous thrombosis. *Thromb. Haemostas.*, **47**, 269–274.

SUNDT, T.M. & WALTZ, A.G. (1966). Experimental cerebral infarction: retro-orbital extradural approach for occluding the middle cerebral artery. *Mayo Clin. Proc.*, **41**, 159–168.

TALBOT, M.D., AMBLER, J., BUTLER, K.D., FINDLAY, V.S., MITCHELL, K.A., PETERS, R.F., TWEED, M.F. & WALLIS, R.B. (1989). Recombinant desulphatohirudin (CGP 39393) Anticoagulant and antithrombotic properties in vivo. *Thromb. Haemostas.*, **61**, 77–80.

THIEMERMANN, C., THOMAS, G.R. & VANE, J.R. (1989). Defibrotide reduces infarct size in a rabbit model of experimental myocardial ischaemia and reperfusion. *Br. J. Pharmacol.*, **97**, 401–408.

THIEMERMANN, C., MAY, G.R., PAGE, C.P. & VANE, J.R. (1990). Endothelin-1 inhibits platelet aggregation *in vivo*: a study with ^{111}indium-labelled platelets. *Br. J. Pharmacol.*, **99**, 303–308.

TRACY, P.B. (1988). Regulation of thrombin generation at cell surfaces. *Sem. Thromb. Hemostas.*, **14**, 227–233.

ZIMMERMAN, G.A., MCINTYRE, T.M., MEHRA, M. & PRESCOTT, S.M. (1990). Endothelial cell-associated platelet-activating factor: a novel mechanism for signaling intercellular adhesion. *J. Cell Biol.*, **110**, 529–540.

(Received July 2, 1991
Revised January 20, 1992
Accepted January 24, 1992)

Br. J. Pharmacol. (1992), **106**, 139–142 © Macmillan Press Ltd, 1992

Opposing roles for 5-HT_{1B} and 5-HT_3 receptors in the control of 5-HT release in rat hippocampus *in vivo*

[1]Keith F. Martin, Serina Hannon, Ian Phillips & David J. Heal

Boots Pharmaceuticals Research Department, Nottingham NG2 3AA

1 Intracerebral microdialysis was used to determine whether 5-hydroxytryptamine (5-HT) release in the ventral hippocampus of rats anaesthetized with chloral hydrate was modulated by 5-HT_3 receptors.

2 It was confirmed that 5-methoxy-3-(1,2,3,6-tetrahydro-4-pyridinyl)-1H-indole (RU 24969), a selective 5-HT_{1B} receptor agonist, decreased 5-HT release in a dose- and concentration-related manner when administered i.p. (1 and 5 mg kg^{-1}) or via the dialysis probe (0.1 and 1 μM) respectively. The effect of RU 24969 infusion (1 μM) was attenuated by concurrent infusion of metitepine (10 μM) into the hippocampus.

3 When infused into the hippocampus for 15 min, the selective 5-HT_3 receptor agonist, 2-methyl-5-hydroxytryptamine (2-methyl-5-HT; 0.1– 10 μM) increased dialysate 5-HT levels in a concentration-related manner; an effect which was abolished by concurrent infusion of 3-tropanyl-3,5-dichlorobenzoate (1 μM, MDL 72222), a selective 5-HT_3 antagonist.

4 MDL 72222 had no effects on hippocampal 5-HT release when administered via the dialysis probe (1 or 10 μM).

5 The data show that 5-HT_3 and 5-HT_{1B} receptors have opposing roles in the control of 5-HT release in the hippocampus, with 5-HT_3 receptors facilitating and 5-HT_{1B} receptors inhibiting 5-HT efflux, respectively. They also indicate that the facilitatory 5-HT_3 receptors are not tonically activated.

Keywords: 5-HT release; 5-HT_3 receptors; hippocampus; intracerebral microdialysis

Introduction

Radioligand binding and pharmacological studies have revealed several subtypes of 5-hydroxytryptamine (5-HT) receptor in the mammalian CNS. These receptors have been classified as 5-HT_1-like, 5-HT_2 and 5-HT_3 (Bradley *et al.*, 1986). Recently, 5-HT_4 receptors have also been identified (Bockaert *et al.*, 1990). The 5-HT_1-like receptor has been further subdivided into at least four subtypes: 5-HT_{1A}, 5-HT_{1B}, 5-HT_{1C} and 5-HT_{1D} (Pazos *et al.*, 1985; Pazos & Palacios, 1985). It is now widely accepted that in the rat, 5-HT_{1B} receptors subserve the role of nerve terminal autoreceptors (Middlemiss, 1984; Engel *et al.*, 1986; Martin & Marsden, 1988). Furthermore, the 5-HT_{1A} receptor has also been shown to be located on 5-HT neurone cell bodies where it exerts an inhibitory action on 5-HT neurone firing (De Montigny *et al.*, 1984; Verge *et al.*, 1985; Sprouse & Aghajanian, 1987).

Although 5-HT_3 receptors are present in the CNS in fairly low concentrations, their relative distribution is high in the frontal cortex and the hippocampus (Kilpatrick *et al.*, 1987). Furthermore, the physiological role of 5-HT_3 receptors in the CNS is not clearly defined. It is known, however, that these receptors are linked to a monovalent cation channel (Derkach *et al.*, 1989) and that stimulation leads to depolarization of the membrane. It has also been suggested that 5-HT_3 receptors are involved in the control of cortical acetylcholine release (Barnes *et al.*, 1989) and, more recently, Galzin *et al.* (1990) have shown that the release of [^{3}H]-5-HT from guinea-pig frontal cortex slices is enhanced by 5-HT_3 receptor agonists. These findings suggest that 5-HT_3 receptors may play an important role in controlling the release of neurotransmitters, and in particular, may act as facilitatory autoreceptors in the 5-hydroxytryptaminergic system.

The purpose of the experiments described here, therefore, was to determine whether 5-HT_3 receptors are involved in the control of 5-HT release in rat hippocampus *in vivo*.

[1]Author for correspondence.

Methods

Animals

Male Wistar rats (Charles River) weighing 280–300 g were used. They were housed in pairs on a 12:12 h light:dark cycle (lights on: 07 h 00 min) in an ambient temperature of 21°C and had free access to food and water.

Implantation of dialysis probes

Rats were anaesthetized with chloral hydrate (600 mg kg^{-1}, i.p.) and then held in a stereotaxic frame (David Kopf). A concentric microdialysis probe (500 μm o.d., CMA/Microdialysis) with a membrane 3 mm long was then implanted into the ventral hippocampus (co-ordinates for probe tip: anterior-posterior (AP) −4.4 mm, medio-lateral (ML) −4.2 mm, from bregma and dorso-ventral (DV) −8.6 mm from skull surface according to Paxinos & Watson, 1982). The probe was continuously perfused at a flow rate of 1 μl min^{-1} with an artificial CSF solution containing NaCl 147 mM, KCl 4 mM, $CaCl_2$ 4 mM and the selective 5-HT reuptake inhibitor, citalopram 1 μM. Anaesthesia was maintained throughout the experiment with supplementary doses of chloral hydrate (30 mg i.p.) when required. At the end of each experiment, the brain was removed and dialysis probe placement visually confirmed.

Perfusate analysis

Perfusates were collected every 30 min for the first 2 h after probe implantation and then every 15 min throughout the experiment. They were analysed for their 5-HT content by high performance liquid chromatography (h.p.l.c.) with electrochemical detection. Separation was achieved by reversed-phase liquid chromatography using a 10 cm × 2 mm column with Hypersil ODS2 3 μm packing (Technicol) and a mobile phase of 0.1 M phosphate, 0.93 M sodium octane sulphonic acid, 0.07% v/v dibutylamine and 12% v/v methanol

(pH 3.0). A Coulochem electrochemical detector with a Coulochem 5011 dual electrode analytical cell (ESA) was used. Electrode 1 was set at +0.1 V and electrode 2 at +0.28 V. The signal from electrode 2 was used to quantify the amount of 5-HT present. The detection limit for 5-HT was approximately 2 fmol on column.

Experimental protocol

Following a 2 h stabilization period, two 15 min baseline samples were obtained before any intervention. Drugs were then administered peripherally by the i.p. route. Alternatively, they were infused directly into the ventral hippocampus via the dialysis probe for one 15 min collection period.

Statistical analysis

Data were analysed by Dunnett's test or Student's *t* test. Where more than one experimental group was compared with a single control group the null hypothesis was rejected where $P<0.01$.

Drugs

All chemicals used were analytical or h.p.l.c. grade. The following drugs were used: 2-methyl-5-hydroxytryptamine (2-methyl-5-HT), 3-tropanyl-3,5-dichlorobenzoate (MDL 72222) (Research Biochemicals Inc.), 5-methoxy-3(1,2,3,6-tetrahydro-4-pyridinyl)-1H-indole (RU 24969) (Roussel Uclaf), citalopram (Lundbeck), metitepine and chloral hydrate (Sigma).

Results

Basal levels of 5-HT in the dialysate before any intervention were 21.94 ± 0.72 fmol per 15 min sample ($n = 58$).

Effects of RU 24969 on dialysate 5-hydroxytryptamine

Peripheral administration of the 5-HT_1-like receptor agonist, RU 24969, decreased the concentration of 5-HT in hippocampal dialysates in a dose-related manner (Figure 1a). The decrease was maximal 75 min after administration.

When RU 24969 was infused directly into the hippocampus via the dialysis probe for 15 min, there was a rapid, concentration-related decrease in 5-HT output (Figure 1b). For example, following infusion of RU 24969 at a concentration of 1 μM, 5-HT concentrations decreased by 47% in the 15 min period following the infusion. Extracellular 5-HT returned to basal values 60 min after cessation of the infusion. Concurrent infusion of the 5-HT receptor antagonist, metetipine (10 μM), with RU 24969 (1 μM) abolished the decrease in 5-HT release induced by RU 24969 alone (Figure 1c).

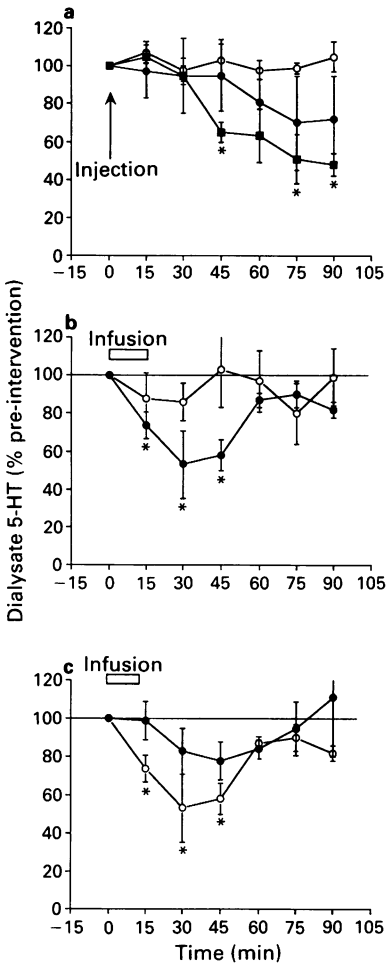

Figure 1 The effects of RU 24969 on rat hippocampal dialysate 5-hydroxytryptamine (5-HT) content. Concentric microdialysis probes were perfused with a solution containing NaCl 147 mM, KCl 4 mM, $CaCl_2$ 4 mM and citalopram 1 μM. Data are expressed as a percentage of the amount of 5-HT in the dialysate collected in the 15 min period immediately before the intervention. Each point represents the mean value with s.e. mean shown by vertical bars. *$P<0.01$ compared to control (Student's *t* test). (a) Saline (○, $n = 6$) or RU 24969 at dose 1(●, $n = 5$) and 5 mg kg^{-1} (■, $n = 5$) were injected i.p. at time zero. (b) RU 24969 at concentrations of 0.1 μM (○, $n = 5$) or 1 μM (●, $n = 5$) was infused into the hippocampus via the dialysis probe for the 15 min period indicated by the horizontal bar. (c) RU 24969 1 μM (○, $n = 5$) or metitepine, 10 μM, plus, RU 24969, 1 μM (●, $n = 4$) was infused directly into the hippocampus via the dialysis probe for the period indicated by the horizontal bar.

Effect of 2-methyl-5-hydroxytryptamine and MDL 72222

The dialysate level of 5-HT was significantly increased, in a concentration-related manner, by local infusion of the 5-HT_3 receptor agonist, 2-methyl-5-HT (Richardson *et al.*, 1985; Figure 2a). Levels of 5-HT were increased 40% and 50% during the infusion of 1 μM and 10 μM, respectively (Figure 2a). Following the infusion of the higher concentration, the levels of 5-HT continued to rise to a maximum increase of 100% in the next 15 min period. Following infusion of 2-methyl-5-HT at 1 μM, levels remained elevated for the 45 min post-infusion. By contrast, the levels of 5-HT rapidly returned to baseline following infusion of 2-methyl-5-HT at 10 μM. Infusion of 2-methyl-5-HT at a concentration of 0.1 μM was without effect (Figure 2a).

Local infusion of the 5-HT_3 receptor antagonist, MDL 72222 (0.1 and 1 μM), via the dialysis probe was without effect on the level of 5-HT measured in the dialysate (Figure 2b).

Infusion of MDL 72222 (1 μM) with 2-methyl-5-HT (1 μM) into the hippocampus via the probe completely prevented the increase in dialysate 5-HT concentrations observed following an infusion of 2-methyl-5-HT alone (Figure 2c).

Discussion

This study has used the technique of intracerebral microdialysis to determine whether 5-HT_3 receptors modulate the release of 5-HT in the hippocampus. The major finding of the experiments is that 5-HT_3 receptors facilitate 5-HT release in the ventral hippocampus of the anaesthetized rat.

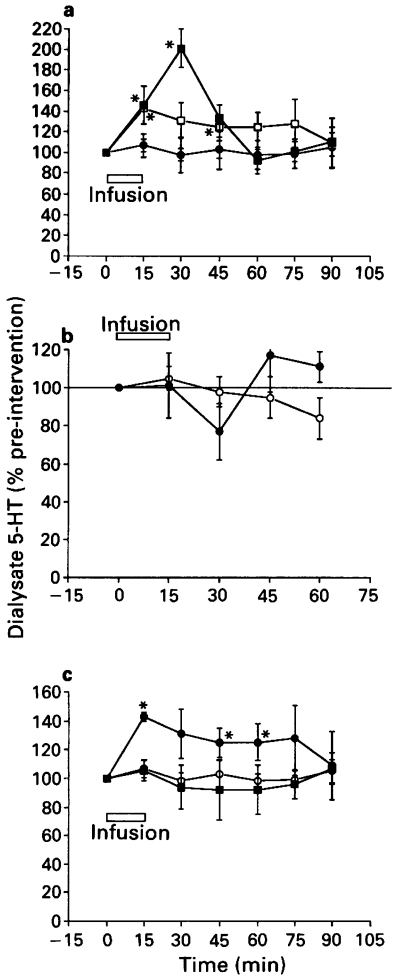

Figure 2 Effects of the 5-HT_3 receptor agonist, 2-methyl-5-HT, and antagonist, MDL 72222, on rat hippocampal dialysate 5-hydroxytryptamine (5-HT) content. (a) 2-Methyl-5-HT, 0.1 μM (●, $n = 5$), 1 μM (□, $n = 4$) or 10 μM (■, $n = 4$) was infused directly into the hippocampus as described in (b); control values (○, $n = 5$). *$P<0.01$ compared to control (Student's t test). (b) MDL 72222, 1 μM (○, $n = 4$) or 10 μM (●, $n = 4$), was infused directly into the hippocampus via the dialysis probe for the 15 min period indicated by the horizontal bar. (c) Either 2-methyl-5-HT, 1 μM (●, $n = 4$) or MDL 72222, 1 μM, plus 2-methyl-5-HT, 1 μM (■, $n = 4$) was infused into the hippocampus via the dialysis probe for 15 min as indicated by the horizontal bar; control values (○, $n = 6$). *$P<0.05$ compared to control (Dunnett's test). Each point represents the mean with s.e. mean indicated by vertical bars. See legend to Figure 1 for further details.

Furthermore, we have shown that these receptors do not appear to be tonically activated.

In the experiments described here, we have used rats anaesthetized with chloral hydrate and have included the specific 5-HT re-uptake inhibitor, citalopram, in the dialysate. Previous studies have clearly shown that under these experimental conditions, a significant proportion of the 5-HT measured results from depolarization-evoked, calcium-dependent release from 5-HT-containing neurones (Sharp *et al.*, 1991).

The observations that peripheral and local administration of RU 24969 inhibited 5-HT release are in close agreement with previous findings (Sharp *et al.*, 1989a; Auerbach *et al.*, 1991). We have also shown that the effects of locally applied RU 24969 were attenuated by metitepine, a 5-HT receptor antagonist which has some selectivity for 5-HT_1-like sites (Hibert & Middlemiss, 1986). Similar findings have also been reported using *in vivo* voltammetry; Martin & Marsden (1986) found that the effects of RU 24969 on 5-HT release and metabolism in the rat suprachiasmatic nucleus were specifically mediated by 5-HT_1-like receptors. These authors also showed that this effect involved 5-HT_{1B}, but not 5-HT_{1A}, receptors located in the nerve terminal region (Martin & Marsden, 1988). Furthermore, using *in vitro* techniques, Middlemiss (1984) has demonstrated that the nerve terminal autoreceptor in the rat is of the 5-HT_{1B} subtype. In view of the above, and because RU 24969 has marginally more affinity for 5-HT_{1B} receptors than 5-HT_{1A} receptors (Hoyer *et al.*, 1985), it is probable that the inhibition described here, is also due to its agonist effect at terminal 5-HT_{1B} receptors.

The physiological role of 5-HT_3 receptors is still not fully understood. However, it has been claimed that these sites are involved in the control of cortical acetylcholine release (Barnes *et al.*, 1989; Bianchi *et al.*, 1990), where they exert an inhibitory effect. In addition, it has also been reported that the *in vitro* release of cortical [^{3}H]-5-HT is increased by 5-HT_3 receptor activation (Galzin *et al.*, 1990). The present data are in agreement with these latter findings. The 5-HT_3 receptor agonist, 2-methyl-5-HT (Richardson *et al.*, 1985), concentration-dependently increased dialysate 5-HT levels. This effect was abolished by an equimolar concentration of MDL 72222, a highly selective 5-HT_3 receptor antagonist (Fozard, 1984). Although these data clearly indicate that 5-HT_3 receptors located in a 5-HT neurone terminal field facilitate 5-HT release, they do not allow firm conclusions to be drawn concerning the anatomical location of these sites. However, we postulate that they may be located on 5-HT nerve terminals, but further experimentation is required to confirm this hypothesis. The 5-HT_3 receptor antagonist, MDL 72222, failed to alter 5-HT release when given directly into the hippocampus. This finding indicates that the 5-HT_3 receptors responsible for mediating the effects of 2-methyl-5-HT are not tonically activated by endogenous 5-HT, under which circumstance, MDL 72222 would have been predicted to decrease 5-HT release.

The facilitation of 5-HT release by 2-methyl-5-HT is not unexpected because several authors have previously shown that 5-HT_3 receptors have stimulatory effects on target neurones where they facilitate the release of neurotransmitters (Gaddum & Piccarelli, 1957; Fozard & Mobarak Ali, 1978; Hagen *et al.*, 1987; Carboni *et al.*, 1989). However, this is the first demonstration that endogenous 5-HT release is facilitated by 5-HT_3 receptor stimulation. In conclusion, the data presented in this paper, demonstrate that *in vivo*, 5-HT_{1B} and 5-HT_3 receptors have opposing roles in the control of rat hippocampal 5-HT release.

References

AUERBACH, S.B., RUTTER, J.J. & JULIANO, P.J. (1991). Substituted piperazine and indole compounds increase extracellular serotonin in rat diencephalon as determined by in vivo microdialysis. *Neuropharmacol.*, **30**, 307–311.

BARNES, J.M., BARNES, N.M., COSTALL, B., NAYLOR, R.J. & TYERS, M.B. (1989). 5-HT_3 receptors mediate inhibition of acetylcholine release in cortical tissue. *Nature*, **338**, 762–763.

BIANCHI, C., SINISCALCHI, A. & BEANI, L. (1990). 5-HT_{1A} agonists increase and 5-HT_3 agonists decrease acetylcholine efflux from the cerebral cortex of freely moving guinea-pigs. *Br. J. Pharmacol.*, **101**, 448–452.

BOCKAERT, J., SEBBEN, M. & DUMUIS, A. (1990). Pharmacological characterization of 5-hydroxytryptamine$_4$ (5-HT_4) receptors positively coupled to adenylate cyclase in adult guinea pig hippocampal membranes: effects of substituted benzamide derivatives. *Molec. Pharmacol.*, **37**, 408–411.

BRADLEY, P.B., ENGEL, G., FENIUK, W., FOZARD, J.R., HUMPHREY, P.P.A., MIDDLEMISS, D.N., MYLECHARANE, E.J., RICHARDSON, B.P. & SAXENA, P.R. (1986). Proposals for the classification and nomenclature of functional receptors for 5-hydroxytryptamine. *Neuropharmacol.*, **25**, 563–576.

CARBONI, E., ACQUAS, E., FRAU, R. & DI CHIARA, G. (1989). Differential inhibitory effects of a 5-HT_3 antagonist on drug-induced stimulation of dopamine release. *Eur. J. Pharmacol.*, **164,** 515–519.

DE MONTIGNY, C., BLIER, P. & CHAPUT, Y. (1984). Electrophysiologically-identified serotonin receptors in rat CNS: effect of antidepressant treatment. *Neuropharmacol.*, **23,** 1511–1520.

DERKACH, V., SURPRENANT, A. & NORTH, R.A. (1989). 5-HT_3 receptors are membrane ion channels. *Nature*, **339,** 706–709.

ENGEL, G., GÖTHERT, M., HOYER, D., SCHLICKER, E. & HILLENBRAND, K. (1986). Identity of inhibitory presynaptic 5-hydroxytryptamine (5-HT) autoreceptors in the rat brain cortex with 5-HT_{1B} binding sites. *Naunyn-Schmiedebergs Arch. Pharmacol.*, **332,** 1–7.

FOZARD, J.R. (1984). MDL 72222: a potent and highly selective antagonist at neuronal 5-hydroxytryptamine receptors. *Naunyn-Schmiedebergs Arch. Pharmacol.*, **326,** 36–44.

FOZARD, J.R. & MOBARAK ALI, A.T.M. (1978). Receptors for 5-hydroxytryptamine on the sympathetic nerves of rabbit heart. *Naunyn-Schmiedebergs Arch. Pharmacol.*, **301,** 223–235.

GADDUM, J.H. & PICARELLI, Z.P. (1957). Two kinds of tryptamine receptor. *Br. J. Pharmacol. Chemother.*, **12,** 323–328.

GALZIN, A.M., PONCET, V. & LANGER, S.Z. (1990). 5-HT_3 receptor agonists enhance the electrically-evoked release of [^{3}H]5-HT in guinea pig frontal cortex slices. *Br. J. Pharmacol.*, **100,** 307P.

HAGEN, R.M., BUTLER, A., HILL, J.M., JORDAN, C.C., IRELAND, S.J. & TYERS, M.B. (1987). Effect of the 5-HT_3 receptor antagonist, GR 38032F, on the response to injection of a neurokinin agonist into the ventral tegmental area of the rat brain. *Eur. J. Pharmacol.*, **138,** 303–305.

HIBERT, M. & MIDDLEMISS, D.N. (1986). Stereoselective blockade at the 5-HT autoreceptor and inhibition of radioligand binding to central 5-HT recognition sites by the optical isomers of methiothepin. *Neuropharmacol.*, **25,** 1–4.

HOYER, D., ENGEL, G. & KALKMAN, H.O. (1985). Molecular pharmacology of 5-HT_1 and 5-HT_2 recognition sites in rat and pig brain membranes: radioligand binding studies with [^{3}H]5-HT, [^{3}H]8-OH-DPAT, (−)[^{125}I]cyanopindolol, [^{3}H]mesulergine and [^{3}H]ketanserin. *Eur. J. Pharmacol.*, **118,** 13–23.

KILPATRICK, G.J., JONES, B.J. & TYERS, M.B. (1987). Identification and distribution of 5-HT_3 receptors in rat brain using radioligand binding. *Nature*, **330,** 746–748.

MARTIN, K.F. & MARSDEN, C.A. (1986). *In vivo* voltammetry in the suprachiasmatic nucleus of the rat: effects of RU 24969, methiothepin and ketanserin. *Eur. J. Pharmacol.*, **121,** 135–140.

MARTIN, K.F. & MARSDEN, C.A. (1988). *In vivo* identification of the serotonin (5-HT) autoreceptor in the rat suprachiasmatic nucleus (SCN). In *New Concepts in Depression* ed. Briley, M. & Fillion, G. pp. 66–68. Basingstoke: Macmillan Press.

MIDDLEMISS, D.N. (1984). The putative 5-HT_1 receptor agonist, RU 24969, inhibits the efflux of 5-hydroxytryptamine from rat frontal cortex slices by stimulation of the 5-HT autoreceptor. *J. Pharm. Pharmacol.*, **37,** 434–437.

PAXINOS, S. & WATSON, C. (1982). *The Rat Brain in Stereotaxic Co-ordinates.* Sydney: Academic Press.

PAZOS, A. & PALACIOS, J.M. (1985). Quantitative autoradiographic mapping of serotonin receptors in the rat brain. 1. Serotonin receptors. *Brain Res.*, **346,** 205–230.

PAZOS, A., HOYER, D. & PALACIOS, J.M. (1985). The binding of serotonergic ligands to the choroid plexus: characterization of a new type of serotonin recognition site. *Eur. J. Pharmacol.*, **106,** 539–546.

RICHARDSON, B.P., ENGEL, G., DONATSCH, P. & STADLER, P.A. (1985). Identification of serotonin M-receptor subtypes and their specific blockade by a new class of drugs. *Nature*, **316,** 126–131.

SHARP, T., BRAMWELL, S.R. & GRAHAME-SMITH, D.G. (1989a). 5-HT_1 agonists reduce 5-hydroxytryptamine release in rat hippocampus *in vivo* as determined by brain microdialysis. *Br. J. Pharmacol.*, **96,** 283–290.

SHARP, T., BRAMWELL, S.R., HJORTH, S. & GRAHAME-SMITH, D.G. (1989b). Pharmacological characterization of 8-OH-DPAT-induced inhibition of rat hippocampal 5-HT release *in vivo* as measured by microdialysis. *Br. J. Pharmacol.*, **98,** 989–997.

SHARP, T., BRAMWELL, S.R. & GRAHAME-SMITH, D.G. (1991). Release of endogenous 5-hydroxytryptamine in rat ventral hippocampus evoked by electrical stimulation of the dorsal raphe nucleus as detected by microdialysis: sensitivity to tetrodotoxin, calcium and calcium antagonists. *Neuroscience*, **39,** 629–637.

SPROUSE, J.S. & AGHAJANIAN, G.K. (1987). Electrophysiological responses of serotonergic dorsal raphe neurons to the 5-HT_{1A} and 5-HT_{1B} agonists. *Synapse*, **1,** 3–9.

VERGE, D., DAVAL, G., PATEY, A., GOZLAN, H., EL MESTIKAWY, S. & HAMON, M. (1985). Presynaptic 5-HT autoreceptors on serotonergic cell bodies and/or dendrites, but not terminals, are of the 5-HT_{1A} subtype. *Eur. J. Pharmacol.*, **113,** 463–464.

(Received January 15, 1992
Revised February 3, 1992
Accepted February 5, 1992)

Br. J. Pharmacol. (1992), **106**, 143–150 © Macmillan Press Ltd, 1992

Endothelium-dependent relaxation to acetylcholine in the rabbit basilar artery: importance of membrane hyperpolarization

Victoria E. Rand & [1]C.J. Garland

Department of Physiology & Pharmacology, University of Southampton, Bassett Crescent East, Southampton, SO9 3TU

1 Muscarinic stimulation of isolated, preconstricted segments of the basilar artery, with either acetylcholine or carbachol, was followed by endothelium-dependent smooth muscle relaxation and membrane hyperpolarization.

2 Smooth muscle relaxation to acetylcholine was stimulated in the presence of lower concentrations than the associated hyperpolarization (EC_{50} values 3.2 μM and 31.6 μM, respectively), and was sustained during agonist application, while the hyperpolarization was relatively transient.

3 Repeated exposure to acetylcholine was associated with loss of membrane hyperpolarization, while smooth muscle relaxation was unaltered. Following a second exposure to 100 μM acetylcholine, mean hyperpolarization was markedly depressed from 8.5 to 2 mV, and subsequent exposures failed to induce any hyperpolarization. Relaxations with a similar amplitude and rate of development, were recorded with each subsequent addition of acetylcholine.

4 The competitive substrate inhibitors for nitric oxide synthase, L-N^G-monomethyl arginine (100 μM L-NMMA) or L-N^G-nitro arginine methyl ester (100 μM L-NAME), modified the form and amplitude of both the relaxation and the hyperpolarization to acetylcholine. In the majority of experiments, both the hyperpolarization and the relaxation were almost totally abolished.

5 Neither nitric oxide, applied directly in physiological salt solution, nor sodium nitroprusside, produced smooth muscle hyperpolarization except in high concentrations. Reproducible, small amplitude (around 2 mV) hyperpolarization followed the application of either NO gas (15 μM) or sodium nitroprusside (100 μM), both of which induced almost maximal smooth muscle relaxation.

6 These data show that muscarinic stimulation of endothelial cells in the rabbit basilar artery is followed by both smooth muscle hyperpolarization and relaxation. They indicate that nitric oxide is involved in both of these responses, but that the smooth muscle hyperpolarization is not an essential component of the relaxation.

Keywords: Vascular smooth muscle; endothelial cells; EDHF; nitric oxide; sodium nitroprusside; L-N^G-nitro arginine methylester (L-NAME); L-N^G-monomethylarginine (L-NMMA); membrane potential

Introduction

As well as relaxing vascular smooth muscle in an endothelium-dependent fashion (by releasing endothelium-derived relaxing factor (EDRF)), acetylcholine and other muscarinic agonists also stimulate endothelium-dependent smooth muscle hyperpolarization (Bolton *et al.*, 1984; Chen *et al.*, 1988; Feletou & Vanhoutte, 1988; Brayden, 1990; Garland & McPherson, 1991; McPherson & Angus, 1991). Smooth muscle hyperpolarization to acetylcholine, like the relaxation, is mediated, at least in part, by the release of a diffusible factor (Feletou & Vanhoutte, 1988; Chen *et al.*, 1991).

Whether or not the endothelium-dependent hyperpolarization to acetylcholine is mediated in any way by nitric oxide, which either is or is closely related to EDRF, is currently the subject of some controversy. In contrast to the relaxation induced by acetylcholine in the rat aorta and pulmonary artery, hyperpolarization was not blocked by either oxyhaemoglobin or methylene blue, leading to the suggestion that a separate hyperpolarizing factor (EDHF) was released simultaneously with EDRF (Chen *et al.*, 1988; Taylor & Weston, 1988). The concept of a separate hyperpolarizing factor was supported by the failure of exogenous nitric oxide to induce smooth muscle hyperpolarization in concentrations which induced marked relaxation in a number of vascular preparations (Komori *et al.*, 1988; Huang *et al.*, 1988; Brayden, 1990). Also, hyperpolarization to acetylcholine was not reduced by inhibitors of nitric oxide synthase in both the guinea-pig coronary artery and rat small mesenteric artery (Chen *et al.*, 1991; Garland & McPherson, 1992).

However, pronounced smooth muscle hyperpolarization and relaxation was demonstrated to exogenous nitric oxide in the guinea-pig uterine artery (Tare *et al.*, 1990a) and the rat small mesenteric artery (Garland & McPherson, 1992). In addition, Tare and co-workers were able to reduce both the hyperpolarization and relaxation to acetylcholine with the nitric oxide synthase inhibitor, L-N^G-monomethyl arginine (L-NMMA), indicating that nitric oxide may contribute to both the hyperpolarization and relaxation induced by this agonist.

The present study investigated the role of nitric oxide in the smooth muscle relaxation and hyperpolarization to muscarinic stimulation in the rabbit basilar artery. Some of these results have been communicated in a preliminary form (Rand & Garland, 1991a,b).

Methods

White rabbits of either sex (2–3 kg) were anaesthetized with i.v. sodium pentobarbitone (60 mg kg^{-1}) and killed by rapid exsanguination. The brain was removed and placed in physiological salt solution (PSS) at room temperature. The basilar artery was carefully removed and cut into cylindrical

[1] Author for correspondence.

segments 1–2 mm in length. Segments were then mounted in a tissue chamber for recording changes in smooth muscle membrane potential and tension, as previously described (Garland, 1987). Briefly, two tungsten wires (each of 25 μm diameter) were passed through the segment's lumen and each wire attached to a small plastic foot. One foot was coupled to an isometric force transducer (Harvard Biosciences, 52-9529) and the other to a microdrive (Prior, code 71). The segment was stretched between the wires, under a previously determined optimal pre-load of 500 mg and superfused (at 1–3 ml min^{-1}) with PSS which had been gassed with 95% O_2 + 5% CO_2 and warmed to 36°C. Concentration-response curves were constructed from responses to single concentrations of agonist. Both agonists, antagonists and enzyme inhibitors were equilibrated with the superfusate before it entered the tissue chamber. In the case of nitric oxide gas, PSS containing the gas (usually 200 μl) was injected close to the artery segment from a gas-tight syringe. In some experiments, endothelial cells were destroyed by carefully passing a blunt syringe needle (25 gauge) through the artery lumen, and then cutting and mounting segments as described above. The success of this manoeuvre was confirmed by a loss of relaxation and, in some cases, hyperpolarization to acetylcholine. In addition, in a number of experiments, the loss of the endothelium was confirmed histologically by staining with haematoxylin and eosin.

Electrophysiology

Measurement of smooth muscle membrane potential was made with a glass microelectrode, advanced through the adventitial surface of the artery segment. The electrodes were filled with 2 M KCl and had resistances of 80–120 MΩ. Membrane electrical events were recorded through a high-input impedance d.c. preamplifier (Neurology 102G) and digitized, together with data from the isometric transducer, and stored on disc.

Solutions and drugs

Experiments were made in physiological salt solution (PSS) of the following composition (mM): NaCl 122, $NaHCO_3$ 25.5, KCl 5.2, $MgSO_4$ 1.2, $CaCl_2$ 1.6, disodium EDTA 0.027, ascorbate 0.114 and glucose 9.4. At the end of an experiment contraction was stimulated with 100 mM K-PSS. This solution was prepared by direct replacement of NaCl with KCl.

Drugs used were acetylcholine chloride (BDH); noradrenaline bitartrate (arterenol, Sigma); atropine sulphate (Sigma); carbamylcholine chloride (carbachol, Sigma); histamine acid phosphate (Sigma); D-monomethyl-L-arginine and N^G-monomethyl-L-arginine (gifts from Dr H. Hodson, Wellcome Foundation); N^G-nitro L-arginine methyl ester and sodium nitroprusside (both Sigma).

Preparation of nitric oxide solution

Nitric oxide (BDH) was injected, with a gas tight syringe, into PSS which had been bubbled with research grade helium (BOC) for 45–60 min. The PSS contained an appropriate concentration of noradrenaline, in order to prevent local dilution artifacts during injection. Nitric oxide solution was then injected into the tissue chamber in volumes of 100–200 μl, with a gas tight syringe. Control injections of helium gassed PSS, containing noradrenaline, were always performed to assess the extent of potential injection artifacts.

Analysis of data

Relaxations are expressed as a percentage decrease in the initial tone to noradrenaline, and in some cases histamine. Data are expressed as mean ± s.e. mean. The significance between mean values was calculated by Student's *t* test, with rejection of the null hypothesis at the 5% level.

Results

Endothelium-dependent responses to acetylcholine

Acetylcholine (0.01–100 μM) hyperpolarized smooth muscle cells in the basilar artery, when applied either in the presence or absence of noradrenaline to depolarize and contract the muscle cells. Figure 1 summarizes the relaxant and hyperpolarizing responses obtained in the presence of noradrenaline, which was applied in variable concentrations (between 10 and 100 μM) in order to stimulate similar-sized contraction and depolarization in each experiment. Acetylcholine was applied against a mean background contraction and depolarization of 2.5 ± 0.3 mN and 6 ± 0.5 mV ($n = 53$), respectively. Threshold relaxation was obtained with 0.1 μM acetylcholine, and relaxation increased with increasing concentrations of acetylcholine, until contraction was totally reversed in the presence of 1 mM acetylcholine. Hyperpolarization, in contrast, was only recorded with acetylcholine concentrations in excess of 1 μM, and increased to 10 ± 1.0 mV in the presence of 1 mM acetylcholine. Hyperpolarization was not observed in artery segments after the endothelium had been rubbed, which also markedly reduced acetylcholine-induced relaxation (> 70%).

In the continued presence of acetylcholine, smooth muscle relaxation was sustained, whereas the membrane hyperpolarization was relatively transient. Although smooth muscle hyperpolarization was always initiated (1–9 s) before relaxation, the membrane potential had returned to pre-stimulation levels within approximately 10–15 min (742 ± 106 s, mean ± s.e. mean; $n = 5$) Figure 2a.

In addition, smooth muscle hyperpolarization, but not relaxation, desensitized rapidly with repeated application of acetylcholine. Figure 2b illustrates this point. Exposure to 100 μM acetylcholine was associated with a mean reversal of noradrenaline-induced contraction by 93 ± 2% and a hyperpolarization of 8.5 ± 1.0 mV ($n = 5$ paired observations in each case). After 60 min wash-out, re-exposure to the same concentration of acetylcholine stimulated relaxation of a similar size and rate (90% reversal of contraction), but now the hyperpolarization was significantly reduced, 1.9 ± 0.42 mV ($P < 0.001$; $n = 9$). Subsequent exposure to acetylcholine every 60 min, over a period of 2–3 h, was followed by relaxation which again developed at the same rate and had the same amplitude as the first response. However, after the second exposure to acetylcholine, no hyperpolarization was detected, and hyperpolarization did not return during the period of the experiment.

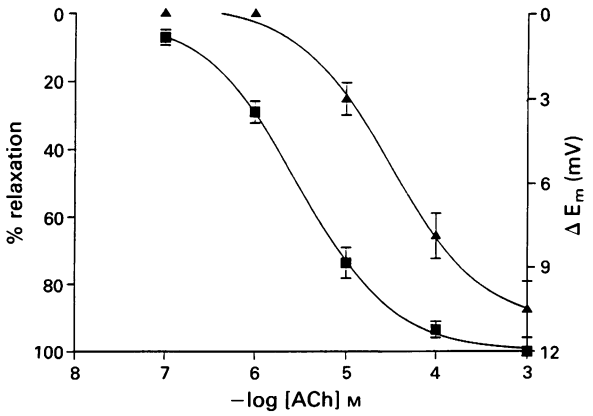

Figure 1 Mean concentration-response curves to acetylcholine in the rabbit basilar artery. Points show the mean hyperpolarization (▲) and relaxation (■) recorded from arteries preconstricted with noradrenaline. Points are the mean from at least five separate experiments; s.e. mean shown by vertical bars.

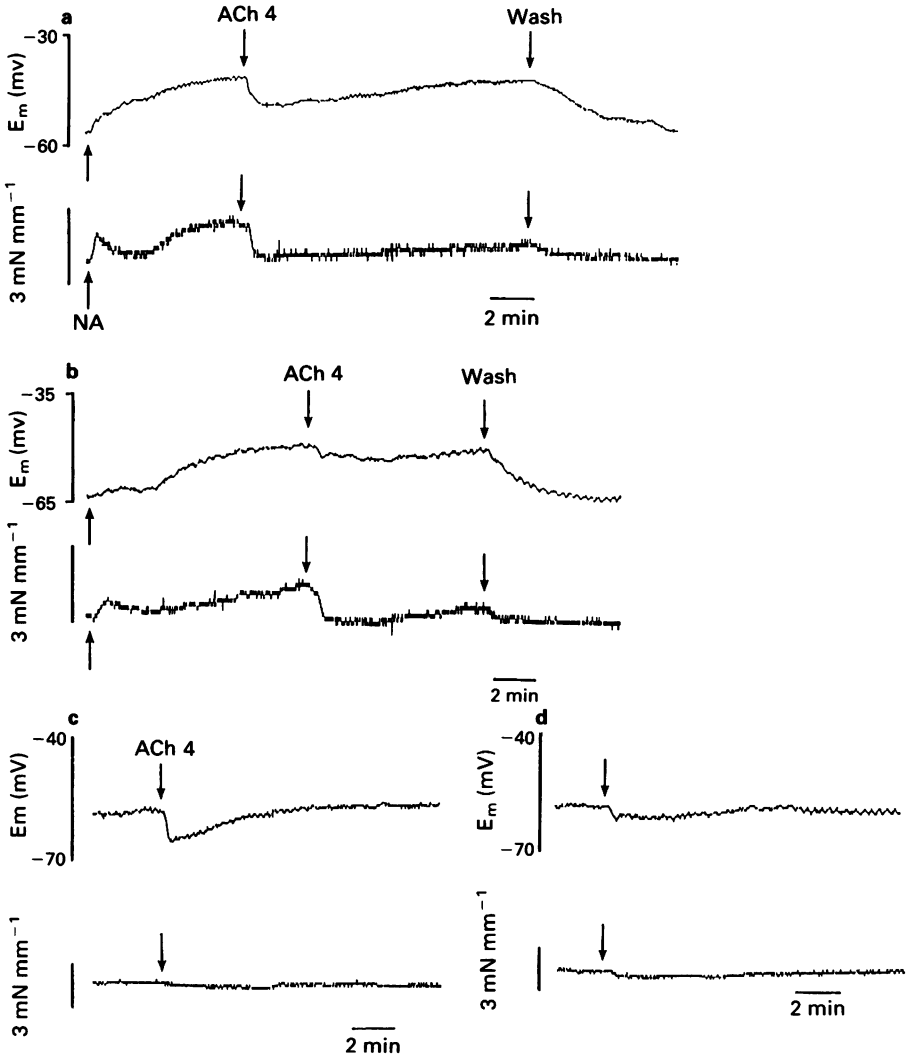

Figure 2 (a,b,c,d) Representative trace showing the response to acetylcholine (ACh) in the presence (a,b) and absence (c,d) of noradrenaline (NA) to induce contraction. Acetylcholine (-log M) hyperpolarized and relaxed smooth muscle in the basilar artery (a), when reapplied to the same artery 60 min later (b), the hyperpolarization, but not the relaxation, was markedly depressed. In the absence of contraction, acetylcholine hyperpolarized the smooth muscle cell (c), and this hyperpolarization was also depressed when acetylcholine was reapplied to the cell 60 min later (d).

Similar membrane responses were observed in the absence of prior smooth muscle stimulation. Acetylcholine (100 μM) stimulated hyperpolarization which had a similar amplitude range (7–8.5 mV in 2 separate experiments) and time course to the responses obtained in the presence of noradrenaline (Figure 2c). Again, desensitization of the hyperpolarization was marked after a single exposure to acetylcholine (Figure 2d).

Effect of carbachol and atropine

Carbachol (0.01–100 μM) produced endothelium-dependent smooth muscle hyperpolarization and relaxation which was very similar to the response obtained with acetylcholine. The hyperpolarization to 100 μM carbachol was of similar amplitude (6.3 ± 0.6 mV, $n = 5$) to that observed with an equivalent concentration of acetylcholine (8.5 ± 1.0 mV, $n = 5$). Hyperpolarization also preceded the onset of relaxation by a similar time (3 ± 0.7 vs 4 ± 1.0 s, $n = 5$), took a similar period to reach maximum (33.4 ± 9.0 vs 38.0 ± 3.0 s, $n = 5$ separate experiments in each case), and was reduced to a similar level after an initial exposure to carbachol (2.1 ± 1.0 vs 2.0 ± 0.4 mV, $n = 5$ and 9, respectively). However, in the continued presence of carbachol, the membrane potential returned to pre-stimulation levels more rapidly than was the case with acetylcholine (382.0 ± 42.0 s; range 292–514 s, $n = 5$). The relaxant potency of carbachol was slightly less than that of acetylcholine (EC_{50} values 14 μM and 2.7 μM, respectively), but both agents induced maximal relaxation.

Atropine (0.1 μM) reversibly blocked the smooth muscle relaxation to acetylcholine, the mechanical effects of 10 μM acetylcholine being reduced from 60% to 8%, while those to 100 μM acetylcholine were reduced from 86% to 27% (each $n = 5$). Hyperpolarization to 100 μM acetylcholine was totally abolished by the presence of atropine ($n = 5$).

Effects of L-NMMA and L-NAME

Competitive substrate inhibitors for nitric oxide synthase reduced both the hyperpolarization and the relaxation to acetylcholine. However, the extent of the observed inhibition was variable (Table 1). In some cases, only a minimal hyperpolarization and relaxation remained (group1, Table 1), while in other tissues the form of the hyperpolarization became biphasic, while relaxation was only minimally reduced (group 2, Table 1). These effects are illustrated in Figure 3. Apart from the extent of the inhibition of responses to acetylcholine, the only other apparent difference between the two groups of tissues was in the size of the additional contraction produced by the synthase inhibitors. Significant blockade of

Table 1 The effects of L-N^G-monomethyl arginine (L-NMMA) and L-N^G-nitro arginine methyl ester (L-NAME) on the endothelium-dependent hyperpolarization and relaxation of the rabbit basilar artery to acetylcholine

	Group I			*Group II*	
	L-NMMA		*L-NAME*	*L-NMMA*	
	10^{-5}M	10^{-4}M	10^{-4}M	10^{-5}M	10^{-4}M
	$n=6$	$n=5$	$n=4$	$n=3$	$n=4$
Resting membrane potential (mV)	59 ± 5	64 ± 5	56 ± 2	61 ± 4	54 ± 3
Contraction to noradrenaline (mN)	4.6 ± 2.0	4.1 ± 1.6	3.5 ± 1.3	3.4 ± 2.5	3.8 ± 2.5
Depolarization to noradrenaline (mV)	13 ± 5.0	17 ± 7.0	8 ± 1.0	12 ± 3.0	7 ± 1.0
Contraction:inhibitor + noradrenaline (mN)	9.4 ± 1.8	16.5 ± 3.1	15.0 ± 1.9	6.1 ± 3.8	8.8 ± 4.0
Additional depolarization (mV)	2 ± 1.0	3 ± 0.9	3.1 ± 1.3	2 ± 1.0	2 ± 0.8
% relaxation to 100 μM acetylcholine	38 ± 6	37 ± 5	32 ± 3	90 ± 10	91 ± 6
Hyperpolarization to 100 μM acetylcholine	3 ± 1.0	2.5 ± 0.5	3.1 ± 1.0	7.5 ± 1.5	9 ± 1.4
Contraction to 100 mM K^+ (mN)	27.1 ± 2.7	29.3 ± 3.1	29.8 ± 3.0	31 ± 2.0	28.3 ± 1.9

Each value is the mean derived from the stated number (n) of observations ± s.e. mean.

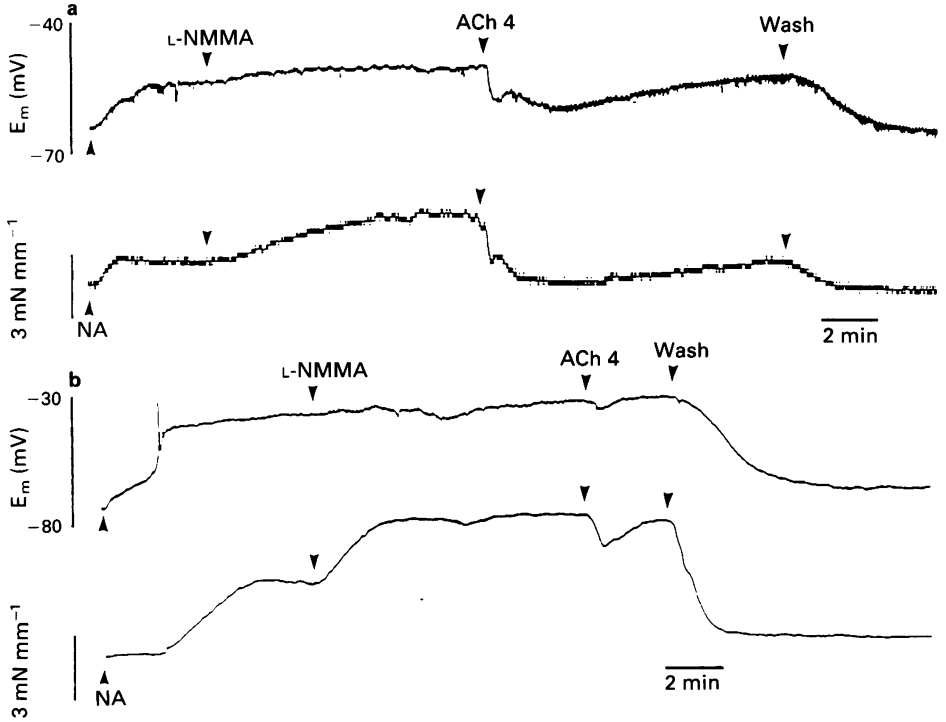

Figure 3 Representative traces showing the different responses obtained in the presence of the nitric oxide synthase inhibitor L-N^G-monomethyl arginine (L-NMMA, 100 μM) with smooth muscle depolarization and contraction induced with noradrenaline (NA). In a small number of arteries, the hyperpolarization and relaxation to acetylcholine (ACh, -log M) had a similar magnitude to control (Figure 2a), but both responses became biphasic (a). In the majority of arteries tested, both the hyperpolarization and the relaxation to acetylcholine were markedly reduced following the application of L-NMMA (b).

the responses to acetylcholine was associated with a large additional tissue contraction to either L-NMMA or L-NAME (group 1). This phenomenon is, however, unlikely to underlie the differences in the extent of the inhibition of responses to acetylcholine by the nitric oxide synthase inhibitors, for two reasons. First, both groups developed a similar contraction when subsequently stimulated with 100 mM K^+-PSS, indicating that the smaller responses to L-NMMA in group 2 did not reflect damaged tissue. Second, the larger contractions produced by L-NMMA and L-NAME in group 1 would

not in themselves reduce the subsequent responses to acetylcholine, as in control experiments acetylcholine produced >90% relaxation in artery segments contracted to between 40 and 60% of the response to 100 mM K^+-PSS, with either histamine ($n = 15$) or noradrenaline ($n = 6$).

D-NMMA (100 μM) did not alter the tension or the membrane potential in artery segments pre-contracted with noradrenaline, nor did it modify the subsequent relaxation and hyperpolarization to acetylcholine ($n = 3$).

Membrane and tension responses to nitric oxide

Nitric oxide, applied either as a gas in solution or via the application of sodium nitroprusside, stimulated endothelium-independent relaxation in segments of basilar artery contracted with noradrenaline. Over the concentration range 0.1 μM–100 μM, sodium nitroprusside produced sustained relaxation, which reversed the noradrenaline-induced contraction by 92.6 ± 1.4% ($n = 6$). Nitric oxide gas, injected close to the tissue, initiated a transient relaxation. At the highest concentration tested (15 μM), nitric oxide reversed the noradrenaline-induced contraction by 74.7 ± 6.1% ($n = 8$), a response which decayed within 20 s. The EC_{50} values for sodium nitroprusside and nitric oxide gas were not different (3 ± 0.9 vs 2.2 ± 0.8 μM; Figure 4a).

Membrane hyperpolarization was only recorded with high concentrations of nitric oxide (15 μM), concentrations which were associated with almost maximal tissue relaxation. Hyperpolarizations with an amplitude of 3 ± 0.3 mV were stimulated by 100 μM sodium nitroprusside applied to smooth muscle with a membrane potential of 43.5 ± 1.7 mV and contracted by 3.8 ± 1.0 mN in the presence of noradrenaline ($n = 5$). The hyperpolarizations were reproducible (up to 3 determinations), slow to peak and lagged behind the onset of smooth muscle relaxation by around 15 s. Larger hyperpolarizations could be induced with 10 mM sodium nitroprusside, which produced a slow, but reproducible hyperpolarization of 19 ± 2 mV and which totally relaxed the arterial segments ($n = 3$). No cross-desensitization of either hyperpolarization or relaxation was observed between acetylcholine and sodium nitroprusside. This was the case whether sodium nitroprusside was applied before or after acetylcholine ($n = 3$).

The highest concentration of nitric oxide gas tested (15 μM), produced only a weak hyperpolarization of 2.2 ± 0.4 mV ($n = 5$). As with sodium nitroprusside, the hyperpolarizations could be reproduced (at least three applications), and were associated with marked smooth muscle relaxation Figure 4b. If nitric oxide was applied to unstimulated smooth muscle cells (membrane potential of 61 ± 7 mV; $n = 4$), hyperpolarizations were recorded which had a similar size to those observed in the presence of noradrenaline.

Discussion

These data indicate very clearly that the membrane hyperpolarization which is induced by muscarinic stimulation in the rabbit basilar artery, does not make an important contribution to the concurrent smooth muscle relaxation. The most direct evidence for this statement comes from the experiments involving repeated application of acetylcholine. After three exposures to acetylcholine, membrane hyperpolarization was completely abolished, but the relaxation was unaltered, both in the amplitude attained and the rate at which it developed. A further indication that membrane hyperpolarization is not required for smooth muscle relaxation to acetylcholine in the basilar artery, comes from the absence of a correlation between the concentration of acetylcholine required for hyperpolarization and relaxation, and from the time course for both of these responses. In the latter, the membrane potential returned to prestimulation levels in the continued presence of either acetylcholine or carbachol, while relaxation was sustained.

Overall, these observations contrast with other arteries, in that they argue against an important role for smooth muscle hyperpolarization in relaxation. For example, in the aorta and the pulmonary and mesenteric arteries from the rat, there is a close correlation between acetylcholine-induced smooth muscle hyperpolarization and relaxation (Taylor *et al.*, 1988; Chen & Suzuki, 1989; Garland & McPherson, 1992). As marked smooth muscle relaxation follows membrane hyperpolarization, either induced by current injection (Makata, 1986) or by potassium channel openers (Bray *et al.*, 1987; Nakao *et al.*, 1988; McPherson & Angus, 1990), hyperpolarization to acetylcholine will also provide an important drive to relaxation. This concept is supported by the finding that smooth muscle hyperpolarization to acetylcholine, which reflects an increase in membrane potassium conductance, can be abolished in the presence of raised extracellular potassium (Chen & Suzuki, 1989). Raised extracellular potassium, in addition to abolishing hyperpolarization, also blocked relaxation by 30–50% (Taylor & Weston, 1988; Nagao & Vanhoutte, 1991). The fact that both the smooth muscle hyperpolarization and the relaxation were suppressed, is a further indication that both events are causally linked. Extrapolating from this evidence to the basilar artery, hyperpolarization would most probably cause relaxation were it not for the fact that it is not induced, except with high concentrations of acetylcholine, concentrations which stimulate maximal relaxation. At this stage, relaxation driven by a parallel process, presumably the activation of guanylyl cyclase, will mask any influence exerted by hyperpolarization.

The majority of the evidence available from other arteries, suggests that the hyperpolarization observed in response to cholinomimetics is not stimulated by nitric oxide. This assertion is based on a number of observations, including the fact that endothelium-dependent smooth muscle relaxation can be blocked independently of hyperpolarization, with either methylene blue (blocks guanylyl cylase which is activated by nitric oxide) or oxyhaemoglobin (binds and inactivates nitric oxide). Also, Chen *et al.* (1991) demonstrated that the relaxation, but not the hyperpolarization to acetylcholine in the guinea-pig coronary artery, could be significantly reduced by the nitric oxide synthase inhibitor, nitroarginine; while a number of studies, including the present investigation, have failed to show any significant hyperpolarization in response to exogenous nitric oxide concentrations which stimulate maximal smooth muscle relaxation (Komori *et al.*, 1988; Huang *et al.*, 1988; Brayden, 1990). Although these observations indicated that nitric oxide had very little effect on smooth muscle membrane potential, recent work has clearly demonstrated hyperpolarization to exogenous nitric oxide in vessels from a number of different species (Tare *et al.*, 1990a, b; Garland & McPherson, 1991; 1992). This raises the possibility that, at least in some vessels, nitric oxide may contribute to the acetylcholine-induced hyperpolarization, and hence to smooth muscle relaxation. In the guinea-pig uterine artery, this does seem to be the case, as both the hyperpolarization and relaxation in response to acetylcholine were reduced with the nitric oxide synthase inhibitor, L-NMMA (Tare *et al.*, 1990a).

However, the ability of nitric oxide to induce smooth muscle hyperpolarization, and thereby contribute to relaxation, is not a general property of the endothelium-dependent responses of arteries to acetylcholine. A variation between arteries was demonstrated by observations on the rat mesenteric artery, where the hyperpolarizations to either acetylcholine or nitric oxide were shown to have very different characteristics. Principally, the nitric oxide-induced hyperpolarization could be blocked, either by prior membrane depolarization or with glibenclamide, whereas depolarization increased the amplitude of the hyperpolarization to acetylcholine, and hyperpolarization was not modified in the presence of glibenclamide (McPherson & Angus, 1991;

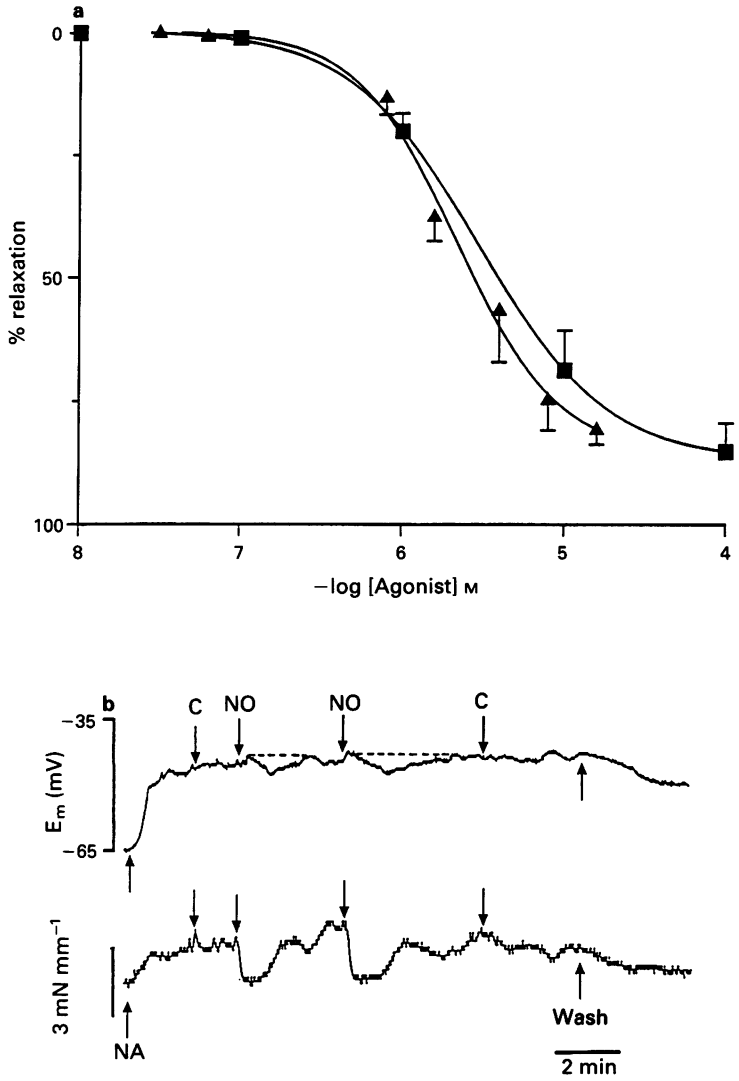

Figure 4 (a) Mean concentration-relaxation curve for the action of sodium nitroprusside (■, $n = 6$) and nitric oxide gas (▲, $n = 8$) against contraction to noradrenaline in the rabbit basilar artery. Points show means with s.e. mean indicated by vertical bars. (b) Representative trace showing a simultaneous record of membrane potential change and relaxation to nitric oxide gas, injected in PSS, in a basilar artery stimulated with noradrenaline (NA, 100 μM). Injection of PSS alone (200 μl, C) did not modify the membrane potential or the tension, while PSS-containing nitric oxide (200 μl of a 15 μM NO solution) reversed contraction and induced a small, reproducible hyperpolarization.

Garland & McPherson, 1992).

It may be the case that high concentrations of nitric oxide can induce hyperpolarization in most blood vessels, as suggested by Tare *et al.* (1990a), but that a separate endothelium-derived hyperpolarizing factor also contributes to a variable extent in different blood vessels. A general failure to demonstrate hyperpolarization to exogenous nitric oxide, may then reflect the concentration applied and/or the method of application. The concentration of exogenous nitric oxide which is available to stimulate smooth muscle cells will be continually decreasing as nitric oxide is oxidised. So while the available concentration of nitric oxide is still sufficient to stimulate marked relaxation, it may have fallen below the threshold for activating membrane hyperpolarization.

In the present study, the highest concentration of nitric oxide gas tested was equivalent to adding around 0.1 μmol to the tissue chamber. This amount was only sufficient to induce a small hyperpolarization of about 2 mV and is close to the threshold for hyperpolarization (3 mV increase in potential) to nitric oxide in the rat mesenteric artery, in which tissue 1 μmol was required to increase the membrane potential by nearly 10 mV (Garland & McPherson, 1992). If nitric oxide and EDHF do make a variable contribution to the hyperpolarization in different arteries, this may then partly explain the somewhat variable hyperpolarizations to acetylcholine which have been recorded in arteries. For example, in the rabbit ear and femoral artery (Suzuki, 1988; Huang *et al.*, 1988), the rat pulmonary (Chen *et al.*, 1988) and the canine mesenteric arteries (Komori *et al.*, 1988) acetylcholine induces only a small, transient hyperpolarization, whereas in the rat mesenteric artery (McPherson & Angus, 1991), feline middle cerebral artery (Brayden & Wellman, 1989), canine coronary artery (Chen *et al.*, 1989) and the guinea-pig basilar artery (Nishiye *et al.*, 1989) large hyperpolarizations of as much as 25 mV have been reported.

If this hypothesis is correct, the rabbit basilar artery may represent an artery which releases only nitric oxide in response to acetylcholine. Exposure to a high concentration of acetylcholine will release enough nitric oxide to stimulate marked smooth muscle relaxation and hyperpolarization, with both responses susceptible to the blocking action of nitric oxide synthase inhibitors. Acetylcholine-induced relaxation and hyperpolarization were blocked or modified by the nitric oxide synthase inhibitors in this tissue, although the action of L-NMMA was somewhat variable, when compared with the blocking action of L-NAME. The reason for the

relatively variable effect of L-NMMA is not clear, but this may be related to the ability of nitric oxide synthase to utilize L-NMMA, but not nitro-arginine, as a substrate (Hecker *et al.*, 1990). If the release of nitric oxide from endothelial cells in the basilar artery is slightly reduced on a second exposure to acetylcholine, the nitric oxide concentration may be sufficient to stimulate maximal smooth muscle relaxation, but the concentration fall below the threshold for hyperpolarization. Feedback control of the release of nitric oxide has been shown in other studies. Nitric oxide can increase the concentration of guanosine 3':5'-cyclic monophosphate (cyclic GMP) in endothelial cells, and elevated levels of cyclic GMP may be responsible for the reduced release of EDRF from endothelial cells in culture, when they are stimualted with atrial natriuretic peptide (Busse *et al.*, 1988; Boulanger *et al.*, 1990).

In contrast to the rabbit basilar artery, vessels such as the rat small mesenteric artery, may represent arteries which release only, or predominantly EDHF. In the mesenteric artery, acetylcholine stimulates marked and reproducible endothelium-dependent hyperpolarization, which is mediated by membrane mechanisms different from those responsible for the hyperpolarization induced with exogenous nitric oxide. In such a tissue, hyperpolarization to acetylcholine is closely linked to, and probably largely responsible for the smooth muscle relaxation. Furthermore, both the hyperpolarization and the relaxation to acetylcholine are resistant to the blocking action of L-nitroarginine, oxyhaemoglobin and glibenclamide (Garland & McPherson, 1992).

In summary, muscarinic stimulation of the rabbit basilar artery is followed by smooth muscle hyperpolarization and relaxation. Both events appear to be mediated by the endothelium-dependent release of nitric oxide, or a related substance. In contrast to other blood vessels, the smooth muscle hyperpolarization appears to make a negligible contribution to relaxation. In the context of studies on other vessels, this raises the intriguing possibility that nitric oxide and a separate EDHF may vary in their contribution to the endothelium-dependent relaxation which occurs in different parts of the circulation.

This work was made possible by financial support from the Wellcome Trust.

References

BOLTON, T.B., LANG, R.J. & TAKEWAKI, T. (1984). Mechanisms of action of noradrenaline and carbachol on smooth muscle of guinea-pig anterior mesenteric artery. *J. Physiol.*, **351**, 549–572.

BOULANGER, C., SCHINI, V.B., MONCADA, S. & VANHOUTTE, P.M. (1990). Stimulation of cyclic GMP production in cultured endothelial cells of the pig by bradykinin, adenosine diphosphate, calcium ionophore A23187 and nitric oxide. *Br. J. Pharmacol.*, **101**, 152–156.

BRAY, K.M., NEWGREEN, D.T., SMALL, R.C., SOUTHERTON, J.S., TAYLOR, S.G., WEIR, S.W. & WESTON, A.H. (1987). Evidence that the mechanism of the inhibitory action of pinacidil in rat and guinea-pig smooth muscle differs from that of glyceryl trinitrate. *Br. J. Pharmacol.*, **91**, 421–429.

BRAYDEN, J.E. (1990). Membrane hyperpolarization is a mechanism of endothelium-dependent cerebral vasodilation. *Am. J. Physiol.*, **259**, H668–H673.

BRAYDEN, J.E. & WELLMAN, G.C. (1989). Endothelium-dependent dilation of feline cerebral arteries: Role of membrane potential and cyclic nucleotides. *J. Cerebral Blood Flow Metab.*, **9**, 256–263.

BUSSE, R., LUCKHOFF, A.L., MULSCH, A. & BASSENGE, E. (1988). Modulation of EDRF release assessed by guanylate cyclase assay. In *Vascular Neuroeffector Mechanisms* ed. Bevan, J.A., Majewski, H.M., Maxwell, R.A. & Storey, D.F. pp. 111–118. Oxford: IRL Press.

CHEN, G. & SUZUKI, H. (1989). Some electrical properties of the endothelium-dependent hyperpolarization recorded from rat arterial smooth muscle cells. *J. Physiol.*, **410**, 91–106.

CHEN, G., SUZUKI, H. & WESTON, A.H. (1988). Acetylcholine releases endothelium derived hyperpolarizing factor and EDRF from rat blood vessels. *Br. J. Pharmacol.*, **95**, 1165–1174.

CHEN, G., HASHITANI, H. & SUZUKI, H. (1989). Endothelium-dependent relaxation and hyperpolarization of canine coronary artery smooth muscle in relation to electrogenic Na-K pump. *Br. J. Pharmacol.*, **98**, 950–956.

CHEN, G., YAMAMOTO, Y., MIWA, K. & SUZUKI, H. (1991). Hyperpolarization of arterial smooth muscle induced by endothelial humoral substances. *Am. J. Physiol.*, **260**, H1888–H1892.

FELETOU, M. & VANHOUTTE, P.M. (1988). Endothelium-dependent hyperpolarization of canine coronary artery smooth muscle. *Br. J. Pharmacol.*, **93**, 515–524.

GARLAND, C.J. (1987). The role of membrane depolarization in the contractile response of the rabbit basilar artery to 5-hydroxytryptamine. *J. Physiol.*, **392**, 333–348.

GARLAND, C.J. & MCPHERSON, G.A. (1991). Nitric Oxide and acetylcholine hyperpolarize smooth muscle cells in the rat small mesenteric artery by different mechanisms. *Br. J. Pharmacol.*, **104**, 296P.

GARLAND, C.J. & MCPHERSON, G.A. (1992). Evidence that nitric oxide does not mediate the hyperpolarization and relaxation to acetylcholine in the rat small mesenteric artery. *Br. J. Pharmacol.*, **105**, 429–435.

HECKER, M., MITCHELL, J.A., HARRIS, H.J., KATSURA, M., THIEMERMANN, C. & VANE, J.R. (1990). Endothelial cells metabolize N^G-monomethyl-L-arginine to L-citrulline and subsequently to L-arginine. *Biochem. Biophys. Res. Commun.*, **167**, 1037–1043.

HUANG, A.H., BUSSE, R. & BASSENGE, E. (1988). Endothelium-dependent hyperpolarization of smooth muscle cells in rabbit femoral arteries is not mediated by EDRF (nitric oxide). *Naunyn-Schmiedebergs Arch. Pharmacol.*, **338**, 438–442.

KOMORI, K., LORENZ, R.R. & VANHOUTTE, P.M. (1988). Nitric oxide, ACh and electrical and mechanical properties of canine arterial smooth muscle. *Am. J. Physiol.*, **24**, H207–H212.

MCPHERSON, G.A. & ANGUS, J.A. (1990). Characterization of responses to cromakalim and pinacidil in smooth and cardiac muscle by use of selective antagonists. *Br. J. Pharmacol.*, **100**, 201–206.

MCPHERSON, G.A. & ANGUS, J.A. (1991). Evidence that acetylcholine mediated hyperpolarization of the rat small mesenteric artery does not involve the K^+ channel opened by cromakalim. *Br. J. Pharmacol.*, **103**, 1184–1190.

MEKATA, F. (1986). The role of hyperpolarization in the relaxation of the monkey coronary artery. *J. Physiol.*, **371**, 257–265.

NAGAO, T. & VANHOUTTE, P.M. (1991). Hyperpolarization contributes to endothelium-dependent relaxations to acetylcholine in femoral veins of rats. *Am. J. Physiol.*, **261**, H1034–1037.

NAKAO, K., OKABE, K., KITAMURA, K., KURIYAMA, H. & WESTON, A.H. (1988). Characteristics of cromakalim-induced relaxations in the smooth muscle of guinea-pig mesenteric artery and vein. *Br. J. Pharmacol.*, **95**, 795–804.

NISHIYE, E., NAKAO, K., ITOH, T. & KURIYAMA, K. (1989). Factors inducing endothelium-dependent relaxation in guinea-pig basilar artery as estimated from the actions of haemoglobin. *Br. J. Pharmacol.*, **96**, 645–655.

RAND, V.E. & GARLAND, C.J. (1991a). Endothelium-dependent hyperpolarization and relaxation to acetylcholine in rabbit isolated cerebral arteries. *Br. J. Pharmacol.*, **102**, 128P.

RAND, V.E. & GARLAND, C.J. (1991b). Relaxation to nitric oxide does not require smooth muscle hyperpolarization in the rabbit isolated basilar artery. *Br. J. Pharmacol.*, **104**, 411P.

SUZUKI, H. (1988). The electrogenic Na-K pump does not contribute to endothelium dependent hyperpolarization in the rabbit ear artery. *Eur. J. Pharmacol.*, **156**, 195–197.

TARE, M., PARKINGTON, H.C., COLEMAN, H.A., NEILD, T.O. & DUSTING, G.J. (1990a). Hyperpolarization and relaxation of arterial smooth muscle caused by nitric oxide derived from the endothelium. *Nature*, **346**, 69–71.

TARE, M., PARKINGTON, H.A., COLEMAN, H.A., NEILD, T. O. & DUSTING, G.J. (1990b). Actions of endothelium-derived nitric oxide include hyperpolarization of vascular smooth muscle. In *Nitric Oxide from L-Arginine: a Bioregulatory System* ed. Moncada, S. & Higgs, E.A. pp. 73–80. Elsevier Science Publishers.

TAYLOR, S.G. & WESTON, A.H. (1988). Endothelium derived hyperpolarizing factor: an endogenous inhibitor released from the vascular endothelium. *Trends Pharmacol. Sci.*, **9**, 272–274.

(Received January 6, 1992
Accepted January 28, 1992)

Br. J. Pharmacol. (1992), **106**, 151–156 © Macmillan Press Ltd, 1992

Kinetic modulation of guinea-pig cardiac L-type calcium channels by fendiline and reversal of the effects of Bay K 8644

[1]Wolfgang Schreibmayer, *Onkar Tripathi & Helmut A. Tritthart

Institute of Medical Physics and Biophysics, Karl-Franzens University, A-8010 Graz, Austria, and *Department of Physiology, Central Drug Research Institute, Lucknow-226001, India

1 The modulation of L-type calcium channel current (I_{Ca}) by fendiline, a diphenylalkylamine type of calcium channel blocker was investigated on guinea-pig ventricular myocytes by use of the whole-cell patch-clamp technique.

2 Fendiline-induced block of I_{Ca} is accompanied by modulation of the channel kinetics in a complex manner. The time course of I_{Ca} inactivation is significantly faster and the channel availability (f_∞) curve is shifted considerably to more negative potentials by fendiline. These findings can be interpreted qualitatively in terms of a modulated receptor.

3 When the 1,4-dihydropyridine agonist (4**R**, 4S)-Bay K 8644 was added in presence of 30 μM fendiline a further reduction of I_{Ca} instead of the expected stimulatory effect was observed.

4 A similar 'paradoxical' inhibition of I_{Ca} was produced by the pure agonist enantiomer (4S)-Bay K 8644. Thus this novel effect of Bay K 8644 cannot be attributed to changes in affinity of the 1,4-dihydropyridine receptor site for (4**R**)-Bay K 8644 during fendiline action.

5 The IC_{50} for fendiline was reduced to 3.0 ± 0.1 μM (control value: 17.0 ± 2.4 μM) and the Hill slope in its presence was increased to 1.90 ± 0.1 (control value: 1.39 ± 0.23) by 1 μM (4**R**, 4S)-Bay K 8644.

6 (4**R**,4S)-Bay K 8644 caused the expected stimulation of I_{Ca} in the presence of verapamil, diltiazem and nifedipine, overcoming the inhibitory effect of these calcium channel blockers.

7 The 'paradoxical' inhibitory effect of the agonist Bay K 8644 can be explained in terms of an allosteric interaction between fendiline and the dihydropyridine agonist.

Keywords: L-type Calcium channel; fendiline; Bay K 8644; guinea-pig ventricular myocytes

Introduction

The diphenylalkylamine type of agents have long been attributed a weak calcium antagonist activity (Fleckenstein, 1981) but the mechanism of their inhibitory effect on calcium channels is not yet properly understood. Fendiline, a prototype of this group, already in clinical use as an anti-anginal drug, is reported to have inhibitory effects on calcium channels (Fleckenstein *et al.*, 1977; Tritthart & Koidl, 1985) as well as calmodulin and calmodulin-dependent enzymes (Johnson & Fugman, 1983; Spedding, 1983; Bayer & Mannhold, 1987) indicating a multiplicity of sites of action. In a recent study undertaken to clarify this controversy we observed that fendiline indeed directly inhibits the L-type calcium channel activity in guinea-pig ventricular myocytes following its extracellular application (Tripathi, Schreibmayer & Tritthart, unpublished). The main objective of the present study was to investigate the detailed kinetic interactions of fendiline with L-type calcium channels and to compare it with the other classical organic calcium channel blockers by use of Bay K 8644, a calcium channel agonist, which acts differently from the β-adrenoceptor agonist, isoprenaline (Tsien *et al.*, 1986). (4**R**,4S)-Bay K 8644 as well as its agonist isomer (4S)-Bay K 8644, were found to bring about a paradoxical additive inhibition of the calcium channel current (I_{Ca}) in the presence of fendiline. In the presence of nifedipine, verapamil, and diltiazem, however, (4**R**,4S)-Bay K 8644 produced its usual agonist effect. Some of these findings have been presented in preliminary form (Schreibmayer *et al.*, 1991).

[1] Author for correspondence.

Methods

Solutions used

The following solutions were used in the present study (composition in mM, if units not given):
Culture medium: foetal calf serum 1 ml, penicillin-G 1.2 mg, streptomycin 2 mg, made up to 20 ml with medium M199.
Physiological salt solution (Na-PSS) in mmol l^{-1}: NaCl 137, KCl 5.4, $CaCl_2$ 1, $MgCl_2$ 2, glucose 10 and HEPES 10; buffered with NaOH to pH 7.4. Physiological salt solution containing tetrodotoxin (TTX-PSS): Na-PSS containing various concentrations of TTX.
Collagenase-PSS in mmol l^{-1}: NaCl 137, KCl 5.4, $CaCl_2$ 0.125, $MgCl_2$ 2, glucose 10 and HEPES 10; buffered with NaOH to pH 7.4, collagenase 100 u ml^{-1}.
Choline-PSS in mmol l^{-1}: choline chloride 137, KCl 5.4, $CaCl_2$ 1, $MgCl_2$ 2, glucose 10 and HEPES 10; buffered with KOH to pH 7.4.
Caesium containing pipette solution (CPS) in mmol l^{-1}: CsCl 110, EGTA 11, $MgCl_2$ 2, $CaCl_2$ 1, HEPES 10, K-ATP 63 mg to 25 ml; buffered with KOH to pH 7.4.

Stock solutions of all the drugs used in this study were prepared in dimethylsulphoxide (DMSO) and subsequently diluted in choline-PSS before application to the myocytes.

Preparation of adult guinea-pig ventricular cells

Adult guinea-pigs injected with heparin (3000 iu kg^{-1}, s.c.) were killed by cervical dislocation and the heart immediately removed and mounted on a Langendorff apparatus. Retrograde intra-arterial perfusion was performed with physiological salt solution (PSS; 37°C; for composition of the solutions see above) bubbled with O_2 containing 5% CO_2. The ventricular myocytes were prepared by collagenase

dispersion essentially according to the method described earlier for rat heart cells (Schreibmayer *et al.*, 1985). Briefly, the perfusion of heart was switched over from Na-PSS to the oxygenated collagenase-PSS (37°C) to disaggregate the cells which were then gently dispersed by chopping. The suspension was filtered through a nylon filter, the filtrate centrifuged at 500 r.p.m. for 1 min and the extracellular calcium concentration raised to normal. This suspension was centrifuged at 500 r.p.m. for 1 min. The resulting cells were added to the culture medium and stored in a CO_2 incubator for up to 72 h at 37°C. Immediately before the electrophysiological experiments were performed, an aliquot of the culture medium containing ventricular myocytes was transferred to a plastic petri-dish, surrounded by a peltier element for appropriate temperature control (Patch Clamp Tower, List Medical Instruments, F.R.G.). After the cells had settled to the bottom of the petri-dish, superfusion with Na-PSS (20°C) was begun and continued until complete exchange of the culture medium.

Recording of the L-type calcium channel current (I_{Ca}) and data evaluation

Macroscopic I_{Ca} was recorded by the whole-cell configuration of the patch-clamp technique (Hamill *et al.*, 1981). Voltage jump protocols were applied across the cell membrane via a TL-125 computer interface (Axon Instruments, Inc., U.S.A.) controlled by an AT-386 based personal computer (Steiner Computer, Austria). The resulting currents were amplified with a patch-clamp amplifier (Model 8900, Dagan Corporation, U.S.A.) at the maximum possible series resistance compensation. Current signals were low-pass filtered by the amplifier's built-in Bessel filters at approximately 1/5th of the sampling frequency and subsequently digitized by the TL-125 interface. The software used for generating voltage jump protocols, data acquisition and evaluation was a considerably custom modified version of pClamp 5.5 (Axon Instruments, Inc., U.S.A.). The patch pipettes were pulled from standard soft glass (micro-haematocrit tubes No. 564, Assistent, Germany) with a microelectrode puller (Model L/M-3P-A, List Medical Instruments, Germany) and had final tip resistance between 1 and 2 MΩ with the pipette-solution used.

Different types of voltage-pulse protocols were employed according to the experimental requirements as described in the legends to Figures 1a, 2a and 3a.

Determination of steady-state inactivation ($f\infty$) of calcium channels

The steady-state inactivation of calcium channels was determined from the values of peak ($I_{Ca(peak)}$) elicited by voltage-pulses following conditioning prepulses at different test potentials (E_m; Figure 2a). A least squares-fit of $I_{Ca(peak)}$ expressed as a function of E_m was carried out according to the following equation (Trautwein *et al.*, 1975):

$$I_{Ca(peak)}\ (E_m) = I_{Ca(peak)}\ (max) \times [1 + \exp(E_m - E_{0.5})/k]^{-1} \quad (1)$$

where I_{Ca} (max) is the maximal I_{Ca} in a given experiment, $E_{0.5}$, the conditioning membrane potential when $I_{Ca}\ (E_m) = I_{Ca}$ (max)/2 and k is the slope of the function at $E_{0.5}$. $f\infty(E_m)$ was then calculated according to the following equation:

$$f\infty(E_m) = I_{Ca(peak)}\ (E_m)/I_{Ca(peak)}\ (max) \quad (2)$$

Statistical analysis

Significance of the observations was determined by Student's *t* test.

Chemicals

Chemicals used were of reagent grade unless otherwise stated. M199 was purchased from Flow Laboratories and collagenase from Worthington (Type CI-28). TTX and nifedipine were procured from Sigma Chemical Company (Germany), fendiline from Thiemann Arzneimittel GmbH (Germany), verapamil from Knoll AG (Germany), diltiazem from Gödecke AG (Germany), and Bay K 8644 (methyl 1, 4-dihydro-2,6-dimethyl-3-nitro-4-(2-trifluoromethylphenyl)-pyridine -5-carboxylate) from Bayer AG (Germany).

Results

Assessment of I_{Ca}

Calcium inward current was recorded from ventricular myocytes bathed in Na-PSS, TTX-PSS containing 10 μM TTX, or choline-PSS. No obvious difference was seen in the magnitude of peak I_{Ca} ($I_{Ca(peak)}$)in these three extracellular media using K^+-free and Cs^+ and ATP containing pipette solution (CPS, not illustrated). However, in Na-PSS small residual fast inward currents could be seen at clamp potentials too low to elicit a prominent I_{Ca}, probably due to an incomplete inactivation of the fast sodium system. In order to avoid this artifact all subsequent experiments included in this study were carried out with choline-PSS as extracellular medium and CPS in the patch-pipette.

Activation and inactivation kinetics

Measurement of the time course of calcium channel activation and inactivation was accomplished by fitting single exponential functions through the onset and the decaying phases of the currents elicited by the voltage pulse protocol of Figure 1a. Selected current traces obtained before and after superfusion with 30 μM fendiline (Figure 1b and c, respectively) show an acceleration of inactivation but not activation time course. The mean time constants of activation and inactivation calculated for a voltage range between − 10 and + 30 mV (Figure 1d) clearly demonstrated reduction of the latter by fendiline.

Steady-state inactivation

Altered gating kinetics suggest conformation-dependent binding of a drug (Hondeghem & Katzung, 1977; Starmer & Grant, 1985). Therefore, the effect of fendiline on steady-state inactivation ($f\infty$) was investigated by use of the voltage pulse protocol as illustrated in Figure 2a (see Methods). Direct inspection of resulting I_{Ca} recordings reveals that the availability of calcium channels is shifted considerably to more negative potentials by fendiline (Figure 2b and c). Accordingly, the $f\infty$ curve shows a significant shift to the left (Figure 2d). $E_{0.5}$ were -18.5 ± 9.3 mV (mean ± standard deviation, s.d. $n = 6$) for control calcium currents and -46.4 ± 15.8mV ($n = 4$, $P < 0.001$) for calcium currents recorded in the presence of 30 μM fendiline.

Paradoxical block of fendiline-modified calcium channels by Bay K 8644

I_{Ca} was elicited every 5 s as shown in Figure 3a. Superfusion of the cells with Choline-PSS containing 30 μM fendiline brought about a submaximal inhibition of I_{Ca} (Figure 3). After the block developed by fendiline reached an equilibrium state, superfusion was changed to Choline-PSS containing 30 μM fendiline and 1 μM (4**R**,4**S**)-Bay K 8644 (Figure 3b and c). Fendiline (30 μM) alone led to a reduction of $I_{Ca(peak)}$ to $32.9 \pm 15.7\%$ of control ($n = 14$). Surprisingly, the addition of 1 μM (4**R**,4**S**)-Bay K 8644 resulted in a further reduction of $I_{Ca(peak)}$ to $1.0 \pm 1.6\%$ ($n = 6$) instead of the anticipated stimulation. Application of 1 μM (4**R**,4**S**)-Bay-K 8644 alone resulted in the usual increase of $I_{Ca(peak)}$ to $293.0 \pm 107.9\%$ ($n = 4$, Figure 3d) under the present experimental conditions. This paradoxical inhibition of I_{Ca} by

(4R,4S)-Bay K 8644 in the presence of fendiline occurred even at concentrations as low as 10 nM (Figure 3e).

A cumulative dose-response curve for the effect of fendiline in the presence of 1 μM (4R,4S)-Bay K 8644 was recorded taking $I_{Ca(peak)}$ stimulated by the agonist as 100% (Figure 4). This curve was also monophasic and sigmoidal. The IC_{50} value for fendiline in presence of 1 μM (4R,4S)-Bay K 8644 was calculated to be 3.0 ± 0.1 μM (mean ± s.e.mean) with a Hill slope of $n = -1.90 \pm 0.10$ (mean ± s.e.mean). These values were significantly different from those for fendiline alone which were 17.0 ± 2.4 μM and $n = -1.39 \pm 0.23$ (Tripathi *et al.*, unpublished).

(4R,4S)-Bay K 8644 is known to be a mixture of an agonist and an antagonist enantiomer, namely (4S)-Bay K 8644 and (4R)-Bay K 8644, respectively (Franckowiak *et al.*, 1985). Therefore, the pure stereoenantiomeric forms of Bay K 8644 were also tested for their effects in the presence of fendiline. I_{Ca} was first blocked submaximally by 30 μM fendiline and then 1 μM of either of the two enantiomers was applied. It was noted that (4R)-Bay K 8644 decreased $I_{Ca(peak)}$ to 1.0 ± 0.9% of control (mean ± s.d., $n = 4$) as did also the dihydropyridine agonist (4S)-Bay K 8644. An overall further reduction of $I_{Ca(peak)}$ (4.7 ± 1.1% of control (mean ± s.d., $n = 4$; Figure 5a, b and f) was observed in the presence of the agonist enantiomer.

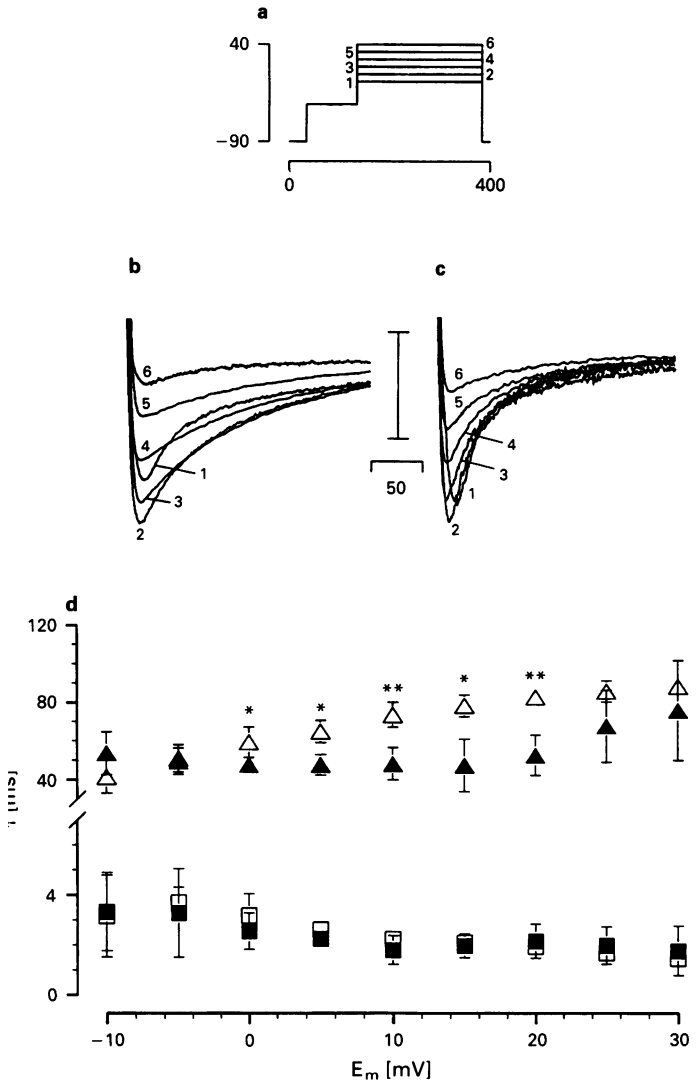

Figure 1 Effects of fendiline on the kinetics of L-type calcium channel current (I_{Ca}): (a) Voltage jump protocol employed to generate the family of I_{Ca}. Holding potential (− 90 mV for 2 s) was followed by a step potential to − 40 mV for 100 ms. Then a command potential of 250 ms incremented by 5 mV steps up to the final value of + 110 mV was applied. (b) Superimposed I_{Ca} recordings elicited in a cell by the command potentials numbered correspondingly in (a). (c) Superimposed I_{Ca} recordings from the same cell as (b) but under equilibrium effect of 30 μM fendiline. Note that the vertical bar denotes 0.5 nA for (b) and 0.25nA for (c) in order to make the change in time course of inactivation stand-out prominently. (d) Mean values of the time constants of activation (t_a, rectangles) and inactivation (t_i, triangles) of I_{Ca} obtained from four different cells plotted as a function of the command potential under control conditions (open symbols) and in presence of fendiline (30 μM; closed symbols). Time constants were fitted as single exponential functions to the individual current traces. Standard deviations are indicated by vertical bars. Statistically significant differences were observed for t_i before and after fendiline action (*$P<0.05$ and **$P<0.01$).

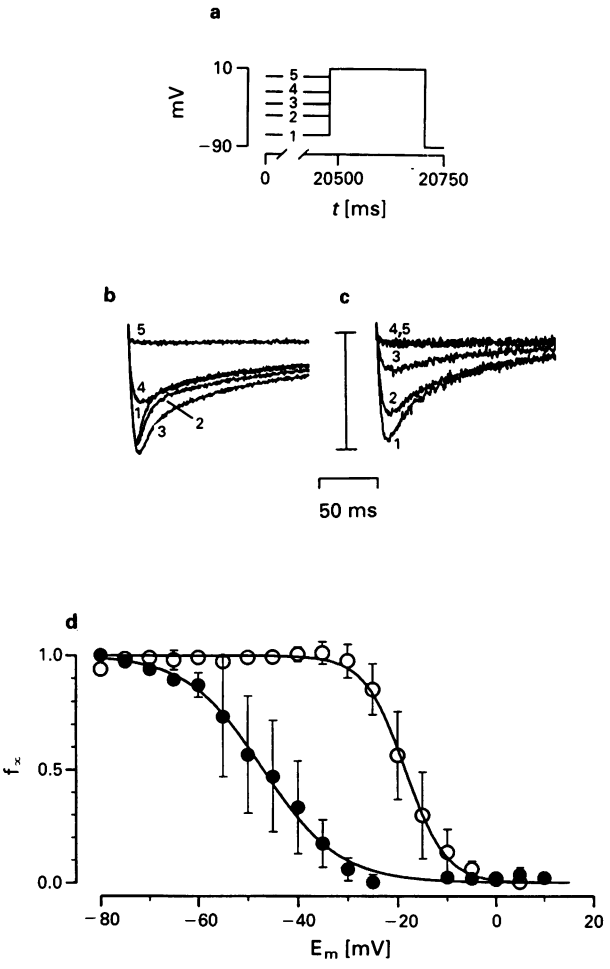

Figure 2 Effect of fendiline on the availability (f∞) of L-type calcium channels. (a) Voltage jump protocol consisted of holding potential of − 90 mV. Varying conditioning membrane potentials (20 s) starting from − 80 mV were increased in 5 mV steps to final value of + 10 mV. Subsequently, a command potential of + 10 mV was delivered for 250 ms to elicit I_{Ca}. (b) and (c) Superimposed I_{Ca} recordings numbered corresponding to (a), under control conditions (b) and in presence of 30 μM fendiline (c). The vertical bar between (b) and (c) represents 1.0 and 0.5 nA for the two records, respectively. (d) I_{Ca} availability curves ($n = 4$) showing mean f∞ values, calculated as outlined under Results under control conditions (○) and in presence of 30 μM fendiline (●). Standard deviations exceeding the symbol size are shown by vertical bars. The solid line represents a least-squares fit through the data according to equations (1) and (2) in the Methods.

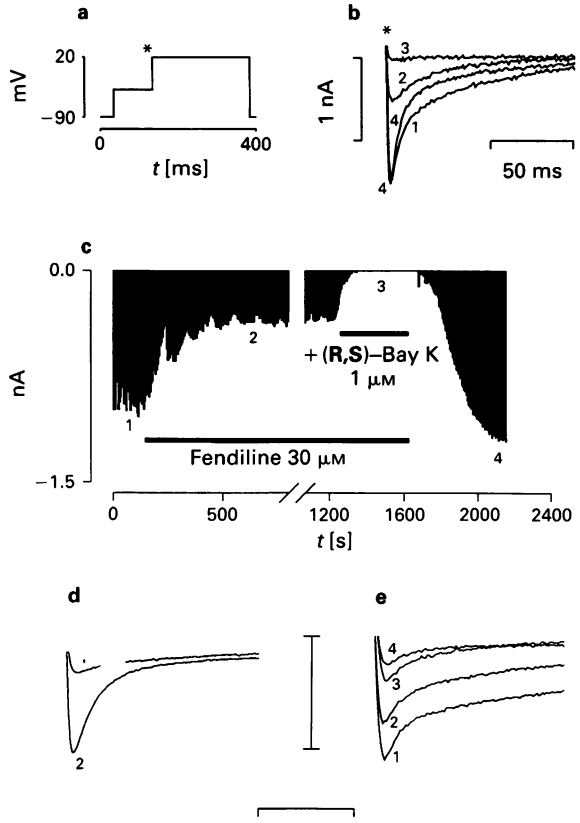

Figure 3 The paradoxical inhibition of I_{Ca} by (4R,4R)-Bay K 8644 in presence of fendiline. (a) Voltage pulse protocol to elicit peak I_{Ca} ($I_{Ca,peak}$): holding potential was − 90 mV, followed by a prepotential of − 40 mV (100 ms) and then a command potential of + 10 mV (250 ms) delivered recurrently at 5 s intervals. (b) Superimposed records of I_{Ca} showing the effects of fendiline (30 μM) and (4R,4S)-Bay K 8644 in the presence of fendiline, numbered to correspond to the points in (c). (c) Time-dependent changes in the magnitude $I_{Ca(peak)}$ following the application of fendiline (30 μM) and (4R,4S)-Bay K 8644 (1 μM) in the presence of fendiline. The drugs applied during the periods indicated by bars were washed-out later showing recovery of I_{Ca}. (d) I_{Ca} recorded under control conditions (1) and in presence of 1μM (4R,4S)-Bay K 8644 (2). (e) I_{Ca} recorded under control conditions (1) and in presence of 30 μM fendiline (2–4). (4R,4S)-Bay K8644 was present in concentrations of 10 nM (3) and 30 nM (4).

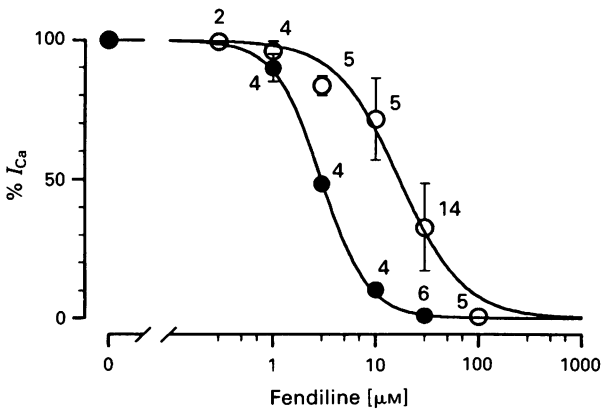

Figure 4 Cumulative dose-response curves for fendiline added alone (○, data from Tripathi *et al.*, unpublished) or in presence of 1 μM (4R,4S)-Bay K 8644 (●) on $I_{Ca(peak)}$: pulse protocol as depicted in Figure 3a. Effect of fendiline (%I_{Ca}) as % of $I_{Ca(peak)}$ under control conditions. Mean values with vertical bars showing standard deviations, number of experiments given adjacent to data points. Solid lines represent dose-response curve fitted through the data points.

Interaction of (4R,4S)-Bay K 8644 with other L-type calcium channel blockers

In view of this 'inverse' effect of Bay K 8644 on calcium channels blocked by fendiline, it was of interest to investigate whether Bay K 8644 in combination with other known organic calcium channel blockers gives rise to a similar phenomenon under our experimental conditions. Diltiazem, verapamil and nifedipine were first administered at submaximal doses. An additional administration of 1 μM (4R,4S)-Bay K 8644 led to the expected increase of $I_{Ca(peak)}$ in presence of all these three calcium channel blockers as shown in Figure 5c–f.

Discussion

Different extra- and intracellular solutions were tested for appropriate voltage clamp recording of the L-type cardiac calcium current (I_{Ca}). Replacement of most of the intracellular K^+ by Cs^+ and addition of ATP to the pipette solution proved useful in preventing rundown of I_{Ca} for up to 1–2 h. Elimination of the fast sodium current by TTX-blockade, substitution of Na^+ by choline$^+$ and/or predepolarization to − 40 mV for 100 ms was found necessary to obtain unimpaired I_{Ca} recordings. The possibility of contamination of the recorded current by activation of T-type calcium channels (which are reported to exist in guinea-pig ventricular cells, Tytgat *et al.*, 1990) would also be eliminated by the predepolarization.

Fendiline, prenylamine and other diphenylalkylamines were initially classified as 'weak' calcium-antagonists (Fleckenstein, 1981). At a later stage, however, these agents were shown to act on other sites, e.g. calmodulin (Johnson & Fugmann, 1983; Spedding, 1983; Bayer & Mannhold, 1987). Vaghy *et al.* (1982) have shown that fendiline acts as a selective inhibitor of the Na^+/Ca^{2+}-antiporter in rabbit heart mitochondria at an IC_{50} of 13 μM. Moreover, Motulsky *et al.* (1983) found a selective displacement of [^{3}H]-yohimbine by fendiline in human platelets suggesting its action on α_2-receptors with a K_D value of 2.6 μM. These reports led to the belief that fendiline was not a specific inhibitor of L-type calcium channels. The direct blocking effect of fendiline upon extracellular application on the voltage-sensitive calcium channel has nevertheless been demonstrated recently by Schreibmayer *et al.* (1991).

Modulation of I_{Ca} by fendiline

Electrophysiological observations on the interaction of most of the organic compounds with the cardiac calcium channel can be readily interpreted by the assumption of a 'modulated' receptor (modulated receptor hypothesis (MRH), Hondeghem & Katzung, 1977; Bean, 1984; Uehara & Hume, 1985). Additional assumptions have been made to account for occasionally observed complex behaviour of the channel. These are for instance the assumption of (i) a second open state ('modal' gating, Hess *et al.*, 1984) and (ii) two or more 1,4-dihydropyridine binding sites on one calcium channel unit (Lacerda & Brown, 1989).

A marked shift of the availability curve to more negative membrane potentials is common to 1,4-dihydropyridines, phenylalkylamines and benzothiazepines (Uehara & Hume, 1985). This indicates a high affinity of the inactivated channel state for these drugs in terms of the MRH. A high affinity of 1,4-dihydropyridines for the inactivated channel state in comparison to the rested state has been demonstrated more directly by dose-response curves for I_{Ca}-inhibition at different membrane potentials (Bean, 1984; Brown *et al.*, 1987). We observed a significant shift of the f_∞ curve to more negative potentials in the presence of fendiline (Figure 2), indicating thereby, that the inactivated channel state also has high

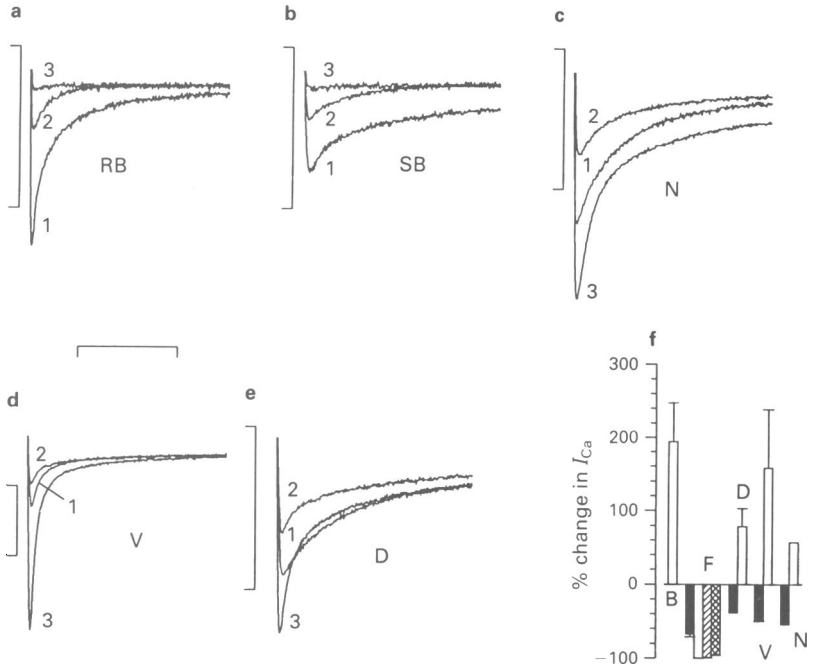

Figure 5 Effects of combination of various drugs on I_{Ca}: pulse protocol as in Figure 3. (a–e) Vertical bar: 1 nA; horizontal bar: 70 ms; (1) control I_{Ca}, (2) I_{Ca} recorded in presence of calcium antagonist (30 μM fendiline in a,b; 0.3 μM nifedipine (N) in c; 3 μM verapamil (V) in d; 3 μM diltiazem (D) in e); (3) I_{Ca} in additional presence of 1 μM (4**R**)-Bay K 8644 (a), 1 μM (4**S**)-Bay K 8644 (b) and 1 μM (4**R**,4**S**)-Bay K 8644 (c–e). (f) Diagram of %change in $I_{Ca(peak)}$ (mean with s.e. shown by vertical bars): B, addition of 1 μM (4**R**,4**S**)-Bay K 8644 ($n = 4$); F, 30 μM fendiline alone (solid column, $n = 14$), in combination with 1 μM (4**R**,4**S**)-Bay K 8644 (open column, $n = 5$), 1 μM (4**R**)-Bay K 8644 (hatched column, $n = 4$) and 1 μM (4**S**)-Bay K 8644 (cross-hatched column, $n = 4$); D, 3 μM diltiazem alone (solid column) and in combination with 1 μM (4**R**,4**S**)-Bay K 8644 (open column, single experiment); V, 3 μM verapamil alone (solid column) and with 1 μM (4**R**,4**S**)-Bay K 8644 (open column, $n = 3$); N, 0.3 μM nifedipine alone (solid column) and with 1 μM (4**R**,4**S**)-Bay K 8644 (open column, single experiment).

affinity for this drug. A peculiar feature of the inhibitory effect of fendiline is the observation of significant hastening of I_{Ca} inactivation (Figure 1). Also a similar decrease in inactivation time constant has been observed for some antagonistic 1,4-dihydropyridines (Lee & Tsien, 1983; Sanguinetti & Kass, 1984, but see Brown *et al.*, 1986). This appears to be a common feature of 1,4-dihydropyridine agonists (Hess *et al.*, 1984; Lacerda & Brown, 1989). In terms of the MRH this indicates a high affinity of the drug for the open and inactivated states of the channel. A fast 'on'-rate of the drug to the open state has been directly demonstrated for nifedipine by use of a special double-pulse protocol (Uehara & Hume, 1985). In the same study it has been demonstrated that the corresponding 'on'-rates for diltiazem and D-600 are much slower and the apparent drug binding occurs mainly via the inactivated state.

The time course of activation was found to be unaffected by fendiline (Figure 1), similar to phenylakylamines and benzothiazepines (Lee & Tsien, 1983; Uehara & Hume, 1985). Antagonist 1,4-dihydropyridines have been shown either not to affect the time course of activation (Lee & Tsien, 1983; Uehara & Hume, 1985), or to speed it up slightly (Hess *et al.*, 1984). Agonist 1,4-dihydropyridines, on the other hand, have been reported generally to speed up activation accompanied by a shift of the steady state activation curve to more negative potentials (Hess *et al.*, 1984; Lacerda & Brown, 1989; Patmore *et al.*, 1990). These observations are suggestive of an 'on'-reaction of agonist dihydropyridines with some pre-open state.

In view of these reports our findings lead us to suggest that the functional modulation of I_{Ca} by fendiline most closely resembles that observed for 1,4-dihydropyridine blocking drugs, which do not affect the time course of activation of I_{Ca}.

Interaction of Bay K 8644 with fendiline

The most striking observation of our study was a 'paradoxical' reversal of the agonist effect of Bay K 8644 on I_{Ca} in presence of fendiline (Figures 3 and 5). Such a comodulation of an ion channel seems not to have been described previously.

Our results clearly indicate that despite a resemblance in functional modulation of calcium channels by fendiline and 1,4-dihydropyridines their sites of action are distinct. It has been discussed in the literature (see Brown *et al.*, 1986, for example), that two physically distinct 1,4-dihydropyridine sites exist on one L-type calcium channel protein: one mediating agonist and the other the antagonist action. In order to produce the paradoxical effect, Bay K 8644 might have acted on the former and fendiline on the latter site. This hypothesis is rendered unlikely as (4**R**,4**S**)-Bay K 8644 in the presence of the antagonist nifedipine does not induce effects comparable to the paradoxical one observed in the presence of fendiline. Instead the normal reversal of the antagonist action of nifedipine by Bay K 8644 was observed (Figure 5).

Bay K 8644 is in fact a racemic mixture of one high affinity agonist ((4**S**)-Bay K 8644) and one antagonist ((4**R**)-Bay K 8644) with lower affinity (Franckowiak *et al.*, 1985). Under the experimental protocol used by us, the racemic mixture by itself, acted as an agonist (Figure 3d). If this agonist action was due to competition of the two enantiomers for one site, fendiline could well have altered their apparent affinities in an allosteric manner, leading to increased affinity for the antagonist isomer. As the pure agonist as well as the antagonist isomers exerted a similar inhibitory effect in combination with fendiline as observed with the racemic form (Figure 5a and b) the above hypothesis is ruled out.

Positive cooperativity is clearly indicated by (i) the shift of the dose-response curve for fendiline to lower concentrations and (ii) the definite increase in the Hill coefficient in the presence of 1 μM Bay K 8644 (Figure 4). Our findings also provide a mechanistic explanation for the observations of Spedding & Berg (1984) that Bay K 8644 could not reverse the inhibitory effect of fendiline in calcium-induced contractions of guinea-pig taenia preparations.

Based on chemical structure and radioligand binding properties, organic calcium channel blockers are currently classified into five subgroups (see for example Grassegger *et al.*, 1989) without a separate one for diphenylalkylamines. In view of the unique paradoxical effect of fendiline in combination with Bay K 8644 observed by us, one has to take into consideration that diphenylalkylamines might act on an altogether different site on the voltage-dependent calcium channel.

We thank Prof. R.A. Chapman (Bristol, U.K.) for critical correction of the manuscript and Prof. H. Glossman (Innsbruck, Austria), Dr K. Groschner (Graz, Austria) and Dr B. Wagner (Freiburg, Germany) for valuable gifts of some of the organic calcium channel modulators. Mrs B. Spreitzer and Mr A. Russ provided excellent assistance in culturing cells and computer work respectively. We gratefully acknowledge financial support by the Austrian Research Foundation (project No.: S4504B) and Thiemann Pharma (travelling fellowship to O.T.).

References

BAYER, R. & MANNHOLD, R. (1987). Fendiline: A review of its basic pharmacological and clinical properties. *Pharmacother.*, **5**, 103–136.

BEAN, B.P. (1984). Nitrendipine block of cardiac calcium channels: High-affinity binding to the inactivated state. *Proc. Natl. Acad. Sci. U.S.A.*, **81**, 6388–6392.

BROWN, A.M., KUNZE, D.L. & YATANI, A. (1986). Dual effects of dihydropyridines on whole cell and unitary calcium currents in single ventricular cells of guinea pig. *J. Physiol.*, **379**, 495–514.

BROWN, A.M., YATANI, A., LACERDA, A.E., GURROLA, G.B. & POSSANI, L.D. (1987). Neurotoxins that act selectively on voltage-dependent cardiac calcium channels. *Circ. Res.*, **61**, I-6–I-9.

FLECKENSTEIN, A. (1981). Fundamental actions of calcium antagonists on myocardial and cardiac pacemaker cell membranes. In *New Perspectives on Calcium Antagonists*. ed. Weiss, G.B., pp. 51–81: Bethesda MD: American Physiological Society.

FLECKENSTEIN, A., FLECKENSTEIN-GRÜN, G. & BYON, Y.K. (1977). Fundamentale Herz- und Gefäßwirkungen des Ca^{++}-antagonistischen Koronartherapeutikums Fendilin (Sensit^R) *Drug Res.*, **29**, 230–246.

FRANCKOWIAK, G., BECHEM, M., SCHRAMM, M. & THOMAS, G. (1985). The optical isomers of the 1,4-Dihydropyridine Bay-K-8644 show opposite effects on calcium channels. *Eur. J. Pharmacol.*, **114**, 223–226.

GRASSEGGER, A., STRIESSNIG, J., WEILER, M., KNAUS, H.G. & GLOSSMANN, H. (1989). [^{3}H]HOE166 defines a novel calcium antagonist drug receptor – distinct from the 1,4 dihydropyridine binding domain. *Naunyn Schmiedebergs Arch. Pharmacol.*, **340**, 752–759.

HAMILL, O.P., MARTY, A., NEHER, E., SAKMANN, B. & SIGWORTH, F. (1981). Improved patch-clamp techniques for high resolution current recording from cells and cell-free membrane patches. *Pflügers Arch.*, **391**, 85–100.

HESS, P., LANSMAN, J.B. & TSIEN, R.W. (1984). Different modes of calcium channel gating behaviour favoured by dihydropyridine calcium agonists and antagonists. *Nature*, **311**, 538–544.

HONDEGHEM, L.M. & KATZUNG, B.G. (1977). Time- and voltage dependent interaction of antiarrhytmic drugs with cardiac sodium channels. *Biochem. Biophys. Acta.*, **472**, 373–398.

JOHNSON, J.D. & FUGMAN, D.A. (1983). Calcium and calmodulin antagonists binding to calmodulin and relaxation of coronary segments. *J. Pharmacol. Ther.*, **226**, 330–334.

LACERDA, A.E. & BROWN, A.M. (1989). Nonmodal gating of cardiac calcium channels as revealed by dihydropyridines. *J. Gen. Physiol.*, **93**, 1243–1273.

LEE, K.S. & TSIEN, R.W. (1983). Mechanism of calcium channel blockade by verapamil, D600, diltiazem and nitrendipine in single dialysed heart cells. *Nature*, **302**, 790–794.

MOTULSKY, H.J., SNAVELY, M.D., HUGHES, R.J. & INSEL, P.A. (1983). Interaction of verapamil and other calcium channel blockers with a1- and a2-adrenergic receptors. *Circ. Res.*, **52**, 226–231.

PATMORE, L., DUNCAN, G.P., CLARKE, B., ANDERSON, A.J., GREENHOUSE, R. & PFISTER, J.R. (1990). RS 30026: a potent and effective calcium channel agonist. *Br. J. Pharmacol.*, **99**, 687–694.

SANGUINETTI, M.C. & KASS, R.S. (1984). Voltage-dependent block of calcium channel current in the calf cardiac purkinje fiber by dihydropyridine calcium channel antagonists. *Circ. Res.*, **55**, 336–348.

SCHREIBMAYER, W., TRITTHART, H.A., ZERNIG, G. & PIPER, H.M. (1985). Single voltage-dependent and outward rectifying potassium channels in isolated rat heart cells. *Eur. Biophys. J.*, **11**, 259–263.

SCHREIBMAYER, W., TRIPATHI, O. & TRITTHART, H.A. (1991). Block of cardiac calcium channels by fendiline in guinea pig ventricular cells. *Biophys. J.*, **59**, 552a.

SPEDDING, M. (1983). Direct inhibitory effects of some 'calcium-antagonists' and trifluoroperazine on the contractile proteins in smooth muscle. *Br. J. Pharmacol.*, **79**, 225–231.

SPEDDING, M. & BERG, C. (1984). Interactions between a 'calcium channel agonist', Bay-K-8644, and calcium antagonists differentiate calcium antagonist subgroups in K^+-depolarized smooth muscle. *Naunyn Schmiedebergs Arch. Pharmacol.*, **328**, 69–75.

STARMER, C.F. & GRANT, A.O. (1985). Phasic ion channel blockade. A kinetic model and parameter estimation procedure. *Mol. Pharmacol.*, **28**, 348–356.

TRAUTWEIN, W., McDONALD, T.F. & TRIPATHI, O. (1975). Calcium conductance and tension in mammalian ventricular muscle. *Pflügers Arch.*, **354**, 55–74.

TRITTHART, H.A. & KOIDL, B. (1985). Das pharmakologische Wirkungsprinzip von Calciumantagonisten: Fendilin im Vergleich zu Nifedipin, Verapamil und Diltiazem. In *Calmodulin und Calciumantagonismus*. ed. Luethy, E. pp. 41–52. New York: Gustav Fischer.

TSIEN, R.W., BEAN, B.P., HESS, P., LANSMAN, J.B., NILIUS, B. & NOWYCKY, M.C. (1986). Mechanisms of calcium channel modulation by beta-adrenergic agents and dihydropyridine calcium agonists. *J. Mol. Cell. Cardiol.*, **18**, 691–710.

TYTGAT, J., VEREECKE, J. & CARMELIET, E. (1990). A combined study of sodium current and T-type calcium current in isolated cardiac cells. *Pflügers Arch.*, **417**, 142–148.

UEHARA, A. & HUME, J.R. (1985). Interactions of organic calcium channel antagonists with calcium channels in single frog atrial cells. *J. Gen. Physiol.*, **85**, 621–647.

VAGHY, P.L., JOHNSON, J.D., MATLIB, M.A., WANG, T. & SCHWARTZ, A. (1982). Selective inhibition of Na^+-induced Calcium release from heart mitochindria by diltiazem and certain other calcium antagonist drugs. *J. Biol. Chem.*, **257**, 6000–6002.

(Received November 22, 1991
Revised January 27, 1992
Accepted January 30, 1992)

Br. J. Pharmacol. (1992), **106**, 157–165 © Macmillan Press Ltd, 1992

Contractions induced by potassium-free solution and potassium relaxation in vascular smooth muscle of hypertensive and normotensive rats

[1]Pertti Arvola, Ilkka Pörsti, Pauli Vuorinen, Anu Pekki & Heikki Vapaatalo

Department of Biomedical Sciences, University of Tampere, P.O. Box 607, SF-33101, Tampere, Finland

1 Vascular contractions induced by K^+-free solution and relaxation responses following the return of K^+ to the organ bath were studied in mesenteric arterial rings from spontaneously hypertensive rats (SHR) and normotensive Wistar-Kyoto rats (WKY) with particular focus on the role of vascular adrenergic nerve-endings and endothelium.

2 In endothelium-denuded rings the omission of K^+ from the incubation medium resulted in gradual contractions, the rate of which was slower in SHR than WKY. Nifedipine (1 μM) inhibited the contractions more effectively in SHR than WKY.

3 Adrenergic denervation *in vitro* with 6-hydroxydopamine reduced the contractions induced by the K^+-free medium in endothelium-denuded rings. The remaining contractions after denervation were markedly greater in SHR than WKY.

4 The presence of intact vascular endothelium attenuated the K^+-free contractions in both strains, the attenuation being smaller in SHR than WKY. N^G-nitro-L-arginine methyl ester (L-NAME, 0.1 mM) and methylene blue (10 μM), but not indomethacin (10 μM), abolished the attenuating effect of endothelium on the K^+-free contractions. L-Arginine (1 mM) reversed the effect of L-NAME in WKY but not in SHR.

5 The re-addition of K^+ after full K^+-free contractions dose-dependently relaxed the rings. The rate of this K^+-induced relaxation was significantly slower in SHR than WKY at all K^+ concentrations (0.1–5.9 mM) studied, whether the endothelium or functioning adrenergic nerve-endings were present or not. Ouabain (1 mM) totally inhibited the K^+ relaxation in SHR but only partially in WKY.

6 Vascular smooth muscle contractions induced by high concentrations of potassium were comparable between the strains. The EC_{50} for noradrenaline-induced contractions was lower in SHR than WKY, but the maximal forces did not differ significantly.

7 In conclusion, the contractile response in K^+-free solution more clearly differentiates vascular rings from SHR and WKY than the responses induced by the classical contractile agents noradrenaline and high concentrations of potassium. The depressant effect of the presence of intact endothelium on the K^+-free contractions, which was smaller in SHR than WKY, is mediated via the endothelium-derived relaxing factor. Neurotransmitter release from vascular adrenergic nerve-endings participates less in the K^+-free contractile response in SHR than WKY. Moreover, the contractile response is more dependent on calcium entry through nifedipine-sensitive calcium channels in SHR than WKY. The greater K^+-free contractions of denervated endothelium-denuded rings and the reduced K^+ relaxation rate in SHR when compared to WKY suggest increased cell membrane permeability and decreased activity of vascular Na^+, K^+-ATPase, respectively, in this type of genetic hypertension.

Keywords: Adrenergic nerve-endings; endothelium; potassium; potassium-free contraction; potassium relaxation; spontaneously hypertensive rat; vascular smooth muscle; Wistar-Kyoto rats

Introduction

Increased responses to the classical contractile agents noradrenaline and high concentrations of KCl and decreased relaxation have been described in arterial smooth muscle of spontaneously hypertensive rats (SHR) (Field & Soltis, 1985). However, the findings in different investigations have been somewhat inconsistent, and not all studies have been able to demonstrate increased sensitivity to vasoconstrictor agents in experimental forms of hypertension (see Bohr & Webb, 1984). The controversial results and rather small changes between hypertensive and normotensive blood vessels suggest that the study of vasoconstrictor sensitivity alone does not reveal all alterations in arterial smooth muscle function associated with hypertension.

Bohr *et al.* (1988) have suggested that a generalized membrane defect is associated with genetic hypertension. Increased membrane permeability both in vascular smooth muscle (Hopp *et al.*, 1986) and in non-vascular cells (Tamura *et al.*, 1985; Furspan *et al.*, 1989) has been demonstrated in hypertensive animals. The contractile response induced by inhibition of vascular Na^+, K^+-ATPase with K^+-free medium has commonly been used as a tool to study smooth muscle permeability to ions in both hypertensive and normotensive rats (Bohr *et al.*, 1988; Lamb *et al.*, 1988). However, since these investigations involved endothelium-intact preparations, different endothelial influences on the contractile responses in hypertensive and normotensive blood vessels may have affected the results. In addition, the participation of adrenergic nerve-endings in vascular contractions induced by N^+, K^+-ATPase inhibition via endogenously released noradrenaline (NA) (Vanhoutte & Lorenz, 1984) may alter responses differently in hypertensive and normotensive arteries.

Vascular endothelium has a basal release of the endothelium-derived relaxing factor (EDRF), which stimulates

[1] Author for correspondence:

soluble guanylate cyclase and elevates guanosine 3':5'-cyclic monophosphate (cyclic GMP) in vascular smooth muscle cells (Furchgott & Vanhoutte, 1989), and is thus capable of controlling vascular tone (Pique *et al.*, 1989; Kelm & Schrader, 1990; Vane *et al.*, 1990). EDRF has been identified as nitric oxide (Moncada *et al.*, 1991) or a closely related substance (Myers *et al.*, 1990) synthesized from L-arginine, and the synthesis can be inhibited with arginine analogues such as N^G-nitro-L-arginine methyl ester (L-NAME) (Ishii *et al.*, 1990).

We have previously found that the contractile response induced by K^+-free solution and the K^+ relaxation clearly differentiate vascular smooth muscle of hypertensive and normotensive rats (Pörsti *et al.*, 1992). The aim of the present study was to investigate in greater detail the vascular smooth muscle responses induced by alterations in organ bath K^+ concentration in SHR and their normotensive controls Wistar-Kyoto rats (WKY). Special attention was paid to the modulatory role of adrenergic nerve-endings and endothelium.

Methods

Animals

Male SHR of the Okamoto-Aoki strain and WKY (Møllegaard's Breeding Centre, Ejby, Denmark) were used at the age of 22–25 weeks (weight 370–410 g in SHR, 370–430 g in WKY). The rats were housed four animals a cage in a room maintained at 22°C and illuminated from 06 h 00 min to 18 h 00 min and had free access to drinking fluid (tap water) and food pellets (Ewos, Södertälje, Sweden). The systolic blood pressures of the unanaesthetized rats were measured by the tail cuff method at 28°C (Model 129 Blood Pressure Meter; IITC Inc., Woodland Hills, Ca., U.S.A.).

The experimental design of the study was approved by the Animal Experimentation Committee of the University of Tampere.

Vascular responses in vitro

The animals were decapitated and the mesenteric arteries excised and cleaned of connective tissue. Three successive sections (3 mm in length) of the artery from each animal were cut, beginning 1 cm distally from the mesenteric artery-aorta junction. The vascular endothelium was removed by gently rubbing with a scuffed injection needle. The mesenteric arterial rings were placed between stainless steel hooks and mounted in an organ bath chamber in physiological salt solution (PSS) (pH 7.4) of the following composition (mM): NaCl 119.0, $NaHCO_3$ 25.0, glucose 11.1, $CaCl_2$ 1.6, KCl 4.7, KH_2PO_4 1.2, $MgSO_4$ 1.2, and aerated with 95% O_2: 5% CO_2. The rings were equilibrated for 1 h at 37°C with a resting tension of 1.5 g. The force of contraction was measured with an isometric force-displacement transducer (Grass FT03) and registered on a polygraph (Model 7 E Polygraph; Grass Instrument Co., Quincy, Ma., U.S.A.).

The absence of endothelium was confirmed by the lack of relaxation response to 1 μM acetylcholine (ACh) in vascular rings precontracted with 1 μM NA. If any relaxation was observed, the endothelium was further rubbed. After a 30 min stabilization period, cumulative concentration-response curves for NA and KCl were determined. In solutions containing high concentrations of K^+ (20–125 mM), NaCl was substituted with KCl on an equimolar basis.

After another 30 min of stabilization, K^+ was omitted from the PSS. The K^+-free buffer solution (pH 7.4) was prepared by substituting KH_2PO_4 and KCl with NaH_2PO_4 and NaCl, respectively, on an equimolar basis. The baths were rinsed with fresh K^+-free solution every 20 min. The K^+-free solution resulted in a gradual contraction in all vascular rings. After the contraction had reached a plateau, a single dose of K^+ was re-added to the baths and the subsequent relaxation registered.

The K^+-free contraction and K^+ relaxation procedure was also performed in endothelium-denuded rings after chemical adrenergic denervation and in the presence of ouabain (1 mM), and in endothelium-intact rings as such and in the presence of the competitive EDRF synthesis inhibitor L-NAME (0.1 mM) with or without L-arginine (1 mM). The effect of soluble guanylate cyclase inhibition by methylene blue (10 μM) on K^+-free contractions was studied in endothelium-intact rings. The cyclo-oxygenase inhibitor, indomethacin (10 μM), was used to examine the possible effects of endothelial prostacyclin on K^+-free contractions. The effect of the Ca^{2+} antagonist, nifedipine (1 μM), on contractions was investigated in endothelium-denuded rings. The endothelium-denuded rings were denervated *in vitro* by exposing them to a buffer-free solution containing 1.2 mM 6-hydroxydopamine, and vigorously gassing them with nitrogen for 15 min, followed by a 2 h recovery period in normal PSS (Aprigliano & Hermsmeyer, 1976). L-NAME, L-arginine and indomethacin were added to the baths 15 min before, and the other compounds simultaneously with the introduction of K^+-free solution.

To test the dependence of K^+-free contractions on organ bath Ca^{2+} and Na^+ concentrations, further experiments with endothelium-denuded mesenteric arterial rings were made with the K^+-free, Ca^{2+}-free solution (Ca^{2+} omitted from K^+-free solution) and the K^+-free, low Na^+ solution (Na^+ 25 mM, NaCl substituted with LiCl on an equimolar basis). Some endothelium-denuded rings from SHR and WKY were also exposed to 1 mM ouabain in normal PSS. In an additional series, concentration-response curves for ACh-induced relaxations were determined cumulatively in 1 μM NA-precontracted mesenteric arterial rings with intact endothelium.

Morphological studies

To test the adequacy of our mechanical endothelium denudation, both endothelium-denuded and -intact mesenteric arterial rings from WKY were prepared for electron microscopy. The rings were fixed in 2% glutaraldehyde at 4°C and postfixed in 2% osmiumtetroxide. After washing, they were stained with 1% uranyl acetate and dehydrated with acetone series. Thereafter the samples were embedded in Epon (LX-112 Resin, Ladd, Burlington, Vt., U.S.A.). Ultrathin sections were stained with 4% uranyl acetate and 0.2% lead citrate and examined under a Jeol JEM 1200 electron microscope (Jeol Ltd., Tokyo, Japan) at 60 kV accelerating voltage.

Drugs

The following drugs were used: acetylcholine chloride, 6-hydroxydopamine, indomethacin, N^G-nitro-L-arginine methyl ester hydrochloride, ouabain octahydrate (Sigma Chemical Co., St. Louis, Mo., U.S.A.), L-arginine, methylene blue (E. Merck AG, Darmstadt, Germany), nifedipine (Orion Pharmaceutical Co., Espoo, Finland) and (−)-noradrenaline L-hydrogentartrate (Fluka Chemie AG, Buchs SG, Switzerland). The stock solutions were dissolved in distilled water, with the exception of indomethacin (in 1.5 mM Na_2CO_3), nifedipine (in 50% ethanol), 6-hydroxydopamine and ouabain (in PSS). All solutions were freshly prepared and protected from light.

Analysis of results

EC_{50} for NA and KCl in each ring was calculated from the plots of the concentration of agonist versus the percentage of maximal contraction response. IC_{50} for ACh-induced relaxations was calculated correspondingly. Contractile responses in K^+-free solution were normalized by comparing them to the maximal response induced by 125 mM KCl. After re-addition of K^+ the greatest reduction in smooth muscle

contractile force during a 1 min period was considered the maximal relaxation rate, which was normalized by comparing it to the maximal 125 mM KCl-induced contraction, or by relating it to the pre-existing maximal K^+-free contraction or tissue dry weight.

Statistical analysis was carried out by one-way analysis of variance (ANOVA) supported by Bonferroni confidence intervals. Differences were considered significant when $P<0.05$. BMDP Statistical Software (Los Angeles, Ca., U.S.A.) was used. All results are expressed as mean ± s.e.mean.

Results

K^+-free contractions of endothelium-denuded vascular rings

Typical tracings of the K^+-free contraction and K^+ relaxation procedure in endothelium-denuded rings from SHR and WKY (systolic blood pressures 215–250, 120–165 mmHg, respectively) are presented in Figure 1. The rate of K^+-free contraction was significantly slower in SHR than in WKY, while the maximal forces were comparable (Table 1, Figures 1 and 2). The time from K^+ omission to the onset of rise in contractile force did not differ between the two strains (7.3 ± 0.5 min in SHR, 6.7 ± 0.4 min in WKY).

If Ca^{2+} was omitted from the K^+-free solution the endothelium-denuded rings of neither strain contracted. The re-addition of Ca^{2+} to the K^+-free, Ca^{2+}-free solution resulted in a steep rise in the contractile force, rapidly reaching the level of the normal K^+-free contraction (Figure 1). When the Na^+ concentration of the K^+-free solution was lowered to 25 mM practically no contractions were induced in WKY, whereas some were seen in SHR. After changing the K^+-free, low Na^+ solution to the normal K^+-free solution the rings gradually reached the normal level of K^+-free contraction (Figure 1).

The Ca^{2+} antagonist, nifedipine (1 μM), inhibited the K^+-free conctractions more effectively in SHR than WKY (Table 1). Nifedipine prolonged the time to maximal contraction by approximately 90% and 30%, and reduced the maximal force by approximately 75% and 60% in SHR and WKY, respectively. Na^+, K^+-ATPase inhibition with high concentrations of ouabain (1 mM) abolished the difference between SHR and

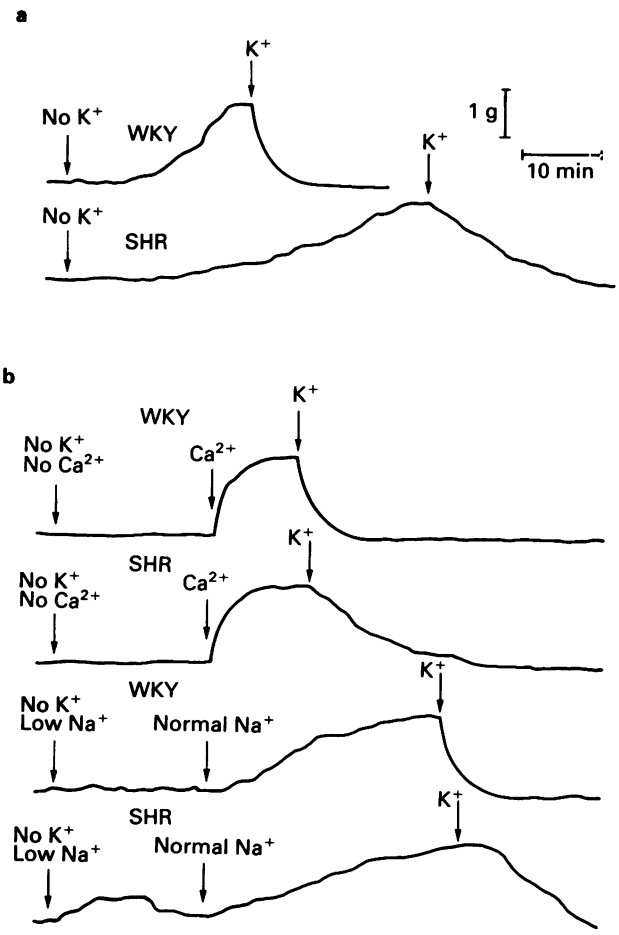

Figure 1 Typical responses (representative of 6–16 experiments) of endothelium-denuded mesenteric arterial rings from spontaneously hypertensive rats (SHR) and Wistar-Kyoto rats (WKY) (a) in K^+-free solution followed by relaxations induced by 1.0 mM potassium; (b) in K^+-free, Ca^{2+}-free solution and in K^+-free, low Na^+ solution (Na^+ 25 mM), the responses following the return of normal calcium and sodium, respectively, to the organ baths and subsequent relaxations induced by 1.0 mM potassium.

Table 1 Parameters of contractile responses induced by K^+-free solution in mesenteric arterial rings from spontaneously hypertensive (SHR) and Wistar-Kyoto rats (WKY)

		K^+-free contraction	
		Time to maximum (min)	*Maximal force* (% of 125 mM KCl)
Endo –	SHR	44.4 ± 2.5*	57.6 ± 5.1
	WKY	23.0 ± 1.2	60.6 ± 3.1
Endo –	SHR	83.9 ± 2.4* +	14.4 ± 1.1* +
+ nifedipine (1 μM)	WKY	30.3 ± 2.9	25.6 ± 2.3 +
Endo –	SHR	21.8 ± 1.3 +	59.0 ± 5.9
+ ouabain (1 mM)	WKY	20.1 ± 0.7	63.4 ± 3.7
Endo –	SHR	74.8 ± 5.4* +	55.0 ± 4.2*
+ adrenergic denervation	WKY	98.6 ± 7.2 +	23.5 ± 6.9 +
Endo +	SHR	49.2 ± 1.0*	47.5 ± 2.2*
	WKY	26.7 ± 2.6	28.2 ± 2.7 +
Endo +	SHR	42.7 ± 1.7*	53.9 ± 6.1
+ L-NAME (0.1 mM)	WKY	29.7 ± 6.2	69.6 ± 6.0
Endo +	SHR	51.9 ± 3.3*	58.4 ± 3.4*
+ L-NAME (0.1 mM) + L-arginine (1 mM)	WKY	27.7 ± 4.5	33.1 ± 2.5 +
Endo +	SHR	41.8 ± 3.2*	52.3 ± 7.7
+ methylene blue (10 μM)	WKY	17.7 ± 0.7	71.8 ± 3.6

Endo – = endothelium-denuded rings, Endo + = endothelium-intact rings. Values are mean ± s.e.mean from 6–16 experiments. *$P<0.05$ versus WKY, +$P<0.05$ versus corresponding parameter in Endo – rings (ANOVA).

WKY in K^+-free contraction rate (Table 1). Ouabain shifted the K^+-free contractile responses of SHR towards that of WKY, whereas the responses of WKY with and without ouabain did not deviate.

Effect of adrenergic denervation on K^+-free contractions of endothelium-denuded vascular rings

Chemical adrenergic denervation suppressed the K^+-free contractions of endothelium-denuded SHR and WKY rings, but the effect was smaller in SHR (Table 1 and Figure 2). Strikingly, no contractions were observed in WKY during the time in which the corresponding non-denervated rings had already reached their maximum. In denervated rings the time from K^+ omission to the onset of contraction was 4.6 ± 0.8 and 52.5 ± 5.0 min in SHR and WKY, respectively ($P < 0.05$). The rate of K^+-free contractions was also slower in denervated SHR rings when compared to rings with intact nerve-endings, but there was no significant difference in the maximal contractile force.

Effect of intact vascular endothelium on K^+-free contractions

The presence of intact vascular endothelium slowed the rate of K^+-free contractions in both strains. The maximal force of contraction was also decreased in WKY, but not in SHR, as compared to the contractions of corresponding endothelium-denuded rings (Table 1 and Figure 3).

L-NAME (0.1 mM), an inhibitor of EDRF synthesis, abolished the attenuation of K^+-free contraction in the presence of endothelium (Table 1 and Figure 3). The effect of L-NAME was reversed in WKY, but not in SHR, by 1 mM L-arginine. Methylene blue (10 μM), which inhibits soluble guanylate cyclase and thus the effects of EDRF, exerted an effect similar to that of L-NAME (Table 1). Indomethacin (10 μM) did not affect the K^+-free contractions of endothelium-intact rings from either strain.

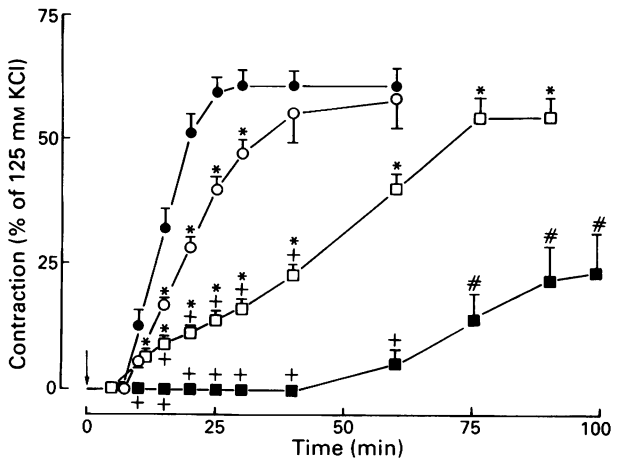

Figure 2 Contractile responses induced by K^+-free solution (100% represents the maximal force attained by 125 mM KCl) in endothelium-denuded mesenteric arterial rings with intact nerve-endings (○) and after adrenergic denervation (□) from spontaneously hypertensive rats (open symbols) and Wistar-Kyoto rats (closed symbols). Symbols indicate mean from 12–16 experiments; vertical bars show s.e.mean. $^*P < 0.05$ versus Wistar-Kyoto rats, $^+P < 0.05$ versus corresponding response in rings with intact nerve-endings, $^\#P < 0.05$ versus corresponding maximal response in rings with intact nerve-endings (ANOVA).

K^+ relaxation

The rate of relaxation induced by K^+ upon K^+-free contractions was slower in SHR than WKY in endothelium-denuded mesenteric arterial rings (Table 2 and Figure 4). The difference was seen with all K^+ concentrations studied. Small concentrations of K^+ (0.1 mM) elicited no relaxation in SHR, while the rings of WKY still expressed a clear relaxation.

Ouabain (1 mM) abolished the relaxations induced by 1.0 and 5.9 mM K^+ totally in SHR, but only partially in WKY,

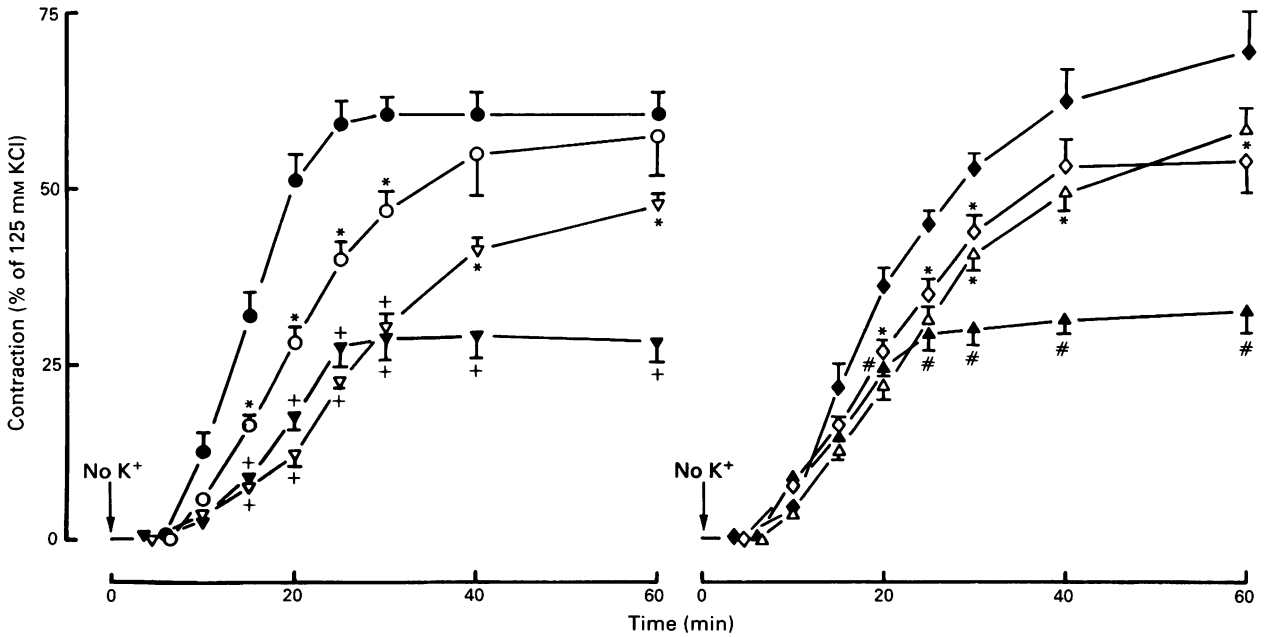

Figure 3 Contractile responses induced by K^+-free solution (100% represents the maximal force attained by 125 mM KCl) in endothelium-denuded (○) and endothelium-intact (▽) mesenteric arterial rings from spontaneously hypertensive rats (open symbols) and Wistar-Kyoto rats (closed symbols); and the effect of 0.1 mM N^G-nitro-L-arginine methyl ester (L-NAME) alone (◇) and with 1 mM L-arginine (△) on the responses in endothelium-intact rings. Symbols indicate mean from 8–16 experiments; vertical bars show s.e.mean. $^*P < 0.05$ versus Wistar-Kyoto rats, $^+P < 0.05$ versus corresponding response in endothelium-denuded rings, $^\#P < 0.05$ versus corresponding response in the presence of L-NAME alone (ANOVA).

in endothelium-denuded rings (Table 2 and Figure 4). In denervated and endothelium-intact preparations the difference between SHR and WKY in relaxation induced by 1.0 mM K^+ remained (Table 2). The relaxation rates in these rings tended to be slower than in corresponding endothelium-denuded non-denervated rings.

Other smooth muscle responses

Ouabain (1 mM) in normal PSS (K^+ 5.9 mM) elicited contractions resembling those induced by the K^+-free solution in SHR but not in WKY (Table 3). The concentration-response curves of contractions induced by KCl in endothelium-denuded rings did not differ significantly between the strains. The EC_{50} for NA was lower in SHR than WKY, but the maximal NA-induced contractions were comparable. The relaxations induced by ACh were attenuated in SHR and the time required for total relaxation after 125 mM KCl (the wash-out time) was longer in SHR than WKY (Table 3).

Morphological studies

The absence of endothelium in mechanically endothelium-denuded rings was confirmed by electron microscopy, which also showed the undamaged underlying smooth muscle cells in these preparations. The unrubbed rings had a well preserved endothelial cell monolayer (Figure 5).

Discussion

The omission of K^+ from the incubation medium results in an almost total inhibition of Na^+, K^+-ATPase (Mulvany, 1985), which can affect intracellular Ca^{2+} and promote smooth muscle contraction in many ways: (1) The inhibition causes depolarization and increases the influx of Ca^{2+} through voltage-dependent channels (Mulvany, 1985). (2) The depolarization of vascular adrenergic nerve-endings releases NA, which activates α-adrenoceptors and contributes to smooth muscle contraction (Vanhoutte & Lorenz, 1984). (3) Passive Na^+ leak through the cell membrane during Na^+, K^+-ATPase inhibition also increases intracelluar Na^+ and decreases the plasmalemmal Na^+ gradient, thus reducing the extrusion of Ca^{2+} by the Na^+, Ca^{2+} exchange mechanism and leading to increased intracellular Ca^{2+} (Blaustein, 1977).

In the present study, the K^+-free contractions of endothelium-denuded mesenteric arterial rings clearly differed between SHR and WKY, while there was no difference between the contractions induced by high concentrations of KCl, and only a modest increase in sensitivity to NA in SHR. Since the K^+-free contractile responses were strikingly attenuated after adrenergic denervation in WKY, they were predominatly mediated by intrinsic NA release. Adrenergic nerve-endings participated much less markedly in the K^+-free contractions of SHR rings, the remaining contractions after denervation being significantly greater in SHR than WKY. Therefore, other mechanisms of contraction must be operative in SHR.

Increased Ca^{2+} influx to the vascular smooth muscle cells of SHR has been shown to occur through the 'leak' channels, the receptor-operated channels and the voltage-sensitive

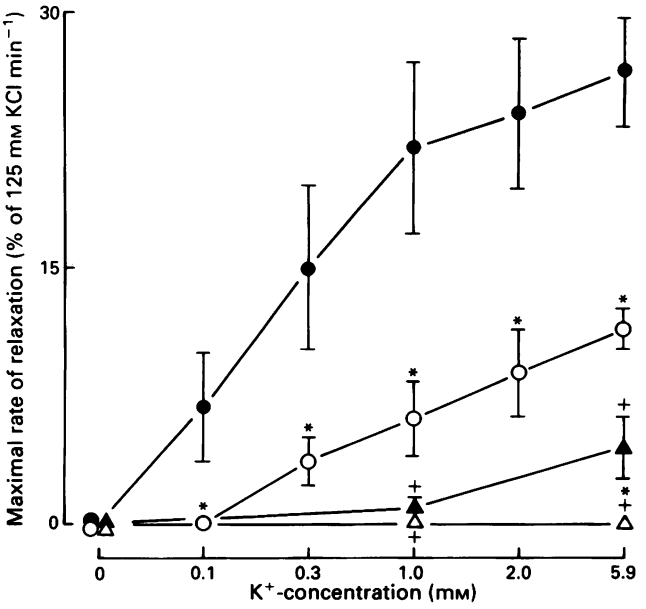

Figure 4 The maximal rates of K^+ relaxation (related to the maximal force induced by 125 mM KCl) in endothelium-denuded mesenteric arterial rings in the absence (○) and presence (△) of 1 mM ouabain in spontaneously hypertensive rats (open symbols) and Wistar-Kyoto rats (closed symbols). Symbols indicate mean from 8–16 experiments; vertical bars show s.e.mean. $^*P<0.05$ versus Wistar-Kyoto rats, $^+P<0.05$ versus corresponding response without ouabain (ANOVA).

Table 2 Parameters of relaxation responses induced by K^+ (1.0 mM) after full K^+-free contractions in mesenteric arterial rings from spontaneously hypertensive (SHR) and Wistar-Kyoto rats (WKY)

		K^+-relaxation rate	
		Related to maximal K^+-free contraction (% min^{-1})	*Related to tissue dry weight* ($g\ mg^{-1}\ min^{-1}$)
Endo –	SHR	13.2 ± 4.0*	0.31 ± 0.06*
	WKY	38.4 ± 5.3	1.17 ± 0.14
Endo –	SHR	no relaxation	no relaxation
+ ouabain (1 mM)	WKY	1.5 ± 1.0 +	0.06 ± 0.02 +
Endo –	SHR	5.1 ± 1.5* +	0.12 ± 0.02* +
+ adrenergic denervation	WKY	22.9 ± 4.1 +	0.22 ± 0.04 +
Endo +	SHR	4.7 ± 2.1* +	0.14 ± 0.03* +
	WKY	32.8 ± 3.5	0.95 ± 0.16
Endo +	SHR	6.1 ± 1.9* +	0.14 ± 0.03* +
+ L-NAME (0.1 mM)	WKY	33.7 ± 2.8	1.00 ± 0.19
Endo +	SHR	5.2 ± 0.4* +	0.20 ± 0.03* +
+ L-NAME (0.1 mM) + L-arginine (1 mM)	WKY	31.9 ± 3.2	0.92 ± 0.15

Endo – = endothelium-denuded rings, Endo + = endothelium-intact rings. Values are mean ± s.e.mean from 6–16 experiments. $^*P<0.05$ versus WKY, $^+P<0.05$ versus corresponding parameter in Endo – rings (ANOVA).

Table 3 Parameters of contraction and relaxation responses in mesenteric arterial rings from spontaneously hypertensive (SHR) and Wistar-Kyoto rats (WKY)

	SHR	*WKY*
Contraction		
EC_{50}		
Noradrenaline (nM)	495 ± 69*	729 ± 64
Potassium chloride (mM)	45.3 ± 1.8	43.5 ± 2.0
Maximal force		
(g mg^{-1} tissue dry weight)		
Noradrenaline (0.1 mM)	5.75 ± 0.51	6.64 ± 0.54
Potassium chloride (125 mM)	5.83 ± 0.32	6.70 ± 0.55
Ouabain (1 mM)	3.28 ± 0.35	no contraction
Relaxation		
Acetylcholine		
IC_{50} (nM)	103 ± 11*	18 ± 3
Maximal response to 10 μM ACh (% of pre-existing tension)	74 ± 7*	100 ± 2
Washout time after 125 mM KCl (min)	17.2 ± 1.3*	7.5 ± 0.6

Values are mean ± s.e.mean from 8–16 experiments. *$P<0.05$ versus WKY (ANOVA). Rings were endothelium-denuded, except those for acetylcholine (ACh) responses.

channels (Van Breemen *et al.*, 1986). Furthermore, the membranes of SHR can bind less Ca^{2+} than those of WKY and are more permeable to Ca^{2+} and Na^+ (Dominiczak & Bohr, 1990). In the present study nifedipine inhibited the K^+-free contractions more in SHR than WKY, suggesting that a greater proportion of the contraction results from Ca^{2+} influx through nifedipine-sensitive Ca^{2+} channels in SHR. The results support the concept of increased sensitivity to dihydropyridine Ca^{2+} antagonists in SHR, as reported previously by ourselves (Pörsti, 1992) and others (Lederballe *et al.*, 1978; Bohr & Webb, 1984). This is also in agreement with results of Rusch & Hermsmeyer (1988) showing that the relative proportions of voltage-dependent Ca^{2+} currents are different between SHR and WKY smooth muscle. The long-lasting current, sensitive to dihydropyridines (Bean *et al.*, 1986; Loirand *et al.*, 1986), is greater in SHR, whereas the transient current (dihydropyridine-resistant) predominates in WKY. Additionally, an altered Na^+, Ca^{2+} exchange mechanism could be hypothesized to explain the greater contractions of endothelium-denuded denervated rings in SHR. The Na^+, Ca^{2+} exchange mechanism has been found in large arteries (Ashida & Blaustein, 1987), but its role appears to be marginal in smaller vessels (Mulvany *et al.*, 1984; Hermsmeyer & Harder, 1986). Accordingly, the Na^+, Ca^{2+} exchange does not noticeably affect smooth muscle tone in our mesenteric preparations in either SHR or WKY (unpublished observations). Hence, this mechanism does not play a significant role in our experimental conditions. Taken together, the greater K^+-free contractions in endothelium-denuded denervated rings from SHR when compared to WKY are most probably caused by increased permeability of the cell membrane to ions and increased voltage-dependent Ca^{2+} entry to the smooth muscle cells.

Ouabain abolished the difference between SHR and WKY in the rate of K^+-free contractions in endothelium-denuded rings by changing the response of SHR towards that of WKY. The membranes of SHR have been shown to be more permeable to K^+ (Bohr *et al.*, 1988). In the K^+-free solution enhanced K^+ efflux could occur in SHR, transferring K^+ into the solution in amounts sufficient to activate Na^+, K^+-ATPase, and thus resist contraction. When ouabain causes an additional inhibition of Na^+, K^+-ATPase, the pump cannot be activated even in the presence of leaked K^+. However, the high concentration of ouabain (1 mM) used may have exerted some unspecific effects and the mechanism of the effect by ouabain remains to be clarified.

Modulation of the effects of Na^+, K^+-ATPase inhibition by epithelial cells has previously been shown in isolated tracheas (Raeburn & Fedan, 1989). In our experiments, the presence of intact vascular endothelium attenuated the K^+-free contractions in both SHR and WKY. This attenuation could be abolished with L-NAME and methylene blue, indicating that the basal release of EDRF inhibited the contractile responses induced by the K^+-free solution. The fact that the attenuation was clearly smaller in SHR than WKY suggests impaired endothelial function in this type of genetic hypertension. This is in agreement with previous results showing diminished ACh-elicited endothelium-dependent relaxations in SHR (Shirasaki *et al.*, 1988; Watt & Thurston, 1989), a finding which was also confirmed in the present study. The effect of L-NAME could be reversed with L-arginine in WKY but not in SHR. This may indicate impaired utilization of exogenous L-arginine by the endothelial cells of SHR (e.g. decreased uptake of L-arginine, or reduced affinity of L-arginine for EDRF-synthase). Alternatively, at this advanced stage of hypertension the EDRF synthesizing enzyme might be different from that of WKY. Recently, at least two distinct forms of enzyme responsible for EDRF biosynthesis, with differing susceptibility to inhibition by different arginine analogues, have been described (Gross *et al.*, 1991; Smith *et al.*, 1991). However, at the moment differences between SHR and WKY in EDRF-synthases remain speculative and need further investigation. Rubanyi & Vanhoutte (1988) have previously reported that the action, but not the release of EDRF can be prevented by K^+-free solution. This does not seem to be the case in our experimental conditions. Since indomethacin did not affect the contractions of endothelium-intact rings, the products of the cyclo-oxygenase pathway cannot be involved in the attenuation of K^+-free contractions in the presence of endothelium. This is in agreement with the observation that K^+-free solution does not modulate endothelial production of prostacyclin (Boeynaems & Ramboer, 1989).

K^+ relaxation is an indirect method for the evaluation of vascular Na^+, K^+-ATPase activity. When K^+ is returned to the organ bath, the activation of Na^+, K^+-ATPase repolarizes the cell membrane (Bonaccorsi *et al.*, 1977; Webb & Bohr, 1979), thereby initiating smooth muscle relaxation with Ca^{2+} extrusion and sequestration, and contractile protein dephosphorylation (Johns *et al.*, 1987). Controversial results on Na^+, K^+-ATPase in hypertension have been reported, demonstrating sometimes a decrease (Overbeck *et al.*, 1974; Chen & Lin-Shiau, 1986; Manjeet & Sim, 1987) and sometimes an increase (Webb & Bohr, 1979; Syme *et al.*, 1990; Sakai & Inazu, 1991) in Na^+, K^+-ATPase activity. In the present study, the rate of smooth muscle relaxation after the

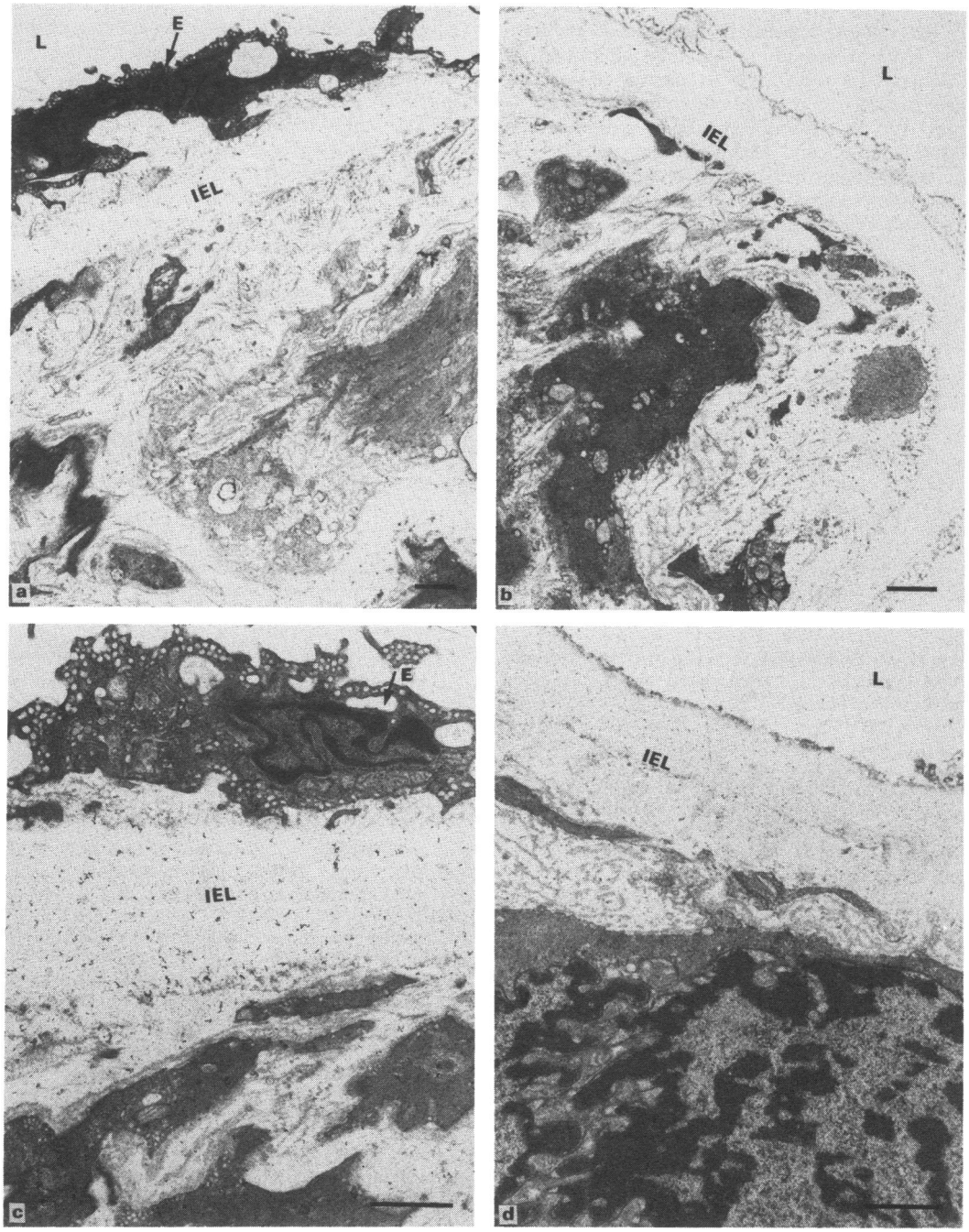

Figure 5 Electron microscopy of Wistar-Kyoto rat mesenteric arterial rings, where vascular endothelium was left intact (a and c) or mechanically denuded by gentle rubbing (b and d). L = lumen, E = endothelial cell and IEL = internal elastic lamina. Calibration bar = 1 μM.

re-addition of K^+ was slower in SHR than WKY with all K^+ concentrations studied. Ouabain (1 mM) totally inhibited the K^+ relaxations in SHR but not in WKY, and small K^+ concentrations (0.1 mM) failed to elicit any relaxation in SHR while clear relaxations were still seen in WKY. Furthermore, the inhibition of Na^+, K^+-ATPase with ouabain in a medium with normal K^+ (5.9 mM) induced contractions only in SHR, not in WKY. The conclusion from these results, although indirect in nature, supports the concept of reduced Na^+, K^+-ATPase activity in SHR vascular smooth muscle.

In addition to the activity of vascular Na^+, K^+-ATPase, the rate of K^+ relaxation probably also reflects contractile protein dephosphorylation and re-establishment of resting intracellular free Ca^{2+} concentration in smooth muscle. This is indicated by the relatively slow K^+ relaxation (minutes) observed, while the repolarization induced by the re-addition of K^+ would be anticipated to be quite rapid (seconds). Thus, the general mechanisms of smooth muscle relaxation appear to be impaired in SHR, which interpretation is also supported by the markedly prolonged wash-out time after maximal 125 mM KCl-induced contractions in SHR when compared to WKY.

The rate of K^+ relaxation was also clearly slower in SHR than WKY in the presence of intact vascular endothelium and after adrenergic denervation. However, when compared to the corresponding endothelium-denuded non-denervated rings, the rate of K^+ relaxation tended to be somewhat slower in preparations with an intact endothelium or destroyed adrenergic nerve-endings in both strains. Intact endothelium forms a barrier between the organ bath space and

the smooth muscle cells, and may prevent the repleted K^+ from reaching the smooth muscle. In the case of chemical denervation the reduced relaxation rate may be caused by some subtle damage (possibly due to anoxia during the 15 min nitrogen gassing) to the smooth muscle cells.

In conclusion, vascular smooth muscle contractions induced by K^+-free solution and the mechanisms of contraction were distinctly different between SHR and WKY, while only little to neglible changes were seen in response to the classical contractile agents noradrenaline and high concentrations of potassium. Increased sensitivity to the Ca^{2+} entry blockade by nifedipine, and decreased neural and endothelial influences on the K^+-free contractions were observed in SHR smooth muscle. The results suggest increased permeability of smooth muscle cell membranes to Ca^{2+} through dihydropyridine–sensitive voltage-dependent channels in genetic hypertension. They further suggest impaired endothelial function via EDRF in SHR. The attenuated K^+ relaxation rate in SHR indicates both decreased activity of Na^+, K^+-ATPase and impaired relaxation mechanisms in vascular smooth muscle. Thus, the clear differences between SHR and WKY in both contractions induced by the K^+-free solution and K^+ relaxation responses suggest that these alterations in organ bath K^+ concentration offer a useful tool for studying vascular pathophysiology in hypertension.

This study was supported by the Academy of Finland (P.V. & H.V.) and the University of Tampere (I.P.).

References

APRIGLIANO, O. & HERMSMEYER, K. (1976). *In vitro* denervation of the portal vein and caudal artery of the rat. *J. Pharmacol. Exp. Ther.*, **94**, 325–334.

ASHIDA, T. & BLAUSTEIN, M.P. (1987). Regulation of cell calcium and contractility in mammalian arterial smooth muscle: The role of sodium-calcium exchange. *J. Physiol.*, **392**, 617–635.

BEAN, B.P., STUREK, M., PUGA, A. & HERMSMEYER, K. (1986). Calcium channels in muscle cells isolated from rat mesenteric arteries: modulation by dihydropyridine drugs. *Circ. Res.*, **59**, 229–235.

BLAUSTEIN, M.P. (1977). Sodium ions, calcium ions, blood pressure regulation, and hypertension: a reassessment and a hypothesis. *Am. J. Physiol.*, **232**, C165–C173.

BOEYNAEMS, J.M. & RAMBOER, I. (1989). Effects of changes in extra- and intracellular K^+ on the endothelial production of prostacyclin. *Br. J. Pharmacol.*, **98**, 966–972.

BOHR, D.F., BRUNER, C.A., LAMB, F.S. & WEBB, R.C. (1988). Physiology of vascular smooth muscle in relation to hypertension. *Acta Physiol. Scand.*, **133**, (suppl. 571), 15–24.

BOHR, D.F. & WEBB, R.C. (1984). Vascular smooth muscle function and its changes in hypertension. *Am. J. Med.*, **77**, 3–16.

BONACCORSI, A., HERMSMEYER, K., APRIGLIANO, O., SMITH, C.B. & BOHR, D.F. (1977). Mechanisms of potassium relaxation of arterial muscle. *Blood Vessels*, **14**, 261–276.

CHEN, C.-C. & LIN-SHIAU, S.-Y. (1986). Decreased Na^+-K^+-ATPase activity and [^{3}H]ouabain binding sites in various tissues of spontaneously hypertensive rats. *Eur. J. Pharmacol.*, **122**, 311–319.

DOMINICZAK, A.F. & BOHR, D.F. (1990). Cell membrane abnormalities and the regulation of intracellular calcium concentration in hypertension. *Clin. Sci.*, **79**, 415–423.

FIELD, F.P. & SOLTIS, E.E. (1985). Vascular reactivity in the spontaneously hypertensive rat: effect of high pressure stress and extracellular calcium. *Hypertension*, **7**, 228–235.

FURCHGOTT, R.F. & VANHOUTTE, P.M. (1989). Endothelium-derived relaxing and contracting factors. *FASEB J.*, **3**, 2007–2018.

FURSPAN, P.B., RINALDI, G.J., HOFFMAN, K. & BOHR, D.F. (1989). Dietary calcium and cell membrane abnormality in genetic hypertension. *Hypertension*, **13**, 727–730.

GROSS, S.S., JAFFE, E.A., LEVI, R. & KILBOURN, R.G. (1991). Cytokine-activated endothelial cells express an isotype of nitric oxide synthase which is tetrahydrobiopterin-dependent, calmodulin-independent and inhibited by arginine analogs with a rank order of potency characteristic of activated macrophages. *Biochem. Biophys. Res. Commun.*, **178**, 823–829.

HERMSMEYER, K. & HARDER, D. (1986). Membrane ATPase mechanism of K^+-return relaxation in arterial muscles of stroke-prone SHR and WKY. *Am. J. Physiol.*, **250**, C557–C562.

HOPP, L., KHALIL, F., TAMURA, H., KINO, M., SEARLE, B.M., TOKUSHIGE, A. & AVIV, A. (1986). Ouabain binding to cultured vascular smooth muscle cells of the spontaneously hypertensive rat. *Am. J. Physiol.*, **250**, C948–C954.

ISHII, K., CHANG, B., KERWIN, J.F., HUANG, Z.-J. & MURAD, F. (1990). N^{ω}-nitro-L-arginine: a potent inhibitor of endothelium-derived relaxing factor formation. *Eur. J. Pharmacol.*, **176**, 219–223.

JOHNS, A., LEIJTEN, P., YAMAMOTO, H., HWANG, K. & VAN BREEMEN, C. (1987). Calcium regulation in vascular smooth muscle contractility. *Am. J. Cardiol.*, **59**, 18A–23A.

KELM, M. & SCHRADER, J. (1990). Control of coronary vascular tone by nitric oxide. *Circ. Res.*, **66**, 1561–1575.

LAMB, F.S., MORELAND, R.S. & WEBB, R.C. (1988). Calcium and contractile responses to ouabain and potassium-free solution in aortae from spontaneously hypertensive rats. *J. Hypertens.*, **6**, 821–828.

LEDERBALLE PEDERSEN, O., MIKKELSEN, E. & ANDERSSON, K.-E. (1978). Effects of extracellular calcium on potassium and noradrenaline induced contractions in the aorta of spontaneously hypertensive rats – increased sensitivity to nifedipine. *Acta Pharmacol. Toxicol.*, **43**, 137–144.

LOIRAND, G., PACAUD, P., MIRONNEAU, C. & MIRONNEAU, J. (1986). Evidence for two distinct calcium channels in rat vascular smooth muscle cells in short-term primary culture. *Plügers Arch.*, **407**, 566–568.

MANJEET, S. & SIM, M.K. (1987). Decreased Na^+K^+ATPase activity in the aortic endothelium and smooth muscle of the spontaneously hypertensive rats. *Clin. Exp. Hypertens.*, **9**, 797–812.

MONCADA, S., HIGGS, E.A., HODSON, H.F., KNOWLES, R.G., LOPEZ-JARAMILLO, P., MCCALL, T., PALMER, R.M.J., RADOMSKI, M.W., REES, D.D. & SCHULZ, R. (1991). The L-arginine:nitric oxide pathway. *J. Cardiovasc. Pharmacol.*, **17** (suppl. 3), S1–S9.

MULVANY, M.J. (1985). Changes in sodium pump activity and vascular contraction. *J. Hypertens.*, **3**, 429–436.

MULVANY, M.J., AALKJÆR, C. & PETERSEN, T.T. (1984). Intracellular sodium, membrane potential, and contractility of rat mesenteric small arteries. *Circ. Res.*, **54**, 740–749.

MYERS, P.R., MINOR, R.L., GUERRA, R.Jr., BATES, J.N. & HARRISON, D.G. (1990). Vasorelaxant properties of the endothelium-derived relaxing factor more closely resemble S-nitrosocysteine than nitric oxide. *Nature*, **345**, 161–163.

OVERBECK, H.W., DERIFIELD, R.S., PAMNANI, M.B. & SÖZEN, T. (1974). Attenuated vasodilator responses to K^+ in essential hypertensive men. *J. Clin. Invest.*, **53**, 678–686.

PIQUE, J.M., WHITTLE, B.J.R. & ESPLUGUES, J.V. (1989). The vasodilator role of endogenous nitric oxide in the rat gastric microcirculation. *Eur. J. Pharmacol.*, **174**, 293–296.

PÖRSTI, I. (1992). Arterial smooth muscle contractions in spontaneously hypertensive rats on a high calcium diet. *J. Hypertens.*, (in press).

PÖRSTI, I., ARVOLA, P., WUORELA, H. & VAPAATALO, H. (1992). High calcium diet augments vascular potassium relaxation in hypertensive rats. *Hypertension*, **19**, 85–92.

RAEBURN, D. & FEDMAN, J.S. (1989). The effects of alterations in electrogenic Na^+/K^+-pumping in guinea-pig isolated trachealis: their modulation by the epithelium. *Br. J. Pharmacol.*, **98**, 343–350.

RUBANYI, G.M. & VANHOUTTE, P.M. (1988). Potassium-free solution prevents the action but not the release of endothelium-derived relaxing factor. *Eur. J. Pharmacol.*, **145**, 351–355.

RUSCH, N.J. & HERMSMEYER, K. (1988). Calcium currents are altered in the vascular muscle cell membrane of spontaneously hypertensive rats. *Circ. Res.*, **63**, 997–1002.

SAKAI, Y. & INAZU, M. (1991). Sodium pump activity and contraction of renal artery from spontaneously hypertensive rats. *Eur. J. Pharmacol.*, **200**, 227–231.

SHIRASAKI, Y., KOLM, P., NICKOLS, G.A. & LEE, T.J.-F. (1988). Endothelial regulation of cyclic GMP and vascular responses in hypertension. *J. Pharmacol. Exp. Ther.*, **245**, 53–58.

SMITH, R.E.A., PALMER, R.M.J. & MONCADA, S. (1991). Coronary vasodilatation induced by endotoxin in the rabbit isolated perfused heart is nitric oxide-dependent and inhibited by dexamethasone. *Br. J. Pharmacol.*, **104,** 5–6.

SYME, P.D., DIXON, R.M., ARONSON, J.K., GRAHAME-SMITH, D.G. & RADDA, G.K. (1990). Evidence for increased *in vivo* sodium-potassium pump activity and potassium-efflux in skeletal muscle of spontaneously hypertensive rats. *J. Hypertens.*, **8,** 1161–1166.

TAMURA, H., KINO, M., TOKUSHIGE, A., SEARLE, B.M. & AVIV, A. (1985). Increased membrane permeability of skin fibroblasts from the spontaneously hypertensive rat. *Hypertension*, **7,** 300–305.

VAN BREEMEN, C., CAUVIN, C., JOHNS, A., LEIJTEN, P. & YAMAMOTO, H. (1986). Ca^{2+} regulation of vascular smooth muscle. *Fed. Proc.*, **45,** 2746–2751.

VANE, J.R., ÄNGGÅRD, E.E. & BOTTING, R.M. (1990). Regulatory functions of the vascular endothelium. *N. Engl. J. Med.*, **323,** 27–36.

VANHOUTTE, P.M. & LORENZ, R.R. (1984). Na^+, K^+-ATPase inhibitors and the adrenergic neuroeffector interaction in the blood vessel wall. *J. Cardiovasc. Pharmacol.*, **6** (suppl. 1), S88–S94.

WATT, P.A.C. & THURSTON, H. (1989). Endothelium-dependent relaxation in resistance vessels from the spontaneously hypertensive rats. *J. Hypertens*, **7,** 661–666.

WEBB, R.C. & BOHR, D.F. (1979). Potassium relaxation of vascular smooth muscle from spontaneously hypertensive rats. *Blood Vessels*, **16,** 71–79.

(Received November 7, 1991
Accepted January 7, 1992)

Br. J. Pharmacol. (1992), **106**, 166–172 © Macmillan Press Ltd, 1992

Effects of peptidase inhibition on angiotensin receptor agonist and antagonist potency in rabbit isolated thoracic aorta

[1]Mark J. Robertson, Mootoosamy P. Cunoosamy & Kenneth L. Clark

Peripheral Pharmacology Department, Glaxo Group Research, Ware, Herts

1 Experiments were performed with peptidase inhibitors on rabbit aortic strip preparations, to determine whether endogenous peptidase activity can influence the potency estimates for angiotensin receptor agonists and antagonists in this tissue.

2 Angiotensin II (A II) and angiotensin III (A III) both induced concentration-related contractions of rabbit aortic strip preparations. A III was approximately 38 fold less potent than A II, and the gradient of the A III concentration-response curve (1.00 ± 0.04) was significantly more shallow than that (1.76 ± 0.05) of the A II curve.

3 Neither the aminopeptidase-A and -M inhibitor, amastatin, nor the aminopeptidase-B and -M inhibitor, bestatin, affected the potency of, or the maximum response to, A II. In contrast, the potency of A III was increased by both amastatin and bestatin. Amastatin had the most marked effect and at 10 μM caused approximately a 12 fold increase in the potency of A III (EC_{50} values, 102 nM and 8.6 nM in the absence and presence of amastatin, respectively), and also significantly steepened the gradient of the A III concentration-response curve. Amastatin did not affect the position or shape of the concentration-response curve to the α_1-adrenoceptor agonist, phenylephrine. Finally, the carboxypeptidase-N inhibitor, D-L-mercaptomethyl-3-guanidine-ethylpropanoic acid (MERGETPA) did not change the position or shape of the concentration-response curves to either A II or A III.

4 In the presence of amastatin, the potency of the peptide angiotensin receptor antagonist, Ile^7-A III (100 nM–1 μM), was increased approximately 13 fold (pA_2, with A II as the agonist, 7.0 ± 0.1 and 8.1 ± 0.1, in the absence and presence of amastatin, respectively). However, the potency of the non-peptide angiotensin receptor antagonist, DuP 753 (30–300 nM), was little affected by amastatin (pA_2, 8.2 ± 0.1 and 8.1 ± 0.1 in the absence and presence of amastatin, respectively).

5 The results of this study suggest that endogenous aminopeptidase activity in the rabbit thoracic aorta can profoundly affect estimates of the potency of peptide angiotensin receptor agonists and antagonists. A suitable aminopeptidase inhibitor should therefore be included in studies, using this tissue, which aim to classify angiotensin receptor subtype(s) based on the rank order of peptide angiotensin receptor agonist and/or antagonist potencies.

Keywords: Angiotensin II, III; peptidase inhibition; rabbit aorta; DuP 753; Ile^7-A III; amastatin

Introduction

The renin-angiotensin system exerts its many effects predominantly via angiotensin II (A II). This octapeptide, which plays a major role in the maintenance of blood pressure, and in salt and water retention, is formed following the action of angiotensin converting enzyme on the weakly active precursor, angiotensin I (Reid *et al.*, 1978; Ferrario, 1990). The potent contractile effect of A II on vascular smooth muscle both *in vitro* and *in vivo* has been well documented (Peach, 1977).

The degradative enzyme, aminopeptidase A, can cleave the N-terminal amino acid (aspartate) from A II (Ahmad & Ward, 1990), resulting in formation of the heptapeptide, angiotensin III (A III). This can be further degraded at its N-terminal by aminopeptidase-B or aminopeptidase-M (Sullivan *et al.*, 1988; Ahmad & Ward, 1990; see Figure 1)to produce a hexapeptide with less biological activity (Peach, 1977; Dostal *et al.*, 1990). A II and A III may also be cleaved at the C-terminal by the action of carboxypeptidase enzymes (Peach, 1977; Magnan & Regoli, 1977). Although A III retains considerable activity as a contractile agent on vascular smooth muscle, estimates of its potency relative to A II have varied (e.g. see Waugh & Bales, 1978; Trachte & Peach, 1983).

It is common practice to investigate receptor heterogeneity by comparing the relative potencies of agonists and/or antagonists. Despite this, few studies have been carried out to determine the extent to which differential degrees of enzymatic degradation may have influenced the estimates of the potency of A II or A III (e.g. Peach, 1977; Trachte & Peach, 1977; Freer *et al.*, 1980). Moreover, until recently, the only angiotensin receptor antagonists available have been peptides based closely on the structures of A II and A III. Consequently, these antagonists are also likely to be subject to degradation by peptidase enzymes.

Current angiotensin receptor classification is defined by the selectivity of the non-peptide ligands, DuP 753 (losartan) and PD 123177 for what have been ascribed AT_1 and AT_2 receptors (Bumpus *et al.*, 1991). The vast majority of functional responses to A II appear to be mediated via AT_1 receptors (see Wong *et al.*, 1990). Clues to the possible locations of further subtypes of the AT_1 receptor may be obtained by differences in the relative potencies of agonists or antagonists in various tissues and vascular beds. Thus, if progress is to be made in the future sub-classification of angiotensin receptors, it is essential to investigate whether endogenous peptidase activity can influence these potency estimates. The aim of the present work was to address this question using the rabbit isolated thoracic aortic strip preparation.

In this study, the contractile effects of A II and A III in rabbit aortic strips were compared in the absence and presence of either the aminopeptidase-A and -M inhibitor, amastatin (Aoyagi *et al.*, 1978; Palmieri *et al.*, 1989; Ahmad & Ward, 1990), the aminopeptidase-B and -M inhibitor,

[1]Author for correspondence.

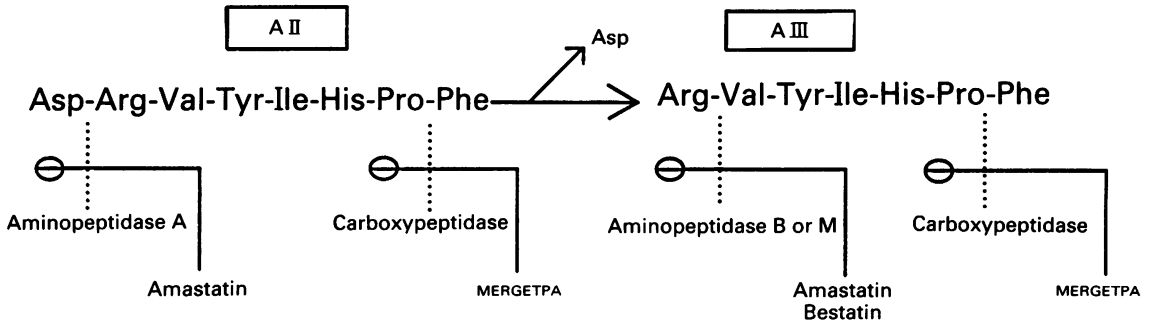

Figure 1 Putative pathway for the breakdown of angiotensin II and III (A II and A III) by various peptidases, and how peptidase inhibitors may interfere with the degradation processes. Dotted lines show the proposed point of cleavage by enzymes. ⊖ shows sites where amastatin, bestatin or D-L-mercaptomethyl-3-guanidino-ethylpropanoic acid (MERGETPA) are believed to interfere with these enzymes.

bestatin (Umezawa *et al.*, 1976; Sullivan *et al.*, 1988), or the carboxypeptidase-N inhibitor, D-L-mercaptomethyl-3-guanidino-ethylpropanoic acid (MERGETPA) (Ward *et al.*, 1987). In addition, the potencies of two angiotensin receptor antagonists were determined, against first A II and then A III-induced contractions, in both the presence and absence of amastatin. One of the antagonists used, Ile^7-A III, is a peptide. The other, DuP 753 (losartan), has a non-peptide heterocyclic structure, and has high affinity for A II binding sites in a variety of animal and human tissues including vascular smooth muscle, adrenal cortex and kidney cortex (see Timmermans *et al.*, 1991). A preliminary account of these findings has been published in abstract form (Robertson *et al.*, 1991).

Methods

Preparation of the rabbit aorta

Male, New Zealand White rabbits (2–3 kg) were killed by captive bolt. The descending thoracic aorta was rapidly removed on a perspex rod, then cleaned of connective tissue in a Petri dish containing physiological salt solution (at room temperature) of the following composition (mM) :Na^+ 143.4, K^+ 5.9, Mg^{2+} 0.6, Ca^{2+} 1.3, Cl^- 124.5, $H_2PO_4^-$ 1.2, SO_4^{2-} 0.6, HCO_3^- 25 and glucose 11.1, bubbled with 95% O_2/5% CO_2. The physiological salt solution also contained indomethacin (30 μM, to prevent the formation of endogenous cyclo-oxygenase products) and ascorbic acid (100 μM, as an anti-oxidant). Each aorta, with the endothelium removed, was cut into a spiral strip as described by Furchgott & Bhadrakom (1953), and then cut into 4–8 smaller strips each measuring 1.5–2.0 cm in length and 3–4 mm in width. Individual strips were suspended vertically in glass tissue chambers (10 or 20 ml) containing the physiological salt solution at 37°C (pH = 7.4). Each strip was connected by a cotton thread to a force displacement transducer (Dynamometer, UF1) and a resting tension of 0.5 g was applied to each tissue. Changes in isometric tension were displayed on an 8-channel pen recorder (Lectromed, MT8P).

Experimental design: construction of angiotensin II and III concentration-response curves

Fifteen minutes after adjusting the applied tension on the tissues to 0.5 g, KCl (80 mM) was added to the bathing fluid to depolarize the smooth muscle and thereby determine the contractile viability of the preparations. Once the contraction had reached a plateau, the tissues were washed. After 10 min, the tension was mechanically re-adjusted to 0.5 g and 5 min later, a cumulative 10 fold priming concentration-response curve to A II (0.1–100 nM) or to A III (1 nM–10 μM) was constructed. After washing, the preparations were allowed to equilibrate for 30 min before re-adjusting the basal tension to 0.5 g. After a further 15 min, a cumulative 3 fold concentration-response curve to A II (0.3–100 nM) or A III (1 nM–10 μM) was constructed. After washing and equilibrating as before, another cumulative 3 fold concentration-response curve to A II or A III was obtained (pretest curve) and the concentration of agonist required to elicit a 50% maximum response (EC_{50}) in the pretest curve was calculated.

Effects of peptidase inhibitors on contractile responses to angiotensin II and III

The pretest curves for either A II or A III were constructed as described above. After washing, three preparations were then exposed to a different concentration of either amastatin (3, 10 or 30 μM), bestatin (3, 10 or 30 μM), MERGETPA (10, 30 or 100 μM), or a combination of amastatin (10 μM) and bestatin (10 μM), whilst a fourth preparation was exposed to vehicle alone. Forty-five minutes later, a final cumulative, 3 fold A II or A III concentration-response curve (test curve) was constructed. In separate experiments, the specificity of action of amastatin (3, 10 or 30 μM) was assessed. The protocol in these studies was the same as described above, with the exception that phenylephrine (10 nM–30 μM) was used to contract the tissues in place of A II or A III.

Determination of angiotensin receptor antagonists potencies in the absence or presence of amastatin

The pretest curve for A II or A III was constructed as before. After washing, three preparations were then exposed to different concentrations of angiotensin receptor antagonist DuP 753, (30, 100 or 300 nM) or Ile^7- A III (100, 300 or 1000 nM), whilst a fourth preparation was exposed to vehicle alone. Forty-five minutes later a final cumulative 3 fold A II or A III concentration-response curve (test curve) was constructed. In this series of experiments and those described in the previous paragraph there was a tendency for the maximal response to A II and A III in the test curves to increase slightly in vehicle-treated preparations, although the concentration-range over which each agonist was effective was unchanged. Where angiotensin curves obtained in the presence of the antagonists were parallel with the control curves, angiotensin concentration-ratios were calculated. To do this, the concentration of agonist in the test curve, which produced the same response as that caused by the EC_{50} in the pretest curve, was divided by the EC_{50}. The concentration-ratio values from the drug-treated preparations were divided by the concentration-ratio value from the vehicle-treated preparations to correct for any spontaneous changes in sensitivity. These results were plotted graphically in the form of a Schild plot as log (agonist concentration-ratio − 1) versus log antagonist concentration (mol l^{-1}), and pA_2 values were derived (Arunlakshana & Schild, 1959). In some experiments

with A III as the agonist, curves obtained in the presence of the antagonists, although parallel with each other, were not parallel with the control A III curve. However, to obtain an approximate measure of their potency, pA_2 values were calculated as described above. The potency of each antagonist was also determined in the presence of amastatin. In these experiments, antagonist pA_2 values were obtained by use of the protocol described above, with the exception that amastatin (10 μM) was added to all the tissues following the KCl challenge at the beginning of the experiment, and was then present at this concentration in the bathing fluid for the remainder of the study.

Expression of results and statistical analysis

Mean EC_{50} values and mean concentration-ratios were expressed in the results as geometric means with 95% confidence intervals. For each individual preparation, the contractile responses to A II or A III in the test curve were expressed as a percentage of the maximum response to A II or A III in the pretest curve, and the results plotted graphically. pA_2 values and Schild plot slopes, and mean changes in contractile tension are expressed as the arithmetic mean ± s.e.mean. The gradients of the A II and A III concentration-response curves are calculated by use of the non-linear unweighted ALLFIT curve-fitting programme (De Lean *et al.*, 1978). Differences between groups of pA_2 values were tested for statistical significance by Student's unpaired t test. In all analyses the level of statistical significance was taken as $P<0.05$.

Drugs used

A III, amastatin hydrochloride, bestatin hydrochloride, phenylephrine hydrochloride, Ile^7-A III, indomethacin, and ascorbic acid were obtained from Sigma. A II and MERGETPA (D-L-mercaptomethyl-3-guanidino-ethylpropanoic acid) were obtained from Novabiochem and Calbiochem, respectively. DuP 753 (2-n-butyl-4-chloro-5-hydroxymethyl-1-[2'(1H-tetrazol-5-yl)biphenyl-4-yl)methyl]imidazole) potassium salt, was a gift from DuPont de Nemours (Delaware, USA). All drugs were dissolved in distilled water with the exception of indomethacin which was dissolved in 100 μl NaOH (2 M). The stock solutions of amastatin, bestatin and MERGETPA were all 10 mM. A II and A III were stored frozen as aliquots (1 mM or 10 mM), which were defrosted as required on the day of experimentation. Dilutions of all drugs were made in distilled water. All chemicals for the physiological salt solution were of Analar grade and obtained from BDH Ltd., England.

Results

Contractile effects of angiotensin II and III

In most experiments, the maximum contractile response to both A II and A III became progressively greater in consecutive curves. This was particularly apparent between the first and second A II or A III curve. On a few occasions, consecutive A II and A III curves became smaller. These experiments were abandoned. Rarely, all aortic preparations from a single rabbit failed to respond to either A II or A III after having shown a normal contractile response to the depolarizing KCl solution.

Cumulative addition of A II (0.3 nM – 100 nM) or A III (1 nM – 10 μM) to the rabbit isolated aortic strips caused concentration-related contractions (Figure 2) with a similar maximal contractile response (A II, 0.99 ± 0.07 g, $n = 33$; A III, 1.03 ± 0.05 g, $n = 36$). The concentration (geometric mean and 95% confidence interval) of A III in the test curve, required to elicit a response equal to 50% of the maximum response observed in the pretest curve, was 139.9 (106.5–183.9) nM ($n = 36$). The corresponding concentration of A II was 3.7 (3.0–4.4) nM ($n = 33$). Thus, A III was approximately 38 fold less potent than A II. Figure 2 also illustrates that the effects of A III occurred over a wider concentration-range than those of A II. Statistical comparison of the gradients of the concentration-response curves for A II and A III revealed that the mean gradient of the A III curve (1.00 ± 0.04), was significantly lower ($P<0.001$, unpaired t test) than that of the A II curve (1.76 ± 0.05). Thus, only 3 or 4 cumulative three fold concentrations of agonist were typically required to produce the maximum contractile response for A II, whilst 6 or 7 concentration increases were needed for A III. Additionally, as shown in Figure 3, the peak contractile response to each concentration of A III was achieved more rapidly than that to A II.

Effects of peptidase inhibitors on contractile responses to angiotensin II and III

Neither the potency, nor the maximum contractile response to A II, was affected by the aminopeptidase-A and -M inhibitor, amastatin (3–30 μM, Figure 2a). In contrast, the potency of A III was increased to a similar extent in the presence of 3, 10, or 30 μM amastatin (Figure 2b). The geometric mean concentration of A III, required to cause 50% of the maximum response (relative to the pretest curve), before and after amastatin (10 μM) was 102.2 (40.0–260.0) nM and 8.6 (3.6–20.5) nM, respectively. Thus, amastatin (10 μM) increased the potency of A III by approximately 12 fold. Ama-

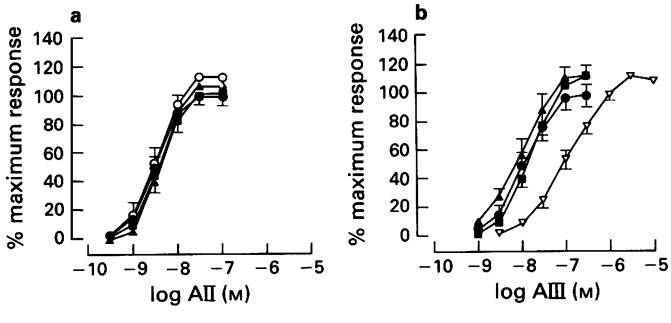

Figure 2 Concentration-response curves to (a) angiotensin II (A II) and (b) A III in separate rabbit aortic strip preparations, before (○, A II; ▽, A III), and after treatment with amastatin (■, 3; ▲, 10 and ●, 30 μM) $n = 5$–7. Results are shown as mean response to A II or A III in the test curve, expressed as a % of the maximum response to A II or A III, respectively, in the pretest curve. Vertical bars show s.e.mean.

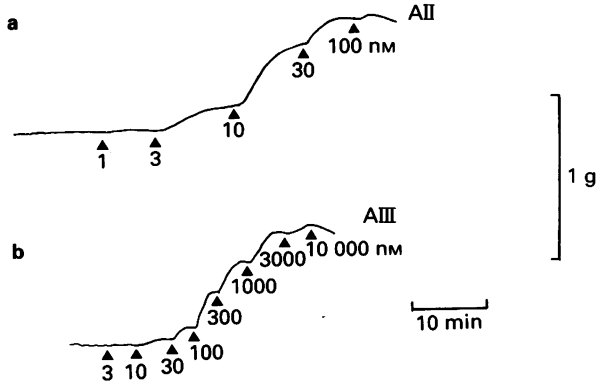

Figure 3 Representative tracings from two rabbit aortic strip preparations showing that less cumulative concentrations of angiotensin II (A II) (a) than A III (b) are required to produce their respective maximal contractile responses. Each change in the bath concentration of A II or A III is indicated (▲).

statin also caused a significant increase in the mean gradient of the A III concentration-response curve, although it was still significantly less ($P<0.05$:paired t test) than the mean gradient of the A II curve:the mean gradients ($\pm$ s.e.mean) of the A III concentration-response curves, before and after amastatin (10 μM, $n=7$), were 0.92 ± 0.06 and 1.40 ± 0.13, respectively. Additionally, in the presence of amastatin, the time to peak response for each concentration of A III was increased, such that the contractile responses to A III more closely resembled those to A II. Amastatin (3–30 μM) had no effect on the position (<2 fold displacement), shape or size of the α_1-adrenoceptor agonist, phenylephrine, concentration-response curve (data not shown).

Like amastatin, although the aminopeptidase -B and -M inhibitor, bestatin (3, 10 or 30 μM), did not affect the potency of A II (Figure 4a), it did significantly ($P<0.05$) increase the potency of A III (Figure 4b). The increase in the potency of A III was similar (approximately 3–10 fold) at each concentration of bestatin tested. Incubation of tissues with a combination of both amastatin (10 μM) and bestatin (10 μM) had no effect on the potency of A II, and produced no greater increase in the potency of A III than was observed in the presence of amastatin (10 μM) alone.

Finally, the carboxypeptidase-N inhibitor, MERGETPA (10–100 μM; $n=4$–5) had no effect on the potency (<2 fold displacement), or maximum contractile effect, of either A II or A III (data not shown).

Potency of angiotensin receptor antagonists in the absence or presence of amastatin

The previous experiments showed that of the peptidase inhibitors tested, amastatin (10 μM) caused the greatest increase in A III potency. For this reason, the potency of the peptide angiotensin receptor antagonist, Ile^7-A III, and the non-peptide angiotensin receptor antagonist, DuP 753 (Chiu *et al.*, 1990), as antagonists of A II- and A III-induced contractions, were determined in the absence and presence of amastatin (10 μM). The pA_2 and slope estimates are shown in Table 1.

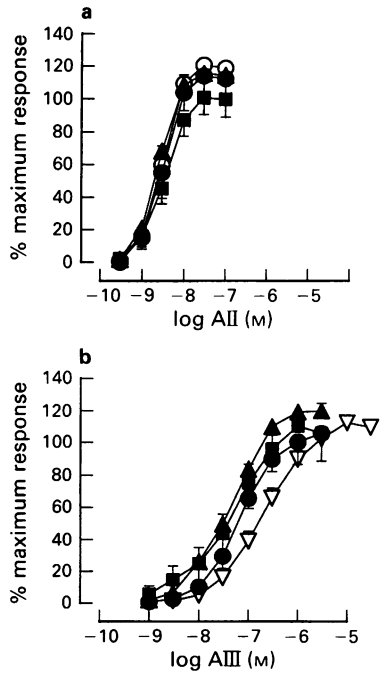

Figure 4 Concentration-response curves to (a) angiotensin II (A II) and (b) A III in rabbit aortic strip preparations, before (○, A II; ▽, A III), and after treatment with bestatin (■, 3; ▲, 10 and ●, 30 μM), $n=4$–6. Expression of results is as for Figure 2.

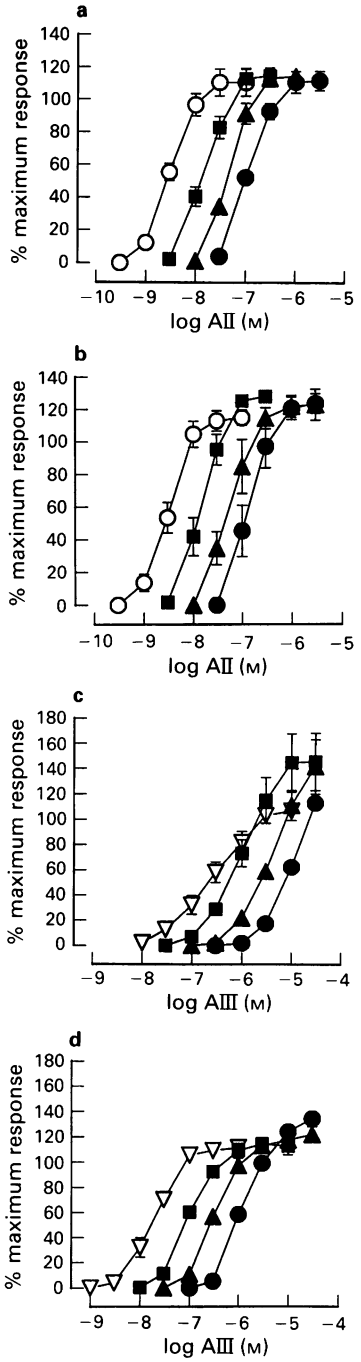

Figure 5 The effect of DuP 753 on concentration-response curves to (a) angiotensin II (A II), (b) A II in the presence of amastatin (10 μM), (c) A III and (d) A III in the presence of amastatin (10 μM). For each panel, curves shown are in the absence (○ A II, ▽ A III) or presence of DuP 753 (■, 30 nM; ▲, 100 nM and ●, 300 nM), $n=4$. Results are shown as mean response to A II or A III in the test curve, expressed as a % of the maximum response to A II or A III, respectively, in the pretest curve. Vertical bars show s.e.mean.

DuP 753

DuP 753 (30, 100 or 300 nM) caused concentration-related, parallel, rightward displacements of A II concentration-response curves without change in the maximum response, in both the absence (Figure 5a) and presence (Figure 5b) of amastatin (10 μM).

Similarly, over the same concentration-range, DuP 753 also caused concentration-related rightward shifts of A III concentration-effect curves in the absence (Figure 5c) and

Table 1 Angiotensin receptor antagonist potency in the absence and presence of amastatin (10 μM)

	DuP 753		*Ile⁷-A III*	
	− Amastatin	*+ Amastatin*	*− Amastatin*	*+ Amastatin*
A II	8.2 ± 0.1	8.1 ± 0.1	7.0 ± 0.1	8.1 ± 0.1
	SL = 1.1 ± 0.1	SL = 1.0 ± 0.1	SL = 1.4 ± 0.1	SL = 1.2 ± 0.1
A III	7.9 ± 0.2	8.1 ± 0.1	7.2 ± 0.2	7.9 ± 0.03
	SL = 1.2 ± 0.05	SL = 1.1 ± 0.05	SL = 1.1 ± 0.1	SL = 1.0 ± 0.2

Values are pA_2 with slope (SL) calculated as arithmetic mean ± s.e.mean ($n = 4$).

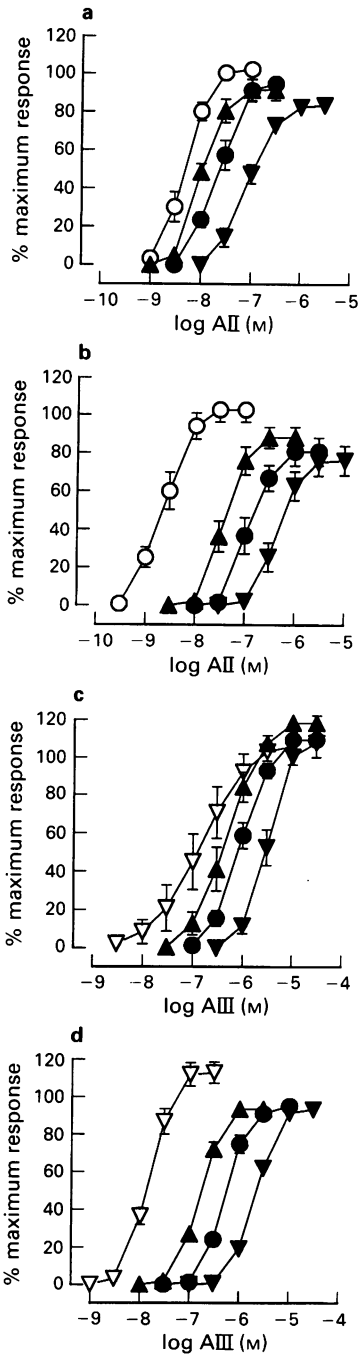

Figure 6 The effect of Ile⁷-A III on concentration-response curves to (a) angiotensin II (A II), (b) A II in the presence of amastatin (10 μM), (c) A III and (d) A III in the presence of amastatin (10 μM). For each panel, curves shown are in the absence (○ A II, ▽ A III) or presence of Ile⁷-A III (▲, 100 nM; ●, 300 nM; and ▼, 1000 nM), $n = 4$. Expression of results is as for Figure 5.

presence (Figure 5d) of amastatin (10 μM). In the presence of amastatin, A III concentration-response curves were shifted in a parallel manner by DuP 753. In contrast, Figure 5c shows that, although A III curves were shifted to the right by DuP 753 in the absence of amastatin, the gradient of the curves also appeared to increase, as did the maximum response (by approximately 40%). Thus, in the presence of DuP 753, A III curves were parallel with each other, but were not parallel with the A III curves generated from the corresponding vehicle-treated preparations. Despite this, calculated at the pretest curve EC_{50} level, the affinity estimate (pA_2 values, Table 1) for DuP 753 against A III was not significantly altered by the addition of amastatin.

Table 1 also shows that the potency of DuP 753 was similar against both A II and A III, in the absence or presence of amastatin.

Ile⁷-A III

Ile⁷-A III (100, 300 and 1000 nM) caused concentration-related, rightward displacements of A II concentration-response curves, with some suppression (up to about 20%) of the maximum response, in both the absence (Figure 6a) and presence (Figure 6b) of amastatin. In contrast to DuP 753, the potency of Ile⁷-A III against A II was significantly increased ($P < 0.005$), approximately 13 fold (Table 1), in the presence of amastatin.

Ile⁷-A III (100, 300 and 1000 nM) also caused rightward, concentration-related displacements of A III concentration-response curves in the absence (Figure 6c) and presence (Figure 6d) of amastatin. In the presence of amastatin, Ile⁷-A III caused parallel shifts in A III curves with some suppression (approximately 20%) of the maximum response (Figure 6d). However, as had been observed with DuP 753, in the absence of amastatin, Ile⁷-A III seemed to cause more displacement at the bottom, than at the top, of A III concentration-response curves, and did not suppress the maximum response (compare Figures 6c and 5c).

As with A II, the potency of Ile⁷-A III against A III-induced contractions was significantly ($P < 0.05$) increased (approximately 6 fold) in the presence of amastatin (Table 1). Hence, similar to DuP 753, the potency of Ile⁷-A III was independent of the agonist used (A II or A III), in the absence or presence of amastatin.

Discussion

The physiological and pathophysiological importance of the renin-angiotensin system in cardiovascular homeostasis is established. It is accepted that the main biologically active components of this system, A II and A III, exert their effects via specific angiotensin receptors. In the conventional pharmacological manner, attempts to classify angiotensin receptors have often been carried out by determining relative potencies of agonist and/or antagonists within a given tissue (e.g. Samenen *et al.*, 1988) or between tissues (Moore *et al.*, 1976; Trachte & Peach, 1983). However, for the results of such experiments to be meaningful, it is important to ensure that, as far as possible, potency measurements are obtained

under optimal and uniform conditions (Furchgott, 1972).

In the current study, the possibility that endogenous peptidases may degrade angiotensin receptor agonists and antagonists, and therefore interfere with estimates of their potency, was considered with respect to the rabbit isolated aorta. This preparation has been used widely to investigate contractile responses to A II and A III, largely because the preparation is robust, and consecutive agonist concentration-response curves do not readily develop tachyphylaxis (e.g. see Trachte & Peach, 1983).

Initial results of the present study showed that A II and A III each elicited concentration-related contractions of rabbit aortic strips, producing a similar maximum response. However, in addition to A III being less potent (approximately 38 fold) than A II, the gradient of the A III concentration-response curve was found to be shallower than that of the A II curve. Furthermore, the time to peak response for each concentration of A III was shorter than for A II (Figure 3).

One explanation for these differences is simply that the concentration of A III (especially at lower concentrations), but not that of AII, declines rapidly following penetration into the tissue biophase because of its enzymatic degradation. This steady removal of A III from the biophase could also explain why each A III-induced contraction reaches a plateau more quickly than A II. In contrast A II will penetrate further into the biophase and therefore take longer to reach equilibrium. This hypothesis is supported by two further observations in the present study. Firstly, responses to A II were unaffected by amastatin. Thus, in rabbit isolated aorta, A II does not appear to be metabolized by aminopeptidase-A. Secondly, in contrast to its lack of effect against A II, amastatin markedly enhanced the potency of A III, steepened the A III concentration-response curves, and increased the time to peak response for each concentration, making A III- and A II-induced contractions appear similar. These findings may be explained by the ability of amastatin to inhibit aminopeptidase-M. This enzyme is present on vascular smooth muscle membranes, can metabolize A III but not A II, and is inhibited by amastatin (Palmieri *et al.*, 1989). The present data are consistent with those of Ahmad & Ward (1990), who found that pressor responses to A III, but not A II, were enhanced in the presence of amastatin. Finally, amastatin was found not to affect contractile responses to the α_1-adrenoceptor agonist, phenylephrine. This provided further confirmation of the specificity of this peptidase inhibitor.

Like aminopeptidase-M, the enzyme aminopeptidase-B can also degrade A III at the N-terminal amino acid. Bestatin, an inhibitor of both aminopeptidase-B and -M, had, like amastatin, no effect on the potency of A II, but increased the potency of A III. Again, this effect of bestatin is probably due to its ability to inhibit aminopeptidase-M (rather than aminopeptidase-B), since a combination of amastatin and bestatin caused no greater enhancement of the potency of A III than did amastatin alone (not shown).

In some tissues, angiotensins are also susceptible to metabolism at the C-terminal by carboxypeptidase enzymes (Peach, 1977). Based on chromatographic evidence, Magnan & Regoli (1977) suggested that carboxypeptidase activity was important in the metabolism of A II in rabbit aorta. Furthermore, Regoli *et al.* (1986) have shown that MERGETPA (8 μM) completely inhibits the contractile effect of bradykinin in rabbit aorta, where the contractile activity depends on the conversion of bradykinin to the metabolite, des-Arg^9-bradykinin, by carboxypeptidase-N. However, the present results showed that MERGETPA, (up to 100 μM) was without effect on contractile responses to A II or A III. It is therefore possible that A II and A III (unlike bradykinin) are poor substrates for carboxypeptidase-N; however, it cannot be ruled out that a C-terminal specific carboxypeptidase, other than carboxypeptidase-N, but capable of degrading angiotensin, is present in rabbit aorta.

To summarise, the present results are consistent with the presence of aminopeptidase-M in isolated strips of the rabbit thoracic aorta. This enzyme appears to be capable of degrading A III, but not A II. Failure to inhibit this enzyme results in an underestimation of both the potency of A III, and the gradient of the A III concentration-response curve.

Since the data indicated that A III was subject to metabolism by aminopeptidase-M, experiments were subsequently carried out to determine whether this enzyme could also degrade angiotensin receptor antagonists. Thus, using A II and A III separately as agonists, the effects of amastatin on the antagonist potencies of the peptide, Ile^7-A III, and of the non-peptide, DuP 753, were measured. In the absence of amastatin, a pA_2 value of 8.2 was obtained for DuP 753 with A II as the agonist, which is comparable with data published in recent literature (Chiu *et al.*, 1990). Unlike DuP 753, Ile^7-A III tended to reduce the maximum of the A II concentration-response curve. This insurmountable antagonism of A II responses in smooth muscle preparations by peptide antagonists is well documented (e.g. Freer *et al.*, 1980; Chiu *et al.*, 1988).

DuP 753 and Ile^7-A III, as well as causing a rightward displacement of A II and A III concentration-response curves, also steepened the A III curves, and increased the maximum response to A III. In amastatin-treated tissues, however, these phenomena were not apparent. Here, the gradient of the pre-antagonist A III curve was already increased as a consequence of aminopeptidase inhibition. It is tempting to speculate, therefore, that the angiotensin receptor antagonists can, like amastatin, reduce the degradation of A III. However, this is unlikely to constitute the whole explanation because neither amastatin nor bestatin increased the maximum response to A III. Thus, at present, the reason for the angiotensin receptor antagonist-induced increase in the maximum response to A III is uncertain. Although the potency of DuP 753 was little affected by amastatin, the potency of Ile^7-A III was markedly increased. This is not particularly surprising since Ile^7-A III differs in structure from A III only by the replacement of the C-terminal amino acid, phenylalanine, by isoleucine. Consequently, Ile^7-A III may well be subject to metabolism by aminopeptidase-M in this preparation. As one might expect, it would appear that the non-peptide structure of DuP 753 makes it a poor substrate for peptidase enzymes. Whether amastatin was present or not, the respective potencies of both antagonists were independent of the agonist used. However, it should be emphasised that in the absence of amastatin, the antagonist affinities may be slightly underestimated because the antagonist-induced displacements of the A III concentration-response curves lacked parallelism. In the presence of amastatin, the antagonist-induced displacements of A II and A III concentration-response curves are more in keeping with that expected for competitive antagonism (Figures 5b, 5d, 6b and 6d). In this situation, the antagonist affinity estimates are consistent with the idea that A II and A III act via a single class of angiotensin receptors in rabbit thoracic aorta.

In conclusion, the study has demonstrated that endogenous aminopeptidase activity can profoundly influence estimates of peptide agonist and antagonist potency at angiotensin receptors in rabbit aorta. Future studies using this preparation to assess either peptide agonist or antagonist potency should routinely include amastatin (or another suitable aminopeptidase-M inhibitor) in the assay system. The present results also serve as a reminder that for any study of angiotensin receptors *in vitro*, an assessment should first be made of whether endogenous peptidase enzymes are active in the tissue being studied. This seems essential before valid comparisons of agonist or antagonist potencies can be made between different preparations, and thus allow meaningful receptor subclassification.

The authors wish to thank Dr G.M. Drew for editorial comments.

References

AHMAD, S. & WARD, P.E. (1990). Role of aminopeptidase activity in the regulation of the pressor activity of circulating angiotensins. *J. Pharmacol. Exp. Ther.*, **252**, 643-649.

AOYAGI, T., TOBE, H., KOJIMA, F., HAMADA, M., TAKEUCHI, T. & UMEZAWA, H. (1978). Amastatin, an inhibitor of aminopeptidase A, produced by actinomycetes. *J. Antibiotics*, **31**, 636-638.

ARUNLAKSHANA, O. & SCHILD, H.O. (1959). Some quantitative uses of drug antagonists. *Br. J. Pharmacol. Chemother.*, **14**, 48-58.

BUMPUS, F.M., CATT, K.J., CHIU, A.T., DEGASPARO, M., GOODFRIEND, T., HUSAIN, A., PEACH, M.J., TAYLOR, D.G. & TIMMERMANS, P.B.M.W.M. (1991). Nomenclature for angiotensin receptors. *Hypertension*, **17**, 720-721.

CHIU, A.T., CARINI, D.J., JOHNSON, A.L., MCCALL, D.E., PRICE, W.A., THOOLEN, M.J.M.C., WONG, P.C., TABER, R.I. & TIMMERMANS, P.B.M.W.M. (1988). Non-peptide angiotensin II receptor antagonists. II. Pharmacology of S-8308. *Eur. J. Pharmacol.*, **157**, 13-21.

CHIU, A.T., MCCALL, D.E., PRICE, W.A., WONG, P.C., CARINI, D.J., DUNCIA, J.V., WEXLER, R.R., YOO, S.E., JOHNSON, A.L. & TIMMERMANS, P.B.M.W.M. (1990). Nonpeptide angiotensin II receptor antagonists. VII. Cellular and biochemical pharmacology of DuP 753, an orally active antihypertensive agent. *J. Pharmacol. Exp. Ther.*, **252**, 711-718.

DE LEAN, A., MUNSON, P.J. & RODBARD, D. (1978). Simultaneous analysis of families of sigmoidal curves: application to bioassay, radioligand assay, and physiological dose-response curves. *Am. J. Physiol.*, **4**, E97-E102.

DOSTAL, D.E., MURAHASHI, T. & PEACH, M.J. (1990). Regulation of cytosolic calcium by angiotensins in vascular smooth muscle. *Hypertension*, **15**, 815-822.

FERRARIO, C.M. (1990). The renin-angiotensin system: importance in physiology and pathology. *J. Cardiovasc. Pharmacol.*, **15**, (Suppl. 3), S1-S5.

FREER, R.J., SUTHERLAND, J.C. & DAY, A.R. (1980). Synthesis and pharmacology of a noncompetitive antagonist of angiotensin-induced contractions of vascular smooth muscle. *Circ. Res.*, **46**, 720-725.

FURCHGOTT, R.F. & BHADRAKOM, S. (1953). Reactions of strips of rabbit aorta to epinphrine, isopropylarterenol, sodium nitrate and other drugs. *J. Pharm. Pharmacol.*, **108**, 129-143.

FURCHGOTT, R.F. (1972). The classification of adrenoceptors (adrenergic receptors). An evaluation from the standpoint of receptor theory. In *Catecholamines. Handb. exp. Pharmacol.*, N.S. Vol. 33, ed. Blaschko, H. & Muscholl, E. pp 283-335. Berlin and Heidelberg: Springer-Verlag.

MAGNAN, J. & REGOLI, D. (1977). Metabolism of angiotensin II and some analogs in intact strips and in muscle preparations of rabbit aortae. *Can. J. Physiol. Pharmacol.*, **56**, 39-47.

MOORE, A.F., HALL, M.H. & KHAIRALLAH, P.A. (1976). A comparison of the effects of angiotensin II and heptapeptide on smooth muscle (vascular and uterine). *Eur. J. Pharmacol.*, **39**, 101-107.

PALMIERI, F.E., BAUSBACK, H.H. & WARD, P.E. (1989). Metabolism of vasoactive peptides by vascular endothelium and smooth muscle aminopeptidase M. *Biochem. Pharmacol.*, **38**, 173-180.

PEACH, M.J. (1977). Renin-angiotensin system: Biochemistry and mechanisms of action. *Physiol. Rev.*, **57**, 313-369.

REGOLI, D., DRAPEAU, G., ROVERO, P., DION, S., RHALEB, N.E., BARABE, J., D'ORLEANS-JUSTE, P. & WARD, P. (1986). Conversion of kinins and their antagonists into B_1 receptor activators and blockers in isolated vessels. *Eur. J. Pharmacol.*, **127**, 219-224.

REID, I.A., MORRIS, B.J. & GANONG, W.F. (1978). The Renin-Angiotensin System. *Annu. Rev. Physiol.*, **40**, 377-410.

ROBERTSON, M.J., CUNOOSAMY, M.P. & CLARK, K.L. (1991). Aminopeptidase inhibition selectively increases the potency of some angiotensin receptor agonists and antagonists in rabbit isolated aorta. *Br. J. Pharmacol.*, **102**, 186P.

SAMENEN, J., BRANDEIS, E., NARINDRAY, D., ADAMS, W., CASH, T., YELLIN, T. & REGOLI, D. (1988). The importance of residues 2 (arginine) and 6 (histidine) in high-affinity angiotensin II antagonists. *J. Med. Chem.*, **31**, 737-741.

SULLIVAN, M.J., HARDING, J.W. & WRIGHT, J.W. (1988). Differential effects of aminopeptidase inhibitors on angiotensin-induced pressor responses. *Brain Res.*, **456**, 249-253.

TIMMERMANS, P.B.M.W.M., WONG, P.C., CHIU, A.T. & HERBLIN, W.F. (1991). Nonpeptide angiotensin II receptor antagonists. *Trends Pharmacol. Sci.*, **12**, 55-62.

TRACHTE, G.J. & PEACH, M.J. (1983). A potent noncompetitive angiotensin II antagonist induces only competitive inhibition of angiotensin III responses. *J. Cardiovasc. Pharmacol.*, **5**, 1025-1033.

UMEZAWA, H., AOYAGI, T., SUDA, H., HAMADA, M. & TAKEUCHI, T. (1976). Bestatin, an inhibitor of aminopeptidase B, produced by actinomycetes. *J. Antibiotics*, **24**, 97-99.

WARD, P.E., BAUSBACK, H.E. & ODYA, C.E. (1987). Kinin and angiotensin metabolism by purified renal post-proline cleaving enzyme. *Biochem. Pharmacol.*, **36**, 3187-3193.

WAUGH, W.H. & BALES, T.E. (1978). Myotropic affinities of angiotensin II and des-Asp^1-angiotensin II in rabbit aorta and femoral artery by microassay. *Can. J. Physiol. Pharmacol.*, **57**, 1256-1266.

WONG, P.C., HART, S.D., ZASPEL, A.M., CHIU, A.T., ARDECKY, R.J., SMITH, R.D. & TIMMERMANS, P.B.M.W.M. (1990). Functional studies of nonpeptide angiotensin II receptor subtype-specific ligands: DuP 753 (AII-1) and PD123177 (AII-2). *J. Pharmacol. Exp. Ther.*, **255**, 584-592.

(Received July 31, 1991
Revised December 1, 1991
Accepted December 23, 1991)

Br. J. Pharmacol. (1992), **106**, 173–179 © Macmillan Press Ltd, 1992

Influence of N^G-nitro-L-arginine on non-adrenergic non-cholinergic relaxation in the guinea-pig gastric fundus

[1]R.A. Lefebvre, E. Baert & A.J. Barbier

Heymans Institute of Pharmacology, University of Gent Medical School, De Pintelaan 185, B-9000 Gent, Belgium

1 The influence of N^G-nitro-L-Arginine (L-NNA) on non-adrenergic non-cholinergic (NANC) relaxations induced by electrical field stimulation was investigated in circular muscle strips of the guinea-pig gastric fundus.

2 In the presence of 10^{-6} M atropine and 4×10^{-6} M guanethidine, electrical field stimulation (40 V, 1 ms, 0.125–16 Hz) with 10 s trains at 5 min intervals induced short-lasting, frequency-dependent relaxations. Continuous stimulation, with cumulative increase of the stimulation frequency, induced sustained frequency-dependent relaxations. Both types of response were abolished by 3×10^{-6} M tetrodotoxin.

3 L-NNA (10^{-5} M and 10^{-4} M) concentration-dependently reduced both types of NANC response. Pre-incubation with 2×10^{-3} M L-arginine prevented the inhibitory action of 10^{-5} M L-NNA and partially antagonized that of 10^{-4} M L-NNA. D-arginine (2×10^{-3} M) did not protect against the inhibitory effect of L-NNA.

4 L-NNA did not consistently influence the basal tone of the tissues. L-Arginine and D-arginine likewise did not influence basal tone; they also had no influence on the electrically-induced NANC relaxations.

5 NO (10^{-6}–10^{-4} M) induced short-lasting concentration-dependent relaxations, while vasoactive intestinal polypeptide (VIP, (10^{-9}–10^{-7} M) induced more sustained relaxations, that developed at a slower rate. The NO- and VIP-induced relaxations were not influenced by 10^{-4} M L-NNA.

6 These results suggest that NO is involved in NANC neurotransmission of the guinea-pig gastric fundus; its contribution to sustained NANC relaxation in the guinea-pig gastric fundus is much more important than in the rat.

Keywords: Guinea-pig gastric fundus; NANC neurotransmission; N^G-nitro-L-arginine (L-NNA); NO; vasoactive intestinal polypeptide (VIP)

Introduction

Inhibitory non-adrenergic non-cholinergic (NANC) neurones are present throughout the gastrointestinal tract. Both purines and peptides, especially vasoactive intestinal polypeptide (VIP), have been proposed as possible mediators in different parts of the gut (McKirdy, 1988; Taylor & Bywater, 1989). Recent data suggest that nitric oxide (NO) is also an inhibitory NANC neurotransmitter. In several tissues such as the opossum lower oesophageal sphincter (Tøttrup *et al.*, 1991), the canine lower oesophageal sphincter and ileocolonic junction (Boeckxstaens *et al.*, 1990; De Man *et al.*, 1991) and the human ileum (Maggi *et al.*, 1991), NO synthesis inhibitors reduce electrically-induced NANC relaxations. Furthermore, the release of a vasorelaxant factor with the characteristics of a nitrovasodilator has been shown upon stimulation of the NANC nerves in the canine ileocolonic junction (Bult *et al.*, 1990), and NO synthase-like immunoreactivity has been observed in the myenteric plexus of the rat intestine (Bredt *et al.*, 1990). These data support the idea that NO has a more general transduction role in addition to endothelium-derived relaxation (Moncada *et al.*, 1991).

The NANC inhibitory neurones of the gastric fundus are involved in the receptive relaxation of the stomach during food intake (Abrahamsson, 1986). In the rat gastric fundus, NANC relaxation induced by prolonged electrical field stimulation is reduced in the presence of peptidases and VIP antiserum, but the initial component persists; this suggests that in addition to VIP, another, non-peptide, neurotransmitter is involved (De Beurme & Lefebvre, 1987; 1988). It was then shown that NANC relaxation induced by short train (10 s) field stimulation was greatly reduced by the NO synthesis inhibitors N^G-monomethyl-L-arginine (L-NMMA) and N^G-nitro-L-arginine (L-NNA), especially at lower frequencies of stimulation (Li & Rand, 1990; Boeckxstaens *et al.*, 1991). Both NO and VIP might thus be inhibitory NANC transmitters in the rat gastric fundus, whereby NO is released with short trains or low frequencies of stimulation, while VIP release is elicited by longer periods or higher frequencies of stimulation. NO and VIP might also be inhibitory transmitters in the guinea-pig trachea (Tucker *et al.*, 1990; Li & Rand, 1991). VIP has been proposed as the neural mediator of the NANC relaxation in the guinea-pig gastric fundus (Grider *et al.*, 1985; Grider & Makhlouf, 1987; Grider, 1990); the NANC relaxation induced by field stimulation with 10 s trains at lower frequencies in this tissue was almost abolished in the presence of VIP antiserum (Grider *et al.*, 1985). Recently, it was shown that adaptive relaxation in response to increased gastric pressure in a guinea-pig isolated stomach model is antagonized by NO synthesis inhibitors, suggesting that NO is released from the inhibitory NANC neurones in the guinea-pig stomach (Desai *et al.*, 1991). We have now investigated the influence of L-NNA on NANC relaxation, induced by short train and prolonged field stimulation, in the guinea-pig gastric fundus. Our results suggest that both during short-lasting and continuous stimulation, NO is involved in the inhibitory NANC neurotransmission of the guinea-pig gastric fundus. A preliminary account of the results was given at the second international meeting on the biology of NO (Lefebvre *et al.*, 1991).

Methods

Tissue preparation

Guinea-pigs of either sex (weight 320–670 g) were fasted for 24 h and were killed by a blow on the head and bleeding.

[1]Author for correspondence.

The stomach was removed and after careful removal of the mucosa by sharp dissection, 2 circular muscle strips (length 2 cm) were prepared from the ventral part of the fundus. The strips were mounted under a load of 1 g in 6 ml (for the experiments with VIP) or 18 ml organ baths containing Krebs solution of the following composition (mM): NaCl 118.5, KCl 4.8, KH_2PO_4 1.2, $MgSO_4$ 1.2, $CaCl_2$ 1.9, $NaHCO_3$ 25.0 and glucose 10.1. The Krebs solution always contained 10^{-6}M atropine and 4×10^{-6}M guanethidine; it was maintained at 37°C and bubbled with 95% O_2:5%CO_2. The guinea-pig gastric fundus is a spontaneous tone preparation; thus it is not necessary to raise tone in order to observe relaxant responses (Sahyoun et al., 1982). Electrical stimulation at supramaximal voltage was applied by two parallel platinum electrodes with an S88 Grass stimulator and a constant current unit. Changes in length were recorded isotonically with Bioscience T_3 transducers and registered on a Graphtec Linearcorder FWR 3701. For the experiments with VIP in the 6 ml organ baths, response were recorded auxotonically (Harvard heart – smooth muscle transducer) on a Graphtec Multicorder MC6625. The tissues were equilibrated for 1 h with rinsing every 15 min. Frequency-response curves to electrical field stimulation (40 V, 1 ms, 0.125–16 Hz) were obtained by stimulating the tissues either with 10 s trains at 5 min intervals (non-cumulative train stimulation) or continuously with stepwise increases of the frequency, once the response to a given frequency had become maximal (cumulative stimulation). At the end of each experiment a maximal relaxation was induced by administration of 10^{-4} M papaverine.

Protocols

To study the influence of L-NNA on the electrically-induced relaxations, and the modification of the effect of L-NNA by L- and D-arginine, four parallel tissues were studied, in which three non-cumulative or cumulative frequency-response curves (0.125–16 Hz) were obtained. Drugs were not added in the control strip; L-NNA (10^{-5} and 10^{-4}M) was added 10 min before the second and third curve respectively. L-Arginine (2×10^{-3}M) and D-arginine (2×10^{-3}M) were added 5 min before L-NNA. The influence of 10^{-4}M L-NNA was also studied on the relaxations induced by electrical stimulation at 0.5 and 4 Hz, both applied for 10 s and 3 min within the same strip; between the stimulus trains, an interval with rinsing was given to allow the tone of the strips to recover.

In an additional series of experiments, the influence of 3×10^{-6}M tetrodotoxin (TTX; incubated for 10 min), 2×10^{-3}M L-arginine and 2×10^{-3}M D-arginine (both incubated for 15 min) on non-cumulative and cumulative frequency-response curves was studied; the 2 types of stimulation were applied in different tissues. Also in these experiments, 3 frequency-response curves were constructed and TTX, L-arginine or D-arginine was added between the second and third curve.

In a last series, concentration-response curves were constructed for NO (10^{-6}–10^{-4}M; non-cumulative administration) and VIP (10^{-9}–10^{-7}M; cumulative administration) and repeated 10 min after adding 10^{-4}M L-NNA. In the control tissues, L-NNA was not added. The influence of NO was also studied when it was continuously administered to the tissue for 5 min; in view of the short half-life of NO, the amount yielding 10^{-5}M, when administered in bolus, was infused into the organ bath over a period of 10 s via a Braun infusion pump.

Drugs

The following drugs were used: atropine sulphate (Boehringer Ingelheim, Germany), D-arginine hydrochloride (Sigma, St. Louis, MO, U.S.A.), L-arginine hydrochloride (Sigma), bacitracin (Sigma), bovine serum albumin (Sigma), guanethidine sulphate (Ciba-Geigy, Groot-Bijgaarden, Belgium), N^{ω}-nitro-L-Arginine (Sigma), tetrodotoxin (TTX; Janssen Pharmaceutica, Beerse, Belgium) and vasoactive intestinal polypeptide (VIP; CRB, Northwich, U.K.). A saturated NO solution was prepared as described by Kelm & Schrader (1988) from NO gas (l'Air Liquide, Belgium). Drugs were dissolved and diluted with distilled water. Atropine, guanethidine, bacitracin and bovine serum albumin were added to the Krebs solution reservoir. Stock solutions of 10^{-3}M TTX and 10^{-3}M VIP were kept frozen at −20°C and dilutions were made the day of the experiment.

Statistical analysis

All relaxant responses are expressed as a percentage of the papaverine-induced relaxation. Results are given as means ± s.e.mean. Results were compared by the Wilcoxon signed-ranks test, P values of less than 0.05 being considered statistically significant.

Results

Stimulation with 10 s trains induced frequency-dependent relaxations (Figures 1, 2). Upon stimulation, tone very quickly declined; at the end of the 10 s stimulus train, a biphasic recovery of tone was evident in some tissues, an initial rapid phase being followed by a second slower phase (Figure 1). In other tissues, recovery was monophasic, with tone rising at a slower rate than it had declined (Figure 2). For calculations, the amplitude of the first phase of relaxation was taken into account. TTX (3×10^{-6}M) nearly abolished the relaxation induced by train stimulation at all frequencies tested. The relaxation induced by stimulation at 16 Hz was abolished in 3 strips and reduced from 47 to 10% in a fourth strip, while the response was well maintained in control tissues.

A representative experiment showing the influence of L-NNA on NANC relaxations induced by train stimulation is given in Figure 1, while the mean results are given in Figure 3. In the control tissues, the NANC response increased somewhat from the first to the second curve but then remained stable. L-NNA concentration-dependently reduced the electrically-induced relaxations. The administration of L-NNA did not consistently increase the basal tension of the strips. Administration of 2×10^{-3}M L-arginine prevented the inhibitory action of 10^{-5}M L-NNA; as in the control tissues, the responses increased from the first to the second frequency-response curve. L-Arginine partially antagonized the inhibitory effect of 10^{-4}M L-NNA. The inhibitory effect of L-NNA in the presence of 2×10^{-3}M D-arginine was similar to that in the absence of D-arginine, although the concentration-dependency was less clear. Neither L-arginine nor D-arginine influenced the NANC relaxations induced by train stimulation *per se* ($n = 4$ for each compound), nor did they influence basal tone.

Continuous stimulation with cumulative increases of the stimulation frequency induced sustained relaxations (Figure 4). The maximal relaxation was reached at 8 Hz as some contraction occurred when the stimulation frequency was increased to 16 Hz. The maximal relaxation, ranging between 60 to 90% of the papaverine-induced relaxation, was more pronounced than the maximal effect induced by 10 s train stimulation (40 to 50%). As with the trains, this type of relaxant response was nearly abolished by 3×10^{-6}M TTX:the relaxation obtained at a stimulation frequency of 8 Hz was reduced from 80 ± 2% to 5 ± 1% ($n = 4$). L-NNA reduced the sustained relaxations in a concentration-dependent manner (Figures 4, 5). The relaxation induced by stimulation at 8 Hz was reduced from 61 ± 11% to 33 ± 10% and 14 ± 5% in the presence of 10^{-5} and 10^{-4}M L-NNA respectively. In the presence of the higher concentration of L-NNA, some contraction started to occur at a stimulation

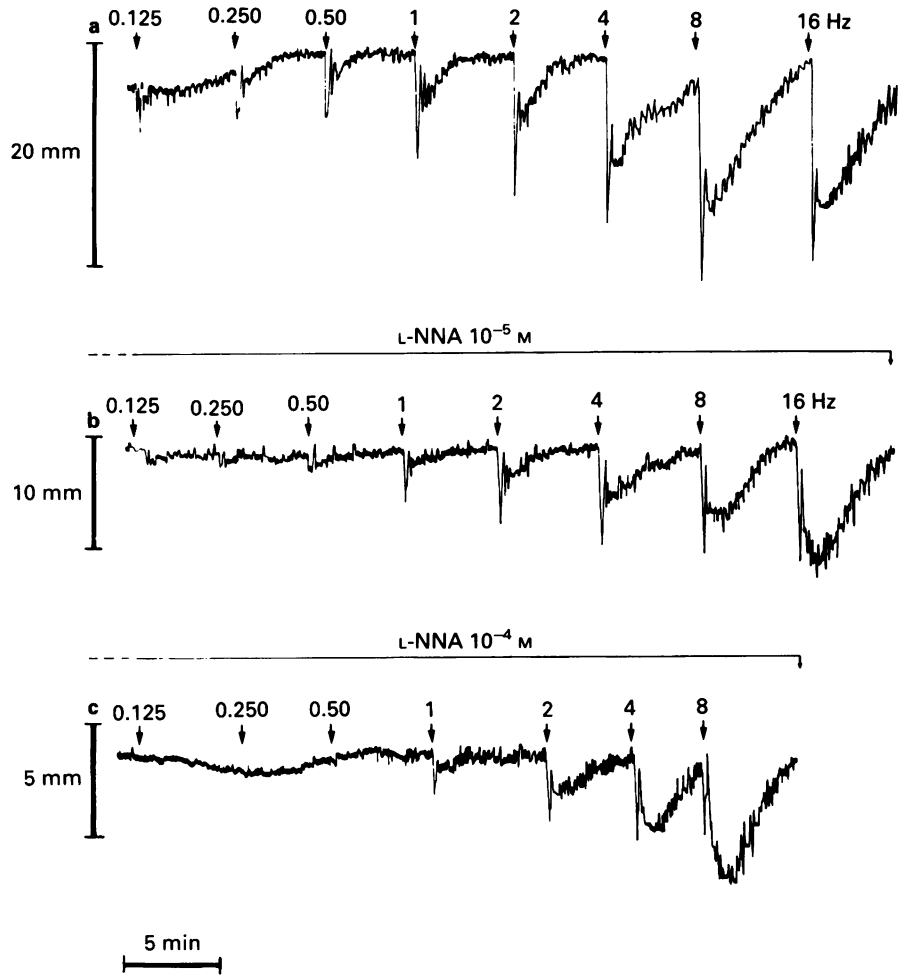

Figure 1 Original recording of a circular muscle strip of the guinea-pig gastric fundus, showing the isotonic responses to electrical stimulation (40 V, 1 ms) with 10 s trains (0.125–16 Hz) at 5 min intervals in the absence (a) and in the presence of 10^{-5}M (b) and 10^{-4}M (c) N^G-nitro-L-arginine (L-NNA). L-NNA was added 10 min before stimulation. Between (b) and (c), the sensitivity of the recorder was increased by a factor of 2.

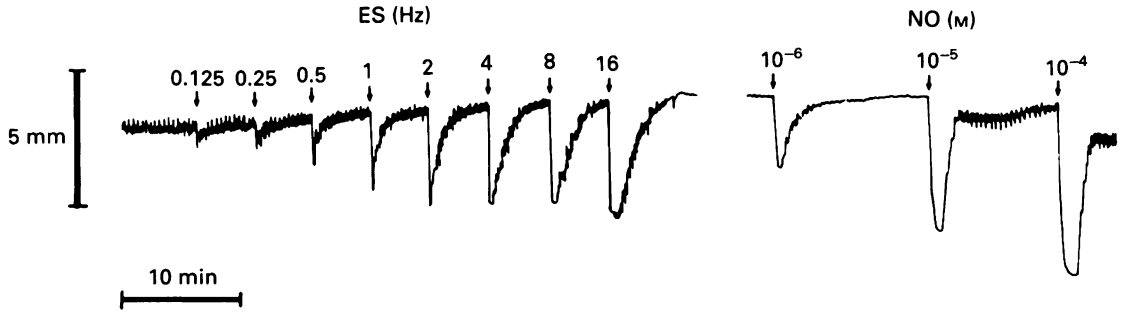

Figure 2 Original recording of a circular muscle strip of the guinea-pig gastric fundus, showing the isotonic responses to electrical stimulation (ES, 40 V, 1 ms) with 10 s trains at 5 min intervals and to NO.

frequency of 8 Hz. L-Arginine (2×10^{-3}M) prevented the inhibitory effect of 10^{-5}M L-NNA, although the latter still induced some non-significant inhibition at the lower stimulation frequencies. D-Arginine did not influence the effect of L-NNA. When incubated alone, L-arginine ($n = 7$) and D-arginine ($n = 4$) did not change the electrically-induced sustained relaxations. Also, when sustained stimulation (3 min) at a given frequency was performed in isolation and not as part of a cumulative frequency-response curve (experiments with stimulation at 0.5 and 4 Hz), the elicited relaxation was antagonized by 10^{-4}M L-NNA. The relaxation induced by stimulation for 3 min at a frequency of 0.5 Hz was reduced from 30 ± 6% to 2 ± 1% ($n = 6$, $P<0.05$), while that at 4 Hz was reduced from 49 ± 9% to 6 ± 3% ($n = 6$, $P<0.05$). When a 10 s train was used for stimulation the values were 13 ± 3% and 1 ± 1% ($n = 6$, $P<0.05$) for 0.5 Hz and 25 ± 5% and 7 ± 1% ($n = 6$, $P<0.05$) for 4 Hz.

NO, administered in bolus, induced short-lasting concentration-dependent relaxations, similar to the NANC responses obtained with short train stimulation (Figure 2). The

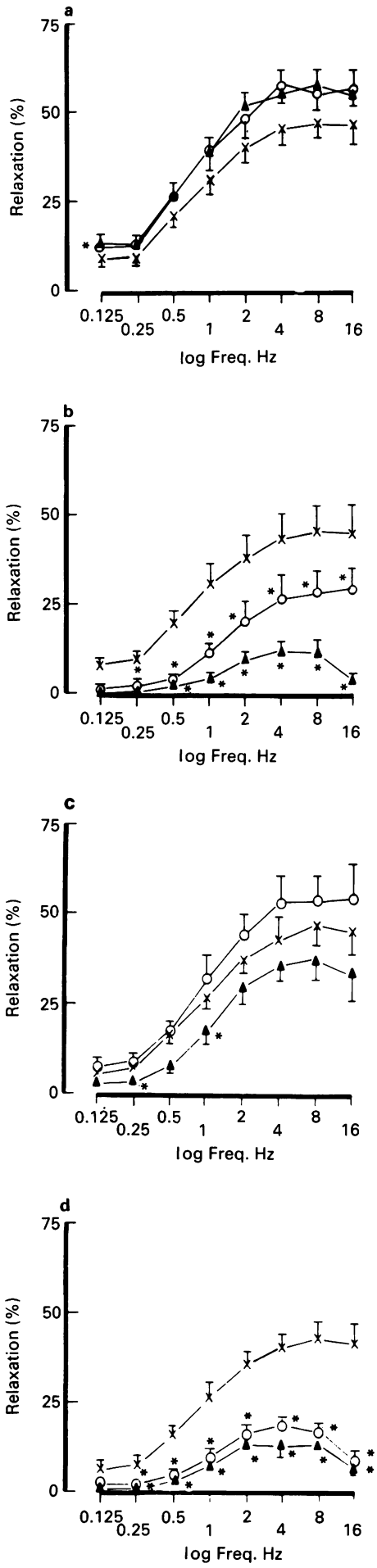

maximal relaxation was about 60% of that induced by papaverine. The NO-induced relaxations were not influenced by 10^{-4}M L-NNA (Figure 6). VIP induced a more sustained relaxation of the tissues, resembling the picture obtained by continuous stimulation. Sustained relaxation was, however, also obtained by infusing NO into the organ bath ($n = 4$). The relaxant effect by the highest concentration of VIP used (10^{-7}M) was only 33% ($n = 14$). The VIP-induced relaxations were not influenced by 10^{-4}M L-NNA. The results with VIP were obtained in the absence of bovine serum albumin and bacitracin, as an additional series showed that the presence of 50 mg l^{-1} bovine serum albumin, to prevent adhesion of VIP to the glassware, and 30 mg l^{-1} bacitracin, to prevent VIP metabolism by peptidases, in the Krebs solution did not significantly increase the relaxant effect of VIP.

Discussion

N^G-nitro-L-arginine (L-NNA) has been shown to be a potent inhibitor of NO biosynthesis (Ishii *et al.*, 1990; Moore *et al.*,

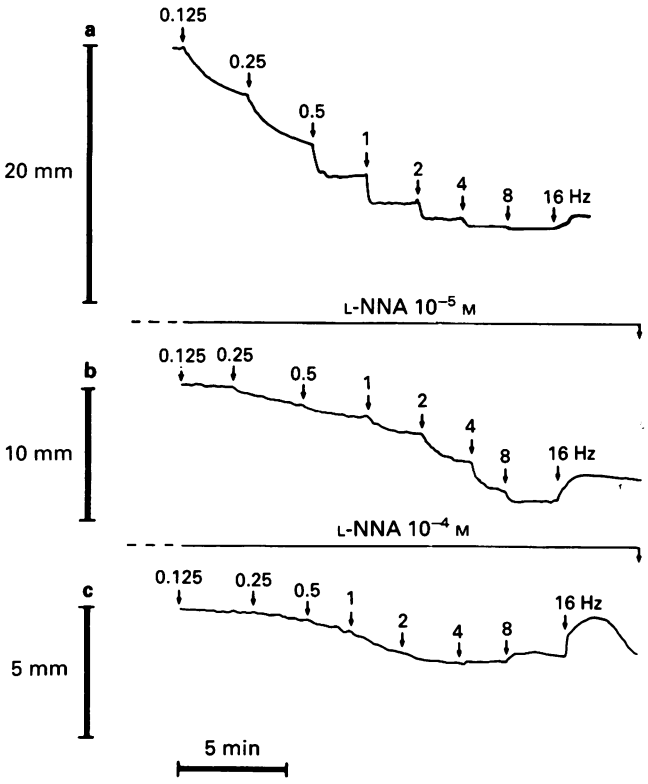

Figure 4 Original recording of a circular muscle strip of the guinea-pig gastric fundus, showing the responses to continuous electrical stimulation (40 V, 1 ms) at increasing frequency in the absence (a) and in the presence of 10^{-5}M (b) and 10^{-4}M (c) N^G-nitro-L-arginine (L-NNA). L-NNA was added 10 min before stimulation. Between (b) and (c) the sensitivity of the recorder was increased by a factor of 2.

Figure 3 Relaxation responses to electrical stimulation (40 V, 1 ms) with 10 s trains at 5 min intervals. (a) In control tissues, 3 frequency-response curves were constructed without addition of drugs (×, 1st curve; O, 2nd curve; ▲, 3rd curve). (b) Responses in the absence (×) and in the presence of 10^{-5}M (O) and 10^{-4}M (▲) N^G-nitro-L-arginine (L-NNA). (c) As in (b) but tissues were incubated with 2×10^{-3}M L-arginine before L-NNA was administered. (d) As in (b) but tissues were incubated with 2×10^{-3}M D-arginine before L-NNA was administered. Mean of $n = 5$ to 6; vertical bars show s.e.mean. *$P<0.05$: significantly different from the control values (signed-ranks test).

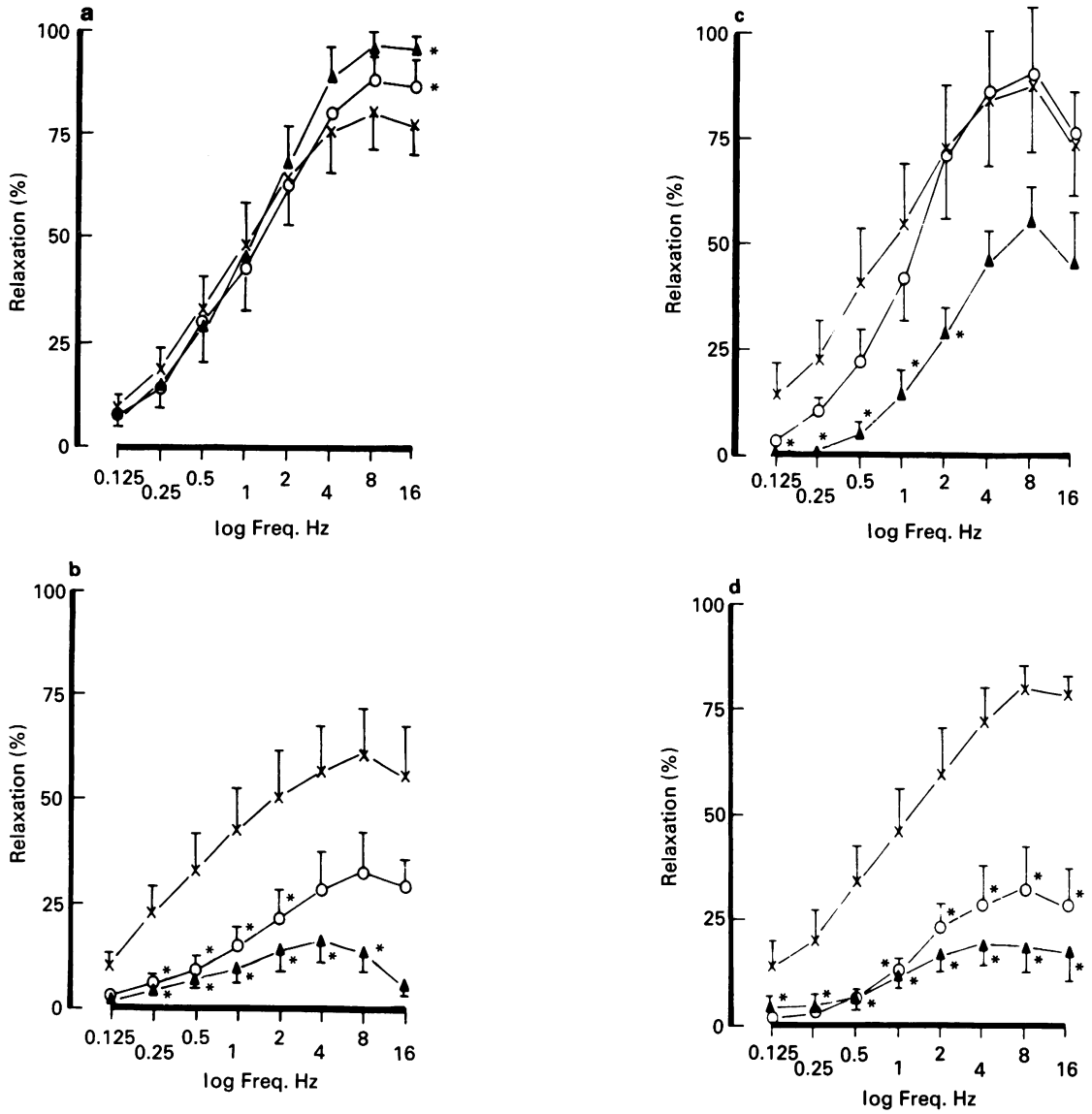

Figure 5 Responses to continuous electrical stimulation (40 V, 1 ms) at increasing frequency. (a) In control tissues, 3 frequency-response curves were constructed without addition of drugs (×, 1st curve; O, 2nd curve; ▲, 3rd curve). (b) Responses in the absence (×) and in the presence of 10^{-5}M (O) and 10^{-4}M (▲) N^G-nitro-L-arginine (L-NNA). (c) As in (b) but tissues were incubated with 2×10^{-3}M L-arginine before L-NNA was administered. (d) As in (b) but tissues were incubated with 2×10^{-3}M D-arginine before L-NNA was administered. Mean of $n = 5$ (c, d) or 6 (a, b); vertical bars show s.e.mean. *$P<0.05$ (one tailed in c and d because $n = 5$): significantly different from the control values (signed-ranks test).

1990; Mülsch & Busse, 1990). In the present study, L-NNA concentration-dependently reduced NANC relaxations in the guinea-pig gastric fundus, induced by short train and continuous stimulation. Both types of response were blocked by TTX, illustrating their neurogenic nature. The tendency to contraction at 16 Hz, occurring at the end of a cumulative frequency-response curve might be due to acetylcholine overcoming the atropine-mediated blockade of the muscarinic receptors in a very relaxed tissue or to release of a non-cholinergic contractile transmitter at higher frequencies. The inhibition by L-NNA was stereospecifically prevented by L-arginine and seemed not due to a non-specific effect at the muscular level as the NO- and VIP-induced relaxations were not influenced by L-NNA. This suggests that NO or a related compound is an important component of the inhibitory NANC neurotransmission of the guinea-pig gastric fundus.

The concentration-dependent reduction of the NANC relaxations, induced by short trains (10 s) of stimulation, by L-NNA corresponds to the effect of L-NNA and other NO synthase inhibitors on similar responses in many other gastrointestinal tissues such as the opossum (Tøttrup *et al.*, 1991) and canine (De Man *et al.*, 1991) lower oesophageal sphincter, the rat gastric fundus (Li & Rand, 1990; Boeckxstaens *et al.*, 1991), the human ileum (Maggi *et al.*, 1991), the canine ileocolonic junction (Boeckxstaens *et al.*, 1990) and the mouse (Gibson *et al.*, 1990) and rat (Gillespie *et al.*, 1989) anococcygeus muscle. It is difficult to correlate the observation that L-NNA completely blocked the NANC relaxations induced by 10 s train stimulation at lower frequencies (0.125–0.5Hz) with the finding of Grider *et al.* (1985) that these responses are completely blocked in the presence of VIP-antiserum. Our results were similar to those of Li & Rand (1991) who found that NANC relaxations induced by field stimulation at 1 Hz are completely blocked by N^G-nitro-L-arginine methyl ester in the guinea-pig trachea. In sheep cerebral arteries, VIP was proposed as the mediator of neurally mediated vasodilatation, whereby VIP would act via synthesis of NO (Gaw *et al.*, 1991). A similar mechanism in the guinea-pig gastric fundus could explain our findings and those of Grider *et al.* (1985) but this is unlikely

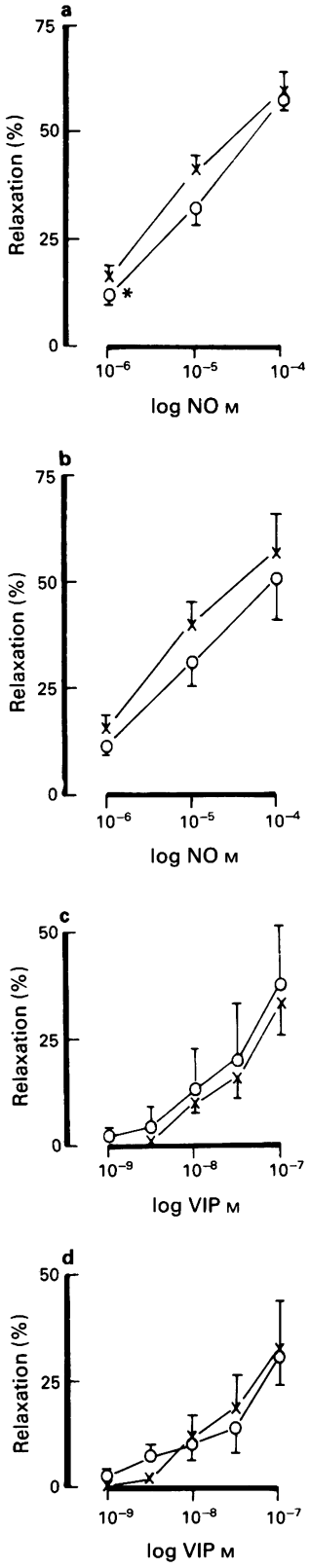

Figure 6 Concentration-response curves to NO (a, b) and vasoactive intestinal polypeptide (VIP, c, d). (a, c) In control tissues, 2 concentration-response curves were constructed without addition of drugs (×, 1st curve; O, 2nd curve). (b, d) Responses in the absence (×) and in the presence (O) of 10^{-4}M N^G-nitro-L-arginine (L-NNA). Mean of $n = 6-8$; vertical bars show s.e.mean. *$P<0.05$: significantly different from the value in the 1st curve (signed-ranks test).

since the VIP-induced relaxations in the guinea-pig gastric fundus are not antagonized by L-NNA. The latter was also observed in the rat gastric fundus (Boeckxstaens *et al.*, 1991) and the opossum lower oesophageal sphincter (Tøttrup *et al.*, 1991). The opposite mechanism, that NO would release VIP, is also unlikely since the VIP-induced relaxations have a different shape from the NANC relaxations induced by train stimulation. In contrast to VIP, the shape and the maximal amplitude of relaxations induced by bolus administration of NO were similar to those induced by the short trains of stimulation. NO has been reported to be more potent in inducing relaxation of vascular than of non-vascular smooth muscle (Buga *et al.*, 1989; Boeckxstaens *et al.*, 1990). Between different non-vascular tissues, the sensitivity can also differ (Buga *et al.*, 1989). In the guinea-pig gastric fundus, the sensitivity to NO was somewhat lower than in the rat gastric fundus (Boeckxstaens *et al.*, 1991) but similar to that in the canine lower oesophageal sphincter (De Man *et al.*, 1991) and ileocolonic junction (Boeckxstaens *et al.*, 1990).

In the rat gastric fundus, the amplitude of NANC relaxations induced by more sustained trains of field stimulation at higher frequencies is not reduced by NO synthase inhibitors (see Li & Rand, 1990, where N^G-monomethyl-L-arginine was tested versus the response induced by stimulation at 5 Hz, and Boeckxstaens, 1991, who tested L-NNA versus the response induced by stimulation at 16 Hz). In the presence of the NO synthase inhibitors, the relaxation developed at a slower rate; VIP antiserum (Li & Rand, 1990) and trypsin (Boeckxstaens, 1991) reduced this type of NANC response, corroborating our suggestion (De Beurme & Lefebvre, 1988) that VIP is involved in this type of NANC relaxation in the rat gastric fundus. Surprisingly, in the guinea-pig gastric fundus, the amplitude of NANC relaxations induced by sustained stimulation was greatly reduced in the presence of L-NNA, even at the higher frequencies of stimulation. The reduction of the responses at higher frequencies was not related to the use of a frequency-response curve as the response to an isolated stimulation at 4 Hz during 3 min was also very clearly antagonized by L-NNA. This result suggests that the role of NO in sustained NANC relaxation is more important in the guinea-pig than in the rat gastric fundus. The observation that infusion of NO is able to induce sustained relaxation corroborates the thesis that NO, when continuously released from nerves to smooth muscle cells, can be responsible for the sustained relaxation observed during continuous field stimulation. Still, our results do not allow us to exclude that NO, released during sustained stimulation, would subsequently release VIP or would be important for the release of VIP as cotransmitter.

In the mouse anococcygeus muscle, L-arginine increased the electrically induced NANC relaxations (Gibson *et al.*, 1990), suggesting that the amount of L-arginine available for NO synthesis during nerve stimulation is limited. No such effect of L-arginine was observed in the guinea-pig gastric fundus. L-NNA did not influence the basal tone of the tissue. The influence of NO synthesis inhibitors on the basal tone of non-vascular smooth muscle preparations differs between tissues, e.g. in the rat anococcygeus muscle (Gillespie *et al.*, 1989), the canine ileocolonic junction (Boeckxstaens *et al.*, 1990) and the rat gastric fundus (Li & Rand, 1990; Boeckxstaens *et al.*, 1991), the NO-synthesis inhibitors induce contraction; inhibition of a tonic production of NO is a possible mechanism. In contrast, the NO synthesis inhibitors do not influence basal tone in the guinea-pig trachea (Li & Rand, 1991), canine lower oesophageal sphincter (De Man *et al.*, 1991) and the rat duodenum (Irie *et al.*, 1991).

In conclusion, our results suggest that NO or a related compound is involved in NANC inhibitory neurotransmission in the guinea-pig gastric fundus, both when elicited by brief periods of stimulation and when stimulation was sustained. These results corroborate the finding that NO is important for the adaptive relaxation of the guinea-pig stomach (Desai *et al.*, 1991).

R.A.L. is a Senior Research Associate and A.J.B. is a Research Assistant of the National Fund for Scientific Research (Belgium).

The study was financially supported by Grant No. 3.0012.86 of the Fund for Medical Scientific Research.

References

ABRAHAMSSON, H. (1986). Non-adrenergic non-cholinergic nervous control of gastrointestinal motility patterns. *Arch. Int. Pharmacodyn. Ther.*, **280**, Suppl., 50–61.

BOECKXSTAENS, G.E. (1991). In vitro study on the nature of the inhibitory non-adrenergic non-cholinergic neurotransmitter in the gut. *Ph. D. Thesis, University of Antwerp*, Belgium.

BOECKXSTAENS, G.E., PELCKMANS, P.A., BOGERS, J.J., BULT, H., DE MAN, J.G., OOSTERBOSCH, L., HERMAN, A.J. & VAN MAERCKE, Y.M. (1991). Release of nitric oxide upon stimulation of nonadrenergic noncholinergic nerves in the rat gastric fundus. *J. Pharmacol. Exp. Ther.*, **256**, 441–447.

BOECKXSTAENS, G.E., PELCKMANS, P.A., BULT, H., DE MAN, J.G., HERMAN, A.G. & VAN MAERCKE, Y.M. (1990). Non-adrenergic non-cholinergic relaxation mediated by nitric oxide in the canine ileocolonic junction. *Eur. J. Pharmacol.*, **190**, 239–246.

BREDT, D.S., HWANG, P.M. & SNYDER, S.H. (1990). Localization of nitric oxide synthase indicating a neural role for nitric oxide. *Nature*, **347**, 768–770.

BUGA, G.M., GOLD, M.E., WOOD, K.S., CHAUDHURI, G. & IGNARRO, L.J. (1989). Endothelium-derived nitric oxide relaxes nonvascular smooth muscle. *Eur. J. Pharmacol.*, **161**, 61–72.

BULT, H., BOECKXSTAENS, G.E., PELCKMANS, P.A., JORDAENS, F.H., VAN MAERCKE, Y.M. & HERMAN, A.G. (1990). Nitric oxide as an inhibitory non-adrenergic non-cholinergic neurotransmitter. *Nature*, **345**, 346–347.

DE BEURME, F.A. & LEFEBVRE, R.A. (1987). Influence of α-chymotrypsin and trypsin on the non-adrenergic non-cholinergic relaxation in the rat gastric fundus. *Br. J. Pharmacol.*, **91**, 171–177.

DE BEURME, F.A. & LEFEBVRE, R.A. (1988). Vasoactive intestinal polypeptide as possible mediator of relaxation in the rat gastric fundus. *J. Pharm. Pharmacol.*, **40**, 711–715.

DE MAN, J.G., PELCKMANS, P.A., BOECKXSTAENS, G.E., BULT, H., OOSTERBOSCH, L., HERMAN, A.G. & VAN MAERCKE, Y.M. (1991). The role of nitric oxide in inhibitory non-adrenergic non-cholinergic neurotransmission in the canine lower oesophageal sphincter. *Br. J. Pharmacol.*, **103**, 1092–1096.

DESAI, K.M., SESSA, W.C. & VANE, J.R. (1991). Involvement of nitric oxide in the reflex relaxation of the stomach to accommodate food or fluid. *Nature*, **351**, 477–479.

GAW, A.J., ABERDEEN, J., HUMPHREY, P.P.A., WADSWORTH, R.M. & BURNSTOCK, G. (1991). Relaxation of sheep cerebral arteries by vasoactive intestinal polypeptide and neurogenic stimulation: inhibition by L-N^G-monomethyl arginine in endothelium-denuded vessels. *Br. J. Pharmacol.*, **102**, 567–572.

GIBSON, A., MIRZAZADEH, S., HOBBS, A.J. & MOORE, P.K. (1990). L-N^G-monomethyl arginine and L-N^G-nitro arginine inhibit non-adrenergic non-cholinergic relaxation of the mouse anococcygeus muscle. *Br. J. Pharmacol.*, **99**, 602–606.

GILLESPIE, J.S., LIU, X. & MARTIN, W. (1989). The effects of L-arginine and N^G-monomethyl L-arginine on the response of the rat anococcygeus muscle to NANC nerve stimulation. *Br. J. Pharmacol.*, **98**, 1080–1082.

GRIDER, J.R. (1990). Identification of neurotransmitters by selective protection of postjunctional receptors. *Am. J. Physiol.*, **258**, G103–G106.

GRIDER, J.R., CABLE, M.B., SAID, S.I. & MAKHLOUF, G.M. (1985). Vasoactive intestinal peptide as a neural mediator of gastric relaxation. *Am. J. Physiol.*, **248**, G73–G78.

GRIDER, J.R.. & MAKHLOUF, G.M. (1987). Prejunctional inhibition of vasoactive intestinal peptide release. *Am. J. Physiol.*, **253**, G7–G12.

IRIE, K., MURAKI, T., FURUKAWA, K. & NOMOTO, T. (1991). L-N^G-nitro-arginine inhibits nicotine-induced relaxation of isolated rat duodenum. *Eur. J. Pharmacol.*, **202**, 285–288.

ISHII, K.B., CHANG, B., KERWIN, J.F., JR, HUANG, Z.-J. & MURAD, F. (1990). N^ω-nitro-L-arginine: a potent inhibitor of endothelium-derived relaxing factor formation. *Eur. J. Pharmacol.*, **176**, 219–223.

KELM, M. & SCHRADER, J. (1990). Control of coronary vascular tone by nitric oxide. *Circ. Res.*, **66**, 1561–1575.

LEFEBVRE, R.A., BAERT, E. & BARBIER, A.J. (1991). Influence of N^G-nitro-L-arginine on non-adrenergic non-cholinergic relaxation in the guinea-pig gastric fundus, Abstract book, *Second Int. Meeting on Biology of Nitric Oxide*, London, 30.9–2.10, p. 149.

LI, C.G. & RAND, M.J. (1990). Nitric oxide and vasoactive intestinal polypeptide mediate non-adrenergic, non-cholinergic inhibitory transmission to smooth muscle of the rat gastric fundus. *Eur. J. Pharmacol.*, **191**, 303–309.

LI, C.G. & RAND, M.J. (1991). Evidence that part of the NANC relaxant response of guinea-pig trachea to electrical field stimulation is mediated by nitric oxide. *Br. J. Pharmacol.*, **102**, 91–94.

MAGGI, C.A., BARBANTI, G., TURINI, D. & GIULIANI, S. (1991). Effect of N^G-monomethyl L-arginine (L-NMMA) and N^G-nitro L-arginine (L-NOARG) on non-adrenergic non-cholinergic relaxation in the circular muscle of the human ileum. *Br. J. Pharmacol.*, **103**, 1970–1972.

McKIRDY, H.C. (1988). Novel autonomic neurotransmitters and upper gastrointestinal function. *Pharmacol. Ther.*, **38**, 429–452.

MONCADA, S., PALMER, R.M.J. & HIGGS, E.A. (1991). Nitric oxide: physiology, pathophysiology and pharmacology. *Pharmacol. Rev.*, **43**, 109–142.

MOORE, P.K., ALSWAYEH, O.A., CHONG, N.W.S., EVANS, R.A. & GIBSON, A. (1990). L-N^G-nitro arginine (L-NOARG), a novel, L-arginine reversible inhibitor of endothelium-dependent vasodilatation in vitro. *Br. J. Pharmacol.*, **99**, 408–412.

MÜLSCH, A. & BUSSE, R. (1990). N^G-nitro-L-arginine (N^5-[imino(nitroamino)methyl]-1-ornithine) impairs endothelium-dependent dilations by inhibiting cytosolic nitric oxide synthesis from L-arginine. *Naunyn-Schmiedebergs Arch. Pharmacol.*, **341**, 143–147.

SAHYOUN, H.A., COSTALL, B. & NAYLOR, R.J. (1982). On the ability of domperidone to selectively inhibit catecholamine-induced relaxation of circular smooth muscle of guinea-pig stomach. *J. Pharm. Pharmacol.*, **34**, 27–33.

TAYLOR, G.S. & BYWATER, R.A.R. (1988). Novel autonomic neurotransmitters and intestinal function. *Pharmacol. Ther.*, **40**, 401–438.

TØTTRUP, A., SVANE, D. & FORMAN, A. (1991). Nitric oxide mediating NANC inhibition in opossum lower esophageal sphincter. *Am. J. Physiol.*, **260**, G385–G389.

TUCKER, J.F., BRAVE, S.R., CHARALAMBOUS, L., HOBBS, A.J. & GIBSON, A. (1990). L-N^G-nitro arginine inhibits non-adrenergic, non-cholinergic relaxations of guinea-pig isolated tracheal smooth muscle. *Br. J. Pharmacol.*, **100**, 663–664.

(Received October 28, 1991
Revised January 2, 1992
Accepted January 7, 1992)

Br. J. Pharmacol. (1992), **106**, 180–186 © Macmillan Press Ltd, 1992

Effects of the neutral endopeptidase inhibitor, SQ 28,603, on regional haemodynamic responses to atrial natriuretic peptide or proendothelin-1 [1-38] in conscious rats

[1]S.M. Gardiner, P.A. Kemp & T. Bennett

Department of Physiology and Pharmacology, University of Nottingham Medical School, Queen's Medical Centre, Nottingham NG7 2UH

1 Regional haemodynamic responses to atrial natriuretic peptide (ANP, 0.5 nmol kg^{-1}) or proendothelin-1 [1-38] (1.0 nmol kg^{-1}) were assessed in the same conscious Long Evans rats before and 20 min after administration of the novel neutral endopeptidase (NEP) inhibitor, SQ 28,603 (50 mg kg^{-1}, i.v.). In a separate experiment, responses to endothelin-1 (0.5 nmol kg^{-1}), angiotensin I (0.25 nmol kg^{-1}) and angiotensin II (0.12 nmol kg^{-1}) were measured before and after administration of SQ 28,603.

2 SQ 28,603 alone had no significant cardiovascular effects but caused significant prolongation of the hypotensive, tachycardic and renal and mesenteric vasoconstrictor effects of ANP. However, the early vasodilator and late vasoconstrictor responses in the hindquarters were not affected significantly.

3 SQ 28,603 caused significant attenuation of the pressor effects of proendothelin-1 [1-38] but the associated bradycardia was unchanged. SQ 28,603 caused a significant inhibition of the renal and mesenteric vasoconstrictor effects of proendothelin-1 and also inhibited the initial vasodilator and subsequent vasoconstrictor responses in the hindquarters vascular bed.

4 SQ 28,603 had no significant effects on the haemodynamic responses to endothelin-1, angiotensin I, or angiotensin II.

5 The results are consistent with SQ 28,603 not only inhibiting NEP that is involved in the degradation of ANP, but also suppressing activity of the enzyme involved in the conversion of proendothelin-1 [1-38] to endothelin-1.

Keywords: Rat atrial natriuretic peptide [1-28]; proendothelin-1 [1-38]; neutral endopeptidase inhibitor; SQ 28,603; haemodynamics

Introduction

In vivo, phosphoramidon suppresses the hypertensive effects of proendothelin-1 [1-38] and proendothelin-1 [1-39], but not of endothelin-1 (Matsumura *et al.*, 1990; Fukuroda *et al.*, 1990; McMahon *et al.*, 1991). These observations are consistent with the pressor effects of exogenous proendothelin-1 *in vivo* being due to its conversion to endothelin-1 by neutral endopeptidase, EC 3.4.24.11 (NEP), or a related enzyme. The latter possibility is consistent with the finding that the pressor effects of proendothelin-1 [1-39] are inhibited less effectively by thiorphan or kelatorphan than by phosphoramidon (McMahon *et al.*, 1991).

The studies cited above were concerned only with measurements of blood pressure and heart rate in anaesthetized animals and, hence, did not show whether or not the *in vivo* effects of proendothelin-1 [1-38] in different vascular beds were influenced to different extents by phosphoramidon. However, in a recent study (Gardiner *et al.*, 1991) we found that phosphoramidon could suppress the bradycardic and renal and hindquarters vasoconstrictor effects of proendothelin-1 under conditions in which the potent mesenteric vasoconstrictor action of this peptide was not changed significantly. These findings are consistent with a local conversion of proendothelin-1 [1-38] to endothelin-1. Furthermore, they indicate that phosphoramidon-resistant enzyme system(s) could be involved in the conversion of proendothelin-1 [1-38] to endothelin-1 in the mesenteric vascular bed.

Recently, it has been found that several novel inhibitors of NEP cause a reduction in mean arterial blood pressure in hypertensive rats, together with natriuresis and diuresis, and an enhancement of responses to exogenous atrial natriuretic peptide (ANP) (Seymour *et al.*, 1989; 1991; Sybertz *et al.*, 1990). While these effects are consistent with inhibition of the degradation of ANP (Gerbes & Vollmar, 1990), it is not known if these NEP inhibitors also suppress the production of endothelin-1 from proendothelin-1 [1-38]. Furthermore, the influence of these NEP inhibitors on the regional haemodynamic responses to exogenous ANP have not been delineated. Therefore, in the present work we examined the regional haemodynamic responses to ANP and to proendothelin-1 [1-38] in the same conscious, Long Evans rats before and after administration of the novel NEP inhibitor, SQ 28,603 (N-[2-(mercaptomethyl)-1-oxo-3-phenylpropyl]-β-alanine) (Seymour *et al.*, 1991).

In order to cover the possibility that any effects of SQ 28,603 on responses to proendothelin-1 [1-38] were not specific to that agonist, in a separate experiment we assessed the effects of endothelin-1, angiotensin I and angiotensin II, before and after administration of SQ 28,603.

Methods

Male, Long Evans rats (350–450 g) were anaesthetized (sodium methohexitone, 60 mg kg^{-1}; i.p., supplemented as required) and had pulsed Doppler probes (Haywood *et al.*, 1981) implanted to permit monitoring of renal, mesenteric and hindquarters blood flows (Gardiner *et al.*, 1990a,c,d). Animals were given an i.m. injection of ampicillin (Penbritin, Beecham, 7 mg kg^{-1}) and allowed to recover for at least 7 days in individual home cages. After that time animals in good health and with acceptable signals from all 3 probes had intravascular catheters implanted (under brief sodium methohexitone anaesthesia, 40 mg kg^{-1}, i.p.). Animals were

[1] Author for correspondence.

then returned to their home cages to recover for at least 24 h, with free access to food and water.

Experiments were run in conscious, unrestrained animals over a period of 3 days. In the first experiment animals ($n = 7$) were randomized to receive ANP (0.5 nmol kg^{-1}, i.v. bolus) or proendothelin-1 [1-38] (1 nmol kg^{-1}, i.v. bolus) in the absence of, or 20 min after (Seymour *et al.*, 1989; 1991), injection of SQ 28,603 (50 mg kg^{-1}, i.v. bolus). This dose of SQ 28,603 was used because in pilot experiments in 3 animals SQ 28,603 at a dose of 25 mg kg^{-1} had no discernible effects on the responses to ANP.

In the second experiment animals ($n = 8$) were randomised to receive endothelin-1 (0.5 nmol kg^{-1}), angiotensin I (0.25 nmol kg^{-1}) and angiotensin II (0.12 nmol kg^{-1}) before and after SQ 28,603. Six of these animals also received proendothelin-1 [1-38] before and after SQ 28,603, to ensure responses were similar to those in the first experiment.

Before any intervention baseline measurements were made for 30 min to ensure steady state haemodynamics had been achieved. Thereafter, cardiovascular variables were monitored continuously and measurements (averaged over 20 s) made at 1, 5, 10, 15, 20, 30 and 60 min after injection of ANP or proendothelin-1. The pulsed Doppler system used (VF-1; Crystal Biotech, Holliston, U.S.A.) was modified to run with a pulse repetition frequency of 125 kHz to avoid aliasing (Gardiner *et al.*, 1990b). The mean Doppler shift signals were divided by mean arterial blood pressure to provide estimates of changes (%) in vascular conductances (Gardiner *et al.*, 1990c,d).

Data analysis

Changes (%) relative to baseline were analysed by Friedman's test (Theodorsson-Norheim, 1987). Comparison of responses to ANP or proendothelin-1 in the absence and after SQ 28,603 were made by Wilcoxon's ranks sums test applied to areas under or over curves (AUC and AOC, respectively) measured over the 60 min time period following each injection (Gardiner *et al.*, 1990d); a P value <0.05 was taken as significant.

Drugs and peptides

ANP (rat, 1-28), human proendothelin-1 [1-38], endothelin-1, angiotensin I, and angiotensin II were obtained from Bachem (U.K.). All peptides were dissolved in isotonic saline (157 mmol l^{-1} NaCl) containing 1% bovine serum albumin (Sigma) the solutions were divided into aliquots (100 µl) and frozen (−80°C) until required. SQ 28,603 was dissolved in 2.5% $NaHCO_3$ and deep frozen (as above). All injections were given as 100 µl volumes and flushed in with 150 µl of isotonic saline.

Results

Experiment 1

Resting values for cardiovascular variables before (control) and after injection of SQ 28,603 are shown in Table 1. SQ 28,603 caused no significant cardiovascular effects, i.e. there were no significant differences in the two conditions. However, administration of SQ 28,603 caused marked increases in grooming activity, but this was not assessed formally. Vehicle injections had no significant effects and, furthermore, in preliminary experiments repeated injections of ANP or proendothelin-1 [1-38] on consecutive days had reproducible actions.

Responses to ANP before and after administration of SQ 28,603

ANP caused a modest, but prolonged, fall in mean arterial blood pressure (AOC, 387 ± 82 mmHg min) (Figure 1). There was an early tachycardia (AUC, 616 ± 104 beats) but this had waned by 10 min (Figure 1). Renal blood flow showed a sustained decrease (AOC, 1245 ± 234% min), whereas there was a reduction in mesenteric blood flow (AOC, 896 ± 234% min) that was less prolonged (Figure 1). Hindquarters flow increased initially (AUC, 138 ± 34% min) and then decreased (AOC, 1147 ± 194% min) (Figure 1). Hence, there was a sustained reduction in renal vascular conductance (AOC, 1000 ± 206% min), a transient mesenteric vasoconstriction (AOC, 703 ± 212% min) and an early hindquarters vasodilatation (AUC, 253 ± 90% min) followed by a vasoconstriction (AOC, 941 ± 175% min) (Figure 1).

Following SQ 28,603, administration of ANP had significantly enhanced hypotensive (AOC, 694 ± 141 mmHg min) and tachycardic (AUC, 1210 ± 288 beats) effects (Figure 1). The reductions in renal blood flow (AOC, 2123 ± 167% min) and mesenteric blood flow (AOC, 2043 ± 152% min) were also significantly increased (Figure 1). However, neither the initial increase (AUC, 113 ± 30% min) nor the subsequent decrease (AOC, 1583 ± 142% min) in hindquarters flow were significantly different from the changes before SQ 28,603. In the presence of the latter, ANP had significantly enhanced renal and mesenteric vasoconstrictor effects (AOC, 1710 ± 158 and 1598 ± 140% min, respectively), but the changes in hindquarters vascular conductance were not significantly affected (vasodilatation AUC, 174 ± 41% min; vasoconstriction AOC, 1158 ± 89% min) (Figure 1).

Responses to proendothelin-1 [1-38] before and after SQ 28,603

Proendothelin-1 [1-38] caused a marked hypertension of long duration (AUC, 2216 ± 209 mmHg min) (Figure 2). There was an initial, transient tachycardia (AUC, 209 ± 103 beats) followed by a profound bradycardia (AOC, 3568 ± 387 beats) (Figure 2). Renal and mesenteric blood flows showed marked reductions (AOC, renal 1836 ± 226% min; mesenteric 2453 ± 266% min) (Figure 2). There was an initial, transient increase (AUC, 231 ± 79% min) followed by a sustained decrease (AOC, 2067 ± 212% min) in hindquarters flow (Figure 2). Hence there were substantial and sustained reductions in renal and mesenteric vascular conductances (AOC, 2710 ± 127 and 3235 ± 218% min, respectively), whereas there was an early hindquarters vasodilatation (AUC, 156 ± 61% min) followed by a vasoconstriction (AOC, 2924 ± 229% min) (Figure 2).

Table 1 Cardiovascular variables before (control) and 20 min after administration of SQ 28,603 (50 mg kg^{-1}, i.v. bolus) in the same conscious, Long Evans rats ($n = 7$)

	Heart rate (beats min^{-1})	*Mean arterial blood pressure* (mmHg)	*Doppler shift* (kHz) *Renal*	*Mesenteric*	*Hindquarters*	*Vascular conductance* ([kHz $mmHg^{-1}$]10^3) *Renal*	*Mesenteric*	*Hindquarters*
Control	332 ± 3	105 ± 2	11.0 ± 1.1	6.9 ± 0.5	3.7 ± 0.4	104 ± 7	66 ± 6	35 ± 3
+ SQ 28,603	362 ± 6	113 ± 3	11.5 ± 1.4	6.3 ± 0.3	3.7 ± 0.5	101 ± 6	56 ± 8	32 ± 2

Values are mean ± s.e.mean.

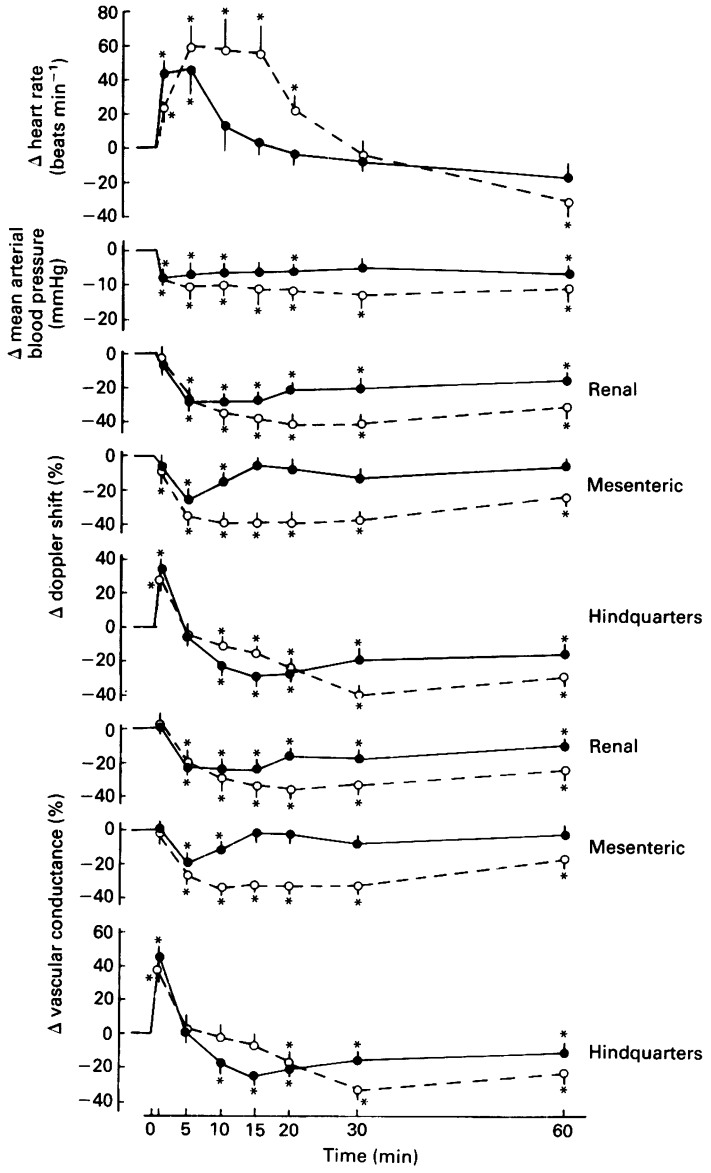

Figure 1 Changes in cardiovascular variables in response to atrial natriuretic peptide (0.5 nmol kg^{-1}, i.v. bolus) in the same conscious Long Evans rats ($n = 7$) before (●) and 20 min after SQ 28,603 (○). Values are mean with s.e.mean shown by vertical lines. $^*P < 0.05$ versus baseline. Statistics for comparisons between responses (areas under or over curves) in the two conditions are given in the text.

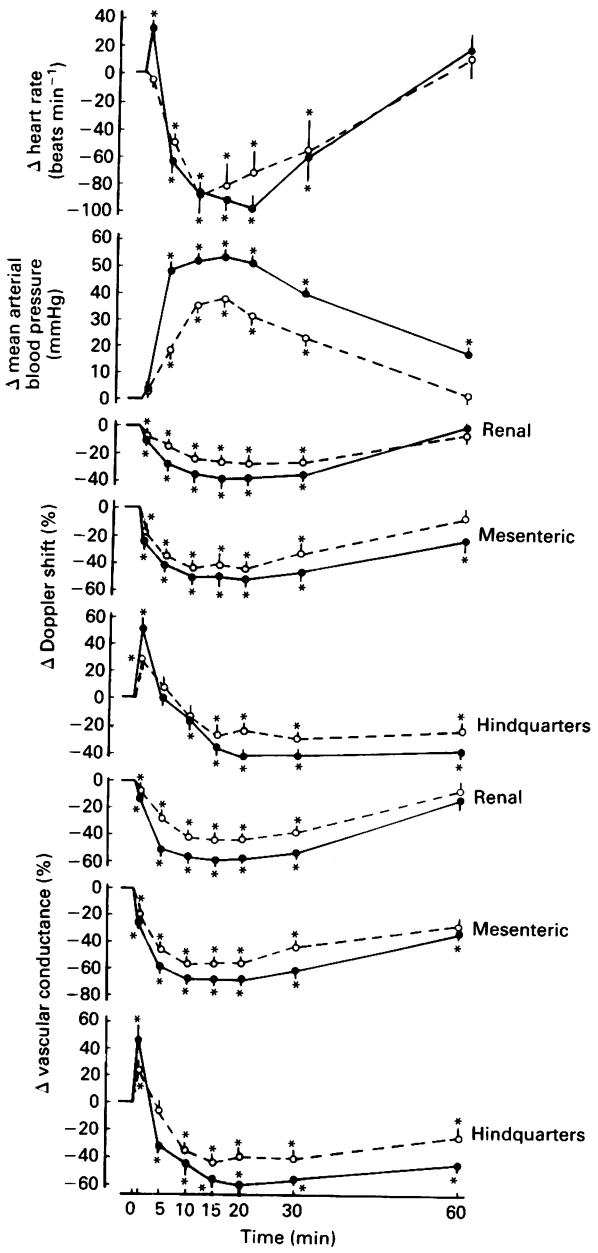

Figure 2 Changes in cardiovascular variables in response to proendothelin-1 [1-38] (1.0 nmol kg^{-1}, i.v. bolus) in the same conscious Long Evans rats ($n = 7$) before (●) and 20 min after SQ 28,603 (○). Values are mean with s.e.mean shown by vertical lines. $^*P < 0.05$ versus baseline. Statistics for comparisons between responses (areas under or over curves) in the two conditions are given in the text.

Following SQ 28,603 the hypertensive effect of proendothelin-1 [1-38] was significantly attenuated (AUC, 1322 ± 98 mmHg min) and slower in onset. Although the initial tachycardic response was lost (AUC 42 ± 39 beats), the bradycardia (AOC, 3414 ± 794 beats) was not significantly affected (Figure 2). Changes in blood flow in response to proendothelin-1 [1-38] before and after SQ 28,603 were not compared because of the marked differences in mean systemic arterial blood pressure. However, in the presence of SQ 28,603 there was significant attenuation of the renal (AOC, 1930 ± 153% min) and mesenteric (AOC, 2472 ± 217% min) vasoconstrictor effects of proendothelin-1 [1-38], and of the initial hindquarters vasodilator (AUC, 73 ± 11% min) and subsequent vasoconstrictor (AOC, 2021 ± 171% min) responses to this peptide (Figure 2).

Experiment 2

The responses to proendothelin-1 were similar to those in experiment 1, consisting of hypertension (AUC, 1897 ± 187 mmHg min) accompanied by reductions in renal and mesenteric vascular conductances (AOC renal, 2637 ± 85% min; mesenteric, 2857 ± 169% min). There was an initial increase followed by a decrease in hindquarters vascular conductance (AUC, 53 ± 28, AOC, 2506 ± 182% min). After administration of SQ 28,603 there was significant attentuation of the pressor effects (AUC, 953 ± 49 mmHg min) and reductions in renal (AOC, 1297 ± 239% min), mesenteric (AOC, 1876 ± 249% min) and hindquarters (1489 ± 248% min) vascular conductances seen with proendothelin-1. In contrast, SQ 28,603 had no significant effects on the responses to endothelin-1, angiotensin I, or angiotensin II (Tables 2–4).

Discussion

SQ 28,603 alone, at a dose of 50 mg kg^{-1}, was without significant effect on any cardiovascular variables in the con-

Table 2 Changes in cardiovascular variables following endothelin-1 (0.5 nmol kg^{-1}, i.v. bolus) before (control) or 20 min after SQ 28,603 in the same, conscious Long Evans rats ($n = 8$)

Time (min)			0.25	0.5	1	5	10	15	20	30	60
Heart rate (beats min^{-1})		Control	88 ± 8*	115 ± 6*	94 ± 17*	−22 ± 6*	−53 ± 10*	−36 ± 17	−33 ± 14*	−15 ± 10	−13 ± 4*
		+ SQ 28,603	83 ± 12*	107 ± 12*	99 ± 22*	−29 ± 11*	−49 ± 15*	−42 ± 15*	−41 ± 15*	−33 ± 10*	−21 ± 11
Mean arterial blood pressure (mmHg)		Control	−34 ± 2*	−23 ± 3*	6 ± 3	27 ± 2*	30 ± 2*	23 ± 4*	21 ± 4*	15 ± 3*	3 ± 1
		+ SQ 28,603	−31 ± 3*	−17 ± 3*	6 ± 3	27 ± 3*	28 ± 3*	21 ± 3*	19 ± 4*	15 ± 5*	0 ± 3
Vascular conductance (%)	Renal	Control	−23 ± 5*	−41 ± 5*	−53 ± 5*	−57 ± 4*	−56 ± 4*	−52 ± 6*	−48 ± 5*	−32 ± 6*	−9 ± 9*
		+ SQ 28,603	−26 ± 4*	−46 ± 5*	−54 ± 5*	−56 ± 5*	−54 ± 4*	−50 ± 5*	−45 ± 5*	−31 ± 8*	1 ± 6
	Mesenteric	Control	−1 ± 9	−12 ± 6	−16 ± 6*	−59 ± 3*	−56 ± 3*	−50 ± 3*	−47 ± 3*	−36 ± 3*	−12 ± 3*
		+ SQ 28,603	7 ± 7	−17 ± 4*	−12 ± 4*	−60 ± 4*	−57 ± 3*	−48 ± 4*	−45 ± 4*	−35 ± 6*	−13 ± 5*
	Hindquarters	Control	125 ± 8*	132 ± 7*	30 ± 4*	−20 ± 4*	−16 ± 4*	−10 ± 7	−14 ± 6	−6 ± 4	−1 ± 4
		+ SQ 28,603	107 ± 11*	102 ± 12*	6 ± 5	−25 ± 6*	−27 ± 4*	−17 ± 7*	−16 ± 7	−12 ± 6	8 ± 6

Values are mean ± s.e.mean.
*$P < 0.05$ versus baseline.

Table 3 Changes in cardiovascular variables following angiotensin I (0.25 nmol kg^{-1}, i.v. bolus) before (control) or 20 min after SQ 28,603 in the same, conscious, Long Evans rats ($n = 8$)

Time (min)			0.25	1	2	3	4	5	10
Heart rate (beats min^{-1})		Control	−88 ± 11*	−90 ± 14*	−70 ± 15*	−43 ± 14*	−27 ± 6*	−19 ± 5*	−8 ± 3
		+ SQ 28,603	−84 ± 8*	−89 ± 9*	−61 ± 10*	−18 ± 8	−7 ± 9	−6 ± 9	4 ± 11
Mean arterial blood pressure (mmHg)		Control	54 ± 4*	50 ± 3*	30 ± 5*	18 ± 3*	12 ± 2*	8 ± 2*	3 ± 2
		+ SQ 28,603	54 ± 3*	51 ± 3*	32 ± 4*	12 ± 3*	7 ± 2*	6 ± 2*	1 ± 2
Vascular conductance (%)	Renal	Control	−92 ± 1*	−73 ± 2*	−45 ± 5*	−28 ± 3*	−19 ± 2*	−14 ± 2*	−7 ± 3
		+ SQ 28,603	−92 ± 1*	−73 ± 1*	−44 ± 2*	−23 ± 2*	−14 ± 3*	−13 ± 3*	−8 ± 3*
	Mesenteric	Control	−81 ± 1*	−64 ± 2*	−31 ± 5*	−17 ± 4*	−12 ± 4*	−11 ± 3*	−7 ± 3
		+ SQ 28,603	−83 ± 2*	−64 ± 2*	−30 ± 4*	−16 ± 3*	−10 ± 3*	−11 ± 2*	−6 ± 3
	Hindquarters	Control	−26 ± 7*	−35 ± 5*	−29 ± 7*	−18 ± 8	−12 ± 6	−4 ± 7	−2 ± 6
		+ SQ 28,603	−23 ± 5	−33 ± 6*	−25 ± 5*	−12 ± 3*	−3 ± 4	−2 ± 4	−1 ± 5

Values are mean ± s.e.mean.
*$P < 0.05$ versus baseline.

Table 4 Changes in cardiovascular variables following angiotensin II (0.12 nmol kg^{-1}, i.v. bolus) before (control) or 20 min after SQ 28,603 in the same conscious, Long Evans rats ($n = 8$)

Time (min)			0.25	1	2	3	4	5	10
Heart rate (beats min^{-1})		Control	−69 ± 4*	−58 ± 10*	−11 ± 12	−7 ± 13*	−6 ± 10	−3 ± 10	−2 ± 9
		+ SQ 28,603	−81 ± 6*	−73 ± 11*	−33 ± 7*	14 ± 13	8 ± 10	9 ± 11	4 ± 18
Mean arterial blood pressure (mmHg)		Control	49 ± 3*	36 ± 3*	16 ± 3*	9 ± 2*	7 ± 2*	5 ± 1*	0 ± 1
		+ SQ 28,603	47 ± 3*	40 ± 5*	14 ± 4*	6 ± 3	3 ± 3*	3 ± 3	1 ± 4
Vascular conductance (%)	Renal	Control	−87 ± 1*	−54 ± 3*	−26 ± 3*	−14 ± 3*	−7 ± 4	−3 ± 3	7 ± 5
		+ SQ 28,603	−90 ± 1*	−56 ± 5*	−25 ± 6*	−12 ± 4*	−5 ± 5	−2 ± 4	2 ± 5
	Mesenteric	Control	−81 ± 1*	−49 ± 3*	−20 ± 3*	−12 ± 3*	−9 ± 3	−7 ± 3	−3 ± 3
		+ SQ 28,603	−79 ± 2*	−47 ± 5*	−15 ± 5*	−9 ± 4	−4 ± 5	−3 ± 4	−5 ± 6
	Hindquarters	Control	−15 ± 6	−20 ± 4*	−8 ± 7	−6 ± 3	−4 ± 4	−2 ± 4	−4 ± 2
		+ SQ 28,603	10 ± 6	−26 ± 8*	−14 ± 5*	−9 ± 4	−4 ± 5	−3 ± 4	−5 ± 6

Values are mean ± s.e.mean.
*$P < 0.05$ versus baseline.

scious normotensive rats in the present study. These results are consistent with those from previous investigations using SQ 28,603 (Seymour *et al.*, 1991) or other novel NEP inhibitors (Sybertz *et al.*, 1990), although only mean arterial blood pressure was measured in those experiments. However, it is clear that the dose of SQ 28,603 we used was exerting effects on NEP because the regional haemodynamic responses to exogenous ANP were significantly enhanced, in spite of the fact that clearance receptors for ANP have a particularly important influence on its pharmacokinetics (Almeida *et al.*, 1989; Chiu *et al.*, 1991).

Although ANP is an effective vasorelaxant *in vitro*, its hypotensive actions *in vivo* are more probably attributable to a reduction in cardiac output, since regional vasoconstrictions usually accompany the fall in mean arterial blood pressure (e.g. Lappe *et al.*, 1985; Hofbauer *et al.*, 1986; Gardiner *et al.*, 1988a,b; 1989a; Lappe, 1988). It has been suggested that the vasoconstrictor responses to ANP are reflex in origin, and are not seen with bolus injections (Lappe, 1988). However, we have found bolus injections of ANP can elicit regional vasoconstrictions (Gardiner *et al.*, 1988a,b), and there is evidence that factors other than reflex sympathetic effects may be involved in the vasoconstrictor responses to ANP *in vivo* (Allen, 1990; Barbee *et al.*, 1990; Shen *et al.*, 1990).

In the present work, bolus injection of ANP in conscious, Long Evans rats caused hypotension, tachycardia, renal and mesenteric vasoconstrictions and an initial hindquarters vasodilatation followed by a vasoconstriction, as observed previously (Gardiner *et al.*, 1988a). Except for the changes in hindquarters haemodynamics, all these effects of ANP were enhanced after SQ 28,603. However, the enhancement was due to a prolongation of responses, rather than to changes in the maximum responses (see also Seymour *et al.*, 1989). Thus, it is likely that the initial high plasma level of ANP achieved with bolus injection was unaffected by NEP inhibition with SQ 28,603, probably because the high capacity clearance receptors for ANP buffered the effects of inhibiting ANP hydrolysis (Almeida *et al.*, 1990; Chiu *et al.*, 1991). Similar peak plasma levels of ANP could account for the similar initial hindquarters hyperaemic vasodilator effects of ANP before and after SQ 28,603.

Under conditions in which we found SQ 28,603 caused significant prolongation of the effects of ANP we demonstrated that most of the responses to proendothelin-1 [1-38] were significantly attenuated. This latter finding is qualitatively similar to the effects obtained with phosphoramidon (Gardiner *et al.*, 1991), but those effects were seen at a 10 fold lower dose (5 mg kg^{-1}) than that of SQ 28,603 used in the present work, and were more pronounced. Thus, it is feasible that the conversion of proendothelin-1 [1-38] to endothelin-1 is brought about by an enzyme related to NEP that is less inhibited by SQ 28,603 than it is by phosphoramidon. This proposition is consistent with other findings showing that the effects of proendothelin-1 are inhibited less by thiorphan than by phosphoramidon, although both are inhibitors of NEP (McMahon *et al.*, 1991; Pollock & Opgenorth, 1991).

In order to demonstrate that the effects of SQ 28,603 were not due to a non-specific reduction in cardiovascular reactivity, we also assessed responses to endothelin-1, angiotensin I and angiotensin II before and after administering SQ 28,603. The lack of effect of SQ 28,603 on responses to endothelin-1 supports the suggestion that the diminution in the respones to proendothelin-1 [1-38] was due to inhibition of its conversion to endothelin-1. In addition, the failure of SQ 28,603 to affect responses to endothelin-1 might indicate that this drug does not inhibit the NEP that is involved in the degradation of endothelin-1 (Sokolovsky *et al.*, 1990; Vijayaraghavan *et al.*, 1990), but other experiments would need to be performed to cover that point.

We included angiotensin I and angiotensin II in the protocol of the second experiment in case SQ 28,603 suppressed

responses to the former by inhibiting angiotensin-converting enzyme. In the event, responses to both peptides were unchanged by SQ 28,603, providing additional evidence for the selectivity of its inhibitory action against the effects of proendothelin-1 [1-38].

It is notable that SQ 28,603 reduced the initial hindquarters vasodilator effects of proendothelin-1 [1-38] and abolished its tachycardic action. This finding is consistent with the NEP inhibitor suppressing the rapid production of endothelin-1 following the bolus injection of proendothelin-1 [1-38], because it is only when endothelin-1 levels rise rapidly that tachycardic and hindquarters vasodilator responses are seen (Gardiner *et al.*, 1989b; 1990a). Since endothelin-1 is a potent stimulus for ANP release (Fukuda *et al.*, 1988; Winquist *et al.*, 1989), and since the initial hindquarters vasodilator responses to bolus injections of ANP (Gardiner *et al.*, 1988a,b), endothelin-1 (Gardiner *et al.*, 1989b; 1990a) and proendothelin-1 [1-38] (this study) are similar, it could be argued that ANP mediates the initial responses to the latter two peptides. However, other evidence indicates that ANP is not likely to be the agent responsible for the early vasodilator effects of endothelin-1 or proendothelin-1 [1-38] (Gardiner *et al.*, 1990a; Fozard & Part, 1990; Ohlstein *et al.*, 1991).

The ability of SQ 28,603 to leave intact the bradycardic effects of proendothelin-1 [1-38], whilst inhibiting the pressor effects of this peptide, is interesting in the light of the fact that phosphoramidon can inhibit the bardycardic effects of proendothelin-1 [1-38] at a dose that has no significant influence on its pressor action (Gardiner *et al.*, 1991). These findings indicate that the bradycardic effects of proendothelin-1 [1-38] are not due simply to baroreflex mechanisms. As suggested previously (Gardiner *et al.*, 1991), it is feasible that local conversion of proendothelin-1 [1-38] to endothelin-1 contributes to its negative chronotropic effects. If this is the case it is possible that SQ 28,603 and phosphoramidon differ in their effects on the cardiac conversion of proendothelin-1 [1-38] to endothelin-1, with phosphoramidon being more potent in this respect also.

It appeared that SQ 28,603 caused similar, albeit modest, degrees of antagonism of the renal, mesenteric and hindquarters vasoconstrictor effects of proendothelin-1 [1-38]. This picture is quite different from that seen with phosphoramidon, which reduced the renal and hindquarters vasoconstrictor effects of the peptide more than it did the mesenteric vasoconstriction (Gardiner *et al.*, 1991). The present results with SQ 28,603 could be explained if this compound inhibited a NEP that was responsible for generating endothelin-1 from exogenous proendothelin-1 [1-38] at a site that resulted in systemic delivery of endothelin-1 to all vascular beds. Thus, for example, if SQ 28,603 antagonized, selectively, the generation of endothelin-1 from proendothelin-1 [1-38] in the lungs, due to suppression of NEP at this site (Seymour *et al.*, 1991), it could produce similar degrees of attenuation of the vasoconstrictor responses to exogenous proendothelin-1 [1-38], while leaving intact the vasoconstrictor responses due to local conversion of the peptide. At present it is not known if the local conversion of exogenous proendothelin-1 [1-38] to endothelin-1 is dependent on the same enzyme that is responsible for the conversion of endogenous proendothelin-1 [1-38] to endothelin-1. The latter appears to occur intracellularly (Sawamura *et al.*, 1991), whereas it is feasible that conversion of exogenous proendothelin-1 [1-38] to endothelin-1 occurs extracellularly.

In conclusion, the present work has shown that SQ 28,603 at a dose of 50 mg kg^{-1} attenuates, selectively, the haemodynamic responses to exogenous proendothelin-1 [1-38] whilst enhancing the effects of exogenous ANP. Although SQ 28,603 does not appear very potent in these respects, compared to phosphoramidon, it seems feasible that any haemodynamic effects it might have in the clinical setting could be due to inhibition of the production of endothelin-1 in addition to suppression of the degradation of ANP.

We are grateful to Squibb (U.S.A.) for the gift of SQ 28,603.

References

ALLEN, D.E. (1990). Effect of sympathectomy on renal and circulatory action of atrial natriuretic peptide. *Am. J. Physiol.*, **259**, R1274–R1280.

ALMEIDA, F.A., SUZUKI, M., SCARBOROUGH, R.M., LEWICKI, J.A. & MAACK, T. (1989). Clearance function of type C receptors of atrial natriuretic factor in rats. *Am. J. Physiol.*, **256**, R469–R475.

BARBEE, R.W., HARRISON-BERNARD, L., ZIMMERMAN, R.S., TRIPPODO, N.C. & FROHLICH, E.D. (1990). Sympathectomy fails to reveal prominent vasodilation by atrial natriuretic factor. *Hypertension*, **15**, 888–893.

CHIU, P.J.S., TETZLOFF, G., ROMANO, M.T., FOSTER, C.J. & SYBERTZ, E.J. (1991). Influence of C-ANF receptor and neutral endopeptidase on pharmacokinetics of ANF in rats. *Am. J. Physiol.*, **260**, R208–R216.

FOZARD, J.R. & PART, M.L. (1990). No major role for atrial natriuretic peptide in the vasodilator response to endothelin-1 in the spontaneously hypertensive rat. *Eur. J. Pharmacol.*, **180**, 153–159.

FUKUDA, Y., HIRATA, Y., YOSHIMI, H., KOJIMA, T., KOBAYASHI, Y., YANAGISAWA, M. & MASAKI, T. (1988). Endothelin is a potent secretagogue for atrial natriuretic peptide in cultured rat atrial myocytes. *Biochem. Biophys. Res. Commun.*, **155**, 167–172.

FUKURODA, T., NOGUSHI, K., TSUCHIDA, S., NISHIKIBE, M., IKEMOTO, F., OKADA, K. & YANO, M. (1990). Inhibition of biological actions of big endothelin-1 by phosphoramidon. *Biochem. Biophys. Res. Commun.*, **172**, 390–395.

GARDINER, S.M., COMPTON, A.M. & BENNETT, T. (1988a). Regional haemodynamic effects of depressor neuropeptides in conscious, unrestrained, Long Evans and Brattleboro rats. *Br. J. Pharmacol.*, **95**, 197–208.

GARDINER, S.M., COMPTON, A.M. & BENNETT, T. (1988b). Regional hemodynamic effects of atrial natriuretic peptide or captopril in Brattleboro rats. *Am. J. Physiol.*, **255**, R737–R743.

GARDINER, S.M., COMPTON, A.M. & BENNETT, T. (1989a). Regional hemodynamic effects of calcitonin gene-related peptide. *Am. J. Physiol.*, **256**, R332–R338.

GARDINER, S.M., COMPTON, A.M. & BENNETT, T. (1989b). Regional hemodynamic effects of endothelin-1 in conscious, unrestrained, Wistar rats. *J. Cardiovasc. Pharmacol.*, **13**, Suppl 5, S202–S204.

GARDINER, S.M., COMPTON, A.M. & BENNETT, T. (1990a). Regional haemodynamic effects of endothelin-1 and endothelin-3 in conscious Long Evans and Brattleboro rats. *Br. J. Pharmacol.*, **99**, 107–112.

GARDINER, S.M., COMPTON, A.M., BENNETT, T. & HARTLEY, C.J. (1990b). Can pulsed Doppler technique measure changes in aortic flow in conscious rats? *Am. J. Physiol.*, **259**, H448–H456.

GARDINER, S.M., COMPTON, A.M., KEMP, P.A. & BENNETT, T. (1990c). Regional and cardiac haemodynamic effects of N^G-nitro-L-arginine methyl ester in conscious, Long Evans rats. *Br. J. Pharmacol.*, **101**, 625–631.

GARDINER, S.M., COMPTON, A.M., KEMP, P.A. & BENNETT, T. (1990d). Regional and cardiac haemodynamic responses to glyceryl trinitrate, acetylcholine, bradykinin and endothelin-1 in conscious rats: effects of N^G-nitro-L-arginine methyl ester. *Br. J. Pharmacol.*, **101**, 632–649.

GARDINER, S.M., COMPTON, A.M., KEMP, P.A. & BENNETT, T. (1991). The effects of phosphoramidon on the regional haemodynamic responses to human proendothelin [1-38] in conscious rats. *Br. J. Pharmacol.*, **103**, 2009–2015.

GERBES, A.L. & VOLLMAR, A.M. (1990). Degradation and clearance of atrial natriuretic factors (ANF). *Life Sci.*, **47**, 1173–1180.

HAYWOOD, J.R., SHAFFER, R., FASTENOW, C., FINK, G.D. & BRODY, M.J. (1981). Regional blood flow measurement with pulsed Doppler flowmeter in conscious rat. *Am. J. Physiol.*, **241**, H273–H278.

HOFBAUER, K.G., CRISCIONE, L., SONNENBURG, C., MUIR, A. & MAH, S.C. (1986). Actue and chronic hemodynamic and natriuretic effects of atriopeptin II in conscious rats. *J. Hypertens.*, **4** (Suppl 2), S41–S47.

LAPPE, R.W. (1988). The *in vivo* vascular actions of atrial natriuretic factor. In *Advances in Atrial Peptide Research*. ed. Brenner, B.M. & Laragh, J.H. Vol II, pp. 91–100. New York: Raven Press.

LAPPE, R.W., SMITS, J.F.M., TODT, J.A., DEBETS, J.J.M. & WENDT, R.L. (1985). Failure of atriopeptin II to cause arterial vasodilation in the conscious rat. *Circ. Res.*, **56**, 606–612.

MATSUMURA, Y., HISAKI, K., TAKAOKA, M. & MORIMOTO, S. (1990). Phosphoramidon, a metalloprotease inhibitor, suppresses the hypertensive effect of big endothelin-1. *Eur. J. Pharmacol.*, **185**, 103–106.

MCMAHON, E.G., PALOMO, M.A., MOORE, W.M., MCDONALD, J.F. & STERN, M.K. (1991). Phosphoramidon blocks the pressor activity of porcine big endothelin-1-[1-39] *in vivo* and conversion of big endothelin-1-[1-39] to endothelin-1-[1-21] *in vitro*. *Proc. Natl. Acad. Sci. U.S.A.*, **88**, 703–707.

OHLSTEIN, E.H., VICKERY, L., SAUERMELCH, C. & WILLETTE, R.N. (1990). Vasodilation induced by endothelin: role of EDRF and prostanoids in rat hindquarters. *Am. J. Physiol.*, **259**, H1835–H1841.

POLLOCK, D.M. & OPGENORTH, T.J. (1991). Evidence for metalloprotease involvement in the *in vivo* effects of big endothelin 1. *Am. J. Physiol.*, **261**, R257–R263.

SAWAMURA, T., KASUYA, Y., MATSUSHITA, Y., SUZUKI, N., SHINMI, O., KISHI, N., SUGITA, Y., YANAGISAWA, M., GOTO, K., MASAKI, T. & KIMURA, S. (1991). Phosphoramidon inhibits the intracellular conversion of big endothelin-1 to endothelin-1 in cultured endothelial cells. *Biochem. Biophys. Res. Commun.*, **174**, 779–784.

SEYMOUR, A.A., NORMAN, J.A., ASAAD, M.M., FENNELL, S.A., LITTLE, D.K., KRATUNIS, V.J. & ROGERS, W.L. (1991). Antihypertensive and renal activity of SQ 28,603, an inhibitor of neutral endopeptidase. *J. Cardiovasc. Pharmacol.*, **17**, 296–304.

SEYMOUR, A.A., SWERDEL, J.N., FENNELL, S.A., DRUCKMAN, S.P., NEUBECK, R. & DELANEY, N.G. (1989). Potentiation of the depressor responses to atrial natriuretic peptides in conscious SHR by an inhibitor of neutral endopeptidase. *J. Cardiovasc. Pharmacol.*, **14**, 194–204.

SHEN, Y.-T., YOUNG, M.A., OHANIAN, J., GRAHAM, R.M. & VATNER, S.F. (1990). Atrial natriuretic factor-induced systemic vasoconstriction in conscious dogs, rats and monkeys. *Circ. Res.*, **66**, 647–661.

SOKOLOVSKY, M., GALRON, R., KLOOG, Y., BDOLAH, A., INDIG, F.E., BLUMBERG, S. & FLEMINGER, G. (1990). Endothelins are more sensitive than sarafotoxins to neutral endopeptidase: possible physiological significance. *Proc. Natl. Acad. Sci. U.S.A.*, **87**, 4702–4706.

SYBERTZ, E.J., CHIU, P.S., WATKINS, R.W. & VEMULAPALLI, S. (1990). Neutral metalloendopeptidase inhibition: a novel means of circulatory modulation. *J. Hypertens.*, **8**, Suppl. 7, S161–S167.

THEODORSSON-NORHEIM, E. (1987). Friedman and Quade tests: BASIC computer program to perform non-parametric two-way analysis of variance and multiple comparisons on ranks of several related samples. *Comput. Biol. Med.*, **17**, 85–99.

VIJAYARAGHAVAN, J., SCICLI, A.G., CARRETERO, O.A., SLAUGHTER, C., MOOMAW, C. & HERSH, L.B. (1990). The hydrolysis of endothelins by neutral endopeptidase 24.11 (enkephalinase). *J. Biol. Chem.*, **265**, 14150–14155.

WINQUIST, R.J., SCOTT, A.L. & VIASUK, G.P. (1989). Enhanced release of atrial natriuretic factor by endothelin in atria from hypertensive rats. *Hypertension*, **14**, 111–114.

(Received May 21, 1991
Revised December 16, 1991
Accepted January 15, 1992)

Br. J. Pharmacol. (1992), **106**, 187–195 © Macmillan Press Ltd, 1992

Haemodynamic and abdominal motor reflexes elicited by neurotensin in anaesthetized guinea-pigs

[1]Francis Rioux & Margot Lemieux

Centre de Recherche de l'Université Laval, Hôtel-Dieu de Québec, 11 Côte du Palais, Québec G1R 2J6, Canada

1 Single intraperitoneal (i.p.) injections of neurotensin (NT) (0.14– 140 nmol kg^{-1}) in anaesthetized guinea-pigs were found to trigger transient abdominal wall contractions (TAWC) accompanied by relatively sustained increases of systemic blood pressure (BP) and heart rate (HR). The modification of the latter NT effects by various drugs and surgical manipulations was examined to obtain some insight into the nature of, and possible relationship between, these responses.

2 The abdominal motor response (i.e. TAWC) to i.p. NT (14 nmol kg^{-1}) was inhibited by prior i.v. injection of the guinea-pigs with pancuronium (0.27 μmol kg^{-1}), morphine (1.5 and 15 μmol kg^{-1}), clonidine (0.34 μmol kg^{-1}), by concomitant i.p. injection of procaine 2% w/v, or by acute spinalization. It was potentiated by naloxone (2.8 and 28 μmol kg^{-1}), but not affected by i.v. injection of autonomic drugs (i.e. pentolinium, prazosin, yohimbine and atropine), by capsaicin desensitization, or by acute bilateral cervical vagotomy. In spinalized animals a sustained abdominal wall contraction (SAWC) was unmasked, which was resistant to i.v. morphine, clonidine or baclofen but suppressed by i.v. pancuronium or i.p. lignocaine 2% w/v.

3 Haemodynamic responses to i.p. NT were not affected by i.v. pancuronium, morphine, naloxone, atropine, or by vagotomy. They were inhibited by i.v. pentolinium or clonidine (BP, HR), i.v. prazosin (BP), i.p. procaine 2% w/v (BP, HR), capsaicin desensitization or acute spinalization (BP, HR). Yohimbine (i.v.) potentiated BP and HR increases caused by i.p. NT.

4 These results suggest that: (1) the haemodynamic and TAWC responses to i.p. NT in this animal model, are two independent, neurally-mediated reflexes which are likely to originate from the abdominal cavity and require a functionally intact spinal cord for their full expression; (2) the neural pathways subserving both types of responses appear to be different from each other. The nature and time-response characteristics of the reflexes caused by i.p. NT, raise the possibility that i.p. NT is a noxious stimulus, at least in guinea-pigs.

Keywords: Neurotensin; abdominal muscle; motor reflexes; haemodynamic effects

Introduction

Intraperitoneal (i.p.) injection of a low volume (i.e. 0.3 ml) of saline (i.e. 0.9% w/v NaCl), added with increasing amounts of neurotensin (NT), in the anaesthetized guinea-pigs with the abdomen opened, was previously shown to cause dose-dependent increases of systemic blood pressure (BP) and heart rate (HR) (Rioux *et al.*, 1989). Similar haemodynamic effects were also elicited by topical application of minute volumes (i.e. 10 to 20 μl) of NT solution to discrete areas of the visceral peritoneum of various organs (e.g. stomach, ileum, liver). Detailed pharmacological analysis led these authors to propose that NT, directly and/or indirectly, activates abdominal visceral afferents scattered in the peritoneum, and secondarily triggers sympathetically-mediated increases of BP and HR (Rioux *et al.*, 1989). More recently, using guinea-pigs with closed-abdomen rather than opened-abdomen and commercial, isotonic peritoneal dialysis solutions instead of saline as NT vehicle for i.p. injection, the same team showed that the amplitude of the increases of BP and HR caused by single i.p. injection of NT solution is directly related to NT concentrations, whereas the duration of both effects tended to increase with the volume of NT solution used (Rioux *et al.*, 1990a). The abdominal visceral afferents believed to be the target site of action of i.p. NT in guinea-pigs were tentatively identified as capsaicin-sensitive (i.e. small diameter, tachykinins-containing afferents) (Buck & Burks, 1986), based on the blockade of i.p. NT-induced haemodynamic effects by pretreatment of the animals with capsaicin (Rioux *et al.*, 1990a). Besides causing pressor effects and tachycardia, i.p. injection of NT in the anaesthetized guinea-pig with opened-abdomen was also claimed (i.e. based on visual observation) to induce transient, clonic-like movements of the trunk sometimes associated with partial expulsion of intestinal loops out of the abdomen (Rioux *et al.*, 1989). In anaesthetized, closed-abdomen guinea-pigs the latter motor effects of i.p. NT were also observed, although in this condition, they were clearly seen as transient abdominal wall contractions (Rioux *et al.*, 1990a).

In the present study we examined the effect of various drugs (e.g. opioids, autonomic blockers, capsaicin and others) and surgical manipulations (i.e. vagotomy, spinalization) on both the abdominal motor and cardiovascular responses to i.p. NT in anaesthetized guinea-pigs. The main objective of the study was to obtain some insight into the nature of this motor response and examine the potential relationship between the haemodynamic and abdominal motor responses to i.p. NT.

Methods

General procedures

All experiments were done on female Albino guinea-pigs (325–375 g) purchased from Charles River Canada Inc., St-Constant, Québec, Canada. The animals were housed 4–6 per cage, given guinea-pig purina chow and tap water *ad libitum*, and kept under stable environmental conditions for a few days before use.

[1] Author for correspondence.

The animals were anaesthetized with sodium pentobarbitone (0.22 mmol kg^{-1}, i.p.), tracheotomized and artificially ventilated at a constant rate of 50 strokes min^{-1} (2.8–3 ml stroke) with ambient air from rodent ventilators (New England Medical Instr., Inc.). A polyethylene catheter (PE 50) filled with saline was introduced into the left jugular vein for intravenous (i.v.) drug injection. A second catheter filled with sodium heparin (200 u ml^{-1} of saline) was inserted into the right carotid artery for direct BP recording. BP was measured with arterial pressure transducers (Spectramed P 23 XL) connected to a Grass polygraph (Model 79). HR was derived from the BP signal. Body temperature was monitored with a rectal thermoprobe coupled to a telethermometer (Yellow Spring Instr.) and kept constant at 38.0–39.0°C with a lamp (100 W) hung over the animal. A third catheter (PE 90) was introduced into the urinary bladder (via the urethra) to prevent overdistension of the bladder and ease micturition. A fourth catheter (PE 190) was implanted in the peritoneal cavity for i.p. injection of NT or its solvent as described previously (Rioux *et al.*, 1990a). A thread was attached to the skin of the animal right lower abdominal quadrant (i.e. inguinal region) and linked almost vertically, under a resting tension of 2.5–3 g, to a force displacement transducer (Grass F 103) coupled to a Grass polygraph (Model 79), to monitor the changes of basal abdominal wall tension (AWT) (i.e. an index of abdominal muscle tension), and the number of transient (i.e. ~100–300 ms duration) (twitch-like) abdominal wall contraction (TAWC) induced by i.p. injection of NT. Both animal hindlimbs were secured to the bench with tape to prevent lateral displacement of the animal body during volleys of TAWC caused by i.p. NT. Additional doses of anaesthetic were given intravenously to animals during preparatory procedures only (total doses: 0.1–0.12 mmol kg^{-1}, i.v.) to stabilize the anaesthesia level (as judged by suppression of corneal reflexes and stability of BP recording). The time interval between the last dose of anaesthetic and testing of NT effects was set at 40–45 min throughout the study.

Dose-response curves and kinetics

Once the preparation of animals was over and all parameters stabilized, each animal was given a single i.p. injection of 0.14, 1.4, 14 or 140 nmol kg^{-1} of NT (each dose in a volume of 9 ml) or of an equal volume of NT solvent (i.e. PDS). Each solution was pre-warmed at 38°C before injection. Twelve (12) s were needed to complete an i.p. injection. The basal mean arterial pressure (MAP) (i.e. MAP = diastolic pressure + 1/3 pulse pressure), heart rate (HR) and abdominal wall tension (AWT) were measured before (i.e. 30–60 s) and at different times (i.e. 10, 20, 30, 60 s, 2, 5, 10, 15 min) after i.p. injection of NT or its solvent. Changes (Δ) of MAP, HR, or AWT caused by i.p. injection of NT or its solvent were used to build dose-response curves (MAP, HR) and/or describe kinetics (MAP, HR, AWT) of NT effects. Other parameters measured were, the number of animals showing TAWC (n_1), and the number of TAWC per animal (TAWC/animal), caused by i.p. injection of NT or its solvent, over a 15 min post-i.p. injection period. These parameters were easily obtained from AWT tracings (Figure 2). The percentage of animals exhibiting TAWC and TAWC/animal values were used for describing dose- or time-response relationships. In parallel studies the animals were challenged with i.p. injection of either bradykinin (BK) or substance P (SP) (14, 140 or 1400 nmol kg^{-1}) (each dose given in a volume of 9 ml), to assess the response selectivity of the experimental animal model.

Animal pretreatment with selected drugs

A first series of experiments was conducted with animals pretreated with various doses of morphine, a potent analgesic drug known to suppress various nociceptive reflexes (Jaffe & Martin, 1990) or of naloxone, an opioid receptor antagonist known to potentiate various reflexes (Duggan, 1983). A second series of experiments involved animal pretreatment with various drugs known to interfere with adrenergic and/or cholinergic neural pathways, such as pentolinium (nicotinic receptor antagonist and ganglion blocker), prazosin (α-adrenoceptor antagonist), clonidine (α_2-adrenoceptor agonist, and centrally and peripherally acting sympatholytic), yohimbine (α_2-adrenoceptor antagonist), atropine (muscarinic receptor blocker), and pancuronium (nicotinic receptor antagonist and neuromuscular blocker). All drugs were given by i.v. bolus injection 30 min before single i.p. injection of NT (14 nmol kg^{-1}). Only one type of drug and one drug dose were tested per animal. The volume of each injection was 0.1–0.2 ml, followed by 0.2 ml of saline, to rinse the catheter. Each experimental series had its own control group (i.e. animals given i.v. bolus injection of drug solvent). All these studies involved comparing, ΔMAP, ΔHR, n_1 and TAWC/animal values in control animals (i.e. drug solvent-pretreated animals) with those measured in drug-pretreated animals.

Intraperitoneal injection of a local anaesthetic

The experiments involved comparing ΔMAP, ΔHR, n_1 and TAWC/animal values measured in animals given single i.p. injection of NT (14 nmol kg^{-1}) plus procaine solvent (i.e. 0.5 ml of PDS) (control) (total volume injected: 9 ml), to those measured in animals given single i.p. injection of NT (as above) plus procaine 2% w/v. Parallel experiments involved measurement and comparison of peak pressor and tachycardic responses to i.v. bolus injection of dimethylphenylpiperazinium (DMPP) (310 nmol kg^{-1}), a ganglion stimulant, in animals first given (i.e. 2 min before) either i.p. procaine 2% w/v (as above) or i.p. procaine solvent.

Capsaicin treatment

Experimental animals were given s.c. injection of capsaicin suspension (0.08 mmol kg^{-1}, once a day for two consecutive days). All treatments were done under anaesthesia with a mixture of ketamine (0.16 mmol kg^{-1}) and xylazine (0.02 mmol kg^{-1}) given intramuscularly (i.m.). All animals were given prophylactic doses of salbutamol (210 nmol kg^{-1}, s.c. and aminophylline (0.06 mmol kg^{-1}, i.p.) 15 min before capsaicin, to prevent respiratory distress due to capsaicin-induced bronchospasms (Lundberg *et al.*, 1985). Control animals received similar amounts of capsaicin solvent (i.e. 0.4 ml of a mixture of ethanol 10% w/v, Tween 80 10% v/v and saline), and the same drug treatments (i.e. anaesthetics, bronchodilators) as experimental animals, except that no capsaicin was given. ΔMAP, ΔHR, n_1 and TAWC/animal following i.p. injection of NT were then measured in both animal groups and compared.

Vagotomy and spinalization

Acute bilateral vagotomy (at the cervical level) or complete transection of the spinal cord (between C2 and C3) (i.e. spinalization) were performed under anaesthesia according to procedures recently described (Beauchamp *et al.*, 1991). Control animals were sham-operated (i.e. exposed to the same surgical procedures except for the vagotomy or spinalization). These surgical interventions were made 45–50 min before i.p. injection of NT (14 nmol kg^{-1}) or its solvent. ΔMAP, ΔHR, n_1 and TAWC/animal values following i.p. injection of NT were then measured in both animal groups and compared to those measured in their respective controls. Additional experiments were done with spinalized guinea-pigs which, 30 min before being challenged with i.p. NT (14 nmol kg^{-1}), were given i.v. bolus injection of saline (control) or of one of the following drugs (doses in μmol kg^{-1}): pancuronium (0.27), morphine (15.0), clonidine (0.34) or baclofen (10.0). Other experiments in this series involved pre-addition

of procaine or lignocaine 2% w/v to NT solution before i.p. injection in spinalized guinea-pigs. The purpose of the latter experiments was to define better the mechanism of the relatively more sustained abdominal wall contraction observed in spinalized guinea-pigs (Figure 3) given i.p. injection of NT. Finally peak changes of MAP or HR caused by i.v. bolus injection of either noradrenaline, DMPP or pentolinium were compared in spinalized guinea-pigs and sham-operated animals to rule out any non-specific effect of spinalization on the cardiovascular or sympathetic nervous system.

Drugs, solutions and statistics

Drugs used in this study were: neurotensin triacetate (NT) (Peninsula), capsaicin, (−)-noradrenaline. HCl (NA), pentolinium tartrate, sodium heparin, procaine HCl, dimethylphenylpiperazinium iodide (DMPP), atropine methylnitrate, yohimbine HCl (all from Sigma), morphine sulphate and sodium pentobarbitone (Sabex Inc.), naloxone HCl (Endo Lab. Inc.), clonidine HCl (Boehringer), prazosin HCl (Pfizer), lignocaine HCl (Xylocard) (Astra), ketamine HCl (Rogar/STB. Inc.), xylazine (Rompun) (Bayvet), theophylline (Aminophylline) (Abbot), baclofen (lioresal) (Ciba), and salbutamol sulphate (Allen & Hanburys). Most drugs were dissolved in saline or distilled water, except for capsaicin which was dissolved in absolute ethanol. Drug solutions were made fresh daily. Drug dilutions for i.v. injections were made in saline. Drug dilutions for i.p. injections were made in commercial, sterile, isotonic peritoneal dialysis solution (PDS) (Dianeal PD 101 CAPD PDS with 0.5% dextrose) (Baxter), the composition of which was (in mM): dextrose 28.0, Na^+ 132.0, Ca^{2+} 1.62, Mg^{2+} 0.75, Cl^- 101.7, lactate 35.0. KCl (4 mM) was added to PDS solution. The pH and osmolality of PDS were 5.2 and 306 mOs l^{-1}, respectively. Solutions of NA were acidified to pH 4.0 with HCl and added with ascorbic acid (0.5 mM) to prevent oxidation. Drug doses are given in nano-, micro-, or millimol of the salt per kg of the animal body weight, except for local anaesthetics (in %).

Statistical significances of results were determined by one-way analysis of variance (ANOVA) followed by the Dunnett's test, or by the Chi-square test or Student's *t* test for unpaired data (Tallarida & Murray, 1981). *P* values of 0.05 or less were considered significant.

Results

Dose-response curves and time courses of neurotensin effects

Single i.p. injection of 9 ml of PDS (i.e. NT solvent) in anaesthetized guinea-pigs, caused no significant changes of mean arterial pressure (MAP) or heart rate (HR), and no transient abdominal wall contraction (TAWC). However it evoked a sudden, persistent decrease of basal abdominal wall tension (AWT) (an artefactual consequence of abdominal distension caused by i.p. injection of 9 ml of fluid, in this case of PDS). On the other hand, single i.p. injection of NT (0.14, 1.4, 14 or 140 nmol kg^{-1}) (each dose given in a volume of 9 ml) elicited dose-dependent increases of MAP, HR, number of animals showing TAWC, and number of TAWC/animal. These results are shown in Figure 1. A typical tracing illustrating the changes of BP or AWT, and the occurrence of TAWC following single i.p. injection of NT (14 nmol kg^{-1}), is illustrated in Figure 2. Data describing the time sequence of cardiovascular and abdominal motor responses to i.p. injection of NT (14 nmol kg^{-1}) are presented in Table 1. Note the rapid onset (i.e. <10 s) and short times to peak effect for all the measured parameters. The basal AWT decreased to the same extent, although at a slightly lower rate in animals given i.p. injection of NT than in animals given the NT solvent. Eight (8) out of 8 animals (100%)

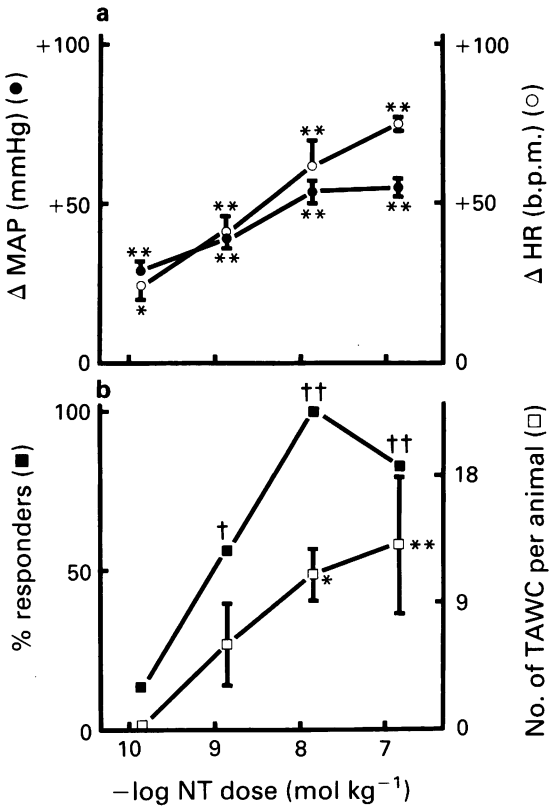

Figure 1 (a) Dose-response curves of pressor and tachycardic responses to single intraperitoneal (i.p.) injection of neurotensin (NT, 0.14, 1.4, 14 and 140 × 10^{-9} mol kg^{-1}, $n = 8$, 7, 8 and 6, respectively), in anaesthetized guinea-pigs. Ordinates: peak increases (+) (irrespective of time to peak) of basal mean arterial pressure (ΔMAP) (●) or heart rate (ΔHR) (○). Abcissae: −log NT dose. mmHg, millimeters of mercury; b.p.m., heart beat min^{-1}. Points are mean values with s.e.mean shown by vertical bars. (b) Dose-response curves showing the percentage (%) of animals exhibiting transient abdominal wall contraction (TAWC) (% responders) (■) or number of TAWC/animal (□), following single i.p. injection of NT in anaesthetized guinea-pigs (same animals as above). Ordinates: % responders or number of TAWC/animal; abcissae: −log NT dose. (■) % of responders; (□) number of TAWC per animal; mean values ± s.e.mean.
*$P<0.05$; **$P<0.01$ when compared to control values (i.e. values measured in animals given single i.p. injection of NT solvent) (Dunnett's test)
†$P<0.05$; ††$P<0.005$ when compared to control values (Chi-square test)

challenged with i.p. injection of 14 nmol kg^{-1} of NT exhibited TAWC. ΔTAWC/animal became significant 60 s post-i.p. injection of the latter NT dose.

Single i.p. injection of bradykinin (BK) (14, 140 or 1400 nmol kg^{-1}), in anaesthetized guinea-pigs, elicited significant pressor effects (peak ΔMAP values: + 14.3 ± 4.1, + 13.2 ± 5.0, + 30.5 ± 4.0 mmHg, $n = 6$, 6 or 8, respectively), but only modest, variable levels of tachycardia (peak ΔHR values: + 10 ± 3, + 7 ± 5, + 21 ± 6 b.p.m.). TAWC were seen only in 1 out of 20 animals given i.p. injection of BK. Single i.p. injection of substance P (SP) (same dose as for BK) elicited slight decreases of MAP (peak ΔMAP values − 3.3 ± 1.1, − 8.3 ± 1.7, − 11.5 ± 1.6 mmHg, $n = 6$, 6 and 6, respectively) and HR (peak ΔHR values: − 7 ± 2, − 8 ± 4, − 13 ± 3 b.p.m.), but no TAWC was seen in any of these animals.

Effects of morphine and naloxone

The pressor and tachycardic responses to single i.p. injection of 14 nmol kg^{-1} of NT were not affected by prior animal

treatment with i.v. bolus injection of 1.5 or 15.0 μmol kg^{-1} (i.e. 1 and 10 mg kg^{-1}) of morphine. On the other hand, the number of animals exhibiting TAWC (n_1) and the number of TAWC/animal, following i.p. NT, were markedly reduced by morphine. These results are summarized in Table 2. A lower dose of morphine (i.e. 0.15 μmol kg^{-1}) was not effective in reducing the abdominal motor response to i.p. NT ($n = 8$, data not shown). Animal pretreatment with i.v. bolus injection of 2.8 or 28.0 μmol kg^{-1} (i.e. 1 and 10 mg kg^{-1}) of naloxone, was found to markedly increase n_1 and TAWC/animal values, without altering the pressor and tachycardic responses to i.p. NT (Table 2). A lower dose of naloxone (i.e. 0.28 μmol kg^{-1}) did not modify the abdominal motor responses to i.p. NT ($n = 8$, data not shown). Combined i.v. administration of morphine (15 μmol kg^{-1}) and naloxone (28.0 μmol kg^{-1}) gave results suggesting inhibition of the morphine suppressive effect on abdominal motor responses by naloxone (Table 2).

Animal pretreatment with i.v. bolus injection of naloxone (2.8 μmol kg^{-1}) tended to increase the abdominal motor response to a single i.p. injection of a low NT dose (0.14 nmol kg^{-1}). In control (naloxone-free) animals, 1 out of 8 animals exhibited TAWC, whereas 3 out of 8 animals pretreated with naloxone, exhibited TAWC (TAWC/animal = 0.1 ± 0.1 in control animals and 17 ± 9 in naloxone-pretreated animals).

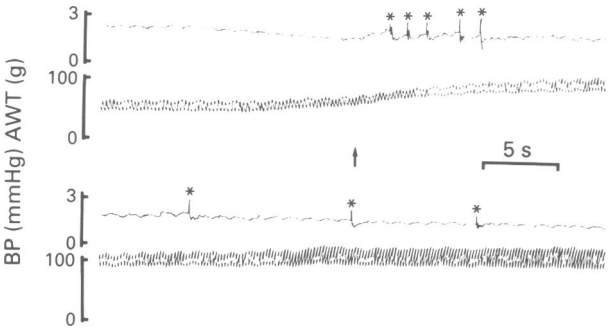

Figure 2 Typical tracing showing the time course of changes of basal abdominal wall tension (AWT) (1st tracing from the top) and systemic blood pressure (BP) (2nd tracing from the top) in anaesthetized guinea-pigs following single i.p. injection of neurotensin (NT) (14 nmol kg^{-1}). The 3rd and 4th tracing (from the top) are continuations of 1st and 2nd tracings, respectively. The arrow indicates the end of i.p. injection of NT. Note the rapid onset of the pressor effect and occurrence of transient abdominal wall contractions (TAWC) (*) at different times after i.p. injection of NT. The slight, gradual decrease of AWT during filling of the peritoneal cavity is mainly an artefact reflecting fluid-induced distension of the abdomen. Small waves 'contaminating' AWT tracings are due to animal respiratory (i.e. diaphragm) movements. mmHg: millimeters of mercury; g, grams.

Effect of drugs interfering with cholinergic and/or adrenergic mechanisms

The results of these experiments are compiled in Table 3. Animals pretreatment with i.v. bolus injection of either pentolinium, prazosin or clonidine reduced the pressor effect elicited by i.p. injection of NT (14 nmol kg^{-1}). Pentolinium and clonidine also inhibited the tachycardic responses to i.p. NT. Of the latter 3 drugs, only clonidine was able to inhibit to some extent the abdominal motor responses to i.p. NT. The pressor and tachycardic responses to i.p. NT were increased in animals pretreated with yohimbine, but the latter drug did not affect the abdominal motor response to i.p. NT. Animal pretreatment with atropine did not affect pressor, tachycardic and abdominal motor responses to i.p. NT, whereas pancuronium completely suppressed the abdominal motor responses, without affecting the cardiovascular responses, to i.p. NT. The suppressive effect of clonidine (0.34 μmol kg^{-1}) on abdominal motor and cardiovascular responses to i.p. NT was reversed in animals given yohimbine (5.1 μmol kg^{-1}) simultaneously with clonidine.

Effects of procaine, vagotomy, capsaicin or spinalization

The results of these 4 series of experiments are shown in Table 4. The pressor, tachycardic and abdominal motor (i.e. TAWC) responses to single i.p. injection of (14 nmol kg^{-1}) were reduced (pressor) or abolished (tachycardic, TAWC), when NT solution was pre-mixed with procaine 2% w/v. On the other hand, peak pressor and tachycardic responses to i.v. bolus injection of DMPP (310 nmol kg^{-1}) in 4 animals first given (i.e. 2 min before) i.p. injection of 9 ml of procaine 2% w/v (ΔMAP and ΔHR values: +34.7 ± 3.3 mmHg and +45 ± 12 b.p.m., respectively), were similar to those measured in 4 animals first given i.p. injection of 9 ml of procaine solvent (i.e. PDS) (ΔMAP and ΔHR values: +29.0 ± 3.8 mmHg and +40 ± 8 b.p.m., respectively).

The pressor, tachycardic and TAWC responses to i.p. NT were of similar amplitude in vagotomized animals as in their controls. Animals pretreated 4 to 5 days previously with capsaicin (see Methods) exhibited reduced cardiovascular

Table 1 Time-related changes (Δ) of MAP, HR, AWT and TAWC/animal associated with i.p. injection of neurotensin (NT) in anaesthetized guinea-pigs[a]

Time after i.p. injection	*ΔMAP* (mmHg)	*ΔHR* (b.p.m.)	*ΔAWT* (g)	*ΔTAWC/animal*
0	0	0	0	0
10 s	+22.1 ± 4.9¶	+12 ± 6†	−0.6 ± 0.2†	+3 ± 2
20 s	+30.4 ± 4.2**	+21 ± 7§	−0.6 ± 0.2*	+2 ± 1
30 s	+32.7 ± 4.7**	+25 ± 8§	−1.0 ± 0.1	+2 ± 1
60 s	+46.0 ± 4.9**	+40 ± 10**	−1.2 ± 0.1	+3 ± 1†
2 min	+52.9 ± 3.9**	+49 ± 7**	−1.0 ± 0.1	+2 ± 1
5 min	+40.2 ± 4.1**	+56 ± 10**	−0.9 ± 0.1	0
10 min	+32.4 ± 3.3**	+54 ± 10**	−0.8 ± 0.1	0
15 min	+28.6 ± 3.3**	+54 ± 9**	−0.8 ± 0.2	0
ANOVA	$P<0.01$	$P<0.01$	$P<0.01$	$P<0.05$

[a]Each animal was given a single intraperitoneal (i.p.) injection of NT (14 nmol kg^{-1}) (volume of NT solution injected = 9 ml). ΔMAP, ΔHR, ΔAWT and ΔTAWC/animal indicate increases (+) or decreases (−) of basal mean arterial pressure (MAP), heart rate (HR), abdominal wall tension (AWT) and in the number of abdominal wall contractions per animal (TAWC/animal) respectively, as measured in 8 anaesthetized guinea-pigs at different times after i.p. injection of NT. Results are expressed as mean ± s.e.mean. mmHg, millimeter of mercury; b.p.m., heart beats min^{-1}; g, grams. Basal values of MAP, HR, AWT and TAWC/animal (i.e. before i.p. injection) were respectively 39.9 ± 1.8 mmHg, 254 ± 7 b.p.m., 2.4 ± 0.2 g and 0.
*$P<0.05$; †$P<0.02$; §$P<0.01$; ¶$P<0.005$; **$P<0.001$ when compared to corresponding control values (i.e. values measured in animals given single i.p. injection of 9 ml of NT solvent) (Student's t test)

Table 2 Effect of morphine and naloxone on pressor, tachycardic and abdominal motor responses to single i.p. injection of neurotensin (NT) in anaesthetized guinea-pigs[a]

Treatment (μmol kg^{-1})	n	*MAP* (mmHg)	*ΔMAP* (mmHg)	*HR* (b.p.m.)	*ΔHR* (b.p.m.)	n_1	*TAWC/animal*
Control	8	39.9 ± 1.8	+53.2 ± 4.1	254 ± 7	+61 ± 9	8	11 ± 2
Morphine (1.5)	6	39.5 ± 1.5	+58.5 ± 4.5	268 ± 10	+42 ± 8	2†	0.3 ± 0.2*
Morphine (15.0)	10	33.3 ± 1.1*	+57.1 ± 3.5	237 ± 6	+61 ± 8	0††	0*
Naloxone (2.8)	6	38.2 ± 3.3	+51.7 ± 2.8	252 ± 5	+62 ± 10	6	43 ± 3¶
Naloxone (28.0)	8	39.5 ± 2.0	+56.4 ± 4.0	251 ± 4	+64 ± 8	8	53 ± 4¶
Morphine (15.0) + naloxone (28.0)	6	33.5 ± 1.0	+56.2 ± 2.4	237 ± 4	+60 ± 4	6§	27 ± 5¶§
ANOVA		$P<0.05$	NS	$P<0.05$	NS		$P<0.01$

[a]Animals were given single i.v. bolus injection of either saline (drug vehicle, control), morphine or naloxone 30 min before being given single i.p. injection of NT (14 nmol kg^{-1}). Results are expressed as mean ± s.e.mean. *n*, number of animals tested. MAP, basal mean arterial pressure (i.e. before i.p. injection of NT); HR, basal heart rate. ΔMAP and ΔHR indicate peak increases (+) of MAP or HR (irrespective of time to peak) over the 15 min period which follows i.p. injection of NT. mmHg, millimeters of mercury; b.p.m. heart beat per min. n_1, number of animals exhibiting transient abdominal wall contraction (TAWC) during the 15 min period of observation after i.p. injection of NT. TAWC/animal, number of TAWC per animal. NS, not statistically significant.
*$P<0.05$; ¶$P<0.01$ when compared to the control value (Dunnett's test)
†$P<0.01$; ††$P<0.005$ when compared to the control value (Chi-square test)
§$P<0.01$ when compared to the values measured in animals pretreated with morphine (15 μmol kg^{-1}) alone (Student's *t* test or Chi-square test)

Table 3 Effect of various drugs on pressor tachycardic and abdominal motor responses to single i.p. injection of neurotensin (NT) in anaesthetized guinea-pigs[a]

Treatment (μmol kg^{-1})	n	*MAP* (mmHg)	*ΔMAP* (mmHg)	*HR* (b.p.m.)	*ΔHR* (b.p.m.)	n_1	*TAWC/animal*
Control	8	35.5 ± 1.5	+47.2 ± 1.9	250 ± 4	+49 ± 5	8	11 ± 2
Pentolinuim (2.8)	8	27.4 ± 1.4*	+17.8 ± 1.7†	229 ± 6	+19 ± 4*	6	9 ± 3
Prazosin (1.9)	6	31.7 ± 1.7	+14.5 ± 2.7†	263 ± 6	+68 ± 12	5	15 ± 5
Clonidine (0.34)	8	39.0 ± 1.6	+1.6 ± 1.8†	215 ± 6†	+7 ± 5†	2§§	3 ± 3
Yohimbine (5.1)	11	38.2 ± 1.6	+66.1 ± 3.2†	259 ± 9	+93 ± 10†	9	15 ± 3
Atropine (4.1)	6	35.7 ± 2.4	+54.0 ± 4.4	245 ± 8	+68 ± 3	5	11 ± 3
Pancuronium (0.27)	5	38.6 ± 2.7	+51.2 ± 4.8	266 ± 7	+64 ± 8	0§§	0
Clonidine (0.34) + yohimbine (5.1)	8	31.0 ± 3.3	+53.8 ± 4.0§	211 ± 3†	+80 ± 11*§	6¶	10 ± 2
ANOVA		$P<0.01$	$P<0.01$	$P<0.01$	$P<0.01$		$P<0.05$

[a]Animals were given single i.v. bolus injection of saline (drug vehicle, control) or of one of the drugs listed above, 30 min before being given single i.p. injection of 14 nmol kg^{-1} of NT. Results are expressed as mean ± s.e.mean. *n*, number of animals tested. MAP, basal mean arterial pressure (i.e. before i.p. injection of NT); HR, basal heart rate. ΔMAP and ΔHR indicate peak increases (+) of MAP or HR (irrespective of time to peak) over the 15 min period which follows i.p. injection of NT. mmHg, millimeters of mercury; b.p.m., heart beat per min. n_1, number of animals exhibiting transient abdominal wall contraction (TAWC) during the 15 min period of observation after i.p. injection of NT. TAWC/animal indicates the number of TAWC per animal.
*$P<0.05$; †$P<0.01$ when compared to respective control value (Dunnett's test)
§$P<0.001$ when compared to corresponding values of clonidine-pretreated animals (Student's *t* test)
§§$P<0.005$ when compared to the control value (i.e. saline-pretreated animals) (Chi-square test)
¶$P<0.05$ when compared to corresponding values of clonidine-pretreated animals (Chi-square test)

Table 4 Effect of various drug treatments or surgical interventions on pressor, tachycardic and abdominal motor responses to single i.p. injection of neurotensin (NT) in anaesthetized guinea-pigs[a]

Exp. No.	*Treatment*	*n*	*MAP* (mmHg)	*ΔMAP* (mmHg)	*HR* (b.p.m.)	*ΔHR* (b.p.m.)	n_1	*TAWC/animal*
1	Control	6	35.5 ± 1.8	+55.5 ± 3.0	250 ± 5	+52 ± 5	6	19 ± 4
	Procaine	6	38.3 ± 2.8	+20.0 ± 4.0§	257 ± 2	−23 ± 10§	0**	0§
2	Control	8	36.1 ± 2.0	+56.6 ± 2.6	245 ± 4	+74 ± 5	8	21 ± 6
	Vagotomy	8	32.9 ± 2.1	+52.4 ± 4.1	251 ± 6	+60 ± 7	8	10 ± 2
3	Control	8	41.4 ± 2.0	+50.6 ± 1.9	257 ± 6	+50 ± 7	8	16 ± 3
	Capsaicin	8	35.5 ± 1.9*	+16.2 ± 3.0§	250 ± 5	+20 ± 5¶	6	17 ± 4
4	Control	8	41.2 ± 1.8	+54.0 ± 5.6	258 ± 10	+67 ± 9	7	7 ± 2
	Spinalized	8	34.7 ± 1.4†	−1.5 ± 1.9§	245 ± 10	0 ± 6§	0**	0¶

[a]All animals received single i.p. injection of 14 nmol kg^{-1} of NT. Exp. no. 1: i.p. NT solution was added with procaine 2% w/v or an equivalent volume of procaine solvent (control). Exp. no. 2: animals underwent vagotomy or sham operation (control) 45–50 min before i.p. NT. Exp. no. 3: animals were pretreated 4 days previously with capsaicin or its solvent (control) (see Methods) before i.p. NT. Exp. no. 4: animals underwent spinalization or sham operation (control) (see Methods), 45–50 min before i.p. NT. Results are expressed as mean ± s.e.mean. Other abbreviations as in Table 3.
*$P<0.05$; †$P<0.02$; ¶$P<0.005$ and §$P<0.001$ when compared to respective control value (Student's *t* test)
**$P<0.005$ when compared to respective control value (Chi-square test)

(MAP, HR) responses to i.p. injection of NT, but TAWC responses were not affected. Acute transection of the spinal cord (between C2–C3) 45–50 min before, completely suppressed the cardiovascular and TAWC responses to i.p. NT. Interestingly, slowly developing, relatively sustained abdominal wall contractions (SAWC) occurred in spinalized guinea-pigs given i.p. NT (Figure 3). This unexpected response was not seen in sham-operated animals. The latter animals rather exhibited the usual decrease of AWT associated with i.p. NT (see Figure 4b and Table 1). Single i.p. injection of 9 ml of NT solvent (i.e. PDS) in spinalized guinea-pigs elicited similar decreases of AWT as in sham-operated (control) animals (Figure 4a).

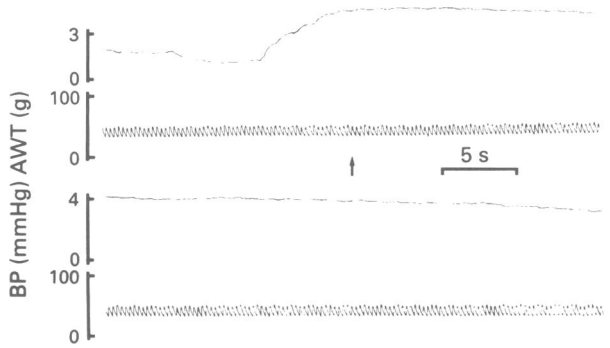

Figure 3 Typical tracing showing the time course of changes of basal abdominal wall tension (AWT) (1st tracing from the top) and systemic blood pressure (BP) (2nd tracing from the top) in anaesthetized, spinalized (i.e. acute transection of the spinal cord at the C2–C3 level) guinea-pigs, following single i.p. injection of neurotensin (NT) (14 nmol kg^{-1}). The 3rd and the 4th tracing are continuations of 1st and 2nd tracings, respectively. The arrow indicates the end of i.p. injection of NT. Note the slowly developing, relatively sustained contraction of the abdominal wall starting before the i.p. injection is over, the absence of transient abdominal wall contractions (or twitches) and absence of pressor effect after i.p. injection of NT (see Figure 1 for comparison). mmHg, millimeters of mercury; g, grams.

Effect of selected drugs on sustained abdominal wall contractions

Various drugs were tested as potential inhibitors of SAWC in anaesthetized, spinalized guinea-pigs given i.p. NT (14 nmol kg^{-1}). Results are compiled in Table 5. Animal pretreatment with i.v. bolus injection of pancuronium or pre-addition of lignocaine 2% w/v to NT solution for i.p. injection, abolished SAWC. Neither i.v. morphine, clonidine or baclofen, nor pre-addition of procaine 2% w/v to NT solution for i.p. injection, modified the amplitude of SAWC.

Effect of naloxone in spinalized animals

Intravenous bolus injection of naloxone (5.6 μmol kg^{-1}) in anaesthetized, spinalized guinea-pigs (see Methods) partially restored the pressor (ΔMAP), tachycardic (ΔHR) and TAWC responses to i.p. injection of NT (14 nmol kg^{-1}). Peak ΔMAP values in 9 naloxone-treated spinalized animals were $+15.3 \pm 3.4$ mmHg vs -1.5 ± 1.9 mmHg in 8 control (i.e. saline-pretreated) spinalized animals ($P<0.001$) (Student's t test). Peak ΔHR values in 9 naloxone-treated spinalized animals were $+26 \pm 12$ b.p.m. vs 0 ± 6 b.p.m. in 8 control animals ($P>0.05$). Basal (i.e. pre-i.p. NT) MAP and HR values in naloxone-treated spinalized animals were 35.9 ± 2.0 mmHg and 233 ± 4 b.p.m. ($n=9$), respectively. Corresponding values in naloxone-free spinalized animals were 34.7 ± 1.4 mmHg and 245 ± 10 b.p.m. ($n=8$). Three (3) out of 9 naloxone-treated spinalized animals exhibited TAWC (TAWC/animal: 9 ± 4, $P<0.05$, Student's t test), whereas 0 out of 8 naloxone-free, spinalized animals exhibited TAWC. Naloxone treatment did not modify the amplitude or time course of SAWC caused by i.p. NT in spinalized guinea-pigs.

Effect of i.v. bolus injection of NA, DMPP or pentolinium in spinalized guinea-pigs

Peak pressor and tachycardic responses to single i.v. bolus injection of noradrenaline (NA) (7.3 nmol kg^{-1}) or DMPP (310 nmol kg^{-1}) in anaesthetized spinalized guinea-pigs were similar to those measured in control (sham-operated) guinea-pigs (ΔMAP and ΔHR values for NA in 5 control guinea-pigs: $+39.6 \pm 2.1$ mmHg and $+54 \pm 7$ b.p.m.; corresponding values in 5 spinalized guinea-pigs: $+42.0 \pm 3.1$ mmHg and $+58 \pm 10$ b.p.m.; ΔMAP and ΔHR values for DMPP in 4 control guinea-pigs: $+37.2 \pm 6.2$ mmHg and $+38 \pm 9$ b.p.m.; corresponding values in 4 spinalized guinea-pigs: $+36.5 \pm 2.4$ mmHg and $+35 \pm 10$ b.p.m.). Peak hypotensive and bradycardic responses to single i.v. bolus injection of pentolinium (3.7 μmol kg^{-1}) in 6 anaesthetized spinalized guinea-pigs (ΔMAP and ΔHR: -13.5 ± 1.3 mmHg and -23 ± 2 b.p.m.) were similar to those measured in 6 sham-operated (control) guinea-pigs (ΔMAP and ΔHR values: -14.8 ± 2.7 mmHg and -32 ± 5 b.p.m.).

Table 5 Effect of various drug treatments on basal abdominal wall tension (AWT) associated with single i.p. injection of neurotensin (NT) in anaesthetized, spinalized guinea-pigs[a]

		ΔAWT (g)				
Treatment	*AWT* (g)	*5 s*	*10 s*	*20 s*	*30 s*	*60 s*
Control (8)	2.6 ± 0.1	$+1.8 \pm 0.3$	$+1.6 \pm 0.4$	$+1.4 \pm 0.4$	$+1.0 \pm 0.4$	$+0.4 \pm 0.3$
PCR (6)	2.9 ± 0.1*	-1.0 ± 0.1†	-0.9 ± 0.1†	-0.3 ± 0.1†	-0.4 ± 0.1†	-0.5 ± 0.1*
Mor (4)	2.9 ± 0.1	$+2.5 \pm 0.7$	$+2.1 \pm 0.6$	$+1.7 \pm 0.5$	$+1.5 \pm 0.4$	$+1.1 \pm 0.2$
Clo (6)	2.8 ± 0.1	$+1.5 \pm 0.7$	$+1.8 \pm 0.7$	$+1.9 \pm 0.5$	$+1.5 \pm 0.4$	$+0.7 \pm 0.4$
Bac (4)	2.9 ± 0.1*	$+2.5 \pm 0.7$	$+1.6 \pm 0.7$	$+1.2 \pm 0.5$	$+0.8 \pm 0.4$	$+0.5 \pm 0.4$
Pro (6)	2.7 ± 0	$+0.6 \pm 0.3$	$+1.1 \pm 0.3$	$+1.1 \pm 0.2$	$+0.6 \pm 0.1$	$+0.1 \pm 0.1$
Lig (6)	2.8 ± 0.1	-0.3 ± 0.3*	-0.1 ± 0.2*	-0.4 ± 0.1†	-0.6 ± 0.1†	-0.5 ± 0.1*
ANOVA	$P<0.05$	$P<0.01$	$P<0.01$	$P<0.01$	$P<0.01$	$P<0.01$

[a]All animals had their spinal cord completely transected (between C2–C3) 45–50 min before receiving single i.p. injection of NT (14 nmol kg^{-1}). Thirty (30) min before i.p. NT, the animals received i.v. bolus injection of either saline (control) or of one of the following drugs (doses in μmol kg^{-1}): pancuronium (PCR) (0.27), morphine (mor) (15.0), clonidine (Clo) (0.34), or baclofen (Bac) (10.0). Procaine (Pro) (2% w/v) or lignocaine (Lig) (2% w/v) were added to NT solution before i.p. injection. AWT, basal abdominal wall tension; ΔAWT indicates increases (+) or decreases (−) of AWT at different times (over a 60 s period) after i.p. NT. g, grams. Results are expressed as mean ± s.e.mean; the number of animals per group is given in parentheses on the left.
*$P<0.05$; †$P<0.01$ when compared to the corresponding control value (Dunnett's test)

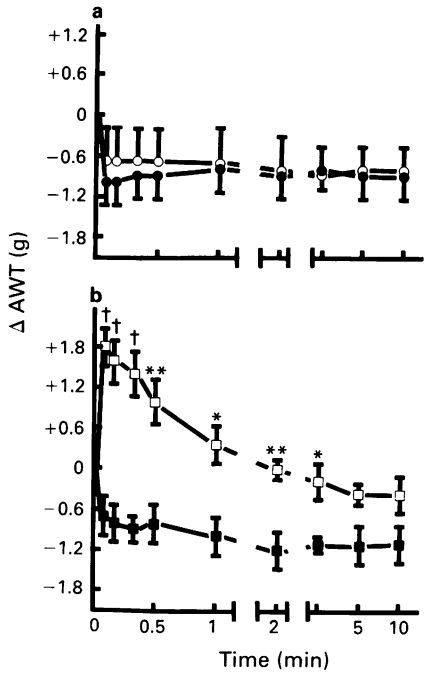

Figure 4 (a) Time courses of the decreases (−) of basal abdominal wall tension (AWT) in anaesthetized, sham-operated (control) (●) ($n = 4$) or spinalized (○) ($n = 4$) guinea-pigs at different times after single i.p. injection of neurotensin (NT) solvent (i.e. PDS). Ordinate scale: changes of AWT (ΔAWT); abscissa scale: time after i.p. injection of NT solvent. g, grams. Note the similar effect of i.p. injection of NT solvent on AWT in both animal groups. (b) Time courses of the decreases (−) or increases (+) of AWT in anaesthetized, sham-operated (control) (■) ($n = 8$) or spinalized (□) ($n = 8$) guinea-pigs, following single i.p. injection of NT (14 nmol kg^{-1}). Ordinate and abcissae scales, as above. Note the relatively sustained contraction of the abdominal wall in spinalized guinea-pigs compared to controls, following i.p. NT.
$^{*}P<0.02$; $^{**}P<0.005$; †$P<0.001$ when compared to corresponding control values (Student's t test).

Discussion

The ability of i.p. NT to induce TAWC in anaesthetized guinea-pigs, is a relatively novel observation (see Introduction). Evidence presented in this paper suggests that TAWC is a neurally-mediated reflex response that originates within the peritoneal cavity and involves the contraction of abdominal muscles. This conclusion is based on several facts. First, TAWC are suppressed by animal pretreatment with pancuronium, a neuromuscular blocker that inhibits nicotinic receptors, thus indicating that TAWC result from the activation of cholinergic motoneurones that innervate abdominal muscles. Second, the concomitant i.p. injection of procaine, a local anaesthetic, and NT, prevents TAWC caused by i.p. NT, thus suggesting that i.p. NT caused TAWC by means of activation of abdominal visceral afferents presumably making mono- and/or polysynaptic contacts with cholinergic motoneurons innervating abdominal muscles. Third, TAWC were dose-dependently suppressed by i.v. morphine, a potent opioid agonist known to suppress various nociceptive reflexes (Jaffe & Martin, 1990). Fourth, animal pretreatment with naloxone, a potent opioid receptor antagonist which potentiates various reflexes (Duggan, 1983), was shown to markedly increase the number of TAWC/animal, and to suppress the effect of morphine on TAWC. Fifth, acute spinalization was found to suppress TAWC as well as pressor and tachycardic responses caused by i.p. NT, thus indicating that the spinal cord is likely to be an important relay centre for the pressor, tachycardic and TAWC responses to i.p. NT. Whether or not supraspinal centres are involved in the latter reflexes could not be determined in the present study, for acute transection of the spinal cord is known to cause spinal shock. However, based on the ability of naloxone to restore partially pressor, tachycardic and TAWC responses to i.p. NT in spinalized guinea-pigs, it seems reasonable to hypothesize that these reflex responses are subserved by spinal cord neural circuitry. The mechanism of the beneficial effect of naloxone in spinal shock has been discussed previously (Holaday & Faden, 1980; Faden *et al.*, 1981).

Several observations suggest that haemodynamic and TAWC responses to i.p. NT are independent reflexes that do not share the same neural pathways. This conclusion is based on the following facts: (1) animal pretreatment with pancuronium inhibits TAWC, but not haemodynamic responses to i.p. NT; (2) morphine suppresses, and naloxone potentiates, TAWC, without altering haemodynamic NT effects; (3) pentolinium, prazosin and capsaicin treatment markedly reduced haemodynamic responses to i.p. NT, without affecting TAWC. The results of capsaicin experiments also indicate that abdominal visceral afferents involved in TAWC, are unlikely to be small diameter, tachykinins-containing (i.e. capsaicin-sensitive) primary afferents (Buck & Burks, 1986), in contrast to those subserving reflex haemodynamic responses to i.p. NT (Rioux *et al.*, 1990a; this paper). That vagal afferents are not involved in TAWC (this paper) or haemodynamic responses to i.p. NT (Rioux *et al.*, 1990a; this paper), is well supported by the persistence of these responses in vagotomized animals. That acute spinalization did not inhibit the cardiovascular response to i.p. NT by causing a nonspecific depression of the cardiovascular system is indicated by the absence of amplitude differences between pressor and tachycardic responses to i.v. NA or DMPP in spinalized guinea-pigs compared to control. The similar amplitude of hypotensive effect of i.v. pentolinium in spinalized and sham-operated (i.e. control) guinea-pigs also suggests that spinalization did not completely suppress the activity of preganglionic sympathetic neurones, despite the spinal shock.

Besides inhibiting haemodynamic and TAWC responses to i.p. NT, acute spinalization was also shown to reveal a different type of abdominal motor response, which we called SAWC (i.e. slowly developing, sustained abdominal wall contration) (Figure 3). This type of abdominal motor response was absent in sham-operated or intact guinea-pigs after i.p. NT. The ability of NT to elicit SAWC is, to our knowledge, a novel biological property for NT. Various drugs were tested to unravel the mechanism by which i.p. NT causes SAWC in spinal guinea-pigs. The results showed that i.v. pancuronium, or i.p. lignocaine 2% w/v (i.e. pre-added to i.p. NT solution), completely prevent SAWC, whereas i.v. morphine, naloxone, clonidine or baclofen, or i.p. procaine 2% w/v, exert no effect. The suppression of SAWC by pancuronium clearly indicates that cholinergic motoneurones innervating abdominal muscles are involved, whereas SAWC suppression by i.p. lignocaine suggests the participation of abdominal visceral afferents. This interpretation is consistent with the fact that NT does not cross the blood-brain barrier (Nemeroff *et al.*, 1977). Consequently, the activation by i.p. NT of abdominal visceral afferents making synaptic contacts at the spinal level (i.e. presumably the ventral horn) with cholinergic motoneurones innervating abdominal muscles, is the most probable means by which i.p. NT causes SAWC in spinal guinea-pigs. However the possibility that i.p. lignocaine inhibits i.p. NT-induced SAWC by additional mechanisms (i.e. inhibition of transmission at neuromuscular junction) cannot be dismissed without further studies. The superiority of i.p. lignocaine over i.p. procaine in suppressing SAWC, is likely to reflect the difference of potency and efficacy between these 2 local anaesthetics (Ritchie & Greene, 1990). It also raises the possibility that abdominal visceral afferents subserving SAWC in spinal guinea-pigs, are less easily reached than those involved in TAWC. The inability of i.v. morphine, naloxone or clonidine to affect SAWC (in spinalized animals) even when used at doses that effectively modify TAWC (in

intact animals), suggests that the mechanism (e.g. neural circuitry) of these two types of responses may be different. Alternatively, the latter results might reflect the fact that morphine, naloxone and clonidine must act supraspinally to modify SAWC (i.e. via the activation of descending inhibitory neural pathways). Assuming that SAWC are true reflex responses, then, why do they occur in spinalized guinea-pigs, but not in sham-operated animals? In our opinion the abdominal distension associated with i.p. injection of a relatively large volume of NT solution (i.e. 9 ml), contributes to mask the detection of SAWC in sham-operated or intact guinea-pigs given i.p. NT. This hypothesis is supported by the fact that SAWC can easily be detected in intact animals given i.p. NT when lower volumes (i.e. 1 or 3 ml) of NT solution are utilized (Rioux, F., Lemieux, M., unpublished). The reason why spinalization unmasks SAWC responses to i.p. NT, despite fluid-induced abdominal distension is not clear. One possible explanation is that proprioceptive reflexes are triggered by abdominal distension, which promote abdominal muscle relaxation in intact animals, whereas such reflexes are absent in spinalized guinea-pigs (due to spinal shock), thus revealing SAWC.

The pressor and tachycardic responses to i.p. NT in anaesthetized guinea-pigs were not affected by animal pretreatment with morphine or naloxone. On the other hand TAWC responses to i.p. NT were suppressed by morphine and potentiated by naloxone. These results suggest that TAWC might be the motor component of a morphine-sensitive nociceptive reflex, whereas haemodynamic responses might be the circulatory component of the same reflex, which would involve morphine-insensitive neural pathways. The potentiation of TAWC responses (i.e. increase of the number of TAWC/animal) to i.p. NT by naloxone, also suggest that neural pathways involved in TAWC are somehow negatively regulated by endogenous opioid peptides, which could, theoretically, be released within the spinal cord following NT-induced activation of abdominal visceral afferents. This interpretation is consistent with the presence of opioid peptides in dorsal root ganglia, peripheral and central ends of primary sensory neurones, as well as in the dorsal horn of the spinal cord (Weihe *et al.*, 1988; Ribeiro da Silva *et al.*, 1990). The possibility of a tonic inhibition by endogenous opioid peptides of neural pathways involved in TAWC responses to i.p. NT cannot be ruled out completely. However, based on the inability of i.v. naloxone to elicit TAWC in animals not given NT (Rioux, F., Lemieux, M., unpublished), this last hypothesis seems less likely than the former one.

The response selectivity of our experimental model was good, for i.p. injection of BK or SP were either inactive (SP) or weakly active (BK) in mimicking the effects of i.p. NT. The weak potency of BK was somewhat surprising since BK is considered a potent algesic substance in mammals (Garrison, 1990), and i.p. injection of BK in conscious dogs or human subjects was previously reported to be painful (Lim *et al.*, 1967; Sancilio & Cheung, 1978). Besides, BK (or SP) is known to stimulate abdominal visceral afferents in cats (Lew & Longhurst, 1986) and guinea-pigs (Beauchamp *et al.*, 1991). The precise reason for the absence of effect of i.p. SP and low potency of i.p. BK in our animal model is unknown.

The response sensitivity of our animal model to i.p. NT was probably affected by the anaesthesia and surgical stress, as barbiturates are known to depress transmission in autonomic ganglia and at the neuromuscular junction (Rall, 1990). Therefore the amplitudes of haemodynamic and abdominal motor responses to i.p. NT were probably attenuated by the anaesthesia, for both types of responses utilized barbiturate-sensitive neural pathways. On the other hand the negative influence of anaesthesia on haemodynamic responses to i.p. NT was probably counterbalanced by concomitant reductions of baroreceptor-mediated cardiovascular reflexes. In addition, the low basal systemic BP level observed in barbiturate-anaesthetized guinea-pigs, certainly contributed to enhance pressor responses to i.p. NT, for high initial BP levels tend to attenuate the latter responses (Rioux *et al.*, 1990b). Surgical stress is the second factor which potentially modified the sensitivity of our animal model to i.p. NT, for noxious stimuli (i.e. surgery) are known to activate endogenous antinociceptive mechanisms that are known to reduce the amplitude and/or duration of nociceptive reflexes (Lumb, 1986; Besson & Chaouch, 1987). In addition the putative role of opioid peptidergic mechanisms in stress-induced analgesia (Terman *et al.*, 1984) raises the possibility that the potentiating action of naloxone on TAWC responses to i.p. NT, may depend to a large extent upon inhibition of opioid peptidergic mechanisms activated by surgical stress (Dubois *et al.*, 1981; Jaffe & Martin, 1990). The last technical point to be discussed is the use of i.p. procaine (or lignocaine) as a pharmacological tool to infer the participation of abdominal visceral afferents in haemodynamic and abdominal motor responses to i.p. NT. One could argue that i.p. procaine, in addition to causing conduction blockade in abdominal visceral afferents, also caused paralysis of cholinergic motoneurones and pre- and postganglionic sympathetic nerves, effects which could also explain the blockade of reflex haemodynamic and TAWC responses to i.p. NT. Although no direct proof is yet available to rule out this possibility, we believe that conduction blockade of abdominal visceral afferents is the most likely mechanism subserving the prevention of reflex haemodynamic and TAWC responses to i.p. NT by i.p. procaine. Our conviction is based on the following facts: (1) both the onset of NT effects and their blockade by i.p. procaine (i.e. procaine was pre-added to NT solution before i.p. injection of the latter) occurred rapidly (i.e. within seconds) after i.p. injection of NT solution, so that peritoneal visceral afferents are more likely than cholinergic motoneurones to have been reached rapidly by i.p. procaine; (2) peak pressor and tachycardic responses to i.v. bolus injection of DMPP, a ganglion stimulant, in anaesthetized guinea-pigs that first received (i.e. 2 min before) i.p. injection of 9 ml of procaine 2% w/v, were similar in amplitude to those measured in control animals (i.e. animals given i.p. injection of 9 ml of procaine solvent 2 min before i.v. DMPP), thus indicating that postganglionic noradrenergic neurones were still pharmacologically excitable 2 min after i.p. procaine; (3) reflex pressor and tachycardic responses to topical application of microlitre volumes of NT solution to discrete small area of the visceral peritoneum were previously shown, in the same animal model, to be reduced by prior (i.e. 30 s before) topical application of similar volume of lignocaine solution to the same sites as NT (Rioux *et al.*, 1989).

In conclusion, i.p. injection of NT in anaesthetized guinea-pigs caused dose-dependent pressor, tachycardic and abdominal motor responses (i.e. TAWC). Evidence were provided that haemodynamic and TAWC responses are both reflex in nature and not causally related. Both types of reflexes appear to result from the activation by i.p. NT of abdominal visceral afferents making synaptic contacts with spinal neurones. The pathophysiological significance of these results, if any, is unknown at present. However, given the nature and time-response characteristics of the reflexes elicited by i.p. NT, it seems reasonable to hypothesize that i.p. NT could be a noxious stimulus in guinea-pigs.

The authors wish to thank the Medical Research Council of Canada (Grant MT-6550) and the Canadian Heart Foundation for their financial support, and Mrs Gaétane Rioux for typing the manuscript.

References

BEAUCHAMP, J.-F., LEMIEUX, M., DRAPEAU, G. & RIOUX, F. (1991). Mechanism of the pressor response to intraperitoneal injection of bradykinin in guinea pigs. *Peptides*, **12**, 513–521.

BESSON, J.-M. & CHAOUCH, A. (1987). Peripheral and spinal mechanisms of nociception. *Physiol. Rev.*, **67**, 67–186.

BUCK, S.H. & BURKS, T.F. (1986). The neuropharmacology of capsaicin. Review of some recent observations. *Pharmacol. Rev.*, **38**, 180–226.

DUBOIS, M., PICKAR, D., COHEN, M.R., ROTH, Y.F., MACNAMARA, T. & BUNNEY, JR, W.E. (1981). Surgical stress in humans is accompanied by an increase in plasma beta-endorphin immunoreactivity. *Life Sci.*, **29**, 1249–1254.

DUGGAN, A.W. (1983). Electrophysiology of opioid peptides and sensory systems. *Br. Med. Bull.*, **39**, 65–70.

FADEN, A.I., JACOB, T.P. & HOLADAY, J.W. (1981). Opiate antagonist improves neurologic recovery after spinal injury. *Science*, **211**, 493–494.

GARRISON, J.C. (1990). Histamine, bradykinin, 5-hydroxytryptamine, and their antagonists. In *The Pharmacological Basis of Therapeutics*. ed. Goodman Gilman, A., Rall, T.W., Nies, A.S. & Taylor, P., pp. 575–599. New York: Pergamon Press.

HOLADAY, J.W. & FADEN, A.I. (1980). Naloxone acts at central opiate receptors to reverse hypotension, hypothermia and hypoventilation in spinal shock. *Brain Res.*, **189**, 295–299.

JAFFE, J.H. & MARTIN, W.R. (1990). Opioid analgesics and antagonists. In *The Pharmacological Basis of Therapeutics*. ed. Goodman Gilman, A., Rall, T.W., Nies, A.S. & Taylor, P. pp. 485–521. New York: Pergamon Press.

LEW, W.Y.W. & LONGHURST, J.C. (1986). Substance P, 5-hydroxytryptamine, and bradykinin stimulate abdominal visceral afferents. *Am. J. Physiol.*, **250**, R465–R473.

LIM, R.K.S., MILLER, D.G., GUZMAN, F., RODGERS, D.W., ROGERS, R.W., WANG, S.K., CHAO, P.Y. & SHIH, T.Y. (1967). Pain and analgesia evaluated by the intraperitoneal bradykinin-evoked pain method in man. *Clin. Pharmacol. Ther.*, **8**, 521–542.

LUMB, B.M. (1986). Brainstem control of visceral afferent pathways in the spinal cord. In *Prog. Brain Res.*, vol. 67, pp. 279–293. New York: Elsevier Science Publ., B.V.

LUNDBERG, J.M., FRANCO-CERECEDA, A., HUA, X.-Y., HOKFELT, T. & FISCHER, J.A. (1985). Co-existence of substance P and calcitonin gene-related peptide-like immunoreactivities in sensory nerves in relation to cardiovascular and broncho-constrictor effects of capsaicin. *Eur. J. Pharmacol.*, **108**, 315–319.

NEMEROFF, C.B., BISSETTE, G., PRANGE, JR, A.J., LOOSEN, P.T., STEVEN BARLOW, T. & LIPTON, M.A. (1977). Neurotensin: central nervous system effects of a hypothalamic peptide. *Brain Res.*, **128**, 485–496.

RALL, T.W. (1990). Hypnotics and sedatives; ethanol. In *The Pharmacological Basis of Therapeutics*. ed. Goodman Gilman, A., Rall, T.W., Nies, A.S. & Taylor, P. pp. 345–382. New York: Pergamon Press.

RIBEIRO-DA-SILVA, A., PIORO, E.P. & CLAUDIO CUELLO, A. (1991). Substance P- and enkephalin-like immunoreactivities are colocalized in certain neurons of the substantia gelatinosa of the rat spinal cord: an ultrastructural double-labeling study. *J. Neurosci.*, **11**, 1068–1080.

RIOUX, F., LEMEIUX, M., KEROUAC, R., BERNOUSSI, A. & ROY, G. (1989). Local application of neurotensin to abdominal organs triggers cardiovascular reflexes in guinea pigs: possible mechanisms. *Peptides*, **10**, 647–655.

RIOUX, F., LEMIEUX, M. & LEBEL, M. (1990a). Further observations on the mechanism of the cardiovascular reflexes caused by exposure of the peritoneum to neurotensin. *Peptides*, **11**, 805–816.

RIOUX, F., LEMIEUX, M. & LEBEL, M. (1990b). Effect of initial blood pressure level on cardiovascular reflexes caused by intraperitoneal neurotensin. *Peptides*, **11**, 921–926.

RITCHIE, J.M. & GREENE, N.M. (1990). Local anesthetics. In *The Pharmacological Basis of Therapeutics*. ed. Goodman Gilman, A., Rall, T.W., Nies, A.S. & Taylor, P. pp. 311–331. New York: Pergamon Press.

SANCILIO, L.F. & CHEUNG, S. (1978). Analysis of the bradykinin response in dogs and its antagonism by analgesic drugs. *J. Pharmacol. Exp. Ther.*, **207**, 469–475.

TALLARIDA, R.J. & MURRAY, R.B. (1981). *Manual of Pharmacologic Calculations with Computer Programs*. New York: Springer-Verlag.

TERMAN, G.W., SHAVIT, Y., LEWIS, J.W., CANNON, J.T. & LIEBESKIND, J.C. (1984). Intrinsic mechanisms of pain inhibition: activation by stress. *Science*, **226**, 1270–1277.

WEIHE, E., NOHR, D. & HARTSCHUH, W. (1988). Immunohistochemical evidence for a co-transmitter role of opioid peptides in primary sensory neurons. In *Progress in Brain Research*, vol. 74. ed. Hamann, W. & Iggo, A. pp. 189–199. New York: Elsevier Science Publishers B.V.

(Received May 30, 1991
Revised January 8, 1992
Accepted January 10, 1992)

Br. J. Pharmacol. (1992), **106**, 196–198 © Macmillan Press Ltd, 1992

The effect of monoclonal antibodies to calcitonin gene-related peptide (CGRP) on CGRP-induced vasodilatation in pig coronary artery rings

[1]N.E. Shaw, R. Foulkes, *D.P. Andrew, *D.T. Brown & B. Hughes

Department of Pharmacology and *Cell Biology, Celltech Limited, 216 Bath Road, Slough, Berkshire SL1 4EN

1 The modification of the vasodilator effect of calcitonin gene-related peptide (CGRP) by a panel of monoclonal antibodies (MAbs), which map to discrete epitopes on the CGRP molecule, was investigated in pig coronary artery rings (PCA). The preparations were pre-constricted with acetylcholine (3×10^{-7}M) and concentration-response curves to CGRP (2×10^{-10}–2.56×10^{-8}M) were obtained in the presence or absence of each MAb.

2 CGRP caused a concentration-dependent relaxation of PCAs which reached a maximum ($98.2 \pm 4.8\%$, $n = 25$) at 1.28×10^{-8}M and gave an EC_{50} of $3.8 \pm 0.8 \times 10^{-9}$M.

3 Two MAbs which map to the N-terminal, CN1 and CRA3, did not affect the CGRP response whilst a third, CRA5, significantly inhibited its effect.

4 The C-terminal MAb, CRA2, did not modify the CGRP response whilst, in contrast, CB3 (C-terminal) potentiated its effect. A similar augmentation of the CGRP-induced vasodilatation was seen in the presence of the middle-region MAb, CRA8.

5 These results suggest that regional specific MAbs can modify the vasodilator effect of CGRP causing either inhibition (CRA5, N-terminal) or potentiation (CB3, C-terminal; CRA8, middle region).

Keywords: Calcitonin gene-related peptide (CGRP); vasodilatation; pig coronary artery; monoclonal antibodies

Introduction

Calcitonin gene-related peptide (CGRP) is an endogenous 37 amino-acid peptide the effects of which are receptor-mediated (Sano *et al.*, 1989) causing vasodilatation in the pig isolated coronary artery preparation (Beny *et al.*, 1989). Although previous work has shown the peptide fragment CGRP (8–37) to be an antagonist of CGRP in rat liver plasma membranes (Chiba *et al.*, 1989), *in vivo* in conscious rats (Gardiner *et al.*, 1990) and in pig isolated arteries (Foulkes *et al.*, 1991) little is known about the location of the active region of the peptide. A more conventional pharmacological approach to investigate this problem may involve the study of structure-activity relationships using sequence analogues to CGRP. However, such methods of investigation, utilising amino-acid substitutions, deletions and insertions, can lead to gross distortions in tertiary structure and loss of function. As a possible alternative strategy, the use of a panel of monoclonal antibodies (MAbs) which bind and possibly inhibit specific functional regions of a peptide may yield information regarding the active site of the molecule. In this study the modification of the vasodilator effect of CGRP by a panel of MAbs (Andrew *et al.*, 1990) was investigated in the pig coronary artery ring preparation.

Methods

Isolated coronary artery preparations

Pig coronary artery rings (PCAs) of diameter < 1 mm were obtained from a section of the left anterior descending coronary artery of the pig heart, near to the apical region. Previous workers (Beny *et al.*, 1989) have shown in this preparation that the response to CGRP is endothelium-independent; however, the endothelium of each ring was removed by gentle rubbing of the lumen with a dissection needle to obtain a more stable tissue. Rings that gave a relaxation greater than 20% on addition of bradykinin (10^{-7}M) were discarded. Each ring was mounted in a 10 ml organ bath containing Krebs Ringer solution of the following composition (in mM): NaCl 118, $NaHCO_3$ 25, D-glucose 11, KCl 4.7, $CaCl_2$ 2.5, KH_2PO_4 1.2 and $MgSO_4.7H_20$ 1.2. The Krebs solution was maintained at 37 ± 1°C and gassed with $95\%O_2$ and $5\%CO_2$. Any changes in tension were measured by a Grass FTO3 force-displacement transducer and displayed on a Gould BS 273 flat-bed recorder. A resting tension of 2 g was applied to all the tissues which were allowed to equilibrate for 90 min. The optimal resting tension was chosen from force developed/applied tension curves previously obtained in these laboratories (data not shown). The tissues were initially pre-constricted with a sub-maximal concentration of acetylcholine (ACh, 3×10^{-7}M). In each experiment a control concentration-response curve (CRC) to CGRP was obtained by cumulative administration of CGRP between the range of 2×10^{-10}–2.56×10^{-8}M, with a dose cycle of 6 min. The rings were repeatedly washed and left for 30 min to allow the tissue to recover from each treatment before reconstriction. Further CRCs to CGRP were obtained in the presence of each MAb. Up to three CRCs per tissue were carried out since previous studies have shown tachyphylaxis to CGRP does not occur in the pig small coronary artery ring preparation on repeated administration (Foulkes *et al.*, 1991), nor does the ACh-induced constriction diminish. Prior to use, a stock solution of each MAb was incubated for 30 min with CGRP in a 10 fold molar excess of antibody. The CGRP-MAb mixture was administered to the tissue giving a CGRP range of 10^{-10}–10^{-8}M (the antibody concentration hence remaining at a constant 10 fold excess) and not more than three CRCs per tissue were obtained. Full details of the epitope mapping of the anti-CGRP MAbs have been previously described by Andrew *et al.* (1990). The MAbs used in the present study (and the amino-acid sequence recognised) were: CRA2 (27–37); CB3 (19–37); CRA8 (19– 28); CN1 (1–13); CRA3 (1–13); CRA5 (1–13).

[1] Author for correspondence.

Binding affinity constants

Scatchard analysis of the MAbs CN1, CRA3 and CRA5 was obtained by use of flexible microtitre plates coated with CGRP and blocked with phosphate buffered saline and 5% bovine serum albumin (BSA) over an incubation period of 1 h. Each radiolabelled MAb was then added in serial dilutions to the wells and, following 4 h incubation at room temperature, were washed, dried and counted on a gamma counter. The binding affinity for each antibody was calculated by use of a Scatchard plot of bound/free antibody against bound (mol) antibody.

Statistical analyses

All data from the pig coronary artery ring experiments were expressed as a % reversal of tone induced by ACh (3×10^{-7}M). The EC_{50} value of each CRC was calculated and the differences between values were compared by analysis of variance (ANOVA) and considered significantly different if $P<0.05$.

Materials

The following were used: synthetic human α-CGRP (Celltech); acetylcholine, bradykinin and BSA (obtained from Sigma).

Results

ACh (3×10^{-7}M) caused an increase in tone of 2.21 ± 0.2 g ($n = 53$) which could be maintained for more than 45 min (results not shown). CGRP caused a concentration-dependent relaxation of the PCAs which reached a maximum ($98.2 \pm 4.8\%$, $n = 25$) at 1.28×10^{-8}M and gave an EC_{50} value of $3.8 \pm 0.8 \times 10^{-9}$M.

N-terminal monoclonal antibodies (Figure 1a)

CGRP when incubated with CN1 and CRA3 gave maximum reversal in tone and EC_{50} values that were not significantly different from CGRP alone. However, in the presence of CRA5, the CGRP response was inhibited. Since we were unable to produce enough CRA5, preventing the completion of the CRC, a comparison between CGRP alone and in the presence of CRA5 was made at the level of 25% relaxation which gave values (CGRP, $3.1 \pm 0.7 \times 10^{-9}$M, $n = 12$); CGRP + CRA5, $9.9 \pm 2 \times 10^{-9}$M, $n = 7$) that were significantly different from each other.

C-terminal monoclonal antibodies (Figure 1b)

In the presence of CRA2 the maximum reversal of tone and EC_{50} for CGRP were not significantly different from that of CGRP alone. However, in the presence of CB3 there was a similar maximum vasodilator effect but a potentiation of the vasodilator response compared to CGRP alone was evident. The EC_{50} values in the absence ($2 \pm 0.3 \times 10^{-9}$M, $n = 9$) and in the presence ($7.5 \pm 1.6 \times 10^{-10}$M, $n = 5$) of CB3 were significantly different.

Middle region monoclonal antibodies (Figure 1c)

In the presence of CRA8, there was a potentiation of the vasodilator response to CGRP alone; the two EC_{50} values (CGRP, $2 \pm 0.3 \times 10^{-9}$M, $n = 9$; CGRP + CRA8, $1.1 \pm 0.2 \times 10^{-9}$M, $n = 8$) were significantly different from each other.

The binding affinity constants for N-terminal MAbs were all found to be within a similar range (CRA5, $1.8 \pm 0.2 \times 10^{8}\,M^{-1}$, $n = 3$; CN1, $4.9 \pm 0.6 \times 10^{7}\,M^{-1}$, $n = 3$; CRA3, $4.0 \pm 0.5 \times 10^{7}\,M^{-1}$, $n = 3$). Although CRA5 was marginally (but significant, $P<0.05$) greater than CN1 and CRA3 the binding affinity constants for all three were similar to those obtained previously for other anti-CGRP MAbs (Andrew *et al.*, 1990).

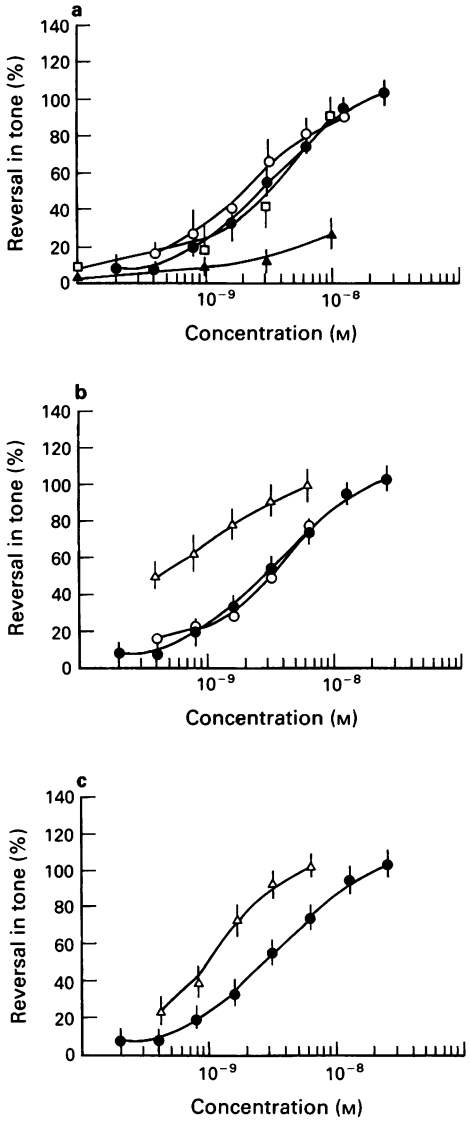

Figure 1 Effects of monoclonal antibodies (MAbs) on the vasodilator response to calcitonin gene-related peptide (CGRP). (a) Concentration-response curves to CGRP alone ($n = 25$), (●) and in the presence of CRA3 ($n = 4$), (○); CN1 ($n = 6$), (□) and CRA5 ($n = 7$), (▲). (b) Concentration-response curves to CGRP alone ($n = 25$), (●) and in the presence of CB3 ($n = 5$), (△) and CRA2 ($n = 7$), (○). (c) Concentration-response curves to CGRP alone ($n = 25$), (●) and in the presence of CRA8 ($n = 8$), (△). Values are mean of n observations (s.e.mean shown by vertical bars; some s.e.means have been omitted for clarity).

Discussion

Previous work investigating the structure-activity relationships of CGRP (Tippins *et al.*, 1986) has shown conservation of the N-terminal to be important for biological activity. Moreover, the N-terminal fragments CGRP-(1-12) and CGRP-(1-15) have been reported to cause CGRP-like vasodilatation in the anaesthetized rat (Maggi *et al.*, 1990), suggesting that, in terms of vasodilatation, the active region of the peptide may well be located in the N-terminal. However, since the potencies of these fragments were 100-1000 fold less than the intact CGRP molecule, it could be argued

that the middle and C-terminal regions are important for maximum peptide-receptor interaction. In light of these findings, this study was undertaken to investigate whether a panel of MAbs to CGRP could influence its vasodilator effect in the PCAs. Our data indicate that in the presence of MAbs that map to different epitope regions along the peptide, the vasodilator effect of CGRP was modified in several ways.

Firstly, some of the MAbs tested did not affect the CGRP response, hence despite their size (molecular wt. 150,000) in comparison to CGRP (molecular wt. 3789), once bound to the peptide they do not prevent receptor coupling. Secondly, of the N-terminal MAbs tested (all binding to epitopes within the first 13 amino acids), CN1 and CRA3 did not significantly affect the CGRP response whilst CRA5 inhibited its vasodilator effect. Although the explanation for this disparity is not clear from the data in the present study, further investigations into the epitope mapping of these MAbs suggest that they see different epitopes in the mutual mapping region. Firstly, of the N-terminal MAbs, only CN1 sees chicken CGRP and β-hCGRP (Andrew *et al.*, 1990). These two forms of CGRP differ from α-hCGRP, within the first 7 amino acids, by a point change from asparganine to aspartic acid at the third amino acid. Hence, CN1 is less specific than CRA5 or CRA3 in binding α-hCGRP. Secondly, CRA5 and CRA3 can also bind the peptide fragment (1–7) but it is important to note that against this fragment a stronger signal was seen with CRA5 than with CRA3, (Andrew, D., personal communication), suggesting that, unlike CRA5, the epitope to CRA3 is not fully contained in the (1–7) peptide.

Previous studies of general peptide mapping (Kabat, 1970) using MAbs have shown sequential epitopes to be in the region of 5–8 residues in length. Although the N-terminal MAbs see an epitope in the (1–13) region of CGRP, they have potentially different hexamer epitopes to which they can bind and so it is not surprising that CRA3 and CN1 differed in their ability to modify the CGRP-induced effect in comparison to CRA5. Furthermore, the calculated binding affinity constants determined suggest that all the N-terminal MAbs bind strongly to the CGRP molecule. When considered together, these results suggest that CRA5 may inhibit the peptide response by binding to a different epitope from CRA3 or CN1 within the mutual mapping region, on the CGRP molecule which is responsible for CGRP-receptor interaction. Although binding studies showed CRA5 to have a higher binding affinity constant than both CN1 and CRA3, it would seem unlikely that the discrepancies of their actions could be solely attributed to at most a 4 fold difference in these values. A further important consideration when discussing the effects of antibody-peptide complexes is the possibility of their dissociation upon administration to the organ bath. This would seem unlikely given the relatively high binding affinity constants for the N-terminal MAbs. Moreover, if dissociation had occurred within the 6 min dose cycle this would have been highlighted by distortion of the CGRP-response curve which was not the case.

Of the C-terminal and middle region MAbs tested, CRA2 (C-terminal) did not modify the CGRP response whilst CB3 (C-terminal) and CRA8 (middle-region) enhanced its effects. The discrepancies of the two C-terminal MAbs can be explained by the antibodies binding to different areas of the CGRP molecule as epitope mapping studies have shown CB3 sees the fragment CGRP (21–37) whilst CRA2 does not (Andrew *et al.*, 1990). Potentiation of the CGRP response could not be attributed to differences in binding affinities as the binding affinity constant determined for CB3 (Andrew *et al.*, 1990) was similar to those obtained for the N-terminal MAbs. Previous workers, investigating solution structures of CGRP by circular dichroism spectroscopy (Hubbard *et al.*, 1991), have shown the N-terminal to contain up to 20% alpha-helix in aqueous solution whilst the C-terminal is less well defined with a random coil structure which exists in a conformational equilibrium. Furthermore, studies of the interactions of CGRP with Fab' fragments of CB3 in solution by nuclear magnetic resonance have shown that a conformational change occurs in the peptide on binding (Hubbard, J., personal communication). Therefore, if the peptide exists in a conformational equilibrium in solution, augmentation of the CGRP response could occur if CB3 or CRA8 are binding to the peptide in such a way as to stabilize the molecule in a particular structural arrangement which is more favourable for receptor coupling.

To summarise, some but not all of the MAbs tested modified the vasodilator effect of CGRP. Those which modified the response have done so by binding to a particular region of the peptide which is important in its activity. Data obtained by use of this novel approach, suggest that the active site of the peptide may be located in the N-terminal and that the C-terminal or middle region of the peptide may play an important role in the structural conformation necessary for peptide-receptor coupling.

References

ANDREW, D.P., BIDGOOD, T.D., BOSE, C., BROWN, D., GALFRE, G. & SHERWOOD, M. (1990). Monoclonal antibodies distinguishing alpha- and beta- forms of calcitonin gene-related peptide. *J. Immunol. Methods*, **134**, 87–94.

BENY, J., BRUNET, P.C. & HUGGEL, H. (1989). Effects of substance P, calcitonin gene-related peptide and capsaicin on tension and membrane potential of pig coronary artery in vitro. *Reg. Pept.*, **25**, 25–36.

CHIBA, T., YAMAGUCHI, A., YAMATANI, T., NAKAMURA, A., MORASHITA, T., INUI, T., FUKASE, M., NODA, T & FUJITA, T. (1989). Calcitonin gene-related peptide receptor antagonist human CGRP–(8–37). *Am. J. Physiol.*, **256**, E331–E335.

FOULKES, R., SHAW, N.E., BOSE, C.C. & HUGHES, B. (1991). Differential vasodilator profile of calcitonin gene-related peptide (CGRP) in large and small diameter pig coronary artery rings and the effect of CGRP (8–37) on these responses. *Eur. J. Pharmacol.*, **201**, 143–149.

GARDINER, R.M., COMPTON, A.M., KEMP, P.A., BENNETT, T., BOSE, C., FOULKES, R. & HUGHES, B. (1990). Antagonistic effect of human α-CGRP (8–37) on the in vivo regional haemodynamic actions of human α-CGRP. *Biochem. Biophys. Res. Commun.*, **171**, 938–943.

HUBBARD, J.A.M., MARTIN, S.R., CHAPLIN, L.C., BOSE, C. & KELLY, S.M. (1991). Solution structures of calcitonin gene-related peptide analogues of calcitonin gene-related peptide and amylin. *Biochem. J.*, **275**, 785–788.

KABAT, E.A. (1970). Heterogeneity and structure of antibody-combining sites. *Ann. N.Y. Acad. Sci.*, **169**, 43–54.

MAGGI, C.A., ROVERO, P., GIULIANI, S., EVANGELISTA, S., REGOLI, D. & MELI, A. (1990). Biological activity of N-terminal fragments of calcitonin gene-related peptide. *Eur. J. Pharmacol.*, **179**, 217–219.

SANO, Y., HIROSHIMA, O., YUZURIHA, T., YAMOTO, C., SAITO, A., KIMURA, S., HIRABAYASHI, T. & GOTO, K. (1989). Calcitonin gene-related peptide-binding sites of porcine cardiac muscles and coronary arteries: solubilization and characterization. *J. Neurochem.*, **52**, 1919–1924.

TIPPINS, J.R., DI MARZO, V., PANICO, M., MORRIS, H.R. & MACINTYRE, I. (1986). Investigation of the structure/activity relationship of human calcitonin gene-related peptide (CGRP). *Biochem. Biophys. Res. Commun.*, **134**, 1306–1311.

(Received September 23, 1991
Revised January 13, 1992
Accepted January 15, 1992)

Br. J. Pharmacol. (1992), **106**, 199–207 © Macmillan Press Ltd, 1992

Actions of arginine polyamine on voltage and ligand-activated whole cell currents recorded from cultured neurones

[1]Roderick H. Scott, †Marva I. Sweeney, †Evgeny M. Kobrinsky, †Hugh A. Pearson, *Graham H. Timms, *Ian A. Pullar, *Susan Wedley & †Annette C. Dolphin

Department of Physiology, St Georges Hospital Medical School, Cranmer Terrace, London SW17 0RE; †Department of Pharmacology, Royal Free Hospital School of Medicine, London NW3 2PF and *Lilly Research Centre Ltd., Eli Lilly and Company, Erl Wood Manor, Windlesham, Surrey, GU20 6PH

1 Toxins from invertebrates have proved useful tools for investigation of the properties of ion channels. In this study we describe the actions of arginine polyamine which is believed to be a close analogue of FTX, a polyamine isolated from the American funnel web spider, *Agelenopsis aperta.*

2 Voltage-activated Ca^{2+} currents and Ca^{2+}-dependent Cl^- currents recorded from rat cultured dorsal root ganglion neurones were reversibly inhibited by arginine polyamine (AP; 0.001 to 100 μM). Low voltage-activated T-type Ca^{2+} currents were significantly more sensitive to AP than high voltage-activated Ca^{2+} currents. The IC_{50} values for the actions of AP on low and high voltage-activated Ca^{2+} currents were 10 nM and 3 μM respectively. AP was equally effective in inhibiting high voltage-activated currents carried by Ba^{2+}, Sr^{2+} or Ca^{2+}. However, AP-induced inhibition of Ca^{2+} currents was attenuated by increasing the extracellular Ca^{2+} concentration from 2 mM to 10 mM.

3 The actions of AP on a Ca^{2+}-independent K^+ current were more complex, 1 μM AP enhanced this current but 10 μM AP had a dual action, initially enhancing but then inhibiting the K^+ current.

4 γ-Aminobutyric acid–activated Cl^- currents were also reversibly inhibited by 1 to 10 μM AP. In contrast N-methyl-D-aspartate currents recorded from rat cultured cerebellar neurones were greatly enhanced by 10 μM AP.

5 We conclude that at a concentration of 10 nM, AP is a selective inhibitor of low threshold T-type voltage-activated Ca^{2+} currents. However, at higher concentrations 1–10 μM AP interacts with ion channels or other membrane constituents to produce a variety of actions on both voltage and ligand gated ion channels.

Keywords: Arginine polyamine; voltage-activated calcium currents; cultured dorsal root ganglion neurones; cultured cerebellar neurones; GABA currents; NMDA currents

Introduction

The main objective of this work was to investigate the actions and selectivity of an arginine polyamine on voltage-activated Ca^{2+} currents. Several different types of neuronal voltage-activated Ca^{2+} channel have been described (Carbone & Lux, 1984; Nowycky *et al.*, 1985; Llinás *et al.*, 1989). Compounds based on natural products, such as invertebrate toxins, may prove useful pharmacological tools to dissect out the physiological functions of the different types of Ca^{2+} channel. So far, peptide toxins including ω-conotoxin GVIA (ω-CgTx) from the marine mollusc *Conus geographus (Olivera et al.*, 1985) and ω-agatoxins (IA and IIIA) from the American funnel web spider, *Agelenopsis aperta* (Adams *et al.*, 1990) have been studied. The inhibition caused by ω-CgTx is usually incomplete (McCleskey *et al.*, 1987; Kasai *et al.*, 1987; Plummer *et al.*, 1989; Scott *et al.*, 1990a) but it remains unclear whether it inhibits a distinct subclass of high voltage-activated Ca^{2+} channel. ω-Agatoxin IA (ω-Aga-IA), although a very potent inhibitor of voltage-activated Ca^{2+} currents did not show much selectivity and differentiated poorly between low voltage-activated T-type current and high voltage-activated Ca^{2+} currents (Scott *et al.*, 1990b). In contrast ω-Agatoxin IIIA did not inhibit T-type current but revealed a pharmacologically distinct high threshold Ca^{2+} current (Mintz *et al.*, 1991). Recently a polyamine FTX, also from *A. aperta* has been shown to inhibit a novel voltage-activated Ca^{2+} channel isolated from the squid giant synapse and cerebellum (Llinás *et al.*, 1989; Lin *et al.*, 1990). It has been suggested that FTX has a structure close to arginine polyamine (AP) (Cherksey *et al.*, 1989), although the complete structure of FTX has yet to be determined, and unfortunately this compound is not yet widely available. However, crude venom from *A. aperta* will contain not only FTX but also the ω-agatoxins and other peptide toxins, and is unlikely to identify selectively novel Ca^{2+} channels. Polyamines are found in the venom of a variety of invertebrates including wasps and spiders (Jackson & Usherwood, 1988). *A. aperta* venom alone contains at least five low molecular weight (489–505) acylpolyamines (α-agatoxins) which show a use-dependent block of e.p.s.ps and glutamate potentials (Adams *et al.*, 1989; Quistad *et al.*, 1990; Jasys *et al.*, 1990). Polyamines have been shown to interact with a variety of glutamate receptors including the N-methyl-D-aspartate (NMDA) type, and produce several different effects (Ransom & Stec 1988; Kerry *et al.*, 1989; Priestly *et al.*, 1989; Williams *et al.*, 1990; Brackley *et al.*, 1990). In addition to studying the actions of AP on voltage and ligand gated currents in rat cultured DRG neurones and a sensory neurone cell line we have also investigated the effect of AP on NMDA currents recorded from cultured cerebellar neurones, to obtain a broad view of its actions.

Methods

Primary cultures

Dorsal root ganglia (DRG) were dissected from 2 or 3 day old rats. The DRG cells were dissociated and plated on

[1] Author for correspondence.

polyornithine-laminin-coated coverslips. The cultures were maintained in a serum-free defined medium (Bottenstein *et al.*, 1980; Winter 1987) for up to 3 weeks, at 37°C in humidified air containing 5% CO_2.

Cerebellar cells were dispersed from cerebella of 6 day old rats (Huston *et al.*, 1990). Cerebellar neurones were plated on 2 cm^2 coverslips at 5×10^6 cells/coverslip and maintained in modified Eagle's medium containing 10% heat-inactivated horse serum, 50 iu ml^{-1} penicillin, 50 $\mu g\ ml^{-1}$ streptomycin, 25 $\mu l\ ml^{-1}$ chick embryo extract, 39 mM glucose, 2 mM glutamine and 23 M KCl. The cerebellar neurones were kept at 37°C in humidified air containing 5% CO_2. After 48 h, fluorodeoxyuridine (80 μM), was added to reduce proliferation of non-neuronal cells. The culture medium was replaced with fresh medium every 4 days and the cells used after 3 weeks in culture.

Cell lines

The sensory neurone × neuroblastoma cell line (ND7–23) was grown in culture as previously described (Wood *et al.*, 1990), and experiments were performed on cells differentiated as described for at least 8 days.

Electrophysiology

The whole cell recording variant of the patch clamp technique (Hamill *et al.*, 1981) was used to record voltage and ligand-gated currents. Low resistance (2–4 MΩ) patch pipettes were used and cells were voltage-clamped with an Axoclamp-2a switching voltage clamp amplifier, operated at a sampling rate of 20–30 kHz or an Axopatch-ID amplifier for experiments on ND7–23 cells. Experiments were conducted at room temperature (21–24°C), and the cells allowed to equilibrate for 5 min following disruption of the membrane patch between the pipette and cytoplasm and entry into the whole cell recording configuration. Voltage-activated currents were evoked at a frequency of 0.1–0.03 Hz. GABA, NMDA and AP were applied by low pressure ejection (less than about 7 kPa) from a micropipette (tip diameter of 10 μm) placed about 100 μm from the cells. Data were stored on a DAT recorder and either digitized at 2–5 kHz for analysis or replayed and plotted with a Gould pen recorder. The voltage-activated currents are shown following digital subtraction of scaled linear leakage and capacitance currents. All data are given as mean ± standard error of the mean (s.e.mean).

Solutions for electrophysiology

Ca^{2+} channel currents and GABA currents in DRG neurones were recorded in a recording medium containing (in mM): choline chloride 130, KCl 3, $MgCl_2$ 0.6, $NaHCO_3$ 1.0, HEPES 10, glucose 4, tetraethylammonium (TEA) bromide 25, tetrodotoxin 0.0025 and $CaCl_2$ 2 or 10, or $BaCl_2$ 2 or $SrCl_2$ 2. Ca^{2+} channel currents in ND7–23 cells were recorded as previously described (Pearson *et al.*, 1991). All recording solutions were adjusted to pH 7.4 with NaOH and to 320 mOsM by addition of sucrose. Sodium currents (I_{Na}) were recorded with a NaCl based recording medium rather than choline chloride, and tetrodotoxin was not present. The same extracellular solution was used to record NMDA currents as voltage-activated Ca^{2+} currents except that $MgCl_2$ was excluded.

Patch electrodes were also filled with different solutions depending on the type of current being studied. Voltage-activated Ca^{2+} and Na^+ channel currents were recorded using a patch solution containing (in mM): CsCl 140, $CaCl_2$ 0.1, EGTA 1.1, $MgCl_2$ 2, ATP disodium dihydrogen salt 2 and HEPES 10. The free Ca^{2+} in this solution was about 1.6×10^{-8} M. The pH was adjusted to 7.2 with Tris and the osmolarity to 310 mOsm with sucrose. The same patch solution as above was used to record voltage-activated K^+ currents but CsCl was replaced with KCl. NMDA currents were also recorded with this patch solution but $MgCl_2$ was omitted.

Chemistry of arginine polyamine

Figure 1 summarizes the synthesis to arginine polyamine VI. *t*-Butoxycarbonylation of the diamine I (Israel *et al.*, 1964) was based on the method of Lurdes *et al.* (1964) using ditert-butyldicarbonate [$(Boc)_2O$] and dimethylaminopyridine (DMAP) to give the nitrile II. Reduction of the nitrile II to the amine III (Nakamura, 1988) was accomplished using Raney nickel (Israel *et al.*, 1964) in the presence of ammonia. Coupling of the amine III with Boc-arg(Boc)-OH IV using dicylohexylcarbodiimide (DCC) and 1-hydroxybenzotriazole (HOBt) (Jasys *et al.*, 1985) provided the penultimate product V, which was readily deprotected by dissolving in ethanolic hydrogen chloride to generate arginine polyamine VI as a hydroscopic solid. ^1H nuclear magnetic resonance (NMR) spectra were obtained on a Bruker AM300 spectrometer with tetramethylsilane or $CDCl_3$ as internal reference. Infrared spectra were recorded on a Bruker FTIR IFS-48 instrument as capillary films or potassium bromide discs. Mass spectra were recorded on a VG 7070E spectrometer and the optical rotation was performed on a Bellingham and Stanley P.70–4 polarimeter. Extracts were washed with water and dried ($MgSO_4$).

[^{125}I]-ω-conotoxin GVIA binding assay

Membrane preparation Membranes from rat cerebral cortex were prepared as described by Wagner *et al.* (1988). Male Wistar rats (275–350 g) were killed by cervical dislocation and their brains rapidly removed and dissected over ice. The cerebral cortices were homogenized, at a concentration of 50 mg wet wt ml^{-1}, in 50 mM HEPES buffer pH 7.4 at 4°C with a Teflon/glass homogenizer (0.01–0.015 mm clearance). After centrifugation at 40,000 *g* for 15 min, the resulting pellet was resuspended in the same volume of 50 mM HEPES pH 7.4 containing 10 mM EDTA and was incubated at 4°C for 30 min. After recentrifugation at 40,000 *g* for 10 min, the tissue was resuspended in HEPES pH 7.4 which had been treated with chelating resin (Na^+ form, Sigma) to give a concentration of 20 mg wet weight ml^{-1}. The protein concentration of the tissue preparation (range 1.0–2.0 mg ml^{-1}) was then estimated (Lowry *et al.*, 1951). Membranes prepared in this manner could be stored at − 20°C for one month without any alteration in the binding of [^{125}I]-ω-CgTx.

Binding assay All solutions and dilutions were made in chelating resin-treated HEPES, pH 7.4, containing 0.1% bovine albumin. Cortical membranes (5 μg) were incubated at 25°C for 30 min with various concentrations of the test substance in a volume of 0.4 ml. After the addition of 100 μl, 125 pM [^{125}I]-ω-CgTx (Amersham International), the mixture was incubated for a further 15 min at 25°C and then filtered, by use of a Brandel cell harvester, through GF/C papers which had been soaked in the filtration buffer (10 mM Tris pH 7.7 containing 160 mM choline chloride and 0.1% bovine albumin). The filters were washed three times with 4 ml of the filtration buffer and, after drying, the bound [^{125}I]-ω-CgTx estimated with a γ-spectrometer.

Results

Action of arginine polyamine on voltage-activated Ca^{2+} channel currents

AP was found to inhibit both low voltage-activated T-type and high voltage-activated Ca^{2+} currents in cultured DRG neurones. These inhibitory effects of AP were dose-dependent (Figure 2a) and reversible. Not all DRG neurones express

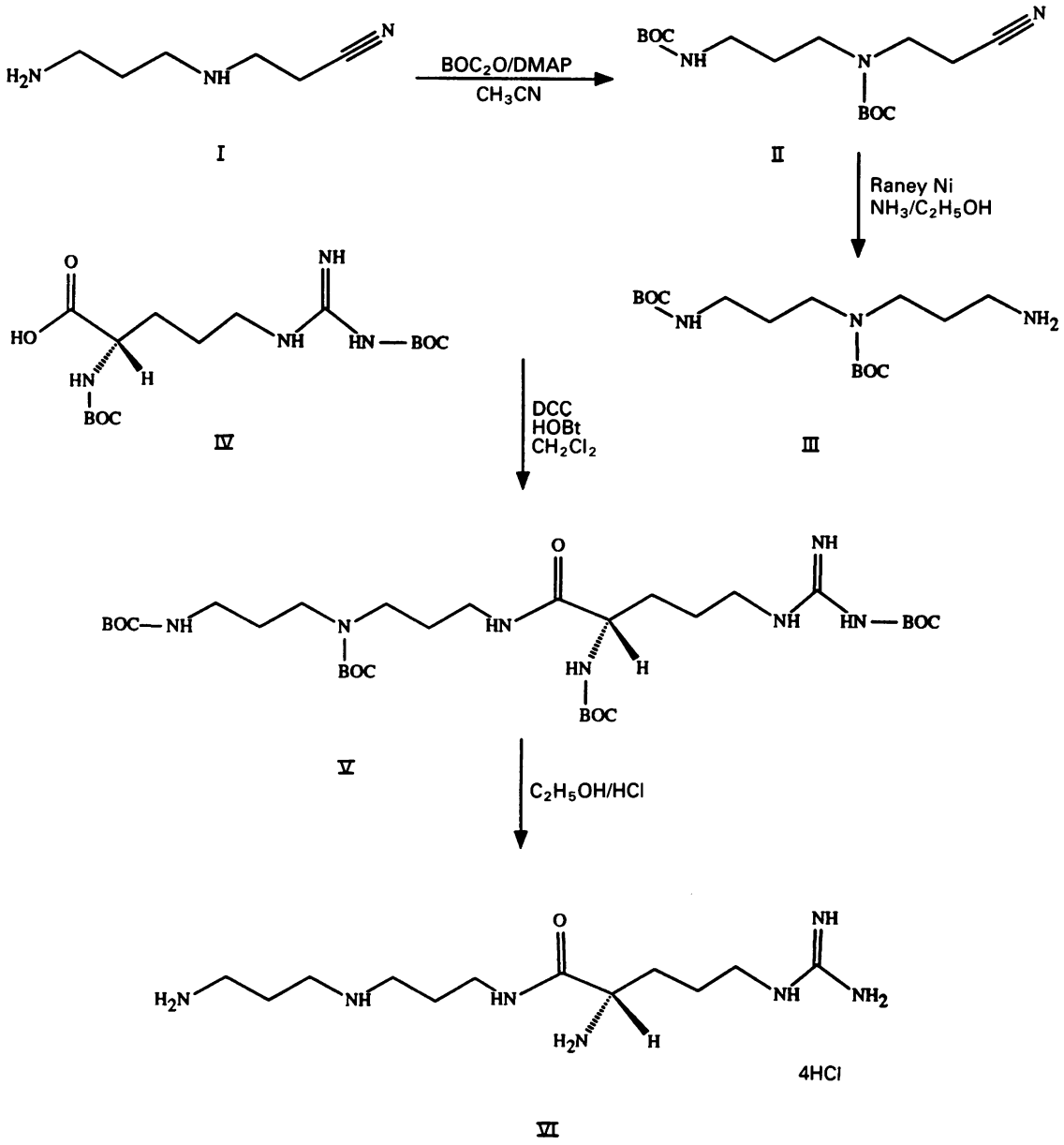

Figure 1 Synthesis of N-(7-amino-4-azaheptyl)-L-argininamide tetrahydrochloride, which is also called N-(4,8-diazoctl)-L-argininamide tetrahydrochloride, depending on the polyamine nomenclature system used: (I) = 7-amino-4-azaheptanonitrile; (II) = N,N^{I}-di (tert-butoxycarbonyl) -7-amino-4-azaheptanonitrile; (III) = N,N^{I}-1,4-di (tert-butoxycarbonyl) -4-azaheptane-1,7-diamine; (IV) = Boc-arg (Boc)-OH; (V) = N-[N,N^{I}-di(tert-butoxycarbonyl)-7-amino-4-azaheptyl]-N^{2},N^{G}-di-(tert-butoxycarbonyl)-L-argininamide tetrahydrochloride; (VI) = N-(7-amino-4-azaheptyl)-L-argininamide tetrahydrochloride.

T-type Ca^{2+} currents, a previous study revealed 55% of cells ($n = 161$) had low threshold T-type Ca^{2+} currents (Scott *et al.*, 1990a). The T-type currents in this study were identified by their low voltage threshold of activation and by their complete inactivation within a 100 ms voltage step command. The low voltage-activated Ca^{2+} currents were significantly more sensitive to AP than the high voltage-activated Ca^{2+} currents. The IC_{50} values (estimated by eye) for low and high voltage-activated Ca^{2+} current inhibition by AP were 10 nM and 3 μM respectively (Figure 2a). From a holding potential (V_h) of -90 mV the peak amplitude of the low voltage-activated Ca^{2+} current at a clamp potential (V_c) of -30 mV was -0.35 ± 0.05 nA under control conditions, and -0.18 ± 0.03 nA ($n = 4$) at equilibration following 3 to 5 min application of 10 nM AP. The reduction in low voltage-activated Ca^{2+} current produced by 10 nM AP was not accompanied by any change in voltage-dependence of activation (Figure 2b). At 10 nM AP had no effect on leak currents or high voltage-activated Ca^{2+} currents (Figure 2c).

Inward and outward high voltage-activated Ca^{2+} channel currents were also inhibited by AP but at higher concentrations between 0.1 μM and 100 μM (Figures 2a and 3). The outward Ca^{2+} channel currents have been shown to be carried predominantly by Cs^{+} and K^{+} leaving the cell through Ca^{2+} channels when the membrane potential was depolarized to a V_c of 100 mV (Bean, 1989; Dolphin & Scott, 1990). Three to five minutes application of 10 μM AP reduced the inward Ca^{2+} currents ($V_c = 0$mV) and outward current ($V_c = 100$ mV) by $62 \pm 4\%$ and $53 \pm 9\%$ ($n = 5$) respectively. AP (10 μM) inhibited equally the inward and outward Ca^{2+} channel currents measured at the peak and end (last 5 ms) of 100 ms voltage step commands. The control inward Ca^{2+} current had a mean amplitude of -1.08 ± 0.2 nA which inactivated during the 100 ms voltage step command to -0.61 ± 0.08 nA. In the presence of 10 μM AP the mean inward Ca^{2+} current was reduced to -0.37 ± 0.06 nA and

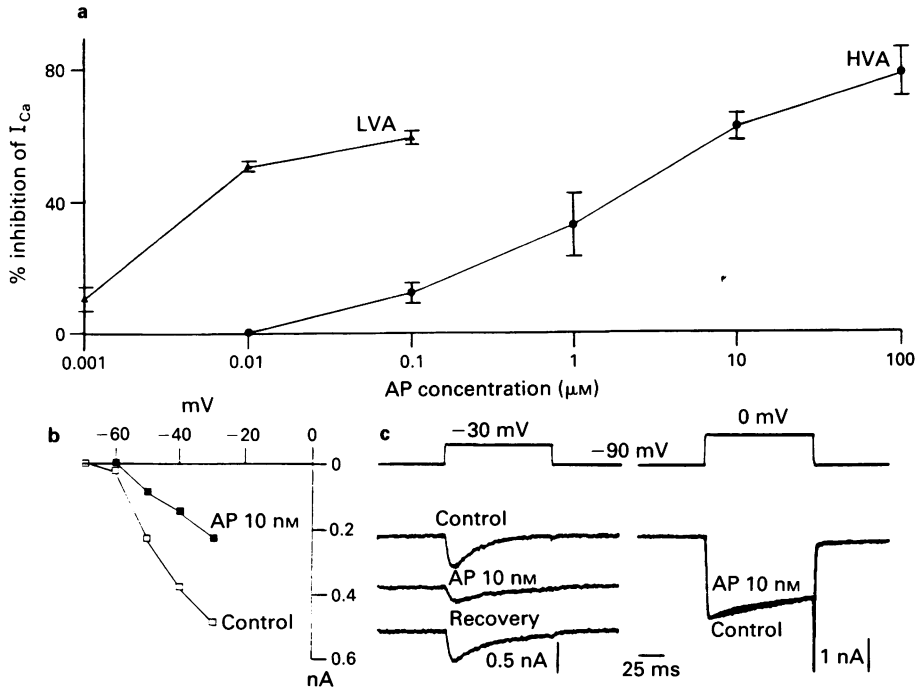

Figure 2 Effect of arginine polyamine (AP) on voltage-activated Ca^{2+} currents recorded from DRG neurones. (a) Dose-response relationships for low voltage-activated (LVA) T-type Ca^{2+} current and high voltage-activated (HVA) Ca^{2+} current and inhibition by AP. Currents were recorded from cells bathed in recording medium containing 2 mM Ca^{2+}. Each value on the dose-response curve was derived from 5 to 7 separate applications to different DRG neurones. (b) Current-voltage relationship for low voltage-activated T-type current showing the inhibition produced by 10 nM AP. (c) Traces of low voltage-activated T-type current activated from a V_h of − 90 mV by 100 ms voltage step commands to − 30 mV. Currents are illustrated under control conditions, and after 3 min continuous application of 10 nM AP. Low and high voltage-activated Ca^{2+} currents illustrated were recorded from the same DRG neurone.

− 0.2 ± 0.04 nA ($n = 5$) for current measured at the beginning and end of the voltage step. The mean control outward Ca^{2+} channel current at a V_c of 100 mV was + 1.12 ± 0.29 nA and the current did not decay significantly during a 100 ms voltage step. AP (10 μM) reduced the mean outward current to + 0.47 ± 0.06 nA ($n = 5$). The activation curves for high voltage-activated Ca^{2+} currents showed that AP did not significantly shift the voltage-dependence of activation.

The inhibitory action of AP (10 μM) was similar at a depolarized holding potential (V_h − 30 mV). The mean amplitude of Ca^{2+} currents activated from V_h of − 30 mV at V_c of 0 mV was − 0.39 ± 0.05 nA under control conditions and − 0.11 ± 0.02 nA ($n = 7$) in the presence of 10 μM AP. These values give a mean percentage inhibition produced by 10 μM AP of 67 ± 5% ($n = 7$). The outward Ca^{2+} channel current activated from V_h of − 30 mV by depolarizing to V_c of + 100 mV was similarly reduced by 62 ± 5% ($n = 5$) by AP (10 μM).

Application of 10 μM AP also reduced the input conductance of the DRG neurones which was calculated from leak currents activated at a V_c of − 150 mV (Figure 3) by 0.8 ± 0.4 nS ($n = 9$) from a resting level of 5.4 ± 0.5 nS. All data shown are given following leak subtraction to take into account the reduction in leak current. Although 10 μM AP inhibited Ca^{2+} currents when applied to the extracellular environment, inclusion of 100 μM AP in the patch solution did not attenuate inward high voltage-activated Ca^{2+} channel currents ($n = 6$). Initial Ca^{2+} currents were compared with currents measured 5 min after entering the whole cell recording configuration, the mean percentage change was 20 ± 12% ($n = 6$) and this apparent increase was not significant. Surprisingly, the mean outward Ca^{2+} channel current was significantly attenuated by intracellular AP. The initial outward current at V_c + 100 mV from V_h − 80 mV was reduced from + 1.07 ± 0.27 nA to + 0.66 ± 0.13 nA ($n = 6$; paired Student's t test, $P < 0.03$) over 5 min with patch pipettes containing AP. In contrast, no significant change in outward current occurred over the first 5 min of recording in control cells.

The inhibitory action of extracellular AP on both low and high voltage-activated Ca^{2+} currents was attenuated by elevating the extracellular Ca^{2+} concentration from a normal level of 2 mM to 10 mM (Figure 4a). In recording medium containing 10 mM Ca^{2+}, the peak inward Ca^{2+} current activated from V_h of − 90 mV by 100 ms voltage step commands ($V_c = 0$ mV) was − 2.01 ± 0.29 nA and − 1.34 ± 0.25 nA ($n = 7$) in the absence and presence of 10 μM AP respectively. Although the data were variable the mean percentage inhibition of Ca^{2+} current produced by AP (10 μM) applied for 3 to 5 min was 32 ± 10% ($n = 7$) with 10 mM extracellular Ca^{2+} and this was significantly less than 62 ± 4% ($n = 5$) inhibition observed with 2 mM extracellular Ca^{2+} (unpaired Student's t test, $P < 0.02$). Similar observations were made when studying T-type current which was completely blocked by 10 μM AP ($n = 2$) when 2 mM extracellular Ca^{2+} was present, but when the cells were bathed with recording medium containing 10 mM Ca^{2+}, AP (10 μM) only reduced the T-type current by 52 ± 10% ($n = 3$).

To investigate the actions of AP further, we studied the inhibitory effect of 10 μM AP on barium and strontium currents. Inward and outward Ca^{2+} channel currents recorded in the presence of extracellular Ca^{2+}, Ba^{2+} or Sr^{2+} were all equally inhibited by AP (10 μM) (Table 1).

Ca^{2+}-activated Cl^- currents were observed as slowly decaying inward tail currents following activation of Ca^{2+} currents by 100 ms depolarizing voltage step commands to 0 mV, in cells loaded with CsCl patch solution. The Ca^{2+}-dependent Cl^- tail currents were found to have a reversal potential at the Cl^- equilibrium potential and were sensitive to the Cl^-

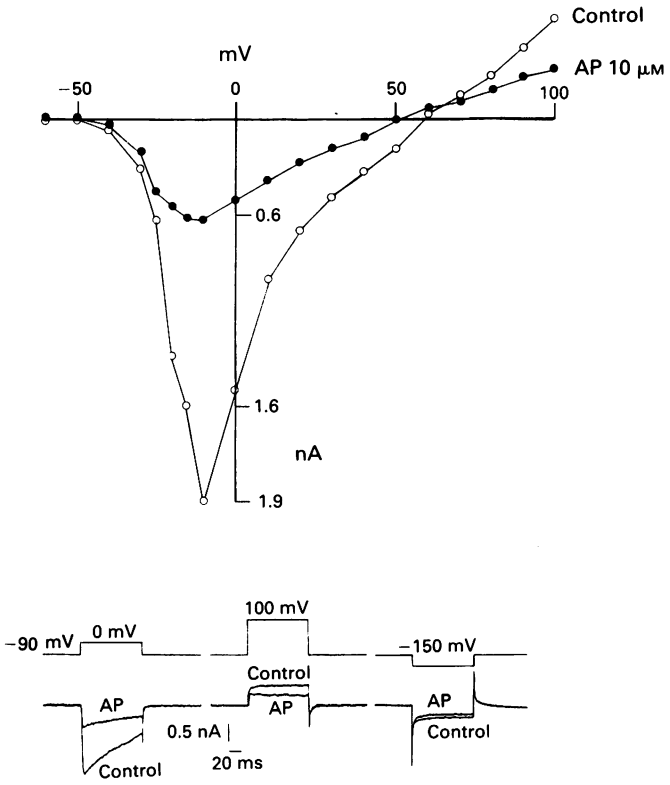

Figure 3 A current-voltage relationship illustrating arginine polyamine (AP)-induced inhibition of voltage-activated Ca^{2+} currents. Inward and outward Ca^{2+} channel currents activated from V_h − 90 mV are inhibited by 10 μM AP. Inset traces show inhibition of the maximum inward Ca^{2+} current and the outward current activated at a V_c of + 100 mV. The third inset trace shows AP-induced reduction in the leak current generated by hyperpolarizing voltage step commands to a V_c of − 150 mV. No low voltage-activated T-type current was expressed in this cell.

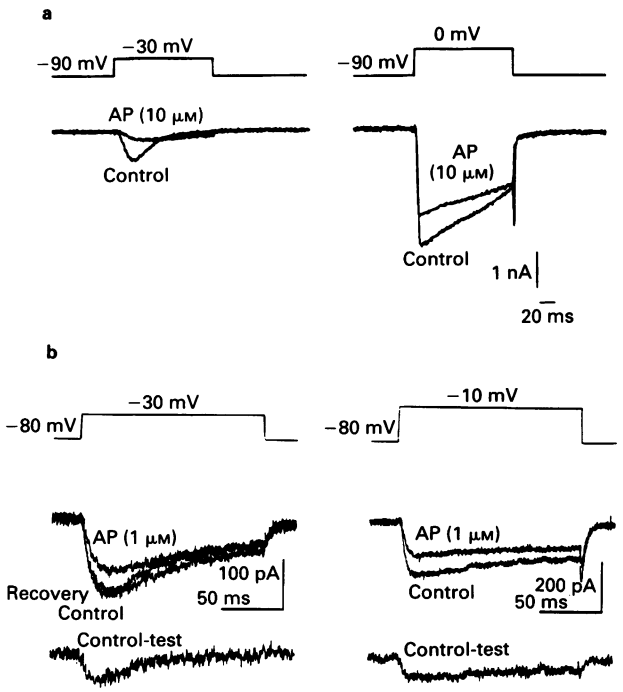

Figure 4 (a) Traces show inhibition of voltage-activated Ca^{2+} currents recorded from DRG neurones bathed in recording medium containing 10 mM Ca^{2+}. Arginine polyamine (AP, 10 μM)-induced inhibition of Ca^{2+} currents was less apparent with elevated extracellular Ca^{2+}. (b) Inhibition of Ba^{2+} currents in ND7–23 cells produced by 1 μM AP. The recording medium contained 2.5 mM Ba^{2+}. Current records show the effect of AP on a low voltage-activated current (left) and a high voltage-activated current (right). The difference current inhibited by AP is shown beneath the current traces.

Table 1 Action of arginine polyamine (10 μM) on inward and outward Ca^{2+} channel currents recorded with 2 mM extracellular Ca^{2+} Ba^{2+} or Sr^{2+}

Divalent Cation	*% inhibition of inward current* (Vc = 0 mv)	n	*% inhibition of outward current* (Vc = 100 mV)	n
Ca^{2+}	62 ± 4	5	53 ± 9	5
Ba^{2+}	51 ± 12	5	50 ± 8	4
Sr^{2+}	64 ± 8	7	53 ± 8	5

All results are mean ± s.e.mean.

channel blocker 5-nitro 2-(3-phenylpropylamino) benzoic acid (NPPB; 10 μM) (Currie & Scott, 1991).

As expected, given the inhibition of Ca^{2+} currents by AP, 10 μM-AP also reduced Ca^{2+}-activated Cl^- tail currents. The mean amplitude of Ca^{2+}-activated Cl^- tail currents measured 20 ms after the end of the voltage step command was reduced by 58 ± 8% ($n = 4$) by 10 μM AP. AP (1 μM) had no significant action on voltage-activated Na^+ currents recorded from DRG neurones held at a V_h of − 90 mV ($n = 6$).

The effect of arginine polyamine on voltage-activated Ca^{2+} channel currents in ND7–23 cells

The ability of AP to inhibit voltage-activated Ca^{2+} channel currents was confirmed in ND7–23 cells. When 2.5 mM Ba^{2+} was used as the charge carrier, low voltage-activated currents were observed in all differentiated ND7–23 cells examined. The mean current amplitude at V_c − 30 mV from V_h − 100 or − 80 mV was 102 ± 13 pA ($n = 17$). AP (1 μM) inhibited low voltage-activated currents by 44.5 ± 3.9% ($n = 17$) ($P < 0.001$). Where it was examined, in five experiments, recovery of 83.5 ± 10.2% was observed. High voltage-activated currents recorded at V_c 0 mV from V_h − 100 or − 80 mV were observed in 23% of cells ($n = 5$), and the mean current amplitude measured at the end of a 150 ms pulse was 50 ± 11 pA. This current was smaller than the low voltage-activated current, one reason being that smaller cells were used in these experiments, to obtain adequate space clamp. AP (1 μM) produced 29.5 ± 6.8% inhibition ($n = 5$), ($P < 0.02$) (Figure 4b). Complete reversal was observed in two cells.

The effect of arginine polyamine on ω-conotoxin GVIA binding

Under the conditions used, the binding of ω-CgTx to its sites on cortical membranes was irreversible and thus equilibrium conditions could not be established within the assay. AP inhibited the association of [^{125}I]-ω-CgTx with these sites giving an IC_{50} value of 18 ± 3 μM (Table 2). Other polybasic compounds such as the aminoglycosides (Knaus *et al.*, 1987; Wagner *et al.*, 1988) and the polyamine, spermine (Pullan *et al.*, 1990) have been shown to inhibit the binding of ω-CgTx to brain tissue. The IC_{50} obtained for AP is similar to that of spermine and streptomycin (Table 2) but it is an order of magnitude less active than the most active of the aminoglycosides, neomycin, which gave an IC_{50} of 1.4 ± 0.2 μM.

Table 2 Effect of arginine polyamine and other polybasic compounds on the binding of [^{125}I]-ω-conotoxin GVIA to rat cortical membranes

Compound	*IC_{50} (μM)*	n
Arginine polyamine	18 ± 3	3
Spermine	14 ± 4	6
Neomycin	1.4 ± 0.2	7
Streptomycin	28 ± 4	5

Results are mean ± s.e.mean.

Action of arginine polyamine on Ca^{2+}-independent K^+ currents

More complex actions of AP (1 and 10 μM) were observed when studying its effects on Ca^{2+}-independent K^+ currents. A large K^+ current can be recorded from about 60% of DRG neurones bathed in recording medium containing no added Ca^{2+}. This K^+ current is insensitive to TEA (25 mM) but is markedly inhibited by 4-aminopyridine (500 μM) (Dolphin & Scott, 1986). In this study, Ca^{2+} was usually included in the extracellular recording medium to improve seal formation between the patch pipette and cell membrane and TEA was added to inhibit TEA sensitive Ca^{2+}-activated K^+ currents. AP 1 μM, enhanced the Ca^{2+}-independent K^+ current by 112 ± 49% ($n = 4$). From a V_h of − 90 mV the mean peak amplitude of the K^+ current at a V_c of + 30 mV was increased from 0.95 ± 0.44 nA to 1.64 ± 0.46 nA ($n = 4$) during 3 to 7 min application of 1 μM AP. The substantial enhancement of Ca^{2+}-independent K^+ current by AP did not arise because the inward voltage-activated Ca^{2+} current was inhibited, for two reasons. Firstly, the K^+ current was studied at a V_c of + 30 mV or + 50 mV (Figure 5). At these voltages inward Ca^{2+} currents were small or not observed because the null potential (where there is no net inward or outward current) for Ca^{2+} currents is close to + 50 mV (Figure 3). Secondly, preliminary experiments carried out in recording medium with no added Ca^{2+} showed that 1 μM AP enhanced the Ca^{2+}-independent K^+ current by 89% ($n = 2$). Application of 10 μM AP produced dual responses, initially enhancing the K^+ current and subsequently reducng it to less than control levels. After 30 s application of 10 μM AP, the peak K^+ current activated at V_c of + 30 mV was increased by 24 ± 6% ($n = 5$). Continuing application of 10 μM AP for 5 min resulted in a mean percentage inhibition of the peak K^+ current compared with controls of 28 ± 15% ($n = 5$). This K^+ current under control conditions did not run-down over the first 10 min of recording.

Arginine polyamine modulates ligand-gated ion channels

DRG neurones have both $GABA_A$ receptor chloride ion channel complexes and $GABA_B$ receptors (Dunlap, 1981). $GABA_B$ receptors are linked via G-proteins to voltage-activated Ca^{2+} channels and when activated do not cause any change in membrane potential or input conductance in DRG neurones (Dolphin & Scott, 1987).

Large inward Cl^- currents activated by γ-aminobutyric acid (GABA) can be recorded from DRG neurones loaded with CsCl patch solution. Under our experimental conditions the Cl^- equilibrium potential (E_{Cl}) was shifted to around − 1 mV. A 100 ms pulse of 100 μM GABA produced a − 1.20 ± 0.22 nA ($n = 12$) inward current which decayed during GABA application. The $t_{\frac{1}{2}}$ values for the rise of the inward GABA currents were about 100 ms, and GABA currents were activated from a V_h of − 90 mV at a rate of 1 every 3 min. Cells were washed between applications of GABA by low pressure perfusion of fresh saline. In spite of potential problems with desensitization we have clear evidence of dose-dependent inhibition of GABA currents by AP (1 and 10 μM). Simultaneous application of GABA (100 μM) and AP (1 μM) produced a 38 ± 5% ($n = 7$) smaller mean inward current compared to the mean control GABA currents derived by applying GABA alone before and after the experimental applications. A higher concentration of 10 μM AP produced greater inhibition of the GABA currents, reducing the peak amplitude by 58 ± 9% ($n = 5$) (Figure 6). AP, 10 nM, was found to have no action on GABA currents ($n = 2$).

Non-NMDA glutamate currents could also be activated in DRG neurones which had been maintained in culture for 1 week. The mean amplitude of these currents activated from a V_h of − 90 mV by 100 μM glutamate was 0.27 ± 0.03 nA ($n = 7$). The mean peak amplitude of glutamate currents was not significantly reduced by simultaneous application of glutamate and 10 μM AP (Figure 7a).

We were unable to obtain any NMDA currents from our DRG neurones maintained in culture for 1 or 3 weeks. However, cultured cerebellar neurones in culture for 2 to 3 weeks produced large NMDA responses when using Mg^{2+}-free intracellular and extracellular solutions. The type of cerebellar neurones used in this part of the study were likely not to be granule or Purkinje neurones, given their size, shape and low density. We believe that the NMDA-sensitive cells, which had round cell bodies with diameters of approximately 35 μM, were Basket cells, but this awaits further investigation. Of 10 cells investigated, 5 cells produced inward currents in response to a 100 ms pulse of 100 μM NMDA. The mean amplitude of the inward NMDA current-activated from a V_h of − 60 mV was − 0.73 ± 0.16 nA

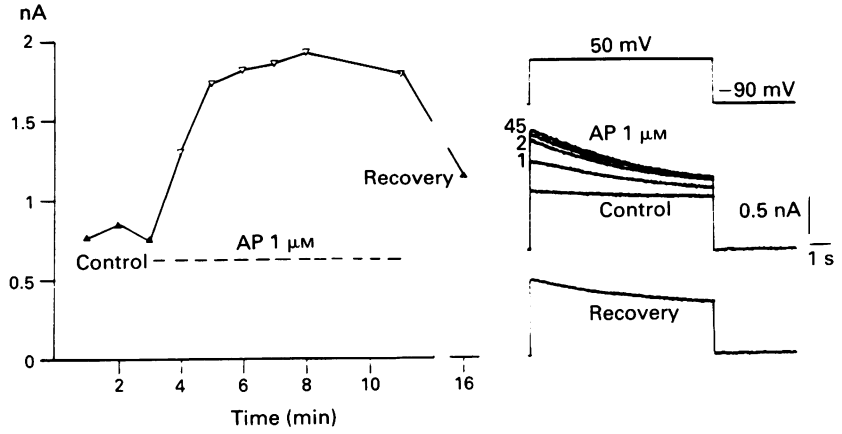

Figure 5 Action of arginine polyamine (AP, 1 μM) on voltage-activated Ca^{2+}-independent K^+ current. Graph shows time course of enhancement of K^+ current and partial recovery 6 min after removal of the AP pipette. Inset traces show a control K^+ current and the enhanced currents recorded 1,2,4 and 5 min in the presence of 1 μM AP, and partial recovery of the current. All currents are shown following subtraction of scaled leak currents.

($n = 6$) and the currents rapidly decayed. To limit problems with rapid NMDA current decay and overloading neurones with Ca^{2+}, the currents were activated 3 to 5 min apart and the cells microperfused with fresh saline between applications. Simultaneous application of 100 μM NMDA and 10 μM AP gave rise to a greatly enhanced inward current (Figure 7b), comparing the NMDA currents recorded before and after the response to the combined application of NMDA and AP. At a V_h of − 60 mV, NMDA currents had a mean peak amplitude of 0.44 ± 0.14 nA ($n = 3$), whereas the current enhanced by AP had a mean amplitude of 1.17 ± 0.58 nA ($n = 3$). AP, 10 nM, was found to have no action on NMDA currents ($n = 2$).

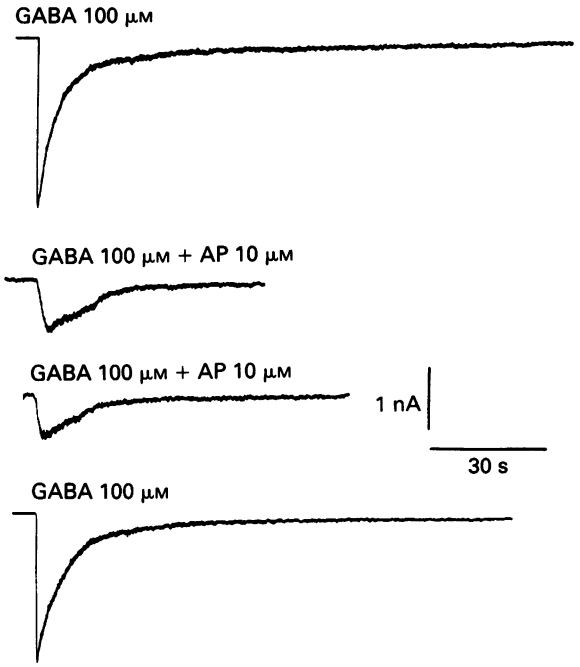

Figure 6 γ-Aminobutyric acid (GABA)-activated Cl^- currents are attenuated by 10 μM arginine polyamine (AP). Inward GABA-activated Cl^- curents were produced by 100 ms pulsed microperfusion of 100 μM GABA applied to DRG neurones loaded with CsCl patch solution. Simultaneous application of GABA and AP resulted in reduced inward Cl^- currents as illustrated by the central two traces. The bottom trace shows recovery of the GABA response, which is similar to the initial control current. DRG neurones were held at a V_h of − 90 mV for these experiments.

Discussion

AP produced diverse effects on a variety of different voltage-activated and ligand gated whole cell currents. However AP (1–10 nM) is a selective inhibitor of DRG neurone low voltage-activated T-type Ca^{2+} currents. This action highlights some similarities between DRG neurone T-type Ca^{2+} channels and the novel P-type channels described by Llinás and colleagues (Llinás *et al.*, 1989). Other properties that T- and P-type Ca^{2+} channels have in common include low threshold of activation, lack of irreversible inhibition by ω-CgTx, and small unitary conductance of the channels (Llinás *et al.*, 1989). However the use of crude venom to identify novel Ca^{2+} channels is complicated by the additional presence of the ω-agatoxins which have been shown also to inhibit voltage-activated Ca^{2+} channel currents in DRG neurones. There is clear overlap between ω-Aga-IA and both ω-CgTx and 1,4-dihydropyridine-sensitive components of high voltage-activated DRG Ca^{2+} channel currents (Scott *et al.*, 1990b). Higher concentrations of AP (0.1–100 μM) also inhibited high voltage-activated Ca^{2+} currents in DRG neurones. Differential inhibition was also seen of low voltage-activated Ba^{2+} currents by 1 μM AP in ND7–23 cells. DRG neurones and ND7–23 cells differ in their sensitivity to AP, suggesting some degree of heterogeneity of either voltage-activated Ca^{2+} channels or another site with which AP interacts. The reduction in both inward and outward Ca^{2+} channel currents is indicative of inhibition of ion permeation rather than a drug-induced shift in voltage-dependence. Inhibition of Ca^{2+}-activated Cl^- currents is consistent with inhibition of Ca^{2+} currents and previously reported inhibitory effects of FTX (Lin *et al.*, 1990).

The multiple effects of AP on a variety of whole cell currents suggests that AP has a number of sites of action. There is evidence from binding studies that NMDA receptor ion channel complexes have distinct polyamine binding sites.

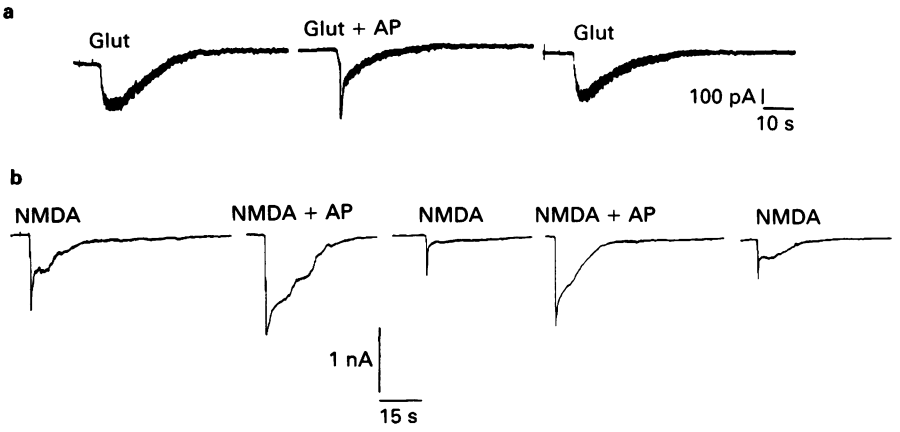

Figure 7 (a) Traces show the action of 10 μM arginine polyamine (AP) on non-N-methyl-D-aspartate (NMDA) glutamate responses recorded from DRG neurones maintained in culture for 1 week. Glutamate (Glut, 100 μM) responses were activated from a V_h of − 90 mV. The middle trace shows the glutamate current activated when glutamate and AP (10 μM) were simultaneously applied. Similar results were achieved when AP was also present in the bath. Five minutes recovery was allowed between each application of glutamate. (b) AP (10 μM) increases NMDA response recorded from cerebellar neurones. Inward NMDA currents were activated by 100 ms pulsed microperfusion of 100 μM NMDA. The cerebellar neurones were recorded in a medium containing no added Mg^{2+} and the cells voltaged clamped at a V_h of − 60 mV. All records are from the same cell and show responses to 100 μM NMDA applied alone and with 10 μM AP. With 3 to 5 min washing, a recovery occurred between each current. AP greatly enhanced the NMDA currents and recovery from the action of AP is apparent.

These polyamine binding sites have been shown to be allosterically linked to binding sites for other modulators and glutamate (Ransom & Stec, 1988; Williams *et al.*, 1990). A binding site also appears to be associated with voltage-activated Ca^{2+} channels given the effect of AP on ω-CgTx binding described in this study, and that FTX affinity gels have been used in the isolation of a protein with Ca^{2+} channel activity (P channel) (Llinás *et al.*, 1989).

However, less selective actions may also account for some of the responses to AP. The polyamine spermine has been shown to cross-link phospholipids, and thus stabilize cell membranes (Ballas *et al.*, 1983). Polyamine toxins may have similar actions (Bruce *et al.*, 1990) and so by virtue of reducing membrane fluidity and interacting with lipid as well as protein structures affect the activity of a variety of ion channels. Raising extracellular Ca^{2+} may reduce the membrane stabilizing action of AP and therefore reduce the inhibition of voltage-activated Ca^{2+} currents. In this study we also report that AP actions are not restricted to effects on cation channels, since GABA-activated Cl^- currents are also markedly inhibited. It would be perhaps surprising if AP interacts with both anion and cation channels directly, given that the ion-selective filters and other properties of these channels are so different. Indirect interactions may occur which allow some access of AP molecules to the extracellular mouth of the channels. Channel blocking by polyamines may account for the inhibitory component of the dual effects observed in this study, where AP produced dual responses on voltage-activated Ca^{2+}-independent K^+ current. Dual responses have also previously been described for the action of spermine on NMDA currents (Williams *et al.*, 1990). Intracellular application of AP also reduced outward Ca^{2+} channel currents but not inward Ca^{2+} currents. This may also involve restricted monovalent ion access or shielding of charged groups at the channel opening.

Ca^{2+} influx into neurones via voltage-activated Ca^{2+} channels may contribute to Ca^{2+} overload in hypoxic conditions (Choi, 1988). The actions of AP on voltage-activated Ca^{2+} currents and Ca^{2+}-independent K^+ currents in DRG neurones raised the possibility that AP might have neuroprotective properties. However, like spermine and synthetic philanthotoxin (Brackley *et al.*, 1990), AP enhanced NMDA currents suggesting that AP would increase NMDA receptor-mediated neuronal damage. This action of AP is in contrast to that of the polyamine toxin, Argiotoxin-636 which has predominantly inhibitory effects on NMDA currents (Priestly *et al.*, 1989).

We conclude that AP (10 nM) selectively inhibits low threshold T-type channels. It remains to be determined if T-type current inhibition by AP is caused by AP binding to a high affinity site on this Ca^{2+} channel or whether T-type Ca^{2+} channels are particularly sensitive to the fluidity of their lipid environment. However, the variety of effects observed at higher concentrations of AP probably involve a number of different interactions with membrane constituents. It will be interesting in the future to investigate other polyamines with regard to Ca^{2+} entry through both voltage and ligand-gated ion channels.

We thank the British and Canadian medical research councils for their support, Ms E. Huston for help with the cell culture and Drs M. Adams, M. Sansom and I. Duce for useful discussions. We thank Dr John Wood (Sandoz Institute for Medical Research, London) for the ND7-23 cell line.

References

ADAMS, M.E., BINDOKAS, V.P., HASEGAWA, L. & VENEMA, V.J. (1990). ω-Agatoxins: novel calcium channel antagonists from funnel web spider (*Agelenopsis aperta*) venom. *J. Biol. Chem.*, **265**, 861-867.

ADAMS, M.E., HEROLD, E.E. & VENEMA, V.J. (1989). Two classes of channel-specific toxins from funnel web spider venom. *J. Comp. Physiol. A Sens. Neural Behav. Physiol.*, **164**, 333-342.

BALLAS, S.K., MOHANDAS, N., MARTIN, L.J. & SHOET, S.B. (1983). Stabilization of erythrocyte membranes by polyamines. *Proc. Natl Acad. Sci. U.S.A.*, **80**, 1942-1946.

BEAN, B.P. (1989). Neurotransmitter inhibition of neuronal calcium currents by changes in channel voltage-dependence. *Nature*, **340**, 153-156.

BOTTENSTEIN, J.E., SKAPER, S.D., VARON, S.S. & SATO, G.H. (1980). Selective survival of neurones from chick embryo sensory ganglionic dissociates utilising serum-free supplemented medium. *Exp. Cell Res.*, **125**, 183-190.

BRACKLEY, P., GOODNOW, R., NAKANISHI, K., SUDAN, H.L. & USHERWOOD, P.N.R. (1990). Spermine and philanthotoxin potentiate excitatory amino acid responses of xenopus oocytes injected with rat and chick brain RNA. *Neurosci. Lett.*, **114**, 51-56.

BRUCE, M., BUKOWNIK, R., ELDEFRAWI, A.T., ELDEFRAWI, M.E., GOODNOW, R., KALLIMOPOULOS, T., KONNO, K., NAKANISHI, K., NIWA, M. & USHERWOOD, P.N.R. (1990). Structure-activity relationships of analogues of the wasp toxin philanthotoxin: non-competitive antagonists of quisqualate receptors. *Toxicon*, **28**, 1333-1346.

CARBONE, E. & LUX, H.D. (1984). A low voltage-activated fully inactivating Ca channel in vertebrate sensory neurones. *Nature*, **310**, 501-502.

CHERKSEY, B., LLINÁS, R., SUGIMORI, M. & LIN, J.-W. (1989). Preliminary molecular structure of FTX and synthesis of analogs that block I_{Ca} in the squid giant synapse. *Biol. Bull.*, **177**, 321-322.

CHOI, D.W. (1988). Calcium-mediated neurotoxicity: relationship to specific channel types and role in ischemic damage. *Trends Neurosci.*, **11**, 465-469.

CURRIE, K.P.M. & SCOTT, R.H. (1991). Ca^{2+} dependent tail currents in cultured rat dorsal root ganglion (DRG) neurones. *Eur. J. Neurosci.*, Supplement 4, **209**, abstract 3222.

DOLPHIN, A.C. & SCOTT, R.H. (1986). Inhibition of calcium currents in cultured rat dorsal root ganglion neurones by (-)-baclofen. *Br. J. Pharmacol.*, **88**, 213-220.

DOLPHIN, A.C. & SCOTT, R.H. (1987). Calcium channel currents and their inhibition by (-)-baclofen in rat sensory neurones: modulation by guanine nucleotides. *J. Physiol.*, **386**, 1-17.

DOLPHIN, A.C. & SCOTT, R.H. (1990). Activation of calcium channel currents in rat sensory neurons by large depolarisations: effect of guanine nucleotides and (-)-baclofen. *Eur. J. Neurosci.*, **2**, 104-108.

DUNLAP, K. (1981). Two types of γ-aminobutyric acid receptor on embryonic sensory neurones. *Br. J. Pharmacol.*, **74**, 579-585.

HAMILL, O.P., MARTY, A., NEHER, E., SAKMANN, B. & SIGWORTH, F.J. (1981). Improved patch-clamp techniques for high-resolution current recording from cells and cell-free membrane patches. *Pflügers Arch.*, **391**, 85-100.

HUSTON, E.R., SCOTT, R.H. & DOLPHIN, A.C. (1990). A comparison of the effect of calcium channel ligands and $GABA_B$ antagonists on transmitter release and somatic calcium channel currents in cultured neurones. *Neuroscience*, **38**, 721-729.

ISRAEL, M., ROSENFIELD, J.S. & MODEST, E.J. (1964). Analogs of spermine and spermidine. I. Synthesis polymethylenepolyamines by reduction of cyanoethylated alpha, omega-alklenediamines. *J. Med. Chem.*, **7**, 710-716.

JACKSON, H. & USHERWOOD, P.N.R. (1988). Spider toxins as tools for dissecting elements of excitatory amino acid transmission. *Trends Neurosci.*, **11**, 278-283.

JASYS, V.J., KELBAUGH, P.R., NASON, D.N., PHILLIPS, D., SACCOMANO, N.A. & VOLKMANN, R.A. (1988). The total synthesis of argiotoxins 636, 659 and 673. *Tetrahedron Lett.*, **29**, 6223-6226.

JASYS, J.V., KELBAUGH, P.R., NASON, D.M., PHILLIPS, D., ROSNACK, K.J., SACCOMANO, N.A., STROH, J.G. & VOLKMANN, R.A. (1990). Isolation, structure elucidation, and synthesis of novel hydroxylamine - containing polamines from the venom of the *Agelenopsis aperta* spider. *J. Am. Chem. Soc.*, **112**, 6696-6704.

KASAI, H., AOSAKI, T. & FUKUDA, J. (1987). Presynaptic Ca-antagonist omega-conotoxin irreversibly blocks N-type Ca channels in chick sensory neurons. *Neurosci. Res.*, **4**, 228–235.

KERRY, C.J., RAMSEY, R.L., SANSOM, M.S.P. & USHERWOOD, P.N.R. (1988). Single channel studies of non-competitive antagonism of quisqualate-sensitive glutamate receptor by argiotoxin$_{636}$ – a fraction isolated from orb-web spider venom. *Brain Res.*, **459**, 312–327.

KNAUS, H.G., STRIESSNIG, J., KOZA, A. & GLOSSMAN, H. (1987). Neurotoxic aminoglycoside antibiotics are potent inhibitors of [^{125}I]-omega-conotoxin GVIA binding to guinea-pig cerebral cortex membranes. *Naunyn-Schmiedebergs Arch. Pharmacol.*, **336**, 583–586.

LIN, J.-W., RUDY, B. & LLINÁS, R. (1990). Funnel-web spider venom and a toxin fraction block calcium current expressed from rat brain mRNA in xenopus oocytes. *Proc. Natl. Acad. Sci. U.S.A.*, **87**, 4538–4542.

LLINÁS, R., SUGIMORI, M., LIN, J.-W. & CHERKSEY, B. (1989). Blocking and isolation of a calcium channel from neurones in mammals and cephalopods utilizing a toxin fraction (FTX) from funnel-web spider poison. *Proc. Natl. Acad. Sci. U.S.A.*, **86**, 1689 1693.

LOWRY, O.H., ROSEBROUGH, N.J., FARR, A.L. & RANDALL, B.J. (1951). Protein measurement with the Folin phenol agent. *J. Biol. Chem.*, **193**, 265–275.

LURDES, M., ALMEIDA, S., GREHN, L. & RAGNARSSON, U. (1988). Selective protection of polyamines: synthesis of model compounds and spermidine derivatives. *J. Chem. Soc.*, Perkin Trans. **I**, 1905–1911.

MCCLESKEY, E.W., FOX, A.P., FELDMAN, D., CRUZ, L.J., OLIVERA, B.M., TSIEN, R.W. & YOSHIKAMI, D. (1987). Direct and persistent blockade of specific types of calcium channels in neurones but not muscle. *Proc. Natl. Acad. Sci. U.S.A.*, **84**, 4327–4331.

MINTZ, I.M., VENEMA, V.J., ADAMS, M.E. & BEAN, B.P. (1991). Inhibition of N- and L-type Ca^{2+} channels by the spider venom toxin ω-Aga-IIIA. *Proc. Natl. Acad. Sci. U.S.A.*, **88**, 6628–6631.

NAKAMURA, Y. (1988). Actinocinyl-bis(hemin); DNA-intercalating cleavage agent. *Heterocycles*, **27**, 1873–1879.

NOWYCKY, M.C., FOX, A.P. & TSIEN, R.W. (1985). Three types of neuronal calcium currents with different calcium agonist sensitivity. *Nature*, **316**, 440–443.

OLIVERA, B.M., GRAY, W.R., ZEIKUS, R., MCINTOSH, J.M., VICTORIA DI SANTOS, J.R. & CRUZ, L.J. (1985). Peptide neurotoxins from fish-hunting cone snails. *Science*, **230**, 1338–1343.

PEARSON, H.A., KOBRINSKY, E.M. & DOLPHIN, A.C. (1992) Ca^{2+} channel currents in the dorsal root ganglion cell × neuroblastoma hybrid cell line, ND7–23. *J. Physiol*, **446**, 181P.

PLUMMER, M.R., LOGOTHETIS, D.E. & HESS, P. (1989). Elementary properties and pharmacological sensitivities of calcium channels in mammalian peripheral neurons. *Neuron*, **2**, 1453–1463.

PRIESTLY, T., WOODRUFF, G.N. & KEMP, J.A. (1989). Antagonism of responses to excitatory amino acids on rat cortical neurones by the spider toxin, argiotoxin$_{636}$. *Br. J. Pharmacol.*, **97**, 1315–1323.

PULLAN, L.M., KEITH, R.A., LAMONTE, D., STAMPO, R.J. & SALAMA, A.I. (1990). The polyamine spermine affects ω-conotoxin binding and function at N-type voltage-sensitive calcium channels. *J. Auton. Pharmacol.*, **10**, 213–219.

QUISTAD, G.B., SUWANRUMPHA, S., JAREMA, M.A., SHAPIRO, M.J., SKINNER, W.S., JAMIESON, G.C., LUI, A. & FU, E.W. (1990). Structure of paralytic acylpolyamines from the spider *Agelenopsis aperta*. *Biochem. Biophys. Res. Commun.*, **169**, 51–56.

RANSOM, R.W. & STEC, N.L. (1988). Cooperative modulation of (^{3}H) MK-801 binding to the N-methyl-D-aspartate receptor ion channel complex by l-glutamate, glycine and polyamine. *J. Neurochem.*, **51**, 830–836.

SCOTT, R.H.,WOOTTON, J.F. & DOLPHIN, A.C. (1990a). Modulation of neuronal T-type calcium channel currents by photoactivation of intracellular guanosine 5'-0(3-thio)triphosphate. *Neuroscience*, **38**, 285–294.

SCOTT, R.H., DOLPHIN, A.C., BINDOKAS, V.P. & ADAMS, M.E. (1990b). Inhibition of neuronal Ca^{2+} channel currents by the funnel web spider toxin ω-Aga-IA. *Mol. Pharmacol.*, **38**, 711–718.

WAGNER, J.A., SNOWMAN, A.M., BISWAS, A., OLIVERA, B.M. & SNYDER, S.H. (1988). ω-Conotoxin GVIA binding to a High-affinity receptor in brain: Characterization, calcium sensitivity, and solubilization. *J. Neurosci.*, **8**, 3354–3359.

WILLIAMS, K., DAWSON, V.L., ROMANO, C., DICHTER, M.A. & MOLINOFF, P.B. (1990). Characterization of polyamines having agonist, antagonist and inverse agonist effects at the polyamine recognition site of the NMDA receptor. *Neuron*, **5**, 199–208.

WINTER, J. (1987). Characterization of capsaicin-sensitive neurones in adult rat dorsal root ganglion cultures. *Neurosci. Lett.*, **80**, 134–190.

WOOD, J.N., BEVAN, S.J., COOTE, P.R., DUNN, P.M., HARMAR, A., HOGAN, P., LATCHMAN, D.S., MORRISON, C., ROUGON, G., THEVENIAU, M. & WHEATLEY, S. (1990). Novel cell lines display properties of nociceptive sensory neurones. *Proc. R. Soc. B.*, **241**, 187–194.

(Received October 9, 1991
Revised January 16, 1992
Accepted January 17, 1992)

Br. J. Pharmacol. (1992), **106**, 208–214 © Macmillan Press Ltd, 1992

Effects of cyclopiazonic acid, a novel Ca^{2+}-ATPase inhibitor, on contractile responses in skinned ileal smooth muscle

Yoshiaki Uyama, [1]Yuji Imaizumi & Minoru Watanabe

Department of Chemical Pharmacology, Faculty of Pharmaceutical Sciences, Nagoya City University, 3-1 Tanabedori, Mizuhoku, Nagoya 467, Japan

1 Effects of cyclopiazonic acid (CPA), a specific inhibitor of the Ca^{2+}-ATPase in sarcoplasmic reticulum (SR) of skeletal and cardiac muscles, on contractile responses induced by Ca^{2+}-release from intracellular storage sites were examined in the longitudinal smooth muscle strip of the guinea-pig ileum skinned with β-escin.

2 Ca^{2+}-loading of storage sites (Ca^{2+}-uptake) was performed in pCa 6.3 solution. The amount of Ca^{2+} taken up was monitored by use of the amplitude of contraction following application of 25 mM caffeine or 25 μM inositol 1,4,5-trisphosphate (IP_3).

3 Contractile responses to caffeine or IP_3 were reduced or abolished when the preceding Ca^{2+}-uptake was performed in the presence of 0.1–10 μM CPA. The dose of CPA required to inhibit the contraction induced by caffeine or IP_3 by 50% was approximately 0.6 μM. The CPA-sensitive Ca^{2+}-uptake completely depended upon the presence of ATP in the solution during Ca^{2+}-uptake.

4 When 1 μM CPA was added after Ca^{2+}-uptake, the subsequent caffeine- or IP_3-induced contraction was not significantly affected by the presence of CPA.

5 Acetylcholine-induced contraction was also almost abolished when the preceding Ca^{2+}-uptake was performed in the presence of 10 μM CPA.

6 The relationship between pCa and contraction was not affected by the presence of 10 μM CPA in skinned fibres where Ca^{2+} storage sites had been destroyed by treatment with A23187. The enhancement of contraction in pCa 6.0 solution by calmodulin was not affected by 10 μM CPA.

7 These results suggest that CPA selectively inhibits ATP-dependent Ca^{2+}-uptake into intracellular storage sites in skinned ileal smooth muscle strips. CPA appears to be a potent, reversible, and very specific inhibitor of the Ca^{2+}-pump in the storage sites of smooth muscle, and is an extremely valuable pharmacological tool.

Keywords: Cyclopiazonic acid; skinned fibre; smooth muscle; ileum; Ca^{2+}-pump; sarcoplasmic reticulum; Ca^{2+}-ATPase; caffeine; inositol 1,4,5-trisphosphate; β-escin

Introduction

A specific inhibitor of Ca^{2+}-ATPase activity in sarcoplasmic reticulum (SR) of muscle cells is a much needed pharmacological tool for investigation of the mechanism(s) and kinetics of SR Ca^{2+}-uptake and -storage. Cyclopiazonic acid (CPA), a mycotoxin from *Aspergillus* and *Penicillium*, has been described as a highly selective inhibitor of Ca^{2+}-ATPase in skeletal muscle SR (Goeger & Riley, 1989; Seidler *et al.*, 1989). It does not affect the activities of kidney and brain Na^+, K^+-ATPase, gastric H^+, K^+-ATPase, mitochondrial F_1-ATPase, Ca^{2+}-ATPase of erythrocytes or Mg^{2+}-activated ATPase of T-tubules and plasma membrane of rat skeletal muscle. It has also been shown that Ca^{2+}-uptake by SR vesicles prepared from skeletal muscle is inhibited by CPA (Goeger *et al.*, 1988). Recently, the effects of CPA on Ca^{2+}-ATPase in skinned fast-twitch skeletal muscle have been studied (Kurebayashi & Ogawa, 1991). Direct evidence for the inhibition of ATP-dependent Ca^{2+}-uptake into SR by CPA and subsequent failure of Ca^{2+}-release has not been obtained in any skinned muscular preparations, although this possibility has been suggested in intact aortic (Deng & Kwan, 1991) and tracheal smooth muscles (Bourreau *et al.*, 1991). Evidence should be obtained in skinned smooth muscle preparations, where the functions of the sarcolemmal Ca-pump, Na-Ca exchange system and ionic channels can be ignored and thereby Ca^{2+}-mobilization is greatly simplified. The dependence of Ca^{2+}-uptake on ATP can also be directly examined.

The present study was undertaken to evaluate the specificity of the CPA-effects on Ca^{2+} loading into storage sites in chemically skinned ileal smooth muscle fibres. The amount of Ca^{2+}-uptake into these storage sites was monitored by evoked contraction following application of caffeine (Iino, 1989) or IP_3 (Somlyo *et al.*, 1985; Suematsu *et al.*, 1984), procedures which release Ca^{2+} from SR and/or ER by separate mechanisms. The effects of CPA on Ca^{2+}-uptake into caffeine- and IP_3-sensitive storage sites were compared, since heterogeneous Ca^{2+} storage sites with regard to sensitivity to these Ca^{2+} releasing substances have been described (Iino *et al.*, 1988). The direct effects of CPA on the Ca^{2+}-sensitivity of contractile proteins and the antagonistic effect of CPA on calmodulin have also been examined after Ca^{2+} storage function of SR had been destroyed by A23187 (Itoh *et al.*, 1991).

Methods

Male Hartley guinea-pigs weighing about 200 g were killed by a blow on the head. Thin strips 1.5–2.0 mm in length, 150–200 μm in width and less than 100 μm in thickness were prepared from the longitudinal muscle layer of ileum. Each end of the muscle strip was tied to a fine thread of about 10 μm in diameter. The strip was placed horizontally in an organ bath which had a volume of approximately 300 μl. The thread at each end of the strip was connected to a thin pin in the silicon rubber bottom of the bath and to a lever of an isometric force transducer, respectively. The contractile re-

[1] Author for correspondence.

sponse of the intact strip to high K^+ solution was measured two or three times before skinning. The compositon of the standard physiological salt solution was: (in mM) NaCl 125.0, KCl 4.7, $CaCl_2$ 2.0, $MgCl_2$ 1.2, glucose 10.0, tris(hydroxymethyl) aminomethane (Tris) 20.0. The pH was adjusted to 7.5 with HCl. High K^+ solution was prepared by replacing 125 mM NaCl with equimolar KCl. Before skinning, the strip was incubated for 25 min in a relaxing solution containing 2 mM ethyleneglycol-*bis*-(β-aminoethyl)-N,N,N',N'-tetraacetic acid (EGTA) (R2G, see below).

Skinning was performed by incubation in a solution of pCa 6.0 with 60 μM β-escin (Kitazawa & Somlyo, 1990; Kobayashi *et al.*, 1989). The skinning process was monitored by a gradual increase in muscle tone, which reached a steady level after approximately 30 min. The solution was then changed to the relaxing solution (R2G). The composition of R2G was (in mM): K-propionate 130, $MgCl_2$ 4.0, adenosine triphosphate (ATP)-2Na 4.0, creatine phosphate 10, NaN_3 10, Tris 20.0, EGTA 2.0. A solution containing 0.5 mM EGTA (R0.5G) was prepared by reducing the EGTA concentration in R2G from 2.0 to 0.5 mM. The contractile effects of caffeine and IP_3 were tested in R0.5G to avoid the strong Ca chelating effects of higher concentrations of EGTA. The approximate pCa of R0.5G was 7.6 ± 0.4, assuming the contamination of Ca^{2+} to be 10–50 μM. The pH was adjusted to 6.8 with maleic acid. Solutions of pCa 7.0, 6.0, 5.0 and 4.0 were prepared by using Ca^{2+}-EGTA buffer of 3 mM EGTA and corresponding Ca^{2+}. The required Ca^{2+}-concentrations were calculated assuming the apparent binding constant of Ca-EGTA complex to be $1.0 \times 10^6\ M^{-1}$ at pH 6.8 (Saida & Nonomura, 1978). The composition of this solution was the same as that of R2G except for the EGTA concentration. When the Ca sensitivity of the contractile proteins was studied in detail, the intracellular Ca storage sites were destroyed by treatment with 10 μM A23187 (Itoh *et al.*, 1985) for about 20 min in R2G solution after skinning to prevent Ca^{2+}-induced Ca^{2+}-release. Experiments were performed at room temperature in the range between 21 and 24°C. Calmodulin was not added except when mentioned.

β-Escin(Lot. 107F0598), CPA (129F4013, 98F4037), calmodulin, and guanosine 5'-O-(3-thiotriphosphate) (GTPγS) were obtained from Sigma Ltd. ATP was from Oriental. Guanosine triphosphate (GTP) was from Yamasa. A23187 was from Calbiochem. Ltd. EGTA and IP_3 were from Dojin. Caffeine, Tris, Maleic acid and acetylcholine were from Wako Junyaku.

Pooled data are expressed as mean ± s.e.mean. Statistical significance was examined by Student's *t* test and was indicated by * or ** at the *P* level of <0.05 and <0.01, respectively.

Results

Figure 1 shows the effects of cyclopiazonic acid on contraction induced by 25 mM caffeine or 25 μM IP_3 in ileal smooth muscle strips skinned with β-escin. After skinning, application of pCa 6.3 solution evoked a control contractile response (Figure 1A). The tension reached the peak within 5 min and gradually declined thereafter (Kitazawa & Somlyo, 1990). This procedure also resulted in loading of intracellular storage sites with Ca^{2+} (Ca^{2+}-loading or Ca^{2+}-uptake). Subsequent application of 25 mM caffeine in a relaxing solution (R0.5G) induced a transient contraction. A second application of 25 mM caffeine in R0.5G elicited either a very small or no response, confirming that most of the Ca^{2+} which had been loaded into storage sites in pCa 6.3 solution had been released by the first application of caffeine and that the released Ca^{2+} was not re-taken up into storage sites in R0.5G. Since the effect of caffeine appeared to be concentration-dependent in the range of 1 and 20 mM but varied widely between preparations, 25 mM caffeine was used to obtain a stable response. Without this Ca^{2+}-loading, subsequent application of caffeine did not elicit contraction. When a pair of contractions induced by pCa 6.3 and 25 mM caffeine was repeated three times in each preparation (three trials) at an interval of approximately 30 min, the peak amplitude of contractions decreased progressively (Figure 1A). This may have resulted from a gradual decrease in cellular calmodulin content (Kitazawa & Somlyo, 1990) (see Figure 3). In Figure 1B, the second application of pCa 6.3 solution was performed in the presence of 3 μM CPA. CPA *per se* did not change the muscle tone in R0.5G (Figure 1B,b). The relative peak amplitude of the second response to pCa 6.3 compared with the first one was not affected significantly by 3 μM CPA ($P > 0.05$, $n = 6$). The subsequent application of caffeine did not induce any response (Figure 1B,b). In the third trial (Figure 1B,c), a substantial response to caffeine was

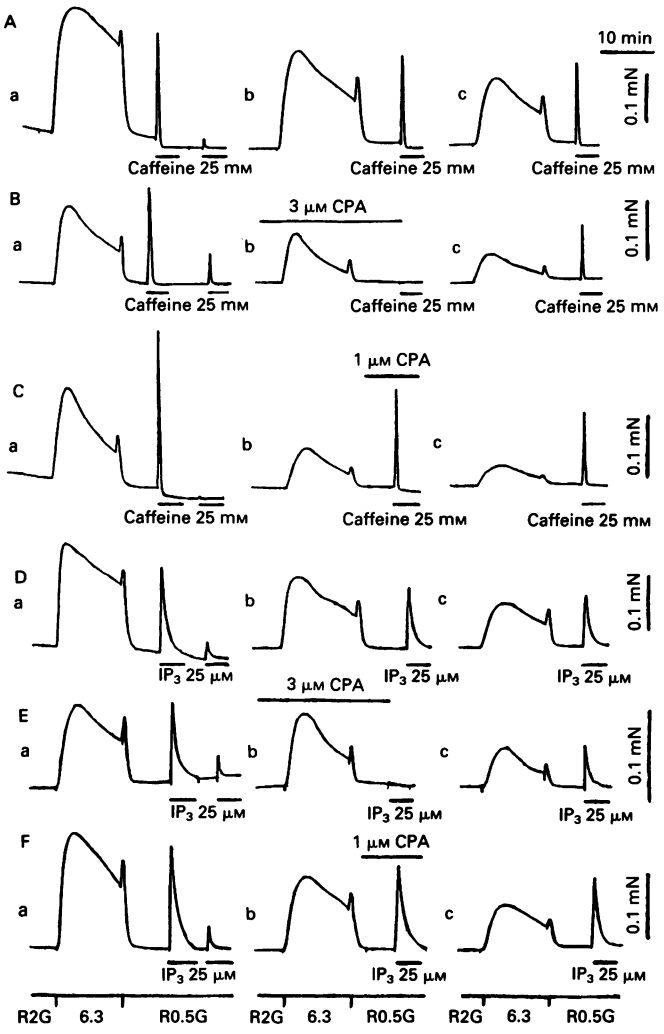

Figure 1 Effects of cyclopiazonic acid (CPA) on 25 mM caffeine- or 25 μM inositol 1,4,5-trisphosphate (IP_3)-induced contraction in skinned smooth muscle strips of guinea-pig ileum. Skinned strips were contracted by changing a relaxing solution (R2G, see Methods) to pCa 6.3 solution as indicated in the line below (F). This was also a Ca^{2+} loading period. Caffeine or IP_3 was applied twice as indicated by bars in the R0.5G period. Note that the second response to caffeine or IP_3 in a paired application was very small. Ca^{2+} loading at pCa 6.3 and subsequent Ca release by caffeine or IP_3 were repeated three times (a,b and c). The amplitude of the responses decreased progressively even in the control (A and D). In (B,b) and (E,b), Ca^{2+} loading was performed in the presence of 3 μM CPA in the second trial. Subsequent application of caffeine or IP_3 in the absence of CPA did not induce contraction, while in the third trial (B,c and E,c) the contractile responses substantially recovered. In (C,b) and (F,b), contraction induced by caffeine or IP_3 was observed in the presence of 1 μM CPA, and not affected significantly by CPA.

observed, indicating a recovery from CPA-induced inhibition following washout.

When 1 μM CPA was added after Ca^{2+}-loading (Figure 1C,b), the subsequent response to caffeine (in the presence of CPA) was very similar to the control (Figure 1A,b). A higher concentration of CPA (> 3 μM) applied after Ca^{2+}-loading for a longer period (> 10 min), caused a small and slow phasic contraction and the subsequent response to caffeine appeared to be smaller than the control (not shown). However, prolonged incubation in R0.5G after Ca^{2+}-loading *per se* progressively reduced the subsequent caffeine-induced contraction. Therefore, the effects of CPA on Ca^{2+}-release mechanisms were examined under fixed conditions: 1 or 3 μM CPA was added just after Ca^{2+}-loading was finished and 25 mM caffeine (or 25 μM IP_3) was added 5 min after the application of CPA as shown in Figure 1C. Under these conditions, CPA did not apparently affect subsequent caffeine-induced contraction (see also Figure 2).

Application of IP_3 at concentrations between 3 and 50 μM after Ca^{2+}-loading elicited contraction in a concentration-dependent manner in skinned ileal fibres. When 25 μM or higher concentrations of IP_3 were used to obtain a stable response, the results were qualitatively very similar to those obtained with 25 mM caffeine. Most of the releasable Ca^{2+} in storage sites sensitive to IP_3 was depleted by the first application of 25 μM IP_3 as shown in Figure 1D,a. The procedure of Ca loading at pCa 6.3 and subsequent application of 25 μM IP_3 in R0.5G was repeated three times in each preparation. The contraction induced by IP_3 was also transient but the decline of tension from the peak was slightly slower than that induced by caffeine. IP_3-induced contraction was almost completely blocked when the preceded Ca loading was performed in the presence of 3 μM CPA (Figure 1E,b) but not when 1 μM CPA was added after the Ca^{2+}-loading (Figure 1F,b).

The responses induced by the third application of caffeine or IP_3 in the control procedure shown in Figure 1A,c and 1D,c were 61.1 ± 6.3 and 56.1 ± 1.6% ($n = 3$ for each) of corresponding first responses (Figure 1A,a and 1D,a), respectively. When 3 μM CPA was added to the Ca-loading solution in the second trial (Figure 1B,b and 1E,b), the responses in the third trial (Figure 1B,c and 1E,c) were 48.4 ± 5.2 and 56.3 ± 7.7% ($n = 3$ for each) which was not significantly different from those in the control ($P > 0.05$ *vs.* 61.1 and 56.1%, respectively), respectively. Therefore, the inhibitory effect of 3 μM CPA can be almost completely removed by washout.

Summarized data are shown in Figure 2. The peak amplitude of contraction induced by the first application of 25 mM caffeine or 25 μM IP_3 was taken as 100%, respectively. The

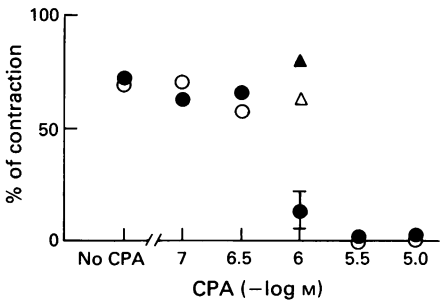

Figure 2 Summarized data shown in Figure 1; dose-response relationships of cyclopiazonic acid (CPA) for caffeine- (open symbols) or inositol 1,4,5-trisphosphate (IP_3)- (closed symbols) induced responses. No CPA on abscissa scale indicates the responses in the second trial in the control (Figure 1A,b and D,b) as a percentage of the first corresponding responses. The number of observations was 3 for each symbol except at CPA dose 0.3 μM where four observations were obtained for each. Triangles indicate the results obtained when caffeine or IP_3 were applied in the presence of 1 μM CPA in the second trial as shown in Figure 1 (C,b) and (F,b).

second responses to caffeine and IP_3 in the control were 70.3 ± 5.6 ($n = 3$) and 73.3 ± 1.8% ($n = 3$) indicated by open and closed circles with 'no CPA', respectively. The second application of caffeine or IP_3 preceded by Ca-loading in the presence of CPA yield dose-dependent decreases in contraction between 0.1 and 3 μM of CPA. Triangles indicate the data obtained when CPA was added after Ca^{2+}-loading (Figure 1C and F). The values shown by open (63.8 ± 2.4%, $n = 3$) and closed triangles (81.0 ± 4.2%, $n = 3$) are not statistically different from those of the open and closed circles with 'no CPA', respectively ($P > 0.05$), demonstrating that 1 μM CPA does not directly reduce Ca release induced by caffeine and IP_3. The approximate half-inhibition dose of CPA for Ca release by caffeine and IP_3 was the same, in spite of the different Ca releasing mechanisms (~0.6 μM).

To examine whether CPA inhibits ATP-dependent Ca^{2+}-uptake into storage sites, the effects of CPA were compared in the presence and absence of ATP and creatine-phosphate (Figure 3). After a standard contraction was obtained in a pCa 6.3 solution, stored Ca^{2+} was depleted by application of 25 mM caffeine. Subsequent removal of ATP and creatine-phosphate induced rigor contraction in R2G solution. Thereafter, a change in bathing solution from R2G solution to pCa 6.3 solution (ATP and creatine-phosphate-free) either did not alter the tone significantly or slightly increased it, suggesting that the tone may not be Ca^{2+}-dependent. During the incubation in pCa 6.3 solution for 15 min, preparations were treated in three different ways; 4.0 mM ATP was added for 10 min (Figure 3a), nothing was added (Figure 3b), or 10 μM CPA and 4.0 mM ATP were added (Figure 3c). The application of ATP induced transient relaxation and subsequent contraction, regardless of the presence of CPA (indicated by arrows in Figure 3a and c). Thereafter, the bathing solution was returned to ATP- and creatine-phosphate-free R2G solution for 1 min and then changed to the standard R2G solution. Finally, the response to 25 mM caffeine was examined in R0.5G solution. A caffeine-induced contraction was observed only in a preparation to which ATP but not CPA was applied during the preceding incubation in pCa 6.3 solution (Figure 3a, 44.1 ± 3.8% of the first contraction induced by caffeine, $n = 3$). These results demonstrate that the Ca^{2+} released by the application of caffeine was previously sequestered into storage sites by an ATP-dependent mechanism and that 10 μM CPA completely inhibited this uptake in a reversible manner.

Although these results strongly suggest that CPA acts on ATP-dependent Ca-uptake into intracellular storage sites, two other mechanisms might be involved; CPA may act as a calmodulin inhibitor, or directly decrease the activity of the contractile apparatus. These possibilities were also examined. To prevent any contribution of Ca^{2+}-induced Ca^{2+}-release, the ability of intracellular sites to store Ca^{2+} was destroyed by treatment with 10 μM A23187 for about 20 min after skinning. Under these conditions, responses to caffeine and IP_3 were abolished.

As mentioned previously, contractile responses in pCa 6.3 solution could be elicited repetitively but the amplitude decreased. Gradual loss of calmodulin from cytoplasm may be, in part, responsible for this phenomenon. In Figure 4a, the control responses to pCa 6.0 solution were observed three times. The fourth application of pCa 6.0 solution, which was performed after 2 μM calmodulin had been added, induced a larger response than the third one (Figure 4a). Summarized data (Figure 4b) show that the fourth response recovered significantly ($P < 0.05$ vs the third one) in the presence of calmodulin. This recovery with calmodulin did not change significantly in the presence of 10 μM CPA ($P > 0.05$) which was added about 5 min before the fourth response.

To test whether CPA could directly affect the contractile proteins, pCa-tension relationships were obtained by stepwise increases in Ca^{2+}-concentration as shown in Figure 5. The maximum response was obtained at pCa 5.0. Further increase to pCa 4.0 or 3.0 did not increase tension significantly, imply-

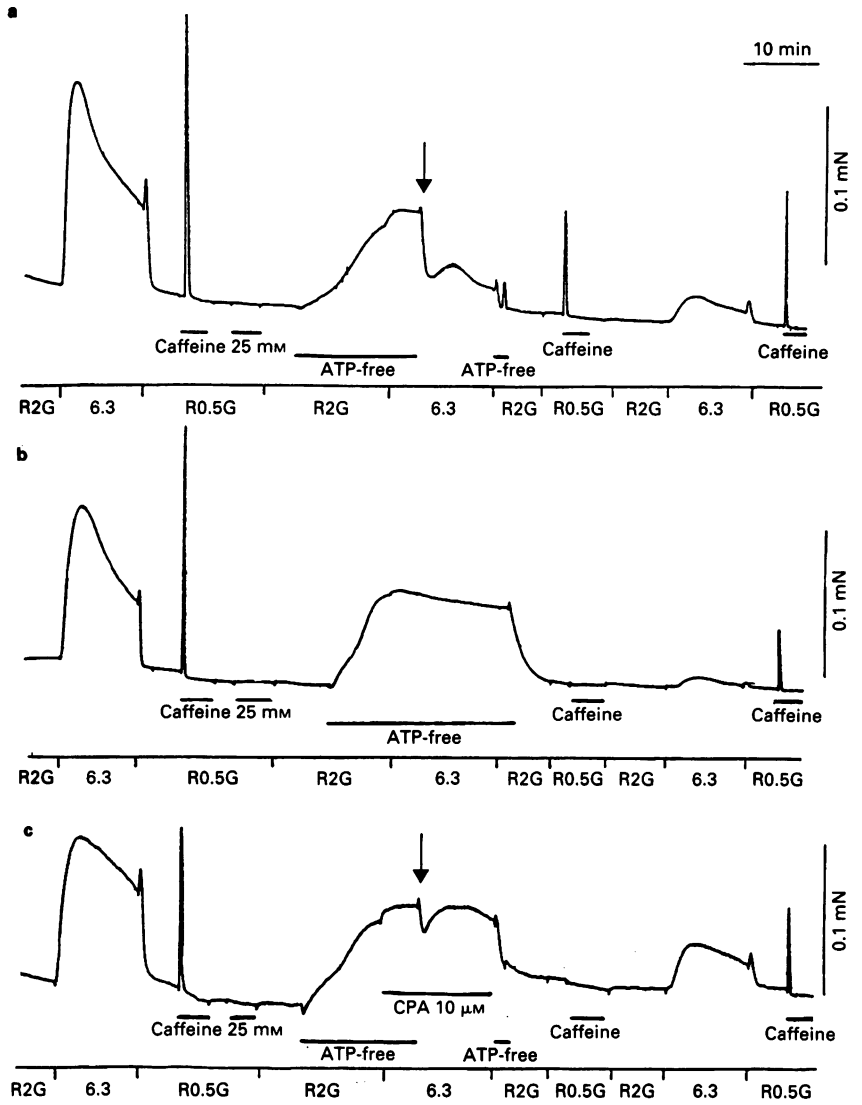

Figure 3 Dependence of cyclopiazonic acid (CPA)-sensitive Ca^{2+}-loading on adenosine 5'-triphosphate (ATP). After loading in pCa 6.3 solution, Ca^{2+} was released by two applications of 25 mM caffeine. Subsequent change to R2G solution which did not contain ATP and creatine-phosphate induced rigor contraction. NaN_3 was present throughout the experiment (see Methods). When rigor contraction reached a steady level, the solution was changed to ATP- and creatine-phosphate-free pCa 6.3 solution. During application of pCa 6.3 solution, the strips were treated in three different ways. (a) ATP (4 mM) was added. (b) Nothing was added. (c) CPA (10 μM) was first added and then 4 mM ATP was added. Addition of ATP-induced relaxation in (a) and (c) as indicated by arrows. Thereafter, the fibre was returned to ATP- and creatine-phosphate-free R2G solution. The solution was then changed to one containing ATP and creatine-phosphate, resulting in a large relaxation from rigor contracture in (b). Subsequent application of 25 mM caffeine was performed in R0.5G solution. Note that a contractile response to caffeine was observed in (a) but not in (b) and (c). After subsequent Ca^{2+} -loading in pCa 6.3 solution, the responses to 25 mM caffeine were observed in (b) and (c), as well as (a).

ing that the contribution of non-skinned cells in the fibre, if any, to the contractile response was negligible. Moreover, maximum contraction in skinned fibres was comparable to or slightly larger than that in 130 mM K solution in intact preparations before skinning ($n > 20$, see Figure 5A). The pCa-tension relationships were examined twice in each preparation. The relative amplitude of contraction at each pCa in the second trial was calculated versus the first maximum response. When the second trial was performed in the presence of 10 μM CPA, the response was not affected significantly, as summarized in Figure 6 ($P > 0.05$; vs. corresponding control at each pCa). Treatment with GTPγS, which is known as a substance increasing the Ca^{2+} sensitivity of contractile proteins (Kitazawa *et al.*, 1991), significantly potentiated the contraction.

A great advantage of skinning with β-escin is that the functions of receptors on the cell membrane and the related intracellular signal transduction are preserved after skinning (Kobayashi *et al.*, 1989; Itoh *et al.*, 1991). In the present study, the response to acetylcholine (ACh, Figure 7) was observed in the presence of 50 μM GTP after skinning. The response to ACh appeared to be dose-dependent in the range of 0.3 to 100 μM. To evaluate the effects of CPA, Ca^{2+}-loading in pCa 6.3 and the subsequent application of 100 μM ACh was repeated three times in each preparation in the same manner shown in Figure 1 for caffeine and IP_3. The response to 100 μM ACh was transient as was that to IP_3. The amplitude of the response to ACh in the control (Figure 7A) was decreased progressively during three trials but not as much as that to pCa 6.3 (see also Figures 1 and 4). When Ca^{2+}-loading was performed in the presence of 10 μM CPA in the second trial, the subsequent response to ACh was almost completely abolished. In the third trial (Figure 7B), CPA was absent during Ca^{2+}-loading and the subsequent response to ACh substantially recovered. The second and third responses to 100 μM ACh were 82.8 ± 7.8 and

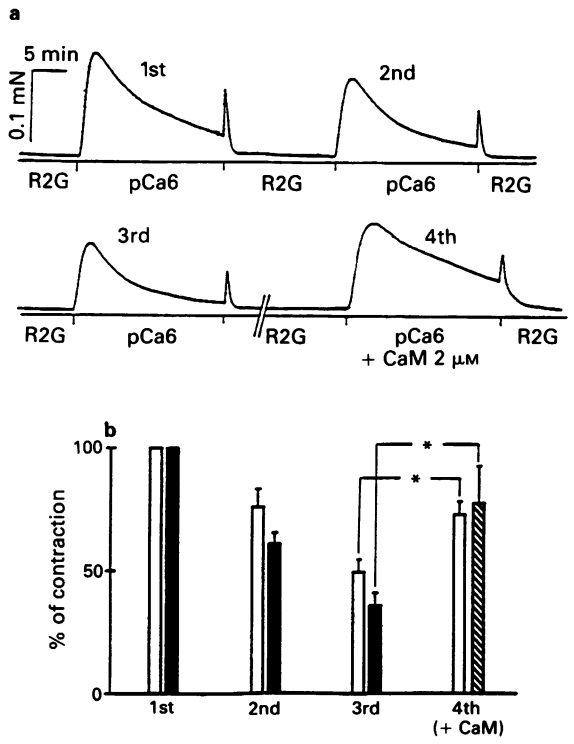

Figure 4 Effect of cyclopiazonic acid (CPA) on calmodulin (CaM) action in the skinned ileal smooth muscle. Intracellular Ca storage sites were destroyed by treatment with 10 μM A23187 for 20 min after skinning. (a) Contraction induced in pCa 6.0 solution was observed four times; in the absence of calmodulin three times and in the presence of 2 μM calmodulin the last time (4th). The amplitude of the response decreased gradually with time but recovered markedly following treatment with calmodulin prior to the fourth contraction. (b) Summarized data for contractions in pCa 6.0 solution. Open and solid columms indicate the data obtained in the absence of CPA (control). The first response was taken as 100%. The hatched column indicates the relative amplitude of the fourth contraction which was induced in the presence of 10 μM CPA as well as 2 μM calmodulin (+ CaM) in the same preparations shown by the closed column. The number of observations was 6, 5 and 5 for open, solid and hatched columns, respectively. Note that the contraction decreased with time and recovered significantly when 2 μM calmodulin was added. This recovery was not affected in the presence of 10 μM CPA.

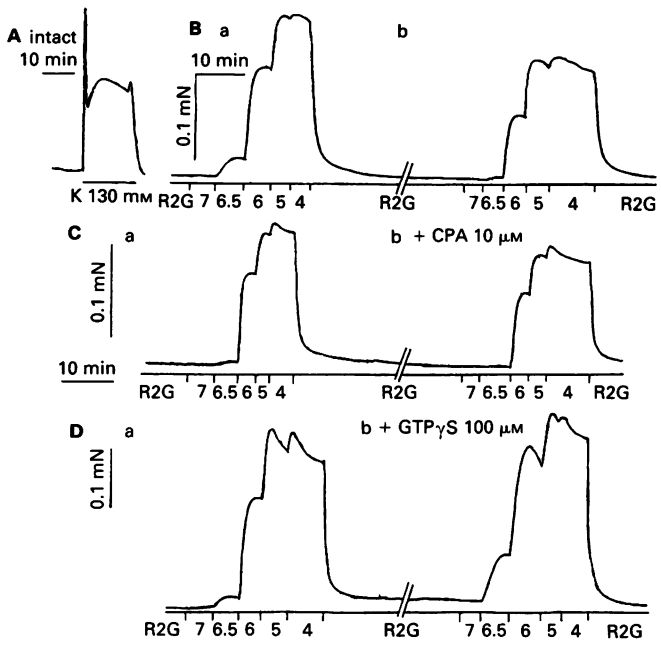

Figure 5 Effects of 10 μM cyclopiazonic acid (CPA) and 100 μM guanosine 5'-0-(3-thiotriphosphate) (GTPγS) on pCa-tension relationship in skinned fibre pretreated with 10 μM A23187. The contractile response to 130 mM K^+ solution was examined in each preparation before skinning as shown in (A). The Ca^{2+} concentration was increased stepwise from pCa 7.0 to 6.5, 6.0, 5.0 and 4.0, twice in each preparation. In (C) and (D) the second trial was performed in the presence of 10 μM CPA or 100 μM GTPγS, respectively. Note that GTPγS did but CPA did not affect the pCa-tension relationship. Calmodulin was not added to the solutions.

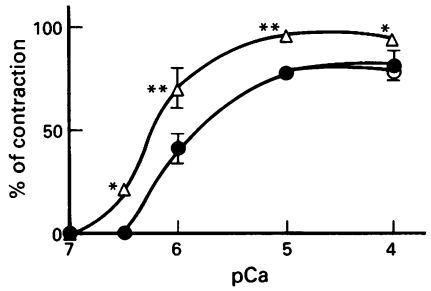

Figure 6 Summarized data shown in Figure 5. Open and closed circles and triangle denote the mean values of the relative amplitude of the contractile response in the control, in the presence of 10 μM cyclopiazonic acid (CPA) or 100 μM guanosine 5'-O-(3-thiotriphosphate) (GTPγS), respectively. The number of observations was 8, 5 and 3 in the control, in the presence of CPA or GTPγS, respectively. Abscissa scale denotes pCa in the solutions. The maximum response in the first trial (see Figure 5) in each preparation was taken as 100%.

65.7 ± 8.8% ($n = 3$), respectively, in the control and 2.10 ± 1.09 ($P < 0.01$ vs 82.8) and 39.1 ± 8.7% ($n = 3$, $P < 0.01$ vs. 2.10), respectively, in the CPA-treated preparations when the first response to ACh was taken as 100% in each preparation. It is clearly shown that Ca^{2+}-uptake by storage sites which is released by application of ACh was also inhibited by CPA. Qualitatively the same results were obtained when 3 μM substance P (SP) was used as an agonist ($n = 2$).

Discussion

Our results show that CPA in a concentration-range between 0.1 and 10 μM decreases the amplitude of contractions induced by caffeine or IP_3 in skinned ileal smooth muscle strips. This effect was observed only when CPA was applied during the preceding Ca^{2+}-loading into the intracellular storage sites. Our results also suggest that 1 μM CPA does not affect the Ca^{2+}-release mechanism itself, whereas inhibition of Ca^{2+}-release by CPA has been reported in SR vesicle of skeletal muscle (Goeger *et al.*, 1988). The CPA-sensitive Ca^{2+}-uptake was due to an ATP-dependent mechanism which is likely to be the SR/ER Ca^{2+}-pump. The Ca sensitivity and the maximum contractile ability of preparations with Ca-storage sites destroyed by A23187 (Itoh *et al.*, 1985) were not affected significantly by 10 μM CPA. CPA did not inhibit the enhanced contraction due to addition of calmodulin. Together, our data indicate that the effect of CPA is quite selective for the ATP-dependent Ca^{2+}-uptake mechanism of intracellular storage sites. This is consistent with previous results showing that CPA is a selective inhibitor of Ca^{2+}-ATPase in skeletal and cardiac muscle SR (Goeger *et al.*, 1988; Goeger & Riley, 1989; Kurebayashi & Ogawa, 1991). The effective concentration-range of CPA for inhibition of caffeine- or IP_3-induced contraction in skinned smooth muscle ($IC_{50} = 0.6$ μM) is also comparable to that reported for

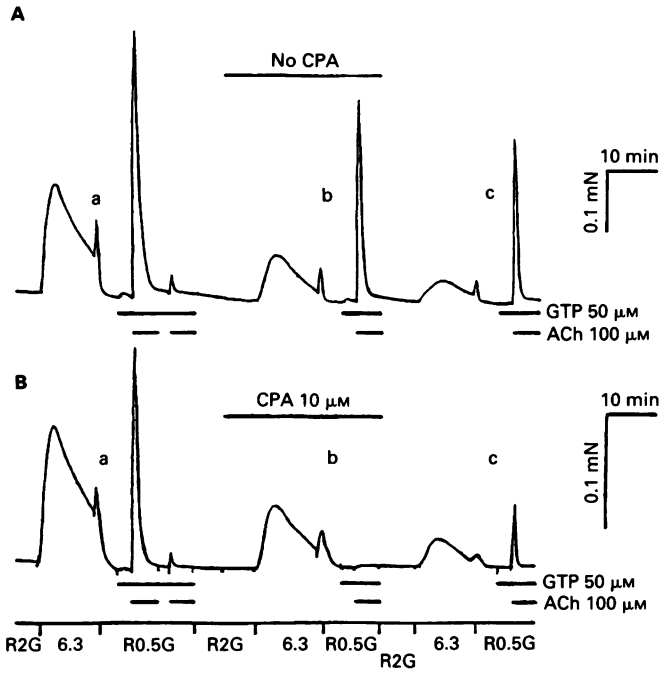

Figure 7 Effects of cyclopiazonic acid (CPA) on acetylcholine (ACh)-induced contraction in skinned ileal strip. The response to 100 μM ACh subsequent to Ca^{2+} -loading in pCa 6.3 solution was observed three times in each preparation. ACh was applied in the presence of 50 μM guanosine triphosphate (GTP) in relaxing solution (R0.5G). Ca^{2+} -uptake in the second trial was performed in the absence or presence of 10 μM CPA in (A) and (B), respectively.

skeletal muscle (~0.2 μM) (Kurebayashi & Ogawa, 1991).

In skinned smooth muscle fibres which showed rigor type contracture in ATP- and creatine-phosphate-free solution, addition of ATP induced transient relaxation followed by contraction at pCa 6.3. The relaxation may be explained by detachment of rigor cross-bridges by ATP which occurs much faster than phosphorylation of the myosin light chain (Somlyo *et al.*, 1988). Although the rate of detachment is much faster than the relaxation, the diffusion rate of ATP into the fibre might be responsible for the slow relaxation and following contraction, since the relaxation is much more transient when ATP is released by laser-flash photolysis (Somlyo *et al.*, 1988).

In most smooth muscle cells, two kinds of intracellular Ca^{2+}-releasing mechanism have been identified; a Ca^{2+}-induced Ca^{2+}-release mechanism which is affected by caffeine or ryanodine and a separate IP_3-induced Ca^{2+}-release mechanism. Two corresponding physically separated storage sites have been postulated; those which are sensitive to IP_3 only and those sensitive to both ryanodine and IP_3 (Iino *et al.*, 1988). Since 10 μM CPA almost completely inhibited both caffeine- and IP_3-induced contractions, the Ca^{2+}-ATPase which is inhibited by CPA may be involved in Ca^{2+}-uptake into both types of storage sites. Thapsigargin which is also known as an inhibitor of Ca^{2+}-ATPase in SR/ER, decreases Ca^{2+}-uptake into IP_3-sensitive storage sites more effectively than that into IP_3-insensitive ones in cultured smooth muscle cells (Bian *et al.*, 1991; Missiaen *et al.*, 1991).

It is well established that ACh activates phospholipase C, increases formation of IP_3 and thereby induces Ca^{2+}-release from SR/ER (Abdel-Latif, 1986). Therefore, the result that Ca^{2+}-uptake into storage sites sensitive to ACh as well as those sensitive to IP_3 were inhibited by CPA is consistent with the proposed mechanism. The possibility that the potency of CPA for inhibiting contraction induced by ACh is different from that by IP_3 has not been examined carefully in the present study. It might be possible since sensitization of contractile proteins to Ca^{2+} by ACh via GTP binding protein has been reported (Kitazawa & Somlyo, 1990).

A series of Ca^{2+}-ATPase isoforms in SR and ER of muscle and non-muscle tissues has been reported. Molecular cloning of smooth muscle SR/ER Ca^{2+}-ATPase has demonstrated that smooth muscle expresses the same gene as slow skeletal muscle, cardiac muscle and non-muscle tissues (Gunteski-Hamblin *et al.*, 1988; Lytton *et al.*, 1989). From this gene, three different mRNAs are transcribed by alternative processing (Eggermont *et al.*, 1990). Recent work has shown that the sensitivity to CPA (and thapsigargin as well) is identical in three types of avian ER/SR Ca^{2+}-ATPase encoded by three distinct cDNAs. These three cDNA sequences have high homology to SERCA1 in fast skeletal muscle, SERCA2a in slow skeletal and cardiac muscles, and SERCA2b in brain and smooth muscle in mammals, respectively (Cambell *et al.*, 1991). The effective concentrations of CPA in our preparation are similar to those required for inhibition of Ca^{2+}-ATPase in skinned fibre of fast skeletal muscle. These results may be consistent with the prediction based upon the molecular biological knowledge that CPA shows similar potency inhibiting Ca^{2+}-uptake into Ca^{2+}-storage sites in skeletal and smooth muscles.

Our results are consistent with the proposal that CPA decreases Ca^{2+}-uptake by inhibition of the Ca^{2+}-pump in the SR/ER, thereby decreasing subsequent Ca^{2+}-release from those storage sites. In the present study, however, Ca^{2+}-ATPase activity *per se* was not measured. Ca^{2+}-ATPase activity in SR of cardiac and smooth muscle is regulated by factors such as phospholamban (Tada *et al.*, 1975; Raeymaekers & Jones, 1986). Moreover, it has been reported that CPA inhibits Ca^{2+}-release from vesicles prepared from skeletal SR as well as Ca^{2+}-uptake. Although phenomena suggesting such kind of action were not found using relatively low concentrations of CPA in the present study, the possibility that higher concentration of CPA (> 3 μM) affects Ca^{2+}-releasing mechanisms remains to be examined. It might be possible that CPA has alternative or additional effects on regulation of the Ca^{2+}-ATPase activity.

One of the most important findings in the present study is that the inhibitory effect of CPA at concentrations less than 3 μM was almost completely reversible by washout in skinned smooth muscle strips. The velocity of Ca^{2+}-uptake which may directly correlate to Ca^{2+}-ATPase activity was not, however, measured in our experiments. Therefore, it is possible that the total amount of Ca^{2+} taken up over 10 min in pCa 6.3 solution was not affected even if the Ca^{2+}-ATPase activity was still partly suppressed by CPA remaining after washout. This has been found in skinned skeletal muscle preparations where inhibition of Ca^{2+}-ATPase activity by CPA was only partly removed by washout (Kurebayashi & Ogawa, 1991). Although the effects of CPA in intact smooth muscle preparations reported so far (Deng & Kwan, 1991; Bourrean *et al.*, 1991) appear to be consistent with our results in skinned fibres, it is not clear whether the effects of CPA are reversible in intact cells. Our preliminary results suggest that the effects of CPA in intact smooth muscle are removed by washout at least in part. Since it has been suggested that another SR/ER Ca^{2+}-ATPase inhibitor, thapsigargin, irreversibly affects Ca^{2+}-uptake in intact smooth muscle (Low *et al.*, 1991), removal of CPA-induced inhibition, even if it is not complete, may be pharmacologically important.

We conclude that CPA is a selective and reversible inhibitor of the Ca^{2+}-pump of intracellular Ca storage sites, mainly SR, in skinned ileal smooth muscle. It therefore is an extremely valuable pharmacological tool for investigation of Ca^{2+}-pumping mechanisms and intracellular Ca^{2+} homeostasis.

A part of this study was supported by the Fujiwara Foundation. We thank Drs Wayne Giles (University of Calgary) and Yasuo Ogawa (Juntendoh Univeristy) for valuable comments about this work.

References

ABDEL-LATIF, A.A. (1986). Calcium-mobilizing receptors, polyphosphoinositides, and the generation of second messengers. *Pharmacol. Rev.*, **38**, 227–272.

BIAN, J., GHOSH, T.K., WANG, J.C. & GILL, D.L. (1991). Identification of intracellular calcium pools. *J. Biol. Chem.*, **266**, 8801–8806.

BOURREAU, J.P., ABELA, A.P., KWAN, C.Y. & DANIEL, E.E. (1991). Acetylcholine Ca^{2+} stores refilling directly involves a dihydropyridine-sensitive channel in dog trachea. *Am. J. Physiol.*, **261**, (Cell Physiol. 30), C497–C505.

CAMBELL, A.M., KESSLER, P.D., SAGARA, Y., INESI, G. & FAMBROUGH, D.M. (1991). Nucleotide sequences of avian cardiac and brain SR/ER Ca^{2+}-ATPase and functional comparisons with fast twitch Ca^{2+}-ATPase. *J. Biol. Chem.*, **266**, 16050–16055.

DENG, H.W. & KWAN, C.Y. (1991). Cyclopiazonic acid is a sarcoplasmic reticulum Ca^{2+}-pump inhibitor of rat aortic muscle. *Acta Pharmacol. Sinca.*, **12**, 53–58.

EGGERMONT, J.A., WUYTACK, F. & CASTEELS, R. (1990). Characterization of the mRNAs encoding the gene 2 sarcoplasmic/endoplasmic-reticulum Ca^{2+} pump in pig smooth muscle. *Biochem. J.*, **266**, 901–907.

GOEGER, D.E. & RILEY, R.T. (1989). Interaction of cyclopiazonic acid with rat skeletal muscle sarcoplasmic reticulum vesicles. Effect on Ca^{2+} binding and Ca^{2+} permeability. *Biochem. Pharmacol.*, **38**, 3995–4003.

GOEGER, D.E., RILEY, R.T., DORNER, J.W. & COLE, R.J. (1988). Cyclopiazonic acid inhibition of the Ca^{2+}-transport ATPase in rat skeletal muscle sarcoplasmic reticulum vesicles. *Biochem. Pharmacol.*, **37**, 978–981.

GUNTESKI-HAMBLIN, A.N., GREEB, J. & SHULL, G.E. (1988). A novel Ca^{2+} pump expressed in brain, kidney, and stomach is encoded by ab alternative transcript of the slow-twitch muscle sarcoplasmic reticulum Ca-ATPase gene. *J. Biol. Chem.*, **263**, 15032–15040.

IINO, M. (1989). Calcium-induced calcium release mechanism in guinea pig taenia caeci. *J. Gen. Physiol.*, **94**, 363–383.

IINO, M., KOBAYASHI, T. & ENDO, M. (1988). Use of ryanodine for functional removal of the calcium store in smooth muscle cells of the guinea-pig. *Biochem. Biophys. Res. Commun.*, **152**, 417–422.

ITOH, T., KANMURA, Y. & KURIYAMA, H. (1985). A23187 increases calcium permeability of store sites more than of surface membranes in the rabbit mesenteric artery. *J. Physiol.*, **359**, 467–484.

ITOH, T., SUZUKI, S. & KURIYAMA, H. (1991). Effects of pinacidil on contractile proteins in high K^+-treated intact, and in β-escin-treated skinned smooth muscle of the rabbit mesenteric artery. *Br. J. Pharmacol.*, **103**, 1697–1702.

KITAZAWA, T. & SOMLYO, A.V. (1990). Desensitization and muscarinic re-sensitization of force and myosin light chain phosphorylation to cytoplasmic Ca^{2+} in smooth muscle. *Biochem. Biophys. Res. Commun.*, **172**, 1291–1297.

KITAZAWA, T., GAYLINN, B.D., DENNEY, G.H. & SOMLYO, A.P. (1991). G-protein-mediated Ca^{2+} sensitization of smooth muscle contraction through myosin light chain phosphorylation. *J. Biol. Chem.*, **266**, 1708–1715.

KOBAYASHI, S., KITAZAWA, T., SOMLYO, A.V. & SOMLYO, A.P. (1989). Cytosolic heparin inhibits muscarinic and α-adrenergic Ca^{2+} release in smooth muscle. *J. Biol. Chem.*, **264**, 17997–18004.

KUREBAYASHI, N. & OGAWA, Y. (1991). Discrimination of Ca^{2+}-ATPase activity of the sarcoplasmic reticulum from acto-myosine-type ATPase activity of myofibrils in skinned mammalian skeletal muscle fibres: distinct effects of cyclopiazonic acid on the two ATPase activities. *J. Muscle Res. Cell Motil.*, **12**, 355–365.

LOW, A.M., GASPAR, V., KWAN, C.Y., DARBY, P.J., BOURREAU, J.P. & DANIEL, E.E. (1991). Thapsigargin inhibits repletion of phenylephrine-sensitive intracellular Ca^{++} pool in vascular smooth muscles. *J. Pharmacol. Exp. Ther.*, **258**, 1105–1113.

LYTTON, J., SARAIN-HERZBERG, A., PERIASAMY, M. & MACLENNAN, D.H. (1989). Molecular cloning of the mammalian smooth muscle sarco(endo)plasmic reticulum Ca^{2+} -ATPase. *J. Biol. Chem.*, **264**, 7059–7065.

MISSIAEN, L., SMEDT, H.D., DROOGMANS, G., DECLERCK, I., PLESSERS, L. & CASTEELS, R. (1991). Uptake characteristics of the $InsP_3$-sensitive and -insensitive Ca^{2+} pools in porcine aortic smooth-muscle cells: different Ca^{2+} sensitivity of the Ca^{2+} sensitivity of the Ca^{2+}-uptake mechanism. *Biochem. Biophy. Res. Commun.*, **174**, 1183–1188.

RAEYMAEKERS, L. & JONES, L.R. (1986). Evidence for the presence of phospholamban in the endoplasmic reticulum of smooth muscle. *Biochem. Biophys. Acta*, **882**, 258–265.

SAIDA, K. & NONOMURA, Y. (1978). Characteristics of Ca^{2+} - and Mg^{2+}-induced tension development in chemically skinned smooth muscle fibres. *J. Gen. Physiol.*, **72**, 1–14.

SEIDLER, N.W., JONA, I., VEGH, M. & MARTONOSI, A. (1989). Cyclopiazonic acid is a specific inhibitor of the Ca2+-ATPase of sarcoplasmic reticulum. *J. Biol. Chem.*, **264**, 17816–17823.

SOMLYO, A.V., BOND, M., SOMLYO, A.P. & SCARPA, A. (1985). Inositol trisphosphate-induced calcium release and contraction in vascular smooth muscle. *Proc. Natl. Acad. USA*, **82**, 5231–5235.

SOMLYO, A.V., GOLDMAN, Y.E., FUJIMORI, T., BOND, M., TRENTHAM, D.R. & SOMLYO, A.P. (1988). Cross-bridge kinetics, cooperatively, and negatively strained cross-bridges in vertebrate smooth muscle. *J. Gen. Physiol.*, **91**, 165–192.

SUEMATSU, E., HIRATA, M., HASHIMOTO, T. & KURIYAMA, H. (1984). Inositol 1,4,5-triphosphate releases Ca^{2+} from intracellular store sites in skinned single cells of porcine coronary artery. *Biochem. Biophys. Res. Commun.*, **120**, 481–485.

TADA, M., KIRCHBERGER, M.A. & KATZ, A.M. (1975). Phosphorylation of a 22,000-dalton component of the cardiac sarcoplasmic reticulum by adenosine 3′,5′-monophosphate-dependent protein kinase. *J. Biol. Chem.*, **250**, 2640–2647.

(Received December 2, 1991
Revised January 13, 1992
Accepted January 16, 1992)

Br. J. Pharmacol. (1992), **106**, 215-221 © Macmillan Press Ltd, 1992

Adenosine A_1-receptor stimulation of inositol phospholipid hydrolysis and calcium mobilisation in DDT_1 MF-2 cells

Teresa E. White, John M. Dickenson, Stephen P.H. Alexander & [1]Stephen J. Hill

Department of Physiology & Pharmacology, Medical School, Queen's Medical Centre, Nottingham NG7 2UH

1. The effect of adenosine receptor-stimulation on inositol phospholipid hydrolysis and calcium mobilization has been investigated in the hamster vas deferens smooth muscle cell line DDT_1 MF-2.

2 Adenosine receptor stimulation increased the accumulation of total [^{3}H]-inositol phosphates in DDT_1 MF-2 cells prelabelled with [^{3}H]-*myo*-inositol. The rank order of agonist potencies was N^6-cyclopentyladenosine > 5'-N-ethylcarboxamidoadenosine > 2-chloroadenosine > adenosine.

3 The response to 2-chloroadenosine was antagonized by the antagonists 8-cyclopentyl-1,3-dipropylxanthine (K_D 1.2 nM), PD 115,199 (K_D 39 nM) and 8-phenyltheophylline (K_D 31 nM).

4 The inositol phosphate response to 2-chloradenosine (10 μM) was not significantly altered when the extracellular Ca^{2+} ion concentration was reduced from 2.4 mM to 1.2 mM or 0.6 mM. Under calcium-free conditions, however, a reduced but still significant response to 2-chloroadenosine was evident (39 ± 10% of the response in calcium-containing medium).

5 The 5-lipoxygenase inhibitor AA861 (10 and 100 μM) inhibited the inositol phosphate response to 2-chloroadenosine by 40 ± 9% and 60 ± 4% respectively. The cyclo-oxygenase inhibitor, indomethacin, however, was without significant effect at 1 μM.

6 2-Chloroadenosine stimulated an increase in intracellular free Ca^{2+} ion concentration in fura-2 loaded DDT_1 MF-2 cells in calcium-free medium containing 0.1 mM EGTA, which could be inhibited by the adenosine A_1-receptor antagonist 8-cyclopentyl-1,3-dipropylxanthine (0.1 μM).

7 These data suggest that adenosine A_1-receptor stimulation results in inositol phospholipid hydrolysis and calcium mobilization from intracellular stores in DDT_1 MF-2 cells.

Keywords: Adenosine; A_1-receptor; inositol phospholipids; calcium mobilisation; DDT_1 MF-2 cells; smooth muscle

Introduction

Extracellular adenosine receptors have been divided into two major subtypes, A_1- and A_2-, on the basis of agonist structure-activity relationships and the use of the antagonists 8-cyclopentyl-1,3-dipropylxanthine (DPCPX) and PD 115, 199 (Daly *et al.*, 1986; Bruns *et al.*, 1987a,b; Rakumar *et al.*, 1990). Thus, for the A_1-receptor the rank order of agonist potencies is such that N^6-derivatives of adenosine are more potent than 5'-analogues such as 5'-N-ethylcarboxamidoadenosine (NECA), while the reverse is true for the A_2-receptor (Daly *et al.*, 1986). Furthermore, DPCPX (which is a selective A_1-receptor antagonist) is more potent than PD 115,199 as an antagonist at the A_1-receptor, but less potent at the A_2-receptor (Bruns *et al.*, 1987a,b). A further subdivision of the A_2-receptor into A_{2A}- and A_{2B}- has also been proposed on the basis of the apparent higher affinities of the agonists 2-phenylaminoadenosine and CGS 21680 and the antagonist PD 115,199 for the A_{2A}-receptor compared to those determined for the A_{2B}-receptor (Bruns *et al.*, 1987b; Jarvis *et al.*, 1989; Alexander *et al.*, 1989b; Hargreaves *et al.*, 1991).

Adenosine A_1 and A_2-receptors can also be distinguished functionally on the basis of their differing effect on adenylate cyclase activity (Van Calker *et al.*, 1979; Londos *et al.*, 1980; Stiles, 1986). Thus, A_2-receptors are positively linked to adenylate cyclase via a G_s GTP-binding protein, while A_1-receptors are generally negatively linked to adenylate cyclase via a pertussis toxin-sensitive G_i protein (Stiles, 1986; Ramkumar *et al.*, 1990). However, recent studies have shown that A_1-receptors can also regulate voltage-sensitive calcium channels (Sperelakis, 1987), atrial potassium channels (Kurachi *et al.*, 1986), guanylate cyclase activity (Kurtz, 1987) and agonist-stimulated inositol phospholipid hydrolysis (Linden & Delahunty, 1989; Hill & Kendall, 1989).

In the central nervous system (CNS), adenosine A_1-receptors can selectively augment histamine H_1-receptor-mediated inositol phospholipid hydrolysis in guinea-pig cerebral cortical slices (Hollingsworth *et al.*, 1986; Hill & Kendall, 1987) and selectively inhibit the histamine response in mouse (Kendall & Hill, 1988) and man (Kendall & Firth, 1989) cerebral cortex. In all three species, however, adenosine-receptor stimulation failed to elicit a direct phosphoinositide response on its own. An inhibition of agonist-induced inositol phospholipid hydrolysis has also been demonstrated in the rat pituitary tumour cell line GH_3 (Delahunty *et al.*, 1988) and the human astrocytoma cell line 1321N1 (Nakahata *et al.*, 1991).

The DDT_1 MF-2 smooth muscle cell line, derived from a steroid-induced leimyosarcoma tumour of the vas deferens of an adult Syrian hamster, has recently been shown to possess high levels of both adenosine A_1- and A_2-receptors that are respectively coupled negatively and positively to adenylate cyclase (Gerwins *et al.*, 1990; Ramkumar *et al.*, 1991). These cells also possess glucocorticoid receptors which following activation can up-regulate adenosine A_1-receptors and down-regulate A_2-receptors (Gerwins & Fredholm, 1991a). We now show that adenosine A_1-receptors can also stimulate inositol phospholipid hydrolysis and intracellular calcium mobilization in this cell line. A preliminary account of some of this work has been presented to the British Pharmacological Society (White & Hill, 1992).

[1] Author for correspondence.

Methods

Cell culture

DDT_1 MF-2 cells (European Cell Collection, Porton Down) were cultured at 37°C in a humidified air/CO_2 (90:10) atmosphere in 75 cm^3 flasks (Costar). The growth medium was Dulbecco's modified Eagle's medium (DMEM) supplemented with 2 mM L-glutamine and 10% (v/v) foetal calf serum (FCS). Cells were passaged twice a week (1:5 split ratio) by vigorous shaking of the flask and fed with fresh growth medium every 48 h. Cells for inositol phospholipid hydrolysis were finally grown in 24 well cluster dishes and cells for $[Ca^{2+}]_i$ determination were grown on 24 mm × 10 mm glass cover slips in 90 mm Petri dishes. All experiments were performed on confluent monolayers (passages 4–12, number assigned after receiving the cell line).

Inositol phospholipid hydrolysis

At confluence, monolayer cultures were loaded with [^{3}H]-*myo*-inositol (37 kBq/well) for 24 h in 24 well cluster dishes in inositol-free DMEM containing 2 mM glutamine and 10% FCS. Prelabelled cells were then washed twice with 1 ml/well Hanks/HEPES (20 mM) buffer pH 7.4 and incubated at 37°C for 30 min in the presence of 20 mM LiCl. Where appropriate, antagonists were added at the beginning of this incubation period. Agonists were then added in 10 µl medium and the incubation continued for 45 min. Incubations were terminated by aspiration of the incubation medium and the addition of 1 ml cold (−20°C) methanol/0.12 M HCl (1:1 v/v). Cells were left a minimum of 2 h at −20°C before isolation of total ^{3}H-inositol phosphates in the supernatant of the disrupted cell monolayers by anion exchange chromatography (Alexander *et al.*, 1989a).

Measurement of intracellular free Ca^{2+}

Intracellular free calcium was measured by loading confluent cell monolayers with the calcium-sensitive fluorescent dye fura-2. Individual coverslips were placed in 35 mm Petri dishes with 1 ml of physiological buffer (composition, mM: NaCl 145, glucose 10, KCl 5, $MgSO_4$ 1, $CaCl_2$ 2, pH 7.45) containing 10% FCS (v/v), 3 µM fura-2/AM and incubated for 30 min at 37°C. After this loading period, the fura-2 containing buffer was replaced with fresh buffer that was free of fura-2 and FCS but contained 0.1% bovine serum albumin, and left at 37°C for a further 15 min. Where appropriate, antagonist drugs were added at the beginning of this 15 min period. Loaded coverslips were then mounted in a specially designed holder which enabled the coverslip to be positioned across the diagonal of a polymethacrylate cuvette. Each cuvette contained 2.9 ml of physiological buffer (containing antagonist drug where appropriate) and agonists were added in 100 µl of medium. Fluorescent measurements were made at 37°C with a Perkin Elmer LS 50 spectrophotometer. The excitation wavelengths were 340 and 380 nm, with emission measured at 500 nm. The slit widths were set at 10 nm for both the excitation and emission wavelengths and the time taken to switch between excitation wavelengths was 0.8 s. Intracellular free $[Ca^{2+}]$ was calculated every 1.6 s from the equation (Grynkiewicz *et al.*, 1985):

$$[Ca^{2+}]_i = \frac{(R - R_{min})}{(R_{max} - R)} \times \beta \times K_d$$

where R is the 340 nm/380 nm ratio of fluorescence values and K_d is the dissociation constant of fura-2 for Ca^{2+} ions (224 nM at 37°C) and β is the ratio of the fluorescent values obtained at 380 nm in the absence and presence of saturating $[Ca^{2+}]_i$. The maximum and minimum R values (R_{max} and R_{min}) were determined on separate cover slips under saturating $[Ca^{2+}]_i$ (achieved by increasing extracellular $[Ca^{2+}]$ to 20 mM followeed by 10 µM ionomycin, pH 7.45) and calcium-free (achieved with 8.3 mM EGTA immediately followed by 25 µl 1.0 M NaOH to compensate for the decrease in pH, in the presence of 10 µM ionomycin) conditions respectively. Corrections for autofluorescence were made by measuring the fluorescence produced by coverslips that had not been loaded with fura-2. Where calcium-free conditions were required, experiments were performed in nominally calcium-free buffer containing 0.1 mM EGTA.

Data analysis

Agonist concentration-response curves and antagonist inhibition curves were fitted to a logistic equation by use of the non-linear regression programme GraphPad (ISI) as described previously (Ruck *et al.*, 1990). Antagonist dissociation constants (K_d) were estimated by a modification of the null method described by Lazareno & Roberts (1987). Briefly, a concentration-response curve to 2-chloroadenosine was generated and a concentration (C; usually 10 µM) of 2-chloroadenosine was chosen which gave a response greater than 50% of the maximum agonist response. The concentration of antagonist (IC_{50}) required to reduce the response of this concentration (C) of 2-chloroadenosine by 50% was then determined. The 2-chloroadenosine concentration-response curve was fitted to a logistic equation as described above and a concentration of 2-chloroadenosine (C') identified which yielded a response equivalent to 50% of that produced by concentration C (in the absence of antagonist). The apparent K_d was then determined from the relationship:

$$C/C' = IC_{50}/K_d + 1$$

Statistical analysis was performed by paired and unpaired *t* tests; *n* in the text refers to the number of separate individual experiments.

Chemicals

Adenosine, 2-chloroadenosine, 5'-N-ethylcarboxamidoadenosine (NECA), N^6-cyclopentyladenosine, indomethacin and 8-phenyltheophylline were purchased from Sigma and 8-cyclopentyl-1,3-dipropylxanthine (DPCPX) from Research Biochemicals Incorporated. [2-^{3}H]-myo-inositol (529 GBq $mmol^{-1}$) was obtained from New England Nuclear. PD 115,199 (N-[2-(dimethylamino)ethyl]N-methyl-4-(1,3-dipropylaxanthine)benzene sulphonamide) and AA861 (2,3,5-trimethyl-6-(12-hydroxy-5,10- dodecadiynyl)1,4 - benzoquinone) were generous gifts from Warner Lambert (Ann Arbor, U.S.A.) and Takeda Chemical Industries (Osaka, Japan) respectively. Ionomycin and fura-2/AM were purchased from Calbiochem.

Results

Adenosine receptor-stimulated [^{3}H]-inositol phosphate accumulation

Adenosine (1 mM, 7.7 ± 0.8 fold over basal levels, $P < 0.05$, $n = 14$) and 2-chloroadenosine (10 µM, 6.8 ± 0.5 fold over basal levels, $P < 0.05$, $n = 26$) produced marked and significant accumulations of total [^{3}H]-inositol phosphates in the DDT_1 MF-2 cell line (Figure 1). Both agents produced a rapid increase in [^{3}H]-inositol phosphate accumulation over the first 10 min of agonist stimulation which began to plateau between 20 and 40 min (Figure 1b). Similar responses were obtained with N^6-cyclopentyladenosine (CPA; 1 µM, 8.5 ± 0.9 fold over basal levels, $n = 7$) and 5'-N-ethylcarboxamidoadenosine (NECA; 100 µM, 7.0 ± 0.8 fold over basal levels, $n = 4$) (Figure 2). Analysis of agonist concentration-response curves gave a rank order of potency which was typical of adenosine A_1-receptors, i.e. CPA > NECA > 2-chloroadenosine > adenosine (Figure 2; Table 1). The

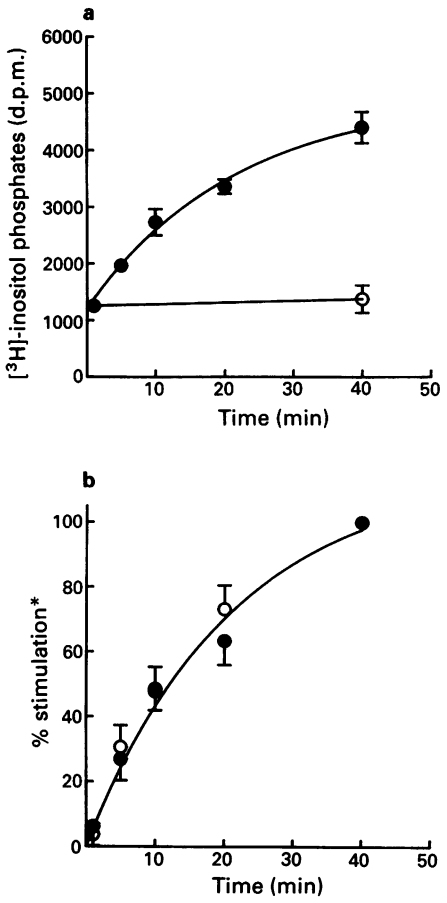

Figure 1 Time course of adenosine- and 2-chloroadenosine-stimulated [^{3}H]-inositol phosphate accumulation in DDT_1 MF-2 cells. (a) Response to 10 μM 2-chloroadenosine (●) added at time zero; (○) unstimulated control. Values represent mean (s.e.mean shown by vertical bars) from quadruplicate determinations in a single experiment. Similar data were obtained in three other experiments. (b) Mean stimulation produced by 10 μM 2-chloroadenosine (○) or adenosine (0.1 mM; ●). *Values represent mean ± s.e.mean of the percentage stimulation (response at 40 min = 100%) of total [^{3}H]-inositol phosphate accumulation (after subtraction of basal levels) obtained in four separate experiments performed in quadruplicate.

Table 1 Agonist potencies of adenosine analogues for stimulation of [^{3}H]-inositol phosphate accumulation in DDT_1 MF-2 cells

Agonist	*Inositol phosphate* (EC_{50} nM)		*A_1-binding** (K_D nM)
CPA	26 ± 4	(6)	58
NECA	290 ± 80	(4)	445
2-Chloroadenosine	480 ± 140	(6)	801
Adenosine	38,000 ± 9,000	(6)	1630

CPA = N^6-cyclopentyladenosine; NECA = 5'-N-ethylcarboxamidoadenosine. Values represent mean ± s.e.mean of the EC_{50} values for total [^{3}H]-inositol phosphate accumulation obtained in 4–6 individual experiments. The actual number of experiments is given in parentheses.
*Values reported (Gerwins *et al.*, 1990) for agonist K_D values from inhibition of [^{3}H]-DPCPX binding to adenosine A_1-receptors in intact DDT_1 MF-2 cells.

involvement of the A_1-class of adenosine receptor was further tested through the use of the selective A_1-receptor antagonist DPCPX (Bruns *et al.*, 1987a) and the high affinity mixed A_1/A_2 receptor antagonist, PD 115,199 (Bruns *et al.*, 1987b) (Figure 3). The apparent K_D values determined from individual inhibition curves for these two antagonists and for 8-phenyltheophylline were in close agreement with the values reported for the binding of these antagonists to the adenosine A_1-receptor in rat brain (Table 2).

Role of extracellular Ca^{2+} and arachidonic acid metabolites

To investigate whether adenosine receptor-stimulation was indirectly linked to inositol phospholipid hydrolysis via an effect on Ca^{2+} ion influx from the extracellular medium or mediated by liberation of cyclo-oxygenase or lipoxygenase products of arachidonic acid metabolism, experiments were performed in the presence of varying extracellular calcium concentrations (Figure 4) or the presence of indomethacin (an inhibitor of cyclo-oxygenase) and AA861 (an inhibitor of lipoxygenase) (Figure 5). In the presence of 0.6 mM and 1.2 mM extracellular calcium, the inositol phospholipid response to 10 μM 2-chloroadenosine was 97 ± 9% and 96 ± 10% of that obtained in normal calcium-containing medium (2.4 mM; $n = 4$, Figure 4). Furthermore, in calcium-free media, a significant response to 2-chloroadenosine

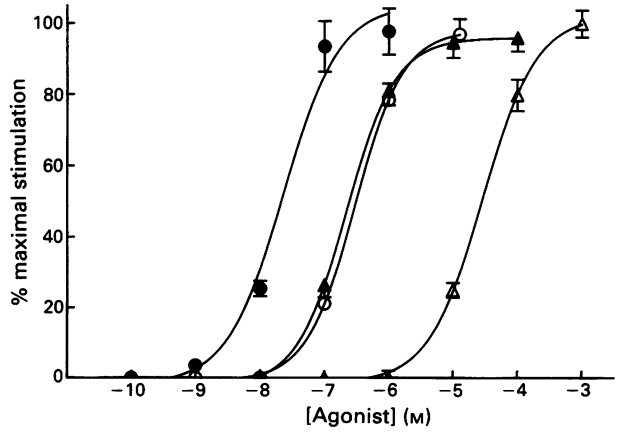

Figure 2 Effect of adenosine-receptor agonists on the accumulation of total [^{3}H]-inositol phosphates in DDT_1 MF-2 cells. Responses to N^6-cyclopentyladenosine (CPA; ●), N-ethylcarboxamidoadenosine (NECA; ▲), 2-chloroadenosine (○) and adenosine (△) are expressed as a percentage (mean with s.e.mean shown by vertical bars) of the maximal stimulation (after subtraction of basal values) from quadruplicate determinations in four (NECA) or six (all others) separate experiments.

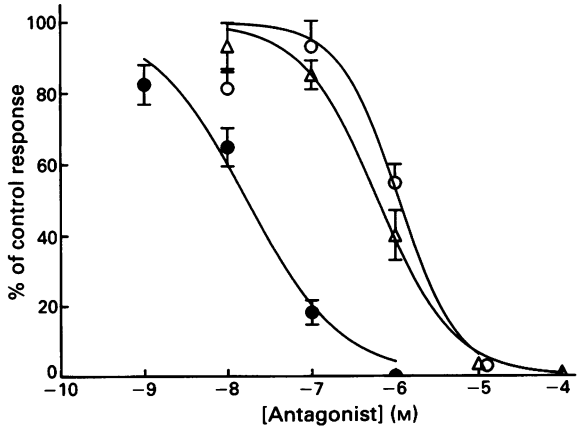

Figure 3 Effect of adenosine-receptor antagonists on 2-chloroadenosine-stimulated inositol phospholipid hydrolysis in DDT_1 MF-2 cells. Antagonism produced by DPCPX (●), 8-phenyltheophylline (△) or PD 115,199 (○) of the response to 10 μM 2-chloroadenosine. Values represent the combined mean (s.e.mean, shown by vertical bars) from quadruplicate determinations in six (8-phenyltheophylline) or four (DPCPX & PD 115,199) separate experiments.

Table 2 Antagonism of 2-chloroadenosine-mediated inositol phosphate accumulation in DDT_1 MF-2 cells

Antagonist	*Inositol phospholipid hydrolysis* IC_{50} (nM)	Apparent K_D (nM)		*Adenosine receptor* A_1*	A_{2A}#	K_D (nM) A_{2B}
DPCPX	37 ± 12	1.2 ± 0.4	(4)	0.5	340	234[a], 163[b]
8-PT	970 ± 350	31 ± 11	(6)	86	850	400[c]
PD 115,199	1200 ± 200	39 ± 7	(4)	14	16	275[a], 395[b]

8-PT = 8-phenyltheophylline. Values for inositol phospholipid hydrolysis represent mean ± s.e.mean of 4–6 determinations (actual number of experiments given in parentheses) of the antagonist IC_{50} values obtained from inhibition of 2-chloroadenosine-stimulated (10 μM) total [^{3}H]-inositol phosphate accumulation in DDT_1 MF-2 cells. Apparent K_D values were calculated from these IC_{50} values as described under Methods. *,#K_D values for inhibition of [^{3}H]-cyclohexyladenosine binding to A_1-receptor (*) or [^{3}H]-NECA binding to A_{2A} receptors (#) in rat brain membranes (Bruns *et al.*, 1987c); [a]K_D values obtained from antagonism of A_{2B}-receptor-mediated relaxation of guinea-pig aorta (Hargreaves *et al.*, 1991) or stimulation of cyclic AMP accumulation in guinea-pig cerebral cortex ([b]Alexander *et al.*, 1989b; [c]Alexander *et al.*, 1989a).

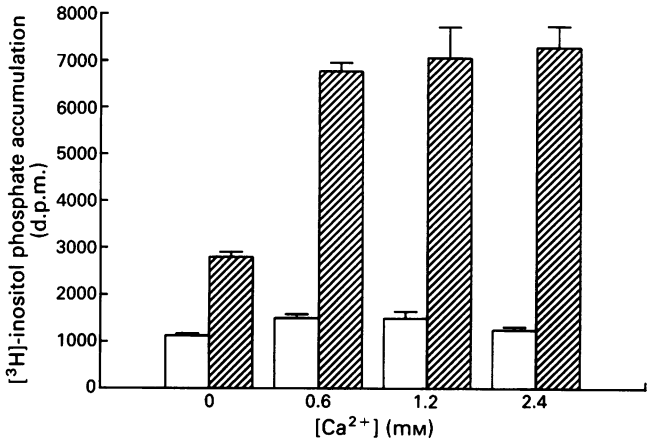

Figure 4 Influence of extracellular Ca^{2+} concentration on A_1-receptor-mediated inositol phospholipid hydrolysis in DDT_1-MF-2 cells. Measurements were made in the absence (open columns) or presence (hatched columns) of 10 μM 2-chloroadenosine. Data represent mean (s.e.mean shown by vertical bars) of quadruplicate determinations in a single experiment. Similar data were obtained in three other experiments and the combined data are summarized in the text.

(39 ± 10% of that obtained in 2.4 mM calcium-containing medium, $P<0.05$, $n=4$) was still evident (Figure 4).

Indomethacin (100 μM; $P<0.05$, $n=4$) and AA861 (100 μM; $P<0.05$, $n=4$) both produced an inhibition of the inositol phosphate response to 10 μM 2-chloroadenosine (Figure 5a), but significant effects with indomethacin were only evident at relatively high concentrations (Figure 5b). AA861 was, however, more potent that indomethacin (Figure 5b) and inhibited inositol phosphate accumulation at concentrations within the same range as that required for inhibition of 5-lipoxygenase (Yoshimoto *et al.*, 1982).

A_1-receptor-mediated release of intracellular Ca^{2+}

Monitoring of intracellular free calcium levels by use of the calcium-sensitive dye, fura-2, allowed the visualisation of an adenosine receptor-mediated increase in intracellular calcium levels in DDT_1 MF-2 cells (Figure 6). The addition of 10 μM 2-chloroadenosine to monolayers of DDT_1 MF-2 cells caused a rapid increase in intracellular free calcium concentrations from 86 ± 8 nM to 306 ± 25 nM (Figure 6a, $n=6$). The response was fairly well maintained and only declined slowly towards basal levels in the presence of extracellular calcium ions. Pretreatment of cells (15 min) with the adenosine A_1-selective antagonist DPCPX (100 nM) completely inhibited

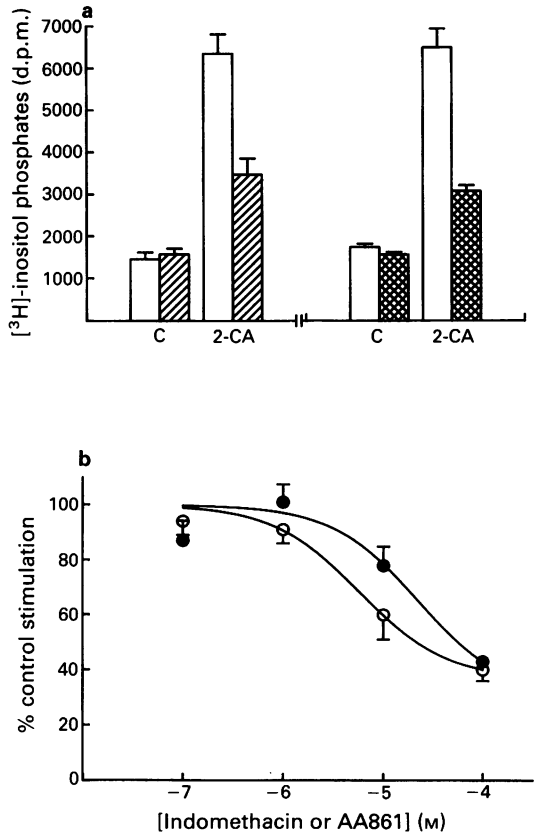

Figure 5 Effect of indomethacin and AA861 on 2-chloroadenosine-stimulated [^{3}H]-inositol phosphate accumulation in DDT_1 MF-2 cells. (a) Control (C) and 2-chloroadenosine (2-CA) responses were measured in the absence (open columns) or presence of 100 μM indomethacin (hatched columns) or 100 μM AA861 (cross-hatched columns). Values represent mean (s.e.mean shown by vertical bars) obtained from quadruplicate determinations in a single experiment. Similar data were obtained in two other experiments. (b) Concentration-response curves for the inhibition of 2-chloroadenosine-stimulated inositol phospholipid hydrolysis in DDT_1 MF-2 cells; (●) indomethacin; (○) AA861. Values represent combined mean (± s.e.mean) of quadruplicate determinations in four separate experiments. Data are expressed as a percentage of the control response to 10 μM 2-chloroadenosine (after subtraction of basal levels). The line through the AA861 data points was fitted to the equation: % control stimulation = $100-[A \times I_{max}/(IC_{50}+A)]$, where A is the concentration of AA861 and I_{max} is the maximal inhibitory effect. The fitted values for log IC_{50} and maximal inhibitory effect of AA861 were -5.23 ± 0.12 and 63.4 ± 4.2% inhibition respectively. The curve for indomethacin was insufficiently well-defined for least squares analysis and was drawn by inspection.

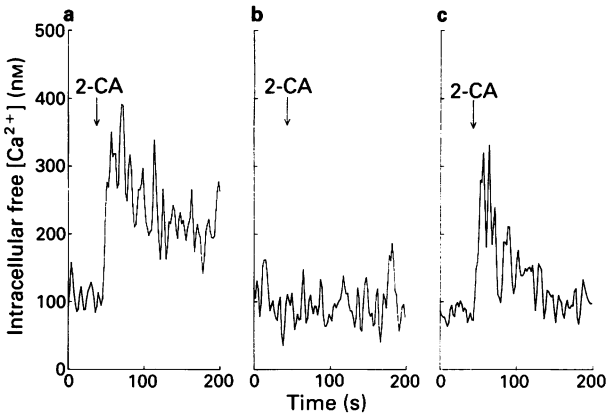

Figure 6 Effect of adenosine-receptor stimulation on intracellular Ca^{2+} concentration in fura-2 loaded DDT_1 MF-2 cells in the presence (a) of extracellular Ca^{2+} (2 mM) and in nominally Ca^{2+}-free buffer containing 0.1 mM EGTA (c). (b) As (a) but cells were incubated with 100 nM DPCPX for 15 min before the addition of 2-chloroadenosine. 2-Chloroadenosine (2-CA, 10 μM) was added where indicated. Similar data were obtained in three other experiments.

the response to a subsequent addition of 2-chloroadenosine (10 μM; Figure 6b). The maintenance of the response to 2-chloroadenosine appeared to be dependent upon influx of extracellular calcium since experiments performed in nominally calcium-free medium containing 0.1 mM EGTA (Figure 6c) resulted in a loss of the maintained phase, leaving the initial transient peak (presumably due to intracellular calcium release) relatively unaffected (90 ± 16% of the response in Ca^{2+}-containing media, $n = 3$).

Discussion

The hamster vas deferens smooth muscle cell line DDT_1 MF-2 has previously been shown to possess a high density of A_1-receptors (Ramkumar *et al.*, 1990; Gerwins *et al.*, 1990). Studies of adenosine 3':5'-cyclic monophosphate (cyclic AMP) accumulation in both intact DDT_1 MF-2 cells (Gerwins *et al.*, 1990) and cell membranes (Ramkumar *et al.*, 1990) have shown that these receptors can negatively couple to adenylate cyclase via a pertussis toxin-sensitive G_i GTP binding protein. The present investigation suggests that A_1-receptors can additionally associate in some way with the activation of phospholipase C leading to inositol phospholipid hydrolysis and mobilization of intracellular calcium.

The A_1-receptor nature of the adenosine-stimulated accumulation of total [^{3}H]-inositol phosphates in DDT_1 MF-2 cells is indicated by both the rank order of agonist potencies and the high affinity of the A_1-receptor selective antagonist DPCPX, deduced from inhibition of 2-chloroadenosine-stimulated inositol phospholipid hydrolysis. Thus, the rank order of agonist potencies is such that the N^6-derivative of adenosine, CPA, is more potent that the 5'-derivative, NECA. Furthermore, the EC_{50} values deduced from inositol phospholipid hydrolysis for the stable analogues of adenosine, namely CPA, NECA and 2-chloroadenosine, agree (within a factor of 2; Table 1) closely with the K_D values obtained for these agonists from inhibition of [^{3}H]-DPCPX binding in intact DDT_1 MF-2 cells (Gerwins *et al.*, 1990).

The most convincing argument for the involvement of an A_1-receptor is, however, provided by the data obtained with antagonists, particularly DPCPX (Table 2). Bruns *et al.* (1987c) have argued that the relative affinities of DPCPX and PD 115,199 provide a useful basis for distinguishing A_1- and A_{2a}-receptor-mediated responses. Thus, DPCPX is 30 times more potent than PD 115,199 at the A_1-receptor, but 20 times less potent than PD 115,199 at the A_{2a} receptor. Furthermore, DPCPX and PD 115,199 are both weak antagonists (K_D *circa* 250 nM) at the A_{2b} receptor in guinea-pig aorta and guinea-pig cerebral cortex (Alexander *et al.*, 1989b; Hargreaves *et al.*, 1991). The data obtained in the present study, where DPCPX is 32.5 fold more potent than PD 115,199, are entirely consistent with the involvement of an A_1-receptor (Table 2). The high affinity of DPCPX (K_D 1.2 nM, Table 2) is similar to that obtained in rat brain membranes (Bruns *et al.*, 1987a) and in good agreement with the K_D (0.95 nM) obtained for A_1-receptor binding in intact DDT_1 MF-2 cells (Gerwins *et al.*, 1990). These data suggest that the receptor involved in the inositol phospholipid response to adenosine in DDT_1 MF-2 cells has the characteristics of a classic A_1-receptor rather than the atypical pharmacology of the adenosine A_1-like receptors involved in modulating histamine-stimulated inositol phospholipid hydrolysis in guinea-pig and mouse brain (Alexander *et al.*, 1989b) or regulating neurotransmission at the frog neuromuscular junction (putative A_3-receptor; Sebastiao & Ribeiro, 1989; 1990), where the K_D values obtained for DPCPX are much higher (10–35 nM).

Stimulation of inositol phospholipid hydrolysis and mobilization of intracellular free calcium by adenosine have also been detected in the rat tumour-derived mast cell line RBL-2H3 (Ali *et al.*, 1990; Hide & Beavan, 1991) and guinea-pig myometrium (Schiemann *et al.*, 1991a,b). In RBL-2H3 cells, the order of adenosine analogue potency indicated an involvement of an A_2-adenosine receptor (Ali *et al.*, 1990). However, adenosine antagonists such as 8-phenyltheophylline and 8-*p*-sulphophenyltheophylline produced only a non-selective antagonism of the NECA-induced inositol phosphate response at high concentrations, indicating the potential involvement of a novel class of adenosine receptor (Ali *et al.*, 1990) which may be related to the atypical adenosine receptor responsible for enhancing mediator secretion from rat peritoneal mast cells (Church *et al.*, 1986).

In oestrogen-primed or pregnant guinea-pig myometrium, adenosine A_1-receptor stimulation can produce smooth muscle contraction and inositol phospholipid hydrolysis via a mechanism which is insensitive to pertussis toxin treatment (Moritoki *et al.*, 1979; Smith *et al.*, 1988; Schiemann *et al.*, 1991a,b). Both of these effects could be completely attenuated by pretreatment of the tissue with cyclo-oxygenase inhibitors suggesting that smooth muscle contraction and inositol-1,4,5-trisphosphate formation may be secondary to the synthesis of prostaglandins from arachidonic acid (Moritoki *et al.*, 1979; Schiemann *et al.*, 1991b). This possibility has also been investigated in DDT_1 MF-2 cells in the present study by use of the cyclo-oxygenase inhibitor indomethacin and the 5-lipoxygenase inhibitor, AA861 (Higgs & Vane, 1983; Yoshimoto *et al.*, 1982; Ashida *et al.*, 1983).

Both agents were able to inhibit the inositol phospholipid response to 2-chloroadenosine by approximately 60% at high concentrations (100 μM) but no significant effect was observed with 1 μM indomethacin, which was sufficient to attenuate completely the A_1-receptor-mediated inositol phosphate response in guinea-pig myometrium (Schiemann *et al.*, 1991b). However, the 5-lipoxygenase inhibitor, AA861, was more potent than indomethacin (Figure 6) and the inhibition of the response to 2-chloroadenosine appeared to plateau at the 60% level. Furthermore, the IC_{50} obtained for AA861-mediated inhibition of 2-chloroadenosine-stimulated inositol phospholipid hydrolysis (5.8 μM) was within the same concentration-range as that required for inhibition of guinea-pig 5-lipoxygenase in cell-free preparations or tissue fragments (Yoshimoto *et al.*, 1982; Ashida *et al.*, 1983). Since indomethacin can inhibit fully cyclo-oxygenase at 1 μM, the inhibitory activity observed at higher concentrations of indomethacin may be accounted for by its effects on lipoxygenase.

These data suggest that lipoxygenase, rather than cyclo-oxygenase, products are involved in the A_1-receptor-mediated inositol phosphate response in DDT_1 MF-2 cells. However, since 40% of the response to 2-chloroadenosine was resistant

to both 100 μM indomethacin and 100 μM AA861, it seems likely that other mechanisms (including the possibility that A_1-receptors are directly coupled to inositol phospholipid hydrolysis via a G-protein) are also involved. Indeed, it is possible that the lipoxygenase products are produced as a consequence of the A_1-receptor-mediated increase in intracellular Ca^{2+} in DDT_1 MF-2 cells (Figure 6) leading to an activation of phospholipase A_2 activity.

Studies in calcium-free media suggest that some 60% of the 2-chloroadenosine-stimulated accumulation of [^{3}H]-inositol phosphates in DDT_1 MF-2 cells is dependent upon an influx of extracellular Ca^{2+} ions. However, experiments in calcium-free medium (containing EGTA) clearly show that adenosine A_1-receptor-stimulation can produce a direct release of Ca^{2+} ions from intracellular stores, presumably as a consequence of the generation of inositol-1,4,5-trisphosphate (Berridge & Irvine, 1989). Interestingly, while this manuscript was in preparation, a short report appeared which demonstrated that the A_1-receptor agonist CPA could increase both inositol-1,4,5-trisphosphate levels and intracellular calcium concentrations in DDT_1 MF-2 via a mechanism which was sensitive to pretreatment with pertussis toxin (Gerwins & Fredholm, 1991b).

In summary, this study provides strong evidence that adenosine A_1-receptors can stimulate inositol phospholipid hydrolysis and release of calcium from intracellular stores in DDT_1 MF-2 cells. It is clear that the A_1-receptor-mediated inositol phospholipid hydrolysis is reduced by either the presence of an inhibitor of lipoxygenase or by removal of extracellular calcium. Consequently, it remains to be established whether A_1-adenosine receptors are directly coupled to phospholipase C via a G-protein or whether inositol phospholipid hydrolysis and calcium mobilization are entirely mediated by indirect mechanisms. However, what is clear is that the DDT_1-MF-2 cell line, in which adenosine A_1-receptors have also been demonstrated to inhibit cyclic AMP accumulation (Gerwins *et al.*, 1991a), will be an important system in which to investigate adenosine receptor-effector coupling mechanisms.

We thank the Wellcome Trust for financial support.

References

ALEXANDER, S.P.H., KENDALL, D.A. & HILL, S.J. (1989a). Differences in the adenosine receptors modulating inositol phosphates and cyclic AMP accumulation in mammalian cerebral cortex. *Br. J. Pharmacol.*, **98**, 1241–1248.

ALEXANDER, S.P.H., HARDING, S.M., RATCLIFFE, K.M. & HILL, S.J. (1989b). DPCPX and PD 115,199 as discriminatory tools for differentiating adenosine receptors in guinea-pig tissues. *Br. J. Pharmacol.*, **98**, 738P.

ALI, H., CUNHA-MELO, J.R., SAUL, W.F. & BEAVAN, M.A. (1990). Activation of phospolipase C via adenosine receptors provides synergistic signals for secretion in antigen-stimulated RBL-2H3 cells: evidence for a novel adenosine receptor. *J. Biol. Chem.*, **265**, 745–753.

ASHIDA, Y., SAIJO, T., KURIKA, H., MAKINO, H., TERAO, S. & MAKI, Y. (1983). Pharmacological profile of AA861, a 5-lipoxygenase inhibitor. *Prostaglandins*, **26**, 955–972.

BERRIDGE, M.J. & IRVINE, R.F. (1989). Inositol phosphates and cell signalling. *Nature*, **341**, 197–205.

BRUNS, R.F., FERGUS, J.H., BADGER, E.W., BRISTOL, J.A., SANTAY, L.A., HARTMAN, J.D., HAYS, S.J. & HUANG, C.C. (1987a). Binding of the A_1-selective adenosine antagonist 8-cyclopentyl-1,3-dipropylxanthine to rat brain membranes. *Naunyn-Schmiedebergs Arch. Pharmacol.*, **335**, 59–63.

BRUNS, R.F., FERGUS, J.H., BADGER, E.W., BRISTOL, J.A., SANTAY, L.A., HARTMAN, J.D. & HAYS, S.J. (1987b). PD 115,199: an antagonist ligand for adenosine A_2 receptors. *Naunyn-Schmiedebergs Arch. Pharmacol.*, **335**, 64–69.

BRUNS, R.F., LU, G.H. & PUGSLEY, T.A. (1987c). Adenosine receptor subtypes: binding studies. In *Topics and Perspectives in Adenosine Research* ed. Gerlach, E. & Becher, B.F. Berlin: Springer-Verlag.

CHURCH, M.K., HUGHES, P.J. & VARDEY, C.J. (1986). Studies on the receptor mediating cyclic AMP-independent enhancement by adenosine of IgE-dependent mediator release from mast cells. *Br. J. Pharmacol.*, **87**, 233–242.

DALY, J.W., PADGETT, W., THOMPSON, R.D., KUSACHI, S., BUGNI, W.J. & OLSSON, R.A. (1986). Structure-activity relationships for N^6-substituted adenosines at a brain A_1-receptor with a comparison to an A_2-adenosine receptor regulating coronary blood flow. *Biochem. Pharmacol.*, **35**, 2467–2481.

DELAHUNTY, T.M., CRONIN, M.J. & LINDEN, J. (1988). Regulation of GH_3-cell formation via adenosine A_1 receptors: inhibition of prolactin release, cyclic AMP production and inositol phosphate generation. *Biochem. J.*, **255**, 69–77.

GERWINS, P. & FREDHOLM, B.B. (1991a). Glucocorticoid receptor activation leads to up-regulation of adenosine A_1 receptors and down-regulation of adenosine A_2 responses in DDT_1 MF-2 smooth muscle cells. *Molec. Pharmacol.*, **40**, 149–155.

GERWINS, P. & FREDHOLM, B.B. (1991b). ATP and its metabolite adenosine act synergistically to mobilize intracellular calcium via the formation of $Ins(1,4,5)P_3$ in a smooth muscle cell line. *Br. J. Pharmacol.*, (in press).

GERWINS, P., NORDSTEDT, C. & FREDHOLM, B.B. (1990). Characterisation of adenosine A_1 receptors in intact DDT_1 MF-2 smooth muscle cells. *Molec. Pharmacol.*, **38**, 660–666.

GRYNKIEWICZ, G., POENIE, M. & TSIEN, R.Y. (1985). A new generation of Ca^{2+} indicators with greatly improved fluorescence properties. *J. Biol. Chem.*, **260**, 3440–3450.

HARGREAVES, M.B., STOGGALL, S.M. & COLLIS, M.G. (1991). Evidence that the adenosine receptor mediating relaxation in dog lateral spahenous vein and guinea-pig aorta is of the A_{2B} subtype. *Br. J. Pharmacol.*, **102**, 198P.

HIDE, M. & BEAVAN, M.A. (1991). Calcium influx in a rat mast cell (RBL-2H3) line. *J. Biol. Chem.*, **266**, 15221–15229.

HIGGS, G.A. & VANE, J.R. (1983). Inhibition of cyclooxygenase and lipoxygenase. *Br. Med. Bull.*, **39**, 265–270.

HILL, S.J. & KENDALL, D.A. (1987). Studies on the adenosine-receptor mediating the augmentation of histamine-induced inositol phospholipid hydrolysis in guinea-pig cerebral cortex. *Br. J. Pharmacol.*, **91**, 661–670.

HILL, S.J. & KENDALL, D.A. (1989). Cross-talk between different receptor-effector systems in the mammalian CNS. *Cell. Signalling*, **1**, 135–141.

HOLLINGSWORTH, E.B., DE LA CRUZ, R.A. & DALY, J.W. (1986). Accumulation of inositol phosphates and cyclic AMP in brain slices: synergistic interactions of histamine and 2-chloroadenosine. *Eur. J. Pharmacol.*, **122**, 45–50.

JARVIS, M.F., SCHULZ, R., HUTCHISON, A.J., HOI DO, U., SILLS, M.A. & WILLIAMS, M. (1989). [^{3}H]-CGS 21680, a selective A_2 adenosine receptor agonist directly labels A_2 receptors in rat brain. *J. Pharmacol. Exp. Ther.*, **251**, 888–893.

KENDALL, D.A. & HILL, S.J. (1988). Adenosine inhibition of histamine stimulated inositol phospholipid hydrolysis in mouse cerebral cortex. *J. Neurochem.*, **50**, 497–502.

KENDALL, D.A. & FIRTH, J.L. (1989). Adenosine inhibition of histamine-stimulated inositol phospholipid hydrolysis in human cerebral cortical slices. *Br. J. Clin. Pharmacol.*, **27**, 109P.

KURACHI, Y., NAKAJIMA, Y. & SUGIMOTO, T. (1986). On the mechanism of activation of muscarinic K^+ channels by adenosine in isolated atrial cells: involvement of GTP-binding proteins. *Pflügers Arch.*, **407**, 264–274.

KURTZ, A. (1987). Adenosine stimulates guanylate cyclase activity in vascular smooth muscle cells. *J. Biol. Chem.*, **262**, 6296–6300.

LAZERENO, S. & ROBERTS, F.F. (1987). Measuring muscarinic antagonist potency using phosphoinositide breakdown in rat cortex slices. *Br. J. Pharmacol.*, **92**, 677P.

LINDEN, J. & DELAHUNTY, M. (1989). Receptors that inhibit phosphoinositide breakdown. *Trends Pharmacol. Sci.*, **10**, 114–120.

LONDOS, C., COOPER, D.M.F. & WOLFF, J. (1980). Subclasses of external adenosine receptors. *Proc. Natl. Acad. Sci. U.S.A.*, **77**, 2551–2554.

MORITOKI, H., TAKEI, M., KASAI, T., MATSUMUAR, Y. & ISHIDA, Y. (1979). Possible involvement of prostaglandins in the action of ATP on guinea-pig uterus. *J. Pharmacol. Exp. Ther.*, **211**, 104–111.

NAKAHATA, N., ABE, M.T., MATSUOKA, I., ONO, T. & NKANISHI, H. (1991). Adenosine inhibits histamine-induced phosphoinositide hydrolysis mediated via pertussis toxin-sensitive G protein in human astrocytoma cells. *J. Neurochem.*, **57**, 963–969.

RAMKUMAR, V., BARRINGTON, W.W., JACOBSON, K.A. & STILES, G.L. (1990). Demonstration of both A_1 and A_2 adenosine receptors in DDT_1 MF-2 smooth muscle cells. *Molec. Pharmacol.*, **37**, 149–156.

RAMKUMAR, V., OLAH, M.E., JACOBSON, K.A. & STILES, G.L. (1991). Distinct pathways of desensitization of A_1- and A_2-adenosine receptors in DDT_1 MF-2 cells. *Molec. Pharmacol.*, **40**, 639–647.

RUCK, A., MILLNS, P., KENDALL, D.A. & HILL, S.J. (1990). Expression of $beta_2$-adrenoceptors mediating cyclic AMP accumulation in astroglial and neuronal cell lines derived from the rat CNS. *Biochem. Pharmacol.*, **40**, 2371–2375.

SCHIEMANN, W.P., DOGGWILER, K.O. & BUXTON, I.L.O. (1991b). Action of adenosine in estrogen-primed nonpregnant guinea-pig myometrium: characterisation of the smooth muscle receptor and coupling to phosphoinositide metabolism. *J. Pharmacol. Exp. Ther.*, **258**, 429–437.

SCHIEMANN, W.P., WESTFALL, D.P. & BUXTON, I.L.O. (1991a). Smooth muscle adenosine A_1-receptors couple to disparate effectors by distinct G proteins in pregnant myometrium. *Am. J. Physiol.*, **261**, E141–E150.

SEBASTIAO, A.M. & RIBEIRO, J.A. (1989). 1,3,8- and 1,3,7-substituted xanthines: relative potency as adenosine receptor antagonists at the frog neuromuscular junction. *Br. J. Pharmacol.*, **96**, 211–219.

SEBASTIAO, A.M. & RIBEIRO, J.A. (1990). Interactions between adenosine and phorbol esters or lithium at the frog neuromuscular junction. *Br. J. Pharmacol.*, **100**, 55–62.

SMITH, M.A., BUXTON, I.L.O. & WESTFALL, D.P. (1988). Pharmacological classification of receptors of adenyl purines in guinea-pig myometrium. *J. Pharmacol. Exp. Ther.*, **247**, 1059–1063.

SPERELAKIS, N. (1987). Regulation of calcium slow channels of cardiac and smooth muscle by adenine nucleotides. In *Cardiac Electrophysiology and Pharmacology of Adenosine and ATP: Basic and Clinical Aspects* ed. Pelleg, A., Michelson, E.L. & Freifus, L.S. New York: Alan R. Liss Inc.

STILES, G.L. (1986). Adenosine receptors: structure, function and regulation. *Trends Pharmacol. Sci.*, **7**, 486–490.

VAN CALKER, D., MUELLER, M. & HAMPRECHT, B. (1979). Adenosine regulates via two different types of receptors, the accumulation of cyclic AMP in cultured brain cells. *J. Neurochem.*, **33**, 999–1005.

WHITE, T.E. & HILL, S.J. (1992). Adenosine-stimulated accumulation of total [^{3}H]-inositol phosphates in DDT_1 MF-2 cells. *Br. J. Pharmacol.*, (in press).

YOSHIMOTO, T., YOKOYAMA, C., OCHI, K., YAMAMOTO, S., MAKI, Y., ASHIDA, Y., TERAO, S. & SHIRAISHI, M. (1982). 2,3,5-trimethyl-6-(12-hydroxy-5,10-dodecadiynyl)1,4-benzoquinone (AA861), a selective inhibitor of the 5-lipoxygenase reaction and the biosynthesis of slow-reacting substance of anaphylaxis. *Biochim. Biophys. Acta*, **713**, 470–473.

(Received January 8, 1992
Revised January 21, 1992
Accepted January 23, 1992)

Br. J. Pharmacol. (1992), **106**, 222–226 © Macmillan Press Ltd, 1992

Effects of a new pteridine derivative on urinary sodium, potassium and magnesium excretion in conscious saline-loaded rats

[1]T. Netzer, *F. Ullrich, H. Priewer, †M. Majewski & E. Mutschler

Department of Pharmacology, University of Frankfurt, Theodor-Stern-Kai 7, Gebäude 75A, D-6000 Frankfurt/M., Germany; *Röhm Pharma GmbH, Dr.-Otto-Röhm-Straße 2-4, D-6108 Weiterstadt, Germany and †Röhm GmbH, Kirschenallee, D-6100 Darmstadt 1, Germany

1 Two recently synthesized pteridine derivatives (RPH 3036; RPH 3038) were tested in conscious saline-loaded rats and showed natriuretic and antimagnesiuretic properties but hardly reduced potassium excretion.

2 In the same model a dose-response curve was performed for RPH 3036. ED_{50} and E_{max} values were calculated for the natriuretic ($ED_{50} = 13.4\ \mu mol\ kg^{-1}$; $E_{max} = 1.08\ mmol\ kg^{-1}$) and antimagnesiuretic ($ED_{50} = 11.3\ \mu mol\ kg^{-1}$; $E_{max} = -0.099\ mmol\ kg^{-1}$) properties of RPH 3036. There were no significant changes of potassium and calcium excretion.

3 After a single dose of RPH 3036 ($100\ \mu mol\ kg^{-1}$) the time course of electrolyte excretion was analysed over 6 h. RPH 3036 did not show any significant effects on renal potassium and calcium excretion whereas a pronounced decrease ($P < 0.01$) in renal magnesium excretion was evident during the 6 h. A moderate increase of sodium excretion was observed only after 3, 5 and 6 h.

4 A selective reduction of magnesium secretion in the late distal tubule and collecting duct was proposed as a possible mechanism of action of RPH 3036. This would explain the fast onset of action as well as the lack of antikaliuretic and anticalciuretic effects. The high selectivity of RPH 3036 makes it potentially valuable for the future investigation of renal magnesium transport.

Keywords: Magnesium-sparing diuretics; potassium-sparing diuretics; pteridine derivatives; triamterene derivatives

Introduction

Increasing attention has been drawn over recent years to diuretic-induced magnesium loss and its consequences (Dyckner & Wester, 1984; Learey & Reyes, 1984). Therapeutic strategies to avoid this magnesium loss primarily consist of the use of potassium-sparing diuretics (Dyckner *et al.*, 1986; Widman *et al.*, 1988; 1990) since there is growing evidence for an antimagnesiuretic effect of these substances (Lim & Jacob, 1978; Devane & Ryan, 1981; 1983).

Triamterene, for example, exerted magnesium-sparing properties in laboratory animals (Mutschler *et al.*, 1981) as well as in man (Hänze & Seyberth, 1967). The lack of antimagnesiuretic activity of triamterene in other studies (van Meyel *et al.*, 1990) was probably due to a different study design. Low water solubility and a high biotransformation rate of triamterene might cause adverse side-effects. Therefore, derivatives with better physico-chemical and pharmacokinetic properties were synthesized several years ago. Some of these derivatives not only showed marked antikaliuretic activity in conscious saline-loaded rats but also exerted pronounced magnesium retaining effects after acute administration (Priewer *et al.*, 1985; Ullrich *et al.*, 1990). The magnesium-sparing effect of these triamterene derivatives was more pronounced than that seen after administration of triamterene itself. These derivatives, however, were potent antikaliuretics like all other diuretic agents with antimagnesiuretic activity.

Recently three new pteridine derivatives (Figure 1) were synthesized and the aim of this study was to test 2,4,7-triamino-6-(*N*,*N*-dimethylaminomethyl)pteridine (RPH 2997), 2,4,7-triamino-6-[2-(*N*,*N*-dimethylamino)ethyl]pteridine (RPH 3036), and 2,4,7-triamino-6-[3-(*N*,*N*-dimethylamino) propyl] pteridine (RPH 3038) for their natriuretic, antikaliuretic, and antimagnesiuretic effects in conscious saline-loaded rats. As will be shown later, RPH 3036 and RPH 3038 are the first magnesium-sparing diuretic compounds that are almost devoid of antikaliuretic activity.

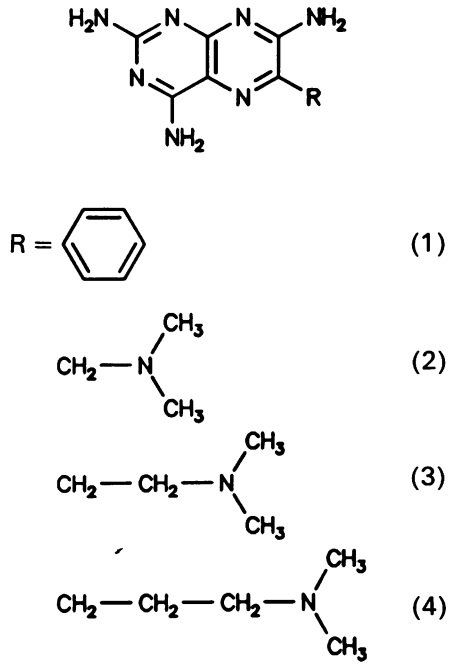

Figure 1 Chemical structures of triamterene (1), RPH 2997 (2), RPH 3036 (3), and RPH 3038 (4).

[1] Author for correspondence.

Methods

Pharmacodynamic experiments

Male Wistar rats weighing 140–210 g were used. Food was withdrawn 18 h before the experiment but tap water was available *ad libitum*. The rats were randomly divided into groups of 5 to 10 animals as indicated in the text. In every experiment the diuretic-treated groups were compared to a control group receiving solvent only. All rats were given by gavage 20 ml kg^{-1} body weight of a 0.9% NaCl solution. Then the test compound (dissolved in 1 ml kg^{-1}) was injected under light ether anaesthesia in one of the caudal veins. The animals were placed in individual metabolism cages without food and water. All experiments were started at 08 h 00 min. Depending on the experiment urine was collected for 2.5 h and 6 h or for 2, 3, 4, 5, and 6 h, respectively.

Analytical methods

To determine its volume the urine was collected in graduated (± 0.1 ml) centrifuge tubes. Sodium and potassium concentrations were analysed by flame emission spectrophotometry and calcium and magnesium concentrations were determined by atomic absorption spectrophotometry with an Elektrolytautomat FL 6 (Zeiss, Oberkochen, Germany) in each case.

Data analysis

Data are expressed as means ± s.e.mean. Significance of differences between means was assessed by the Kruskal-Wallis test for the dose-response experiments and by a two-sided U-test according to Wilcoxon, Mann, Whitney for the rest of the experiments.

The fig.P computer programme (Biosoft, Cambridge, U.K.) was used to fit sigmoid curves to the data points of dose-response experiments and to calculate ED_{50} and E_{max} values. The calculations were based on the following equation:

$$E = E_0 + E_{max} \frac{D^P}{D^P + ED_{50}{}^P}$$

where E_0 is the basal response without any drug, D the dose administered, E the response to the dose D, E_{max} the change of E_0, which is induced by the maximally effective dose, ED_{50} the median of the effective dose and where P is the exponential factor which determines the shape of the curve.

Drugs

Triamterene was a gift from Röhm Pharma GmbH (Weiterstadt, Germany). RPH 2997 was used as the HCl salt. All substances were dissolved or suspended in a solution of 20% polyethylene glycol (PEG) 400 and 80% water.

Syntheses

RPH 2997, RPH 3036 and RPH 3038 are not yet described in the literature and were prepared as follows.

2,4,7-Triamino-6-(N,N-dimethylamino)methylpteridine (RPH 2997): 2,4,7-Triamino-6-methypteridine (1) was synthesized according to Pachter (1963). (1) was converted to 2,4,7-triamino-6-brommethylpteridine (2) by photobromation. Nucleophilic substitution of (2) with diethylamine resulted in RPH 2997.

2,4,7-Triamino-6-(2-N,N-dimethylaminoethyl)pteridine (RPH 3036): Nucleophilic substitution of 3-chlorpropionaldehyde-diethylacetal (Aldrich, Steinheim, Germany) with dimethylamine gave 3-dimethylaminopropionaldehydediethylacetal (1). Using (1) and tetraaminopyrimidine (Aldrich, Steinheim, Germany) RPH 3036 was prepared by the same procedure as described by Pachter (1963) except that hydrochloric acid was used instead of acetic acid as the acetal had to be cleaved. m.p. 286°C (decomp.)

2,4-7-Triamino-6-[3-(N,N-dimethylamino)propyl]pteridine (RPH 3038): RPH 3038 was synthesized in analogy to RPH 3036 starting with the nucleophilic substitution of 2-(3-chlorpropyl)-1,3-dioxolane (Fluka, Neu-Ulm, Germany) with dimethylamine. m.p. 226°C (decomp.)

All compounds wer characterized by ^1H nuclear magnetic resonance (n.m.r.) and ^{13}C n.m.r. measurements as well as by elemental analyses (data not given).

Results

A comparison between the effects of triamterene and the three recently synthesized pteridine derivatives at a dose of 25 μmol kg^{-1} ($n = 10$) is shown in Figure 2. During the first collection period triamterene exerted highly significant diuretic ($P < 0.01$), natriuretic ($P < 0.001$) and antikaliuretic ($P < 0.01$) effects whereas RPH 2997 only reduced potassium excretion ($P < 0.01$) without any significant influence on the other parameters. In contrast to triamterene and RPH 2997, both RPH 3036 and RPH 3038 almost selectively exhibited magnesium-retaining properties ($P < 0.01$). Only after administration of RPH 3036 was a minor natriuretic activity ($P < 0.05$) seen. The effects observed after 6 h were hardly different (data not shown): The increase in magnesium excretion ($P < 0.05$), initially induced by triamterene, was not evident after 6 h. The natriuretic effect of RPH 3036 was attenuated after the longer collection period.

To obtain more information about the selectively anti-magnesiuretic compounds, we chose RPH 3036 to perform a dose-response curve ($n = 6$; Figure 3). Due to significant changes of sodium ($P < 0.1$) and magnesium ($P < 0.01$) excretion ED_{50} and E_{max} values were calculated for natriuretic and antimagnesiuretic effects. The ED_{50} values for both natriuresis ($ED_{50} = 13.4$ μmol kg^{-1}) and antimagnesiuresis ($ED_{50} = 11.2$ μmol kg^{-1}) were almost the same. The maximal increase in sodium excretion (E_{max}) was calculated to be only 1.08 mmol kg^{-1} and the maximal decrease in magnesium excretion was

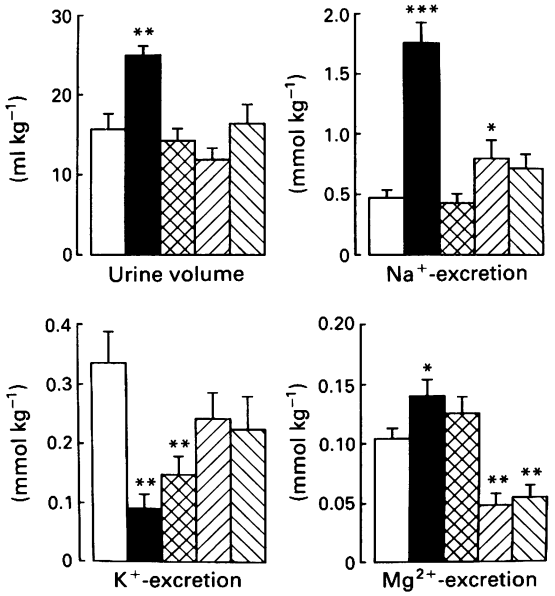

Figure 2 Effects of solvent (□), triamterene (■), RPH 2997 (▩), RPH 3036 (▨), and RPH 3038 (▧) (all 25 μmol kg^{-1}) on urinary volume, sodium, potassium, and magnesium excretion in the conscious saline-loaded rat. Urine was collected over a 2.5 h period. Each column is the mean of $n = 10$ rats/group; s.e.mean shown by vertical bars. *$P < 0.05$ vs. control; **$P < 0.01$ vs. control; ***$P < 0.001$ vs. control.

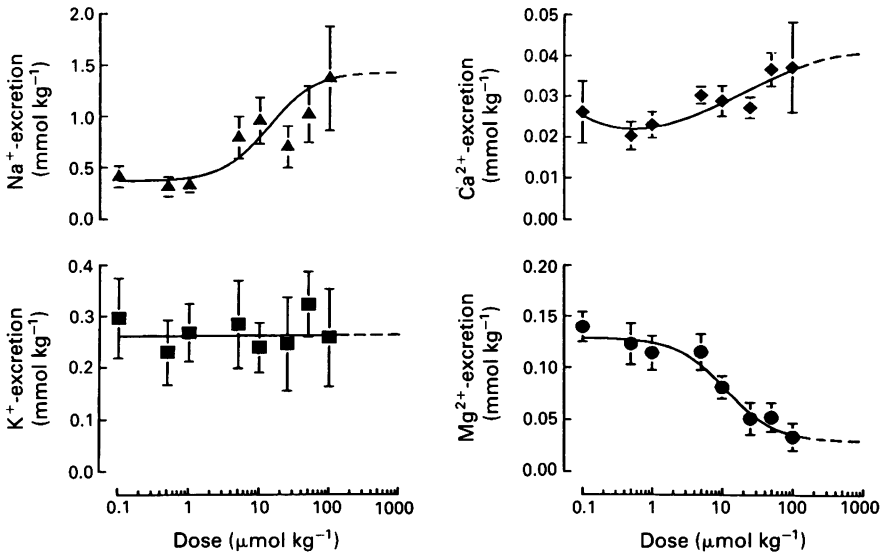

Figure 3 Effects of different doses of RPH 3036 on urinary sodium, potassium, calcium, and magnesium excretion in the conscious saline-loaded rat. Urine was collected over a 2.5 h period. Each point is the mean of $n = 6$ rats/group; s.e.mean shown by vertical bars. A sigmoid curve was fitted to the data of sodium and magnesium excretion by the computer programme fig.P (Biosoft, Cambridge, U.K.). The ED_{50} values of natriuretic and antimagnesiuretic effects were 13.4 μmol kg^{-1} and 11.2 μmol kg^{-1}, respectively.

calculated to be -0.099 mmol kg^{-1}. There were no significant changes in potassium and calcium excretion.

In the last experiment ($n = 5$) the time course of effects on urinary excretion of water, sodium, potassium, calcium, and magnesium was investigated with a high dose (100 μmol kg^{-1}) of RPH 3036 (Figure 4). Sodium excretion was increased after 3 h ($P < 0.05$) and after 5 and 6 h ($P < 0.01$). A pronounced reduction in magnesium excretion ($P < 0.01$) was evident the whole time but no significant potassium-sparing effects were seen. Calcium excretion did not show any significant changes but tended to be slightly higher than the corresponding control values.

Discussion

The results of this study provide evidence that RPH 3036 and RPH 3038 are the first diuretic compounds with prominent antimagnesiuretic but no antikaliuretic or anticalciuretic effects.

In Figure 5 the different potencies, expressed as $-\log ED_{50}$ (mol kg^{-1}), of RPH 3036 were compared to the corresponding values of some other closely related pteridine derivatives such as triamterene, 2,4,7-triamino-6-[4-(3-diamethylamino-2-hydroxypropoxy)phenyl]pteridine (H3), 2,4,7-triamino-6-[4-(3-dimethylaminopropoxy)phenyl]pteridine (B3), ethylamide

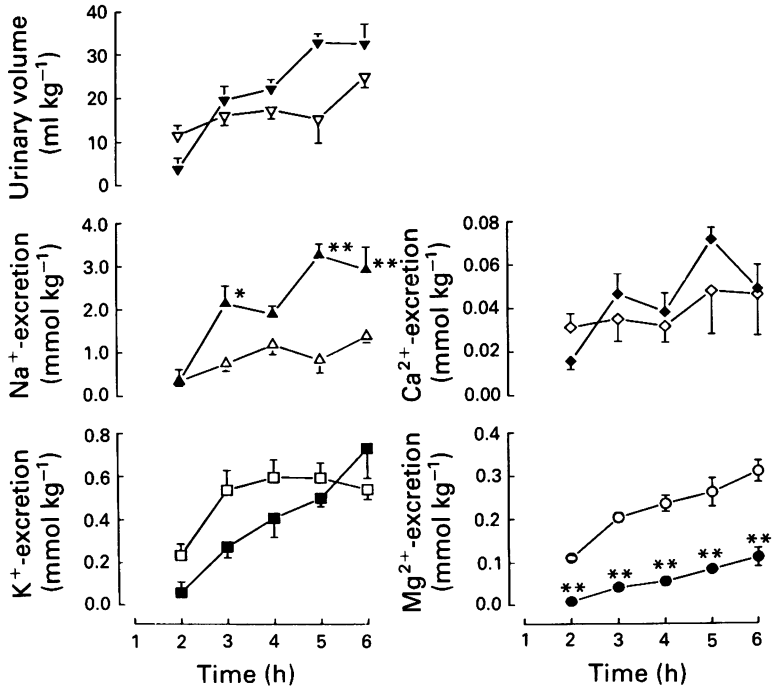

Figure 4 Time-dependent effects of RPH 3036 (100 μmol kg^{-1}; filled symbols) in conscious saline-loaded rats on urinary volume and electrolyte excretion compared to the effects of solvent (open symbols). Each point is the mean of $n = 5$ rats/group; s.e.mean shown by vertical bars. $^{*}P < 0.05$ vs. control; $^{**}P < 0.01$ vs. control.

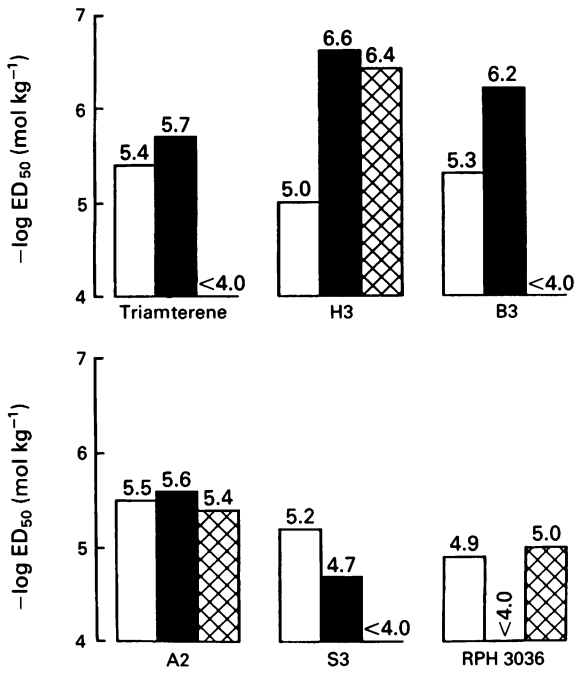

Figure 5 Natriuretic (open columns), antikaliuretic (solid columns), and antimagnesiuretic (cross-hatched) properties of triamterene, H3, B3, A2, S3, and RPH 3036 expressed as $-\log ED_{50}$ (mol kg^{-1}) values.

of 2,4,7-triamino-6-[4-(4-carboxybutoxy)phenyl]pteridine (A2), and 2,4,7-triamino-6-[4-(4-carboxybutoxy)phenyl]pteridine (S3) (data taken from Priewer *et al.*, 1985; 1987).

All compounds shared about the same natriuretic potency whereas antikaliuretic and antimagnesiuretic potencies varied to a great extent. Although among the previous triamterene derivatives some exerted antikaliuretic effects without any influence on magnesium excretion (e.g. B3) none could reduce magnesium excretion without affecting urinary output of potassium. The first compound with this unique profile was RPH 3036 with an antimagnesiuretic potency of 11.2 μmol kg^{-1} but with almost no effect on potassium excretion up to a dose of 100 μmol kg^{-1}.

To explain antimagnesiuretic effects of potassium-sparing diuretics, different mechanisms of action have already been suggested (Devane & Ryan, 1981; Ryan *et al.*, 1984; Ryan, 1986). Due to the differences between RPH 3036 and potassium-sparing diuretics most of these proposed mechanisms cannot account for the effects observed after administration of RPH 3036.

Magnesium-sparing properties of amiloride are thought to be mediated by direct renal action (Devane & Ryan, 1983). A blockade of sodium channels in the late distal tubule and in the collecting duct by potassium-sparing diuretics will result in a reduction of the transepithelial membrane potential (Hendry & Ellory, 1988). This reduces the driving force for potassium exit into the lumen, and thus potassium excretion is attenuated. Some authors suggest (Ryan *et al.*, 1984) that a lower transepithelial potential in this part of the nephron might promote reabsorption of cations such as magnesium, too, thereby reducing their excretion.

This mechanism of action can explain only combined antikaliuretic and antimagnesiuretic effects but it cannot explain a reduction of potassium excretion without reduction of magnesium excretion or selective magnesium-sparing effects. Therefore, the magnesium-retaining effects of RPH 3036 must be mediated by a different mode of action.

RPH 3036 (100 μmol kg^{-1}) only induced excretion of about 50% of the given saline load after 2.5 h (see Figure 3). Thus, it seems to be unlikely that magnesium reabsorption in the proximal tubule was increased due to a reduction in extracellular fluid volume.

The fact that calcium excretion was not influenced by RPH 3036 may be taken as a hint that parathyroid hormone and calcitonin are not involved in the antimagnesiuretic effect of RPH 3036.

Since the effects on magnesium excretion were already evident 2 h after administration of RPH 3036 (Figure 4), a contribution of changes in plasma aldosterone or plasma thyroid hormone concentration to these actions was also unlikely.

The attempt to explain magnesium-retaining effects with an unspecific alkalosis (Ryan, 1986) does not seem to be sufficient as an explanation for the marked and selective effects induced by RPH 3036.

The mode of action which is most consistent with the results of this study is the selective inhibition of magnesium secretion in the late distal tubule and collecting duct. Although it is not unequivocally accepted that magnesium secretion occurs in that part of the nephron (Massry *et al.*, 1969; Alfredson & Walser, 1970) there are hints that magnesium is secreted in the late distal tubule and collecting duct at least during furosemide and saline diuresis (Rios *et al.*, 1977; Lechene & Blouch, 1979). Since our study was performed in saline-loaded rats it is conceivable that magnesium was secreted in the late distal tubule and collecting duct and that blockade of this secretion resulted in a selective reduction of magnesium excretion. Of course further studies are required to determine whether this suggestion holds true.

In conclusion, RPH 3036 and RPH 3038, two recently synthesized pteridine derivatives, exerted in conscious saline-loaded rats natriuretic and antimagnesiuretic effects probably by direct renal action. Due to the fact that these compounds influenced magnesium but not potassium and calcium excretion they might be useful tools for the future investigation of renal magnesium transport.

T.N. thanks the government of Hessen (Germany) for a postgraduate scholarship. This paper contains parts of the Ph.D. thesis of T.N. The authors wish to thank Mr Ch. Gubitz for critical revision of this manuscript.

References

ALFREDSON, K.S. & WALSER, M. (1970). Is magnesium secreted by the rat renal tubule? *Nephron*, **7**, 241–247.

DEVANE, J. & RYAN, M.P. (1981). The effects of amiloride and triamterene on urinary magnesium excretion in conscious saline-loaded rats. *Br. J. Pharmacol.*, **72**, 285–289.

DEVANE, J. & RYAN, M.P. (1983). Evidence for a magnesium-sparing action by amiloride during renal clearance studies in rats. *Br. J. Pharmacol.*, **79**, 891–896.

DYCKNER, T. & WESTER, P.O. (1984). Intracellular magnesium loss after diuretic administration. *Drugs*, **28** (Suppl. 1), 161–166.

DYCKNER, T., WESTER. P.O. & WIDMAN, L. (1986). Effects of spironolactone on serum and muscle electrolytes in patients on long-term diuretic therapy for congestive heart failure and/or arterial hypertension. *Eur. J. Clin. Pharmacol.*, **30**, 535–540.

HÄNZE, S. & SEYBERTH, H. (1967). Untersuchungen zur Wirkung der Diuretika Furosemid, Etacrynsäure und Triamteren auf die renale Magnesium- und Calcium-Ausscheidung. *Klin. Wochenschr.*, **45**, 313–314.

HENDRY, B.M. & ELLORY, J.C. (1988). Molecular sites for diuretic action. *Trends Pharmacol. Sci.*, **9**, 416–421.

LEARY, W.P. & REYES, A.J. (1984). Diuretic-induced magnesium losses. *Drugs*, **28** (Suppl. 1), 182–187.

LECHENE, C. & BLOUCH, K. (1979). Potassium and magnesium secretion occur in the cortical collecting duct. *Kidney Int.*, **16**, 825.

LIM, J. & JACOB, E. (1978). Magnesium-saving property of an aldosterone antagonist in the treatment of oedema of liver cirrhosis. *Br. Med. J.*, **1**, 755–756.

MASSRY, S.G., COBURN, J.W. & KLEEMAN, C.R. (1969). Renal handling of magnesium in the dog. *Am. J. Physiol.*, **216**, 1460–1467.

MUTSCHLER, E., VOLLMER, G. & VÖLGER, K.D. (1981). Diurese und Salurese bei Ratten nach intravenöser Applikation von Pteridinderivaten. *Magnesium-Bull.*, **3**, 46–50.

PACHTER, I.P. (1963). Pteridines. II. Synthesis of 6-substituted 7-aminopteridines from aldehydes. *J. Org. Chem.*, **28**, 1191–1195.

PRIEWER, H., KRAFT, H. & MUTSCHLER, E. (1985). Evidence for an acute antimagnesiuretic effect of triamterene derivatives. *Pharm. Res.*, **2**, 90–93.

PRIEWER, H., WOLF, E., KRAFT, H., KNAUF, H. & MUTSCHLER, E. (1987). Dissociation of the natriuretic and antikaliuretic properties of triamterene derivatives by dose-response experiments. *Pharm. Res.*, **4**, 66–69.

RIOS, L.L., INGRAM, M.J., INGRAM, F.D. & DIBONA, G.F. (1977). Renal tubular secretion of magnesium in the rat. *Clin. Res.*, **25**, 596A.

RYAN, M.P. (1986). Magnesium and potassium-sparing diuretics. *Magnesium*, **5**, 282–292.

RYAN, M.P., DEVANE, J., RYAN, M.F. & COUNIHAN, T.B. (1984). Effects of diuretics on the renal handling of magnesium. *Drugs*, **28** (Suppl. 1), 167–181.

ULLRICH, F., PRIEWER, H. & MUTSCHLER, E. (1990). Magnesium-retaining triamterene derivatives. *Magnesium Res.*, **3**, 311–312.

VAN MEYEL, J.J.M., SMITS, P. & GRIBNAU, F.W.J. (1990). Absence of magnesium sparing effect of a single dose of triamterene in combination with frusemide in healthy male adults. *Br. J. Clin. Pharmacol.*, **30**, 774–777.

WIDMAN, L., DYCKNER, T. & WESTER, P.O. (1988). Effects of triamterene on serum and skeletal muscle electrolytes in diuretic-treated patients. *Eur. J. Clin. Pharmacol.*, **33**, 577–579.

WIDMAN, L., DYCKNER, T. & WESTER, P.O. (1990). Amiloride in the correction of diuretic-induced intracellular potassium and magnesium depletion. *Magnesium-Bull.*, **12**, 118–121.

(Received June 11, 1991
Revised December 16, 1991
Accepted January 4, 1992)

British Journal of Pharmacology

VOLUME 106 (1) MAY 1992

PAPERS

P.I. Thompson, S. Bingham, P.L.R. Andrews, N. Patel, S.P. Joel & M.L. Slevin. Morphine 6-glucuronide: a metabolite of morphine with greater emetic potency than morphine in the ferret 3

D.M. Eckman, J.D. Frankovich & K.D. Keef. Comparison of the actions of acetylcholine and BRL 38227 in the guinea-pig coronary artery 9

Th. Noack, G. Edwards, P. Deitmer, P. Greengrass, T. Morita, P.-O. Andersson, D. Criddle, M.G. Wyllie & A.H. Weston. The involvement of potassium channels in the action of ciclazindol in rat portal vein 17

M.R. Bennett, R. Kerr & G. Khurana. Adenosine modulation of calcium currents in postganglionic neurones of avian cultured ciliary ganglia 25

J.V. Esplugues, Ma.D. Barrachina & J. Esplugues. Modulation by peripheral opioids of basal and distension-stimulated gastric acid secretion in the rat 33

P. Valeri, L.A. Morrone & L. Romanelli. Manifestations of acute opiate withdrawal contracture in rabbit jejunum after μ-, κ- and δ-receptor agonist exposure 39

A. Abdelrahman, Y.-X. Wang, S.D. Chang & C.C.Y. Pang. Mechanism of the vasodilator action of calcitonin gene-related peptide in conscious rats 45

Y. Zhu, W.B. Im, R.A. Lewis & P.F. VonVoigtlander. Comparison of pyrrolidinyl and piperidinyl benzamides for their anticonvulsant activity and inhibitory action on sodium channel 49

S.Y. Lin-Shiau, K.S. Hsu & W.M. Fu. Studies on curare-like action of 2,2',2''-tripyridine in the mouse phrenic nerve-diaphragm 55

L.A. Bishop, V.P. Gerskowitch, R.A.D. Hull, N.P. Shankley & J.W. Black. Combined dose-ratio analysis of cholecystokinin receptor antagonists, devazepide, lorglumide and loxiglumide in the guinea-pig gall bladder 61

K. Fink, R. Schultheiß & M. Göthert. Stimulation of noradrenaline release in human cerebral cortex mediated by N-methyl-D-aspartate (NMDA) and non-NMDA receptors 67

N. Tokutomi, N. Agopyan & N. Akaike. Penicillin-induced potentiation of glycine receptor-operated choride current in rat ventro-medial hypothalamic neurones 73

T. Makki, I. Lartaud, L. Bray-des Boscs, C. Capdeville-Atkinson, J.-M. Chillon, M. Hoffman, J.-P. Nicolas & J. Atkinson. Haemodynamic effects of a new dihydropyridine calcium entry blocker, S-12968-(−), in a rat model of cardiovascular calcium overload 79

G. Kojda, W. Klaus, G. Werner & U. Fricke. Intervascular and stimulus selectivity of nitrendipine and related derivatives in KCl and prostaglandin $F_{2\alpha}$ precontracted porcine arteries 85

M.F.M. Braga, A.J. Anderson, A.L. Harvey & E.G. Rowan. Apparent block of K^+ currents in mouse motor nerve terminals by tetrodotoxin, μ-conotoxin and reduced external sodium 91

J.B. Salom, G. Torregrosa, F.J. Miranda, J.A. Alabadí & E. Alborch. Comparison of the contractile effects of endothelin-1 and sarafotoxin S6b in goat isolated cerebral arteries 95

S. Diamant, T. Eldar-Geva & D. Atlas. Imidazoline binding sites in human placenta: evidence for heterogeneity and a search for physiological function 101

R.M. Henderson, M.L.J. Ashford, L.J. MacVinish & A.W. Cuthbert. Chloride channels and anion fluxes in a human colonic epithelium (HCA-7) 109

L.A. Brown & S.E. Harding. The effect of pertussis toxin on β-adrenoceptor responses in isolated cardiac myocytes from noradrenaline-treated guinea-pigs and patients with cardiac failure 115

H. Morimoto, M. Murai, Y. Maeda, D. Hagiwara, H. Miyake, M. Matsuo & T. Fujii. FR 113680: a novel tripeptide substance P antagonist with NK_1 receptor selectivity 123

J.L. Mehta, D.L. Lawson, B.C. Yang, P. Mehta & W.W. Nichols. Modulation of vascular tone by endothelin-1: role of preload, endothelial integrity and concentration of endothelin-1 127

G.R. May, W. Paul, P. Crook, K.D. Butler & C.P. Page. The pharmacological modulation of thrombin-induced cerebral thromboembolism in the rabbit 133

K.F. Martin, S. Hannon, I. Phillips & D.J. Heal. Opposing roles for $5\text{-}HT_{1B}$ and $5\text{-}HT_3$ receptors in the control of 5-HT release in rat hippocampus *in vivo* 139

V.E. Rand & C.J. Garland. Endothelium-dependent relaxation to acetylcholine in the rabbit basilar artery: importance of membrane hyperpolarization 143

W. Schreibmayer, O. Tripathi & H.A. Tritthart. Kinetic modulation of guinea-pig cardiac L-type calcium channels by fendiline and reversal of the effects of Bay K 8644 151

P. Arvola, I. Pörsti, P. Vuorinen, A. Pekki & H. Vapaatalo. Contractions induced by potassium-free solution and potassium relaxation in vascular smooth muscle of hypertensive and normotensive rats 157

M.J. Robertson, M.P. Cunoosamy & K.L. Clark. Effects of peptidase inhibition on angiotensin receptor agonist and antagonist potency in rabbit isolated thoracic aorta 166

R.A. Lefebvre, E. Baert & A.J. Barbier. Influence of N^G-nitro-L-arginine on non-adrenergic non-cholinergic relaxation in the guinea-pig gastric fundus 173

S.M. Gardiner, P.A. Kemp & T. Bennett. Effects of the neutral endopeptidase inhibitor, SQ 28,603, on regional haemodynamic responses to atrial natriuretic peptide or proendothelin-1 [1-38] in conscious rats 180

F. Rioux & M. Lemieux. Haemodynamic and abdominal motor reflexes elicited by neurotensin in anaesthetized guinea-pigs 187

N.E. Shaw, R. Foulkes, D.P. Andrew, D.T. Brown & B. Hughes. The effect of monoclonal antibodies to calcitonin gene-related peptide (CGRP) on CGRP-induced vasodilatation in pig coronary artery rings 196

R.H. Scott, M.I. Sweeney, E.M. Kobrinsky, H.A. Pearson, G.H. Timms, I.A. Pullar, S. Wedley & A.C. Dolphin. Actions of arginine polyamine on voltage and ligand-activated whole cell currents recorded from cultured neurones **199**

Y. Uyama, Y. Imaizumi & M. Watanabe. Effects of cyclopiazonic acid, a novel Ca^{2+}-ATPase inhibitor, on contractile responses in skinned ileal smooth muscle **208**

T.E. White, J.M. Dickenson, S.P.H. Alexander & S.J. Hill. Adenosine A_1-receptor stimulation of inositol phospholipid hydrolysis and calcium mobilisation in DDT_1 MF-2 cells **215**

T. Netzer, F. Ullrich, H. Priewer, M. Majewski & E. Mutschler. Effects of a new pteridine derivative on urinary sodium, potassium and magnesium excretion in conscious saline-loaded rats **222**

SPECIAL REPORTS

The purpose of *Special Reports* is to provide rapid publication for **new** and **important** results which the Editorial Board considers are likely to be of special pharmacological significance. (Please note that Short Communications are no longer acceptable for publication.) *Special Reports* will have publication priority over all other material and so authors are asked to consider carefully the status of their work before submission.

In order to speed publication there is normally no revision allowed beyond very minor typographical or grammatical corrections. If significant revision is required, the Board may either invite rapid re-submission or, more probably, propose that it be re-written as a Full Paper and be re-submitted for consideration. In order to reduce delays, proofs of *Special Reports* will be sent to authors but **essential corrections must reach the Production Office within 48 hours of receipt.** Authors should ensure that their submitted material conforms exactly to the following requirements.

Special Reports should normally occupy no more than two printed pages of the Journal; two illustrations (Figures or Tables, with legends) are permitted. As a guideline, with type face of 12 pitch and double-line spacing, a page of A4 paper could contain about 400 words. The absolute maximum length of the *Special Report* is 1700 words. For each Figure or Table, please deduct 200 words. The manuscript should comprise a Title page with key words (maximum of 10), a Summary consisting of a single short paragraph, followed by Introduction, Methods, Results, Discussion and References (maximum of 10). In all other respects, the requirements are the same as for Full Papers (see current 'Instructions to Authors').

Edited for the British Pharmacological Society by

A.T. Birmingham *(Chairman)*
R.W. Horton *(Secretary)*
W.A. Large *(Secretary)*

EDITORIAL BOARD

J.A. Angus Prahran, Australia
M.L.J. Ashford Cambridge
G.W. Bennett Nottingham
T. Bennett Nottingham
W.C. Bowman Glasgow
N.G. Bowery London
Alison F. Brading Oxford
S.D. Brain London
K.T. Bunce Ware
G. Burnstock London
K.D. Butler Horsham
M. Caulfield London
M.K. Church Southampton
S.J. Coker Liverpool
R.A. Coleman Ware
G.A. Cottrell St Andrews
A.J. Cross London
V. Crunelli Cardiff
T.C. Cunnane Oxford
F. Cunningham London
A. Dray London
J.M. Edwardson Cambridge
W. Feniuk Ware
J.R. Fozard Basle, Switzerland
C.J. Garland Southampton
L.G. Garland Beckenham
A. Gibson London
R. Gristwood Barcelona, Spain
P.E. Hicks Leuville-sur-Orge, France
S.J. Hill Nottingham
J.C. Hunter Cambridge
K.A. Kane Glasgow
P. Keen Bristol
D.A. Kendall Nottingham
P. Leff Loughborough
D. Lodge Surrey
H.D. Lux Planegg, Germany
R. McMillan Macclesfield
J. Maclagan London
G. Martin Beckenham
W. Martin Glasgow
D.N. Middlemiss Harlow
R.C. Miller Strasbourg, France
P.K. Moore London
R.J. Naylor Bradford
C.D. Nicholson Newhouse
C.P. Page London
R.M.J. Palmer Beckenham
B.K. Park Liverpool
A.N. Payne Beckenham
F.L. Pearce London
M.H.T. Roberts Cardiff
P.J. Roberts Southampton
C. Robinson London
G.J. Sanger Harlow
M.A. Simmonds London
J.M. Sneddon Sunderland
M. Spedding Edinburgh
K. Starke Freiburg, Germany
I.P. Stolerman London
P.V. Taberner Bristol
M.D. Tricklebank Harlow
M.B. Tyers Ware
S.P. Watson Oxford
A.H. Weston Manchester
B.J.R. Whittle Beckenham
Eileen Winslow Newhouse

CORRESPONDING EDITORS

P.R. Adams Stony Brook, U.S.A.
C. Bell Melbourne, Australia
F.E. Bloom La Jolla, U.S.A.
A.L.A. Boura Clayton, Australia
N.J. Dun Toledo, U.S.A.
R.F. Furchgott New York, U.S.A.
T. Godfraind Brussels, Belgium
S.Z. Langer Paris, France
R.J. Miller Chicago, U.S.A.
R.C. Murphy Denver, U.S.A.
E. Muscholl Mainz, Germany
R.A. North Portland, U.S.A.
M. Otsuka Tokyo, Japan
M.J. Rand Melbourne, Australia
S. Rosell Södertalje, Sweden
P. Seeman Toronto, Canada
L. Szekeres Szeged, Hungary
B. Uvnas Stockholm, Sweden
P.A. Van Zwieten Amsterdam, Netherlands
V.M. Varagič Belgrade, Yugoslavia
G. Velo Verona, Italy
Wang Zhen Gang Beijing, China
M.B.H. Youdim Haifa, Israel

Papers will be considered for publication on all aspects of pharmacology, including chemotherapy.

Manuscripts (two copies) should be sent to Editorial Office, British Journal of Pharmacology, St. George's Hospital Medical School, Cranmer Terrace, London SW17 0RE. Authors should consult the Instructions to Authors in Vol. 105, 245–251 (1992) and the Nomenclature Guidelines for Authors in Vol. 105, 252–254 (1992). These Instructions and Guidelines also appear with the journal Index for volumes 102–104, 1991.

The *British Journal of Pharmacology* is published monthly by the Scientific & Medical Division, Macmillan Press Ltd.

The journal is covered by *Current Contents*, *Excerpta Medica* and *Index Medicus*.

All business correspondence and reprint requests should be addressed to the Scientific & Medical Division, Macmillan Press Ltd., Houndmills, Basingstoke, Hampshire RG21 2XS, UK. Telephone: (0256) 29242; Fax: (0256) 810526.

Annual subscription prices for 1992 EEC £412, elsewhere £445/US$825 (sterling rate is definitive). Orders must be accompanied by remittance. Cheques should be made payable to Macmillan Press, and sent to: Macmillan Press Ltd., Subscription Department, Brunel Road, Houndmills, Basingstoke, Hampshire RG21 2XS, UK.

Overseas subscribers may make payments into UK Post Office Giro Account No. 5192455. Full details must accompany the payment.

Second Class postage paid at Rahway NJ. US Mailing Agent: Mercury Airfreight International Ltd, Inc., 2323 Randolph Avenue, Avenel, New Jersey, NJ 07001, USA.

Enquiries concerning advertising space or rates should be addressed to: Michael Rowley, Advertisement Manager, Macmillan Press Ltd., 4 Little Essex Street, London WC2R 3LF. Telephone: 071 836 6633; Fax: 071 379 4204.

All rights of reproduction are reserved in respect of all papers, articles, illustrations, etc., published in this journal in all countries of the world.

Authorization to photocopy items for internal or personal use, or the internal or personal use of specific clients, is granted by Macmillan Press Ltd for libraries and other users registered with the Copyright Clearance Center (CCC) Transactional Reporting Service, provided that the base fee of $3.50 per copy is paid directly to CCC, 21 Congress St., Salem, MA 01970, USA.

© The British Pharmacological Society & Macmillan Press Ltd, 1992.
ISSN 0007–1188

0007–1188/92 $3.50 + $0.00

R.H. Scott, M.I. Sweeney, E.M. Kobrinsky, H.A. Pearson, G.H. Timms, I.A. Pullar, S. Wedley & A.C. Dolphin. Actions of arginine polyamine on voltage and ligand-activated whole cell currents recorded from cultured neurones **199**

Y. Uyama, Y. Imaizumi & M. Watanabe. Effects of cyclopiazonic acid, a novel Ca^{2+}-ATPase inhibitor, on contractile responses in skinned ileal smooth muscle **208**

T.E. White, J.M. Dickenson, S.P.H. Alexander & S.J. Hill. Adenosine A_1-receptor stimulation of inositol phospholipid hydrolysis and calcium mobilisation in DDT_1 MF-2 cells **215**

T. Netzer, F. Ullrich, H. Priewer, M. Majewski & E. Mutschler. Effects of a new pteridine derivative on urinary sodium, potassium and magnesium excretion in conscious saline-loaded rats **222**

SPECIAL REPORTS

The purpose of *Special Reports* is to provide rapid publication for **new** and **important** results which the Editorial Board considers are likely to be of special pharmacological significance. (Please note that Short Communications are no longer acceptable for publication.) *Special Reports* will have publication priority over all other material and so authors are asked to consider carefully the status of their work before submission.

In order to speed publication there is normally no revision allowed beyond very minor typographical or grammatical corrections. If significant revision is required, the Board may either invite rapid re-submission or, more probably, propose that it be re-written as a Full Paper and be re-submitted for consideration. In order to reduce delays, proofs of *Special Reports* will be sent to authors but **essential corrections must reach the Production Office within 48 hours of receipt.** Authors should ensure that their submitted material conforms exactly to the following requirements.

Special Reports should normally occupy no more than two printed pages of the Journal; two illustrations (Figures or Tables, with legends) are permitted. As a guideline, with type face of 12 pitch and double-line spacing, a page of A4 paper could contain about 400 words. The absolute maximum length of the *Special Report* is 1700 words. For each Figure or Table, please deduct 200 words. The manuscript should comprise a Title page with key words (maximum of 10), a Summary consisting of a single short paragraph, followed by Introduction, Methods, Results, Discussion and References (maximum of 10). In all other respects, the requirements are the same as for Full Papers (see current 'Instructions to Authors').

PREPARATION OF MANUSCRIPTS

Authors are strongly recommended to read the full *Instructions to Authors* and *Nomenclature Guidelines for Authors* (*Br. J. Pharmacol.* 1992, **105,** 245–254) before submitting a manuscript for publication in the *British Journal of Pharmacology*. The manuscript and cover letter should be checked against the following list before mailing.

The original and one copy of the manuscript must be supplied. Manuscripts must be typed in double-line spacing on one side of A4 paper, in type not smaller than 12 characters per inch or 10 point. Both copies to include Tables and a set of labelled Figures. One set of Figures without numbers or letters is also to be included. The text to be arranged in the following subsections:

1. **Title**—To have no more than 150 characters on a separate page, which should also include a Short Title (50 characters maximum) and the name and address of the author for correspondence.

2. **Summary**—To be arranged in numbered paragraphs (Full Papers) or a single paragraph (Special Reports).
   —to include aims, principal results and conclusions.
   —to include Key words (10 maximum) at end of summary.

3. **Introduction**—To contain concise statements of the problem and the aims of the investigation.

4. **Methods**—To have brief but adequate account of the procedures; *full names of drugs* (*including those referred to by manufacturer's code*), sources of drugs and statistical tests to be stated.

5. **Results**—To have no repetition of data in Figures, Tables and text.

6. **Discussion**—Findings and conclusions to be placed in context of other relevant work.
   NB Simple repetition of results and unwarranted speculation are not acceptable.

7. **Acknowledgments**—Sources of support. Sources of drugs not widely available commercially.

8. **References**—All references in the text to be included in the Reference List and *vice versa*. References in alphabetical order with complete citations; Journals publishing 'in press' papers identified.
   References to manuscripts submitted to other journals but not yet accepted are not allowed.

9. **Tables**—Each on a separate page and prepared in accordance with current requirements of the Journal.

10. **Figures**—Both labelled and non-labelled Figures to be prepared in accordance with current requirements of the Journal (see *Instructions to Authors*, 1992, **105,** 245–251) and provided with Figure Number and Authors' names on back (*in pencil*).
    —each legend to be typed on a separate page and carrying keys to symbols.
    —keys to symbols and histograms must not appear on the figures themselves, but in the respective legends.
    —'box style' figures are not in keeping with the Journal style; line drawings etc must have only left-hand and bottom axes.

11. **Manuscripts**—To be accompanied by a declaration signed by each author that
    (a) results are original
    (b) approval of all persons concerned has been given to submit manuscripts for consideration (see also 12b)
    (c) the same material is neither 'in press' (i.e. is in proof or has definitely been accepted for publication) nor under consideration elsewhere. Furthermore it will not be submitted or published elsewhere before a decision has been reached by the Editorial Board of the *British Journal of Pharmacology* and will not be submitted elsewhere if accepted by the *British Journal of Pharmacology*.
    (d) Copyright assignment is included.

12. **Cover letter**—To state clearly
    (a) Corresponding author's full postal address, telephone, telex or Fax number
    (b) where appropriate, that *either* ethical approval has been given for investigation *or* Company or Institutional permission to publish work has been received.

13. **Reminder**—Packaging to be sufficiently robust to protect Figures and to withstand mailing.

Failure to comply with *Instructions to Authors* may lead to substantial delays in processing, review and publication and may even jeopardize acceptance of the manuscript.

NOMENCLATURE

Authors are reminded that accepted receptor and associated terminology is laid out in *Nomenclature Guidelines for Authors*, as published in the *British Journal of Pharmacology, Br. J. Pharmacol., 1992,* **105,** 245–254.

BRITISH JOURNAL OF PHARMACOLOGY VOLUME 106 (1) 1992

PAPERS

P.I. Thompson, S. Bingham, P.L.R. Andrews, N. Patel, S.P. Joel & M.L. Slevin. Morphine 6-glucuronide: a metabolite of morphine with greater emetic potency than morphine in the ferret 3

D.M. Eckman, J.D. Frankovich & K.D. Keef. Comparison of the actions of acetylcholine and BRL 38227 in the guinea-pig coronary artery 9

Th. Noack, G. Edwards, P. Deitmer, P. Greengrass, T. Morita, P.-O. Andersson, D. Criddle, M.G. Wyllie & A.H. Weston. The involvement of potassium channels in the action of ciclazindol in rat portal vein 17

M.R. Bennett, R. Kerr & G. Khurana. Adenosine modulation of calcium currents in postganglionic neurones of avian cultured ciliary ganglia 25

J.V. Esplugues, Ma.D. Barrachina & J. Esplugues. Modulation by peripheral opioids of basal and distension-stimulated gastric acid secretion in the rat 33

P. Valeri, L.A. Moorone & L. Romanelli. Manifestations of acute opiate withdrawal contracture in rabbit jejunum after μ-, κ- and δ-receptor agonist exposure 39

A. Abdelrahman, Y.-X. Wang, S.D. Chang & C.C.Y. Pang. Mechanism of the vasodilator action of calcitonin gene-related peptide in conscious rats 45

Y. Zhu, W.B. Im, R.A. Lewis & P.F. VonVoigtlander. Comparison of pyrrolidinyl and piperidinyl benzamides for their anticonvulsant activity and inhibitory action on sodium channel 49

S.Y. Lin-Shiau, K.S. Hsu & W.M. Fu. Studies on curare-like action of 2,2',2''-tripyridine in the mouse phrenic nerve-diaphragm 55

L.A. Bishop, V.P. Gerskowitch, R.A.D. Hull, N.P. Shankley & J.W. Black. Combined dose-ratio analysis of cholecystokinin receptor antagonists, devazepide, lorglumide and loxiglumide in the guinea-pig gall bladder 61

K. Fink, R. Schultheiß & M. Göthert. Stimulation of noradrenaline release in human cerebral cortex mediated by N-methyl-D-aspartate (NMDA) and non-NMDA receptors 67

N. Tokutomi, N. Agopyan & N. Akaike. Penicillin-induced potentiation of glycine receptor-operated choride current in rat ventro-medial hypothalamic neurones 73

T. Makki, I. Lartaud, L. Bray-des Boscs, C. Capdeville-Atkinson, J.-M. Chillon, M. Hoffman, J.-P. Nicolas & J. Atkinson. Haemodynamic effects of a new dihydropyridine calcium entry blocker, S-12968-(−), in a rat model of cardiovascular calcium overload 79

G. Kojda, W. Klaus, G. Werner & U. Fricke. Intervascular and stimulus selectivity of nitrendipine and related derivatives in KCl and prostaglandin $F_{2\alpha}$ precontracted porcine arteries 85

M.F.M. Braga, A.J. Anderson, A.L. Harvey & E.G. Rowan. Apparent block of K^+ currents in mouse motor nerve terminals by tetrodotoxin, μ-conotoxin and reduced external sodium 91

J.B. Salom, G. Torregrosa, F.J. Miranda, J.A. Alabadí & E. Alborch. Comparison of the contractile effects of endothelin-1 and sarafotoxin S6b in goat isolated cerebral arteries 95

S. Diamant, T. Eldar-Geva & D. Atlas. Imidazoline binding sites in human placenta: evidence for heterogeneity and a search for physiological function 101

R.M. Henderson, M.L.J. Ashford, L.J. MacVinish & A.W. Cuthbert. Chloride channels and anion fluxes in a human colonic epithelium (HCA-7) 109

L.A. Brown & S.E. Harding. The effect of pertussis toxin on β-adrenoceptor responses in isolated cardiac myocytes from noradrenaline-treated guinea-pigs and patients with cardiac failure 115

H. Morimoto, M. Murai, Y. Maeda, D. Hagiwara, H. Miyake, M. Matsuo & T. Fujii. FR 113680: a novel tripeptide substance P antagonist with NK_1 receptor selectivity 123

J.L. Mehta, D.L. Lawson, B.C. Yang, P. Mehta & W.W. Nichols. Modulation of vascular tone by endothelin-1: role of preload, endothelial integrity and concentration of endothelin-1 127

G.R. May, W. Paul, P. Crook, K.D. Butler & C.P. Page. The pharmacological modulation of thrombin-induced cerebral thromboembolism in the rabbit 133

K.F. Martin, S. Hannon, I. Phillips & D.J. Heal. Opposing roles for $5\text{-}HT_{1B}$ and $5\text{-}HT_3$ receptors in the control of 5-HT release in rat hippocampus *in vivo* 139

V.E. Rand & C.J. Garland. Endothelium-dependent relaxation to acetylcholine in the rabbit basilar artery: importance of membrane hyperpolarization 143

W. Schreibmayer, O. Tripathi & H.A. Tritthart. Kinetic modulation of guinea-pig cardiac L-type calcium channels by fendiline and reversal of the effects of Bay K 8644 151

P. Arvola, I. Pörsti, P. Vuorinen, A. Pekki & H. Vapaatalo. Contractions induced by potassium-free solution and potassium relaxation in vascular smooth muscle of hypertensive and normotensive rats 157

M.J. Robertson, M.P. Cunoosamy & K.L. Clark. Effects of peptidase inhibition on angiotensin receptor agonist and antagonist potency in rabbit isolated thoracic aorta 166

R.A. Lefebvre, E. Baert & A.J. Barbier. Influence of N^G-nitro-L-arginine on non-adrenergic non-cholinergic relaxation in the guinea-pig gastric fundus 173

S.M. Gardiner, P.A. Kemp & T. Bennett. Effects of the neutral endopeptidase inhibitor, SQ 28,603, on regional haemodynamic responses to atrial natriuretic peptide or proendothelin-1 [1-38] in conscious rats 180

F. Rioux & M. Lemieux. Haemodynamic and abdominal motor reflexes elicited by neurotensin in anaesthetized guinea-pigs 187

N.E. Shaw, R. Foulkes, D.P. Andrew, D.T. Brown & B. Hughes. The effect of monoclonal antibodies to calcitonin gene-related peptide (CGRP) on CGRP-induced vasodilatation in pig coronary artery rings 196

R.H. Scott, M.I. Sweeney, E.M. Kobrinsky, H.A. Pearson, G.H. Timms, I.A. Pullar, S. Wedley & A.C. Dolphin. Actions of arginine polyamine on voltage and ligand-activated whole cell currents recorded from cultured neurones 199

Y. Uyama, Y. Imaizumi & M. Watanabe. Effects of cyclopiazonic acid, a novel Ca^{2+}-ATPase inhibitor, on contractile responses in skinned ileal smooth muscle 208

T.E. White, J.M. Dickenson, S.P.H. Alexander & S.J. Hill. Adenosine A_1-receptor stimulation of inositol phospholipid hydrolysis and calcium mobilisation in DDT_1 MF-2 cells 215

T. Netzer, F. Ullrich, H. Priewer, M. Majewski & E. Mutschler. Effects of a new pteridine derivative on urinary sodium, potassium and magnesium excretion in conscious saline-loaded rats 222

Typeset by Elite Typesetting Techniques, Southampton, Hampshire
and printed in Great Britain by Unwin Brothers Ltd., The Gresham Press, Old Woking, Surrey